Faculty of Science and Engineering
Department of Applied Geology

Modern and Neogene Analogues for Productive Subsurface Carbonate Systems in SE Asia

Robert Henry Christopher Madden

This thesis is presented for the Degree of
Doctor of Philosophy

of

Curtin University

January 2013

Declaration

To the best of my knowledge and belief this thesis contains no material previously published by any other person except where due acknowledgement has been made.

This thesis contains no material which has been accepted for the award of any other degree or diploma in any university.

RHC MADDEN

Date: 09-01-2013

ABSTRACT

This combined sedimentological, diagenetic and remote sensing study of SE Asian Cenozoic carbonate systems has implications for the understanding of how depositional and diagenetic conditions unique to the equatorial tropics influence regional hydrocarbon reservoir development. Most modern analogues used to help evaluate carbonate development and their subsurface reservoir potential are from sub-tropical to arid regions. However, within carbonate build-ups some of the world's most prolific hydrocarbon reserves are in Neogene subsurface deposits from SE Asia where the models generated in other regions cannot easily be applied. Modern and Neogene carbonate production is, and was extensive and diverse throughout the tropical waters of SE Asia. Carbonate systems in SE Asia range from mixed carbonate clastic shelves, localised and ephemeral shoals or reefs, a variety of shallow-water platform top settings and deep water and/or reworked carbonates. Despite the economic importance of Neogene carbonate systems as hydrocarbon reservoir targets there are very few studies of analogous modern or Neogene outcrops from SE Asia. This study evaluates the diagenetic alteration of two Neogene carbonate systems: clastic influenced delta-front patch reefs and an isolated platform from a semi enclosed basin. The third part of the study investigates the environmental characterisation, sedimentology and early alteration of modern fringing reef systems developed around isolated carbonate islands. Comparisons are made with other equatorial carbonate systems and subsurface reservoirs, together with those from other climate belts, thereby enhancing understanding of global carbonate development and hydrocarbon potential.

Combined petrographic, geochemical and field studies reveal that mixed carbonate-siliciclastic deposits from humid equatorial coastal settings generally have low reservoir quality, due to the presence of abundant carbonate-siliciclastic matrix and the throughput of undersaturated meteoric fluids that pervasively stabilise and cement the deposits during early burial diagenesis. Also, isolated carbonate platforms that developed in protected and/or subsiding

settings may possess low reservoir qualities due to abundant matrix together with extensive burial compaction, stabilisation and cementation. However, in high energy marginal settings it is likely that early marine cementation may be enhanced, with the potential to provide resistance to burial compaction effects and promote higher reservoir quality if primary porosity and pore throats are not totally occluded. The effects of meteoric dissolution in such isolated subsiding platforms is not pronounced and further mitigated by later cementation. Where reef development may have been impacted upon by potential nutrient influx there is less potential for exposure through building to sea level. Over 75% of the carbonate reservoirs in SE Asia are from isolated pure carbonate platforms. The effects of widespread vadose aragonite dissolution and large-scale reprecipitation of carbonate cements in both the vadose and particularly the phreatic marine realm lead to a layered reservoir development.

A combined remote sensing and modern sedimentological study of a small-scale high energy fringing reef system reveals where grainstone textures predominate. The paucity of fines across the system as a whole is attributed to high wave/current energies, the small size of the islands rendering limited protection, bidirectional monsoon winds and the lack of reef rimmed margins built to sea level. Furthermore seagrass beds acting as baffles promote the minor accumulation of fines. It is anticipated that if early partial cementation is promoted in such grainstone deposits good quality reservoir units may be preserved. The satellite and sedimentology study probably only hints at some of the variability within SE Asia's vast, and virtually unstudied fringing reef systems however, it highlights apparent significant differences between some equatorial fringing reefs and those from the subtropics. The systems studied here reveal the importance of seagrass bed development, the influence of the monsoons and a degree of sediment homogenisation, lack of windward-leeward effects, and a lack of hurricane influence on these equatorial SE Asian fringing reefs.

ACKNOWLEDGEMENTS

A little over three years ago I started this PhD, and now that it is finished I owe thanks to many people, both professionally and personally. To all of you, whether named here or not, thank you.

Firstly, I would like to express my sincere gratitude to my supervisor Moyra Wilson. Thank you for your endless guidance, seemingly tireless patience and generous support throughout this project. I consider myself fortunate to have worked with Moyra for the duration of this PhD. I owe Moyra further thanks for agreeing to take me on after previous teaching and supervision at the University of Durham, and sparking my interest in all things carbonate. Thank you for everything Moyra, both previously and undoubtedly into the future. It has been a pleasure to work with you and I look forward to our future endeavours.

To Katy Evans, thank you for your time and help with all things geochemical. Thank you to Mehrooz Aspandiar and Alex Stevens for continued support and teachings with GIS, you have certainly made a huge part of this PhD possible. Many thanks go out for the rest of the support I have received in the Department of Applied Geology, you have all been great.

To all of my friends both in Australia and back home in the UK, in one way or another you have all provided motivation and drive for me to get this work completed. For this I am grateful to you all. In particular I would like to extend my thanks to Erin Gray, Fiona Mothersole, Matt Koessler, Reilly Evetts and Meagan Burke. Thanks for everything and the best of luck in finishing your own PhD's. To Sue Court-Oak at the Colchester Sixth Form College, thank you for capturing my interest in Geology from the outset (I believe by telling me to lick a rock at open evening!). Thank you for continuously pushing me Sue.

Being so far away from home has made this PhD a challenge at times, but I consider myself to be incredibly lucky to have such a supportive family who have kept me going through a lot of the ups and downs. Mum and Dad, thank you for your endless love, support, encouragement and inspiration. I realise at times I have been (and I quote you Dad) a "rock bore" but I hope above all else that I have made you both proud. Andrew, thanks for the help finishing up my appendices and late night coffee fuelled Skype chats. Stuart, thanks for constantly telling me to get back to work and Saira for all of your encouragements. Thank you Grandpa for checking I have done my homework, and for all the "fags and booze money". Jen Le Marinel you have been the best of friends, your phone calls, messages, post cards, letters and parcels have always put a smile on my face, I can't say thank you enough.

Finally, to Alex, for over three years now you have put up with me, through the highs and lows. I know at times I have been impossibly difficult but you have stood fast by me and supported me through it all. In so many ways I could not have done this without you, you have kept me going through the thick of it and always reminded me that there is life outside of this PhD. Alex you have been wonderful, I love you and will always be grateful to you.

To everyone, thank you again; a piece of this belongs to each one of you.

“I firmly believe that any man’s finest hour, the greatest fulfilment of all that he holds dear, is that moment when he has worked his heart out in a good cause and lies exhausted on the field of battle, victorious.”

Vince Lombardi

List of Publications Included as a Part of this Thesis

This thesis compiles a collection of research papers that were either published, in press or under review at the time of writing this document. The objectives and relationship amongst the different papers are described in the introductory chapter. The final chapter summarises the papers and places them into a wider context.

The research papers contained within this thesis are given below.

Madden, R.H.C., and Wilson, M.E.J., 2012. Diagenesis of Neogene delta-front patch reefs: alteration of coastal siliciclastic-influenced carbonates from humid equatorial regions. Journal of Sedimentary Research 82, 871-888.

Madden, R.H.C., and Wilson, M.E.J., 2013. Diagenesis of a SE Asian Cenozoic carbonate platform margin and its adjacent basinal deposits. Sedimentary Geology 286-287, 20-38.

Madden, R.H.C., Wilson, M.E.J., and O'Shea, M. accepted. Modern fringing reef carbonates from equatorial SE Asia: an integrated environmental, sediment and satellite characterisation study. Marine Geology.

The formatting of each chapter within this thesis may appear to vary, and may differ to the published form based on the requirements and formatting guidelines of each individual journal and this thesis. Due to the nature of this thesis as a composite of published manuscripts there is a degree of repetition throughout.

Statement of Contributions of Others

This thesis has been supported by the Department of Applied Geology, Curtin University. The individual chapters of this thesis, notably those comprising the published works listed above were undertaken in collaboration with Dr Moyra E.J. Wilson at Curtin University. Samples for the entirety of this PhD have been collected by Moyra during previous field excursions. However, as the primary author of this thesis, and all published manuscripts contained within, I declare that I have been responsible for all subsequent research, analysis, interpretation and write up of these samples. A written statement of co-author contribution is provided within the Appendices at the end of this thesis.

RHC MADDEN

Date: 09-01-2013

MEJ WILSON

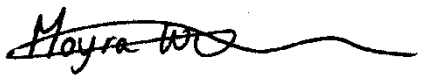

Date: 09-01-2013

TABLE OF CONTENTS

LIST OF FIGURES

is moderately to highly fragmented with coral and foraminifera showing moderate abrasion. Coral clasts are pervasively micritised. (h) Binocular microscope photo of mixed long and short seagrass facies sample Kal17. Sample is very poorly sorted silts to gravel. Characteristic *Halimeda*, imperforate foraminifera and miliolids are dominant with lesser coral and shell allochems. (i) Binocular microscope photograph of mixed coral and seagrass facies sample HGG3. Sample is moderately sorted and dominated by moderately to highly abraded and fragmented shell allochems. Imperforate, perforate and calcarinid foraminifera are present. Calcarinid spines are generally abraded. (j) Thin-section photomicrograph of mixed coral and seagrass facies sample HGG2. Sample shows abraded and micritised coral fragments with well preserved perforate foraminifera. (k) Thin-section photomicrograph of mixed coral and seagrass facies sample Kal3. Sample shows highly abraded and fragmented coral clasts with minor to moderate micritisation. (l) Binocular microscope photo of coral with/without sediment cover facies sample HSB2S-2. Sample is moderately sorted medium sands to gravel. Coral and shell allochems are dominant and show moderate abrasion and fragmentation. Minor alcyonarian sclerites and echinoid spines are present. (m) Binocular microscope photo of reef slope sample PK10. Sample is well sorted and has an overall low degree of micritisation. Sample has high abundances of alcyonarian sclerites, with the abundant coral and shell allochems highly fragmented. (n) Binocular microscope photo of deep water facies sample Kal34. Sample is almost 100% lithic marl with a single fragment of shell material. (o) Binocular microscope photo of deep water facies sample Kal40. Sample is very poorly sorted with high abundances of perforate, imperforate and mililoid foraminifera and shells. Lithic marl clasts comprises the fine grain sizes of this sample. 24

Figure 2.3. Combined environmental transect, field, component and grain size data for the Pak Kasim's transect undertaken on Hoga. The transect location is identified on both the quasi-natural (RGB:123) and false colour (RGB:421) images, with sample locations identified on the highly magnified displays. The environmental transect correlates with the individual pixels

bathyal setting. Clear isopachous fringing cement forming a fibrous rim to large benthic foraminifera (1). Fringing cement has been overgrown in places by bladed calcite cement (2). (D) Sample HP05; Bioclastic grain-rudstone from platform margin. Isopachous fringing cement developed on a larger benthic foraminifera showing replacement by equant blocky calcite (1). Clear equant blocky calcite infills between clasts and areas of matrix (2). (E) Sample HP19; Planktonic foraminifera packstone from ramp type margin (Wilson et al., 2012). Syntaxial overgrowth cement present on echinoderm grain (1). A high amplitude stylolite cross-cuts the lithology. (F) Sample BR75a; Clast supported limestone breccia from platform margin. Recrystallised carbonate clast including a void (shelter porosity) infilled by bladed to equant calcite (1) and micritic sediment (2; includes planktonic foraminifera). 123

Figure 4.4. Plane-polarised thin-section photomicrographs illustrating a range of diagenetic features from the Kedango Limestone. (A) Sample BR53; Recrystalised mud-wacke-floatstone from platform margin deposits. Recrystalised coral with chambers partially cemented and filled by a fine dark micritic sediment (1). Alveolar texture present as irregular pores with a dark brown rim infilled by sparite and micrite (2). (B) Sample PR05; Clast supported limestone breccia from bathyal to upper bathyal setting. Banded cement infilling a karstic dissolution cavity within a reworked clast. (C) Sample GP03; Coral bioclastic grain-rudstone with mechanically deformed alveolinid (imperforate foraminifera; centre of field of view) with development of a concavo-convex grain contact with an echinoid clast with well developed syntaxial overgrowth cement. A perforate heterostegnid foraminifera has a partial rim of fringing cement and is undeformed (top of field of view). (D) Sample GB43; coarse bioclastic pack-rudstone from shallow-water platform top with Heterostegnid*,* *Nummulites* and coralline algae showing grain breakage and irregular suturing at grain-to-grain contacts. The matrix shows development of dissolution seams with concentrations of insoluble dark brown material. (E) Sample GU29; Bioclastic pack-grainstone from shallow-water platform top. Miliolids and bioclasts heavily micritised

LIST OF TABLES

Chapter 1

INTRODUCTION

Most modern analogues used to help evaluate carbonate development and their subsurface reservoir potential are from regions like the Bahamas, Florida, Central America, the South Pacific or the Persian Gulf (Roberts and Murray, 1984; Phillip et al., 1995; Gischler and Lomando, 1999; Rankey, 2002; Gischler et al., 2003; Gischler, 2006, 2011; Farzadi, 2006; Rankey and Reeder, 2010) However, within carbonate build-ups some of the world's most prolific hydrocarbon reserves are in Neogene subsurface deposits from SE Asia (Greenlee and Lehmann, 1993; Doust and Noble, 2008) where models generated in other regions cannot easily be applied (Wilson, 2002; 2012). The hypothesis here is that the study of modern and Neogene systems in SE Asia will allow an evaluation of how depositional and diagenetic conditions unique to the equatorial tropics influence regional reservoir development.

Tomascik et al. (1997) contributes to the knowledge base and understanding of modern SE Asian coral reefs and seas. This review expands on such early works as Kuenen (1933) and Umbgrove (1946, 1947) that were amongst the first studies to address the biology, morphology and controls on reef development. Within the SE Asian region, the highest global biodiversity in modern marine settings exists alongside the most extensive and complete record of equatorial carbonates spanning the Cenozoic (Fulthorpe and Schlanger, 1989; Wilson, 2002, 2008, 2011). Despite recent research endeavours (Wilkinson, 2000; Gordon, 2005, Wilson and Hall, 2010) it is apparent that there is still a gap in our knowledge resulting from a lack of basic research. There is a need to better evaluate the biota, communities, regional conditions, modern carbonate environments and diagenesis of carbonates from SE Asia (cf. Wilson, 2011).

Furthermore, a need for better evaluation of SE Asian carbonate systems is necessary given the complex interplay of environmental influences in the equatorial tropics that are under-evaluated in the currently accepted analogue models from more arid sub-

tropical regions. Throughout the Cenozoic SE Asia has experienced an interplay of: complex tectonics, frequent sea level fluctuations, low marine salinities, fluctuating temperature patterns and sustained nutrient and clastic influx (compared to the more episodic discharge from sub-tropical models) (e.g. Hamilton, 1979; Hall, 1996; Hendry et al., 1999; Wilson and Moss, 1999; Hall and Nichols, 2002; Burton, 2003; Wilson and Hall, 2010; Wilson, 2011).

Key to producing higher resolution models of subsurface heterogeneity within carbonate systems is to improve on the poorly documented spatial-temporal variability in deposition, diagenesis and porosity characteristics. In particular, there is a need for data that demonstrates how primary environmental settings unique to the region relate to primary depositional sediment characteristics and their early alteration. Furthermore, understanding the effects of diagenesis on the development of reservoir quality from a range of carbonate systems is integral to the development of models that help characterise hydrocarbon reservoirs.

1.1 Objectives

The hypothesis here is that the study of a variety of modern and Neogene carbonate systems from SE Asia will allow better understanding of how depositional and diagenetic conditions unique to the equatorial tropics influence regional hydrocarbon reservoir development.

Specific objectives of this study are:

To evaluate how carbonate system morphologies, facies distributions and depositional environments vary from a range of land-attached and isolated modern-carbonate systems in SE Asia.

To assess the potential influence of environments and their sedimentary characteristics on reservoir development.

To assess how variable diagenesis may overprint primary facies characteristics and the resultant influence on associated reservoir characteristics.

To evaluate the major controlling factors influencing platform morphologies, facies characteristics, together with their spatial distributions and how these may impact reservoir potential.

To develop models for reservoir characterisation and heterogeneity that may be utilised by the hydrocarbon industry.

Carbonate–siliciclastic mixing is common in both modern and ancient environments (Mount 1984; Larcombe and Woolfe 1999; Woolfe and Larcombe 1999; Wilson and Lokier 2002; Wilson 2005). In spite of their common occurrence, the diagenesis of siliciclastic-influenced coral reefs and carbonate platforms from equatorial to subtropical settings remains largely unstudied (Hendry et al. 1999; Wilson 2012). Furthermore the diagenesis and development of open marine carbonate platforms from the humid equatorial tropics of SE Asia are relatively well documented, since many comprise hydrocarbon reservoirs in the subsurface (Epting, 1980; Fulthorpe and Schlanger, 1989; Grötsch and Mercadier, 1999; Wilson and Hall, 2010). However the diagenetic variability across platform flank and contemporaneous bathyal deposits, particularly from low to moderate energy carbonate platforms is less well known. The results of these diagenetic studies offer insights into patterns of diagenesis across humid equatorial land-attached and platform carbonate environments that may have regional analogues as well as implications for hydrocarbon exploration.

Aside from the hydrocarbon reservoir aspects of this project there are also significant developments to be made from a carbonate sedimentology perspective. This study contributes to a better understanding of variability in carbonate deposition and diagenesis in a range of pure carbonate and mixed carbonate–siliciclastic systems from the equatorial tropics, with comparison made to marine systems from other climatic belts. As well as generating a better understanding of the sedimentology of this region, a clearer snapshot on modern carbonate systems in terms of facies and their distribution may be useful for habitat and resource management and conservation (e.g. fisheries and reef eco-tourism), biodiversity as well as providing sedimentary "insight" on modern systems.

Understanding the effects of diagenesis on a range of carbonate systems is integral to the development of models that characterise what are typically fickle systems. Each individual study comprising this PhD project has yielded new and publishable results and are currently either published or accepted for publication in international peer reviewed journals.

1.2 Thesis Structure

This thesis opens with an introduction that addresses the ideas behind this study and ends with a conclusion that summarises the major outcomes of this research. A "standard" literature review is not presented within this thesis. Each manuscript, comprising a portion of this study, incorporates relevant background literature to place this research in a wider context, includes discussions of the new findings with respect to the previous studies, and references are cited at the end of each chapter/paper. Through reference to literature, summaries of the regional geological setting and history of the study sites are given together with evaluations of the field of research. Chapters two, three and four comprise the main body of this thesis, and are based on three peer reviewed international manuscripts. Two of these manuscripts are published (chapter 3 in the *Journal of Sedimentary Research* and chapter 4 in *Sedimentary Geology*), and the third is accepted for publication (chapter 2 in *Marine Geology*). Each of the publishing journals is ranked 'A' grade through ERA (Excellence in Research Australia).

Chapter two of this thesis is a accepted for publication in the journal *Marine Geology*.

Madden, R.H.C., Wilson, M.E.J., and O'Shea, M., accepted. Modern fringing reef carbonates from equatorial SE Asia: an integrated environmental, sediment and satellite characterisation study. Marine Geology.

This manuscript explores statistics-based satellite image classifications in conjunction with modern sediment samples from fringing reef systems around carbonate islands in the Tukang Besi Archipelago, Indonesia. Specific study objectives are to: (1) produce a satellite generated environmental facies map using

statistics based methods, (2) identify primary sedimentological and early sediment alteration characteristics of associated carbonate deposits, (3) compare primary sedimentological properties to primary environmental facies and their satellite characteristics and (4) contribute towards a greater understanding of modern humid equatorial carbonate systems highlighting the heterogeneities that may exist.

Chapter three is a manuscript published in the *Journal of Sedimentary Research.*

Madden, R.H.C., and Wilson, M.E.J., 2012. Diagenesis of Neogene delta-front patch reefs: alteration of coastal siliciclastic-influenced carbonates from humid equatorial regions. Journal of Sedimentary Research 82, 871-888.

This study offers insights into the diagenetic alteration of coastal carbonates that formed coevally with nearly continuous siliciclastic influx in a humid equatorial setting. The manuscript evaluates the diagenesis of Miocene delta-front patch reefs from Borneo with the aims of: (1) characterising the extent of diagenesis in these mixed carbonate–siliciclastic patch reefs from coastal settings, (2) developing a paragenetic sequence of the succession in the context of the evolving basin hydrology and the climatic setting, and (3) comparing general aspects of diagenesis of these humid equatorial carbonates with that of humid non-tropical carbonates and arid coastal carbonates

Chapter four, the final manuscript of this thesis, is published in the journal *Sedimentary Geology.*

Madden, R.H.C., and Wilson, M.E.J., 2013. Diagenesis of a SE Asian Cenozoic carbonate platform margin and its adjacent basinal deposits. Sedimentary Geology 286-287, 20-38.

This study provides insights into the diagenesis of a SE Asian Tertiary carbonate platform and the variations in alteration that occur across platform top, margin, slope and adjacent basinal deposits. This manuscript tests the hypothesis that the diagenesis: (1) of bathyal, slope and shallow platform deposits will vary associated with the different syn-, and post-depositional processes affecting the different

environments, and (2) will be influenced by the setting of the platform in a tectonically active, subsiding marine embayment. Also, that there may be significant differences in diagenetic alteration of the platform from other carbonate platforms developed in more open-oceanic and/or non-subsiding settings within SE Asia.

Chapter five presents a discussion on modern and Neogene analogues for productive subsurface carbonate reservoirs. This chapter acts as a "tie-together" of the three journal manuscripts, identifying the significance of the studies in terms of hydrocarbon reservoir characterisation, as well as placing the studies in a global context. This chapter has been included as implications for reservoir quality within the individual manuscripts are only briefly touched upon.

Appendices lie at the back of this thesis and include the classification schemes used throughout the thesis and individual manuscripts. Further manuscript specific material is also presented including, where possible: high resolution thin-section scans, plain polarised light and cathodoluminescent photomicrographs, petrographic observations and binocular microscope photos of modern sediments. Additional "work-books" relevant to satellite image processing are also included. Finally co-author contribution statements are given at the end of the thesis.

1.3 References

Burton, L.M., 2003. Carbonate-siliciclastic interactions: Tertiary examples from Spain. Unpublished Ph.D. thesis; The University of Durham, 396 p.

Doust, H., and Noble, R.A., 2008. Petroleum systems of Indonesia. Marine and Petroleum Geology 25, 103-129.

Epting, M., 1980. Sedimentology of Miocene carbonate buildups, central Luconia, offshore Sarawak. Bulletin of the Geological Society of Malaysia 12, 17-30.

Farzadi, P. 2006. The development of Middle Cretaceous carbonate platforms, Persian Gulf, Iran: Constraints from seismic stratigraphy, well and biostratigraphy. Petroleum Geoscience 12, 59-68.

Fulthorpe, C.S., and Schlanger, S.O., 1989. Paleo-Oceanographic and tectonic settings of early Miocene reefs and associated carbonates of offshore

Southeast-Asia. American Association of Petroleum Geologists, Bulletin 73, 729-756.

Gischler, E., 2006. Sedimentation on Rasdhoo and Ari Atolls, Maldives, Indian Ocean. Facies 52, 341-360.

Gischler, E., 2011. Sedimentary facies of Bora Bora, Darwin's type barrier reef (Society Islands, South Pacific): The unexpected occurrence of non-skeletal grains. Journal of Sedimentary Research 81, 1-17.

Gischler, E. and Lomando, A.J., 1999. Recent sedimentary facies of isolated carbonate platforms, Belize-Yucatan system, Central America. Journal of Sedimentary Research 69, 747-763.

Gischler, E., Hausa, I., Heinrich, K., Scheitel, U., 2003. Characterization of Depositional Environments in Isolated Carbonate Platforms Based on Benthic Foraminifera, Belize, Central America. Palaios 18, 236-255.

Gordon, A.L., 2005. Oceanography of the Indonesian Seas and their throughflow. Oceanography, 18, 14-27.

Greenlee, S.M., and Lehmann, P.J., 1993. Stratigraphic framework of productive carbonate build-ups. In: R.G. Loucks, and J.F. Sarg (Eds.) Carbonate Sequence Stratigraphy, Recent Developments and Applications, American Association of Petroleum Geologists, Memoir 57, 267-290.

Grötsch, J., and Mercadier, C., 1999. Integrated 3-D Reservoir Modeling Based on 3-D Seismic: The Tertiary Malampaya and Camago Buildups, Offshore Palawan, Philippines. American Association of Petroleum Geologists, Bulletin 83, 1703-1728.

Hall, R., 1996. Reconstructing Cenozoic SE Asia. In: Hall, R., Blundell, D.J. (Eds.) Tectonic Evolution of Southeast Asia. Geological Society of London, Special Publication 106, 153-184.

Hall, R., and Nichols, G., 2002. Cenozoic sedimentation and tectonics in Borneo: climatic influences on orogenesis. Geological Society, London, Special Publications 191, 5-22.

Hamilton, W., 1979. Tectonics of the Indonesian region. U.S. Geological Survey, Professional Papers 1078.

Hendry, J.P., Taberner, C., Marshall, J.D., Pierre, C., and Carey, P.F., 1999. Coral reef diagenesis records pore-fluid evolution and paleohydrology of a

siliciclastic basin margin succession (Eocene South Pyrenean foreland basin, northeastern Spain). Geological Society of America, Bulletin 111, 395-411.

Kuenen, P.H., 1933. Geology of Coral Reefs: The Snellius Expedition in the Eastern part of the Netherlands East Indies 1929-1930. Volume 5: Geological Results, part 2. Kemink en Zoon N.V., 125 p & plates.

Larcombe, P., and Woolfe, K.J., 1999. Terrigenous sediments as influences upon Holocene near shore coral reefs, central Great Barrier Reef, Australia. Australian Journal of Earth Sciences 46, 141-154.

Mount, J.F., 1984. Mixing of siliciclastic and carbonate sediments in shallow shelf environments. Geology 12, 432-435.

Philip, J., Borgomano, J. and Al-Maskiry, S., 1995. Cenomanian-Early Turonian carbonate platform of northern Oman: Stratigraphy and Palaeo-environments. Palaeogeography, Palaeoclimatology, Palaeoceology 119, 77-92.

Rankey, E.C., 2002. Spatial patterns of sediment accumulation on a Holocene carbonate tidal flat, northwest Andros Island, Bahamas. Journal of Sedimentary Research 72, 591-601.

Rankey, E. C. and Reeder, S. L., 2010. Controls on platform-scale patterns of surface sediments, shallow Holocene platforms, Bahamas. Sedimentology 57, 1545–1565.

Roberts, H.H., and Murray, S.P., 1984. Developing carbonate platforms: southern Gulf of Suez, northern Red Sea. Marine Geology 59, 165-185.

Tomascik, T., Mah, A.J., Nontji, A., and Moosa, M.K., 1997. The Ecology of the Indonesian Seas. Oxford University Press, Singapore, 1388 p.

Umbgrove, J.H.F., 1946. Evolution of reef corals in East Indies since Miocene times. American Association of Petroleum Geologists, Bulletin 30, 23-31.

Umbgrove, J.H.F., 1947. Coral Reefs of the East Indies. Bulletin of the Geographic Society of America 58, 729-778.

Wilkinson, C.R., 2000. Status of the coral reefs of the world: 2000. Australian Institute of Marine Science, 363 p.

Wilson, M.E.J., 2002. Cenozoic carbonates in Southeast Asia: implications for equatorial carbonate development. Sedimentary Geology 147, 295-428.

Wilson, M.E.J., 2005. Development of equatorial delta-front patch reefs during the Neogene, Borneo. Journal of Sedimentary Research 75, 114-133.

Wilson, M.E.J., 2008. Global and regional influences on equatorial shallow-marine carbonates during the Cenozoic. Palaeogeography, Palaeoclimatology, Palaeoecology 265, 262-274.

Wilson, M.E.J., 2011. SE Asian carbonates: tools for evaluating environmental and climatic change in the equatorial tropics over the last 50 million years. In: Hall, R., Cottam, M.A., and Wilson, M.E.J., (Eds.) The SE Asian Gateway: History and Tectonics of the Australia-Asia Collision. Geological Society of London, Special Publication 355, 347-369.

Wilson, M.E.J., 2012. Equatorial carbonates: an earth systems approach. Sedimentology 59, 1-31.

Wilson, M.E.J., and Lokier, S.W., 2002. Siliciclastic and volcaniclastic influences on equatorial carbonates: insights from the Neogene of Indonesia. Sedimentology 49, 583-601.

Wilson, M.E.J., and Moss, S.J., 1999. Cenozoic palaeogeographic evolution of Sulawesi and Borneo. Palaeogeography, Palaeoclimatology, Palaeoecology 145, 303-337.

Wilson, M.E.J., and Hall, R., 2010. Tectonic influences on SE Asian carbonate systems and their reservoir development. In: Morgan, W.A., George, A.D., Harris, P.M., Kupecz, J.A., and Sarg, J.F., (Eds.) Cenozoic Carbonates of Australasia. SEPM, Special Publication 95, 122-149.

Woolfe, K.J., and Larcombe, P., 1999. Terrigenous sedimentation and coral reef growth: a conceptual framework. Marine Geology 155, 331-345.

Chapter 2

MODERN FRINGING REEF CARBONATES FROM EQUATORIAL SE ASIA: AN INTEGRATED ENVIRONMENTAL, SEDIMENT AND SATELLITE CHARACTERISATION STUDY.

Robert H.C. Madden, Moyra E.J. Wilson and Maeve O'Shea

Department of Applied Geology, Curtin University, GPO Box U1987, Perth, Western Australia 6845, Australia
E-mails: r.madden@dunelm.org.uk, m.wilson@curtin.edu.au

Abstract

Fringing reefs of SE Asia may conservatively comprise ~30% of the world's coral reef area, but remain almost unstudied (White, 1987; Tomascik et al., 1997). This study provides insights into the primary sedimentological and early alteration characteristics of an isolated fringing reef system (Kaledupa-Hoga) from the Tukang Besi Archipelago, SE Asia. A combined multispectral satellite imagery, field and petrographic study allowed for the generation of an environmental facies map, which acts as a model for the distribution of primary sedimentological characteristics in relation to the primary environmental facies. The islands of the Tukang Besi Archipelago are mesotidal (<2 m) affected by strong diurnal and oceanic tidal currents, as well as high wave energy influenced by the bi-directional southeast Asian monsoon. An environmental facies map generated from Landsat-7 imagery and utilising field observations defines ten environmental facies. The facies map generated has a >71% accuracy when compared with field and sedimentary data. With the exception of the reef crest and reef slope that commonly have widths on a sub-imaging resolution (<30 m), the facies map accurately demonstrates the heterogeneous nature of the carbonate system.

Although field and satellite imagery observations reveal ten environmental facies, sedimentological characterisation results in a lower

number of distinctive categories due to the similarity of many deposits. Foreshore/backshore and bare intertidal deposits are distinctive and are composed of reef-derived material that has been reworked shorewards. Seagrass-associated facies all show some fine silt-clay sized material (<8%) with common imperforate foraminifera and pervasive micritisation, but also contain high abundances of reworked coral and shell allochems. Coral-associated reef flat facies are typically low in imperforate but high in perforate foraminifera, and show lesser effects of bioerosion and very low silt contents. The reef slope and crest are characterised by high abundances of gravel sized fragmented corals with the highest abundances of echinoderm material and alcyonarian sclerites. Sediment samples across all fringing reef environments from the Kaledupa-Hoga transects are characterised almost exclusively by grain-rudstone textures, with <2-5% silt and clay size fractions, and minor baffling of fines in seagrass-associated settings (grain-packstones). The paucity of fines across the fringing reef systems as a whole, and the degree of homogenisation of sediment characteristics across the different field- and satellite-identifiable environmental facies are attributed to: (1) high wave/current energies, (2) the small size of the islands rendering limited protection, (3) bidirectional monsoon winds and (4) the lack of reef rimmed margins built to sea level. Absent from these deposits are well developed high energy windward and low energy leeward deposit characteristics and/or an overriding hurricane influence that are commonly seen in fringing reef systems from other areas.

Keywords: sedimentology, modern-carbonates, Landsat, pure-carbonates, coral-reefs, facies mapping.

2.1 Introduction

It has been estimated that the fringing reefs of SE Asia may conservatively comprise ~30% of the world's coral reef area (White, 1987; Tomascik et al., 1997). There is a paucity of knowledge on fringing reefs globally, since almost no remote sensing studies, and very few modern sediment studies have been undertaken on these systems (Lewis, 1969; Hopley and Partain, 1987; Blanchon et al., 1997; Kennedy and Woodruffe, 2002, Purkis et al., 2012). Regionally, despite fringing reefs being

the dominant reef type within SE Asia they remain the least studied (Tomascik et al., 1997; Hewins and Perry, 2006). Here, a combined environmental, satellite and sediment characterisation study of fringing reefs surrounding isolated oceanic islands in central Indonesia aims to contribute to the understanding of this under evaluated, but globally important reef type.

Most modern analogues used to evaluate carbonate development are from sub-tropical to sub-arid regions such as the Bahamas, Central America or South Pacific and are focussed on barrier reef systems and atolls (Gischler and Lomando, 1999; Rankey, 2002; Gischler et al., 2003; Gischler, 2006, 2011; Rankey and Harris, 2008; Harris, 2010; Harris et al., 2010; 2011, Rankey and Reeder, 2010). However, these systems are not wholly analogous to those from equatorial SE Asia and/or to fringing reef systems (Tomascik et al., 1997; Kennedy and Woodruffe, 2002; Wilson, 2002; 2012; Park et al., 2010). Studies of fringing reefs have focussed on their Holocene development, through multiple coring studies and to a certain extent their environmental variability (Hopley and Partain, 1987; Cabioch et al., 1995; Kennedy and Woodruffe, 2002; Montaggioni, 2005), but there are very few detailed studies on their sedimentology (Lewis, 1969; Gabrié and Montaggioni, 1982; Blanchon et al., 1997; Hewins and Perry, 2006). Studies of modern carbonate systems in SE Asia typically focus on their biota and ecology (Tomascik et al., 1997; Cleary et al., 2005; Becking et al., 2006; Renema, 2006a, 2006b). Satellite studies of reefal environments within Indonesia are in their infancy, but are much needed to better understand the regions modern carbonate systems and for their use in 'developing and implementing sound management and conservation policies' (Tomascik et al., 1997; Asriningrum, 2011). Detailed sedimentological studies of modern carbonates from SE Asia are largely restricted to those of Pulau Seribu, on the predominantly siliciclastic shelf offshore Jakarta, Indonesia (Scrutton, 1978; Park et al., 1992; 2010; Jordan, 1998, O'Shea, 2005). These high-energy, small-scale build-ups do not fully encompass the inherent variability of carbonate depositional systems that have developed throughout the region. An additional sedimentological study reviews fringing reef deposits around the 1.5 km across Danjugan Island in the Philippines at the boundary between the equatorial tropics and subtropics (Hewins and Perry, 2006). SE Asian carbonate deposits are dominated by bioclastic assemblages and notably absent are the coated grains and aggregates of their better studied arid to sub-

tropical counterparts (Lees and Buller, 1972; Wilson, 2002; 2012). Furthermore, carbonate development in SE Asia is extensive forming a wide variety of platform types from land attached shelves, isolated platforms to localised and/or ephemeral carbonates (Tomascik et al., 1997; Wilson, 2002). There is a need to better evaluate sedimentological characteristics of modern carbonate environments, and in particular those from fringing reef systems and their facies distributions related to environmental conditions from SE Asia, since models generated from examples outside the equatorial tropics are commonly not wholly applicable (cf. Gischler and Lomando, 1999; Wilson, 2008a; 2011; 2012; Park et al., 2010).

Satellite based remote sensing is widely established as a key tool in the mapping of modern carbonate systems and reef environments (Lyzenga, 1981; Ahmad and Neil, 1994; Gischler and Lomando, 1999; Andréfouët et al., 2001, 2003; Rankey, 2002; Purkis and Pasterkamp, 2004; Harris, 2010; Kaczmarek et al., 2010). Most of these studies detail the variability of modern carbonate environments from classic sub-tropical Atlantic or Pacific examples, with very few studies including examples from the humid equatorial tropics of SE Asia (Harris and Vlaswinkel, 2008).

An important aspect of understanding SE Asian carbonate variability lies in developing models that demonstrate how primary environmental settings unique to the region relate to primary depositional sediment characteristics and their early alteration. SE Asian modern carbonate systems have distinctive characteristics that relate to local environments and water depths, and it is anticipated that these primary environmental differences will be reflected in satellite imagery characteristics that relate to: (1) benthic sedimentological characteristics, (2) benthic biota communities, and (3) water conditions (including depth and clarity); i.e. identifiable "environmental facies".

This study utilises statistics-based satellite image classifications in conjunction with modern sediment samples from fringing reef systems around carbonate islands in the Tukang Besi Archipelago, Indonesia (Fig. 2.1). Specific study objectives are to: (1) produce a satellite generated environmental facies map using statistics based methods, (2) identify primary sedimentological and early sediment alteration characteristics of associated carbonate deposits, (3) compare primary

sedimentological properties to primary environmental facies and their satellite characteristics and (4) contribute towards a greater understanding of modern humid equatorial carbonate systems highlighting the heterogeneities that may exist.

2.2 Regional Setting

The Tukang Besi Archipelago, encompassing the Wakatobi Marine National Park, is situated <20 km southeast of Buton Island in SE Sulawesi, bordered by the Banda Sea to the northeast, and Flores Sea to the southwest (Fig. 2.1). Three linear rows of atolls, raised coral islands and build-ups trending northwest-southeast rise from a broad subsiding platform of possible continental origin that currently lies at 700-1000 m water depth (Smith and Silver, 1991; Koswara and Sukarna, 1994; Milsom et al., 1999). All the modern carbonate systems are largely isolated from siliciclastic input. The Tukang Besi archipelago contains approximately 500 km^2 of coral reef-related environments within a wide diversity of carbonate systems including large-scale atolls (>10 km across), small-scale atolls, small-scale build-ups and barrier or fringing reefs surrounding the four main islands of the archipelago (Tomascik et al., 1997; Wilson, 2008b). The islands of the archipelago preserve a record of Pliocene to Quaternary uplifted coral reefs. These ancient reefs are exposed as a series of stepped terrace levels that have been uplifted to maximum heights of 300 m (Wilson, 2008b). The deposits of each uplifted terrace formed in a variety of shallow marine environments that were associated with coral reefs that built towards sea level (Wilson, 2008b). These shallow water carbonate terraces overlie deeper water marls of Late Miocene and Early Pliocene age (the Ambewa Formation: Koswara and Sukarna, 1994; Wilson, 2008b). Poorly consolidated marl clasts are reworked into the modern carbonate sediment assemblages fringing the islands, but mainly only in regions adjacent to where there is limited or no preservation of Pliocene–Quaternary reef terraces. The archipelago is therefore an excellent location to characterise and evaluate the effects of primary environmental facies on carbonate sediment characteristics in the humid equatorial tropics of SE Asia. This work focuses on differences within the modern island-attached carbonate systems, with further work in preparation to evaluate the variability across the range of carbonate systems from the archipelago (Wilson et al., 2013).

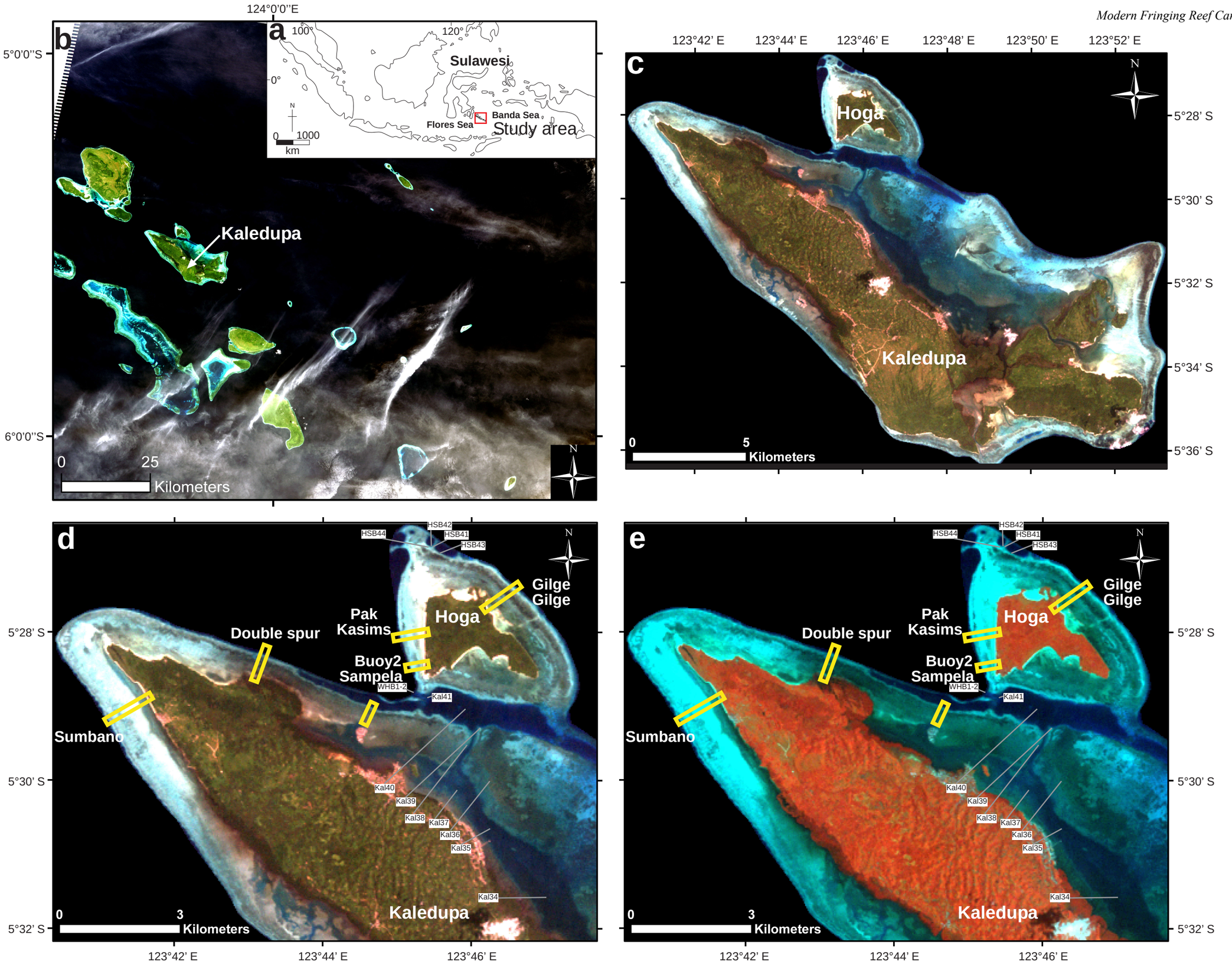

Figure 2.1. Location of the Tukang Besi Archipelago (Wakatobi Marine National Park) offshore SE Sulawesi, Indonesia (a). Landsat 7 image of the Tukang Besi Archipelago captured on 6th February 2009 (b). Subset image of Pulau Kaledupa and Hoga, with pixels outside the area of interest removed (c). Magnified view of sample sites and transect locations utilised in this study, shown in both quasi-natural colour (RGB:123) and false colour (RGB:421) display format (d, e).

The marine environments surrounding the Tukang Besi islands contain amongst the world's highest levels of marine biodiversity (Halford, 2003; Turak, 2003; Pet-Soede and Erdmann, 2003; Bell and Smith, 2004). High biodiversity is not just a feature of the archipelago's coral reefs but also the associated interconnected habitats of seagrass meadows, mangroves, mud flats and algal beds. There are records from within the Wakatobi National Park of at least: 396 species of hermatypic scleractinian hard corals and 10 species of ahermatypic scleractinian corals, 28 species of soft corals, >145 sponge species, nine species of seagrass and upwards of 600 species of fish (Halford, 2003; Turak, 2003; Bell and Smith, 2004; Pet-Soede and Erdmann, 2004; Bell et al., 2010; McMellor and Smith, 2010). Mean coral cover throughout the Wakatobi systems (reef flat, crest and upper slope) is 48.05% with 10.62% macroalgal cover, 2.31% sponge cover and 5.4% dead coral and coral rubble cover (Suharsono et al., 2006; McMellor and Smith, 2010). It is this overall biotic and carbonate systems variability that makes the area ideal to characterise modern SE Asian carbonate deposits. However, with the exception of debates over the morphology and development of the archipelago (Escher, 1920; Hetzel, 1930; Kuenen, 1933a, b; Umbgrove, 1947; van Bemmelen, 1949; Tomascik et al., 1997; Milsom et al., 1999), to date no detailed sedimentological studies have been undertaken (cf. Wilson, 2008b).

The tidal range of the islands and reefs in the archipelago is ~2 m with semi-diurnal tides affecting shallow platforms and very strong oceanic tidal currents between the atolls and islands. Wave energy can be very high and is influenced strongly by the bi-directional monsoon. Very strong south-easterly winds blow between June and August with lesser westerly winds between December and March (Wilson, 2008b). Water temperatures are typically within the range of 27-28 °C with ocean salinities of 35‰ (O'Shea, 2005).

2.3.2 Sample Analysis

All 78 samples were air dried then photographed under a binocular microscope. A proportion of each sample was weighed and separated using a 2 mm sieve, with the <2 mm size fraction analysed for grain size using a Coulter Laser Granulometer. The proportions of components and grain sizes of the >2 mm size fractions were visually estimated. 2.5-3 g of the <2 mm fraction for each sample were placed in test tubes and in the rare samples containing organics 20 ml of 20% Hydrogen Peroxide was added and left overnight in a boiling water bath to allow digestion of the organics. Samples were centrifuged at 2500 rpm for four minutes and half of the supernatant liquid decanted off, then the tubes topped up with water and centrifuged for another 4 minutes to allow degassing and grains to settle. Following decanting off of the supernatant liquid, 20 ml of Sodium Hexametaphosphate solution was added to stop grains clumping then run through the Granulometer. Grain size plots incorporate the results of percentages of the >2 and <2 mm size fractions with grain size divisions from the Udden-Wentworth scheme (Udden, 1914; Wentworth, 1922) and nomenclature on sorting after Pettijohn et al. (1973). Of the 78 samples, 75 were made into thin section grain mounts for petrographic analysis. Half of each thin section was stained with potassium ferricyanide and Alizarin Red S for the identification of ferroan and non-ferroan calcite (Dickson, 1965, 1966). Semi quantitative visual estimates of components were directly comparable with point counting analyses previously undertaken on the Pak Kasim's transect (300 point counts: O'Shea, 2005). Textural classification of the sediments follows the scheme of Dunham (1962), modified by Insalaco (1998)[1]. An early sediment alteration index evaluating abrasion, fragmentation, encrustation, bioerosion and cementation for each thin section is modified after the abrasion and fragmentation index of Beavington-Penney (2004; see Appendix B3).

[1]Insalaco's (1998) scheme is a descriptive expansion, and modification, of the Embry and Klovan (1971) extension to Dunham's classification, and is suited to describing *in situ* reef-related growth fabrics with subdivisions based on dominant growth forms. The subdivisions are domestone (domal and massive colonies), pillarstone (vertical branches), platestone and sheetstone (flattened horizontal forms with a width-to-height ratio of between 30:1–5:1 and > 30:1, respectively) and mixstone (no one growth form dominates). Use of the Insalaco (1998) scheme rather than the Embry and Klovan terms of frame-, baffle-, and bindstone removes potential ambiguity over interpretive nomenclature. For example in the Wakatobi area, seagrass beds act as sediment "baffles", but do not result in bafflestone deposit textures (*sensu* Embry and Klovan), whereas branching coral-rich areas do not appear to act

2.3 Materials and Methods

2.3.1 Fieldwork and Sampling

Modern carbonate settings from across the Tukang Besi archipelago were surveyed and deposits sampled along underwater transects, generally oriented perpendicular to the trend of the reef crest (i.e. from deep forereef areas, passing across the shallow reef crest to inner reef or land areas). Study was through diving and snorkelling with local environmental conditions including substrate and biota types, water depths, water temperatures, slope angles and any wave or current activity recorded along each transect. Surface sediment samples were collected by hand (underwater directly into containers to minimise loss of fines) from the range of local environments and/or at decimetre-spaced intervals along transects, with sampling sites photographed. For regions deeper than 20-30 m additional samples were obtained using a Van Veen sediment grab (with only intact "solid" sediment taken from within the grab sample, again to minimise the loss of fines). In total, 42modern transects were studied from the archipelago, with 390 samples of modern reef-associated sediments collected. From this larger dataset, six key transects and some additional spot sampling sites from around Pulau Kaledupa and its neighbouring "sibling" island of Hoga, were selected for comparison between shallow water environments and their satellite and sediment characterisation. The area of Kaledupa and Hoga was focused on due to: (1) good availability of a range of cloud-free Landsat multispectral data, (2) good sample and transect coverage allowing analysis of much of the range of local environments and variety in satellite characteristics from <20 m water depth in the Wakatobi region to be studied, and (3) the potential to compare between windward versus leeward, or more protected settings. In total, 78 samples were analysed for this study with all from <20 m, and most from <5 m water depth. Out of these 78 samples eight along the Kaledupa centre transect were collected using the Van Veen grab.

as baffles to sedimentation but would have bafflestone deposit textures as defined by Embry and Klovan (1971).

2.3.3 Landsat-7

Modern carbonate systems are ideal for study through satellite based methods as they are typically best developed in shallow (<30 m) relatively clear water marine environments, consistent with the requirements for accurate satellite data collection and their interpretation. Several methods exist for the analysis and interpretation of satellite data sets from modern shallow water carbonate systems (cf. Harris and Kowalik, 1994; Harris, 1996; Gischler and Lomando, 1999; Rankey, 2002; Harris and Vlaswinkel, 2008; Harris et al., 2010; Kaczmarek et al., 2010; Harris et al., 2011). In this study the use of statistical algorithms has been adopted to quantitatively discriminate between combined benthic sediment and biota types across a SE Asian reef-related system.

This study utilises the simplified workflow of Kaczmarek et al. (2010) to generate a Landsat derived facies map of water-bottom characteristics. The methods outlined by Kaczmarek et al. (2010) discriminate between benthic sediment types to produce satellite derived sediment facies maps for carbonate platforms. In satellite imagery, variance in reflection (satellite characteristics) is attributed to variability from three predominant factors: (1) the benthic sediment type, (2) the benthic biota assemblages and (3) water depth. As it is applied to this study the derivative products of satellite analysis are environmental facies maps in which the satellite characteristics are directly related to local benthic communities, sediment types and water conditions.

The methods of Kaczmarek et al. (2010) offer a simple and time efficient way to assess satellite imagery and avoids the use of advanced image processing techniques that arguably would provide little improvement to a low spatial resolution image (cf. Ouillon et al., 2004; Purkis and Pasterkamp, 2004; Kaczmarek et al., 2010). One of the key objectives of this study is to foster a "user friendly" approach to satellite based study, allowing integration of what is possibly an underutilised, yet valuable resource (the Landsat data set), with more traditional sedimentological studies where remote sensing skill sets may be lacking.

A Landsat-derived environmental facies map was produced by combining Landsat multispectral data, statistics-based unsupervised classifications, and field observations of local environmental conditions for the shallow-water fringing reef-related area of Pulau Kaledupa and Hoga from the Tukang Besi Archipelago of SW Sulawesi (Fig. 2.1). A full discussion of the workflow and the Landsat multispectral sensor used to generate this facies map is given in Kaczmarek et al. (2010), with a brief overview outlined below. The Landsat data that forms the basis for the analyses of this study was captured on the 6th February 2009 in seven spectral (thematic) bands with a spatial resolution of 28.5 m^2. The Landsat image of the Tukang Besi Archipelago (delineated to Pulau Kaledupa during image processing) was selected in place of other images collected between 1989 and 2012. The February, 2009 image was chosen as the area of interest was not affected by cloud cover or atmospheric haze and has the most consistent contrast and clarity across the area. Individual spectral bands were combined in the software package ER Mapper to produce a single multispectral composite image for the Tukang Besi Archipelago. Cloud masking and land masking algorithms were applied to the image to reduce the number of spectral classes required to classify the image. To further reduce spectral variability the image has been delineated to an area of interest by assigning pixels outside of a hand drawn polygon (i.e. deep water regions) a null value (Fig.2.1C).

Benthic sediments and biota assemblages are discriminated into distinct thematic classes using the image processing technique "unsupervised classification" within the ER Mapper software package. This image processing utility assesses each pixel in a satellite image by performing a calculation based on a combination of the spectral values of each spectral band. This spectral signature is then used in a binning algorithm which groups pixels into a pre-determined number of spectral classes. Because the unsupervised classification utility groups pixels based on differences between reflection properties, water depth inherently affects classifications. To account for variability due to water depth the unsupervised classification was calibrated so as to group pixels into a large number of classes. Previous studies (e.g. Rankey, 2002; Purkis et al., 2005) have utilised fewer than 10 spectral classes during unsupervised classification, whereas Kaczmarek et al. (2010) suggest that whilst a relatively small number of classes are required to create a satellite based facies map, that the number of spectral classes be significantly (~6x) greater than the number of

classes actually present. As it is applied to this study, ten distinct environmental facies have been identified from field observations across sampling transects, with 50 spectral classes being utilised to produce an environmental facies map.

Areas within the classified image, produced by the ER Mapper unsupervised classification utility, were assigned to environmental facies by linking pixels corresponding to sample locations with field observations of the environment. As a result pixels with similar satellite and field characteristics were automatically grouped together and assigned to the same environmental facies. For pixel groups with no corresponding sample data, environmental facies were assigned based on further field observations (Kaledupa Double Spur Transect; Fig. 2.1D, E), local knowledge, the location of nearby or adjacent environmental facies and the observed geometries of environmental facies groups. Quantification of the accuracy of the environmental facies map has been conducted using the "overall accuracy" metric of Mumby et al (1998; Eq. 1). Overall accuracy reflects the degree to which known pixel values (classes) are represented by the classified image as determined by a point count of correctly classified pixels.

Overall accuracy (%) = (No# correctly classified pixels/No# known pixel classes)*100 (1)

Results of the "overall accuracy" metrics give an indication that the pixels of the classified Landsat image represent the environmental facies on the ground, as determined from field notes and sediment sampling (cf. Kaczmarek et al., 2010).

2.4 Results

Primary sedimentary and environmental results of this study are analysis of sediment components, their early alteration and grain-size variations plotted onto environmental transects for the islands of Pulau Kaledupa and Hoga (Figures 2.2-2.8 and Appendix B3). Results are reported below as environmental and sedimentological descriptions for each environmental facies group identified.

2.4.1 Foreshore/Backshore (Sample References: Kal21, 20, HGG10, 9, PK21, HSB2S-10)

2.4.1.1 Environmental Facies Description. Foreshore/backshore deposits form a <15 m wide rim to the main vegetated landmasses and are bare-sandy deposits composed mainly of material reworked from the reef-flat. Foreshore deposits are supratidal to intertidal and dip 10-20° seaward. At high tide foreshore deposits are affected by breaking waves. In contrast backshore areas are unaffected by all but storm waves, may have the beginnings of colonisation by vegetation and generally include more disseminated land-derived plant material than foreshore areas.

2.4.1.2 Sediment Characteristics. Sediments associated with the foreshore/backshore deposits are dominated by bioclastic carbonate sands with grainstone to grain-rudstone textures. Foreshore/backshore deposits are dominantly moderately to well sorted sands, although there is some variability between the different transects. The foreshore/backshore deposits of Pak Kasim's and Hoga Buoy 2 are coarse to very coarse unimodal to bimodal sands with a minor (~<6%) gravel component (Figs. 2.3, 2.4). Foreshore/backshore deposits of Hoga Gilge Gilge and Sumbano are fine to very coarse bimodal sands with a negligible (<1%) gravel content (Figs. 2.2a, 2.2b, 2.5, 2.6). In all samples silt to clay size fractions are largely absent (<2%). The >2 mm size fraction of these deposits is dominated by shells and/or coral bioclasts which may contribute 60-100% of the material present (Fig. 2.2a). Less abundant bioclasts typically include *Halimeda* and imperforate foraminifera. In thin section the <2 mm size fraction is more variable, but reflects the >2 mm grain components in that coral and shell fragments typically contribute ~50% of the total bioclastic material. Collectively the bioclasts of these foreshore/backshore deposits are highly abraded (e.g. calcarinid spines broken/removed, and truncated to gouged grain margins on clasts) with coral and shell clasts showing pervasive fragmentation. Bioerosion (identified through micritised grain margins) is a variable feature of the deposits. Micritic rims range from 20-50 µm thick and are pervasive features of coral, shell and *Halimeda* fragments from the Hoga Gilge Gilge and Sumbano deposits (Figs. 2.2b, 2.5, 2.6). Non-pervasive micritic rims of up to 20 µm thick are present on coral and shell fragments in deposits from Pak Kasim's and Hoga Buoy 2 (Figs. 2.3, 2.4).

Encrustation by coralline algae and foraminifera is a rare feature of coral clasts from Sumbano and Hoga Buoy 2 (Figs. 2.2b. 2.4, 2.6). Cementation is absent from all foreshore/backshore deposits.

Figure 2.2 (next page). Binocular microscope photographs and Plane Polarised Light (PPL) photomicrographs of unsorted modern sediments from the various environmental facies of Kaledupa-Hoga. (a) Binocular microscope photo of foreshore sample Kal21; well sorted sediment composed dominantly of highly abraded and fragmented shell and coral allochems. (b) Thin-section photomicrograph of foreshore sample HGG10; moderately sorted sediment composed of highly abraded and fragmented shell material. Allochems are highly micritised and in places have been completely destroyed through micritisation by microborers. (c) Binocular microscope photo of sample Kal18, from the intertidal with no seagrass facies. Sample is very poorly sorted sediment with sands and gravels the dominant size fraction. Coral and shell allochems are dominant and highly abraded and fragmented, but also present are whole imperforate foraminifera. (d) Thin-section photomicrograph of sample Kal19 from the intertidal with no seagrass facies, showing high degree of micritisation and the presence of abraded perforate calcarinids. (e) Binocular microscope photo of sample HSB2S-5 from the short seagrass facies. Sample is very poorly sorted, with grain-sizes varying from silt to gravel sized fractions. Coral and shell material is dominant, showing a minor degree of abrasion and moderate fragmentation. Minor imperforate foraminifera and miliolids are also present. (f) Thin-section photomicrograph of short seagrass facies sample HGG7. Sample is moderately to poorly sorted and highly fragmented. Coral and shell allochems are heavily micritised with lesser bioerosion on foraminifera. (g) Thin-section photomicrograph of long seagrass facies sample HGG4. Sample is moderately to highly fragmented with coral and foraminifera showing moderate abrasion. Coral clasts are pervasively micritised. (h) Binocular microscope photo of mixed long and short seagrass facies sample Kal17. Sample is very poorly sorted silts to gravel. Characteristic *Halimeda*, imperforate foraminifera and miliolids are dominant with lesser coral and shell allochems. (i) Binocular microscope photograph of mixed coral and seagrass facies sample HGG3. Sample is moderately sorted and dominated by moderately to highly abraded and fragmented shell allochems. Imperforate, perforate and calcarinid foraminifera are present. Calcarinid spines are generally abraded. (j) Thin-section photomicrograph of mixed coral and seagrass facies sample HGG2. Sample shows abraded and micritised coral fragments with well preserved perforate foraminifera. (k) Thin-section photomicrograph of mixed coral and seagrass facies sample Kal3. Sample shows highly abraded and fragmented coral clasts with minor to moderate micritisation. (l) Binocular microscope photo of coral with/without sediment cover facies sample HSB2S-2. Sample is moderately sorted medium sands to gravel. Coral and shell allochems are dominant and show moderate abrasion and fragmentation. Minor alcyonarian sclerites and echinoid spines are present. (m) Binocular microscope photo of reef slope sample PK10. Sample is well sorted and has an overall low

degree of micritisation. Sample has high abundances of alcyonarian sclerites, with the abundant coral and shell allochems highly fragmented. (n) Binocular microscope photo of deep water facies sample Kal34. Sample is almost 100% lithic marl with a single fragment of shell material. (o) Binocular microscope photo of deep water facies sample Kal40. Sample is very poorly sorted with high abundances of perforate, imperforate and mililoid foraminifera and shells. Lithic marl clasts comprises the fine grain sizes of this sample.

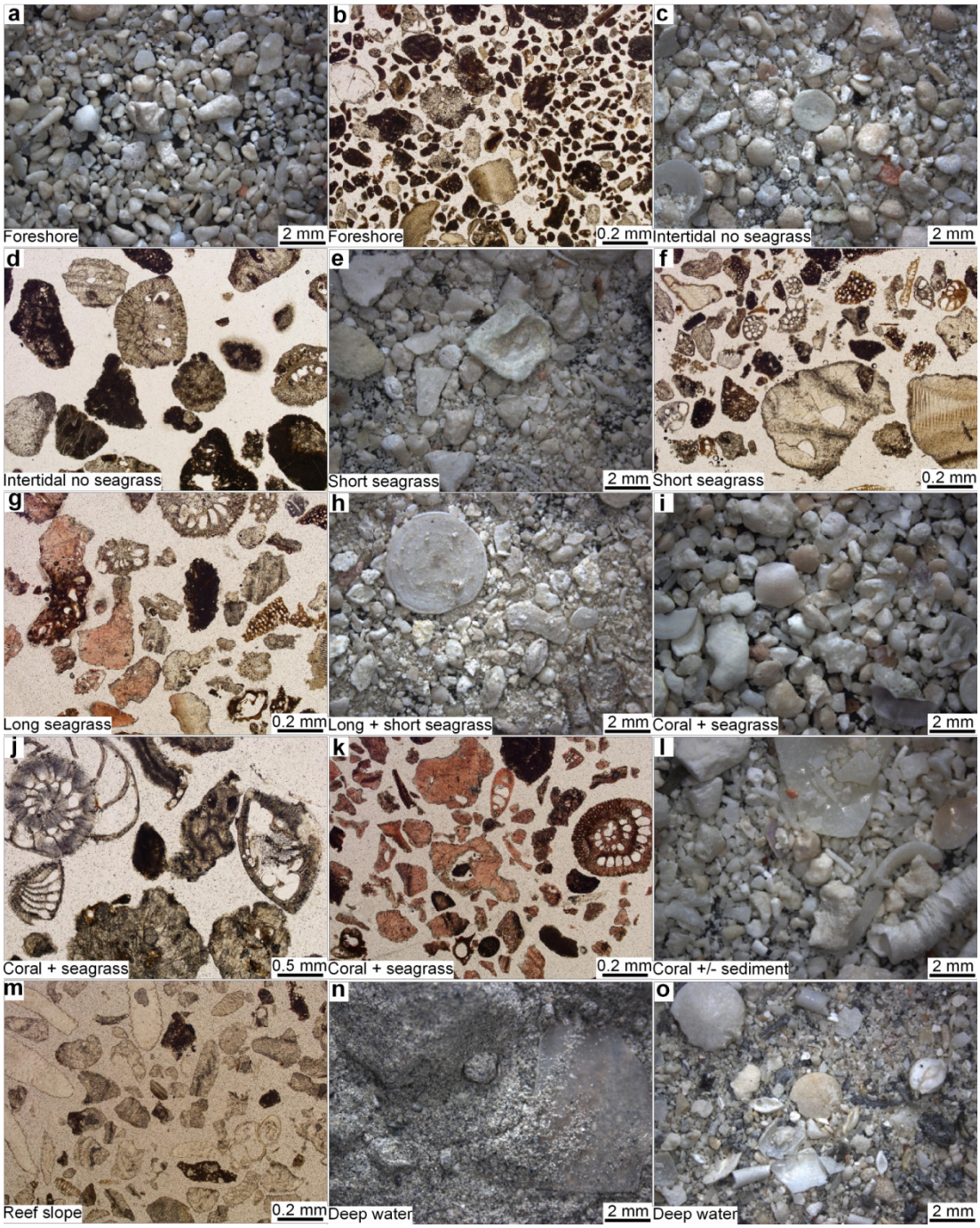

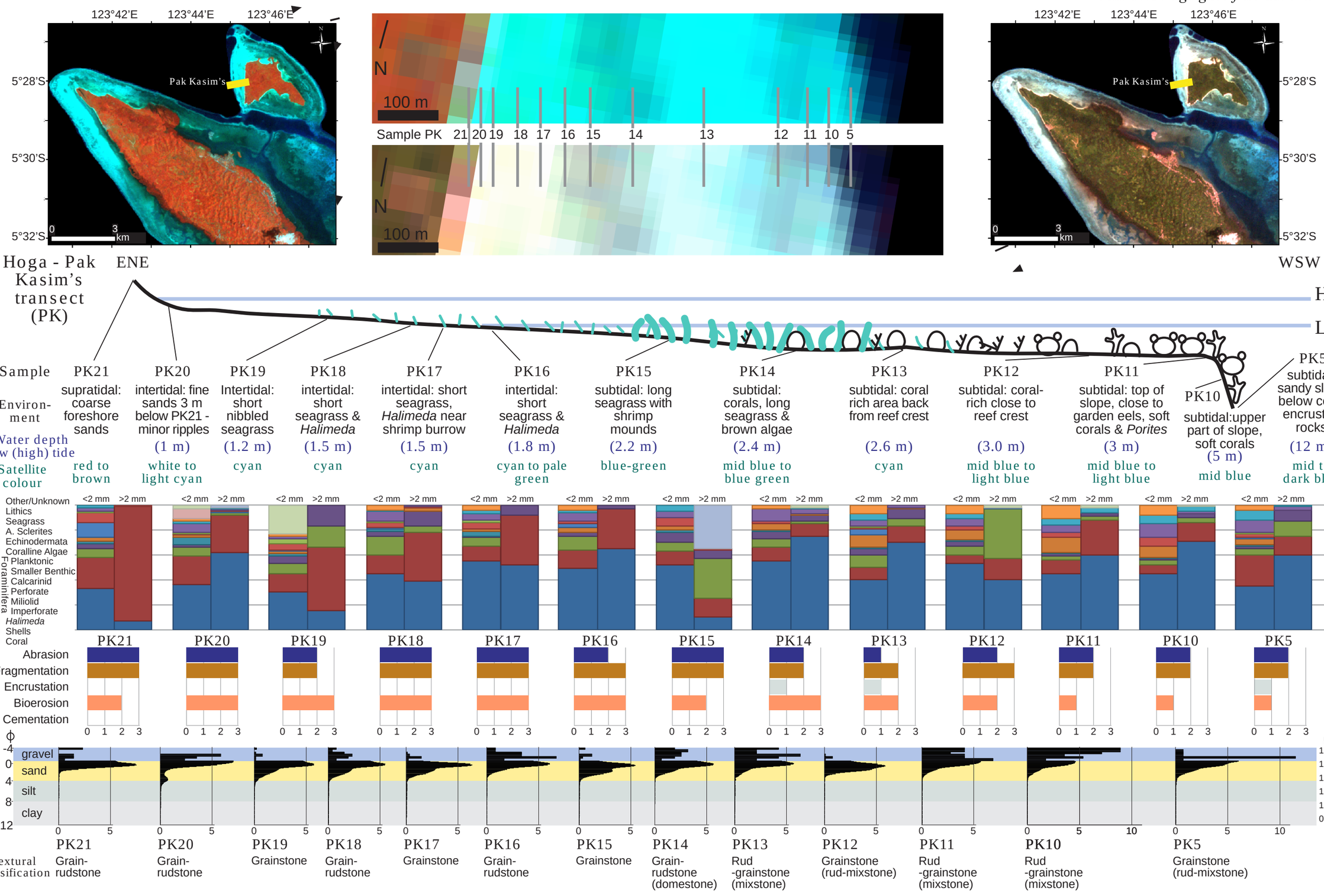

Figure 2.3. Combined environmental transect, field, component and grain size data for the Pak Kasim's transect undertaken on Hoga. The transect location is identified on both the quasi-natural (RGB:123) and false colour (RGB:421) images, with sample locations identified on the highly magnified displays. The environmental transect correlates with the individual pixels identified in the Landsat image, with field observations, detailed component, early alteration and grain size data beneath. Deposit texture characteristics are given at the base of composite image with dominant textures listed first and those identifiable from field characteristics only parenthesised.

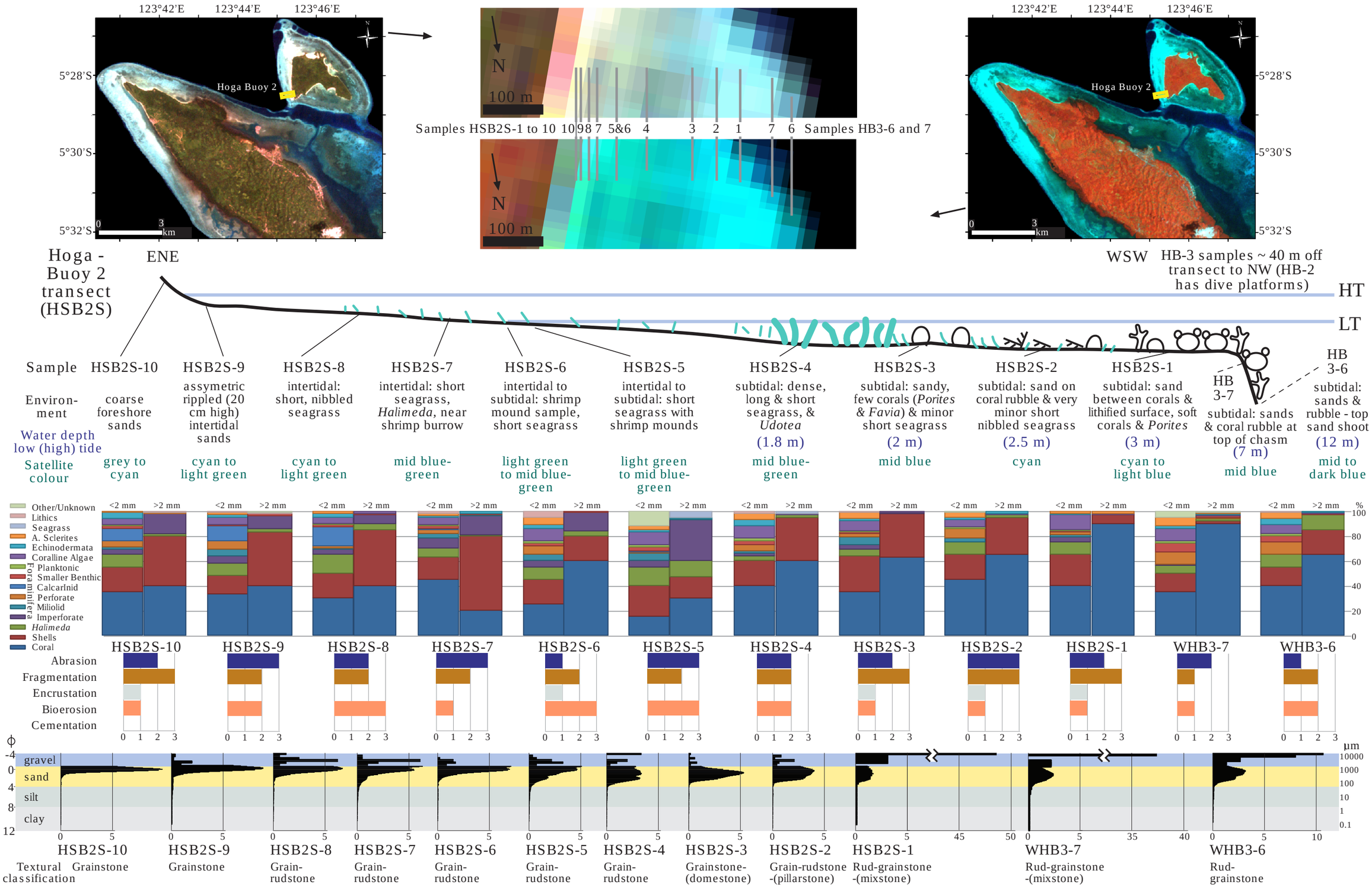

Figure 2.4. Combined environmental transect, field, component and grain size data for the Hoga Buoy 2 transect. The transect location is identified on both the quasi-natural (RGB:123) and false colour (RGB:421) images, with sample locations identified on the highly magnified displays. The environmental transect correlates with the individual pixels identified in the Landsat image, with field observations, detailed component, early alteration and grain size data beneath. Deposit texture characteristics are given at the base of composite image with dominant textures listed first and those identifiable from field characteristics only parenthesised.

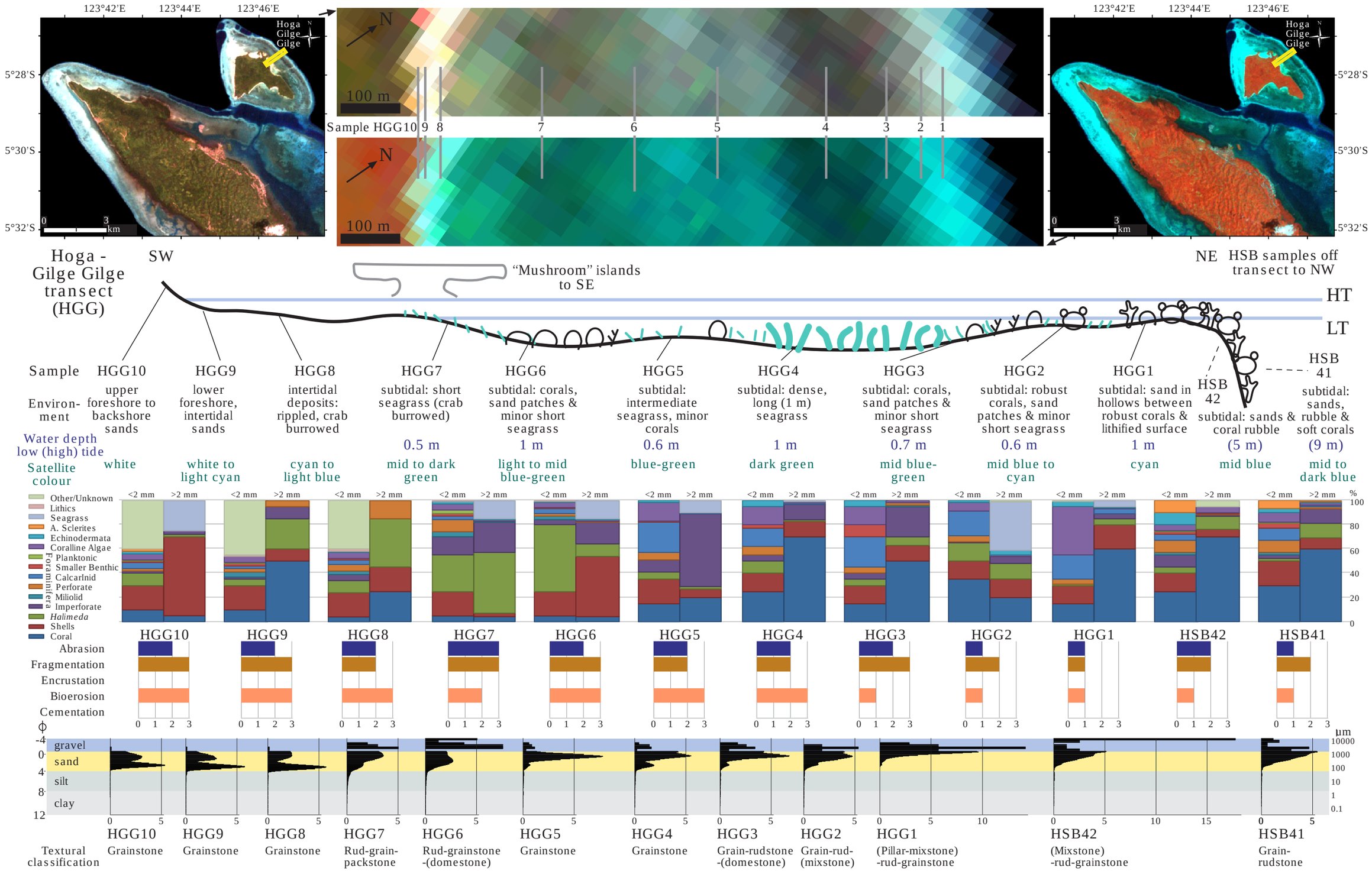

Figure 2.5. Combined environmental transect, field, component and grain size data for the Hoga Gilge Gilge transect. The transect location is identified on both the quasi-natural (RGB:123) and false colour (RGB:421) images, with sample locations identified on the highly magnified displays. The environmental transect correlates with the individual pixels identified in the Landsat image, with field observations, detailed component, early alteration and grain size data beneath. Deposit texture characteristics are given at the base of composite image with dominant textures listed first and those identifiable from field characteristics only parenthesised.

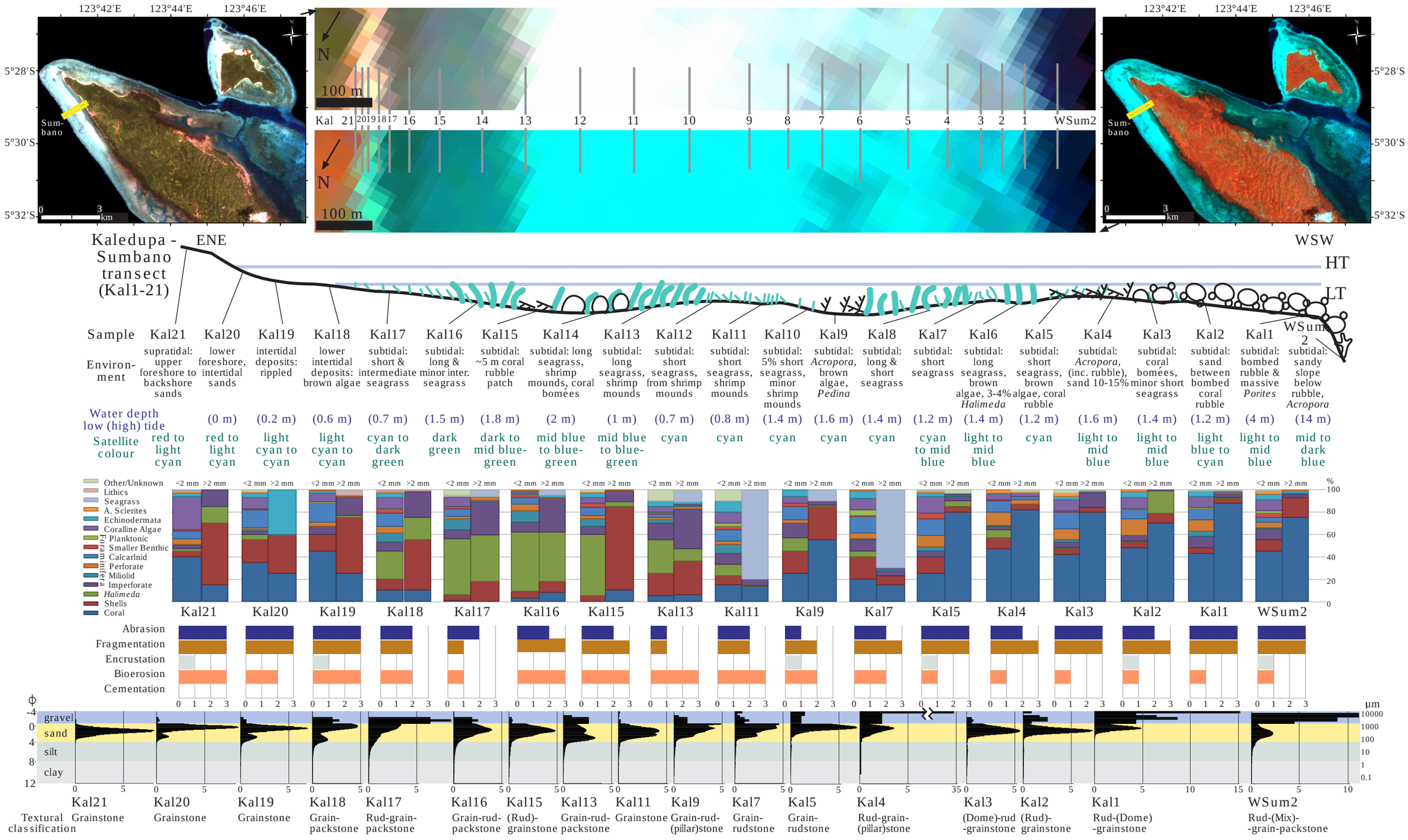

Figure 2.6. Combined environmental transect, field, component and grain size data for the Kaledupa Sumbano transect. The transect location is identified on both the quasi-natural (RGB:123) and false colour (RGB:421) images, with sample locations identified on the highly magnified displays. The environmental transect correlates with the individual pixels identified in the Landsat image, with field observations, detailed component, early alteration and grain size data beneath. Deposit texture characteristics are given at the base of composite image with dominant textures listed first and those identifiable from field characteristics only parenthesised. Detailed sediment characteristics are not shown for samples Kal14, 12, 10, 8 and 6 due to space constraints, but for individual samples are very similar to those directly on their right (i.e. to their ENE).

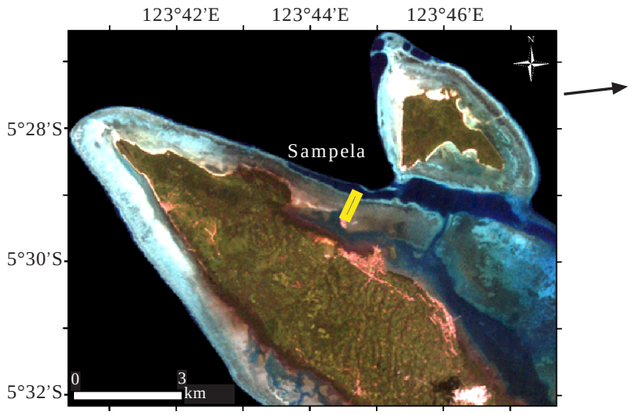

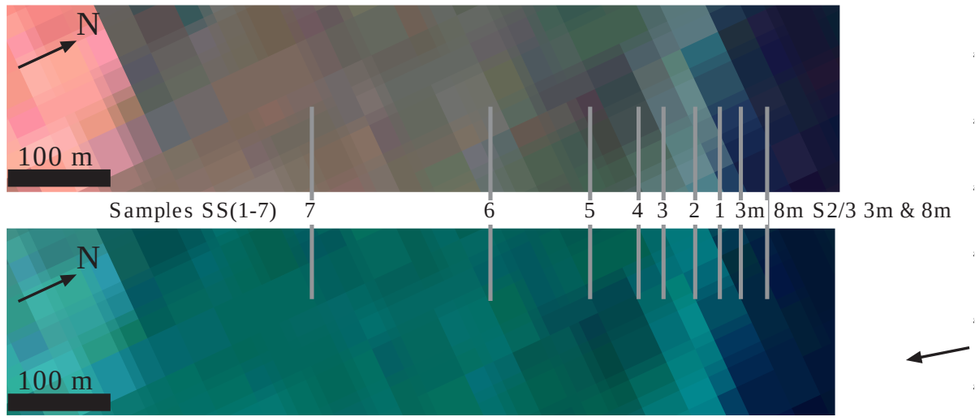

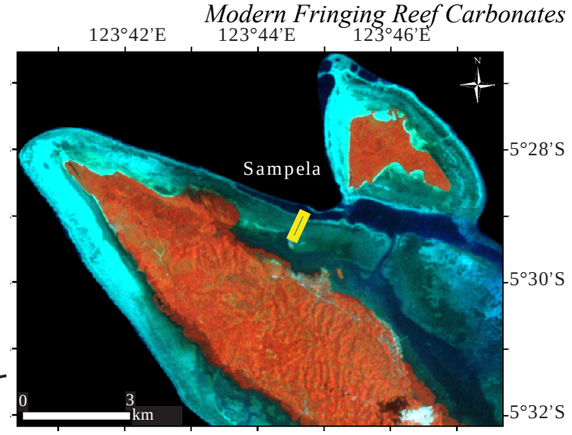

Sampela transect (SS)

SSW

NNE

S2/3 slope transect continuous with SS transect

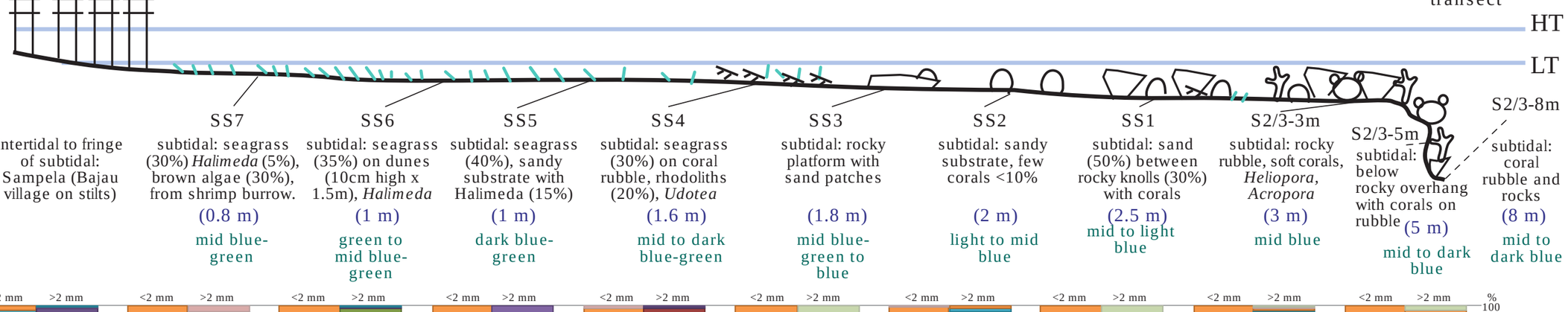

Sample		SS7	SS6	SS5	SS4	SS3	SS2	SS1	S2/3-3m	S2/3-5m	S2/3-8m
Environment	intertidal to fringe of subtidal: Sampela (Bajau village on stilts)	subtidal: seagrass (30%) *Halimeda* (5%), brown algae (30%), from shrimp burrow.	subtidal: seagrass (35%) on dunes (10cm high x 1.5m), *Halimeda*	subtidal: seagrass (40%), sandy substrate with Halimeda (15%)	subtidal: seagrass (30%) on coral rubble, rhodoliths (20%), *Udotea*	subtidal: rocky platform with sand patches	subtidal: sandy substrate, few corals <10%	subtidal: sand (50%) between rocky knolls (30%) with corals	subtidal: rocky rubble, soft corals, *Heliopora*, *Acropora*	subtidal: below rocky overhang with corals on rubble	subtidal: coral rubble and rocks
Water depth low (high) tide		(0.8 m)	(1 m)	(1 m)	(1.6 m)	(1.8 m)	(2 m)	(2.5 m)	(3 m)	(5 m)	(8 m)
Satellite colour		mid blue-green	green to mid blue-green	dark blue-green	mid to dark blue-green	mid blue-green to blue	light to mid blue	mid to light blue	mid blue	mid to dark blue	mid to dark blue

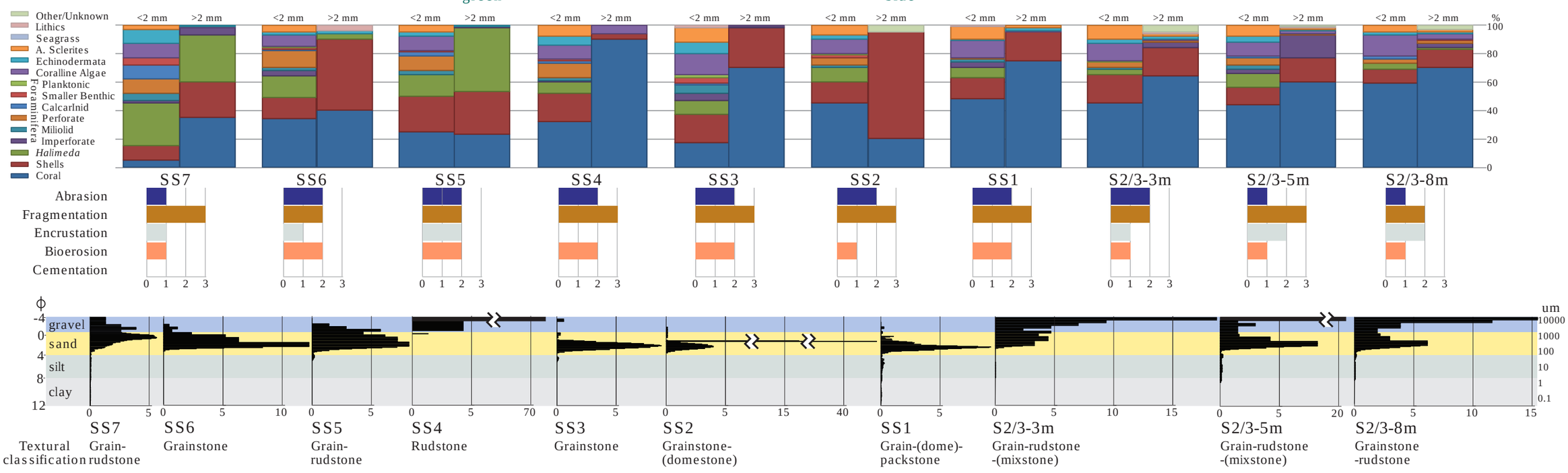

Textural classification	SS7 Grain-rudstone	SS6 Grainstone	SS5 Grain-rudstone	SS4 Rudstone	SS3 Grainstone	SS2 Grainstone-(domestone)	SS1 Grain-(dome)-packstone	S2/3-3m Grain-rudstone -(mixstone)	S2/3-5m Grain-rudstone -(mixstone)	S2/3-8m Grainstone -rudstone

Figure 2.7. Combined environmental transect, field, component and grain size data for the Sampela transect, undertaken on Pulau Kaledupa. The transect location is identified on both the quasi-natural (RGB:123) and false colour (RGB:421) images, with sample locations identified on the highly magnified displays. The environmental transect correlates with the individual pixels identified in the Landsat image, with field observations, detailed component, early alteration and grain size data beneath. Deposit texture characteristics are given at the base of composite image with dominant textures listed first and those identifiable from field characteristics only parenthesised.

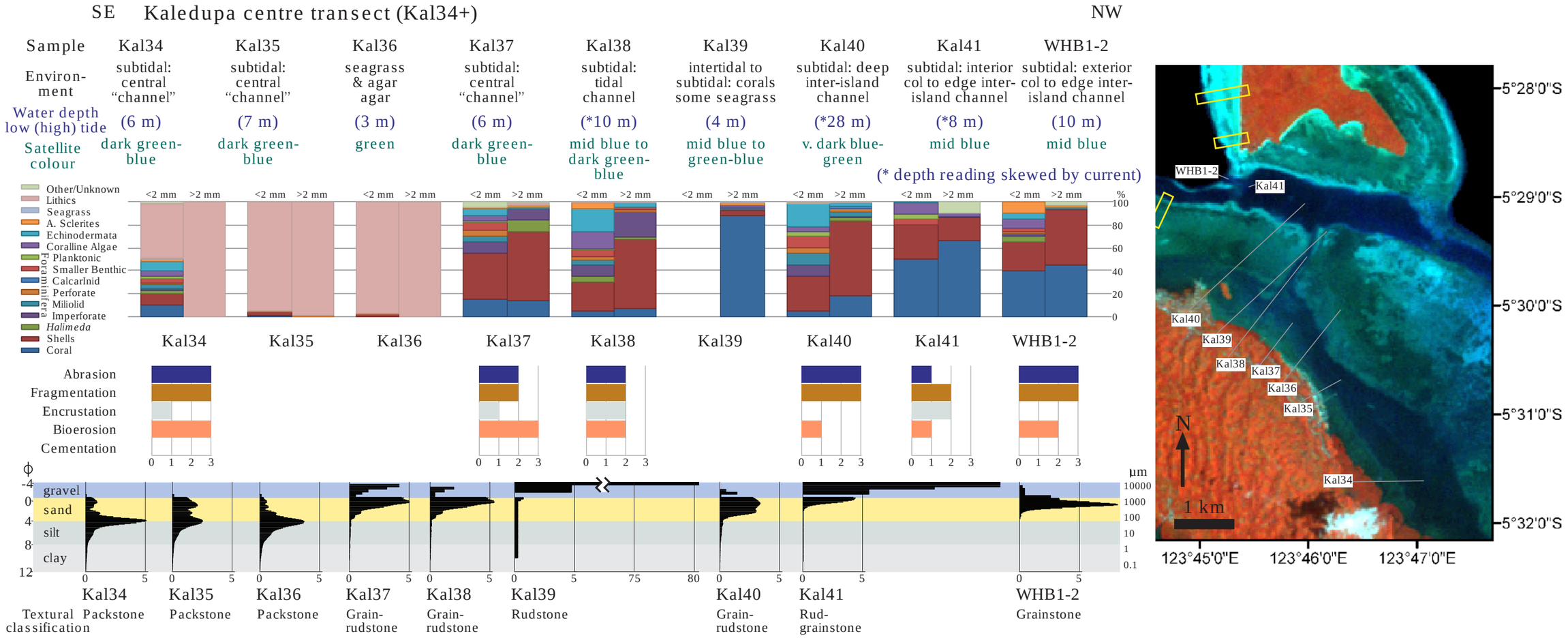

Figure 2.8. Combined environmental transect, field, component and grain size data for the Kaledupa Centre transect, undertaken on the deep water back reef areas of Pulau Kaledupa and the deep water lagoon separating Pulau Kaledupa and Hoga. Sample locations are identified on the false colour image (RGB:421). No environmental transect is shown here due to no underwater surveys being undertaken. The environmental descriptions correlate with the individual pixels identified in the Landsat image, with field observations, detailed component, early alteration and grain size data beneath. Samples in this transect were collected using a sediment grab. Deposit texture characteristics are given at the base of composite image with dominant textures listed first and those identifiable from field characteristics only parenthesised.

2.4.2 Intertidal Reef Flat without Seagrass (Sample References: Kal19, 18, HGG8, PK20, HSB2S-9)

2.4.2.1 Environmental Facies Description. Intertidal reef flat deposits without seagrass coverage form a <30-60 m wide perimeter to the foreshore/backshore deposits. These are bare sand deposits made up of reworked reef-flat material that may have symmetric ripples and may be bioturbated with shrimp mounds. These deposits dip between 1-5° seaward and are intertidal having water depths of 0.2 to 1 m at high tide.

2.4.2.2 Facies and Sediment Characteristics. Sediments associated with the deposits of this environmental facies are dominated by bioclastic carbonate sands with grainstone to grain-rudstone textures. The deposits are poorly to well sorted, with variability between transects. The deposits of the Sumbano transect are bimodal to trimodal fine to very coarse sands with a variable (1-7%) gravel component and consistent (3-7%) silt sized fraction (Fig. 2.6). Deposits from the Hoga Gilge Gilge transect are bimodal very fine to fine and coarse to very coarse-sands with a negligible gravel (<1%) and silt (<2%) content (Fig. 2.5). Deposits from the Pak Kasim's transect are dominantly bimodal coarse to very coarse-sands with gravel (11%) and a minor (<4%) clay-silt fraction (Fig. 2.3). Deposits from the Hoga Buoy 2 transect differ slightly with the other deposits of this environmental facies in that they are very well sorted, unimodal coarse to very coarse sands with minor gravel (<4%) and clay-silt (2%) sized components (Fig. 2.4). The bioclastic content of these deposits, from all transects, exhibits little variability. The >2 mm grain components are dominated by shells and coral bioclasts that may contribute 45-90% of the material present. Less abundant bioclasts include *Halimeda* and imperforate foraminifera (Fig. 2.2c). In thin section the <2 mm grain components are variable but dominated by coral and/or shell bioclasts that make up 20-60% of the bioclasts with *Halimeda* also common (5-25%). The <2 mm grains from the Sumbano transect also have common calcarinids (12-17%) and coralline algae (~10%; Fig. 2.6). Collectively the bioclasts of these intertidal deposits are highly abraded with coral, shell, *Halimeda* and algae clasts showing pervasive fragmentation (Fig. 2.2d). Bioerosion is pervasive throughout these deposits. Coral and shell clasts have micritic rims commonly 50 μm thick, with *Halimeda* clasts showing more variable

20-50 μm thick rims. Minor encrustation by coralline algae is a rare feature of few coral clasts from Sumbano (Fig. 2.6). Cementation is absent from all samples of this facies.

2.4.3 Intertidal/Subtidal Reef Flat with Short Seagrass (Sample References: Kal12, 11, 10, 7, 36, HGG7, PK19, 18, 17, 16, HSB2S-8, 7, 6, 5, SS7, 6, 5)

2.4.3.1 Environmental Facies Description. Reef-flat intertidal/subtidal areas with short seagrass coverage form a <30-~350 m wide sloping to undulating margin to the intertidal deposits without seagrass (above). Short seagrass facies are also located as <100 m wide sections along the Sumbano transect that are adjacent to sections of long seagrass coverage (Fig. 2.6). The deposits are bioclastic sands and are commonly associated with shrimp mounds and bioturbation. These deposits are subtidal to intertidal with water depths of 0.7-1.8 m at high tide. Deposits are near flat lying to gently dipping, generally < 3°, although locally higher dips are present.

2.4.3.2 Facies and Sediment Characteristics. Sediments associated with the deposits of this environmental facies are dominated by bioclastic sands with grain-rudstone to more rarely packstone (Kal36) textures. The deposits are moderately to poorly sorted with some variability between transects. The deposits are dominantly bimodal fine to very coarse sands with a variable gravel (<1-17%) and clay-silt (<1-7%) content (Figs. 2.2e, 2.3-2.7). The sample from Kaledupa Centre transect is a moderately-poorly sorted unimodal silt-very fine sand (<75%) deposit with minor fine to coarse sands and a negligible (<1%) gravel content (Fig. 2.8). The >2 mm size fraction of these deposits is largely consistent across the transects. Coral and shell clasts contribute 13-90% of the bioclasts (Fig. 2.2e), with imperforate foraminifera (3-33%) and *Halimeda* (up to 50%) also dominant constituents. Only the sample from Kaledupa Centre transect differs, where lithic clasts make up 100% of the >2 mm fraction (Fig. 2.8). Lithics are loosely consolidated marl clasts (Fig. 2.2n). In thin section the <2 mm size fraction is composed of variable bioclasts. Coral and shell clasts may be dominant (~50%) with the remaining clasts evenly distributed between common *Halimeda,* imperforate and perforate foraminifera (Fig. 2.2f). Less common components include echinoid plates and spines, alcyonarian sclerites, calcarinids and miliolids. Collectively the bioclasts of these deposits are

moderately abraded and highly fragmented. Again the sample from Kaledupa Centre differs, having a <2 mm size fraction composed of 97% lithics (Fig. 2.8). Encrustation by algae and foraminifera is a rare feature and absent in the Pak Kasim and Sumbano deposits (Figs. 2.3, 2.6). Bioerosion of coral and shell material is pervasive and micritic rims may be 20-50 μm thick (Fig. 2.2f) and rarely up to 100 μm. Bioerosion is less common where coral or shell abundances are lower; with *Halimeda,* calcarinids and larger foraminifera showing 10-30 μm thick micritic rims. Cementation is absent from all deposits.

2.4.4 Subtidal Reef Flat with Long Seagrass (Sample References: Kal16, 13, 6, HGG4, PK15)

2.4.4.1 Environmental Facies Description. Back reef subtidal areas with long seagrass coverage occur along the Sumbano, Hoga Gilge Gilge and Pak Kasim's transects (Figs. 2.3, 2.5, 2.6). These areas form <30-100 m wide sections in relatively deep water areas (1.4-2.2 m) on the reef-flat. Seagrass present in this facies is typically up to 1 m in length, dense and may be associated with shrimp mounds.

2.4.4.2 Facies and Sediment Characteristics. Deposits of this facies are bioclastic sands with grainstone and less commonly grain- to rud- or packstone textures that show some variability between the transects. Deposits of the Sumbano transect are unimodal to trimodal poorly sorted very fine to very coarse sands with minor gravel (<9%) and a low clay-silt sized content (<7%). The >2 mm size fraction of the Sumbano deposits is dominated by *Halimeda* clasts (11-44%) and imperforate foraminifera (30-35%) with coral dominant (60%) from Kal6 adjacent to the subtidal coral deposits (Fig. 2.6). The <2 mm size fraction of the Sumbano deposits is dominantly *Halimeda* (30%), shell fragments (20%) and imperforate foraminifera (15%). The deposits of this facies from the Sumbano transect show only minor abrasion and fragmentation with pervasive micritic rims of 20-30 μm on shell, coral and *Halimeda* fragments. Long seagrass deposits from Hoga Gilge Gilge are poorly sorted trimodal fine to very coarse sands with minor (4<%) gravel and clay-silt sized fractions (Fig. 2.5). The >2 mm size component of the Gilge Gilge deposits is dominated by coral clasts (70%) with less abundant shells and imperforate

foraminifera. The <2 mm fraction of the Gilge Gilge deposits is variable with coral, shell, *Halimeda,* imperforate, perforate and calcarinid foraminifera present in similar abundances. Gilge Gilge deposits of this facies are moderately fragmented and abraded with highly pervasive bioerosion. Coral and *Halimeda* clasts have micritic rims of 10-50 μm (Fig. 2.2g), and shell fragments with rims up to 100 μm thick. The deposits from Pak Kasim's are dominantly bimodal moderately sorted fine to very coarse sands with minor (<3%) gravel and clay-silt size fractions (Fig. 2.3). The >2 mm size fraction of the Pak Kasim's transect is dominated by imperforate foraminifera (35%) and *Halimeda* (32%). In thin section the <2 mm fraction is dominated by corals (52%) and minor imperforate, perforate, calcarinid and miliolid foraminifera. The Pak Kasim's deposit is highly abraded and fragmented with moderate bioerosion.

2.4.5 Subtidal Reef Flat with Mixed Long and Short Seagrass (Sample References: Kal17, 8, HSB2S-4)

2.4.5.1 Environmental Facies Description. The back reef subtidal mixed long and short seagrass facies was sampled in three locations along the Sumbano and Hoga Buoy 2 transects (Figs. 2.4, 2.6). Examples of this facies are 30-100 m wide. Water depths for this facies are 0.7-1.8 m at high tide.

2.4.5.2 Facies and Sediment Characteristics. Deposits of this facies are polymodal poorly sorted fine to very coarse sands with a moderate to high gravel (6-21%) and moderate silt-clay (<3-9%) content (Fig. 2.2h). Sediment textures are grain-rudstones, or in the case of Kal 17 a grain-rud-packstone. The >2 mm size fraction of these deposits is dominated by shell and coral material which may constitute 31-95% of the bioclastic content. Less common bioclasts include *Halimeda*, imperforate foraminifera and seagrass (Fig. 2.2h). In thin section the <2 mm size fraction is dominated by coral (40%) or *Halimeda* (50%) with lesser shell and coralline algae clasts. Minor components include echinoid plates and spines (5%), alcyonarian sclerites (5%), imperforate, perforate, miliolid and smaller benthic foraminifera (<10% respectively). Abrasion and fragmentation are pervasive on coral clasts and echinoderm material with truncated and broken edges and gouged

grain margins. Bioerosion is non-pervasive with <10 μm thick micritic rims to foraminifera and 20-30 μm thick rims to coral and shell fragments.

2.4.6 Subtidal Reef Flat with Mixed Seagrass-Corals (Sample References: Kal14, 5, 3 39, HGG5, 3, 2, HSB2S-3, PK14, SS4)

2.4.6.1 Environmental Facies Description. A few examples of back reef subtidal mixed coral and seagrass facies were sampled along all transects except Kaledupa Centre (Figs. 2.3-2.7). Sections of mixed coral and seagrass are typically 30-100 m wide and located in the deeper water (~2 m, high tide) parts of the back reef, and adjacent to patches of long seagrass or the reef margin. The seagrass present in this mixed facies is generally short and minor, and well-developed brown algae may be present.

2.4.6.2 Facies and Sediment Characteristics. Deposits of the mixed coral and seagrass facies are dominantly moderately sorted medium to very coarse sands with a typically moderate to low gravel (<13%) and silt-clay (<8%) sized fraction, with exception to samples Kal39, and SS4 (Figs. 2.7, 2.8) where the gravel sized fraction constitutes 83-94% of the sample. Hand samples are predominantly grain-rudstones, although in the modern environment domestone or mixstone textures are also present. The >2 mm size faction is dominated mostly by coral and shell bioclasts (commonly 50-90%) with less abundant imperforate foraminifera and seagrass (Fig. 2.2i). In thin section the <2 mm size fraction has a high coral and shell content (typically <50%) with calcarinid and imperforate foraminifera (Fig. 2.2j, k) and coralline algae common components (<20%), together with minor perforate foraminifera and echinoid plates and spines and rarely alcyonarian spicules. Collectively the bioclasts of the mixed coral and seagrass facies are moderately abraded and fragmented with common preservation of elongate coral clasts and calcarinid spines (Fig. 2.2i). Bioerosion is pervasive with micritic rims of up to 100 μm on coral and shell material, and <10-30 μm rims common on other bioclasts. Minor and non-pervasive encrustation by algae is present commonly and cementation is absent from all samples.

2.4.7 Subtidal Reef Flat with Corals and with/without Patchy Sediment Cover

(Sample References: Kal15, 9, 4, 2, HGG6, 1, HSB2S-2, 1, PK13, 12, SS3, 2, 1)

2.4.7.1 Environmental Facies Description. With exception to the Sumbano transect, back reef subtidal areas with coral and patchy sediment cover occurs adjacent to and back from the reef crest/margin. This facies is typically 50-150 m in width. Coral cover is variable ranging from coral rubble to robust massive and branching forms, with a cover of up to 30%, although locally around coral bomées this may be higher. Sand cover may be as high as 60%, occurring between corals, rocky knolls and lithified surfaces. Water depths range from 1-3 m (high tide). The distribution of this facies across the Sumbano transect (Fig. 2.6) is patchy, occurring adjacent to both seagrass and mixed coral/seagrass facies, as well as the reef crest/margin, with typically <30 m wide sections of coral rubble and intact massive and branching corals.

2.4.7.2 Facies and Sediment Characteristics. The deposits of back reef subtidal areas with corals and with or without sediment cover are typified by bimodal, moderately sorted fine to very coarse bioclastic sands to gravels. Sediment samples are rud-grainstones, although pillar-, mix- and domestones are also present in the modern environments. Gravel content is variable (<1-60%) and there is a typically low clay-silt sized fraction (<5%). The >2 mm size fraction of the deposits is variably dominated by coral and shell bioclasts which may comprise 10-90% and 5-75% respectively of a sample (Fig. 2.2l). Less common components may be imperforate foraminifera, *Halimeda* and seagrass, with rare and minor echinoid plates and spines and alcyonarian sclerites. In thin section the <2 mm size fraction is rarely dominated by corals (5-50%) with commonly abundant perforate and calcarinid foraminifera and *Halimeda* (<20%) and less abundant imperforate foraminifera, echinoid material and alcyonarian sclerites (<10%). Collectively the bioclasts of this facies are not highly abraded, shell and coral clasts show minor evidence of abrasion whilst foraminifera, particularly calcarinids show higher levels of abrasion (i.e. spines removed). Clasts from this facies are typically highly fragmented and show little encrustation (Fig. 2.2l). Bioerosion is not a pervasive feature of this facies, micritic rims are commonly 10-30 μm in thickness and

typically only present on coral, shell and echinoderm material. Cements are absent from all deposits of this facies.

2.4.8 Subtidal Reef Crest/Margin (Sample References: Kal1, HSB42, PK11, S2/3-3m)

2.4.8.1 Environmental Facies Description. The reef crest/margin is a narrow (<30 m) rim of coral rubble to massive corals occurring adjacent to the reef slope bordering deeper waters and affected by open oceanic processes (Figs. 2.3, 2.4, 2.6, 2.7). Extensive areas of coral rubble along the reef margin such as at Sumbano, probably at least in part reflect coral bombing and other destructive fishing practices by humans. The reef crest margin is predominantly subtidal, occurring in water depths of 3-5 m (high tide) or more rarely near emergent at low tide (Hoga Gilge Gilge; Fig. 2.5).

2.4.8.2 Facies and Sediment Characteristics. Deposits of the reef crest/margin are typified by bimodal, moderately to poorly sorted coarse sands and gravels. Sediment samples are rud-grainstones but mix- and domestone textures dominate in the modern environments. The gravel content of these deposits is high (25-43%) with a minor silt-clay sized fraction (<2%). The >2 mm size fraction is dominated by coral bioclasts (60-<90%) with less abundant shells, *Halimeda*, echinoid plates and spines and perforate and imperforate foraminifera. In thin section the <2 mm size fraction is largely coral bioclasts (25-45%) with common shell fragments, imperforate, miliolid, perforate and calcarinid foraminifera, echinoid spines and alcyonarian sclerites (<15%). Collectively the bioclasts are moderately to highly abraded and fragmented. Encrustation is not seen in these deposits and bioerosion is minimal. Micritic rims at most are <10 μm and non-pervasive. Cementation is absent from all deposits of the reef crest/margin.

2.4.9 Subtidal Reef Slope (Sample References: WSUM2, HSB41, HB3-7, 6, PK10, 5, S2/3-5m, 8m)

2.4.9.1 Environmental Facies Description. The reef slope environment is a subtidal rocky to sandy slope with hard coral coverage (locally up to 50%), coral

rubble and soft corals (Figs. 2.3-2.7). Selected samples were from water depths from 5-14 m, and from a range of slope environments including sediment collected on ledges from near vertical rocky walls, sediment patches between corals, sand shoots within canyons and sediment aprons below the main reefal development. Studied sections of the reef slope were <30 m wide, with all environments exposed to open oceanic processes.

2.4.9.2 Facies and Sediment Characteristics. The deposits of the reef slope are typically bimodal, moderately to poorly sorted bioclastic gravels and fine to very coarse sands. Rud-grainstone textures comprise the sediment samples, with mixstone textures also present in the modern settings. The coarse gravel content of the deposits is high (12-43%) with a typically low silt-clay sized fraction (<7%). The >2 mm size fraction of the reef slope deposits is dominantly comprised of coral clasts which may contribute 35-75% of the total bioclastic material. Common, less abundant bioclasts include, shell fragments, *Halimeda*, imperforate foraminifera, echinoid plates and spines and alcyonarian sclerites (<10%). In thin section the <2 mm size fraction of the reef slope deposits is largely coral clasts (35-45%) with common shell fragments, perforate foraminifera, echinoderm material and alcyonarian sclerites (Fig. 2.2m). Collectively the bioclasts show moderate to minor abrasion and fragmentation, with coral clasts showing the most pervasive fragmentation. Encrustation and bioerosion are rare and non-pervasive (Fig. 2.2m). No cementation is present in deposits of the reef slope environment.

2.4.10 Platform Interior Channel and/or Deep Water Regions (Sample References: Kal34, 35, 37, 38, 40, 41, WHB1-2)

2.4.10.1 Environmental Facies Description. Turbid and deep water platform interior regions are found in the near-shore back reef 'lagoon' area of northeast Kaledupa and in the semi-enclosed channel that lies between Kaledupa and Hoga (Fig. 2.8). The areas of deep water are 3-<30 m in depth. Complete bottom-water/sediment-surface environmental data is not available along this transect since samples were acquired via a sediment grab. Unlike other transects that are adjacent to onshore areas of limestone the Kaledupan coast proximal to sample locations for Kal34-38 has cliff exposures of marl (deposits rich in carbonate and siliciclastic clay

and silt-sized particles). Turbidity associated with these deposits is commonly high related to suspended particulate matter derived from the marls, terrestrial derived organic matter, plankton and high tidal current velocities in the channels stirring up bottom sediment.

2.4.10.2 Facies and Sediment Characteristics. Deposits of the deep water regions are dominantly bioclastic sands and gravels, however variability exists between the south-eastern deposits (Kal34, 35; Fig. 2.2n, 2.8) and the north-western deposits. South-eastern deposits are bimodal to trimodal, moderately to poorly sorted silts with variable very fine to very coarse sand. Coarse gravel sized material is lacking (<0.2%) and clay-silt comprises 37-51% of the total sediment resulting in packstone textures (Fig. 2.2n). Bioclasts are absent from the small amount of >2 mm size fraction, instead the coarse sediment is 99-100% lithic clasts. In thin section the <2 mm size fraction is 50-95% lithics with minor coral and shell clasts, echinoid material, alcyonarian sclerites and smaller benthic and planktonic foraminifera. The bioclasts that are present are highly fragmented and abraded. Encrustation is a rare feature of larger coral clasts and bioerosion is pervasive. Micritic rims are typically >50 μm in thickness on coral and shell material with other bioclasts showing more variable 10-50 μm rims. The north-western deposits are dominantly unimodal, moderately to well sorted medium-coarse sands to gravel with grain-rudstone textures. The coarse gravel fraction may contribute from 4-54% of the sediment, with a typically low or moderate clay-silt sized fraction (<1-17%). The >2 mm fraction of these deposits is typically dominated by shell material (20-65%) or coral clasts (7-66%). In thin section the <2 mm size fraction is variable with commonly abundant shell (<30%) and echinoderm material (<20%) with less abundant coral, imperforate-, smaller benthic, miliolid- and planktonic-foraminifera, and rare alcyonarian sclerites (Fig. 2.2o). The bioclasts of these deposits are commonly moderately fragmented and abraded, with corals showing the most pervasive fracturing (Fig. 2.2o). Encrustation by coralline algae and rarely foraminifera is common. Bioerosion is common but rarely pervasive, with the best developed micritic rims of 10-40 μm present on coral and shell clasts. Cementation is absent from all deposits.

2.4.11 Satellite Classification Model

A Landsat-7 derived environmental facies map has been created through unsupervised classification processes (Fig. 2.9; see Materials and Methods section). An overall accuracy of pixel classification linked to environmental facies of 71.43% is indicative of good agreement across the Landsat generated facies map (Table 2.1). However, accuracy of classification for most of the subtidal reef flat and intertidal to supratidal facies is >90%. The main source of error in the environmental facies model is due to misclassification of the reef crest-margin and reef slope facies. In all instances these features are at a single pixel or sub-pixel scale (feature width) and are misclassified as either platform interior channel/deep or reef flat subtidal corals with or without sediment cover. Despite attempts to group pixels into a larger number of classes (n=60, 75, 100) it was not possible to correctly identify these features whilst maintaining good agreement in the deep water facies around the Kaledupa Centre transect. To a lesser extent the mixed long and short seagrass facies are a secondary source of error, with only 20% agreement for this class. Misclassification of the mixed seagrass facies places pixels into the short seagrass, long seagrass or mixed coral and seagrass facies. Of the classifiable environmental facies for the classified area: 22.92% are mixed coral and seagrass, 20.53% are short seagrass, 18.43% are coral with or without sediment cover, 16.78% are long seagrass, 13.14% are deep water/turbid, 5.27% are intertidal/subtidal with no seagrass, 2.45% are mixed long and short seagrass and 0.46% are foreshore/backshore (Fig. 2.9).

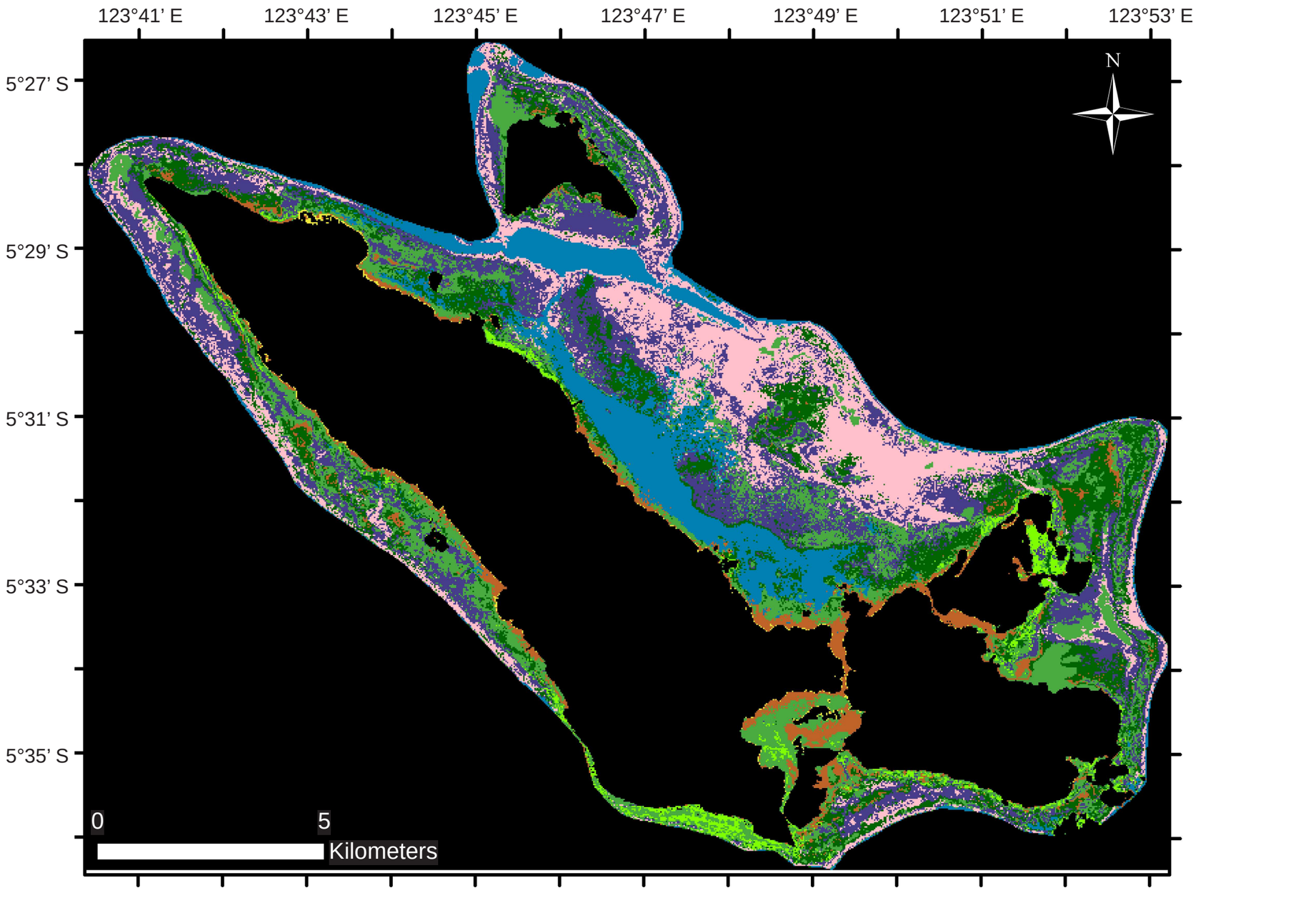

Figure 2.9. Landsat derived environmental facies map, generated through the unsupervised classification utility of ER Mapper software. Land areas at the centre of Kaledupa and Hoga have been masked, along with several small scale areas of cloud cover. Foreshore/backshore facies are relatively sparse and narrow and in few areas have been removed due to the effects of the land masking algorithm applied during image processing.

Table 2.1. Percentage agreement (overall accuracy) metrics as determined through a count of correctly identified Landsat pixels/locations divided by the total number of samples/known pixels available. The overall accuracy has been broken down into individual accuracies for each identified environmental facies. Key sources of error and misclassification of pixels are from the reef slop and reef crest facies.

Class	Environmental Facies	Number of Calibration/Known Pixels	Number of Correctly Classified Pixels	Accuracy/Agreement (No. Know n pixels/No. Correctly classified pixels)*100
10	Deep water	7	7	100.00%
9	Reef slope	8	0	0.00%
8	Reef crest	5	0	0.00%
7	Coral +/- sediment cover	14	13	92.86%
6	Mixed coral and seagrass	13	12	92.31%
5	Mixed long and short seagrass	5	1	20.00%
4	Long seagrass	5	3	60.00%
3	Short seagrass	17	16	94.12%
2	Intertidal no seagrass	2	2	100.00%
1	Foreshore/backshore	1	1	100.00%
TOTAL:		**77**	**55**	**71.43%**

2.4.12 Cluster Analysis

Carbonate sedimentation across the Kaledupa-Hoga system is, for the most part, dominated by the accumulation of skeletal allochems including coral clasts, whole and broken shells, *Halimeda*, foraminifera, coralline algae and echinodermata grains. A comparison of composition (bioclasts and fines) by statistical cluster analysis for the whole data set allows for the identification of four "statistically-defined" sedimentary facies. These four "statistically-defined" facies have textures of; (1) packstone, (2) grainstone, (3) grainstone to grain-rudstone and (4) grain-rudstone to grain-rud-packstone (Fig. 2.10). The dendrogram demonstrates a large degree of sediment homogenisation in that at ~40% dissimilarity the sediments are still largely grouped as the same cluster. The cophenetic correlation coefficient value for the dendrogram at 0.9017 is very high, and indicates that the dendrogram accurately reflects the original sediment characteristics (Fig. 2.10).

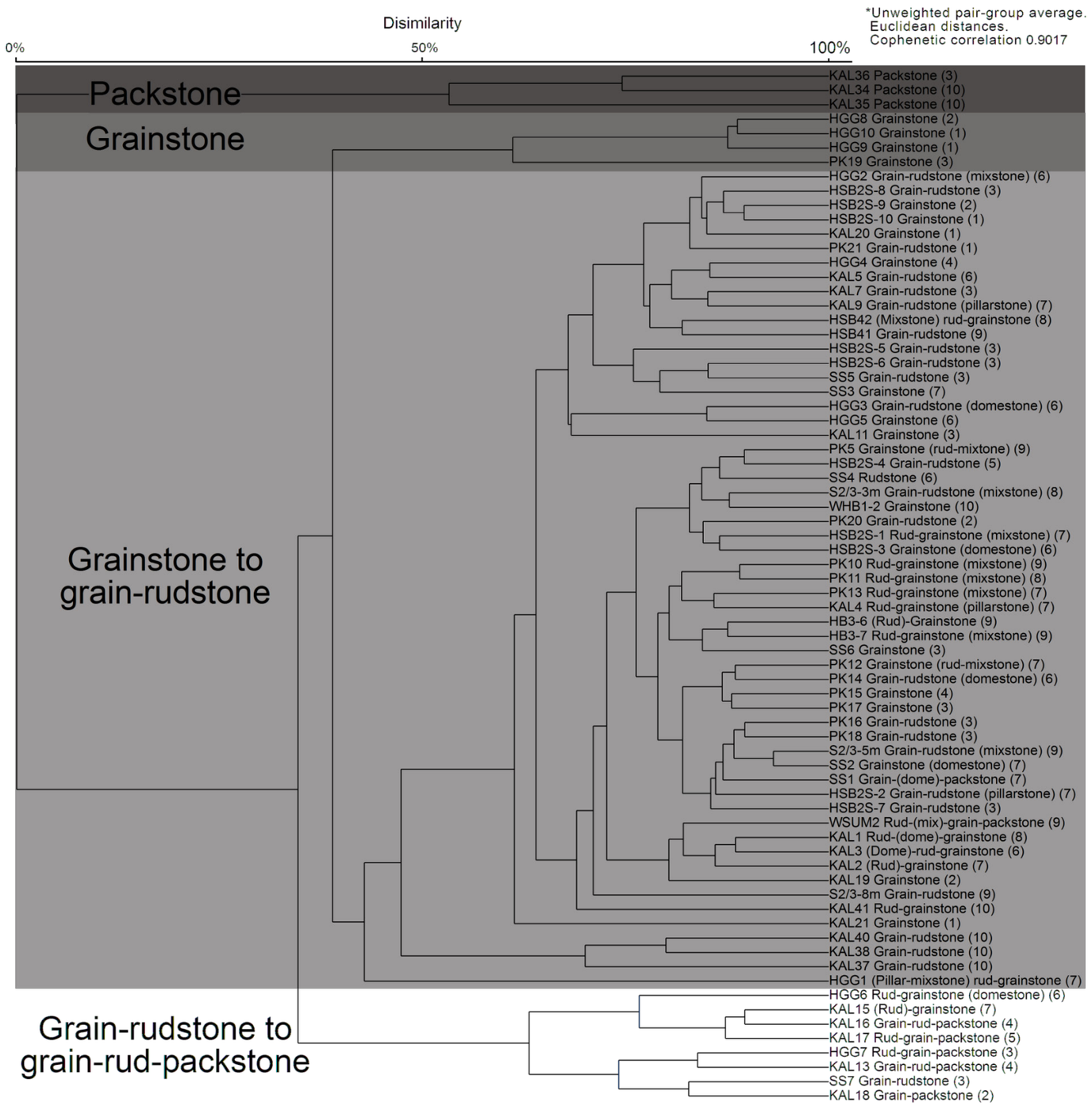

Figure 2.10 (caption on next page)

Figure 2.10. Dendrogram of cluster analysis of sediment data from the Kaledupa-Hoga study area. Represented variables are the abundances of components measured in the <2 mm size fraction and the silt to clay sized sediment fraction of each sample (cf. Figs. 2.3-2.8). The unweighted pair-group average and Euclidean distance algorithms were selected as they generated the most meaningful dendrogram. The dendrogram was generated with PAST (Paleontological Statistics; Hammer et al., 2001). Deposit texture characteristics are given after each sample identifier with dominant textures listed first and those identifiable from field characteristics only parenthesised. The Number in parentheses after each sample is the environmental facies group each sediment has been sampled from (Fig. 2.9).

2.5 Interpretation and Discussion

2.5.1 Environmental facies distributions, sediment characteristics and controlling influences

As is the case for other modern humid equatorial carbonate systems, or indeed those from elsewhere, the distribution of environmental facies and their associated sediments from shallow platforms can be complex (cf. Scrutton, 1978; Park et al., 1992, 2010; Jordan, 1998, O'Shea, 2005). An important consideration for understanding spatial facies patterns well enough to be predictive about their inherent characteristics is whether or not a relationship can be established between observable sedimentary characteristics and the identifiable environmental associations (cf. Harris and Vlaswinkel, 2008). The classification of the Kaledupa- Hoga reef systems demonstrates a heterogeneous distribution of environmental facies. Field observations have identified 10 observable environmental facies. However, although the combined petrographic and sedimentological study allowed subtle deposit variations to be identified for the different environmental facies there is similarity between many of the facies, as corroborated by the cluster analysis of the deposits (Figs. 2.10, 2.11). Sediment characteristics, whilst distinctive would appear to identify broader environmental facies groupings than the facies breakdown presented in the Landsat derived facies map (Figs. 2.9-2.11).

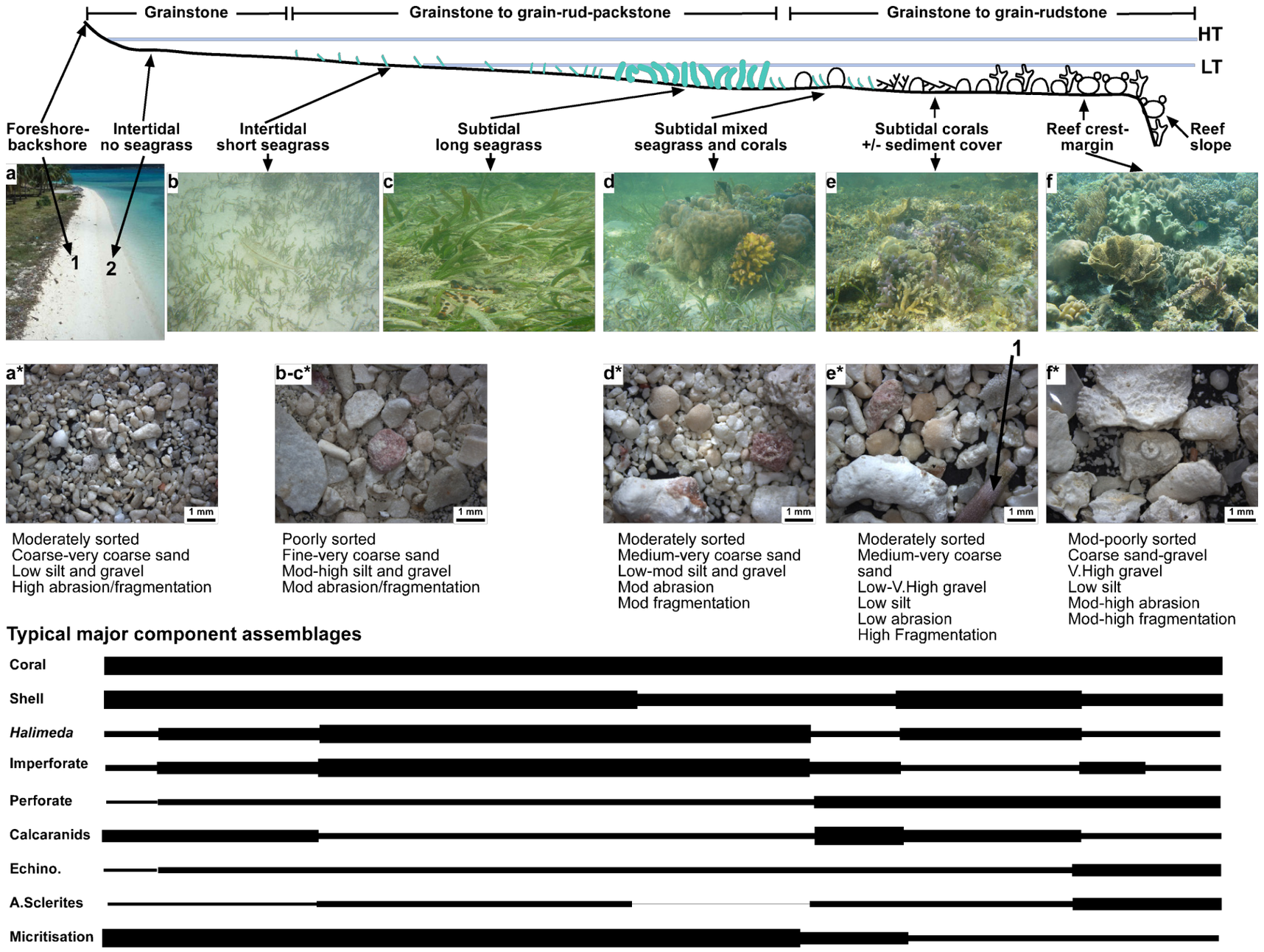

Figure 2.11 (caption on next page)

Figure 2.11. Schematic summary transect of modern environments and their associated sedimentary characteristics, determined from high resolution sediment sampling and field observations from the shallow fringing reefs of Pulau Kaledupa and Hoga. There is similarity between many features and components from the different environments, although subtle variations in biotic assemblages and early alteration features correspond to groupings of environmental facies. a) Modern environment photograph (Hoga beach) showing both foreshore (1) and intertidal with no seagrass (2) environments. (a*) Unsorted modern sediment sample (Kal21), representative of foreshore sediments. (b) Modern environment photograph of short (nibbled) seagrass facies with accumulation of fine sandy material (Hoga Buoy 2). (c) Modern environment photograph (Sampela) of long seagrass facies, with accumulations of both coarse and fine material. (b-c*) Unsorted modern sediment sample (HBS2-7), representative of seagrass facies environments. (d) Modern environment photograph (Pak Kasim's) of mixed coral and seagrass facies. (d*) Unsorted modern sediment sample (Kal5), representative of mixed coral and seagrass facies. (e) Modern environment photograph (Pak Kasim's) showing relatively clear non-turbid waters and minor patchy accumulations of sandy deposits between and around branching coral forms. (e*) Unsorted modern sediment sample (HGG1), representative of coral with or without sediment cover facies deposits, with occurrence of echinoderm spine (1). (f) Modern environment photograph (Hoga Buoy 2) showing typical high energy reef margin, with abundant hard and soft corals. (f*) Unsorted modern sediment sample (HSB41), representative of reef crest and reef slope deposits. Abbreviated component names are; Echino.-Echinodermata and A.ScleritesAlcyonarian sclerites.

Foreshore deposits are a minor component of the Kaledupa-Hoga system, distributed adjacent to the emergent landmasses. The highly abraded allochems, general absence of fine material and fragmented reworked reef debris are due to the accumulation of skeletal sands and coarse coral debris concentrated by wave and storm activity. These same features of foreshore and/or beach deposits are seen regionally, notably in the isolated carbonate systems of Kepulauan Seribu, offshore Jakarta (Jordan, 1998; O'Shea, 2005). The adjacent facies of intertidal reef flat without seagrass form a relatively wide perimeter to the foreshore deposits and are highly distinctive. The accumulation of poorly to well sorted very fine to very coarse sands reflect variable energy settings. The Sumbano deposits, in the lee of Kaledupa Island, having a trimodal grain-size distribution (fine to very coarse sand and low to moderate silts-clays and gravels) reflect the lowest energy depositional conditions. The highest percentage of silts and clays, albeit at only 4-7% (Fig. 2.6), likely reflect the leeside setting and are also a consequence of the broad reef flat, providing limited

protection from wave activity. Although Hoga Buoy 2 is situated in the lee of the smaller island of Hoga the limited width of the reef flat likely contributed to the apparently higher energy, well sorted coarse to very coarse intertidal deposits with minimal silts and clays (<2%; Fig. 2.4). Although the intertidal deposits of Hoga Gilge Gilge are sited in the lee of small offshore "mushroom" islands and inboard of a broad reef flat the paucity of clays and silts (<2%) reflects the windward setting with respect to the strong westerly monsoon (Fig. 2.5). The coral- and shell-rich content of both the foreshore/backshore and intertidal deposits reflect reworking and deposition from the reef flat environments. Micritisation of the intertidal deposits is pervasive and consistent with endolithic micro-borers being most active in moderate to lower energy shallow-photic environments (cf. Swinchatt, 1965; Budd and Perkins, 1980; Perry and Bertling, 2000; Perry and Hepburn, 2008). These foreshore and intertidal deposits are almost exclusively grainstones, a product of strong shoreward reworking of reefal material and localised turbulence and/or winnowing associated with waves breaking at the shore. However, cluster analysis of these samples does not fully resolve these grainstones into their own distinctive facies. Instead, cluster analysis results in a grouping of the heavily micritised foreshore and intertidal deposits of Hoga Gilge Gilge (Fig. 2.10). The remainder of the foreshore and intertidal environmental facies are clustered together with the sedimentary facies of grainstones to grain-rudstones that are pervasive across many environments of the Kaledupa-Hoga fringing reefs; indicating strong homogenisation of the sediments (Fig. 2.10).

Despite the presence of distinct reef flat environmental facies, detectable from field observations and Landsat interpretation, the sedimentological characteristics are less varied. There is a broad similarity of sedimentological features of the back reef in terms of allochem composition, grain size and early alteration characteristics (Figs. 2.2-2.8, 2.10, 2.11). Furthermore the controls of leeward versus windward settings and the effects of sheltering by a broad reef flat that are evident in the foreshore and intertidal deposits are not as apparent in the back reef facies. Reef flat deposits on the basis of their sedimentological characteristics may be grouped into two broad categories: (1) seagrass facies and (2) coral facies.

Seagrass facies are heterogeneous in their distribution and continuity across and between transects, a feature highlighted by their patchy distribution on the Landsat-derived facies map (Fig. 2.9). In general seagrass facies deposits are poorly sorted very fine to very coarse sands, with comparable abundances of clay-silt and gravel sized fractions (typically 3-<10%). This apparent homogenous grain size distribution across both leeward and windward transects and inbound from both broad and narrow reef flats is indicative that the prevailing energy conditions are not the primary controlling factor for the development of high versus low energy deposits, as is the case for foreshore/backshore and intertidal settings. The bioclastic content of the seagrass facies deposits is composed dominantly of moderately abraded and fragmented coral and shell material, lesser imperforate foraminifera and *Halimeda*, and minor miliolid and calcarinid foraminifera, echinoderm material and alcyonarian sclerites. Micritic walled imperforate foraminifera, including miliolids, and calcarinids are associated with the development of seagrass beds where seagrass blades provide renewable substrate upon which such benthic organisms can attach and grow (Ginsburg and Lowenstam, 1958; Renema and Hohenegger, 2005), and where locally protected settings are developed by the baffling effect of the seagrass (e.g. Ginsburg, 1957; Scoffin, 1970; Brasier, 1975; Almasi et al., 1987). These same locally protected settings also act as sediment baffles trapping the highest abundances of silt and clays from the reef flat, resulting in the grain-rud-packstones textures in addition to grain-rudstones. Despite the presence of seagrass facies indicators (poorly sorted sediments, moderate to high silt-clay and imperforate foraminifera) there is an overriding bioclastic signature i.e., a high abundance of reworked corals with accessory echinoids and alcyonarian sclerites. This bioclastic signature is more typical of the coral associated facies occurring seaward of the seagrass facies deposits, although some corals are locally present in the seagrass areas. Reworking of coral reef material into the seagrass facies is attributed to the "wash-over effect" of wave activity and strong diurnal tidal currents promoting the shoreward movement of reef material. The lack of a well-defined or emergent reef crest that would act to protect the back reef areas likely contributed to the shoreward movement of reefal material. Similar to the foreshore/backshore and particularly the intertidal deposits, seagrass facies deposits show high degrees of micritisation consistent with low energy shallow-photic environments, as inferred above.

Coral facies are widespread throughout the study area, comprising 40% of the Landsat classification. The sedimentology of these deposits is reflected in the overall moderately sorted medium to very coarse sands and gravels with a typically low (<5%) silt-clay content and grainstone to grain-rudstone classifications. Coral facies deposits show little variability, with coral contents typically constituting up to 90% of a sample. Less abundant clasts commonly include perforate (including calcarinids) and imperforate foraminifera, *Halimeda*, echinoderm material and alcyonarian sclerites. High abundances of highly fragmented coral with robust forms of perforate foraminifera are distinctive of high energy environments (Hallock and Glenn, 1986; Beavington-Penney and Racey, 2004). However, the presence of non-robust imperforate foraminifera, rare miliolids, calcarinids, and rare highly abraded clasts with pervasive micritisation are indicators of reworking of seagrass facies material into the coral facies deposits. Seaward reworking of sediments is best attributed to the strong semi-diurnal tidal currents in combination with bi-directional monsoonal winds, perhaps in combination with storm-waves, affecting shallow platform environments. Whilst reef crest and slope deposits were not identifiable on the Landsat derived facies map they are perhaps the most distinctive deposits sampled. These deposits are dominantly coarse to very coarse sands with consistently very high (<45%) gravel and low (typically <2%) silt-clay sized fractions, indicative of a high energy platform margin. Despite the inferred high energy setting of the reef crest/slope environments reef slope samples from Hoga Buoy 2 and Sumbano have moderate silt-clay contents of 3 to <6% respectively. This accumulation of some fine sediment is likely the result of their protected leeward setting that is also reflected in the foreshore/intertidal deposits for the same transects.

Despite the presence of identifiable seagrass and coral based environmental facies there is a strong homogenisation of sedimentary characteristics, a result of wash over, bi-directional monsoonal winds and strong semi-diurnal tidal currents. This homogenisation of sedimentary characteristics is clearly highlighted through cluster analysis of the sediments (Fig. 2.10). The dominance of coral and shell material as coarse bioclasts imparts a grainstone to grain-rudstone texture to the majority of the reef flat sediments (Fig. 2.10). However, where seagrass deposits have developed in the lee of Kaledupa (Sumbano transect) and in the more protected settings of

Sampela transect; the concentration of fines allows for the identification of grain-rudstone to grain-rud-packstone sediments which are distinctly representative of locally protected seagrass environmental facies. There is an apparent disconnect between the ability to map environmental facies from satellite imagery and what is preserved in the geologic record i.e., the lack of identifiable reef crest and reef margin facies. The reef crest and margin facies sediments whilst initially appearing as distinctive are still clustered with the largely homogenised sediments of the reef flat, i.e., grainstones-grain-rudstones (Fig. 2.10). These reef crest and margin deposits are likely, however, to be traceable in the rock record through combined component and/or textural class variations, with prior studies detailing the potential of diagenetic overprinting by early marine cements of reef margin sediments (Grötsch and Mercadier, 1999; Wilson and Evans, 2002; Madden and Wilson, 2013). The very small spatial extent of these reef margin and crest deposits and associated inability to detect sub-pixel scale features from this form of satellite imagery is not considered a major failing of this study since the broader sedimentary faceis are still discerned (Figs. 2.9, 2.10).

2.5.2 Kaledupa-Hoga summary and comparisons with other fringing reefs

Sediment samples across all fringing reef environments from the Kaledupa-Hoga transects have almost exclusively grain-rudstone textures, with <2-5% silt and clay size fractions (85% of all samples). Grain-packstone textures (albeit with only up to 7-9% silts and clays) are seen in the seagrass beds and intertidal deposits just from the broader reef flats and predominantly on leeside transects with respect to the predominant monsoonal wind direction. It appears seagrasses are a key baffler of fine grained sediment on these small–scale isolated systems, and are also areas of enhanced biologically-mediated breakdown and alteration of grains (cf. Ginsburg and Lowenstam, 1958). Tomascik et al. (1997) reported that seagrasses are a ubiquitous feature of many Indonesian fringing reefs and that there are important biological, and it now appears sedimentological, dynamics between the reef-seagrass systems (cf. Salinas de León et al., 2010; Unsworth, 2010). Fines in packstones from the Central Kaledupa transect are linked to the physical breakdown of island-derived lithics (marls) and their accumulation in the inter-platform “channel” and deep water “lagoon” area. There may also be anthropogenic influences on environments and

grain sizes, particularly in the Sampela transect (Crabbe and Smith, 2002). The paucity of fines across the Kaledupa-Hoga system as a whole is attributed to: (1) high wave/current energies, (2) the small size of the islands rendering limited protection, (3) bidirectional monsoon winds and (4) the lack of reef rimmed margins built to sea level. Additionally the equatorial tropics unlike the sub-tropics is not a region of significant marine carbonate precipitation, whether in the form of micrite "whitings", ooid formation or cements (Lees and Buller, 1972; Wilson, 2002; 2012), as attested to by the paucity of early cementation throughout the fringing reef deposits. The degree of homogenisation of sediment characteristics across the different field- and satellite-identifiable environmental facies with evidence for both seaward and landward transportation of grains is again attributed to these same four factors listed directly above (cf. Cordier et al., 2012).

Similar features to those described here and a predominance of grain-rudstone sediments across reef flat, crest and slope deposits are also seen regionally in the high-energy, monsoon-influenced carbonate systems of Kepulaun Seribu, offshore Jakarta. In general the reef flat environments with widths of up to 2 km (including seagrass beds, lithified coral flats and patchy coral cover) are characterised by medium to coarse bioclastic sands where coral rubble constitutes 40-70% of the bioclastic material, molluscs 50-70% and minor foraminifera and echinoid material are widespread, and silt-clay size fractions are low (Scrutton, 1976, 1978; Jordan, 1998; O'Shea, 2005; Park et al., 2010). The reef crest and slope environments of Pulau Seribu are dominated by 40-95% coral rubble with a typically poor degree of sorting and <2% silt-clay sediment fraction (Scrutton, 1976, 1978; Jordan, 1998; O'Shea, 2005; Park et al., 2010). The Pulau Seribu system differ from those described here from Kaledupa-Hoga in being shelf patch reefs, with or without coral rubble/sand cays and/or interior lagoons, and in having prominent rampart rims, often with a landward developed moat and lesser seagrass development (Park et al., 1992; 2010; Tomascik et al., 1997; Jordan, 1998). The fringing reef deposits from around the 1.5 km across Danjugan Island in the Philippines, as with those described here, are dominated by sand- to gravel-grade bioclastic grains with homogenisation of grain types across different environments (Hewins and Perry, 2006). Where the Danjugan reefs differ is in showing strong differentiation between "windward, leeward and lagoonal" transects in addition to bathymetric trends, with the systems

as a whole influenced by predominant prevailing winds from the southwest (Hewins and Perry, 2006). Tomascik et al. (1997) noted that some of the variability in SE Asian fringing reef development relates to: (1) geographic location (e.g. continental shelf vs. oceanic), (2) topography and nature (e.g. volcanic or limestone) of the antecedent foundations, and (3) their geomorphological attributes. In the later case this may include the presence of spurs and grooves, lagoons, boat channels, reef crest, reef flats and the angle of the reef slope.

Other fringing reefs from isolated equatorial tropical carbonate systems, such as Mahé in the Seychelles, show similarities to those from the Tukang Besi Archipelago in being dominated by bioclasts, showing similar distinct environmental facies zonations, but in having sediment characteristics in terms of grain-sizes and/or components that may be difficult to relate to their primary environments (Lewis, 1969). As with the Wakatobi region, seagrass beds are zones of accumulation of the finer grained sediments, although rarely more than a few percent silt- or clay-grade material, and mostly in leeside settings (Lewis, 1969). The fringing reefs of Mahé differ from those of Kaledupa-Hoga in showing more distinctive zonation on windward versus leeside reefs, just having predominantly landward transport directions of marine sediments and in showing significant development of outer reef-flat to -crest algal ridges. These differences may reflect the slightly larger size of Mahé at 25 km compared with Kaledupa-Hoga (20 km), the lack of island-transecting tidally-influenced channels, less oceanic-current influence and sea swells mainly during a predominant monsoon season (Lewis, 1969). Kuenen (1933) and Umbgrove (1947) noted that the thick algal sheets and ridges that characterise large areas of the Great Barrier Reef and many Pacific atolls are rare within the Indonesian archipelago, and these features are also not present in Pulau Seribu, Danjugan or Kaledupa-Hoga (cf. Hewins and Perry, 2006; Park et al., 2010).

Fringing reefs in the sub-tropics, such as those from Grand Cayman, New Caledonia or Réunion (Gabrié and Montaggioni, 1982; Cabioch et al, 1995; Blanchon et al., 1997; Blanchon and Jones, 1997), tend to differ significantly from those in the equatorial tropics. At 25 km across Grand Cayman is similar in size to Kaledupa and Mahé but the fringing reefs differ in their zonation, their reef morphology, not developing on leesides, having little seagrass development, being dominated by

zones of coral-cobble rubble underlying the reef crest and in having spur and grove development downslope of the reef crest (Blanchon et al., 1997). An overriding control on fringing reef development in Grand Cayman is inferred to be hurricanes (Blanchon and Jones, 1997; Blanchon et al., 1997): i.e. a process not affecting the equatorial tropics. Braithwaite et al. (2000) and Montaggioni (2005) noted that fringing reefs have a spectrum of development and internal structure related to lower or higher fair-weather energy conditions versus storm severity. Accommodation space and relative sea level change in addition to hurricanes are other important controls on the growth and morphology of fringing reefs (Kennedy and Woodruffe, 2002). The fringing reefs of Kaledupa-Hoga developed under high fair-weather energy, but low storm severity and their development is consistent with the trends described by Braithwaite et al. (2000) and Montaggioni (2005). Fringing reefs with near horizontal reef flats that are partially exposed landward of the reef flat at low tide, as is the case for those of Kaledupa-Hoga, are commonly reported throughout the Indo-Pacific (Kennedy and Woodruffe, 2002). Many of these Indo-Pacific reef flats that dry at low tide appear to have experienced relative sea level fall (Kennedy and Woodruffe, 2002). The fringing reef systems of Kaledupa-Hoga are no exception, surrounding islands with "stepped" coral reef terraces that have been uplifted to maximum heights of 300 m within the last five million years (Wilson, 2008b).

2.5.3 Limitations of, and Comparisons with, Landsat-Derived Environmental Facies Maps

Given the heterogeneous and complex biological and morphological structure of coral reef environments it is perhaps unsurprising that many satellite based facies maps, whether environmentally or sedimentologically focused, typically fall short of 100% accuracy (e.g., Green et al., 2000; Kaczmarek et al., 2010). Discrepancies between the field determined environmental facies and the Landsat derived facies map presented here (i.e. 71.43% agreement) are attributable to several factors. The main source of error in the facies map generated for Kaledupa and Hoga is the misclassification of the reef crest and reef slope environments (Table 2.1, Fig. 2.9). This misclassification of forereef environments is an error inherent to the study area where reef crests and slopes with narrow <30 m wide profiles are juxtaposed against

steep drop-offs and deep water. The occurrence of sub-pixel scale (<30 m) reef features, and the absence of a well defined highly reflective reef crest results in misclassification and placement of these pixels into adjacent thematic classes. It has been suggested that the optimal spatial resolution for most coral reef mapping exercises is 1-10 m (Joyce and Phinn, 2001; Andréfouët et al., 2003). Whilst it is possible to utilise hand digitising, filtering algorithms and/or sub-pixel classification techniques to correct these misclassified pixels the techniques are labour and time intensive. Given the low spatial extent of the observable reef crest and reef margin environments and their sedimentary facies grouping within a broader coral environmental facies (Fig. 2.10) their misclassification does not significantly affect the overall success of the presented facies map (i.e. 86% agreement without the reef crest and slope). Lesser sources of error are likely attributable to the similarity in reflectance of chlorophyll-producing organisms present in the different environmental facies (Kaczmarek et al., 2010), most notably the seagrass environmental facies (Table 2.1, Fig. 2.9). Further sources of error are well established including sampling frequency where the resolution of the transect data is greater than the resolution of the Landsat sensor and local conditions of cloud cover and wave activity which alter the colour and brightness of the satellite image (Harris and Kowalik, 1994; Kaczmarek et al., 2010).

Primary depositional facies are a main controlling factor in the heterogeneity of deposits across a carbonate system. Accurately mapping and constraining primary facies variability is key to understanding resultant sedimentological variability for a system. There are few studies that attempt to characterise the facies and deposit characteristics of modern shallow water carbonate systems, utilising remote sensing data. In one key study, environmental facies are defined and accurately mapped for 19 modern isolated carbonate platforms (Harris and Vlaswinkel, 2008). In this study the colour, texture, shape and relative context of reef features were used to identify, map and hand-digitise nine distinct facies groupings from Landsat images. The resultant facies maps accurately outline the extent of reef environments from a fully aggraded reef crest through to the platform interior. Whilst this subjective method of hand-digitising features provides valuable data on facies metrics and distributions, no links are made between primary environmental facies and primary sedimentological characteristics. Furthermore the use of subjective, hand-digitised facies groupings

may contribute to a limited understanding of facies variability and heterogeneity across smaller scales. Conversely several studies have demonstrated the use of quantitative approaches in producing satellite-based maps of benthic sediments and reef biota (Purkis and Pasterkamp, 2004; Ouillon et al., 2004; Riegl et al., 2007; Kaczmarek et al., 2010). Whilst the approaches of such studies are effective in determining the distribution of benthic biota types or broad sediment observations (i.e. grainstone to mudstone identification) with high accuracies (e.g. >85%; Kaczmarek et al., 2010), such studies do not demonstrate the variability of sediment characteristics in relation to the primary environment of deposition. The Kaledupa-Hoga model presented here demonstrates that primary environmental facies are, for the most part, detectable at the moderate resolution (28.5 m) of the Landsat sensor, and that these environments have some consistent primary sedimentological, and early alteration characteristics (Figs., 2.10, 2.11).

Sub-tropical to tropical isolated carbonate systems are well known from areas such as Central America, the Indian Ocean and south Pacific, with their sedimentology and satellite characterisation well documented (Gischler and Lomando, 1999; Rankey, 2002; Gischler et al., 2003; Gischler, 2006, 2011; Rankey and Harris, 2008; Harris, 2010; Harris et al., 2010; Rankey and Reeder, 2010, Harris et al., 2011). Detailed combined Landsat imagery and sediment studies are lacking from other fringing reef systems globally. The sedimentology of four modern equatorial isolated carbonate platforms from Belize-Yucatan, (Central America) studied utilising Landsat imagery, provides some analogues for comparison with the isolated carbonate system of Kaledupa-Hoga. The composition and texture of surface sediment samples from the modern sedimentary facies of the four isolated carbonate platforms from Belize-Yucatan, define four major sediment types across nine depositional environments (Gischler and Lomando, 1999). A comparison of Landsat images with sediment distribution maps shows that correlations between satellite image characteristics (depositional environments) and sediment composition and/or texture is mostly very good for isolated carbonate systems in Belize-Yucatan (Gischler and Lomando, 1999). I.e. as with Kaledupa-Hoga there is some degree of sediment homogenisation across different field- and satellite-identifiable environmental facies. However, many of the depositional environments that are identified in the Belize-Yucatan systems are not present in the Kaledupa-Hoga

system, nor are the broad sediment types; grainstone, packstone, grain-rich wackestone and mud-rich wackestone of Gischler and Lomando (1999). Instead the sediment types of Kaledupa-Hoga are dominantly homogenous, represented mainly by grainstones to grain-rudstones. Another difference between the Belize-Yucatan platforms, not seen in Kaledupa-Hoga, are the presence of high energy windward versus low energy leeward settings, clearly identifiable through both satellite and sediment characterisation. Near continuous surface breaking reef rims on windward side, characterised by an encrusted and cemented coral rubble build up with a low (<5%) fine sediment (<125 μm) content. The high energy reef rims are absent on the leeward sides of these reef systems where unconsolidated, discontinuous and surface-breaking loose coral-rubble rims are present (Gischler and Lomando, 1999). Back reef lagoonal settings protected by the emergent reef rim in Belize contain high concentrations of shell material, *Halimeda*, and imperforate miliolid foraminifera with fine sediment (<125 μm) fractions as high as >23% (Gischler and Lomando, 1999). However, despite evidence of protected back reef settings redistribution of grains derived from windward margins towards back reef areas produces wide sand aprons that fill into the interior lagoons, and there is corresponding transport towards and across the leeside of the platforms (Gischler and Lomando, 1999). On the easterly side of Kaledupa is a broad coral reef flat partially draped by sediment (Class 7; Fig. 2.9). It is likely that this "apron" has developed due to sediment accumulation and reef progradation in response to the predominant prevailing monsoonal wind direction (cf. Harris and Vlaswinkel, 2008)

2.6 Conclusions

The environments, sediments and satellite image characteristics of fringing reefs surrounding oceanic islands in the Tukang Besi Archipelago of Central Indonesia are detailed for the first time. Ten ground-truthed modern environmental facies were recognised across the fringing reef system, and although these have some distinctive primary depositional characteristics there is a degree of sediment homogenisation across facies. Foreshore/backshore deposits are characterised by moderately sorted, coarse to very coarse sands with a low silt and gravel content and high degrees of abrasion and fragmentation (grainstones). Seagrass-associated facies are typically poorly sorted, fine to very coarse sands with up to 9% silt and some gravel content

together with moderate degrees of fragmentation and abrasion (grain-packstones). Reef flat coral facies are moderately sorted medium to very coarse sands with low silt and typically high gravel contents (grainstones to grain-rudstones). Bioclasts within the coral facies are generally highly fragmented and show some abrasion. Distinctive moderately to poorly sorted coarse sands and abundant gravels with low silt contents are present in fore reef settings (grain-rudstones). The identification of different environmental facies has allowed a Landsat derived facies map to be generated with overall good accuracy. The paucity of fines across the fringing reef systems as a whole and the degree of homogenisation of sediment characteristics across the different field- and satellite-identifiable environmental facies are attributed to: (1) high wave/current energies, (2) the small size of the islands rendering limited protection, (3) bidirectional monsoon winds and (4) the lack of reef rimmed margins built to sea level. This study probably only hints at some of the variability within SE Asia's vast, and virtually unstudied fringing reef systems (>7500 km^2 of Indonesia's coast is fringed by reefs: Tomascik et al., 1997). However, it highlights apparent significant differences between some equatorial fringing reefs and those from the subtropics. The systems studied here reveal the importance of seagrass bed development, the influence of the monsoons and a degree of sediment homogenisation, lack of windward-leeward effects, and a lack of hurricane influence on these equatorial SE Asian fringing reefs. In addition to fostering a time and cost effective method to map system-scale facies distributions, the facies map presented here may have further applications for understanding modern carbonate system heterogeneity and controlling influences. Additional applications are likely for monitoring and assessment of modern coral reef related habitats and ecosystems, and for potential hydrocarbon reservoir analogue modelling.

2.7 Acknowledgements

This research forms a part of Rob Madden's PhD studies, supervised by Moyra Wilson, at Curtin University. Field sampling was undertaken by Moyra through the research and conservation organisation of Operation Wallacea, and the staff, research associates and volunteers of that organisation together with the people of Wakatobi and LIPI, the Indonesian Science Institute are thanked. In particular, Tim Coles, Nigel Deeks, Gareth Fenney, Pippa Mansell, Dave Smith, Richard Unsworth, and

Paul Whipp facilitated, or were involved in, the field sampling of this dataset. Operation Wallacea provided funding for fieldwork and the SE Asia Research Group (Royal Holloway University of London) together with a Sherman A. Wengard Memorial Grant awarded by the AAPG Grants-in-Aid Foundation funded laboratory analysis. Maeve O'Shea undertook the detailed analysis of samples from the Pak Kasim's transect, including component point counting and laser granulometry, as part of her Masters study, again supervised by Moyra whilst based at Durham University, UK. Laser granulometry of samples was run at Durham University with the assistance of Frank Davies and Amanda Hayton with a few additional samples run by Gay Walton and Nancy Hanna at CSIRO, Perth. Most thin sections were made by Neil Holloway at Royal Holloway, University of London. Jim Duggan from Australian Petrographics is gratefully acknowledged for making some further thin sections. Alex Stevens (Curtin) is kindly thanked for her assistance with ER Mapper troubleshooting. The constructive reviews of Eberhard Gischler and Paul (Mitch) Harris and journal editor John T. Wells are gratefully acknowledged.

2.8 References

Ahmad, W., and Neil, D.T., 1994. An evaluation of Landsat Thematic Mapper (TM) digital data for discriminating coral reef zonation: Heron Reef (GBR). International Journal of Remote Sensing 15, 2583-2597.

Almasi, M.N., Hoskin, C.M., Reed, J.K., and Milo, J., 1987. Effects of natural and artificial *Thalassia* on rates of sedimentation. Journal of Sedimentary Petrology 57, 901-906.

Andréfouët, S., Muller-Karger, F.E., Hochberg, E.J., Hu, C., and Carder, K.L., 2001. Change detection in shallow coral reef environments using Landsat 7 ETM+ data. Remote Sensing of Environment 78, 150-162.

Andréfouët, S., Kramer, P., Torres-Pulliza, D., Joyce, K.E., Hochberg, E.J., Garza-Pérez, R., Mumby, P.J., Riegl, B., Yamano, H., White, W.H., Zubia, M., Brock, J.C., Phinn, S.R., Naseer, A., Hatcher, B.G., and Muller-Karger, F.E., 2003. Multi-site evaluation of IKONOS data for classification of tropical coral reef environments. Remote Sensing of Environment 88, 128-143.

Asriningrum, W. 2011. Reef morphology identification in Sikka, NTT using Landsat imagery. Journal of Indonesian Coral Reefs 1, 48-54.

Beavington-Penney, S.J., 2004. Analysis of the effects of abrasion on the test of *Palaeonummulites venosus*: implications for the origin of nummulithoclastic sediments. PALAIOS 19 143–155.

Beavington-Penney, S.J. and Racey, A., 2004. Ecology of extant nummulitids and other larger benthic foraminifera: applications in palaeoenvironmental analysis. Earth Science Reviews 67, 219-265.

Becking, L.E., Cleary, D.F.R., de Voogd, N.J., Renema, W., de Beer, M., van Soest, R.W.M., and Hoeksema, B.W., 2006. Beta diversity of tropical marine benthic assemblages in the Spermonde Archipelago, Indonesia. Marine Ecology 27, 76-88.

Bell, J.J., and Smith, D.J., 2004. Ecology of sponge assemblages (Porifera) in the Wakatobi region, south-east Sulawesi, Indonesia: richness and abundance. Journal of the Marine Biological Association of the United Kingdom 84, 581-591.

Bell, J.J., Berman, J., Powell, A., and Hepburn, L.J., 2010. The ecology of sponges in the Wakatobi National Park. In: Clifton, J., Unsworth, R.K.F. and Smith, D.J. (Eds.) Marine research and conservation in the Coral Triangle The Wakatobi National Park. Nova Science Publishers, New York, 85-109.

Braithwaite, C.J.R., Montaggioni, L.F., Camoin, G.F., Dalmasso, H., Dullo,W.C., and Mangini, A., 2000. Origins and development of Holocene coral reefs: a revisited model based on reef boreholes in the Seychelles, Indian Ocean. International Journal of Earth Sciences 89, 431–445.

Blanchon, P., and Jones, B., 1997. Hurricane control on shelf-edge-reef architecture around Grand Cayman. Sedimentology 44, 479-506.

Blanchon, P., Jones, B., and Kalbfleisch, W. 1997. Anatomy of a fringing reef around Grand Cayman: storm rubble not coral framework. Journal of Sedimentary Research 67, 1-16.

Brasier, M.D., 1975. An outline history of seagrass communities. Palaeontology 18, 681-702.

Budd, D.A., and Perkins, R.D., 1980. Bathymetric zonation and paleoecological significance of microborings in Puerto Rican shelf and slope sediments. Journal of Sedimentary Petrology 50, 881-904.

Cabioch, G., Montaggioni, L.F., and Faure, G., 1995. Holocene initiation and development of New Caledonian fringing reefs, SW Pacific. Coral Reefs 14, 131– 140.

Cleary, D.F.R., Becking, L.E., de Voogd, N.J., Renema, W., de Beer, M., van Soest, R.W.M., and Hoeksema, B.W., 2005. Variation in the diversity and composition of benthic taxa as a function of distance offshore, depth and exposure in the Spermonde Archipelago, Indonesia. Estuarine Coastal and Shelf Science 65, 557-570.

Cordier, E., Poizot, E., and Méar, Y., 2012. Swell impact on reef sedimentary processes: a case study of the La Reunion fringing reef. Sedimentology 59, 2004-2023.

Crabbe, M.J.C., and Smith D.J. 2002. Comparison of two reef sites in the Wakatobi Marine National Park (SE Sulawesi, Indonesia) using digital image analysis. Coral Reefs 21, 242-244.

Dickson, J.A.D., 1965. A modified staining technique for carbonates in thin section. Nature 205, 587.

Dickson, J.A.D., 1966. Carbonate identification and genesis as revealed by staining. Journal of Sedimentary Petrology 36, 491-505.

Dunham, R.J., 1962. Classification of carbonate rocks according to depositional texture. In*:* Ham, W.E. (Ed.), Classification of carbonate rocks. American Association of Petroleum Geologists, Memoir 1, 108-121.

Embry, A.F. and Klovan, J.E. 1971. A late Devonian reef tract on northeastern Banks Island, Northwest Territories. Canadian Petroleum Geologist, Bulletin 19, 730-781.

Escher, M.G., 1920. Atollen in den Nederlandsch-Oost-Indischen Archipel: de riffen in de groep der Toekang Besi-Eilanden. Med Encyclopedisch Bureau, Weltevreden XXII, 17 p.

Gabrié, C., and Montaggioni, L.F., 1982. Sediments from fringing reefs of Réunion Island, Indian Ocean. Sedimentary Geology 31, 281– 301

Ginsburg, R.N., 1957. Early diagenesis and lithication of shallow-water carbonate sediments in South Florida. Regional Aspects of Carbonate Deposition 5, 80-100.

Ginsburg, R.N., and Lowenstam, H.A., 1958. The influence of marine bottom communities on the depositional environments of sediments. Geological

Journal 66, 310-318.

Gischler, E., 2006. Sedimentation on Rasdhoo and Ari Atolls, Maldives, Indian Ocean. Facies 52, 341-360.

Gischler, E., 2011. Sedimentary facies of Bora Bora, Darwin's type barrier reef (Society Islands, South Pacific): The unexpected occurrence of non-skeletal grains. Journal of Sedimentary Research 81, 1-17.

Gischler, E. and Lomando, A.J., 1999. Recent sedimentary facies of isolated carbonate platforms, Belize-Yucatan system, Central America. Journal of Sedimentary Research 69, 747-763.

Gischler, E., Hausa, I., Heinrich, K., Scheitel, U., 2003. Characterization of depositional environments in isolated carbonate platforms based on benthic foraminifera, Belize, Central America. PALAIOS 18, 236-255.

Green, E.P., Mumby, P.J., and Edwards, A.J., 2000. Remote Sensing Handbook for Tropical Coastal Management Sourcebooks 3. UNESCO, Paris, 316 p and plates.

Grötsch, J., and Mercadier, C., 1999. Intergrated 3-D Reservoir Modeling Based on 3-D Seismic: The Tertiary Malampaya and Camago Buildups, Offshore Palawan, Philippines: The American Association of Petroleum Geologists Bulletin, 83, 1703-1728.

Halford, A. 2003. Fish diversity and distribution. In: Pet-Soede, L., and Erdmann, M.V. (Eds.). Rapid ecological assessment Wakatobi National Park. WWF/TNC Joint Publication, Denpasar, Bali, 53-64.

Hallock, P. and Glenn, E.C., 1986. Larger foraminifera: a tool for paleoenvironmental analysis of Cenozoic carbonate depositional facies. PALAIOS 1, 55-64.

Hammer,Ø., Harper, D.A.T., and Ryan, P.D., 2001. PAST: Paleontological statistics software package for education and data analysis. Palaeontologia Electronica 4, 9 p.

Harris, P.M., 1996. Reef styles of modern carbonate platforms: Bulletin of Canadian Petroleum Geology 44, 72-81.

Harris, P.M. 2010. Delineating and quantifying depositional facies patterns in carbonate reservoirs: Insight from modern analogs. American Association of Petroleum Geologists Bulletin 94, 61-86.

Harris, P. M., and Kowalik, W. S., (Eds.) 1994. Satellite images of carbonate depositional settings: Examples of reservoir- and exploration-scale geologic facies variation. AAPG Methods in Exploration Series No. 11, 147 p.

Harris, P.M., and Vlaswinkel, B., 2008. Modern isolated carbonate platforms: Templates for quantifying facies attributes of hydrocarbon reservoirs. In: J. Lukasik and T. Simo, (Eds.) Controls on carbonate platform and reef development: SEPM Special Publication 89, p. 323–341.

Harris, P.M., Ellis, J., and Purkis, S., 2010. Delineating and quantifying depositional facies patterns in modern carbonate sand deposits on Great Bahama Bank; SEPM Short Course Notes No. 54, p, paper p. 1-51, appendix p. 1-31, and 2 DVDs.

Harris, P.M., Purkis, S.J., and Ellis, J., 2011. Analyzing spatial patterns in modern carbonate bodies from Great Bahama Bank: Journal of Sedimentary Research 81, 185-206.

Hetzel, W.H., 1930. Over de Geologie Der Toekang-Besi Eilanden. De Mijningenieur, 11, 51-53.

Hewins, H.R. and Perry, C.T. 2006. Bathymetric and Environmentally influenced patterns of carbonate sediment accummulation in three contrasting reef settings, Danjugan Island, Philippines. Journal of Coastal Research 22, 812-824.

Hopley, D. and Partain, B. 1987. The structure and development of fringing reefs off the Great Barrier Reef Province. In : Baldwin, C.L. (ed.). Fringing Reef Workshop. Great Barrier Reef Marine Park Authority, Townsville. Science, Industry and Management Workshop Series 9, 32 p.

Insalaco, E., 1998, The descriptive nomenclature and classification of growth fabrics in fossil scleractinian reefs. Sedimentary Geology 118, 159-186.

Jordan, C.J., 1998. The sedimentation of Kepuluan Seribu: A modern patch reef complex in the West Java Sea, Indonesia. Indonesian Petroleum Association Field Guide, Jakarta, Indonesia, 81 p.

Joyce, K.E., and Phinn, S.R., 2001. Optimal spatial resolution for coral reef mapping. Proceedings of the International Geoscience and Remote Sensing Symposium volume 2, 619-621.

Kaczmarek, S.E., Hicks, M.K., Fullmer, S.M., Steffen, K.L., and Bachtel, S.L., 2010. Mapping facies distributions on modern carbonate platforms through

integration of multispectral Landsat data, statistics-based unsupervised classifications, and surface sediment data. American Association of Petroleum Geologists Bulletin 94, 1581-1606.

Kennedy, D.M. and Woodroffe, C.D. 2002. Fringing reef growth and morphology: a review. Earth-Science Reviews 57, 255-277.

Koswara, A. and Sukarna, D., 1994. Geology of the Tukang Besi Sheet, Sulawesi. Geological Research and Development Centre, Bandung, Indonesia, 14 p and map.

Kuenen, Ph.H. 1933a. The Geology of Coral reefs. The Snellius Expedition in the eastern part of the Netherlands East Indies 1929-1930. Geological Results. Proc. Kon. Akad. V. Wetensch., Amsterdam 36, 125 p.

Kuenen, Ph.H. 1933b. The formation of the atolls in the Toekang-Besi-group by subsidence. Proc. Kon. Akad. V. Wetensch., Amsterdam 36, 331-336.

Lees, A. and Buller, A.T., 1972. Modern temperate-water and warm-water shelf carbonate sediments contrasted. Marine Geology 13, 67-73.

Lewis, M.S., 1969. Sedimentary environments and unconsolidated carbonate sediments of the fringing coral reefs of Mahé, Seychelles. Marine Geology 7, 95-127.

Lyzenga, D.R., 1981. Remote sensing of bottom reflectance and water attenuation parameters in shallow water using aircraft and Landsat data. International Journal of Remote Sensing 2, 71-82.

Madden, R.H.C., and Wilson, M.E.J., 2013. Diagenesis of a SE Asian Cenozoic carbonate-platform margin and its adjacent basinal deposits. Sedimentary Geology 286-287, 20-38.

McMellor, S. and Smith, D.J. 2010. Coral reefs of the Wakatobi: abundance and biodiversity. In: Clifton, J., Unsworth, R.K.F. and Smith, D.J. (Eds.) Marine research and conservation in the Coral Triangle The Wakatobi National Park. Nova Science Publishers, New York, 11-26.

Milsom, J., Ali, J., and Sudarwono, 1999. Structure and collision history of the Buton continental fragment, Eastern Indonesia. American Association of Petroleum Geologists Bulletin 83, 1666-1689.

Montaggioni, L.F. 2005. History of Indo-Pacific coral reef systems since the last glaciation: Development patterns and controlling factors. Earth Science Reviews 71, 1-75.

Mumby, P.J., Green, E.P., Clark, C.D., and Edwards, A.J., 1998. Digital analysis of multispectral airborne imagery of coral reefs. Coral Reefs 17, 59-69.

O'Shea, M. 2005. Evaluating shallow water variability in equatorial carbonates. Are deposit characteristics distinctive of local environments and water depths? Unpublished Masters Thesis, Durham University, UK, 149 p and Appendices.

Ouillon, S., Douillet, P. and Andréfouët, S. 2004. Coupling satellite data with in situ measurements and numerical modeling to study fine suspended-sediment transport: a study for the lagoon of New Caledonia. Coral Reefs 23, 109-122.

Park, R.K., Siemers, C.T., and Brown, A.A., 1992. Holocene Carbonate Sedimentation, Pulau Seribu, Java Sea, - The Third Dimension. In: Siemers, C.T., Longman, M.W., Park, R.K. and Kaldi, J.G. (Eds.). Carbonate Rocks and Reservoirs of Indonesia, a Core Workshop. Indonesian Petroleum Association, Jakarta, Indonesia, 2-1 - 2-15.

Park, R.K., Crevello, P.D., and Hantoro, W., 2010. Equatorial carbonate depositional systems of Indonesia. In: Morgan, W.A., George, A.D, Harris, P.M., Kupecz, J.A. and Sarg, J.F. (Eds.). Cenozoic Carbonate Systems of Australasia. SEPM Special Publication 95, 41-77.

Perry, C.T., and Bertling, M., 2000. Spatial temporal patterns of macroboring within Mesozoic and Cenozoic coral reef systems. In: Insalaco, E., Skeleton, P.W., and Palmer, T.J., (Eds.). Carbonate Platform Systems: Components and Interactions. Geological Society of London Special Publication 178, 33-50.

Perry, C.T., and Hepburn, L.J., 2008. Syn-depositional alteration of coral reef framework through bioerosion, encrustation and cementation: Taphonomic signatures of reef accretion and reef depositional events. Earth-Science Reviews 86, 106-144.

Pet-Soede, L., and Erdmann, M.V. (Eds.). 2003. Rapid ecological assessment Wakatobi National Park. WWF/TNC Joint Publication, Denpasar, Bali, 187 pp.

Pettijohn, F.J., Potter, P.E., and Siever, R. 1973. Sand and sandstone. Springer, Berlin, 618 p.

Purkis, S.J., and Pasterkamp, R., 2004. Integrating in situ reef-top reflectance spectra with Landsat TM imagery to aid shallow-tropical benthic habitat mapping. Coral Reefs 23, 5-20.

Purkis, S.J., Riegl, B.M., and Andréfouët, S., 2005. Remote sensing of geomorphology and facies on a modern carbonate ramp (Arabian Gulf, Dubai, U.A.E.). Journal of Sedimentary Research 75, 861-876.

Purkis, S.J., Harris, P.M., and Ellis, J., 2012. Patterns of sedimentation in the contemporary Red Sea as an analog for ancient carbonates in rift settings. Journal of Sedimentary Research 82, 859-870.

Rankey, E.C., 2002. Spatial patterns of sediment accumulation on a Holocene carbonate tidal flat, northwest Andros Island, Bahamas. Journal of Sedimentary Research 72, 591-601.

Rankey, E.C., and Harris, P.M., 2008. Remote sensing and comparative geomorphology of Holocene carbonate depositional systems. In Lukasik, J. and Simo, T. (Eds.). Controls on carbonate platform and reef development, SEPM Special Publication No. 89, 317-322 and CD.

Rankey, E. C. and Reeder, S. L., 2010. Controls on platform-scale patterns of surface sediments, shallow Holocene platforms, Bahamas. Sedimentology 57, 1545–1565.

Riegl, B.M., Halfar, J., Purkis, S.J., and Godinez-Ort, L., 2007. Sedimentary facies of the Eastern Pacific's northernmost reef-like setting (Cabo Pulmo, Mexico). Marine Geology 236, 61-77.

Renema, W., 2006a. Habitat variables determining the occurrence of large benthic foraminifera in the Berau area (East Kalimantan, Indonesia). Coral Reefs 25, 351-359.

Renema, W., 2006b. Large benthic foraminifera from the deep photic zone of a mixed siliciclastic-carbonate shelf off East Kalimantan, Indonesia. Marine Micropaleontology 58, 73-82.

Renema W, and Hohenegger J., 2005. On the identity of *Calcarina spengleri* (Gmelin, 1791). Journal of Foraminiferal Research 35:15–21.

Salinas de León, P., Unsworth, R.K.F. and Bell, J.J. 2010. Marine habitat connectivity in the Wakatobi National Park. In: Clifton, J., Unsworth, R.K.F. and Smith, D.J. (Eds.) Marine research and conservation in the Coral Triangle The Wakatobi National Park. Nova Science Publishers, New York, 129-148.

Scoffin, T.P., 1970. The trapping and binding of subtidal carbonate sediments by marine vegetation in Bimini lagoon, Bahamas. Journal of Sedimentary Petrology 40, 249-273.

Scrutton, M.E., 1976. Aspects of Carbonate Sedimentation in Indonesia. Fifth Annual Convention of the Indonesian Petroleum Association 1, 179-194.

Scrutton, M.E., 1978. Modern Reefs in the West Java Sea, Proceedings of the Indonesian Petroleum Association Carbonate Seminar (Special Volume), Jakarta, Indonesia, 14-41.

Smith, R.B., and Silver, E.A., 1991. Geology of a Miocene collision complex, Buton, eastern Indonesia. Geological Society of America Bulletin 103, 660-678.

Swinchatt, J.P., 1965. Significance of constituent composition, texture, and skeletal breakdown in some recent carbonate sediments. Journal of Sedimentary Petrology, 35, 71-90.

Suharsono, Giyanto, Budiyanto, A., and Dehwani, N., 2006. Status and Monitoring of Coral Reefs in Kaledupa Islands, South East Sulawesi, Indonesia. Proceedings of the tenth International Coral Reef Symposium, Japanese Coral Reef Society, Okinawa, 1033-1038.

Tomascik, T., Mah, A.J., Nontji, A., and Moosa, M.K., 1997. The Ecology of the Indonesian Seas. Oxford University Press, 1388 p.

Turak, E., 2003. Coral reef surveys during TNC SEACMPA RAP of Wakatobi National Park, Southeast Sulawesi. Final Report to the Nature Conservancy, Bali. In: Pet-Soede, L., and Erdmann, M.V. (Eds.). Rapid ecological assessment Wakatobi National Park. WWF/TNC Joint Publication, Denpasar, Bali, 33-52.

Udden, J.A. 1914. Mechanical composition of clastic sediments. Geological Society of America Bulletin 25, 655-744.

Umbgrove, J. H. F., 1947. Coral reefs of the East Indies. Bulletin of the Geographic Society of America 58, 729-778.

Unsworth, R.K.F. 2010. Seagrass meadows of the Wakatobi National Park. In: Clifton, J., Unsworth, R.K.F. and Smith, D.J. (Eds.) Marine research and conservation in the Coral Triangle The Wakatobi National Park. Nova Science Publishers, New York, 45-65.

van Bemmelen, R.W., 1949. The Geology of Indonesia. Vol. 1a. Government Printing Office, The Hague, 2nd Edition, 732 p.

Wentworth, C.K., 1922. A scale of grade and class terms for clastic sediments. Journal of Geology 30, 377-394.

White, T.L. 1987. Coral reefs: valuable resources of SE Asia. Volume 1 of ICLARM education series, Issue 1 of Education Series. Issue 386 of ICLARM contribution. International Center for Living Aquatic Resources Management on behalf of the Association of Southeast Asian Nations/United States Coastal Resources Management Project, 1987, 36 p.

Wilson, M.E.J., 2002. Cenozoic carbonates in SE Asia: Implications for equatorial carbonate development. Sedimentary Geology 147, 295-428.

Wilson, M.E.J., 2008a. Global and regional influences on equatorial shallow marine carbonates during the Cenozoic. Palaeogeography, Palaeoclimatology, Palaeoecology, 265, 262-274.

Wilson, M.E.J., 2008b. Reservoir quality of Cenozoic carbonate buildups and coral reef terraces. Proceedings of the 32nd Indonesian Petroleum Association Annual Convention and Exhibition, 8 p.

Wilson, M.E.J., 2011. SE Asian carbonates: tools for evaluating environmental and climatic change in the equatorial tropics over the last 50 million years. In: Hall, R., Cottam, M.A. and Wilson, M.E.J. (Eds.). The SE Asian gateway: history and tectonics of the Australia-Asia collision. Geological Society of London, Spe6cial Publication 355, 347-369.

Wilson, M.E.J., 2012. Equatorial carbonates: an earth systems approach. Sedimentology 59, 1-31.

Wilson, M.E.J., and Evans, M., 2002. Sedimentology and diagenesis of Tertiary carbonates on the Mangkalihat Peninsula, Borneo: implications for subsurface reservoir quality. Marine and Petroleum Geology 19, 873-900.

Wilson, M.E.J, Al Aghbari, A.A.S., Deeks, N.R., Kananan, P., Madden, R.H.C., and Zafir, A. 2013. Modern reef-associated sediments and environments from SE Asia. 30th International Association of Sedimentologists, (Abstract) Manchester, UK.

Chapter 3

DIAGENESIS OF NEOGENE DELTA-FRONT PATCH REEFS: ALTERATION OF COASTAL, SILICICLASTIC-INFLUENCED CARBONATES FROM HUMID EQUATORIAL REGIONS

Robert H.C. Madden and Moyra E.J. Wilson

Department of Applied Geology, Curtin University, GPO Box U1987, Perth, Western Australia 6845, Australia
E-mails: r.madden@postgrad.curtin.edu.au, m.wilson@curtin.edu.au

Abstract

This study offers insights into the diagenetic alteration of coastal carbonates that formed coevally with nearly continuous siliciclastic influx in a humid equatorial setting. A multi-disciplinary petrographic, cathodoluminescent, stable-isotope, trace-element and major-element investigation allowed characterization of diagenetic features, paragenetic sequencing, and an interpretation of diagenetic environments from Neogene patch reefs of the Samarinda region, Mahakam Delta, Borneo, SE Asia. Marine cements are absent from the patch reefs, with grain micritization the only marine diagenetic feature recognized. The predominant diagenetic feature within the patch reefs is pervasive neomorphic stabilization and cementation of aragonite reef components to calcite that pre-dates all compaction features. Meteoric aquifer flow derived from the adjacent landmass is inferred as the main parent diagenetic fluid, since $\delta^{18}O$ V-PDB values of calcite cements of -3.6 to -11.7‰ are consistent with precipitation from SE Asian freshwater, and inconsistent with a wholly marine origin. Late-stage fracturing, cementation, and chemical compaction are relatively minor features and attest to a changing paleohydrologic and diagenetic environment. Evidence for a shallow to moderate burial diagenetic regime for these later features are maximum temperature of 53 °C and burial depths < 1000 m inferred from stable-isotope

values of calcite and late dolomite cements, dolomite crystal fabrics, the onset depth of stylolite or dissolution-seam formation, and regional geothermal gradients. The humid tropical environment and "ever-wet" conditions on the island of Borneo together with rapid Cenozoic uplift likely led to paleoaquifer flow with fluids focused through adjacent deltaic units into the reef carbonates. In these coastal carbonates from the humid Samarinda region, continental groundwater flow has resulted in pervasive stabilization and calcitization, features rare in arid or temperate counterparts

3.1 Introduction

Carbonate–siliciclastic mixing is common in both modern and ancient environments (Mount 1984; Larcombe and Woolfe 1999; Woolfe and Larcombe 1999; Wilson and Lokier 2002; Wilson 2005). In spite of their common occurrence, the diagenesis of siliciclastic-influenced coral reefs and carbonate platforms from equatorial to subtropical settings remains largely unstudied (Hendry et al. 1999; Wilson 2012). The hypotheses tested here are that: (1) the diagenesis of continental margin reef deposits in a region of siliciclastic input will be influenced strongly by basin-margin paleohydrology, and (2) the alteration of coastal carbonates from other climatic regions (cf. Dodd and Nelson 1998; Hendry et al. 1999; Ricketts et al. 2004; Caron and Nelson 2009) may not be directly analogous to that of comparable deposits in the equatorial tropics.

To test these hypotheses, this study evaluates the diagenesis of Miocene delta-front reefs from Borneo, with three aims: (1) to characterize the extent of diagenesis in these mixed carbonate–siliciclastic patch reefs from a coastal setting, (2) to develop a paragenetic sequence of the succession in the context of the evolving basin hydrology and the climatic setting, and (3) to compare general aspects of diagenesis of these humid equatorial carbonates with that of other coastal carbonates from humid-nontropical and arid settings. Here, "coastal carbonate" refers to nearshore marine carbonate development along predominantly siliciclastic coastlines, such as in delta-front, fan-delta, or siliciclastic inner-shelf settings. The results of this study provide insights into patterns of diagenesis in coastal carbonate systems that may

have broad analogs elsewhere (Hendry et al. 1999; Nelson et al. 2003; Wilson and Hall 2010; Wilson 2012).

Neogene carbonates have developed extensively in the tropical marine waters surrounding Borneo, despite abundant sediment runoff from Borneo, the largest island in Indonesia (Fig. 3.1; Wilson et al. 1999; Hall 2002a). Modern and Neogene carbonates exist coevally with major siliciclastic influx from the Mahakam Delta on the eastern side of Borneo (Fig. 1; Roberts and Sydow 1996; Wilson and Lokier 2002; Hook and Wilson 2003; Wilson 2005). Outcrops, with up to 90% exposure, of Miocene patch reefs interbedded with Mahakam Delta deposits crop out onshore East Borneo (Fig. 3.2; Alam et al. 1999; Wilson 2005). The sedimentology and biostratigraphy of these units is well documented, as is the siliciclastic influence on carbonate production, reef growth, and sequence development (BouDagher-Fadel and Wilson 2000; Wilson and Lokier 2002; Wilson 2005; Lokier et al. 2009). The present study extends these results, focusing on the diagenesis of these deposits, by combining outcrop data with petrography, cathodoluminescence, and geochemistry.

3.2 Geological Setting

Tectonic plate convergence and weathering under humid equatorial climatic conditions in Southeast Asia have resulted in high rates of uplift and erosion of the Borneo landmass (Hall 1996; Hall and Nichols 2002). Since at least the Neogene, large volumes of siliciclastic sediments derived from Borneo have been deposited into the deep oceanic basins to the north and east of the island, with associated rapid delta progradation (Fig. 3.1; Hamilton 1979; Wilson and Moss 1999; Hall and Nichols 2002). The Mahakam Delta has been contributing to the Cenozoic sedimentation of the Kutai Basin, in Eastern Borneo, since at least the Early Miocene (van de Weerd and Armin 1992; Allen and Chambers 1998; Moss and Chambers 1999). The eastern Kutai Basin has a Neogene sedimentary section of at least 9 km thickness (Hamilton 1979; Cloke et al. 1999; Hall and Nichols 2002).

The Kutai Basin is one of a series of sedimentary basins that developed around the margins of the Eurasian continental crust during the Paleogene (van de Weerd and Armin 1992; Hall 1996). The cause and exact timing of regional basin initiation is

still debated, but most authors have inferred that the Kutai Basin has rift-related

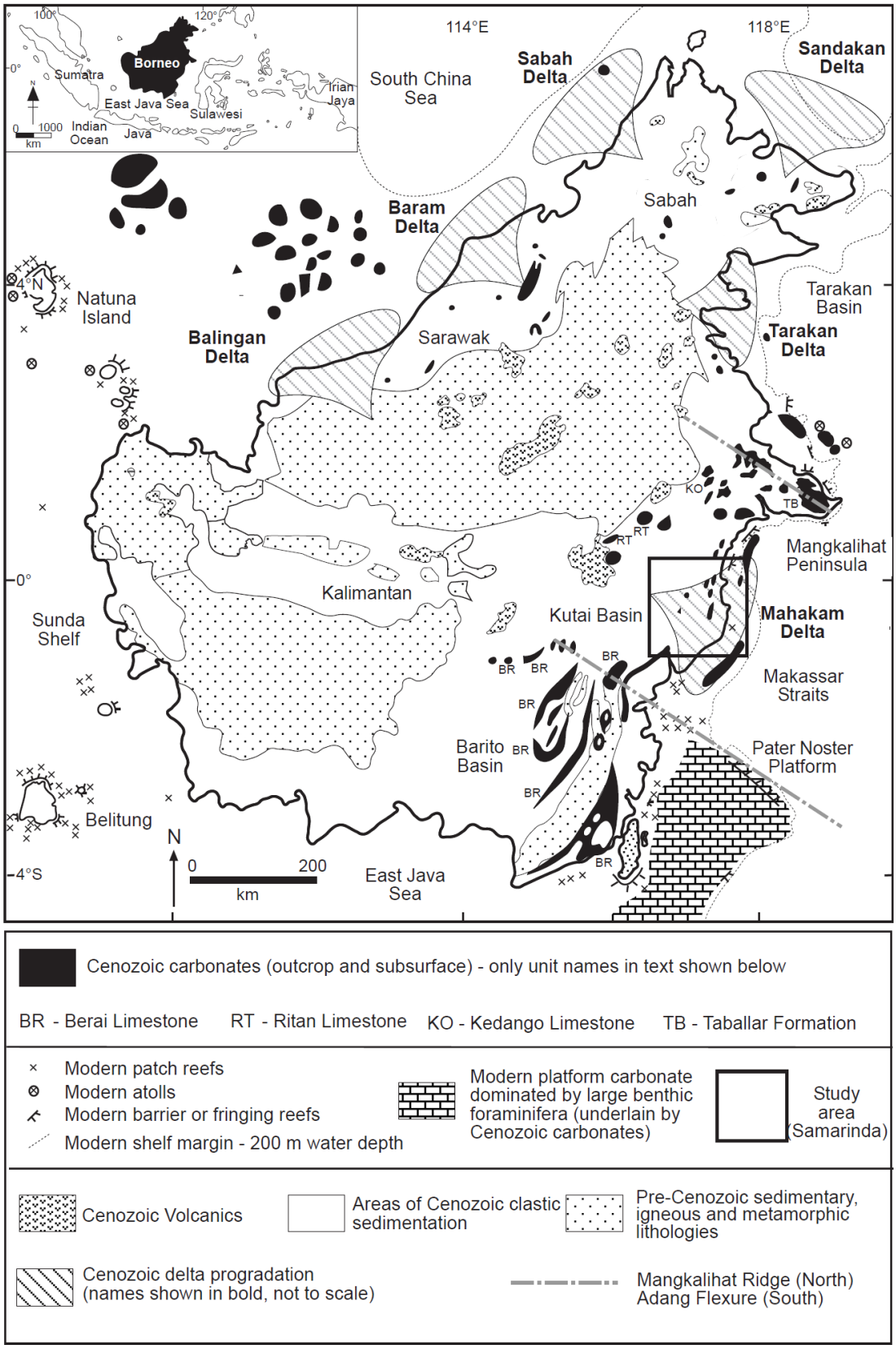

Figure 3.1. Simplified geological map of Borneo. Major outcropping and subsurface Cenozoic and modern carbonates are illustrated, as are areas of Cenozoic delta progradation (modified from Wilson et al. 1999; Wilson 2002).

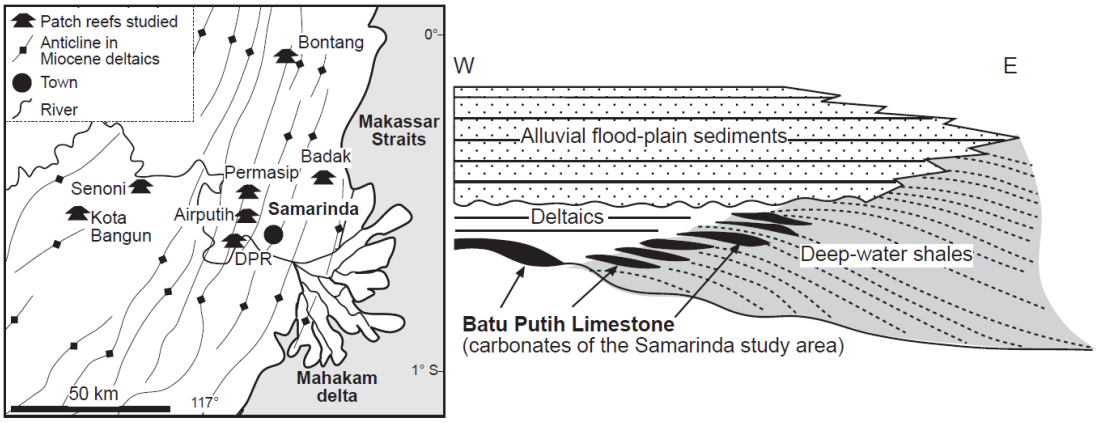

Figure 3.2. Distribution of patch reefs in the Samarinda area and schematic of the stratigraphy and facies of the patch reefs and associated deposits (from Wilson 2005; schematic is modified after Allen and Chambers 1998).

extensional or transtensional origins (van de Weerd and Armin 1992; Moss et al. 1997; Moss and Chambers 1999). Covering a region approximately 165,000 km^2, the Kutai Basin (Fig. 3.1) is the largest and deepest basin in Indonesia, separated from the Tarakan Basin in the north and the Barito Basin in the south by the WNW–ESE-trending Mangkalihat Ridge and Adang Flexure, respectively (van de Weerd and Armin 1992; Alam et al. 1999; Moss and Chambers 1999). Throughout the Cenozoic, carbonates developed on faulted highs at the northern (Fig. 3.1; e.g., the Taballar Formation) and southern (e.g., the Berai Limestone) margins of the Kutai Basin, as well as faulted highs largely isolated from siliciclastic influx within the basin (e.g., the Kedango Limestone and the Ritan Limestone; Moss and Chambers 1999; Wilson et al. 1999). Subsequent to regional subsidence, several Neogene inversion episodes affected the basin, resulting in pulses of rapid delta progradation (Allen and Chambers 1998). Despite a high siliciclastic flux into the Mahakam Delta, Neogene to modern carbonates formed as proximal delta-front patch reefs and more distal shelf accumulations (Roberts and Sydow 1996; Wilson 2005; Saller et al. 2010). These Neogene delta-front patch reefs are the subject of this study.

Based on foraminifera and nannofossils, the western delta-front patch reefs at Senoni and Kota Bangun are of Early Miocene age, older than the Early–Middle Miocene deposits cropping out to the east at Airputih, Dibelakan Parliament (DPR), Permasip, Bontang, and Badak (Fig. 3.3; BouDagher-Fadel and Wilson 2000; Wilson 2005). These Miocene reef deposits are analogous in size, location, and lithology to delta-

front proximal patch reefs, and to a lesser extent more distal shelf carbonates, from the modern and Pleistocene of the Mahakam Delta. These post-Neogene carbonates create platforms and mounds on the northern part of the shelf (Roberts and Sydow 1996). Bioherms in the inner and middle shelf are up to 40 m thick, but they are currently inactive and are covered in a meter-scale layer of clay (Roberts and Sydow 1996). The late Pleistocene-to-modern development of carbonates has been controlled by two factors: (1) the northern delta lobe has a lower rate of sediment supply than the southern lobe, and (2) the Indonesian Throughflow Current flows south at high speed. Both factors favor waters less turbid in the north than in the south (Roberts and Sydow 1996). Miocene carbonates also were concentrated towards the north, and are inferred to have developed best during transgressive phases (Wilson 2005).

3.3 Morphology and Facies of the Miocene Patch Reefs

The outcrops of Miocene patch reefs studied here are up to 2–4 km wide with a post-compactional thickness of up to 40 m (Fig. 3.3; Wilson 2005). The patch reefs overlie, interfinger with, and are overlain by siliciclastic deposits of the Mahakam Delta (Wilson 2005). Corals many in growth position, individually surrounded by a clay-rich and micritic groundmass, dominate the patch-reef deposits. Bioclastic grains including larger benthic foraminifera, coralline algae, mollusks, echinoderms, and *Halimeda* locally contribute to the deposits. None of the samples contain less than 5 weight % admixed siliciclastics, although they may be as high as 80%, suggesting siliciclastic influx contemporaneous with patch-reef development (Wilson 2005). Distinctive zoning of biota and facies within individual patch reefs suggests a dynamic interrelationship between siliciclastic input, nutrient influx, and the carbonate producers (Wilson and Lokier 2002; Wilson 2005; Lokier et al. 2009). Twelve facies were defined from outcrop and petrographic studies on the basis of their constituent components and their textural and lithological features (Wilson 2005). These facies have been grouped into three facies associations, on the basis of their sedimentary and biotic characteristics: (1) siliciclastic facies (> 95% siliciclastics), (2) mixed carbonate–siliciclastic facies (35–80% siliciclastics), and (3) carbonate facies (6–35% siliciclastics; Wilson 2005). The siliciclastic facies association is restricted to the deltaic system and is not considered in the present

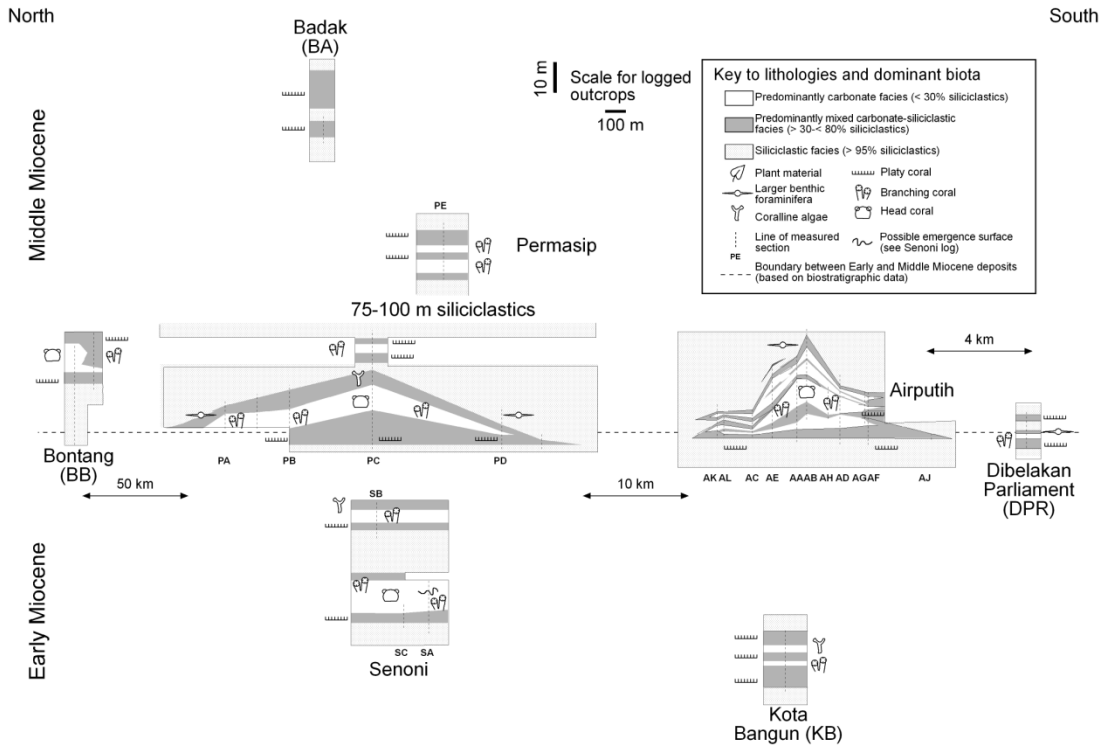

Figure 3.3. Simplified sedimentary logs of patch reefs from the Samarinda region in east Borneo showing their dimensions, ages, and characteristics. The lateral distances between patch reefs are not to scale (from Wilson 2005).

study. Within individual patch reefs a trend of decreasing siliciclastic content is associated with a change from platy to branching to massive corals towards the core of the patch reefs (Figs. 3.3, 3.4). Specifically, mixed carbonate–siliciclastic facies (including common platy coral sheetstones; nomenclature of Insalaco 1998) dominate at the base, top, and margins of the patch reefs and bordering areas where they interfinger with siliciclastics of the delta. Towards the center of the patch reef, carbonate facies change successively from branching coral pillarstones and coral rud-floatstones to head coral mix-domestones as siliciclastic content decreases. Deposits richer in disseminated carbonaceous plant remains include more abundant calcareous algae, echinoderms, and locally larger benthic foraminifera (Wilson and Lokier 2002; Wilson 2005). The change in the faunal assemblage is consistent with a dominance of calcareous algal communities over framework-building reef communities associated with nutrient loading in the modern and the Quaternary (Roberts et al. 1988; Roberts and Sydow 1996). Siliciclastics within the patch-reef deposits are predominantly clay (including kaolinite and smectite) and subsidiary fine sand (Wilson 2005).

3.4 Methods

Mixed carbonate–siliciclastic deposits are exposed in active and disused quarries and unquarried karst through seven patch-reef complexes in Eastern Borneo (Figs. 3.2, 3.3; Wilson 2005). Up to 90% exposure allowed high-resolution sampling, outcrop logging, facies mapping, and section correlation through individual patch reefs (Wilson 2005). Twenty-three sections through the seven reef complexes were logged, and of the 250 samples collected, 117 have been studied petrographically (Appendix C1).

Lithological components, microfacies, diagenetic phases, and the relative timing of diagenetic events were determined through petrographic analysis of the thin sections. Half of each thin section was stained with Alizarin Red S and potassium ferricyanide for identification of dolomites, ferroan calcite, and nonferroan calcite in thin section. The relative abundance of components and diagenetic phases were recorded semi quantitatively (visual estimates: Appendix 3), with the results closely comparable with fully quantitative point counting and acid digestion analyses previously undertaken on 52 of the samples (Wilson 2005; Lokier et al. 2009). Cold cathodoluminescent (CL) microscopy study of 26 polished thin sections utilized a Technosyn 8200 MKII luminoscope (after Witkowski et al. 2000). Samples for CL analysis, selected primarily from thin sections with a variety of coarse (> 250 μm) cements, facilitated investigation of the range of cement phases present. On the basis of the relative timing of petrographically defined diagenetic features, three groups are evident (Appendix C1): (1) pre-fracture, (2) fracture-associated, and (3) post-fracture features.

Stable-isotope analysis ($\delta^{18}O$ and $\delta^{13}C$) is based on 38 samples micro-drilled from the rock off-cut counterpart of thin sections. Drilling sites, matched directly to the off-cuts, represent a range of depositional and diagenetic features identified in thin section. Drilled samples included ferroan and nonferroan cements, and fracture (~ 1 mm) filling cements, dolomites, and bioclastic components. Twenty oxygen and carbon isotope analyses were run on a VG Isocarb automated system online to a VG Isogas Prism II isotope-ratio mass spectrometer at SUERC, East Kilbride. All data have been normalized to NBS-19, and are reported relative to V-PDB. Replicated

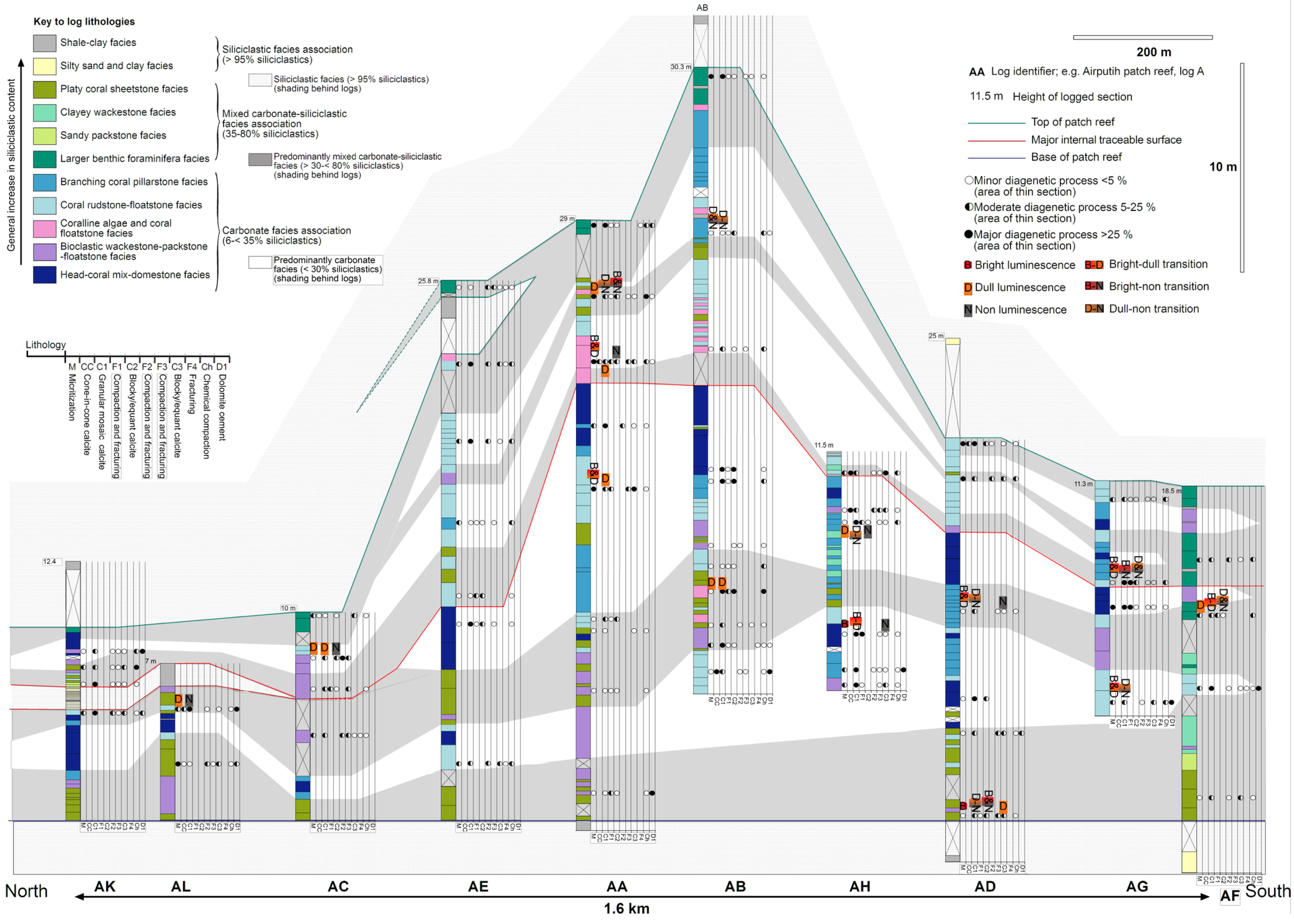
Key to log lithologies
Shale-clay facies
Silty sand and clay facies
Platy coral sheetstone facies
Clayey wackestone facies
Sandy packstone facies
Larger benthic foraminifera facies
Branching coral pillarstone facies
Coral rudstone-floatstone facies
Coralline algae and coral floatstone facies
Bioclastic wackestone-packstone -floatstone facies
Head-coral mix-domestone facies
General increase in siliciclastic content
Siliciclastic facies association (> 95% siliciclastics)
Siliciclastic facies (> 95% siliciclastics) (shading behind logs)
Mixed carbonate-siliciclastic facies association (35-80% siliciclastics)
Predominantly mixed carbonate-siliciclastic facies (> 30-< 80% siliciclastics) (shading behind logs)
Carbonate facies association (6-< 35% siliciclastics)
Predominantly carbonate facies (< 30% siliciclastics) (shading behind logs)
Lithology
M Micritization
CC Cone-in-cone calcite
C1 Granular mosaic calcite
F1 Compaction and fracturing
C2 Blocky/equant calcite
F2 Compaction and fracturing
F3 Compaction and fracturing
C3 Blocky/equant calcite
F4 Fracturing
Ch Chemical compaction
D1 Dolomite cement
200 m
AA Log identifier; e.g. Airputih patch reef, log A
11.5 m Height of logged section
Top of patch reef
Major internal traceable surface
Base of patch reef
10 m
Minor diagenetic process <5 % (area of thin section)
Moderate diagenetic process 5-25 % (area of thin section)
Major diagenetic process >25 % (area of thin section)
B Bright luminescence
B-D Bright-dull transition
D Dull luminescence
B-N Bright-non transition
N Non luminescence
D-N Dull-non transition
AB
30.3 m
29 m
25.8 m
25 m
11.5 m
12.4
10 m
7 m
11.3 m
18.5 m
North
AK
AL
AC
AE
AA
AB
AH
AD
AG
AF
South
1.6 km

Figure 3.4 (previous page): Measured sections through the Airputih patch reef showing key lithologies and facies associations (from Wilson 2005) with petrographically defined diagenetic attributes and cathodoluminescent characteristics. On each measured section, to the right of the lithology column, the diagenetic features in individual thin sections are shown in order of occurrence (left to right — oldest to youngest), with their CL characteristics, where studied, shown directly above. Single letters indicate one CL character, two letters separated by "&" indicates two common characteristics, and two letters separated by "-" indicates a transition from one character to the other (modified from Wilson 2005).

analyses of an internal carbonate standard (Mab2b) were reproducible to ± 0.1‰. An additional 18 oxygen and carbon isotope analyses (samples with the prefix Madden) were run on a GasBench II system coupled online to a stable-isotope-ratio mass spectrometer in continuous flow (Skrzypek and Paul 2006), with all data normalized to NBS-19 and reported relative to V-PDB; these analyses were undertaken at UWA, Perth. External errors for $\delta^{18}O$ and $\delta^{13}C$ were 0.20‰ and 0.10‰, respectively.

Trace-element and major-element analyses on five cement samples and five matrix samples micro-drilled from hand specimen were subject to a four acid (hydrofluoric, nitric, perchloric, and hydrochloric) digestion process. Hydrofluoric acid was used to allow comparison of elemental signatures in the pure carbonate cements (containing no clay) and those of the matrix with admixed micrite and clays. A correction was not applied to account for the dissolution of the silicate fraction. Trace-element and major-element signatures were detected by inductively coupled plasma optical emission spectrometry (ICP-OES). The results were within normal limits (WPR-1 reference standard) and no normalization was required. The results are reported as molar concentrations of the original sample. Precision for each sample is reported as percentage variability at the 95% confidence limit for each element. Precision values have a low variance amongst samples; these values range from 4.5 to 9.3% for Al, 4.2% for Ca, 4.3 to 6.5% for Fe, 4.3 to 6.4% for K, 4.3 to 5.4% for Mg, 4.9 to 6.2% for Mn, 4.4 to 5.4% for Na, and 4.7% for Sr. Variance is greater for S, with a range of 5.8 to 29.5%.

3.5 Diagenetic Characteristics of the Patch Reefs

3.5.1 Petrography of Pre-Fracture Features

3.5.1.1 Micritization

Micritization of bioclastic components is prevalent in 114 of 117 thin sections. Micrite envelopes are visible in plane-polarized light (PL) as narrow (10–60 μm) dark brown rims to bioclasts. Corals show the most pervasive micritization, with rims up to 60 μm thick, and *Halimeda* showing rims of only 10 μm width. The CL properties of the originally calcitic bioclasts (e.g., coralline algae and larger benthic foraminifera) are typically bright to dull luminescent. This CL signature contrasts with that of the micrite envelopes, which are very dull to nonluminescent. The CL character of micritized features is consistent between, and within, individual patch reefs.

3.5.1.2 Cone-in Cone Calcite Cementation

Cone-in-cone calcite, present in approximately 10% of thin sections, is typically nonferroan and is rarely (~ 5% of samples) a dominant cement phase. Cone-in-cone calcite post-dates micritization, but it formed prior to the granular mosaic calcite (C1), since the latter replaces portions of the cones (Fig. 3.5A). This cement is present in samples with abundant fine siliciclastic-rich micritic matrix (25–50% of total rock volume). Cone-in-cone cement has developed within the matrix, and commonly close to the periphery of bioclasts, most notably corals. At Airputih and Permasip (Figs. 3.3, 3.4), cone-in-cone cement is confined to samples from either the top or basal portions of the patch reefs. In comparison, at the < 20-m-thick DPR section, this cement is pervasive throughout. The cone-in-cone cement has a divergent fibrous structure, with cone-shaped bundles of crystalline calcite columns and a displacive habit. Individual crystals are variable in size, typically ranging from 10 to 100 μm in width and up to 500 μm in length. Crystals have an even and regular structure with regular crystal boundaries. Individual crystals are colorless to pale yellow to brown in plane light and are separated by a < 10-μm-thick coating of clay minerals or micrite. Limited CL imagery reveals that in at least one sample, cone-in-

cone cements have the same dull to moderate luminescence as the granular mosaic cements, but with a < 10-μm-thick, brightly luminescent rim to bundles of cones.

3.5.1.3 Granular Mosaic and Blocky Calcite (C1)

Mosaic and blocky calcite cement is a dominant diagenetic feature (up to 50% of the thin section), present in 98% of thin sections. This cement is confined to bioclastic components showing relicts of the original skeletal structure or occurs as minor mosaic cement extending into the chambers of bioclasts (Fig. 3.5B). The cement crystals show a wide variability in size, and where they replace original coral fabric or structure crystal sizes range from 100 to 200 μm up to 600 to 700 μm. The variable but commonly coarse texture contrasts with crystal mosaics found in the chambers of other bioclasts, such as larger benthic foraminifera, where crystal sizes are mostly 100–150 μm. Localized areas of mosaic to granular cement are typified by a uniform mosaic of crystals with irregular crystal boundaries, and little or no evidence of drusy cement morphology. Relicts of the internal skeletal structures and walls of corals are partially preserved through original organic or inorganic inclusions and outlining micrite envelopes. The majority of mosaic cements are nonferroan (stained pink with Alizarin Red S and potassium ferricyanide), with a rare, slight ferroan signature (pale blue stain) in ~ 15% of thin sections. In plane light, these cements are colorless to gray, and have moderate-dull luminescence to nonluminescence in CL or bright CL where C1 blocky calcite grows into primary pore spaces. CL also reveals that these crystals grow crosscutting the micrite envelope and into areas of primary intraparticle porosity within bioclast chambers as outlined by the micritic envelope (Fig. 3.6A/A*).

3.5.2 Petrography of Fracture-Associated Features

3.5.2.1 Grain Breaks and Fractures (F1)

First-phase grain breaks, pre-dating C2 cements, are uncommon (30% of thin sections) and, where present, are mainly associated with regions of C1 cement. Breakage is accommodated via minor crystal or grain fractures, typically on the order of hundreds of μm in length and no more than 20 μm in width. There is minor to no

offset of fractured components. The full extent of minor early fracturing is most evident in CL as fine fracture networks filled with dull-luminescent to nonluminescent (C2) cements that crosscut earlier dull-luminescent C1 cement, and bright-luminescent primary depositional features including micritic matrix (Fig. 3.6A/A*).

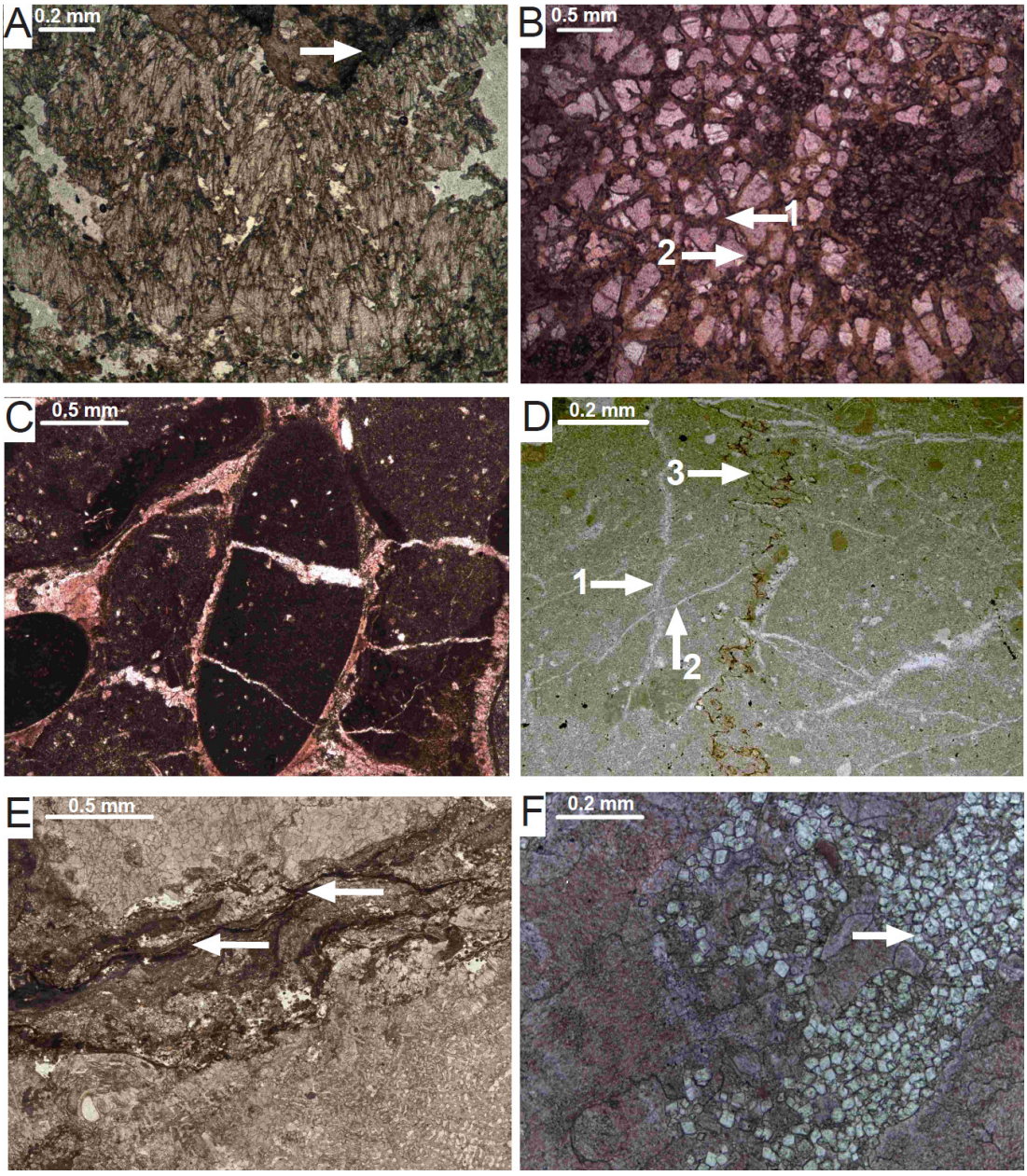

Figure 3.5. Plane-polarized light (PL) thin-sections photomicrographs illustrating a range of diagenetic features in patch-reef deposits. A) Cone-in-cone calcite cement showing fibrous structure arranged into bundles. Darker seams are concentrations of micritic–siliciclastic material. Granular mosaic C1 replacement of cones occurs at the top of the field of view, with the white arrow showing a replacement front. B) Granular mosaic C1 calcite replacing coral chamber walls (1), and contemporaneous blocky calcite cementation of primary porosity (2). C) F1 fractures crosscutting micritic and clay-rich matrix and probable serpulid

worm chamber infill. Fractures are filled by a later stage of C2 calcite cement. Blocky to equant C2 cement includes localized inclusions of dark-colored micritic matrix, attributed to aggrading neomorphism of the matrix. D) Two stages of fractures F2 (arrow 1) and F3 (arrow 2) crosscutting mixed micritic–siliciclastic matrix and filled with C3 calcite cement. Fractures are crosscut by a late-stage stylolite (arrow 3). E) Dissolution seam (arrows) crosscutting micritic matrix and encrusting coralline algae between two corals. F) Micro-dolomite rhombs partially replacing the micritic chamber fill of a coral that has undergone granular mosaic C1 replacement.

3.5.2.2 Blocky to Equant Calcite (C2 and C3)

Thirty-five percent of thin sections show C2 calcite, of which 76% are weakly ferroan to ferroan and 24% are nonferroan. C2 cement fills F1 fractures with some associated growth into, and incorporation of, areas of micritic matrix (Fig. 3.5C), whereas C3 cements fill later F2 and F3 fractures (Fig. 3.5D). Eighty-three percent of thin sections show a C3 calcite, of which 40% are weakly ferroan to ferroan and 60% are nonferroan. In plane light, C2 and C3 cements are colorless to pale yellow and are dull luminescent to nonluminescent in CL. However, C2 cement may show zoning from bright to dull luminescence in larger pores (Fig 3.6B/B*). Both C2 and C3 cements have crystal sizes ranging from 100 to 600 μm, lack a preferred orientation, and have regular to subregular crystal boundaries.

3.5.2.3 Grain Compaction and Fractures (F2, F3 and F4)

Following C2 cementation, a nonpervasive episode of grain compaction and fracturing (F2) occurs, and is evident in ~ 55% of thin sections. F2 fractures have thicknesses of 10 to 100 μm and crosscut matrix (commonly close to bioclasts), bioclasts, and earlier cements. A third stage of grain fracturing (F3) is recognized in 60% of thin sections, where F3 fractures crosscut F2 fractures (Fig. 3.5D). This third set of fractures is more numerous and may form “thread-works” of fractures in areas of micritic or siliciclastic matrix (Fig. 3.5D). Both F2 and F3 fractures are filled by C3 cement with dull luminescence to nonluminescence in CL. Compaction and fracturing did not lead to alignment, rotation, or flattening of grains. F4 fracturing is rare (10% of thin sections), nonextensive and nonpervasive, with fractures typically extending < 500 μm in length and a few tens of μm in width. F4 fractures crosscut earlier cements or, more commonly, contribute to the breakage of previously cemented fractures. F4 fractures are not cemented and remain open.

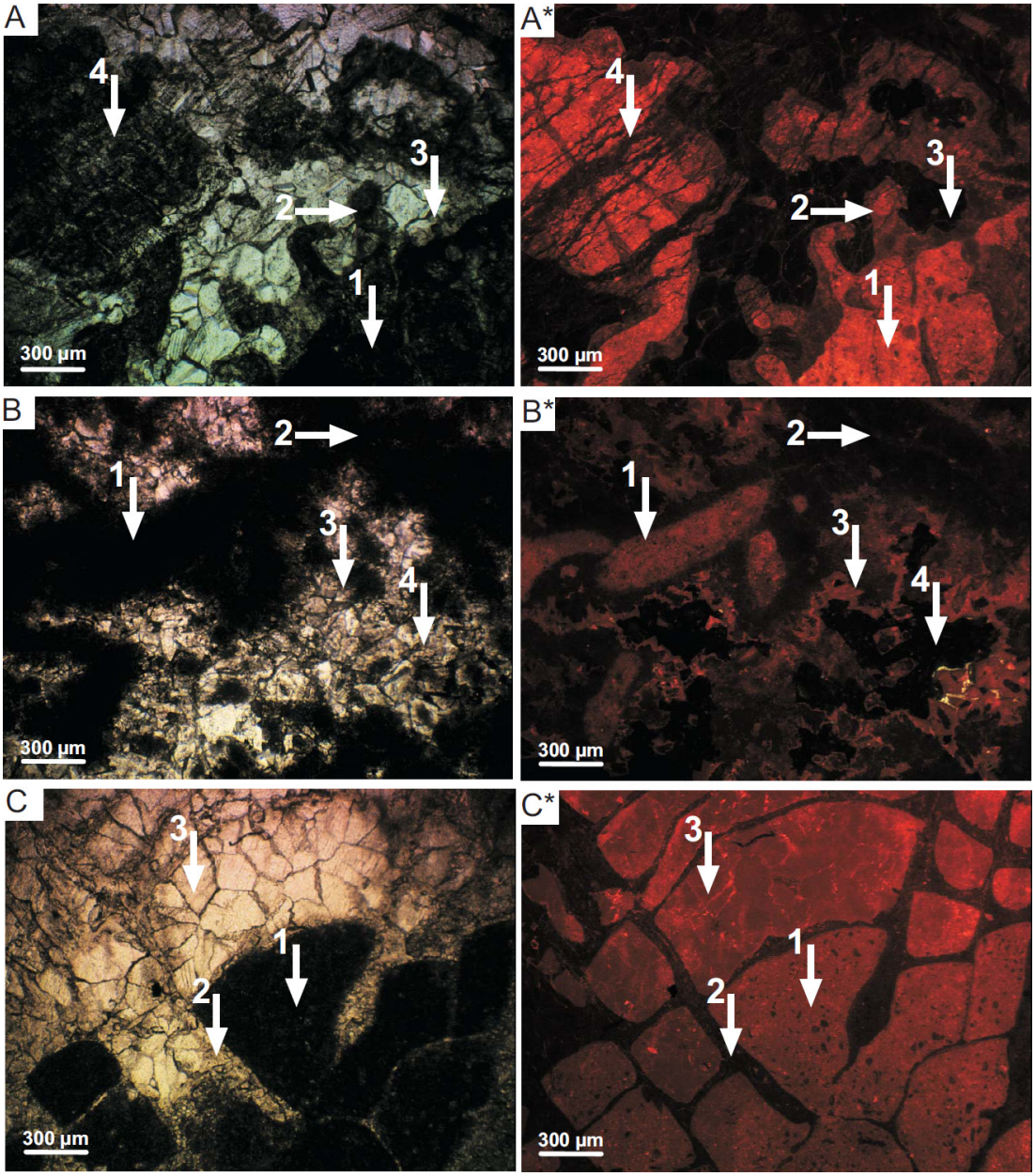

Figure 3.6. PL and CL photomicrograph pairs illustrating different diagenetic features. A/A*) Brightly luminescent micrite fill of coral chamber (1), dull-luminescent granular mosaic C1 replacement of a coral wall (2), contemporaneous blocky C1 calcite growth into cavity with nonluminescence (3) and dull-luminescent C2 calcite filling pervasive fracturing not evident in PL (4). B/B*) Pervasive micritization replacing an originally brightly luminescent bioclast (1), dull-luminescent character of micritic sediment (2) and zoning of C2 blocky calcite cement from bright luminescence (3) into nonluminescence at the center of the cement fill (4). C/C*) Detailed changes within a coral, with bright CL character of micritic chamber infill (1), C1 granular neomorphic cement with dull luminescence to nonluminescence (2) and C1 blocky cement fill of coral chamber (3) showing weak zoning with bright luminescence at the edge of some crystals towards a bright-dull center.

3.5.3 Petrography of Post-Fracture Features

3.5.3.1 Stylolites and Dissolution Seams

Stylolites and dissolution seams are found in 23% and 88% of thin sections, respectively. Stylolites appear as serrated seams (stylolites; Fig. 3.5D), and dissolution seams are smooth and undulating (Fig. 3.5E). Stylolites have amplitudes of up to 1 mm, are several centimeters in length, and are found in areas with minor siliciclastic material in the matrix and with greater cementation. Stylolites crosscut bioclasts, earlier cement phases, and pre-existing fractures. Dissolution seams occur in samples with greater micritic or siliciclastic-rich matrix. Individual samples may have stylolites in calcite-cemented regions that change along length to dissolution seams in matrix-rich areas. Dissolution seams also crosscut older cement phases and fractures, but typically they do not intersect bioclasts, instead commonly going around or between them (Fig. 3.5E). Both features are identified through the concentration of insoluble noncarbonate material, resulting in a dark brown seam in plane light (Figs. 3.5D, 3.5E).

3.5.3.2 Dolomite Cement

Dolomite rhombs are found in < 15% of thin sections, but where present, they commonly are abundant. Mosaics of euhedral to subhedral 10–60 μm micro-dolomite rhombs with regular crystal boundaries typically occur within the micritic matrix infilling bioclast chambers (Fig. 3.5F). Rhombs are also present along dissolution seams and are distributed in the matrix close to seams. In plane light, dolomites are colorless to pale yellow or brown, and in few samples have a cloudy appearance. In CL, they appear as brightly luminescent "spots" or, rarely, dull-luminescent rhombs. There are no crosscutting relationships that suggest that the dolomites were affected by later diagenetic phases.

3.5.4 Cathodoluminescence

CL characteristics are variable at scales from across individual patch reefs (Fig. 3.4) to within isolated corals (Figs. 3.6A/A*, 3.6C/C*), but some trends are evident. For

example, the Airputih and Permasip patch reefs show consistent trends, including: micritic areas typified by bright to dull luminescence, C1 cement with a dull luminescence, and C2/C3 cements with dull luminescence to nonluminescence. There is also a slight tendency for the CL character of carbonate facies (< 35% siliciclastics) to have a brighter luminescence in general than that of mixed carbonate–siliciclastic facies (35–80% siliciclastics). Consistent CL trends are not evident in the patch reefs of Senoni, Bontang, Badak, or Dibelekan Parliament, although CL study was less extensive.

Matrix or cements within large coral chambers have CL characteristics generally brighter than the reef edge or reef core and may show weak zoning within these coral "micro-environments". This trend is evident in C1 cements where nonluminescent C1 cement replacing the coral skeleton changes into dull-luminescent to bright-luminescent pore-filling micrite and blocky C1 cement (Fig. 3.6C/C*).

3.5.5 Stable Isotopes

Stable-isotope composition (Table 3.1, Fig. 3.7) of 31 calcite and six dolomite samples define a tight group, with low variance among individual values of $\delta^{18}O$. These values, ranging from -3.6‰ to -11.7‰ V-PDB, are similar to more negative than that expected from cements derived from Oligo-Miocene southeast Asian marine waters ($\delta^{18}O$ values of -1.5 to -4.2‰; Ali 1995; Wilson and Evans 2002). $\delta^{13}C$ values also lie within a narrow field, generally within to slightly more negative than, the expected range of normal marine waters (+1 to -1‰ $\delta^{13}C$ V-PDB; Ali 1995; Wilson and Evans 2002), where values range from +1.1‰ to -2.6‰ $\delta^{13}C$ V-PDB for all but two samples. Both of the two outlying values at -3.6‰ and -6.2‰ $\delta^{13}C$ V-PDB are from C2 blocky cements.

3.5.6 Trace Elements and Major Elements

The element ratios of magnesium to calcium (Table 3.2) indicate mol % close to a value of 4 mol % Mg, with two C1 and two micritic samples showing a slightly higher concentration of 6 to 7 mol % Mg (intermediate calcite; James 1997). A correction was not applied to account for the dissolution of the silicate fraction in the

Table 3.1. δ13C ‰ VPDB and δ18O‰ VPDB values from samples of the Samarinda patch reefs.

Sample	Name	δ^{13}C‰ VPDB	δ^{18}O‰ VPDB	Phase	Comment
SB10	Madden_SB10	-0.96	-6.87	Larger benthic foraminifera	
AE02	Madden_AE02	-0.09	-9.96	Larger benthic foraminifera	
AB08	Madden_AB08	0.42	-5.79	Larger benthic foraminifera	
AK12	Madden_AK12	1.11	-8.17	Larger benthic foraminifera	
AA26	AA26*0.9	0.57	-7.86	Larger benthic foraminifera	
AC08	AC8*0.6	-1.19	-9.49	Larger benthic foraminifera	
AH09	Madden_AH09	-0.98	-8.61	Cone-in-cone cement	
PE02	Madden_PE02	-0.80	-8.48	Cone-in-cone cement	
AB01	Madden_AB01	-0.45	-10.13	Cone-in-cone cement	
AC08	Madden_AC08	-0.34	-9.15	Cone-in-cone cement	
AL02	Madden_AL02	-0.23	-10.21	Cone-in-cone cement	
AA04a	AA4a*1.1	-1.60	-6.43	Granular mosaic cement (C1)	
AA20	AA20*0.8	-0.79	-7.98	Granular mosaic cement (C1)	
AB01	AB1*1.9	-0.74	-10.01	Blocky equant cement, continuation of granular mosaic (C1)	
AB12a	AB12a*1.5	-1.43	-9.46	Granular mosaic cement (C1)	
AB21a	AA21a*1.9	-0.10	-7.67	Granular mosaic cement (C1)	
DPR04	DPR4*2.2	0.52	-9.10	Granular mosaic cement (C1)	
AD02	AD2*1.2	-0.60	-11.49	Blocky equant cement, continuation of granular mosaic (C1)	
AE05a	AE5a*2.1	0.91	-7.20	Granular mosaic cement (C1)	
AB12a	AB12a*1.0	-1.52	-10.08	Granular mosaic cement (C1)	
AB12a	AB12a*1.0	-1.79	-10.41	Granular mosaic cement (C1)	
AA04b	AA4b*1.9	0.51	-1.64	Blocky equant cement (C2)	contaminated by dolomites or siliciclastics
AB07	AB7*1.3	-6.22	-3.61	Blocky equant cement (C2)	slightly ferroan
AE05b	AE5b*1.5	0.98	-6.27	Blocky equant cement (C2)	
BB05	BB5*0.5	-3.60	-4.86	Blocky equant cement (C2)	
AK02	Madden_AK02	-1.82	-10.74	Vein (Blocky C3 cement filling fracture)	
AA15	Madden_AA15	-0.76	-10.49	Vein (Blocky C3 cement filling fracture)	
PC03	Madden_PC03	-0.41	-7.30	Vein (Blocky C3 cement filling fracture)	
KB07	KB7*0.9	-0.15	-10.04	Vein (Blocky C3 Cement filling fracture)	
AA04	Madden_AA04	-2.62	-7.27	Dolomite	
AH02	Madden_AH02	0.14	-7.31	Dolomite	
PE06	Madden_PE06	0.48	-7.43	Dolomite	
AF06	Madden_AF06	0.49	-6.82	Dolomite	
PC08	Madden_PC08	0.60	-5.99	Dolomite	
AK12	Madden_AK12	1.04	-7.48	Dolomite	

matrix; therefore Mg contents may reflect both the carbonate and siliciclastic content of the matrix. Data reveal several distinctive trends for the trace-element and major-element results within the paired samples of C1 calcite and their associated micritic–siliciclastic matrix. Mn/Ca and Sr/Ca ratios show little variability from matrix to C1 calcite. In contrast, the ratios of Na/Ca, Fe/Ca and Mg/Ca decrease from the matrix to C1 samples. Aluminum content is highly variable, with values of ~ 1 to 13 mol % Al in C1 samples and ~ 27 to 72 mol % Al in micrite. Ratios of Al/Ca are consistent, showing a decreasing concentration from matrix to C1 (Table 3.2).

3.6 Diagenetic, Temperature and Paleohydrology Interpretations

Collectively, the observations reveal a paragenetic sequence with several phases of cementation within the Samarinda patch reefs (Fig. 3.8). The Anderson and Arthur (1983) equation (Equation.1) provides a means to derive Miocene $\delta^{18}O$ seawater values for the region:

$$T=16 - 4.14(\delta^{18}O_{CALCITE} - \delta^{18}O_{SEAWATER}) + 0.13(\delta^{18}O_{CALCITE} - \delta^{18}O_{SEAWATER})^2 \quad (1)$$

A Miocene $\delta^{18}O$ seawater value for the region of -2 to 0‰ V-SMOW has been derived using this equation and the observed range of calcitic bioclast values for SE Asian Oligocene–Miocene seawater and an assumed ocean surface temperature of 25 °C (Neogene of coastal Borneo; Ali 1995). The larger benthic foraminifera in the Samarinda samples ($\delta^{18}O$ V-PDB values of -5.8‰ to -10.0‰) have lower $\delta^{18}O$ values than the known range for SE Asian Oligocene–Miocene calcitic bioclasts, perhaps reflecting: (1) the samples containing contaminating matrix, (2) precipitation out of equilibrium with Miocene sea water, or (3) resetting of the $\delta^{18}O$ during stabilization by meteoric waters or elevated temperatures. Because the deposition of Neogene patch reefs was impacted by terrestrial runoff, the strongly negative $\delta^{18}O$ V-PDB values of the larger foraminifera may partially reflect a brackish signature. Given the uncertainties of the isotopic signatures of the larger foraminifera in the Samarinda patch reefs reflecting marine signatures, estimated Miocene seawater values are used (-1.5‰ to -4.2‰ $\delta^{18}O$ V-PDB; Ali 1995; Wilson and Evans 2002) in deriving a regional V-SMOW seawater value. A $\delta^{18}O$ value of -4 to -8‰ V-SMOW is suggested for meteoric parent fluids on the basis of $\delta^{18}O$ values of meteoric

precipitation in SE Asia of -4 to -6‰ at low elevations (Bowen and Wilkinson 2002) and up to -8‰ for the whole of Borneo (Anderson and Arthur 1983).

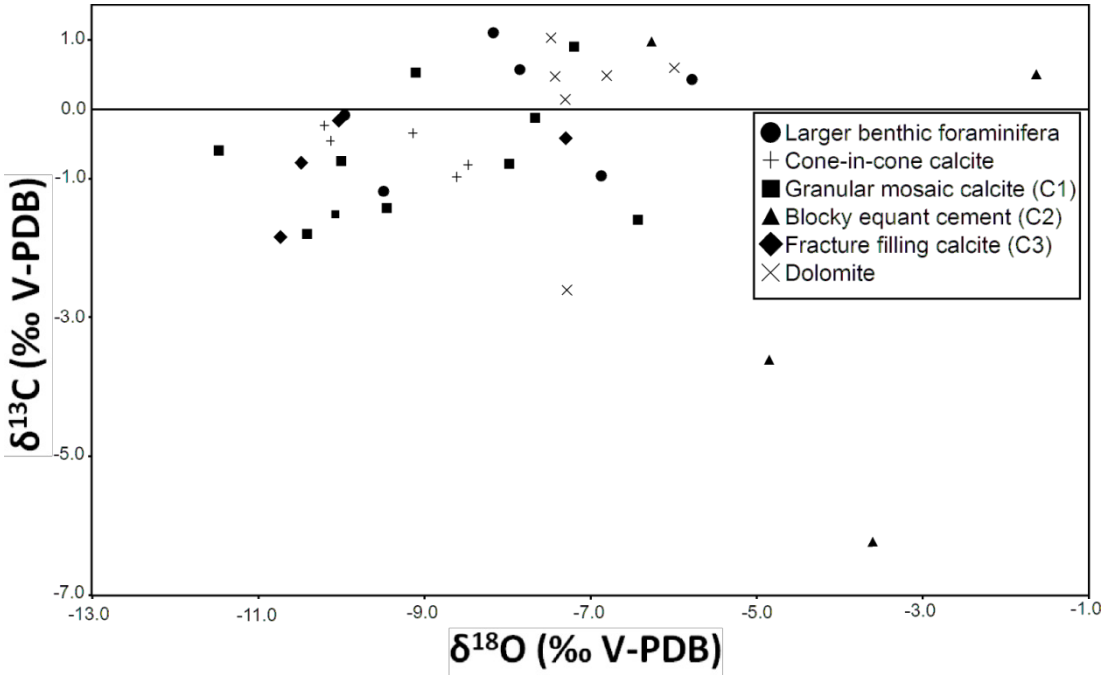

Figure 3.7. Cross-plot of $\delta^{18}O$‰ V-PDB versus $\delta^{13}C$‰ V-PDB for calcite and dolomite components and cements from patch reefs of the Samarinda region. The $\delta^{18}O$ values of -3.6 to -11.7‰ are consistent with precipitation from SE Asian freshwater, and inconsistent with a wholly marine origin at temperatures of 25 to 53 °C (see text for details).

The onset of development of stylolites and dissolution seams occurs in moderate-burial to deep-burial environments of 500–1000 m (Nicolaides and Wallace 1997; Machel 2004). Since all calcite cement precipitation pre-dates development of stylolites and dissolution seams, a maximum burial depth for calcite cementation of the Samarinda patch reefs of 1000 m is inferred. Extrapolation of the eastern Kutai Basins geothermal gradient (27.5 °C/km; Hall 2002b) gives an estimated maximum calcite precipitation temperature of 53 °C.

Table 3.2. Trace-element and major-element molar compositions and molar ratios with respect to calcium from samples of the Samarinda patch reefs. Precision is reported as percentage variability at the 95% confidence limit for each element and each sample.

	Sample	Al	Ca	Fe	K	Mg	Mn	Na	S	Sr
Molar composition	AC01	2.45×10^{-5}	1.77×10^{-3}	1.23×10^{-5}	2.54×10^{-6}	7.46×10^{-5}	4.44×10^{-7}	2.37×10^{-6}	8.36×10^{-6}	8.00×10^{-6}
	AC01M	3.35×10^{-4}	1.24×10^{-3}	6.75×10^{-5}	5.29×10^{-5}	9.92×10^{-5}	1.61×10^{-6}	1.06×10^{-4}	7.62×10^{-5}	2.53×10^{-6}
	PC14	1.27×10^{-4}	1.66×10^{-3}	9.34×10^{-5}	1.01×10^{-5}	4.30×10^{-5}	1.04×10^{-6}	5.19×10^{-5}	1.40×10^{-5}	1.02×10^{-5}
	PC14M	3.86×10^{-4}	1.09×10^{-3}	1.50×10^{-4}	4.54×10^{-5}	7.57×10^{-5}	1.06×10^{-6}	1.65×10^{-4}	1.45×10^{-4}	5.69×10^{-6}
	AH07	4.85×10^{-5}	1.92×10^{-3}	2.54×10^{-5}	7.70×10^{-6}	4.82×10^{-5}	8.10×10^{-7}	2.97×10^{-5}	5.63×10^{-6}	1.36×10^{-5}
	AH07M	4.62×10^{-4}	1.15×10^{-3}	6.58×10^{-5}	5.10×10^{-5}	5.03×10^{-5}	3.64×10^{-7}	3.64×10^{-5}	9.90×10^{-7}	3.66×10^{-6}
	AH05	2.01×10^{-4}	1.55×10^{-3}	4.65×10^{-5}	3.27×10^{-5}	8.15×10^{-5}	1.14×10^{-6}	3.57×10^{-5}	3.79×10^{-6}	1.02×10^{-5}
	AH05M	6.17×10^{-4}	8.55×10^{-4}	1.10×10^{-4}	9.86×10^{-5}	1.44×10^{-4}	7.11×10^{-7}	6.17×10^{-5}	1.88×10^{-6}	5.45×10^{-6}
	AE03	6.94×10^{-5}	1.85×10^{-3}	3.04×10^{-5}	1.13×10^{-5}	1.16×10^{-4}	5.79×10^{-7}	5.57×10^{-5}	1.45×10^{-5}	1.05×10^{-5}
	AE03M	3.09×10^{-4}	8.28×10^{-4}	8.82×10^{-5}	4.81×10^{-5}	4.12×10^{-4}	1.01×10^{-6}	1.24×10^{-4}	2.91×10^{-5}	2.85×10^{-6}

	Sample	Al/Ca	Fe/Ca	K/Ca	Mg/Ca	Mn/Ca	Na/Ca	S/Ca	Sr/Ca
Molar Ratio	AC01	1.38×10^{-2}	6.94×10^{-3}	1.43×10^{-3}	4.21×10^{-2}	2.50×10^{-4}	1.34×10^{-3}	4.71×10^{-3}	4.51×10^{-3}
	AC01M	2.69×10^{-1}	5.42×10^{-2}	4.25×10^{-2}	7.97×10^{-2}	1.29×10^{-3}	8.54×10^{-2}	6.12×10^{-2}	2.04×10^{-3}
	PC14	7.68×10^{-2}	5.64×10^{-2}	6.10×10^{-3}	2.60×10^{-2}	6.30×10^{-4}	3.13×10^{-2}	8.45×10^{-3}	6.16×10^{-3}
	PC14M	3.53×10^{-1}	1.38×10^{-1}	4.16×10^{-2}	6.93×10^{-2}	9.72×10^{-4}	1.51×10^{-1}	1.32×10^{-1}	5.21×10^{-3}
	AH07	2.52×10^{-2}	1.32×10^{-2}	4.01×10^{-3}	2.51×10^{-2}	4.21×10^{-4}	1.54×10^{-2}	2.93×10^{-3}	7.07×10^{-3}
	AH07M	4.02×10^{-1}	5.74×10^{-2}	4.44×10^{-2}	4.38×10^{-2}	3.17×10^{-4}	3.17×10^{-2}	8.62×10^{-4}	3.19×10^{-3}
	AH05	1.30×10^{-1}	3.00×10^{-2}	2.11×10^{-2}	5.27×10^{-2}	7.35×10^{-4}	2.31×10^{-2}	2.45×10^{-3}	6.57×10^{-3}
	AH05M	7.23×10^{-1}	1.29×10^{-1}	1.15×10^{-1}	1.69×10^{-1}	8.32×10^{-4}	7.22×10^{-2}	2.20×10^{-3}	6.37×10^{-3}
	AE03	3.75×10^{-2}	1.64×10^{-2}	6.13×10^{-3}	6.26×10^{-2}	3.13×10^{-4}	3.01×10^{-2}	7.85×10^{-3}	5.65×10^{-3}
	AE03M	3.73×10^{-1}	1.06×10^{-1}	5.18×10^{-2}	4.97×10^{-1}	1.22×10^{-3}	1.49×10^{-1}	3.51×10^{-2}	3.44×10^{-3}

	Sample	Al +/- %	Ca +/- %	Fe +/- %	K +/- %	Mg +/- %	Mn +/- %	Na +/- %	S +/- %	Sr +/- %
Precision at the 95% confidence limit	AC01	9.3	4.2	6.5	6.4	4.8	6.2	5.4	8.3	4.7
	AC01M	4.7	4.2	4.5	4.4	4.7	4.6	4.5	5.9	4.7
	PC14	5.3	4.2	4.4	4.8	5.4	5.0	4.8	7.2	4.7
	PC14M	4.7	4.2	4.3	4.4	4.9	5.0	4.4	5.8	4.7
	AH07	7.1	4.2	5.3	5.0	5.3	5.3	5.3	9.9	4.7
	AH07M	4.6	4.2	4.6	4.4	5.2	6.9	5.1	29.5	4.7
	AH05	4.9	4.2	4.7	4.4	4.8	4.9	5.1	11.8	4.7
	AH05M	4.5	4.2	4.4	4.3	4.5	5.6	4.8	19.0	4.7
	AE03	6.3	4.2	5.2	4.8	4.6	5.9	4.8	7.3	4.7
	AE03M	4.7	4.2	4.4	4.4	4.3	5.0	4.4	6.4	4.7

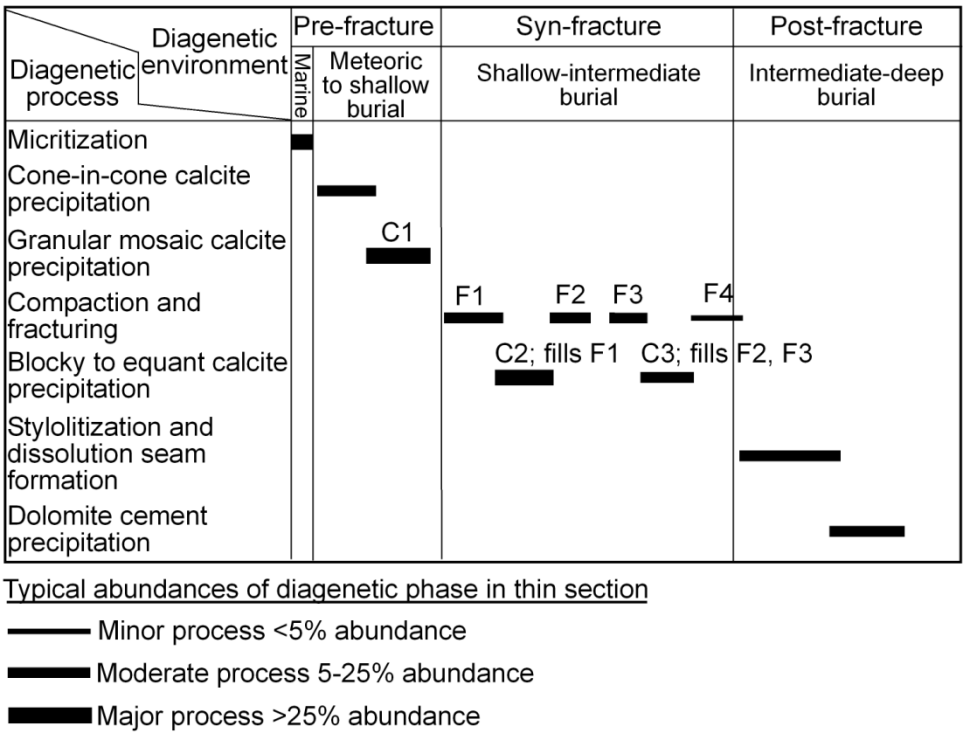

Figure 3.8. Paragenetic sequence of the patch reefs of the Mahakam Delta. Relative timing of events is on the basis of petrographic observations.

3.6.1 Interpretation of Pre-Fracture Features

3.6.1.1 Micritization

Micritization present throughout the samples is the first diagenetic process, on the basis of crosscutting relationships by each of the later features. Skeletal material in shallow-marine environments commonly is micritized due to micrite infilling the micro-borings of endolithic organisms (Bathurst 1966; Gunther 1990; Perry 1999). In particular, in warm and low-energy environments, as is inferred for these samples (Wilson 2005), micritization is commonly recognized as an early marine diagenetic feature (Gunther 1990; Perry 1999). The very dull-luminescent to nonluminescent CL character of the micritic envelopes is consistent with associated marine or oxidizing pore fluids. Alternatively the fine texture of the micritic material may impart a darker CL character.

3.6.1.2 Cone-in-Cone Calcite

Cone-in-cone calcite cement formed prior to the onset of C1 cementation. Well-formed bundles of crystals within the micritic–siliciclastic substrate indicate that the cone-in-cone cement was precipitated prior to lithification of the matrix (cf. Franks 1969; McBride et al. 2003). The predominant distribution of this cement at the top and base of patch reefs adjacent to siliciclastics and in siliciclastic-rich units (Fig. 3.4) may reflect enhanced fluid flow and diffusion from the more permeable siliciclastics, promoting precipitation of the cement (cf. McBride et al. 2003). A dull to moderate CL character of the cone-in-cone cement is suggestive of oxidizing to perhaps slightly reducing conditions (iron derivation from the siliciclastics may have contributed to reducing conditions). $\delta^{18}O$ V-PDB values of -8.5 to -10.2‰ for the cone-in-cone calcite, if precipitated from marine parent fluids, would require temperatures of 50–70 °C at a burial depth of approximately 500–1600 m. This temperature and depth range is unlikely because the cone-in-cone cement precipitated prior to mechanical compaction features (below), and under conditions that were still oxidizing or perhaps slightly reducing. At temperatures of 25 to 35 °C, consistent with shallow burial, the cone-in-cone cements would have formed from pore fluids with $\delta^{18}O$ values of -7.3 to -5.3‰ V-SMOW (Fig. 3.9), suggestive of meteoric fluids with an upland source (Anderson and Arthur 1983). Absent from these cements are the depleted $\delta^{13}C$ values associated with near-surface meteoric precipitation (Allan and Matthews 1982). Instead, relatively high $\delta^{13}C$ values of approximately 0‰ indicate that carbon derived from either sea water or marine carbonate rock was supplied along the fluid flow path (Hendry et al. 1999).

3.6.1.3 Granular Mosaic to Blocky Calcite (C1)

C1 calcite cement, retaining “ghost” internal and external fabrics of aragonitic bioclasts, is indicative of neomorphism rather than of bioclast dissolution and reprecipitation. Crosscutting of micritic rims and partial replacement of cone-in-cone cement (Fig 3.5A): (1) confirms micritization and cone-in-cone cementation asthe earlier processes, and (2) is indicative of contemporaneous neomorphic replacement and growth of pore-filling cement. Neomorphism and contemporaneous cement growth (calcitization) into original porosity is consistent with the granular

mosaic habit and absence of drusy cement morphologies (Fig. 3.10; Hendry et al. 1999). A change from dull luminescence to nonluminescence in neomorphic C1 to dull luminescence to bright luminescence in contemporaneous pore-filling C1 blocky cement in coral-hosted microenvironments is consistent with either: (1) trapping of initially oxidizing neomorphic diagenetic fluids that become more reducing within the pores, or (2) that intra-coral porosity received lower amounts and/or less sustained flushing by diagenetic fluids with a resulting decrease in oxygenation state.

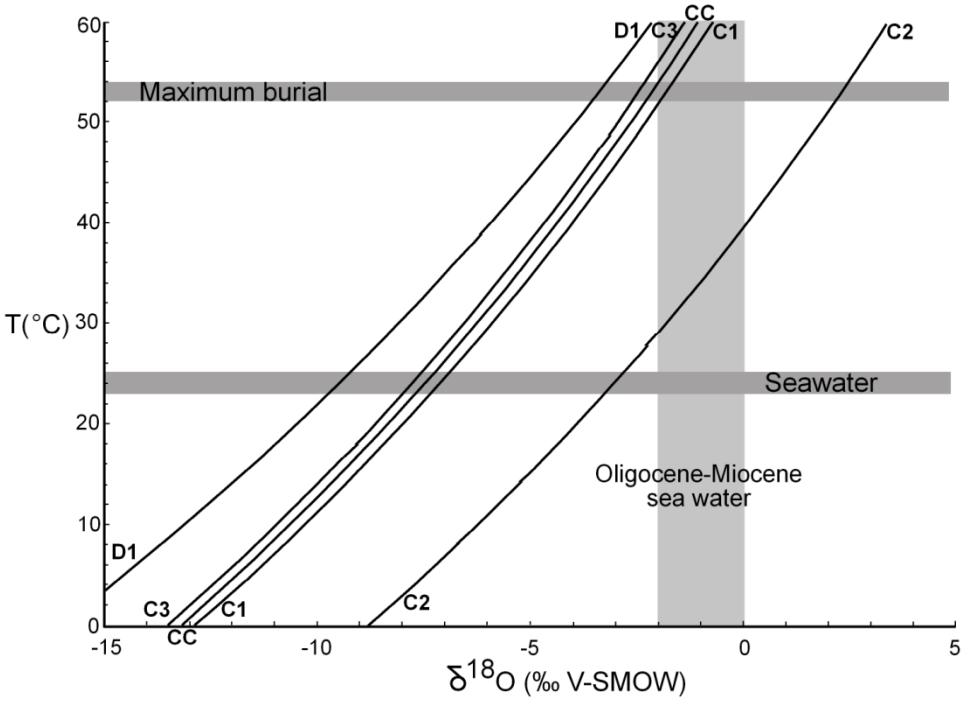

Figure 3.9. Equilibrium oxygen isotope fractionation relationships between calcite and dolomite cements and formation fluids for the Samarinda patch reefs. Calcite curves are based on the equation $10^3 \ln\alpha = 2.78*10^6 T^{-2}-2.89$ (where α is the fractionation factor of calcite–water and T is temperature in K; Friedman and O'Neil 1977) and the dolomite curve is based on the equation $10^3 \ln\alpha = 3.20*10^6 T^{-2}-3.30$ (where α is the fractionation factor of dolomite-water and T is temperature in K; Land 1983). For each cement phase, averaged $\delta^{18}O$ V-PDB compositions were used. CC indicates cone-in-cone cement. C2 cements suggest precipitation from pore fluids with increasing $\delta^{18}O$, or precipitation from meteoric fluids at decreased temperatures than both earlier (CC and C1) and later (C3 and D1) cements

over time. If precipitated from marine parent fluids, cements with stable-isotope values ranging from -6.4 to -11.7‰ $\delta^{18}O$ V-PDB, would require temperatures of 40–80 °C, at a burial depth of approximately 500–1700 m. These temperatures and depths are highly unlikely due to the pre-fracture timing of the C1 cement and potentially still oxidizing precipitation conditions. A formation fluid of -7 to -5‰ V-SMOW at 25 to 35 °C is likely (Fig. 3.9), consistent with early meteoric to shallow-

burial diagenesis and similar to the conditions inferred for the cone-in-cone cement that this C1 cement partially replaces. However, samples with low $\delta^{18}O$ values may be indicative of: (1) mixing marine pore fluids with meteoric water, or (2) meteoric diagenesis at higher rock:water ratios. With the majority of $\delta^{18}O$ values being more negative than -4‰ $\delta^{18}O$ V-PDB, these predominantly reflect an influx of meteoric fluids and lower rock:water ratios. High $\delta^{13}C$ values (-1.6 to 0.9‰) indicate a lack of soil zone processes affecting these meteoric fluids or a rock-derived source of carbon with marine $\delta^{13}C$ values, consistent with the prior cone-in-cone cement.

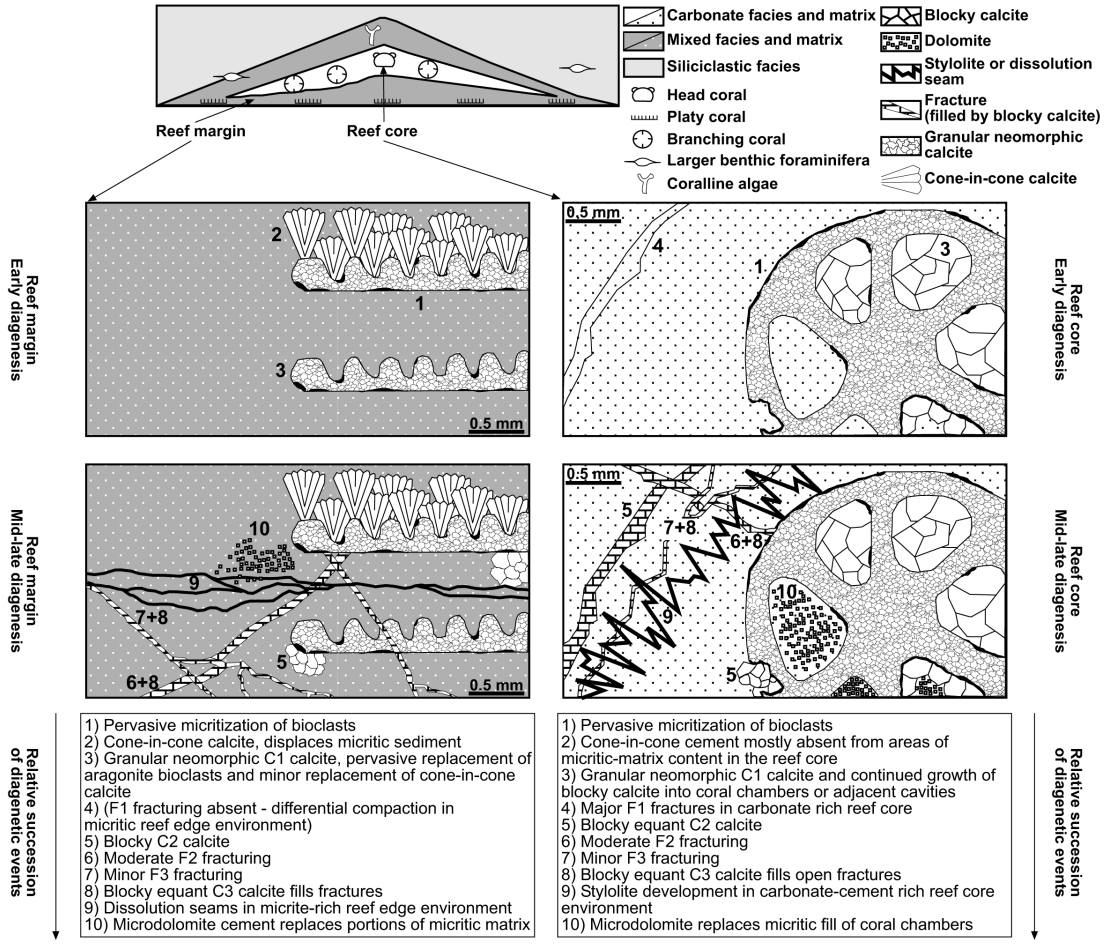

Figure 3.10. Schematic paragenetic scheme from different areas of a patch reef, based on petrographic relationships. Reef margin shows diagenesis of a platy coral-rich section from a mixed carbonate–siliciclastic (35–80% siliciclastics) area of the reef with development of cone-in-cone features, dolomites in the siliciclastic-rich matrix, and dissolution seams. Reef core shows diagenesis of a head or branching coral-rich section containing < 35% siliciclastics in which neomorphic C1 granular to blocky cement is prevalent and stylolites are developed.

Aragonitic scleractinian coral skeletons contain ~ 8000 ppm Sr^{2+} (Milliman 1974; Morrison and Brand 1986). Observations of Sr^{2+} concentrations of 3039 to 4692 ppm for C1 neomorphic calcite (Table 2), and assuming a distribution coefficient for Sr of 0.4 or less (Veizer 1983), suggest Sr removal via an open system, but that inflowing fluids contributed little to the elemental signature (Hendry et al. 1999). The high Sr values of C1 may reflect a partially closed system with less effective elemental removal, perhaps within the coral-hosted microenvironments. Scleractinian-coral aragonite typically contains Mn and Fe element concentrations on the order of tens of ppm at most (Morrison and Brand 1986). Low concentrations of Mn (< 270 ppm) and Fe (typically < 70 ppm) in neomorphic calcite and partition coefficients for both elements of > 1 (i.e. ready ion substitution) are again indicative of elemental removal and fluid throughflow, similar to that inferred for the Sr above. These low Mn and Fe concentrations likely are reflected in the dull-luminescent or nonluminescent CL character of the C1 cements.

Intermediate C1 calcite is affiliated with mixed micrite–siliciclastic matrix, which includes Mg/Ca ratios higher than those of C1. In the tropical marine setting of the patch reefs, it is likely that the primary mineralogy of the micrite was either aragonite or high-Mg calcite (Hoskin 1968; Husseini and Matthews 1972; Andrews et al 1997). The intermediate-Mg calcites may have retained, in part, the precursor elemental composition of the micrite after alteration by undersaturated fluids, or siliciclastic clays might locally contribute magnesium to the elemental signature (Morad et al. 2000).

3.6.2 Interpretation of Syn-Fracture Features

3.6.2.1 Compaction and Fracturing (F1)

The first stage of grain breakage and fracturing (F1) is present mainly in neomorphosed coral-rich bioclastic samples and is interpreted to reflect differential compaction and fracturing of partially lithified matrix, combined with fracturing of more competent cemented components, most notably those units rich in corals (Fig. 3.10). The timing of fracturing, prior to the onset of later-stage chemical

compaction, is also consistent with F1 fractures resulting from mechanical compaction in a shallow burial environment.

3.6.2.2 Blocky to Equant Cement (C2)

Blocky to equant C2 calcite cement infills, and therefore must post-date, F1 fractures. C2 cements also are present in areas of micritic matrix close to bioclasts where differential compaction has generated porosity, and with some cementation attributable to aggrading neomorphism of the matrix, as suggested by micritic inclusions within the cement (Fig. 3.5C). A dull-luminescent to nonluminescent character and largely ferroan to weakly ferroan mineralogy indicates that C2 cement probably was precipitated from oxygenated fluids with Fe ions in solution. A positive shift of $\delta^{18}O$ between cone-in-cone calcite (-8.5 to -10.2‰) and C1 calcite (-6.4 to -11.7‰) to C2 calcite (-3.6 to -6.3‰) suggests either: (1) increasing pore-fluid $\delta^{18}O$, or (2) decreasing temperature. Formation fluid $\delta^{18}O$ values could range from -0.9 to +1.0‰ V-SMOW at 35–45 °C under conditions of increasing burial (Fig. 3.9), consistent with a marine source. If precipitated from meteoric fluids, cements with stable-isotope values ranging from -3.6 to -6.3‰ $\delta^{18}O$ V-PDB would require temperatures of < 20 °C at near-surface burial depths. A burial diagenetic environment is inferred for the C2 cements as evidenced by the prior onset of mechanical fracturing, and indicates that a decreasing formation temperature from C1 to C2 cements is unlikely. Enrichment of the precipitating fluids towards higher $\delta^{18}O$ can be ascribed to: (1) silicate alteration reactions between pore fluids and siliciclastics (Morad 1998), or (2) the introduction of seawater-derived fluids. The depleted $\delta^{13}C$ values (-3.6 to -6.3‰ $\delta^{13}C$ V-PDB) are consistent with carbon derivation from the decay of C_3 and C_4 plants in soil-rich and sediment-rich horizons (Morad 1998), such as occurs in the associated deltaic siliciclastics. The introduction of Fe ions in solution is most reasonably attributed to fluids sourcing Fe ions from siliciclastics along the fluid flow pathway (Morad et al. 2000).

3.6.2.3 Compaction and Fracturing (F2 + F3)

F2 and F3 fractures generally are straighter than the earlier F1 fractures (Figs. 3.5C, 3.5D), indicating that fracturing continued after full lithification of matrix and

bioclasts. The conjugate natures of some of the F2 and F3 fracture sets (Fig. 3.5D) conform to either a compaction or a tectonic origin.

3.6.2.4 Blocky to Equant Cement (C3)

Blocky to equant C3 cementation is confined to, and post-dates, F2 and F3 fractures (Fig. 3.10). The nonluminescence and mostly nonferroan composition of this cement are consistent with oxygenated diagenetic fluids. Stable-isotope values ranging from -7.3‰ to -10.7‰ $\delta^{18}O$ V-PBD would require precipitation at 40–80 °C from marine fluids at a depth of 500–1400 m (based on a regional geothermal gradient of 27.5 °C/km; Hall 2002b), inconsistent with C3 formation prior to the onset of chemical compaction. Formation-fluid $\delta^{18}O$ values range from -5.5 to -2.9‰ V-SMOW at 35–50 °C (Fig. 3.9) at < 1000 m burial depth. At the higher end of this temperature range, formation-fluids for C3 calcite are consistent with precipitation from either marine or meteoric fluids, but lower temperatures and a nonluminescent CL character suggest mixed water compositions. A shift towards higher $\delta^{13}C$ values from C2 to C3 (-1.8 to -0.2‰) cements suggest enrichment of pore fluids by: (1) marine rock-sourced carbon or (2) a lack of soil-zone signatures. An influx of meteoric fluids dissolving marine carbon along its flow path and mixing with residual waters from C2 precipitation is likely with fluids utilizing F2 and F3 fractures as flow pathways.

3.6.2.5 Fracturing (F4)

The final stage of fracturing is minor and poorly developed, likely due to the impact of prior cementation (cf. Purser 1978; Hird and Tucker 1988; Clari and Martire 1996; Railsback 1993a).

3.6.3 Interpretation of Post-Fracture Features

3.6.3.1 Stylolites and Dissolution Seams

Crosscutting all calcite cements and fractures, stylolites and dissolution seams are chemical compaction features that form in moderate to deep burial environments

(Machel 2004) at depths of 500–1000 m (where the onset of stylolitization occurs; Nicolaides and Wallace 1997). A transition from dissolution seams in more siliciclastic-rich samples to stylolites in more calcitic, well-cemented samples as occurs in the Samarinda deposits is a trend well documented in the literature (Wanless 1979; Railsback 1993b). The seams mostly circumvent calcified bioclasts, likely because dissolution was promoted along calcite to clay-rich interfaces (cf. Railsback 1993b).

3.6.3.2 Dolomite Cement

Dolomites are a localized feature found dominantly in areas of micritic matrix (Fig. 3.10). These cements commonly are proximal to dissolution seams in the clay-rich matrix or hosted within coral chambers, with Mg perhaps locally contributed from the compaction of clays (Ali 1995; Carnell and Wilson 2004; Machel 2004). The euhedral microcrystalline and partly cloudy dolomite crystals indicate that they are at least in part replacing the micritic matrix (Warren 2000; Machel 2004). Euhedral rhombic dolomite is indicative of formation temperatures of < 50–60 °C (Warren 2000). $\Delta^{18}O$ values for dolomite (-5.99 to -7.48‰ V-PDB) at 53 to 60 °C convert to formation fluids of -3.4 to -2.3‰ V-SMOW (Fig. 3.9). On the basis of the combined petrographic and stable-isotope evidence, meteoric fluids at moderate burial depths up to ~ 1000 m are interpreted to be the dolomitizing fluids; however, slightly higher $\delta^{18}O$ values may be the result of: (1) mixed marine–meteoric signature similar to C3 fluids, or (2) silicate alteration reactions between pore fluids and siliciclastics (Morad 1998).

3.7 Discussion

3.7.1 Basin Hydrology

Fluids are integral to the diagenesis of sediments, with three primary mechanisms recognized as driving forces for fluid flow through sedimentary successions (Galloway 1984): (1) topography-driven flow, (2) compaction-driven flow, and (3) thermal-convection-driven flow. Given the conditions of shallow burial (< 1 km; based on the onset of stylolitization) and low thermal heat flow (Hall 2002b) for the

Samarinda patch reefs, thermally driven fluid flow is not considered an important factor. Topography-driven flow (established by the elevation of the ground-water table above sea level; Bjørlykke 1993), and compaction-driven flow of trapped marine fluids, appear the more important controls on subsurface flow in the Samarinda area (Fig. 3.11).

Low oxygen isotope values ($\delta^{18}O$ values of -6.4 to -11.7‰ V-PDB) suggest that, at low temperatures, meteoric fluids with an upland source were responsible for the formation of early cone-in-cone and neomorphic C1 cements Involvement of continent-derived fluids in the early diagenesis of the Samarinda patch reefs is consistent with their development adjacent to permeable sands of the Mahakam Delta (Allen and Chambers 1998). The Samarinda patch reefs are underlain by deep-water shales and overlain by alluvial flood-plain sediments (Fig. 3.2).

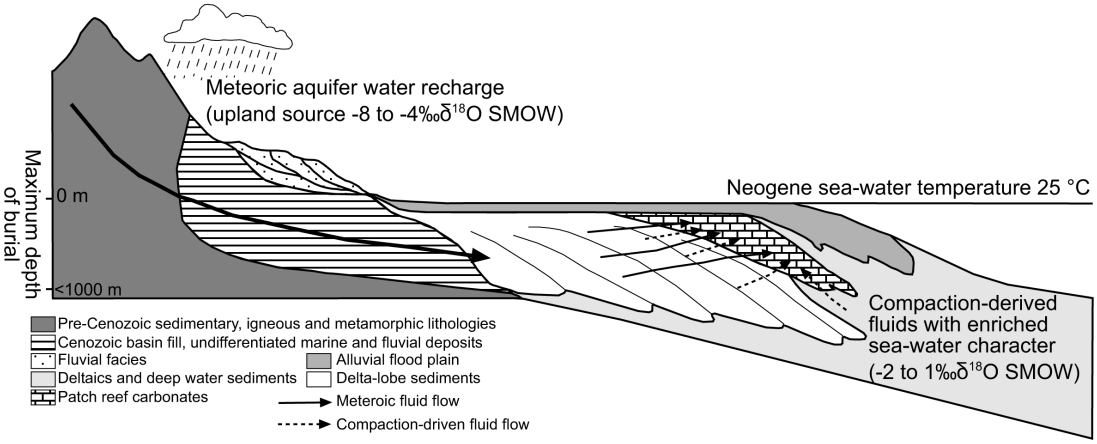

Figure 3.11. Schematic cartoon illustrating paleohydrology dominated by aquifer flow from hinterland areas to the patch reefs with minor contribution from compaction-derived marine fluids. Marine carbonate-sourced fluids (based on stable-isotope evidence; see text) along fluid flow path are derived from within the patch reefs where neomorphism and calcitization occur.

The location of the reefs adjacent to an "ever-wet" elevated continental landmass is inferred to have contributed to the development of a confined paleoaquifer allowing channelling of continent-derived fluids laterally into the patch reefs, dissolving marine carbonate along the flow path, and contributing to the high carbon isotope values of the patch-reef cements (Fig. 3.11). Furthermore, an aquifer system in an "ever-wet" climate would allow replenishment of meteoric fluids capable of pervasive stabilization of the patch reefs through neomorphic replacement and

calcitization. Permeable deltaic units have been shown to be important in the introduction of meteoric diagenetic fluids into carbonates during early diagenesis (Hendry et al. 1999; Taberner et al. 2002). Later cementation, fracturing, and compaction are relatively minor features occurring under the influence of continued burial, rock–water interaction, and the confined aquifer system generated by covering of the patch reefs in flood-plain sediments (Fig. 3.2). Under conditions of increasing burial, the introduction of $\delta^{18}O$-enriched, $\delta^{13}C$-depleted fluids and Fe ions in solution is consistent with dewatering of marine fluids from the underlying deep-water shales possessing an evolved $\delta^{18}O$ seawater character sourcing Fe ions from the shales (Fig. 3.11; cf. Galloway 1984; Hendry et al. 1999).

The diagenesis of a number of SE Asian siliciclastic-influenced coastal carbonates show pervasive early neomorphism of aragonite (Netherwood and Wight 1992; Madden 2008; Wilson 2012), and hint that, similar to the Samarinda patch reefs, their diagenesis is strongly controlled by the role of a continental aquifer driving fluid flow. Few detailed diagenetic studies exist of delta-associated carbonates that developed during the Cenozoic, in humid, temperate, or arid settings. However similarities, and differences, are exhibited between the Samarinda carbonates and delta-associated carbonates from a range of climatic settings from the Cenozoic.

3.7.2 Patterns of Diagenesis of Coastal Carbonates in the Humid Tropics

With respect to early diagenesis and initial basin hydrology, the Samarinda carbonates are sedimentologically and diagenetically comparable to the Eocene Calders reef of the South Pyrenean foreland basin. The Calders reef developed on delta-lobe sand in a warm and humid climatic setting and is the subject of one of the few other detailed diagenetic studies of these types of deposits (Hendry et al. 1999). Reef development occurred contemporaneously with siliciclastic influx, resulting in both admixing and interbedding of mixed carbonate–clastic and siliciclastic lithologies (Hendry et al. 1999; Burton 2003; Lokier et al. 2009). Reef demise is attributed to influx of siliciclastic sediments, now forming low-permeability strata that overlie the Calders reef (Hendry et al. 1999). The Calders reef, like the Samarinda carbonates, was stabilized pervasively early in its diagenetic history via meteoric phreatic to shallow burial diagenesis under the influence of continent-

derived fluids in a confined aquifer system (Hendry et al. 1999). Continental waters with an upland source, indicated by $\delta^{18}O$ SMOW values of -7.9 to -9.0‰, were channeled through the reef by adjacent siliciclastic units and the low-permeability overlying strata. High $\delta^{13}C$ values indicate that marine bicarbonate was sourced from aragonite dissolution along the meteoric-water flow path. This flow was, however, not influenced by the soil zone (Hendry et al. 1999). This pervasive early stabilization and cementation, linked to aquifer flow, appear to be essential elements of conceptual models for diagenesis of humid tropical coastal carbonates (Fig. 3.11; cf. Moore 2001). Nonetheless, the late diagenetic history of the Calders reef differs markedly from the Samarinda patch reefs associated with a postdepositional shift in climate towards more seasonal and arid conditions (Cavagnetto and Anadón 1996). Limited aquifer recharge resulting from an arid climatic shift facilitated late-stage cementation by marine fluids driven off from compacting basinal marls and evaporites at Calders (Hendry et al. 1999; Taberner et al. 2002).

3.7.3 Comparisons with Humid, Temperate Coastal Carbonates

Pliocene limestones (the Te Aute Formation) from the eastern North Island of New Zealand are nontropical, cool-water, skeletal carbonate deposits (Nelson et al. 2003; Caron et al. 2005). Perhaps paradoxically, these coastal cool-water limestones provide further analogs to the Samarinda carbonates; the Te Aute Formation developed as near-shore shelf carbonates in a predominantly siliciclastic setting adjacent to a large elevated continental landmass. The limestones of the Te Aute Formation developed in two settings: (1) under strong, high-energy tidal flow, and (2) with weaker tidal currents, resulting in fine-grained siliciclastic–carbonate admixtures (Beu 1995). The primary low-Mg calcite mineralogy of the cool-water skeletal carbonates contrasts with the more aragonite-rich tropical Samarinda carbonates. However, aragonite locally constitutes 10–60% of the limestones (Hood and Nelson 1996; Nelson et al. 2003; Caron and Nelson 2009). Differential tilting and uplift of the limestones in basin-margin areas allowed temporally and spatially variable contact between the limestone and recharging meteoric waters (Kamp and Nelson 1988; Dodd and Nelson 1998; Nelson et al. 2003). Despite this variable influence of meteoric fluids, and the dominance of metastable low-Mg calcite mineralogy at Te Aute (Caron and Nelson 2009), the aragonite-rich sections of the

Te Aute Formation were strongly affected by selective meteoric dissolution, and, to a lesser degree, neomorphism of aragonite provided a shallow source of carbonate for calcite cements with depleted (meteoric) stable-isotope composition. In comparison, the Samarinda carbonates were stabilized and calcitized by meteoric groundwater fluid flux providing carbonate in solution with a rock-derived, rather than a soil-zone-derived, carbon isotope signature.

3.7.4 Comparisons with Subtropical Arid Coastal Carbonates

Although subtropical arid coastal carbonates are well known from areas such as the Mediterranean and the Red Sea, the diagenesis of these carbonates is not as extensively studied as their sedimentology or stratigraphy (Esteban 1996). The diagenetic characteristics of these arid systems show major differences from humid tropical coastal deposits. Upper Miocene deposits of the Mediterranean region and Middle Miocene strata of the Red Sea include subtropical arid carbonates (Hayward 1982; Burchette 1988; Santisteban and Taberner 1988; Sun and Esteban 1994; Esteban 1996; Burton 2003). Many of these carbonates developed on marginal-marine high-energy fan-delta systems, resulting in intercalated wedges of pure carbonates and siliciclastic sediments due to periodic flash-flood-related influx of terrigenous siliciclastics (Santisteban and Taberner 1988; Wilson and Lokier 2002; Burton 2003). Poor sorting of the intercalated siliciclastics results in limited development of high-permeability aquifers. In contrast with humid equatorial carbonates, the diagenesis of subtropical arid carbonate systems commonly is influenced by flushing of hypersaline brines, leading to extensive dolomitization (Sun 1992; Sun and Esteban 1994; Esteban 1996). Carbonates developed in the semiarid climate of the Lower and Middle Miocene of the Mediterranean show evidence for diagenetic alteration by meteoric fluids. However, unlike the pervasive early stabilization evident in the equatorial humid coastal systems, extensive meteoric leaching and complete dissolution of skeletal aragonite occurs in pure carbonates associated with fan-delta sediments (Burton 2003). Drusy meteoric cements may partially fill primary and secondary porosity, and preserved porosity may be as high as 20–55% (Burton 2003). The Samarinda carbonates are extensively stabilized and cemented by aquifer flow. The development of subtropical carbonates on, and encasement by, poor-aquifer-quality units likely results in nonpervasive and

poorly developed meteoric groundwater flow paths, especially when coupled with an arid climatic setting. Even with preferred flow units, due to the decreased volumes of water flux in subtropical arid coastal carbonates, meteoric aquifer-related stabilization of aragonite is limited and there is good potential for porosity preservation due to limited cementation (cf. James and Choquette 1990; Sun and Esteban 1994).

3.7.5 Conceptual Diagenetic Model of Delta-Associated Carbonates in Humid Tropical Settings

The interpretation of the diagenetic history of patch reefs of this study, as with that of other warm, humid tropical coastal examples (Hendry et al. 1999), suggests a model of continental aquifer flow driving early pervasive stabilization (Fig. 3.11). For the Samarinda carbonates, the lack of subaerial exposure due to early burial by siliciclastics, the presence of permeable siliciclastic units in association with the reefs adjacent to a large landmass, and the humid equatorial climate are the factors contributing to stabilization and pervasive cementation of the reefs. Other carbonates developed in similar humid coastal settings with high siliciclastic influx and, most importantly, continental-aquifer influence also include evidence of pervasive stabilization and calcitization (Ali 1995; Netherwood and Wright 1992; Hook and Wilson 2003; Wilson 2012). Factors that result in less pervasive stabilization in humid coastal carbonates are: (1) high original primary porosity linked to high depositional energy, (2) more common calcitic components, and (3) localized or limited aquifer flow (Hood and Nelson 1996; Nelson et al. 2003; Caron and Nelson 2009).

3.8 Conclusions

3.8.1 Diagenesis

Study of Neogene siliciclastic-influenced patch reefs in Borneo reveals that both pervasive early stabilization of reef components from aragonite to low-Mg calcite and calcite cementation are key diagenetic features of these coastal carbonates from the humid tropics. The early stabilization of reef components and extensive

cementation are attributed to the reefs being flushed by primarily undersaturated meteoric water. Depleted oxygen stable-isotope data indicate a continental meteoric, upland source for the precipitating fluids with a lesser influence from trapped marine fluids expelled with increasing burial. Early diagenesis occurred predominantly in meteoric to shallow-burial environments, with the exception of an initial phase of grain micritization under marine conditions. Late-stage diagenetic processes of fracturing and cementation (also related to aquifer-driven flow) are inferred to have occurred at burial depths of < 1000 m and at temperatures of up to 53 °C prior to chemical compaction. Overall, the diagenesis of the Samarinda patch reefs is inferred to be controlled dominantly by fluid flow from a continental aquifer, one not directly influenced by "soil-zone" processes (as indicated by generally high $\delta^{13}C$), that caused early stabilization and cementation.

3.8.2 Controls on Diagenesis

The diagenesis of these patch reefs from equatorial "ever-wet" climatic settings are strongly controlled by basin-margin paleohydrology. Notably, continental aquifer flow, which drove shallow subsurface flow and early pervasive stabilization of reef components, was driven by the humid "ever-wet" climatic conditions associated with extensive Cenozoic tectonic uplift. Early stabilization and cementation are developed in other carbonates in similar humid mixed carbonate–siliciclastic successions, with large adjacent landmasses, in which extensive meteoric phreatic to shallow-burial fluid flow is the dominant diagenetic process. These findings are of particular relevance to SE Asia, with widespread mixed carbonate–siliciclastic systems developed in coastal settings with a humid equatorial climate, in which models generated in other regions cannot easily be applied.

3.9 Acknowledgments

This research forms a part of Rob Madden's PhD studies, supervised by Moyra Wilson, at Curtin University. Wilson collected samples whilst a member of the SE Asia Research Group at Royal Holloway, University of London. We gratefully acknowledge the support of the SEARG, its funding companies, the Geological Survey of Indonesia, LASMO, John Chambers, and Harry Alam, who made

fieldwork possible. Brain Rosen, Marcelle Fadel, and Ted Finch assisted with paleontological and biostratigraphic input. We thank Francis Witkowski and Neil Holloway (both at Royal Holloway) for help in running the cathodoluminescent analysis, and for producing the thin sections, respectively. Tony Fallick and Terry Donnelly assisted in running the stable-isotope analyses at SUERC, East Kilbride, and Grzegorz Skrzypek at the University of Western Australia, through the John De Laeter Centre, assisted in further stable-isotope work. Frazer Fallons at Genalysis, Perth, WA, helped in the trace-element and major-element study. The constructive reviews of Gene Rankey, Elias Samankassou, Vincent Caron, and an anonymous reviewer are gratefully acknowledged.

3.10 References

ALAM, H., PATERSON, D.W., SYARIFUDDIN, N., BUSONO, I., and CORBIN, S.G., 1999, Reservoir potential of carbonate rocks in the Kutai Basin region, east Kalimantan, Indonesia: Journal of Asian Earth Sciences, v. 17, p. 203-214.

ALI, M., 1995, Carbonate cement stratigraphy and timing of diagenesis in a Miocene mixed carbonate–clastic sequence, offshore Sabah, Malaysia — constraints from cathodoluminescence, geochemistry and isotope studies: Sedimentary Geology, v. 99, p. 191-214.

ALLAN, J.R., and MATTHEWS, R.K., 1982, Isotope signatures associated with early meteoric diagenesis: Sedimentology, v. 29, p. 797-817.

ALLEN, G.P., and CHAMBERS, J.L.C., 1998, Sedimentation in the Modern and Miocene Mahakam Delta: Indonesian Petroleum Association, Jakarta, Field Trip Guidebook, 236 p.

ANDERSON, T.F., and ARTHUR, M.A., 1983, Stable isotopes of oxygen and carbon and their application to sedimentologic and paleoenvironmental problems, *in* Arthur, M.A., Anderson, T.F., Kaplan, I.R., Veizer, J., and Land, L.S., eds., Stable Isotopes in Sedimentary Geology: SEPM, Short Course no. 10, p. 1-1 - 1-151.

ANDREWS, J.E., CHRISTIDIS, S., AND DENNIS, P.F., 1997, Assessing mineralogical and geochemical heterogeneity in the sub 63 micron size fraction of Holocene lime muds: Journal of Sedimentary Research, v. 67, p. 531-535.

BATHURST, R.G.C., 1966, Boring algae, micrite envelopes and lithification of molluscan biosparites: Geological Journal, v. 5, p. 15 - 32.

BEU, A.G., 1995, Pliocene limestones and their scallops: Lower Hutt, New Zealand, Institute of Geological & Nuclear Sciences Limited, Monograph 10, 243 p.

BJØRLYKKE, K., 1993, Fluid flow in sedimentary basins: Sedimentary Geology, v. 86, p. 137-158.

BOUDAGHER-FADEL, M.K., and WILSON, M.E.J., 2000, A revision of some larger foraminifera of the Miocene of southeast Kalimantan: Micropaleontology, v. 46, p. 153-165.

BOWEN, G.J., and WILKINSON, B., 2002, Spatial distribution of $\delta^{18}O$ in meteoric precipitation: Geology, v. 30, p. 315-318.

BURCHETTE, T.P., 1988, Tectonic control on carbonate platform facies distribution and sequence development: Miocene, Gulf of Suez: Sedimentary Geology, v. 59, p. 179-204.

BURTON, L.M., 2003, Carbonate–siliciclastic interactions: Tertiary examples from Spain: unpublished Ph.D. thesis; The University of Durham, 396 p.

CARNELL, A.J.H., and WILSON, M.E.J., 2004, Dolomites in SE Asia–varied origins and implications for hydrocarbon exploration, *in* Braithwaite, C.J.R., Rizzi, G., and Darke, G., eds., The Geometry and Petrogenesis of Dolomite Hydrocarbon Reservoirs: Geological Society of London, Special Publication 235, p. 255 - 300.

CARON, V., and NELSON, C.S., 2009, Diversity of neomorphic fabrics in New Zealand Plio-Pleistocene cool-water limestones: Insights into aragonite alteration pathways and controls: Journal of Sedimentary Research, v. 79, p. 226-246.

CARON, V., NELSON, C.S., and KAMP, P.J.J., 2005, Sequence stratigraphic context of syndepositional diagenesis in cool-water shelf carbonates: Pliocene limestone, New Zealand: Journal of Sedimentary Research, v. 75, p. 231-250.

CAVAGNETTO, C., and ANADÓN, P., 1996, Preliminary palynological data on floristic and climatic changes during the Middle Eocene-Early Oligocene of the eastern Ebro Basin, northeast Spain: Review of Palaeobotany and Palynology, v. 92, p. 281-305.

CLARI, P.A., and MARTIRE, L., 1996, Interplay of cementation, mechanical compaction, and chemical compaction in nodular limestones of the Rosso

Ammonitico Veronese (Middle–Upper Jurassic, Northeastern Italy): Journal of Sedimentary Research, v. 66, p. 447 - 458.

CLOKE, I.R., MOSS, S.J., and CRAIG, J., 1999, Structural controls on the evolution of the Kutai Basin, East Kalimantan: Journal of Asian Earth Sciences, v. 17, p. 137-156.

DODD, J.R., and NELSON, C.S., 1998, Diagenetic comparisons between non-tropical Cenozoic limestones of New Zealand and tropical Mississippian limestones from Indiana, USA: Is the non-tropical model better than the tropical model?: Sedimentary Geology, v. 121, p. 1-21.

ESTEBAN, M., 1996, An overview of Miocene reefs from Mediterranean areas: general trends and facies models, *in* Franseen, E.K., Esteban, M., Ward, W., and Rouchy, J.M., eds., Models for Carbonate Stratigraphy from Miocene Reef Complexes of Mediterranean regions: SEPM, Concepts in Sedimentology and Paleontology no. 5, p. 3-53.

FRANKS, P.C., 1969, Nature, origin, and significance of cone-in-cone structures in the Kiowa Formation (Early Cretaceous) North-Central Kansas: Journal of Sedimentary Petrology, v. 39, p. 1438 - 1454.

FRIEDMAN, I., and O'NEIL, J.R., 1977, Compilation of stable isotope fractionation factors of geochemical interest, *in* Fleischer, M., ed., Data of Geochemistry: U.S. Geological Survey, Professional Paper 440-K, p. 1-12.

GALLOWAY, W.E., 1984, Hydrogeologic regimes of sandstone diagenesis, *in* McDonald, D.A., and Surdam, R.C., eds., Clastic Diagenesis: American Association of Petroleum Geologists, Memoir 37, p. 3 - 13.

GUNTHER, A., 1990, Distribution and bathymetric zonation of shell boring endoliths in recent reef and shelf environments: Cozumel, Yucatan (Mexico): Facies, v. 22, p. 233 - 262.

HALL, R., 1996, Reconstructing Cenozoic SE Asia, *in* Hall, R., and Blundell, D.J., eds., Tectonic Evolution of Southeast Asia: Geological Society of London, Special Publication 106, p. 153-184.

HALL, R., 2002a, Cenozoic geological and plate tectonic evolution of SE Asia and the SW Pacific: computer-based reconstructions, model and animations: Journal of Asian Earth Sciences, v. 20, p. 353-431.

HALL, R., 2002b, SE Asian heat flow: Call for new data: Indonesian Petroleum Association Newsletter, v. 4, p. 20-21.

HALL, R., and NICHOLS, G., 2002, Cenozoic sedimentation and tectonics in Borneo: climatic influences on orogenesis, *in* Jones. S.J., and Frostick, L.E., eds., Sediment Flux to Basins: Causes, Controls and Consequences: Geological Society London, Special Publication 191, p. 5-22.

HAMILTON, W., 1979, Tectonics of the Indonesian region: U.S. Geological Survey, Professional Paper 1078, 345 p.

HAYWARD, A.B., 1982, Coral reefs in a clastic sedimentary environment: Fossil (Miocene, S.W. Turkey) and Modern (Recent, Red Sea) analogues: Coral Reefs, v. 1, p. 109 - 114.

HENDRY, J.P., TABERNER, C., MARSHALL, J.D., PIERRE, C., and CAREY, P.F., 1999, Coral reef diagenesis records pore-fluid evolution and paleohydrology of a siliciclastic basin margin succession (Eocene South Pyrenean foreland basin, northeastern Spain): Geological Society of America, Bulletin, v. 111, p. 395-411.

HIRD, K., and TUCKER, M.E., 1988, Contrasting diagenesis of two Carboniferous oolites from South Wales: a tale of climatic difference: Sedimentology, v. 35, p. 587 - 602.

HOOD, S.D., and NELSON, C.S., 1996, Cementation scenarios for New Zealand Cenozoic nontropical limestones: New Zealand Journal of Geology and Geophysics, v. 39, p. 109-122.

HOOK, J., and WILSON, M.E.J., 2003, Stratigraphic relationships of a Miocene mixed carbonate–siliciclastic interval in the Badak field, East Kalimantan, Indonesia: 29th Indonesian Petroleum Association, Annual Convention, Proceedings, p. 147-161.

HOSKIN, C.M., 1968, Magnesium and strontium in mud fraction of recent carbonate sediment, Alacran Reef, Mexico: American Association of Petroleum Geologists, Bulletin, v.52 p. 2170-2177.

HUSSEINI, S.I., and MATTHEWS, R.K., 1972, Distribution of high-magnesium calcite in lime muds of the Great Bahama Bank: diagenetic implications: Journal of Sedimentary Petrology, v. 42, p. 179-182.

INSALACO, E., 1998, The descriptive nomenclature and classification of growth fabrics in fossil scleractinian reefs: Sedimentary Geology, v. 118, p. 159-186.

JAMES, N.P., 1997, The cool-water carbonate depositional realm, *in* James, N.P., and Clarke, J.D.A., eds., Cool-Water Carbonates: SEPM, Special Publication 56, p. 1–22.

JAMES, N.P., and CHOQUETTE, P.W., 1990, Limestones: The meteoric diagenetic environment, *in* McIlreath, I.A., and Morrow, D.W., eds., Diagenesis: Geoscience Canada Reprint Series 4: Toronto, Geological Association of Canada, p. 35 - 74.

KAMP, P.J.J., and NELSON, C.S., 1988, Nature and occurrence of modern and Neogene active margin limestones in New Zealand: New Zealand Journal of Geology and Geophysics, v. 31, p. 1-20.

LAND, L.S., 1983, The applications of stable isotopes to studies of the origin of dolomite and to problems of diagenesis of clastic sediments, *in* Arthur, M.A., Anderson, T.F., Kaplan, I.R., Veizer, J., and Land, L.S., eds., Stable Isotopes in Sedimentary Geology: SEPM, Short Course no. 10, p. 4-1 – 4-22.

LARCOMBE, P., and WOOLFE, K.J., 1999, Terrigenous sediments as influences upon Holocene near shore coral reefs, central Great Barrier Reef, Australia: Australian Journal of Earth Sciences, v. 46, p. 141-154.

LOKIER, S.W., WILSON, M.E.J., and BURTON, L.M., 2009, Marine biota response to clastic sediment influx: A quantitative approach: Palaeogeography, Palaeoclimatology, Palaeoecology, v. 281, p. 25-42.

MACHEL, H.G., 2004, Concepts and models of dolomitization: A critical reappraisal, *in* Braithwaite, C.J.R., Rizzi, G., and Darke, G., eds., The Geometry and Petrogenesis of Dolomite Hydrocarbon Reservoirs: Geological Society of London, Special Publication 235, p. 7 - 63.

MADDEN, R.H.C., 2008, The effect of diagenesis on the reservoir quality of mixed carbonate–siliciclastics from Sabah, Borneo: Unpublished M.Sci. thesis, The University of Durham, 78 p.

MCBRIDE, E.F., PICARD, M.D., and MILLIKEN, K.L., 2003, Calcite-cemented concretions in Cretaceous sandstone, Wyoming and Utah, U.S.A: Journal of Sedimentary Research, v. 73, p. 462 - 483.

MILLIMAN, J.D., 1974, Marine Carbonates: Berlin, Springer-Verlag, 375 p.

MOORE, C.H., 2001, Carbonate Reservoirs, Porosity Evolution and Diagenesis in a Sequence Stratigraphic Framework: Amsterdam, Elsevier, 444 p.

MORAD, S., 1998, Carbonate cementation in sandstones: distribution patterns and geochemical evolution, *in* Morad, S, ed., Carbonate Cementation in Sandstones: International Association of Sedimentologists Special Publication 26, p. 1-26.

MORAD, S., KETZER, J.M., and ROS, L.F.D., 2000, Spatial and temporal distribution of diagenetic alterations in siliciclastic rocks: implications for mass transfer in sedimentary basins: Sedimentology, v. 47, p. 95-120.

MORRISON, J.O., and BRAND, U., 1986, Geochemistry of recent marine invertebrates: Geoscience Canada, v. 13, p. 237-254.

MOSS, S.J., and CHAMBERS, J.L.C., 1999, Tertiary facies architecture in the Kutai Basin, Kalimantan, Indonesia: Journal of Asian Earth Sciences, v. 17, p. 157-181.

MOSS, S.J., CHAMBERS, J., CLOKE, I., SATRIA, D., ALI, J.R., BAKER, S., MILSOM, J., and CARTER, A., 1997, New observations on the sedimentary and tectonic evolution of the Tertiary Kutai Basin, East Kalimantan, *in* Fraser, A.J., Matthews, S.J. and Murphy, R.W., eds., Petroleum Geology of Southeast Asia: Geological Society of London, Special Publication 126, p. 395 - 416.

MOUNT, J.F., 1984, Mixing of siliciclastic and carbonate sediments in shallow shelf environments: Geology, v. 12, p. 432-435.

NELSON, C.S., WINEFIELD, P.R., HOOD, S.D., CARON, V., PALLENTIN, A., AND KAMP, P.J.J., 2003, Pliocene Te Aute limestones, New Zealand: expanding concepts for cool-water shelf carbonates: New Zealand Journal of Geology and Geophysics, v. 46, p. 407-424.

NETHERWOOD, R., and WIGHT, A., 1992, Structurally-controlled, linear reefs in a Pliocene delta-front setting, Tarakan Basin, Northeast Kalimantan, *in* Siemers, C.T., Longman, M.W., Park, R.K., and Kaldi, J.G., eds., Carbonate Rocks and Reservoirs of Indonesia: Indonesian Petroleum Association, Core Workshop, Notes 1, Ch. 3, p. 3-1 – 3-37.

NICOLAIDES, S., and WALLACE, M.W., 1997, Pressure dissolution and cementation in an Oligo-Miocene non-tropical limestone (Clifton Formation), Otway Basin, Australia, *in* James, N.P. and Clarke, J.A.D., eds., Cool Water Carbonates: SEPM, Special Publication 56, p. 249 - 261.

PERRY, C.T., 1999, Biofilm-related calcification, sediment trapping and constructive micrite envelopes: a criterion for the recognition of ancient grass-bed environments?: Sedimentology, v. 46, p. 33 - 45.

PURSER, B.H., 1978, Early diagenesis and the preservation of porosity in Jurassic limestones: Journal of Petroleum Geology, v. 50, p. 1149 - 1168.

RAILSBACK, L.B., 1993a, Contrasting styles of chemical compaction in the Upper Pennsylvanian Dennis Limestone in the Midcontinent Region, U.S.A: Journal of Sedimentary Petrology, v. 63, p. 61- 72.

RAILSBACK, L.B., 1993b, Lithologic controls on morphology of pressure-dissolution surfaces (stylolites and dissolution seams) in Paleozoic carbonate rocks from the Mideastern United States: Journal of Sedimentary Petrology, v. 63, p. 513 - 522.

RICKETTS, B.D., CARON, V., and NELSON, C.S., 2004, A fluid flow perspective on the diagenesis of Te Aute limestones: New Zealand Journal of Geology and Geophysics, v. 47, p. 823 - 838.

ROBERTS, H.H., and SYDOW, J., 1996, The offshore Mahakam Delta: Stratigraphic response of Late Pleistocene-to-Modern sea level cycle: 25th Indonesian Petroleum Association, Annual Convenetion Proceedings, p. 147-161.

ROBERTS, H.H., AMARON, P., and PHIPPS, C.V., 1988, Morphology and sedimentology of *Halimeda* bioherms from Eastern Java Sea (Indonesia): Coral Reefs, v. 6, p. 61-172.

SALLER, A.H., REKSALEGORA, S., and BASSANT, P., 2010, Sequence stratigraphy and growth of shelf margin and middle shelf carbonates, *in* Morgan, W.A., George, A.D., Harris, P.M., Kupecz, J.A. and Sarg, J.F., eds., Cenozoic Carbonates of Australasia: SEPM, Special Publication 95, p. 147 – 174.

SANTISTEBAN, C., and TABERNER, C., 1988, Sedimentary models of siliciclastic deposits and coral reef interrelation, *in* Doyle, J.L., and Roberts, H.H., eds., Carbonate–Clastic Transitions: Amsterdam, Elsevier, Developments in Sedimentology, v. 42, p. 35–76.

SKRZYPEK, G., and PAUL, D., 2006, $\delta^{13}C$ analysis of calcium carbonate: comparison between the GasBench and elemental analyzer techniques: Rapid Communications In Mass Spectrometry, v. 20, p. 2915 - 2920.

SUN, S.Q., 1992, Skeletal aragonite dissolution from hypersaline seawater: a hypothesis: Sedimentary Geology, v. 77, p. 249–257.

SUN, S.Q., and ESTEBAN, M., 1994, Paleoclimatic controls on sedimentation, diagenesis, and reservoir quality: Lessons from Miocene carbonates: American Association of Petroleum Geologists, Bulletin, v. 78, p. 519 - 543.

TABERNER, C., MARSHALL, J.D., HENDRY, J.P., PIERRE, C., and THIRLWALL, M.F., 2002, Celestite formation, bacterial sulphate reduction and carbonate cementation of Eocene reefs and basinal sediments (Igualada, NE Spain): Sedimentology, v. 49, p. 171-190.

VAN DE WEERD, A.A., and ARMIN, R.A., 1992, Origin and evolution of the Tertiary hydrocarbon-bearing basins in Kalimantan (Borneo), Indonesia: American Association of Petroleum Geologists, Bulletin, v. 76, p. 1778-1803.

VEIZER, J., 1983, Chemical diagenesis of carbonates: Theory and application of trace element techniques, *in* Arthur, M.A., Anderson, T.F., Kaplan, I.R., Veizer, J., and Land, L.S., eds., Stable Isotopes in Sedimentary Geology: SEPM, Short Course no. 10*,* p. 3-1 - 3-100.

WANLESS, H.R., 1979, Limestone response to stress: pressure solution and dolomitization: Journal of Sedimentary Petrology, v. 49, p. 437 - 462.

WARREN, J., 2000, Dolomite: Occurrence, evolution and economically important associations: Earth-Science Reviews, v. 52, p. 1 - 81.

WILSON, M.E.J., 2002, Cenozoic carbonates in Southeast Asia: implications for equatorial carbonate development: Sedimentary geology, v. 147, p. 295-428.

WILSON, M.E.J., 2005, Development of equatorial delta-front patch reefs during the Neogene, Borneo: Journal of Sedimentary Research, v. 75, p. 114-133.

WILSON, M.E.J., 2012, Equatorial carbonates: an earth systems approach: Sedimentology, v. 59, p. 1-31.

WILSON, M.E.J., and EVANS, M.J., 2002, Sedimentology and diagenesis of Tertiary carbonates on the Mangkalihat Peninsula, Borneo: implications for subsurface reservoir quality: Marine and Petroleum Geology, v. 19, p. 873-900.

WILSON, M.E.J., and HALL, R., 2010, Tectonic influences on SE Asian carbonate systems and their reservoir development, *in* Morgan, W.A., George, A.D., Harris, P.M., Kupecz, J.A. and Sarg, J.F., eds., Cenozoic Carbonates of Australasia: SEPM, Special Publication no. 95, p. 122-149.

WILSON, M.E.J., and LOKIER, S.W., 2002, Siliciclastic and volcaniclastic influences on equatorial carbonates: insights from the Neogene of Indonesia: Sedimentology, v. 49, p. 583-601.

WILSON, M.E.J., and MOSS, S.J., 1999, Cenozoic palaeogeographic evolution of Sulawesi and Borneo: Palaeogeography, Palaeoclimatology, Palaeoecology, v. 145, p. 303-337.

WILSON, M.E.J., CHAMBERS, J.L.C., EVANS, M.J., MOSS, S.J., and NAS, D.S., 1999, Cenozoic carbonates in Borneo: case studies from northeast Kalimantan: Journal of Asian Earth Sciences, v. 17, p. 183-201.

WITKOWSKI, F.W., BLUNDELL, D.J., GUTTERIDGE, P., HORBURY, A.D., OXTOBY, N.H., and QING, H., 2000, Video cathodoluminescence microscopy of diagenetic cements and its applications: Marine and Petroleum Geology, v. 17, p. 1085 - 1093.

WOOLFE, K.J., and LARCOMBE, P., 1999, Terrigenous sedimentation and coral reef growth: a conceptual framework: Marine Geology, v. 155, p. 331-345.

Chapter 4

DIAGENESIS OF A SE ASIAN CENOZOIC CARBONATE-PLATFORM MARGIN AND ITS ADJACENT BASINAL DEPOSITS

Robert H.C. Madden and Moyra E.J. Wilson

Department of Applied Geology, Curtin University, GPO Box U1987, Perth, Western Australia 6845, Australia.
E-mails: r.madden@dunelm.org.uk, m.wilson@curtin.edu.au

Abstract

This study provides insights into the diagenesis of a SE Asian Tertiary carbonate platform and the variations in alteration that occur across platform top, margin, slope and adjacent basinal deposits. A petrographic, cathodoluminescent and stable isotopic study allowed evaluation of the diagenesis of the Kedango Limestone of Borneo. The Kedango Carbonate Platform developed as a predominantly low to moderate energy system in the semi-enclosed marine embayment of the Kutai Basin during the Eocene to Miocene. Early alteration through pervasive micritisation and minor isopachous fringing, syntaxial overgrowth and bladed to radiaxial cements was due to marine diagenesis on the basis of limited, relatively enriched stable-isotope compositions and non-luminescent cathodoluminescent (CL) characters. Minor early marine cementation formed just in the shallowest-platform top and margin deposits, and was likely promoted in high energy portions of the platform due to wave and/or current activity. Dissolution cavities, banded calcite cements with variable CL characteristics and depleted stable-isotope compositions, micritic sediment infiltration and alveolar textures are minor features, but together are indicative of localised subaerial emergence and meteoric diagenesis. The most prevalent and pervasive diagenetic feature of the deposits is the neomorphic alteration and replacement of metastable bioclasts and micritic matrix, together with contiguous calcitisation of pore spaces.

Burial fluids with a marine character are inferred as the parent diagenetic fluid, since stable-isotope compositions for the neomorphic spar is largely consistent with precipitation from SE Asian Oligocene Miocene seawater in a burial environment. Tectonic subsidence, the protected semi-enclosed marine embayment setting, and probably terrestrial runoff, together with component variability reflecting local environmental variations, are inferred to have been major controlling influences on the diagenesis of the Kedango Platform. Variations in diagenesis across bathyal, slope and shallow-platform deposits of the Kedango Limestone are not as marked as in other platforms from the region.

4.1 Introduction

The diagenesis and development of open marine Tertiary carbonate platforms from the humid equatorial tropics of SE Asia are relatively well documented, since many comprise hydrocarbon reservoirs in the subsurface (Epting, 1980; Fulthorpe and Schlanger, 1989; Grötsch and Mercadier, 1999; Wilson and Hall, 2010). However the diagenetic variability across platform flank and contemporaneous bathyal deposits, particularly from low to moderate energy carbonate platforms is less well known. In this study a diagenetic assessment of shallow-water platform, slope and bathyal deposits is presented from the Kedango Carbonate Platform. The Kedango Limestone developed as an Eocene to Miocene platform within the semi-enclosed Kutai Basin in Eastern Borneo (Fig. 4.1; Wilson et al., 2012). The hypotheses tested here are that the diagenesis: (1) of bathyal, slope and shallow-platform deposits will vary associated with the different syn-, and post-depositional processes affecting the different environments, and (2) will be influenced by the setting of the platform in a tectonically active, subsiding marine embayment. Also, that there may be significant differences in diagenetic alteration of the Kedango Limestone from other carbonate platforms developed in more open-oceanic and/or non-subsiding settings within SE Asia. The results of this study offer insights into patterns of diagenesis across humid equatorial carbonate platform environments from basin to platform margin deposits that may have regional analogues as well as implications for hydrocarbon exploration.

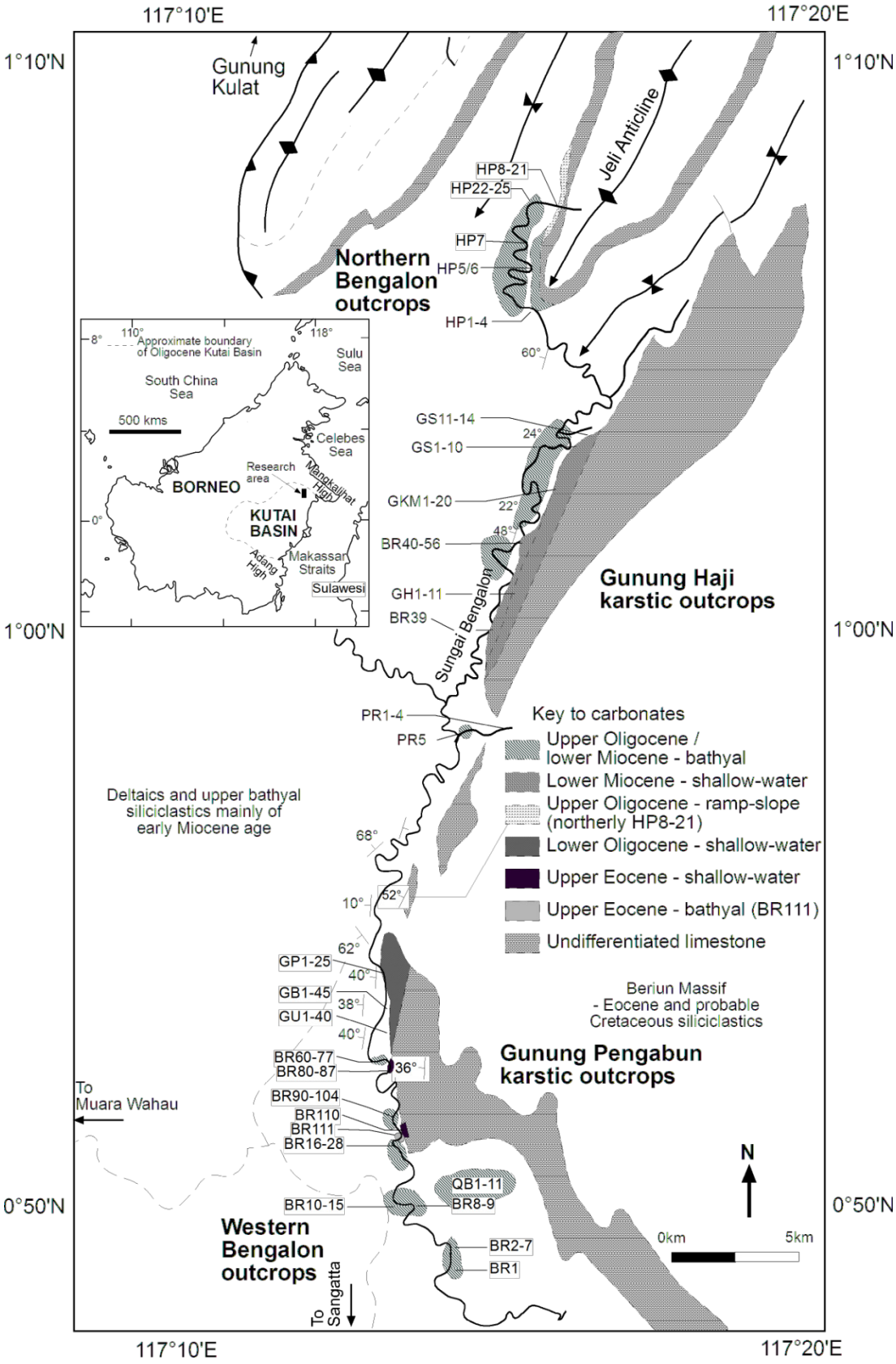

Figure 4.1. Map of the study area, showing locations of studied sections, ages and inferred depositional environments. Inset map of Borneo shows the location of the research area within the Kutai Basin (from Wilson et al., 2012).

Extensive Cenozoic carbonate platforms developed on structural highs away from areas of clastic input on the northern margins of the Kutai Basin in Eastern Borneo (Moss and Chambers, 1999; Wilson et al., 1999; Wilson and Hall, 2010; Wilson, 2011). Carbonates of the Kedango Limestone outcrop extensively in and around the Bengalon Area in East Borneo, with the regional context, sedimentology and biostratigraphy of the formation previously documented (Fig. 4.1; Moss and Chambers, 1999; Wilson et al., 1999; Wilson et al., 2012). The present study expands on these earlier results, focusing on the diagenesis of the deposits through a multidisciplinary outcrop, petrographic, cathodoluminescent and geochemical study. The most influential controls on depositional development and variability along the western margin of the Kedango carbonate platform were tectonic subsidence, active faulting, the protected semi-enclosed marine embayment setting, and probably terrestrial runoff (Wilson et al., 2012). As discussed below, these same factors also had a major impact on diagenesis, together with platform/basin hydrology and component variability reflecting local environmental variations.

4.2 Geological Setting

The Kedango Limestone crops out along the eastern side of the Bengalon River in a largely siliciclastic area close to the northern margin of the Kutai Basin (Wilson et al., 1999; 2012). Tertiary carbonates are common around the margins of the Kutai Basin and the associated widespread basinal area that included Western Sulawesi, the East Java Sea, and much of Eastern Borneo (van de Weerd and Armin, 1992; Wilson et al., 2000; Wilson, 2002; Sharaf et al., 2005). The Kutai Basin developed as one of a series of basins around the margins of the Eurasian continental crust during the Paleogene (van de Weerd and Armin, 1992; Hall, 1996; Moss and Chambers, 1999). The exact cause and timing of regional basin formation is still debated, but many authors infer that the Kutai Basin has rift-related extensional or transtensional origins (van de Weerd and Armin, 1992; Alam et al., 1999; Moss and Chambers, 1999). By the end of the Eocene, extension within the Makassar Strait and in Eastern Borneo had likely ceased, and regional subsidence resulted in marine flooding across the basinal depocentre (Moss et al., 1997; Moss and Chambers, 1999).

Throughout the late Paleogene, extensive carbonate deposition was near-continuous on faulted basement highs at the northern (e.g. the Taballar Formation on the Mangkalihat High) and southern (e.g., the Berai Limestone on the Adang Flexure) margins of the Kutai Basin (van de Weerd and Armin, 1992; Saller et al., 1993; Wilson and Evans, 2002). Shallow-water carbonate production also occurred on small-scale (tens of kilometres across) platforms surrounded by deeper waters largely isolated from siliciclastic influx, and as more localised and ephemeral areas (Moss and Chambers, 1999; Wilson et al., 1999; Wilson, 2002). The north-south trending Kedango Platform is one of these small-scale platforms, developed towards the northern margin of the Kutai Basin in a sheltered embayment setting (Wilson et al., 2012). However, there is uncertainty over whether the Kedango Platform was connected to siliciclastic shelves and land areas to the north and east (Wilson and Evans, 2002; Wilson et al., 2012). Post Miocene basin inversion (Cloke et al., 1999; Moss and Chambers, 1999) resulted in uplift, sedimentary unroofing, and for the Kedango Limestone subaerial exposure and associated tower karst development (Wilson et al., 2012).

A parallel study to this one discusses the Late Eocene to Early Miocene sedimentary evolution and facies of the 30 km long western margin of the >600 km thick Kedango Limestone, providing insights into the variability of a predominantly low to moderate energy platform margin (Wilson et al., 2012). The findings of the depositional study by Wilson et al. (2012) are summarised directly below and set the context for this diagenetic study.

To the east of the Bengalon River, the massive tower karst outcrops of Gunung (mountain) Kulat, Haji and Pengabun form north-south trending exposures of the Kedango Limestone. Both the depositional and diagenetic studies investigated shallow water carbonates forming the western side of Gunung Haji and Gunung Pengabun. The adjacent westerly platform margin and upper bathyal deposits were studied in well-bedded, several metre high outcrops from river and road cuttings in the Western Bengalon area (Fig. 4.1). To the north of Gunung Haji a thin carbonate succession is folded into a series of NNE-SSW trending anticline-syncline pairs in the Northern Bengalon area. The upper part of this carbonate succession was studied

in the northern reaches of the Bengalon River, in exposures of the western limb of the Jeli Anticline (Fig. 4.1).

The platform top deposits of the Kedango Limestone are composed dominantly of shallow-water bioclasts including larger and small benthic foraminifera, coralline algae and some corals mostly in a micritic matrix. During the Oligo-Miocene there was abundant reworking of both these shallow-water bioclasts and lithoclasts from along the ~30 km length of the western platform margin into the adjacent planktonic foraminifera-rich basinal deposits (Wilson et al., 2012). Eleven facies have been defined for the Kedango Limestone on the basis of components, textures and lithological features identified in outcrop and through petrography. These eleven facies have been grouped into four facies associations on the basis of their sedimentary textures and components. The sedimentology and environmental interpretations of these facies are discussed in Wilson et al (2012) and are summarised below:

- Bioclastic Facies Group - contains abundant whole, well-preserved and sometimes fragmented shallow marine bioclasts including corals, foraminifera, algae and molluscs mainly in packstones, grainstones, floatstones and rudstones. Deposition on a shallow-water platform to platform margin setting within the photic zone under normal marine conditions is inferred for most deposits, on the basis of well-preserved light dependant bioclasts such as larger benthic foraminifera and corals. Packstone and wackestone-floatstone textures were likely deposited under moderate to low energy conditions predominantly in shallow-photic depths on the basis of lithological textures and the range of shallow bioclasts. Samples with planktonic foraminifera that lack miliolids are interpreted as deeper photic zone deposits with an open oceanic influence. Packstone-grainstone textures are inferred to have been deposited under moderate to high energy shallow-photic conditions due to the varied bioclasts, their fragmentation and lithological textures. Bioclastic Facies dominate the karstic outcrops of Gunung Haji and Gunung Pengabun to the east of the Bengalon River.

- Mudstone-Wackestone Facies Group - contains few bioclasts and is dominated by micrite in carbonate mudstones, wackestones or floatstones. Mudstone-Wackestone Facies contain well-preserved shallow-marine bioclasts including corals, larger benthic foraminifera, imperforate foraminifera, molluscs, coralline algae, echinoderm plates and minor *Halimeda*. Poor sorting, an abundance of micritic matrix and light dependant bioclasts such as corals and larger benthic foraminifera are indicative of a dominantly low energy, normal marine environment, with deposition on a shallow to moderate photic depth platform. Mudstone-Wackestone Facies are interbedded with the Bioclastic Facies in the karstic outcrops at Gunung Haji and Gunung Pengabun.

- Planktonic Foraminifera Facies Group - contains abundant planktonic foraminifera (>20% and commonly >90% of the total bioclast content) in marls, shaley marls and wackestone-packstones. Marls contain >60-80% mixed clay and micrite content. Fragmented bioclasts including echinoderm debris and reworked shallow water bioclasts or siliciclastic grains may also be present. Planktonic Foraminifera Facies are inferred to have been deposited in open oceanic, bathyal to upper bathyal, slope or outer shelf settings on the basis of abundant planktonic foraminifera and diagnostic small benthic rotaliid foraminifera. Low energy conditions are inferred from the abundant clay and micritic matrix. Lithologies of the Planktonic Foraminifera Facies Group crop out to the south, west and north of the main karstic outcrops, largely in the Western and Northern Bengalon areas.

- Lithoclastic Facies Group - contains abundant reworked, up to 90 cm sized, lithoclasts (>10%) and commonly reworked unlithified shallow marine bioclasts in breccias and graded packstone-grainstones. Lithoclasts are dominated by those of the Bioclastic and Mudstone-Wackestone Facies Groups, although clasts of the Planktonic Foraminifera Facies Group and a range of siliciclastic clasts are also present, the later including arkosic sandstones, siltstones and chert. Reworked material therefore includes abraded shallow water bioclasts derived from the platform top, clasts from older siliciclastics underlying the platform carbonates and lithified slope and

shallow water carbonate clasts. Deposition in slope to bathyal depositional environments with reworking in calciturbidites, debris flows or modified grain flows was inferred from the commonly graded (fining or coarsening upwards) nature of the Lithoclastic Facies together with their interdigitation with Planktonic Foraminifera Facies. The common occurrence of reworked Bioclastic Facies lithologies indicates an erosional platform margin with reworking from the platform top. Lithoclastic Facies Group lithologies are interbedded with Planktonic Foraminifera Facies largely in the Western and Northern Bengalon outcrops.

4.3 Methods

Carbonates of the Kedango Limestone are exposed along the Bengalon River as low riverbank outcrops and massive tower karst. Good exposure allowed high resolution sampling, outcrop sedimentary logging, facies mapping and partial section correlation along the western platform margin and adjacent basinal deposits (Wilson et al., 2012). Twenty-three measured sections were logged and of the 283 samples collected 124 have been studied petrographically.

Lithological components, microfacies, diagenetic phases and the relative timing of diagenetic events were determined through thin-section petrography (Appendix D1 and Fig. 4.2). All carbonate lithologies were impregnated with blue epoxy resin to highlight porosity and half stained with Alizarin Red S and potassium ferricyanide for the identification of dolomites, ferroan and non-ferroan calcite (Dickson, 1965, 1966). The relative abundance of components and diagenetic phases were recorded semi-quantitatively (visual estimates; after Mazzullo and Graham, 1988). Facies nomenclature follows the textural classification scheme of Dunham (1962), modified by Embry and Klovan (1971), with components given in lithology names where they exceed 10-15%. Nomenclature on carbonate cement morphologies follows Flügel (2004). Cold cathodoluminescent (CL) microscopy study of 12 polished sections was via a Technosyn 8200 MkII luminoscope (after Witkowski, 2000). Samples for CL analysis were selected to investigate the range of coarse (>250 μm) cement phases present. Stable-isotope analysis ($\delta^{18}O$ and $\delta^{13}C$) was undertaken on 22 samples micro-drilled from the rock off-cut counterpart of the thin sections. Drilling

sites matched directly to the off-cuts, correspond to a range of depositional and diagenetic features identified in thin section. Drilled samples included a range of cements with varied morphologies and those filling fractures, bioclasts and matrix. Oxygen and carbon isotope analyses were run on a VG Isocarb automated system online to a VG Isogas Prism II isotope-ratio mass spectrometer. All data have been normalised, to NBS-19, which is the primary carbonate standard used to define the V-PDB scale ($\delta^{13}C$ = +1.95‰, $\delta^{18}O$ = -2.2‰). In addition, replicate analyses of an internal carbonate standard (Mab2b) were reproducible to ±0.1‰. An additional nine oxygen and carbon isotope analyses (samples with the prefix Madden) were run on a GasBench II system coupled online to a stable-isotope-ratio mass spectrometer in continuous flow (Skrzypek and Paul, 2006), with all data normalised to NBS-19 and reported relative to V-PDB; these analyses were undertaken at the University of Western Australia, Perth. External errors for $\delta^{18}O$ and $\delta^{13}C$ were ±0.1‰.

4.4 Diagenetic Characteristics

Although the age of the Kedango Limestone varies from Upper Eocene to Lower Miocene (Table 4.1), a broadly comparable set of diagenetic features is seen in many thin sections (Fig. 4.2 and Appendix D1). Depositional environments mentioned below are from Wilson et al. (2012). Figure 4.2 illustrates how the diagenetic features observed in individual samples (Appendix D1) relate to the measured sections of Wilson et al. (2012), and their inferred environments of deposition. Diagenetic features are described below in their relative order of formation, as inferred from petrographic study (Appendix D1 and Fig. 4.2).

Figure 4.2 (next page). Summary measured sedimentological sections for outcrops of the Kedango Limestone studied from the Bengalon Area showing key lithologies, their depositional environments and ages of sections. A generalised paragenetic scheme is given for each thin section studied, with diagenetic and cathodoluminescent features shown. Diagenetic features of individual thin sections are shown in general order of occurrence (left to right; oldest to youngest), with their CL features, where present, shown directly above or below. A comparable figure detailing finer-scale sedimentological attributes is given in Wilson et al. (2012) from which this figure is modified.

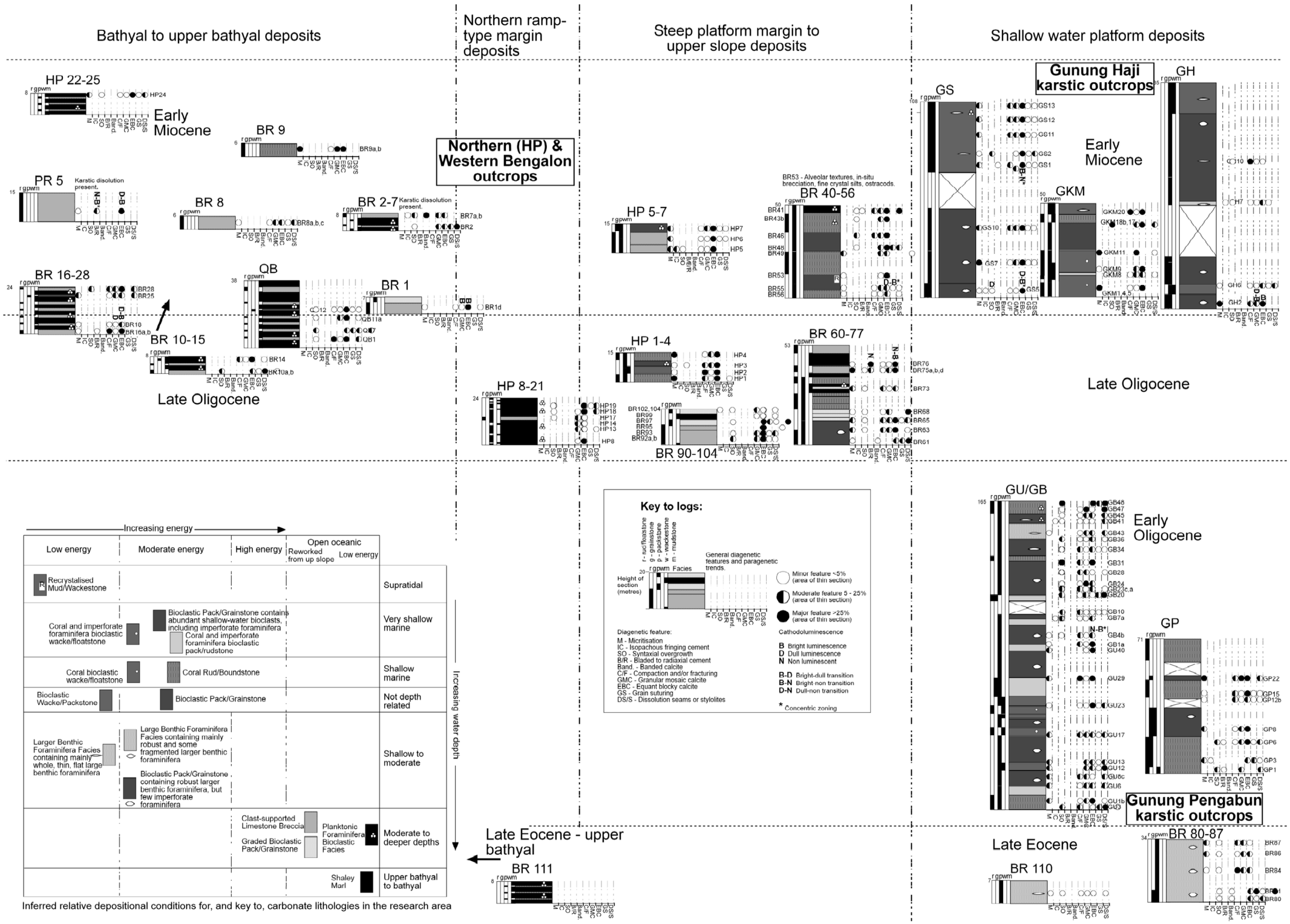

Inferred relative depositional conditions for, and key to, carbonate lithologies in the research area

Table 4.1. Summary of the four study areas (Fig. 4.1), showing ages, facies characteristics and inferred depositional setting.

Area	Carbonate sections	Age range	Carbonate facies group	Inferred depositional setting
Northern Bengalon	Heli Pad (HP)	Oligocene and Lower Miocene	Dominated by Planktonic Foraminifera Facies Group, few Lithoclastic and Bioclastic Facies Group lithologies	Steep platform margin and unrimmed shelf margin deposits with an open oceanic influence
Gunung Haji Karstic	Gunung Semarang (GS)	Lower Miocene	Dominated by lithologies of the Bioclastic Facies Group and few beds of the Mudstone-Wackestone Facies Group	Low to moderate energy shallow-marine shelfal carbonates
	Gunung Kiham (GKM)	Lower Miocene		
	Gunung Haji (GH)	Lower Miocene		
	Bengalon River (BR39-56)	Lower Miocene		
Gunung Pengabun Karstic	Gua Pengabun (GP)	Lower Oligocene	Dominated by lithologies of the Bioclastic Facies Group and fewer beds of the Mudstone-Wackestone Facies Group	Low to moderate energy shallow-marine shelfal carbonates
	Gua Unguk/Bangki (GU/GP)	Lower Oligocene		
	Bengalon River (80-87)	Upper Eocene		
	Bengalon River (BR110)	Upper Eocene		
Western Bengalon	Bengalon River (BR60-77)	Upper Oligocene	Interbedded lithologies of the Planktonic Foraminifera and Lithoclastic Facies Groups	Upper bathyal slope and bathyal deposits into which shallow-water and lithifed carbonate and clastic material has been reworked via sediment gravity flows
	Bengalon River (BR90-104)	Upper Oligocene		
	Bengalon River (BR111)	Upper Eocene		
	Quarry Batu (QB)	Upper Oligocene and Lower Miocene		
	Bengalon River (BR1-9)	Lower Miocene		
	Bengalon River (10-15)	Lower Miocene		
	Bengalon River (BR16-28)	Lower Miocene		

4.4 1 Petrography of Diagenetic Features

4.4.1 1 Micritisation

Micritisation of bioclasts is prevalent in 114 of 124 thin sections. Micrite envelopes are visible in plane-polarised light as narrow (10-50 μm) irregular dark brown rims on bioclasts (Fig. 4.3A, 4.3B). The common bioclasts in packstones, floatstones and wackestones from shallow-water platform deposits show the most consistently pervasive micritisation with micritic rims typically 50 μm thick (Fig. 4.3B). Packstone-grainstones and rudstones from the platform top typically show less pervasive micritisation of bioclasts, having micritic rims mostly <20-30 μm thick. Micritisation was noted from all platform margin deposits studied, with micritic rims on bioclasts most commonly 20-30 μm thick. Micritic rims of 50 μm thickness are only seen in platform margin deposits associated with coral bioclasts and a packstone texture, mainly from the Northern Bengalon area. Micritisation is a rarer feature of bathyal to upper bathyal deposits and rims are the most variable, ranging from 10-50 μm thick. The most pervasive micritisation in bathyal deposits is from reworked shallow water components within Lithoclastic Facies including: (1) bioclastic packstone clasts and (2) coral clasts. Generally larger perforate benthic foraminifera in all three major depositional settings show limited micritisation with rims 10-20 μm thick (Fig. 4.3C, 4.3D). Rare more pervasive micritisation (30-50 μm thick rims) affects larger perforate foraminifera from just the shallow-water platform deposits. The CL signature of the micritic rims is typically dull- to non-luminescent, contrasting slightly with the CL signature of originally calcitic bioclasts that typically

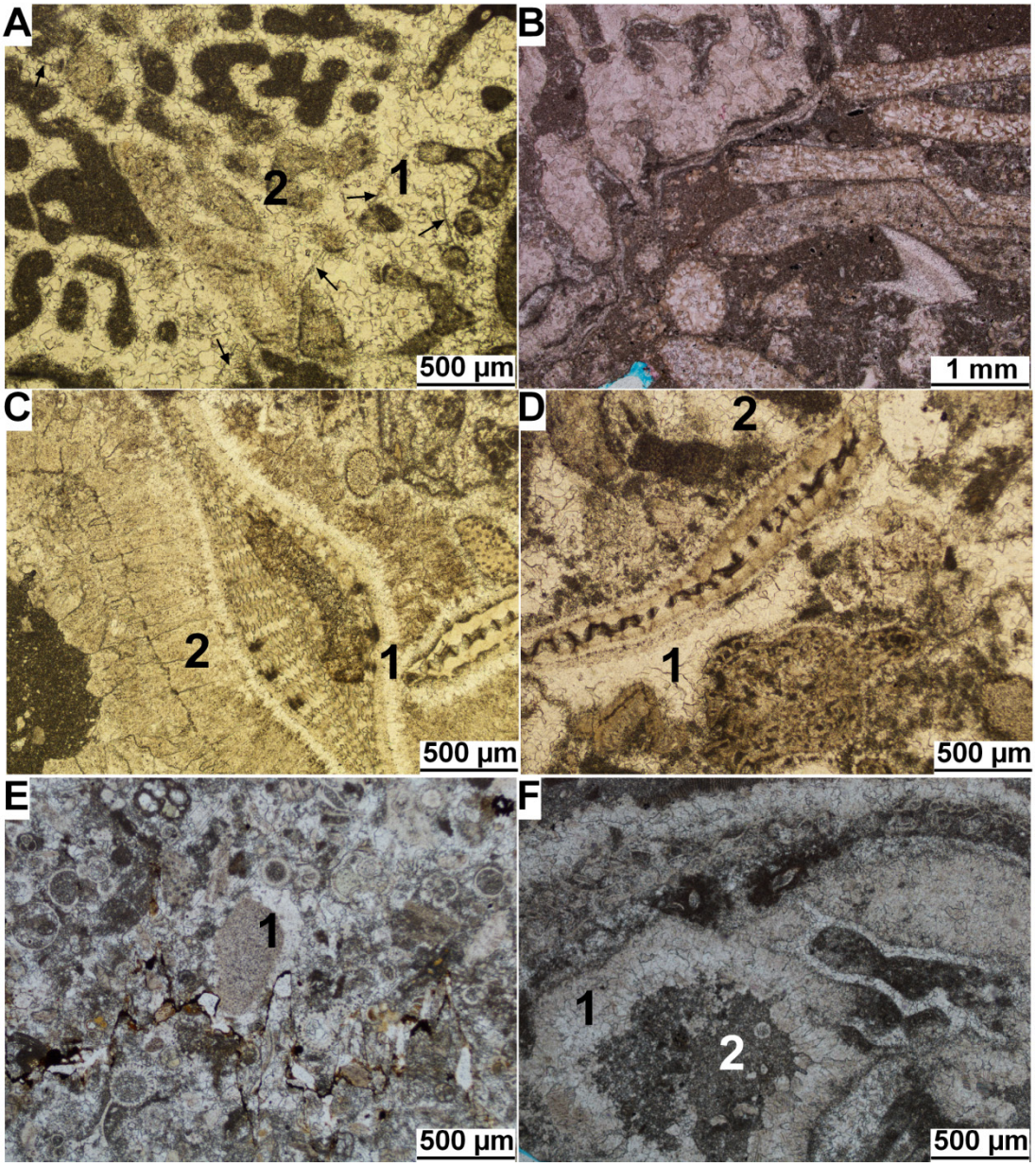

Figure 4.3. Plane-polarised thin-section photomicrographs illustrating a range of diagenetic features from the Kedango Limestone. (A) Sample GP01; Coral fragment from a wackestone-floatstone from the shallow-water platform top. Minor micritisation of coral clast, coral skeleton has been neomorphically replaced by granular mosaic calcite (1) with ghost fabrics present in the neomorphosed coral (arrows) and contiguous cementation of the coral chamber porosity where not filled entirely by micrite. The turbid appearance of contiguous chamber cements (also granular mosaic calcite) is due to likely partial neomorphic replacement of the micritic matrix (2). (B) Sample GKM18b; Bioclastic wacke-pack-floatstone from shallow-water platform top. Abundant *Halimeda* fragments with well developed micritic rims and coral clast with micritic envelope and encrusting algae. The coral skeleton and *Halimeda* have been neomorphically replaced by granular mosaic calcite with infill of bioclast chambers and replacement of matrix both by equant blocky calcite. (C) Sample BR07a; Lithoclast of bioclastic grainstone within clast-supported limestone breccia from bathyal to upper bathyal setting. Clear isopachous fringing cement forming a fibrous rim to large benthic foraminifera (1). Fringing cement has been overgrown in places by bladed calcite cement (2). (D) Sample HP05; Bioclastic grain-rudstone from platform margin. Isopachous fringing cement developed on a larger benthic foraminifera showing

replacement by equant blocky calcite (1). Clear equant blocky calcite infills between clasts and areas of matrix (2). (E) Sample HP19; Planktonic foraminifera packstone from ramp type margin (Wilson et al., 2012). Syntaxial overgrowth cement present on echinoderm grain (1). A high amplitude stylolite cross-cuts the lithology. (F) Sample BR75a; Clast supported limestone breccia from platform margin. Recrystallised carbonate clast including a void (shelter porosity) infilled by bladed to equant calcite (1) and micritic sediment (2; includes planktonic foraminifera).

4.4.1.2 Isopachous Fringing Cement

Non-ferroan isopachous fringing cement is present in 8% of thin sections as minor cement fringes <200 μm wide on bioclasts. Fringing cements have acicular to fibrous crystal habits (Fig. 3C) and are rarely replaced by equant calcite (Fig. 4.3D). Fringing cements are colourless to weakly yellow-brown in plane light and are non-luminescent in CL. Isopachous fringing cements developed in the shallow-water platform deposits are rare in wackestone-packstone lithologies (<1% of a sample, <20 μm wide) but are more common in coarse bioclastic packstone and grainstone lithologies (1-5% of a sample, up to 50 μm wide). Fringing cements mostly occur within bioclast chambers or more rarely fringing bioclasts, notably larger perforate foraminifera. Fringing cements are most abundant (>5% of sample, up to 200 μm wide) in two thin sections of Lithoclastic Facies from the platform margin deposits. These platform margin deposits are a coarse bioclastic grain/rudstone, including carbonate lithic clasts with fringing cements developed on reworked larger perforate benthic foraminifera (Fig. 4.3D). The other occurrence of thick fringing cement from the platform margin deposits is in a reworked grainstone clast from a clast-supported limestone breccia. The only occurrence of isopachous fringing cement from the bathyal deposits is in a reworked grainstone clast from a Lithoclastic Facies limestone breccia (Fig. 4.3C).

4.4.1.3 Syntaxial Overgrowths

Syntaxial overgrowths, present in 19% of thin sections, are common on echinoderm grains (Fig. 4.3E), but are not a dominant cement phase (<1-2% of a sample). Syntaxial overgrowths typically have well-formed crystal shapes, and are only a few tens of microns in width and length. Some overgrowths have a cloudy and inclusion-rich appearance.

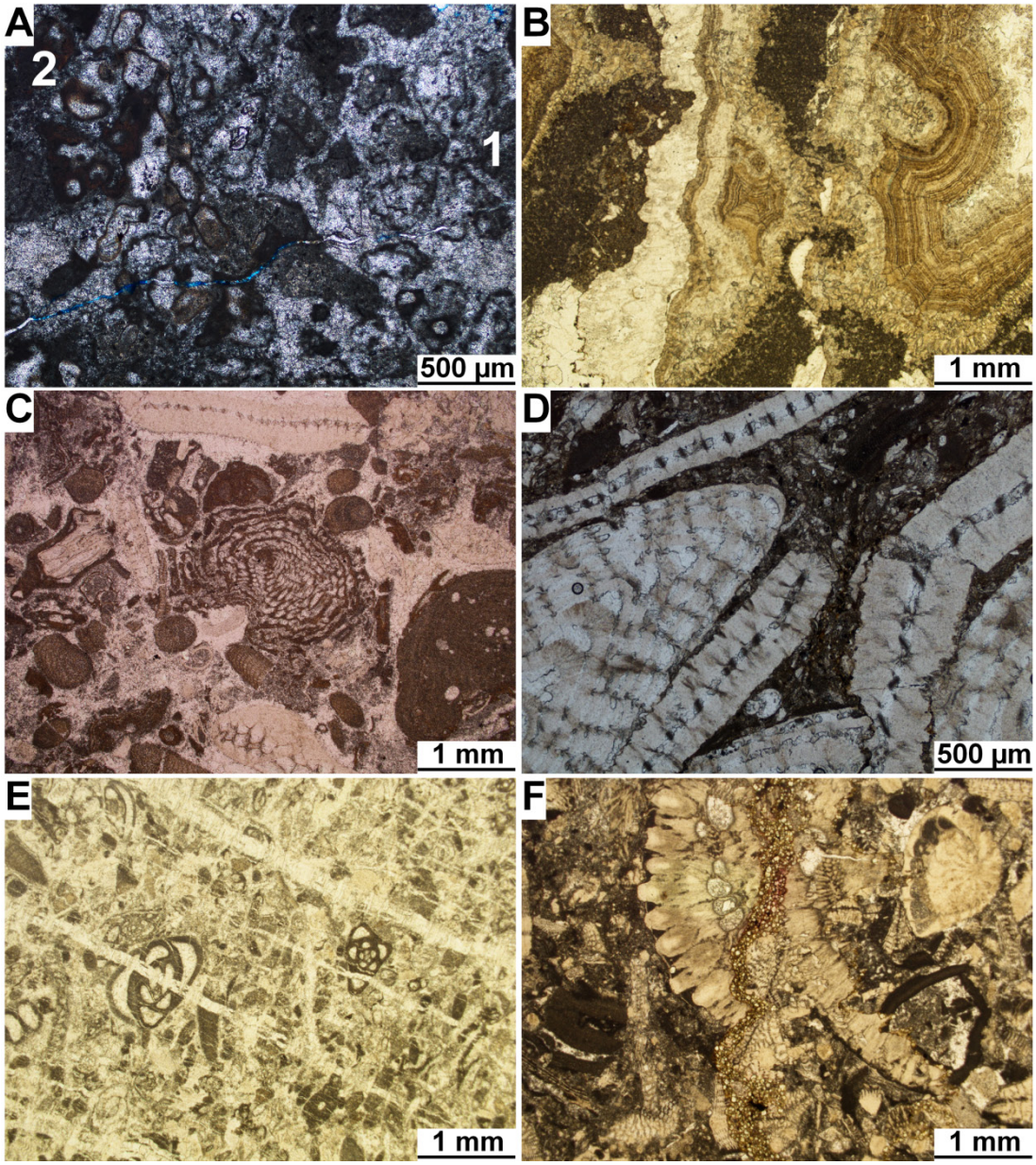

Figure 4.4. Plane-polarised thin-section photomicrographs illustrating a range of diagenetic features from the Kedango Limestone. (A) Sample BR53; Recrystalised mud-wacke-floatstone from platform margin deposits. Recrystalised coral with chambers partially cemented and filled by a fine dark micritic sediment (1). Alveolar texture present as irregular pores with a dark brown rim infilled by sparite and micrite (2). (B) Sample PR05; Clast supported limestone breccia from bathyal to upper bathyal setting. Banded cement infilling a karstic dissolution cavity within a reworked clast. (C) Sample GP03; Coral bioclastic grain-rudstone with mechanically deformed alveolinid (imperforate foraminifera; centre of field of view) with development of a concavo-convex grain contact with an echinoid clast with well developed syntaxial overgrowth cement. A perforate heterostegnid foraminifera has a partial rim of fringing cement and is undeformed (top of field of view). (D) Sample GB43; coarse bioclastic pack-rudstone from shallow-water platform top with Heterostegnid, *Nummulites* and coralline algae showing grain breakage and irregular suturing at grain-to-grain contacts. The matrix shows development of dissolution seams with concentrations of insoluble dark brown material. (E) Sample GU29; Bioclastic pack-grainstone from shallow-water platform top. Miliolids and bioclasts heavily micritised and cross-cut by multiple minor fractures. Fractures are filled by equant blocky calcite cement. (F) Sample BR81; Coarse bioclastic

pack-rudstone from shallow-water platform top. Extensive mechanical compaction has been partially accommodated through chemical compaction at grain-to-grain contacts and dissolution seam formation. Microdolomite rhombs are present along the length of the seam.

Overgrowths post-date micritisation, and pre-date later fracturing since fractures may cross-cut the overgrowths and overgrowths may partially extend over micritic rims. Syntaxial overgrowths are found most commonly in packstone-grainstone lithologies from the shallow-water platform deposits and platform margin deposits. Echinoid spines or plates are most commonly overgrown in shallow-water platform top deposits whereas overgrowths are more common on bifurcating crinoid plates (probably feather stars or Comatulida) in platform margin environments. In general there is a greater abundance of syntaxial overgrowth cement amongst the coarser grainstone lithologies of the platform margin rather than platform top deposits associated with a greater abundance of echinoiderm debris in the former. Syntaxial overgrowths are rare in the bathyal to upper bathyal deposits, but where present are associated with packstone-grainstone lithologies of the Lithoclastic Facies. CL imagery reveals that in at least one sample, of a coarse-gravel grain/rudstone (sample GS05; Fig. 4.2), syntaxial overgrowths have a dull-luminescence.

4.4.1.4 Bladed to Radiaxial Cements

Non-ferroan bladed to radiaxial cements are present in 6 out of 124 thin sections. Bladed cements are formed of individual crystals up to a few millimetres in length and <300 μm in width, with pyramidal to blocky long axis crystal terminations. A radiaxial-bladed to fibrous habit is seen in some crystals displaying sweeping undulose extinction and convergent optic axes. Bladed to radiaxial crystals of 70-100 μm in length were seen in only one coarse bioclastic packstone-grainstone platform top sample where they comprise a very minor phase just coating perforate foraminifera. The other examples of bladed to radiaxial cements are all from platform margin deposits and/or within clasts reworked from the margin present in Lithoclastic Facies. In platform margin deposits bladed to radiaxial cements between 100 μm to 5 mm in length are variously present within or around both bioclasts and lithic clasts (Fig. 4.3C). Bladed to radiaxial cements are only a significant cement phase (15-25% of sample and up to 5 mm long) in two samples of clast supported limestone breccia, one infilling a cavity between lithic clasts (Fig. 4.3F), and the

other around coral clasts. In this later sample the bladed cements formed prior to the reworking of the coral fragments since both cements and corals are sharply truncated and abraded. Bladed cements between 50-250 μm long with crystals truncated at clast margins also formed prior to clast reworking in two other samples from the platform margin and the one lithoclastic sample from bathyal water depths. Bladed to radiaxial cements are colourless to moderately yellow-brown in plane light and may display twinning. These cements were not imaged in CL.

4.4.1.5 Early Fracturing, Crystal Silt and Alveolar Texture

One Lower Miocene bed (BR53; recrystalised wackestone-floatstone) has been affected by early fracturing (brecciation) and fracture infill by fine crystal silt. BR53 is a platform top sample from close to the margin and was deposited just prior to local deepening (Wilson et al., 2012). Fractures are up to 1-2 mm wide and several centimetres in length. Alveolar structure is composed of irregular pores infilled by sparite and separated by interconnecting micrite bridges (Fig. 4.4A). These features of early brecciation, alveolar textures and infill by fine crystal silt, the later including whole and disarticulated thin-shelled ostracods, are not seen elsewhere.

4.4.1.6 Dissolution, Micritic Sediment Infiltration and Banded Calcite Cement

Dissolution features are rare. Irregular cavities up to several millimetres in diameter are present within reworked clasts in just two Lithoclastic Facies samples deposited in a bathyal setting and of Lower Miocene age (PR05 and BR07a; Fig. 4.2). The reworked clasts with dissolution cavities are a: (1) mollusc and imperforate foraminifera wackestone, and (2) bioclastic grainstone. In both samples these cavities are filled by irregular banded-bladed calcite cement and a fine (few tens of microns) non-laminated sediment infill that lacks fossils, although this sediment infill is rare in BR07a. Cement and sediment infills of cavities are sharply truncated at clast boundaries. Banded cements up to 5 mm in width appear as concentric zones or "bands" of crystals, with sharp margins between zones and sometimes a slight bladed habit to crystals (Fig. 4.4B). In plane light the banded cements are moderately yellow-brown. In CL the banded cements display >20 individual alternating bands of non-luminescent and brightly-luminescent zones over a distance of ~ 500 μm (Fig

4.5A/A*). In one sample (BR07a) the banded cements have pendant morphologies where bladed calcite has precipitated around larger perforate benthic foraminifera. The sediment infill of the dissolution cavities is very dark brown in plane light and is typically homogenous.

4.4.1.7 Grain Breakage and Mechanical Compaction

Mechanical breakage and compaction of grains is prevalent throughout the platform deposits and is present in 43% of thin sections. Mechanical compaction effects are seen as grain breakage, internal grain distortion and tangential to concavo-convex grain contacts (Figs. 4.4C, 4.4D). Micritised grain-rims, and to a much lesser extent isopachous cements are both affected by compaction. In the shallow-water platform deposits, grainstone lithologies and coarse-gravel pack/rudstones show preferential compaction features. In these platform top deposits larger perforate benthic foraminifera and algae show common tangential to concavo-convex grain contacts as well as grain breakages, whereas imperforate foraminifera may show considerable internal deformation (Fig. 4.4C). Mudstone-Wackestone Facies have a high micrite content and with sparsely distributed bioclasts do not show extensive compaction features. Platform margin deposits mostly only display pervasive compaction features in grainstone-rudstone lithologies where larger benthic foraminifera or fragmented corals are present. Where isopachous and/or bladed cements are well-developed in platform margin, and to a lesser extent platform top deposits, compaction effects are less prevalent. In platform top deposits where larger perforate foraminifera are rimmed by isopachous cements these allochems may not be affected by compaction, whereas imperforate foraminifera lacking cement rims from the same samples may show significant deformation within the grain and at its margins.

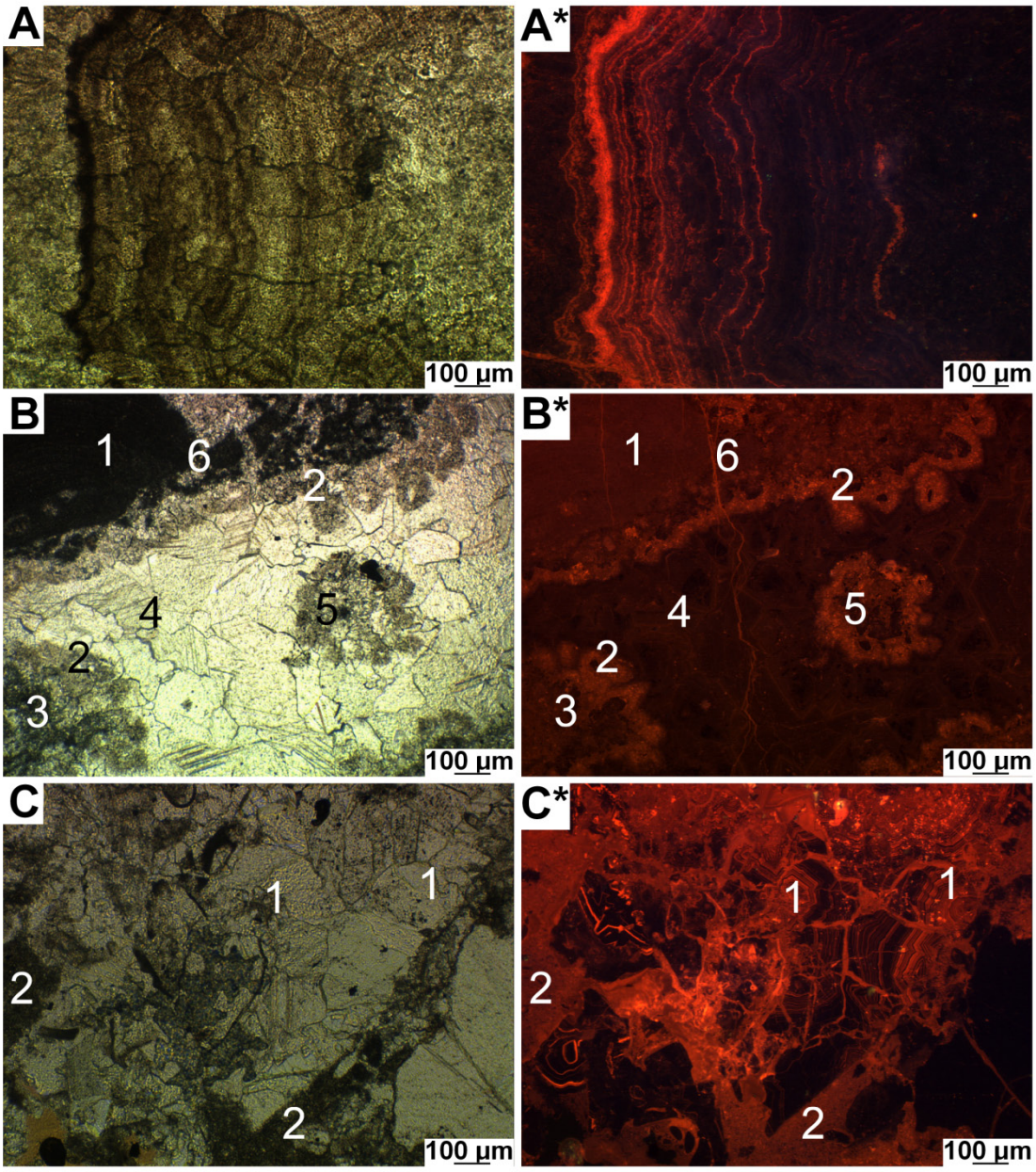

Figure 4.5. PPL and CL photomicrograph pairs illustrating features and trends developed during diagenesis of the Kedango Limestone. (A/A*) Sample PR05; Heavily zoned banded cement, exhibiting zones of non- to dull-luminescence and bright-luminescence. From the right side of the field of view to the left side the contrast in zoning becomes more pronounced as the thickness of bright zones increases. (B/B*) Sample GH02; Dull-luminescence of coralline algae (1) adjacent to cement-filled shelter porosity. Micritic matrix partially infilling original pore space and micritised rims to bioclasts are moderately luminescent (2). The periphery of a coral clast shows dull- to non-luminescence where the original skeletal structure has been neomorphically replaced (3). Zoned non- to dull-luminescent equant blocky calcite fills the remaining original shelter porosity (4), and partially replaces patches of matrix (5), and the original micrite rim (2). A fine fracture filled with moderately- to brightly-luminescent cement, cross-cuts the sample that is not seen in PPL (5). (C/C*) Sample GS01; Non- and brightly-luminescent zoning of equant blocky calcite cement. Dense alternating zones (1) occur during the earlier calcite spar development. Micrite matrix has dull to bright luminescence (2). (Fig. 4.4C). Lithoclastic deposits may show extensive breakage, concavo-convex and tangential contacts associated with larger benthic foraminifera, echinoderm material and lithic clasts in grainstones and breccias. Only minor

compaction effects, including grain breakage, are present in the Planktonic Foraminifera Facies.

4.4.1.8 Fracturing

Minor fracturing of bioclasts, matrix, and rarely prior cement phases, occurs in 69% of thin sections. More pervasive fracturing is common in Lithoclastic Facies derived from the southern part of the platform margin. These fractures are typically less than a few millimetres but may be up to a few centimetres in length, and are commonly <1 mm in width (Fig. 4.4E). Offsets along fractures, if present, are typically 100-500 μm. Fractures cross-cut original fabrics and rarely syntaxial overgrowths and isopachous fringing cements, and are commonly infilled by later granular to equant calcite. However rare examples of fractures cross-cutting and being cross-cut by granular mosaic and equant blocky cements suggest a possible contiguous timing to some of these fractures. Fracturing is prevalent in samples from all three major depositional settings, but is most pervasive and with the largest fracture sizes in lithologies with little micritic matrix i.e., packstone to grainstone lithologies. The full extent of fracturing is seen in CL as fine fracture networks filled with brightly-luminescent granular to equant calcite cements that cross-cut the "background" of moderate- to non-luminescence (Fig. 4.5B/B*).

4.4.1.9 Granular Mosaic Calcite

Non-ferroan granular mosaic calcite is a dominant diagenetic feature, present in 119 of 124 thin sections and accounting for 15-25% of individual samples. Granular mosaic calcite consists of typically small relatively equidimensional crystals with irregular to subhedral crystal margins (Flügel, 2004). This cement affects bioclastic components retaining relicts of original skeletal structure or occurs as mosaic cement extending into bioclast chambers (Figs. 4.3A, 4.3B), or rarely extending into fractures. Granular mosaic calcite crystals vary in size from a few hundred microns, where they replace original skeletal structures, up to 700 μm within bioclast chambers. Relicts of internal skeletal structures and coral walls are partially preserved as original organic or inorganic inclusions or through outlining by micritic envelopes. In plane light granular mosaic calcite is colourless to pale yellow-grey, and has a dull-luminescence in CL.

4.4.1.10 Blocky to Equant Calcite

Non-ferroan blocky to equant calcite is the most dominant diagenetic feature (typically >25% of each sample) and is present in 122 of 124 thin sections. Blocky equant calcite consists of variably sized crystals (up to several millimetres) with commonly distinct euhedral crystal boundaries and an equicrystalline "block like" fabric (Flügel, 2004). This cement occurs between bioclasts and commonly within patches of micrite or more rarely as large areas of cement with micritic inclusions or small relict patches of micritic matrix between or within crystals (Figs. 4.3D, 4.3E, 4.4B, 4.4E, 4.5B/B*). Blocky calcite may extend into bioclast chambers and fractures (continuous from areas of granular mosaic calcite), rarely (<5% of thin sections) with a drusy habit and rarely (8% of thin sections) with isolated crystals of dog tooth calcite. In plane light blocky to equant cements are colourless to pale yellow-grey, but have variable CL characteristics. Blocky calcite from bathyal Lithoclastic Facies deposits show little evidence of zoning and have moderate to bright-luminescence. In both Bioclastic Facies and Lithoclastic Facies from shallow water platform and steep platform margin deposits blocky calcite commonly shows multiple (up to 15) concentric CL bands of dull-luminescence and bright-luminescence (Figs. 4.5B/B*, 4.5C/C*). Both the granular mosaic calcite and blocky to equant calcite are cross-cut by later chemical compaction features and rarely (nine thin sections) very minor non-pervasive fractures which may be filled by an equant calcite spar (Fig. 4.5B/B*).

4.4.1.11 Grain Suturing, Stylolites, and Dissolution Seams

Stylolites are uncommon features (11% of thin sections) appearing as serrated seams. Dissolution seams are common (53% of thin sections), and present as smooth anastomosing seams. Stylolites have amplitudes of up to 1 mm and both stylolites and dissolution seams may be up to several centimetres in length. Some stylolites have developed from intergranular sutures into circum-grain or clast seams. Stylolites are best developed in packstone-grainstone lithologies where there is a low abundance of micritic matrix and greater cementation. Dissolution seams occur in areas where there is a higher proportion of matrix to cement and may transition along their length from dissolution seams in micritic-rich regions to stylolites in cement-

rich regions. Dissolution seams and stylolites cross-cut older cement phases, fractures and depositional features, however dissolution seams most commonly only impact the margins of bioclasts. Both features are identifiable by the concentration of insoluble non-carbonate material, resulting in a dark brown seam in PPL (Figs. 4.3E, 4.4F). In 26% of thin sections the generation of stylolites and dissolution seams has resulted in minor (<1% of sample) dissolution and porosity generation along the features. In two Eocene samples (BR81 and BR110, Bioclastic Facies shallow-water platform deposits; Fig. 2) euhedral micro-dolomite rhombs (<100 μm) have developed along dissolution seams (Fig. 4.4F). In plane light dolomite rhombs are a pale yellow-brown and were not imaged in CL.

4.5 Stable Isotope Analyses

Stable-isotope compositions define a dominantly tight group, with low variance between individual values of $\delta^{18}O$. These values range from -12.0‰ to -1.3‰ V-PDB (Table 4.2, Fig. 4.6), and are similar to more negative than that expected from cements formed from Oligocene-Miocene SE Asian marine waters ($\delta^{18}O$ values of -4.2‰ to -1.5‰; Ali, 1995; Wilson and Evans, 2002). Carbon stable-isotope values lie within a narrow range, commonly within, or slightly more negative than the expected range of normal marine waters (-1‰ to +1‰ $\delta^{13}C$ V-PDB; Ali, 1995; Wilson and Evans, 2002), with values ranging from -4.0‰ to +1.1‰ V-PDB for all but five samples. These outlying samples have $\delta^{13}C$ values within the range of -11.6‰ to -4.7‰ V-PDB, and are from samples of banded (two samples; PR05), blocky equant (adjacent to banded cement; PR05) and fracture filling cements (two samples; GU3 and GB4b (Fig. 4.2)).

4.6 Diagenetic, Temperature, and Paleohydrologic Interpretations

Petrographic observations reveal a paragenetic sequence for diagenetic events affecting the Kedango Platform including several phases of cementation (Figs. 4.2, 4.7). The Anderson and Arthur (1983) equation (Equation 1) provides a means to derive Miocene $\delta^{18}O$ seawater values for the region, and from this the potential to evaluate the possible origins of fluids involved in cement precipitation:

$$T=16 - 4.14(\delta^{18}O_{CALCITE} - \delta^{18}O_{SEAWATER}) + 0.13(\delta^{18}O_{CALCITE} - \delta^{18}O_{SEAWATER})^2 \quad (1)$$

A Miocene $\delta^{18}O$ seawater value for the region of -2‰ to 0‰ V-SMOW has been derived using this equation and the observed range of calcitic bioclast values ($\delta^{18}O$ values of -4.2‰ to -1.5‰; Ali, 1995; Wilson and Evans, 2002) for SE Asian Oligocene-Miocene seawater and an assumed ocean surface temperature of 25 °C (Neogene of coastal Borneo; Ali, 1995). The larger benthic foraminifera in the Kedango Limestone samples (Table 4.2, Fig. 4.6; $\delta^{18}O$ V-PDB values of -6.2‰ to -1.4‰) are in general agreement with the known range of $\delta^{18}O$ values for SE Asian Oligocene-Miocene calcitic bioclasts, perhaps reflecting, precipitation in equilibrium with Miocene seawater. Where the originally calcitic bioclasts are more negative than the known range of $\delta^{18}O$ values for SE Asia it is possible that these may be a reflection of: (1) the samples containing contaminating matrix or (2) precipitation out of equilibrium with Miocene sea water. Alternatively, because there is significant terrestrial runoff into the seas around SE Asia the more negative $\delta^{18}O$ values of the calcitic bioclasts may reflect lower salinities than the global norm (i.e. an apparently slightly brackish signature; Tomascik et al., 1999; Wilson, 2008), indicating that the regional Miocene seawater $\delta^{18}O$ field requires modification. A possible need for modification is suggested by other results from the same region showing more negative $\delta^{18}O$ values, from calcitic bioclasts and marine cements, than the regional seawater field (cf. Wilson and Evans, 2002; Madden and Wilson, 2012). Any meteoric parent fluids potentially involved in diagenetic alteration are suggested to have had $\delta^{18}O$ values of -8‰ to -4‰ V-SMOW on the basis of $\delta^{18}O$ values of meteoric precipitation in SE Asia of -6‰ to -4‰ at low elevations (Bowen and Wilkinson, 2002) and up to -8‰ for the whole of Borneo (Anderson and Arthur, 1983).

The onset of development of stylolites and dissolution seams occurs in moderate to deep burial environments of approximately 1000 m (Finkel and Wilkinson, 1990; Lind, 1993; Railsback, 1993b; Nicolaides and Wallace, 1997; Machel, 2004). Since all calcite precipitation pre-dates the development of stylolites and dissolution seams a maximum burial depth for calcite cementation of the Kedango Limestone of <1000 m is inferred. The prevalence of dissolution seams over stylolites may indicate lesser burial depths; although the occurrence of both features may be more strongly

controlled by the lithology undergoing burial compaction (below). Extrapolation of the Bengalon region's geothermal gradient (24.4 °C/km; Hall, 2002) gives an estimated maximum calcite precipitation temperature of 49.4 °C.

Table 4.2. $\delta^{13}C‰$ VPDB and $\delta^{18}O‰$ V-PDB values from samples of the Kedango Limestone.

Sample	Name	Component	δ13C‰ VPDB	δ18O‰ VPDB
GB43	gb43 0.8	Larger benthic foraminifera	0.12	-2.67
GB45	gb45 0.8	Larger benthic foraminifera	-0.73	-6.19
GP15	gp15 1.0	Larger benthic foraminifera	0.35	-1.37
HP4	hp4a 1.1	Larger benthic foraminifera	-0.06	-1.59
HP4	hp4b 1.1	Larger benthic foraminifera	-0.48	-5.45
BR81	br81a 0.8	Larger benthic foraminifera	0.49	-4.31
GKM20	gkm20a 1.8	Micrite	0.70	-8.68
GKM20	GKM 20B 1.8	Micrite	1.14	-6.51
BR75b	br75b 0.5	Bladed calcite cement	-0.44	-6.60
PR5	pr5b 1.4	Bladed calcite cement (Banded)	-6.62	-10.75
PR5	pr5c 1.9	Bladed calcite cement (Banded)	-11.64	-9.00
GKM8	gkm8a 1.6	Granular mosaic calcite replacing coral	0.91	-8.69
GKM8	gkm8a 1.2	Granular mosaic calcite replacing coral	0.66	-9.20
BR2a	Madden BR2a S.I	Granular mosaic calcite replacing coral	-0.87	-2.37
BR25	Madden BR25 S.I	Granular mosaic calcite replacing coral	-0.07	-1.40
HP6	Madden HP6 S.I	Granular mosaic calcite replacing coral	-4.01	-3.95
BR43b	Madden BR43b S.I	Granular mosaic calcite	0.91	-5.72
GKM8	GKM 8B 1.7	Blocky equant cement (in mollusc)	0.23	-8.83
QB11	qb11 1.5	Blocky cement (within and between clasts)	0.10	-7.70
PR5	pr5a 1.0	Blocky calcite cement	-4.74	-11.98
BR76	Madden BR76 S.I	Blocky calcite cement	0.98	-2.99
BR9a	Madden BR9a S.I	Blocky calcite cement	1.52	-2.53
GU3	Madden GU3 S.I	Blocky calcite cement	0.88	-7.12
GS1	Madden GS1 S.I	Blocky calcite cement	-3.47	-9.72
HP3	Madden HP3 S.I	Blocky calcite cement	-2.54	-1.26
BR95	br95a 1.9	Fracture (thin) filling blocky cement	-0.02	-6.29
BR95	br95a 1.7	Fracture (thin) filling blocky cement	-0.80	-7.67
BR95	br95b 1.7	Fracture filling blocky cement	0.06	-6.20
GU3	GU3 1.6	Fracture filling blocky cement	-7.09	-12.07
GB4b	GB 4b 2.4	Fracture filling blocky cement	-5.88	-10.63
HP2	hp2 1.3	Fracture filling blocky cement	-0.57	-6.50

4.6.1 Interpretation of Pre-Compaction Diagenetic Features

4.6.1.1 Micritisation

Perhaps with the exception of the alveolar texture, micritisation is the first alteration process affecting samples, since micrite envelopes are cross-cut by all other diagenetic features. Bioclastic material in shallow-marine environments may be micritised due to the infilling of micro-borings made by endolithic organisms (Bathurst, 1966; Gunther, 1990; Perry, 1999). Pervasive micritisation of shallow-water platform deposits, particularly those with packstone, floatstone and wackestone textures (Fig. 4.3B), is consistent with endolithic micro-borers being most active in moderate to low energy shallow-photic environments (cf. Swinchatt, 1965; Budd and Perkins, 1980; Perry and Bertling, 2000; Perry and Macdonald, 2002; Perry and Hepburn, 2008). Thick micritic rim development on bioclasts has been related to higher nutrient levels in shallow-photic environments, such as occurs in relatively

protected settings, and/or to constructive micrite envelope development associated with seagrass beds (Golubic et al., 1975; Budd and Perkins, 1980; Tucker and Wright, 1990; Perry, 1998; 1999; Perry and Larcombe, 2003). In the Kedango Limestone the thickest (50 μm) development of micrite rims in wackestones, packstones and floatstones from shallow platform top environments, some associated with inferred seagrass beds, and in northern platform margin deposits closest to the area of terrestrial runoff is consistent with a nutrient and/or specific environmental control on pervasive micritisation. The typically dull-luminescent to non-luminescent CL character of the micritic envelopes is consistent with associated marine waters or oxidising pore fluids. Alternatively the fine texture of the rims may result in a dark CL character.

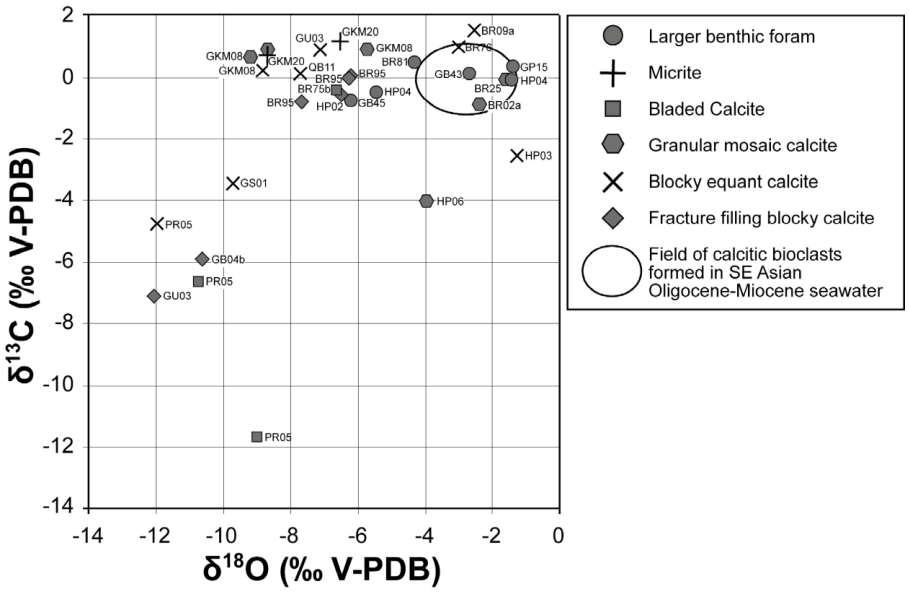

Figure 4.6. Cross-plot of $\delta^{18}O$‰ V-PDB versus $\delta^{13}C$‰ V-PDB for calcite components and cements from the Kedango Limestone of the Bengalon River area, based on the data presented in Table 4.2. The $\delta^{18}O$ values of -12.1‰ to -1.4‰ V-PDB are largely consistent with precipitation from SE Asian Oligocene-Miocene seawater at a temperature range of 25 to 49 °C. A meteoric influence relating to subaerial exposure may also be recorded in the $\delta^{18}O$ and some of the negative $\delta^{13}C$ values although this is likely localised and minor (see text for details)

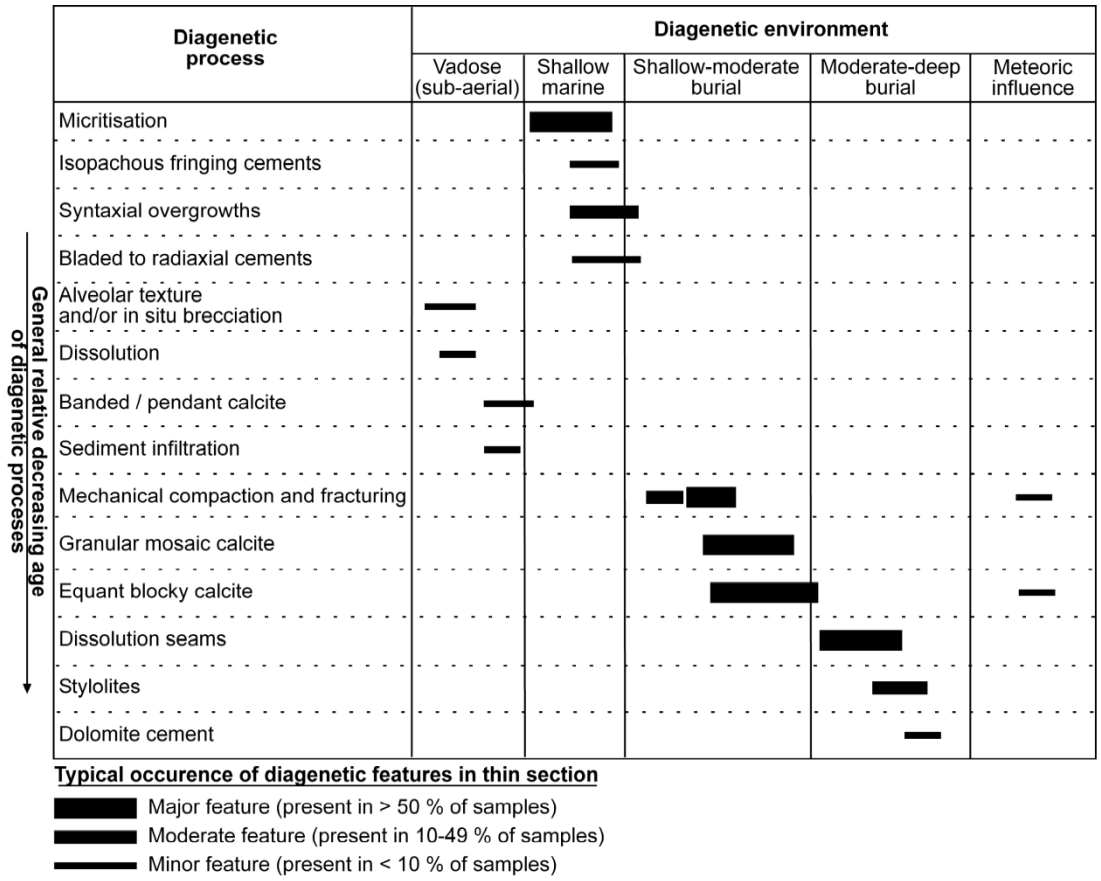

Figure 4.7. Consistent paragenetic scheme of diagenetic events affecting the Kedango Limestones from the Bengalon River area.

4.6.1.2 Isopachous Fringing Cement

Isopachous fringing cements formed after micritisation and prior to late stage cementation, but perhaps with a near-contemporaneous timing to syntaxial overgrowth cements. The CL character of this cement is non-luminescent, consistent with precipitation from marine waters and/or oxidising pore fluids. Although rare, the occurrence of fringing cements is confined dominantly to grainstone lithologies or coarse packstones with an abundance of bioclasts. This distribution of the fringing cement and its non-luminescent character suggests that precipitation was controlled by the availability of marine pore fluids and that the inferred higher depositional energies associated with the open textures of grainstones and coarse bioclastic packstones also resulted in flushing of these deposits by seawater (cf. Tucker and Wright, 1990; Park et al., 1992; Wilson and Evans, 2002; van der Kooj et al., 2010). The slightly greater volume of fringing cements in platform margin deposits suggests that localised enhanced seawater flushing occurred primarily along

the platform margin. Where isopachous cements are present in platform top grainstones these may be associated with intra-bank tidal currents (cf. Rankey and Reeder, 2010; Wilson et al., 2012)

4.6.1.3 Syntaxial Overgrowths

Syntaxial overgrowths formed prior to the onset of later stage granular to equant calcite precipitation, but following micritisation as overgrowths may extend over micritic rims. The cloudy, inclusion-rich appearance to overgrowths, indicates formation most likely in a marine-phreatic environment (Swei and Tucker, 2012). The non-luminescent CL character of the syntaxial overgrowths is also suggestive of oxidising conditions and/or marine pore fluids. The possibility of precipitation during shallow burial cannot be ruled out and in particular may apply to overgrowth cements with a clear inclusion free appearance (Tucker and Wright, 1990; Flügel, 2004). The most common occurrence of overgrowth cements in shallow water and platform margin deposits, and their rarity in bathyal packstone-grainstones is attributed to: (1) primary environmental distributions of echinoderm material and (2) easier pathways for flushing of precipitating pore fluids of probable marine origin in higher energy sections with more open textures (Appendix 4).

4.6.1.4 Bladed to Radiaxial Cements

Bladed to radiaxial calcite cement growth forms are most commonly attributed a marine or shallow-burial marine diagenetic origin (Halley and Scholle, 1985). The occurrence of these cement phases in the Kedango Limestone as a first generation cement with pre-compaction timing, their growth as isopachous rims on marine skeletal substrates, together with their crystal habits are all suggestive of marine origins (cf. Flügel, 2004). Stable-isotope composition of a bladed cement from a platform margin deposit with a $\delta^{18}O$ value of -6.6‰ V-PDB tentatively indicates that at near-surface temperatures of 25-30 °C (cf. Hall, 2002) formation fluids could range from -4.5‰ to -3.5‰ $\delta^{18}O$ V-SMOW, consistent with a marine parent fluid. A carbon stable-isotope value of -0.4‰ $\delta^{13}C$ V-PDB is also consistent with SE Asian Oligocene-Miocene seawater values. That the bladed to radiaxial cements are most abundant in the steep-platform margin deposits and associated with coarse

packstone-grainstone lithologies or Lithoclastic Facies deposits with high primary porosity is attributed to precipitation in a marine phreatic environment where seawater supersaturated with respect to calcium carbonate could be flushed into the carbonate platform.

4.6.1.5 Early Fracturing, Crystal Silt and Alveolar Texture

The alveolar texture in sample BR53 (Fig. 4.2, 4.7) is inferred to be related to alteration along rootlets (Steinen, 1974; Harrison, 1977; Esteban and Klappa, 1983). The localised nature of this feature and its association with auto-brecciation is suggestive of alteration during a period of localised subaerial exposure, desiccation and penetration by rootlets. Corals within the sample are indicative of initial marine depositional conditions. Subaerial exposure is inferred to have occurred shortly after deposition during the Early Miocene since alveolar textures and autobrecciation formed before full lithification and prior to deposition of the overlying marine bed. The presence of abundant ostracods within the fine crystal silt fracture fill are evidence of non-normal marine conditions and may be indicative of brackish or fresh-water conditions (Flügel, 2004) during the early stages of reflooding prior to a return to the normal marine conditions of the overlying strata.

4.6.1.6 Dissolution, Micritic Sediment Infiltration and Banded Calcite Cement

Dissolution cavities are rare features, present in only two examples of reworked clasts derived originally from the platform top (PR05 and BR07a, Fig 4.2; cf. Wilson et al., 2012). Since dissolution cavity margins and their infills of banded cements and fine sediment are all erosionally truncated at clast margins, the formation of these three features pre-dates clast reworking. The non-fossiliferous sediment infill to the cavities is of possible terrestrial origin (see Appendix 2 of Wilson et al., 2012). The depleted $\delta^{13}C$ values (-11.6‰ and -6.6‰ V-PDB) of the banded calcite cements are most reasonably attributed to organic matter degradation associated with soil-zone processes (Saller and Moore, 1991; Nelson and Smith, 1996; Moore, 2001). The dissolution cavities, their banded calcite with partial pendant morphology and fine sediment infills are therefore inferred to be karst-related features associated with subaerial exposure of the platform top prior to reworking of clasts in the Early

Miocene. Stable-isotope values of -10.8‰ to -9.0‰ $\delta^{18}O$ V-PDB for the banded cements are comparatively lighter than most other oxygen stable-isotope compositions across the platform and suggests either: (1) decreased pore-fluid $\delta^{18}O$ or (2) increased temperature. If precipitated from a marine parent fluid, the banded cements would require temperatures of 43-59 °C, corresponding to a burial depth of approximately 700-1400 m (cf. Hall, 2002). This temperature and depth range is unlikely as this cement was precipitated prior to all stages of mechanical or chemical compaction features (below) and in association with likely vadose zone dissolution cavities. At temperatures of 25-30 °C, consistent with a near-surface environment (cf. Hall, 2002), the banded cements would have formed from pore fluids with $\delta^{18}O$ values of -7.9‰ to -6.8‰ V-SMOW, i.e. consistent with meteoric fluids. The likely depleted $\delta^{18}O$ formation fluids and depleted $\delta^{13}C$ values together indicate meteoric fluids with a soil-zone connection (Allan and Matthews, 1982). Distinct CL zoning of this cement indicates changing pore water chemistry, or changing redox conditions during crystal growth, perhaps associated with variable meteoric recharge and or mixed marine-meteoric flushing. A progressively increasing non-luminescent character of the cement perhaps reflects increasingly reducing conditions.

4.6.2 Interpretation of Syn- and Post-Compaction Diagenetic Features

4.6.2.1 Grain Breakage and Mechanical Compaction

Compaction effects post-date micritisation and the early cements mostly of inferred marine origin since micritised margins, isopachous cements and syntaxial overgrowths are affected or broken. Mechanical compaction and grain breakage are interpreted to reflect compaction of the largely unlithified deposits as they underwent progressive burial. Mechanical compaction has been influenced by deposit textures, components and earlier cementation in the following ways. (1) In mudstone and wackestone samples extensive breakage of bioclasts and allochems is mitigated against by abundant micrite matrix and a paucity of grain-to-grain contacts (Fruth et al., 1966). (2) Elongate allochems, such as larger foraminifera or algae, are prone to breakage, whereas micritic walled imperforate foraminifera experienced internal deformation (Figs. 4.4C, 4.4D). (3) Larger perforate foraminifera and/or echinoderm material are preferential sites for early cement precipitation, and as a consequence

may be less affected by breakage and more prone to "impact compactionally" on adjacent uncemented grains (Fig. 4.3C, 4.4C).

4.6.2.2 Fracturing

Fractures mainly pre-date, but are also probably near contemporaneous, and in part post-date granular mosaic calcite and equant blocky calcite precipitation. Fracturing has affected deposits following their partial to full lithification and probably reflects continued progressive burial, but at least in part is also tectonic in origin (Cloke et al., 1999). Extensive reworking from the southern part of the platform margin has been linked to active faulting (Wilson et al., 2012). It may be that the pervasive fracturing affecting Lithoclastic Facies derived from the southern part of the platform, some with fracture offsets, reflects reactivation associated with these same structural lineaments (cf. Cloke et al., 1999).

4.6.2.3 Granular Mosaic Calcite

Granular mosaic calcite retaining relicts of internal and external fabrics of aragonitic bioclasts is indicative of neomorphism rather than dissolution and reprecipitation. Neomorphism and contiguous cementation into original porosity is consistent with the granular mosaic habit and lack of drusy cement fabrics (Hendry et al., 1999). The predominant dull-luminescent CL character of these spars is indicative of oxidising pore fluids. (The close association of neomorphic calcite with likely near-contemporaneous fracturing and contemporaneous (see below) blocky equant calcite indicates that neomorphism and subsequent calcitisation and cementation of the carbonate platform took place in a moderate depth burial environment, progressing towards maximum burial temperatures and depths, where the onset of stylolitisation begins. Precipitation of these cements with stable-isotope values of -9.2‰ to -1.4‰ δ^{18}O V-PDB (av. -5.22‰) at 35-49 °C and burial depths of approximately 400-1000 m (cf. Hall, 2002), suggests parent fluids of -1.2‰ to +1.3‰ δ^{18}O V-SMOW, consistent with marine fluids in a moderate-deep burial environment. Stable-isotope values of -4.0‰ to +0.9‰ δ^{13}C V-PDB indicate a lack of soil zone processes, and that a seawater or rock-derived source of carbon with marine δ^{13}C values was inherited by the precipitating fluids (Hendry et al., 1999; Madden and Wilson, 2012).

4.6.2.4 Blocky to Equant Calcite

The occurrence of blocky equant calcite between bioclasts and within the micritic matrix with relicts and inclusions of micrite, and its apparent continued growth from areas of granular mosaic calcite, suggest that for the most part this cement is a neomorphic replacement of the micritic matrix. However, where a drusy or dog tooth habit is exhibited, or the calcite remains clear and inclusion free, it is likely that this is a separate infill of primary porosity. The moderate-bright luminescence of blocky calcite in bathyal Lithoclastic Facies deposits is suggestive of slightly reducing pore fluids, consistent with depletion of parent fluids under progressive neomorphism. CL zoning in Bioclastic and Lithoclastic Facies from shallow-water platform and platform margin deposits is indicative of a changing pore fluid chemistry. If indeed these cements are contiguous with neomorphic calcite precipitation from marine fluids, then the CL zoning in the equant cements may reflect periodic flushing of the platform margin by marine waters under conditions of increasing burial.

Stable-isotope compositions of the micrite matrix have oxygen values more negative than unaltered bioclasts despite the fact that the micritic portion of the deposits likely accumulated at normal marine temperatures (25 °C). The $\delta^{18}O$ values (-8.7‰ and -6.5‰ V-PDB) of the micritic matrix therefore at least in part reflect alteration by diagenetic fluids despite $\delta^{13}C$ values (+0.7‰ and +1.1‰ V-PDB) in agreement with marine carbon values. Alteration of micrite is consistent with equant blocky calcite being, in part, a neomorphic replacement of the matrix. Alteration of micrite could have taken place after deposition on the sea-floor or up to maximum burial depths (cf. Brachert and Dullo, 2000; Melim et al., 2002; Caron and Nelson, 2009). Diagenetic fluids at temperatures of 25-49 °C suggest parent fluid compositions of -5.5‰ to -1.1‰ $\delta^{18}O$ V-SMOW, suggestive of dominantly marine parent fluids.

Two dominant diagenetic signatures are revealed from equant blocky cements. Non-fracture filling equant blocky calcite just from sample PR05 has a stable-isotope composition of -12.0‰ $\delta^{18}O$ V-PDB and -4.7‰ $\delta^{13}C$ V-PDB. Stable-isotope compositions from other equant blocky calcite samples range from -9.7‰ to -1.3‰ $\delta^{18}O$ V-PDB (av. -5.7‰) and -3.5‰ to +1.5‰ $\delta^{13}C$ V-PDB. Assuming a burial

diagenetic environment, on the basis of prior compaction and fracturing events, then parent fluid compositions at 35-49 °C corresponding to depths of 400-1000 m (cf. Hall, 2002), for sample PR05, were likely -8.0‰ to -5.5‰ δ^{18}O V-SMOW and in conjunction with depleted carbon values; suggest a meteoric derived source, in keeping with meteoric parent fluids for the banded cements in sample PR05. Parent fluids for other equant blocky calcite samples under the same temperature and depth conditions were likely -1.7‰ to +0.8‰ δ^{18}O V-SMOW consistent with a marine composition diagenetic fluid, and in agreement with normal marine carbon values and neomorphic calcite parent fluid values.

Two dominant diagenetic signatures are revealed from equant blocky calcite that infill fractures. Stable-isotope compositions from two shallow-water platform deposits (samples GU4 and GB4b) range from -12.1‰ to -10.6‰ δ^{18}O V-PDB and -7.1‰ to -5.9‰ δ^{13}C V-PDB. Depleted carbon values are suggestive of organically-derived carbon (cf. Morad, 1998; Warrlich et al., 2010). Depleted oxygen values indicate that at burial depths of 400-1000 m and temperatures of 35-49 °C (cf. Hall, 2002) parent fluid compositions were likely -7.4‰ to -4.9‰ δ^{18}O V-SMOW, consistent with meteoric to mixed marine-meteoric fluids. All other fracture filling cements with stable-isotope compositions ranging from -7.7‰ to -6.2‰ δ^{18}O V-PDB and -0.8‰ to +0.1‰ δ^{13}C V-PDB suggest that at 35-49 °C parent fluid compositions were likely -2.6‰ to -1.8‰ δ^{18}O V-SMOW, consistent with marine fluids and marine carbon values.

4.6.2.5 Grain Suturing, Stylolites, and Dissolution Seams

Cross-cutting relationships place these features as the final stages of diagenesis. These features are chemical compaction ones that form in moderate to deep burial environments (Machel, 2004) at depths of approximately 1000 m (Nicolaides and Wallace, 1997). The greater abundance and occurrence of dissolution seams is attributed to a predominance of lower energy wackestone-packstone deposits, especially across the shallow-water platform, promoting dissolution seams in micrite-rich lithologies. Dissolution seams mostly circumvent calcified bioclasts, likely because dissolution was promoted along calcite to clay-rich interfaces (cf. Railsback, 1993b). Under conditions of increasing burial and compaction many

tangential and concavo-convex grain-to-grain contacts have developed into circum grain stylolites. Stylolite development is most common in higher energy packstone-grainstones and Lithoclastic Facies from platform margin and bathyal deposits, reflecting the most competent lithological textures and high numbers of grain-to-grain contacts. The minor occurrence of micro dolomite rhombs along clay rich dissolution seams may indicate a localised source of Mg ions for dolomite cementation (Ali, 1995; Machel, 2004; Carnell and Wilson, 2004).

4.7 Discussion

4.7.1 Diagenetic Summary

Combined petrographic and stable isotope study has revealed a consistent diagenetic trend for the deposits of the Kedango Limestone with some association between diagenetic features and depositional facies (Figs. 4.2, 4.7 and 4.8). Grain micritisation occurred early during marine phreatic diagenesis and is most prevalent in shallow platform wackestones, packstones and floatstones, including those from close to the platform margin that were subsequently reworked down slope. Rare precipitation of isopachous fringing, bladed to radiaxial and syntaxial overgrowth cements is inferred to have taken place in a marine phreatic (to perhaps shallow burial) environment on the basis of cement geometries, non-luminescent CL characters suggestive of oxidising pore fluids, limited stable-isotope data, and a close temporal relationship between micritisation and early cementation. These three early cements are developed best in grain/rudstone lithologies. Fringing and bladed to radiaxial cements are limited to platform margin or margin-derived samples and more rarely shallow-platform top deposits, whereas overgrowths are most prevalent in margin to slope deposits. Grain breakage and other mechanical compaction features are common in most deposits except mudstones, wackestones and floatstones as well as the rare samples with early fringing or radiaxial cements.

Subaerial exposure during the Early Miocene is inferred for just three platform top or margin samples from irregular dissolution cavities in-filled by banded calcite cement and fine non-fossiliferous sediment, their stable isotopic signatures and alveolar textures (samples PR05, BR07a and BR53). The measured section including the

subaerial exposure features in BR53 correlates with a eustatic low at the end of the Early Miocene, although it is unclear whether local variations on the platform top or changes in sea level were responsible for emergence (Wilson et al., 2012).

Although there is some systematic variation in early diagenesis apparently associated with facies and/or environments, later diagenetic feature are more prevalent in the Kedango Limestone and are less facies specific. Late stage diagenesis is dominated by the neomorphic replacement of bioclasts, matrix and contiguous calcitisation into primary pore space followed by the formation of dissolution seams and stylolites from chemical compaction. Fracturing and blocky to equant cementation, are also late stage diagenetic features. Late diagenesis is interpreted to have taken place in a burial environment at temperatures of up to 50 °C, under the influence of dominantly marine composition fluids on the basis of relatively enriched oxygen stable-isotope compositions and carbon stable-isotope compositions in good agreement with marine values. Late diagenetic stabilisation to neomorphic calcite and associated calcitisation, whilst commonly recognised as a feature of meteoric diagenesis, is interpreted to have occurred under: (1) variably recharging marine fluids or (2) from oxidising marine fluids that became reducing with progressive crystallisation and burial. Neomorphism has been shown to act in a range of diagenetic environments, and is not solely associated with meteoric diagenesis (Brachert and Dullo, 2000, Melim et al., 2002, Caron and Nelson, 2009). Overall the effects of pervasive cementation, stabilisation and compaction have led to typical porosities of <1-2% (Appendix 4). In summary although there is some facies-associated early diagenetic variability for the Kedango Limestone, there is an overriding platform-wide later diagenetic overprint. The extent to which the original hypotheses that: (1) cross-platform variations in environments and/or diagenetic processes, and (2) the tectonically-active, but subsiding marine embayment setting of the Kedango Limestone both impacted diagenesis are explored in further detail below.

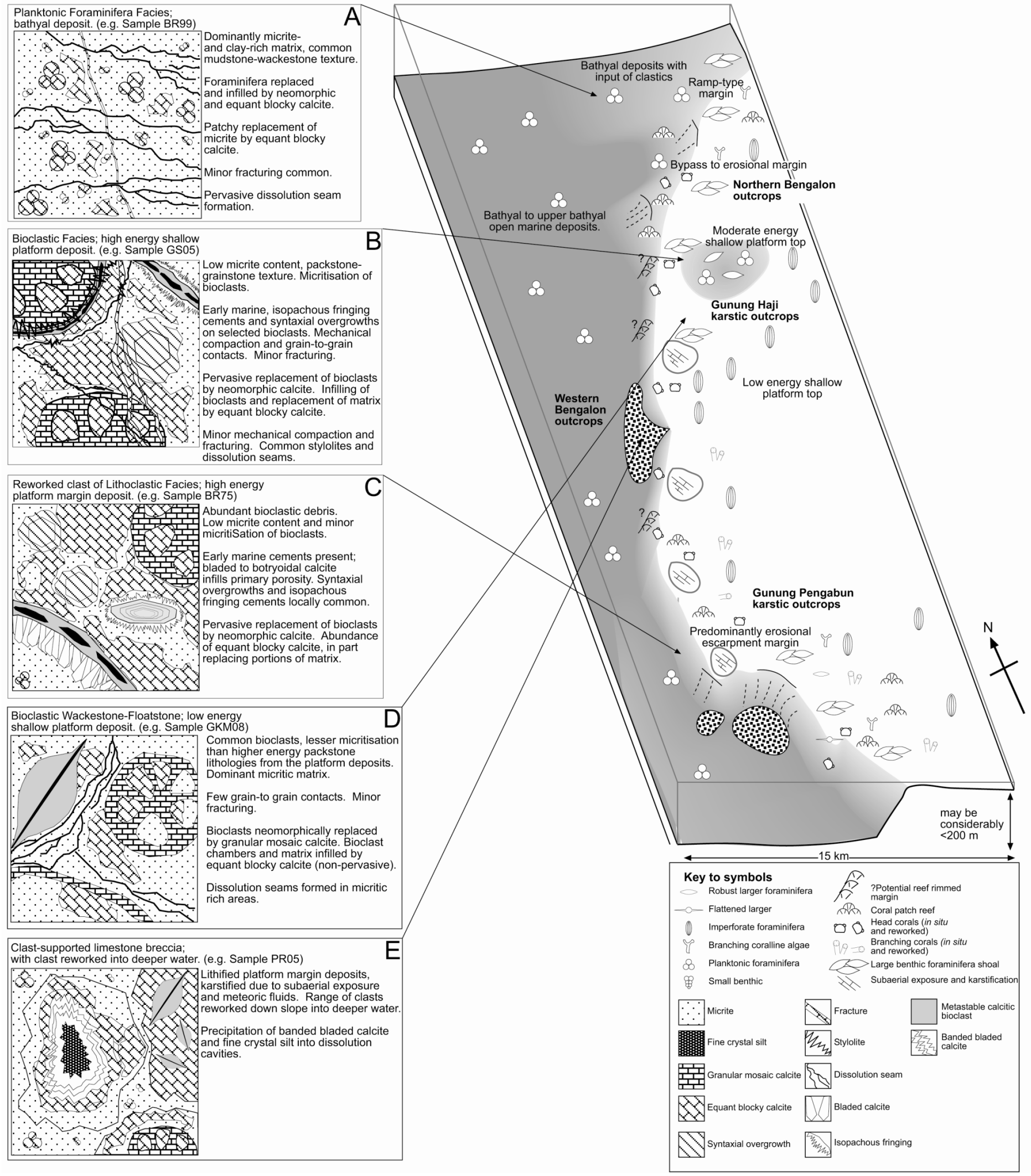

Figure 4.8. Diagenetic summary of various deposits across the Kedango Carbonate Platform. (A) Low energy planktonic foraminifera facies are common background bathyal deposits adjacent to the main platform. Such bathyal deposits do not experience early marine cementation and later burial effects resulted in minor cement precipitation or neomorphism. (B) High energy deposits from the shallow-water platform top are not common, and typically contain whole or fragmented robust bioclasts. Early marine cements are most prevalent in grainstone or coarse packstone textures and sutured grain-to-grain contacts are well developed. C) High energy platform margin deposits are similar to high energy shallow-water platform deposits, but may show development of bladed to radiaxial calcite cements in primary porosity. D) Low energy bioclastic facies to mudstone-wackestone facies are abundant across the platform. These deposits commonly show pervasive micritisation, and are dominated by micrite. Grain breakage, internal deformation of grain, and concavo-convex to tangential grain contacts may all develop prior to stabilisation and calcitisation. Dissolution seams are common through the micritic matrix. E) Rare evidence of subaerial exposure and meteoric diagenesis may be seen in clasts reworked from the platform margin. Schematic layout of the Western Kedango Carbonate Platform is based upon a Lower Miocene reconstruction (Wilson et al. 2012).

4.7.2 Diagenetic Variability and Controlling Influences

As described above there are variations in diagenesis across the different bathyal, slope and shallow-platform deposits of the Kedango Limestone, particularly for the earlier stages of alteration. The most influential controls on depositional development and variability of the western margin of the Kedango carbonate platform were tectonic subsidence, active faulting, the protected semi-enclosed marine embayment setting, and probably terrestrial runoff (Wilson et al., 2012). These same regional controls, together with platform hydrology and component variability reflecting local environmental variations, are also inferred to have been major controlling influences on the diagenesis of the Kedango Platform. However, there are significant differences in diagenesis from other platforms in the broader Borneo-Makassar Straits region that commonly experienced repeated subaerial exposure (Epting, 1980; Fulthorpe and Schlanger, 1989). Also diagenetic variability within the Kedango Limestone is perhaps not as marked as in these other platforms (cf. Park et al., 1992; Grötsch and Mercadier, 1999; Wilson and Evans, 2002; Wilson, 2012) again probably reflecting the setting of the platform in a subsiding, protected semi-enclosed marine embayment as discussed below.

4.7.3 Marine Embayment and Variations in Platform Energy

The low to moderate energy deposits inferred for much of the Kedango Limestone reflect the setting of the western part of the Kedango Platform in the sheltered marine embayment of the Kutai Basin (Wilson et al., 2012). This setting protected the western platform from the high current and wave energies associated with the Indonesian Throughflow Current and the open oceanic conditions of the Celebes Sea by the north-eastern development of the rest of the platform and highs in the Mangkalihat area (Wilson and Moss, 1999; Wilson and Evans, 2002). The generally low energy setting of the Kedango Platform is the dominant control leading to extensive development of micrite-rich deposits throughout the study area (Wilson et al., 2012). The micritisation that is common in all platform top and margin deposits of the Kedango Limestone is also inferred to have been promoted in the generally protected setting of the platform and perhaps by the low-oligotrophy to mesotrophy inferred for the basin (cf. Wilson et al., 2012). The thickest development of micrite

rims (50 μm) in low energy shallow platform top deposits, some associated with inferred seagrass beds, and in northern platform margin deposits closest to the area of terrestrial runoff is consistent with a nutrient and/or specific environmental control on pervasive micritisation. The low-oligotrophy to mesotrophy inferred for the basin probably promoted the abundance of echinoderm debris in platform margin deposits, on which syntaxial overgrowths are promoted.

The general paucity, to localised lack of, isopachous fringing, bladed and other marine cements throughout most platform top and margin deposits is also consistent with the predominant low to moderate depositional energies inferred for the platform as a whole. If easterly winds affected Borneo then it is possible the western margin of the Kedango Platform experienced slightly enhanced wave energies along the platform margin and moderate to higher energies in the shallowest areas of the platform top, in the later case particularly where adjacent to inferred ramp margin development (Wilson et al., 2012). Alternatively, variable occurrences of grainstone and coarse packstone deposits may reflect localised higher energy areas associated with, or between, the patchy coral and seagrass bed development inferred for the shallow-water platform top, such as might be associated with intra-bank tidal currents (cf. Rankey and Reeder, 2010; Wilson et al., 2012). The isopachous fringing and bladed cements are only present generally as minor phases within some of the higher energy deposits, and attests to higher wave or current energy that promotes flushing of the platform with seawater, primarily in the shallowest platform top and platform margin. Marine cements are generally poorly developed in humid equatorial carbonates, perhaps linked to the low salinities of marine waters in the SE Asian region (Wilson, 2002; 2008; 2012). In the Kedango Limestone the general paucity of early marine cements together with the local environment of cement development are both in keeping with those from the region. However, where the Kedango Limestone differs from other Early Miocene examples, such as the Nido Limestone, offshore Palawan and the Taballar Limestone on the Mangkalihat High, is in having far lesser development of marine cements in platform margin deposits (sub-millimetre to mm-scale as opposed to cm-scale thickness fringing cements; cf. Grötsch and Mercadier, 1999; Wilson and Evans, 2002). Although the link between local environments, facies and marine cementation is analogous for the Kedango, Nido and Taballar Limestones the markedly lesser degree of marine cementation in

the Kedango Platform probably relates to its semi-enclosed basinal setting versus the open oceanic facing settings of the other platforms.

4.7.4 Subsidence and Eustasy

It is inferred that the Kedango Limestone was deposited in a largely subsiding area on the basis of the >600 m thick succession of shallow-water carbonates affected by common burial diagenesis (Wilson et al., 2012). Although eustatic fluctuations may have caused localised shallowing and deepening of the platform top during the Oligocene, it is only during the Miocene that there is evidence for highly localised emergence of the platform top (samples BR53, PR05 and BR07a; Figs. 4.1, 4.2), with a eustatic sea level fall a possible cause (Wilson et al., 2012). However active tectonism resulting in uplift and an angular unconformity at the end of the Early Miocene on the adjacent Mangkalihat High is also a possible and likely cause of emergence (cf. Camp et al., 2009; Wilson et al., 2012). The pervasive fracturing affecting Lithoclastic Facies derived from the southern part of the platform may reflect continued fault movement and/or reactivation of structures that are associated with an inferred faulted-escarpment southern margin to the platform and associated down-slope reworking (cf. Cloke et al., 1999; Wilson et al., 2012). Despite eustatic variability, the continued post-rifting sag and subsidence of the Kedango Platform is the most likely reason for the apparent overall lack of subaerial exposure features and meteoric diagenetic effects. The paucity of both early marine or meteoric cementation in the Kedango Limestone together with continued subsidence of, and accumulation on, the platform have resulted in pervasive burial-related stabilisation, cementation, mechanical and chemical compaction.

The Tonasa Limestone Formation (Sulawesi; Wilson, 1996, Wilson et al., 2000) and Kerendan Carbonate Platform (Borneo; Saller and Vijaya, 2002) are diagenetically analogous to the Kedango Limestone in many respects. In these comparable examples meteoric diagenetic effects are negligible and there is a tectonic influence on their development; only being seen as minor features on faulted highs. Instead burial diagenetic features of stabilisation, cementation, mechanical and chemical compaction dominate as in the Kedango Limestone (Wilson, 1996; Saller and Vijaya, 2002). However, there is a marked contrast in the diagenesis of predominantly low

energy platforms developed in subsiding basins, such as the Kedango, Kerenden and Tonasa Limestones to the more typical open-oceanic carbonate platforms that are often the focus of hydrocarbon exploration. Many Miocene carbonate platforms in SE Asia commonly built to sea level and experienced meteoric leaching due to repeated subaerial exposure, with the development of vuggy porosity through leaching commonly preserved and/or enhanced by later leaching (Epting, 1980; Fulthorpe and Schlanger, 1989; Grötsch and Mercadier, 1999; Wilson and Hall, 2010; Wilson, 2012). Despite the effects of widespread vadose aragonite dissolution there is also large-scale reprecipitation of carbonate cements in both the vadose and particularly the phreatic meteoric diagenetic environment (Wilson, 2012). Many of the classic SE Asian carbonate systems (e.g. Luconia, Natuna and Liuhua) have a layered development attributed at least in part to repeated subaerial exposure and leaching in the vadose zone and pervasive phreatic cementation (Epting, 1980; Dunn et al., 1996; Zampetti et al., 2003). Leaching commonly results in porosities of up to 10-40% making such carbonate systems attractive hydrocarbon reservoirs, unlike the Kedango Limestone with <1-2% porosity.

The hypotheses that cross-platform variations in depositional facies and/or environment specific processes influenced diagenesis holds to a limited extent for the Kedango Limestone. Environment specific diagenetic variability is seen as: (1) micritisation being most prevalent in low to moderate energy platform top deposits, (2) minor marine cementation being limited to platform margin or shallowest platform-top deposits, and (3) very limited meteoric diagenesis just affecting a few shallow platform margin samples. Also: (4) syntaxial overgrowth cements are most common in platform margin to slope deposits that are richest in echinoderm debris and had some original primary porosity, and (5) shallow platform-top deposits rich in imperforate foraminifera were affected most by compaction related allochem distortion. However, the subsiding marine embayment setting had the greatest diagenetic impact (i.e. hypothesis 2) resulting in a number of near platform-wide prevalent features that give overall diagenetic homogeneity to the Kedango Limestone. These prevalent diagenetic features include: (1) pervasive micritisation, (2) paucity of early marine or meteoric cements, (3) pervasive neomorphism of aragonite and associated calcitisation, and (4) prevalence of compaction-related features.

4.8 Conclusions

The diagenesis of the Kedango Limestone was strongly controlled by local environmental conditions, depositional facies variations and basin history. The low-energy, subsiding marine embayment setting had the most impact on diagenesis with some cross-platform variability in components, lithological textures and hydrology also influential factors. These facies and environmental influences impact: (1) the degree of micritisation, (2) the location and prevalence of marine isopachous and bladed cements, (3) components and component-specific diagenesis including syntaxial overgrowth cements and the potential for mechanical breakage or compaction of grains, and (4) mineralogies, depositional textures and primary porosities that all influence the potential for burial-related stabilisation, cementation and chemical compaction. However the overall low energy setting of the platform in a semi-enclosed subsiding basin results in a similarity of many features across the whole system, and "masking" of features that are prevalent in many other carbonate systems in SE Asia. I.e. extensive micritisation, together with pervasive burial-related cements and compaction effects dominate in the Kedango Limestone versus volumetrically important marine cements and layered vadose zone leaching. The basinal context and its history influenced the: (a) abundance of micrite; impacting primary porosity, (b) paucity of early cements and (c) prevalence of burial-related stabilisation, cementation and compaction that collectively result in porosities of 1-2% for the Kedango Limestone.

4.9 Acknowledgements

This research forms a part of Rob Madden's PhD studies, supervised by Moyra Wilson, at Curtin University. Initial fieldwork and laboratory analyses for this study were jointly funded by LASMO Runto Ltd, Maersk Oil Indonesia Maratua AS, and the SE Asia Research Group, Royal Holloway University, London. Subsequent analyses were made possible through the Sherman A. Wengard Memorial Grant awarded by the AAPG Grants-in-Aid Foundation together with additional support from Petronas. Fieldwork was undertaken by Moyra Wilson, John Chambers and Dharma S. Nas with the support of Chandra Tiranda and a LASMO field crew. Cathodoluminescent analysis was run with the help of Francis Witkowski at Royal

Holloway. Initial stable isotope analyses were run in collaboration with Tony Fallick and Terry Donnelly at SUERC, East Kilbride. Grzegorz Skrzypek at the University of Western Australia, through the John de Laeter Centre, assisted in further stable-isotope work.

4.10 References

Alam, H., Paterson, D.W., Syarifuddin, N., Busono, I., and Corbin, S.G., 1999. Reservoir potential of carbonate rocks in the Kutai Basin region, east Kalimantan, Indonesia. Journal of Asian Earth Sciences 17, 203-214.

Ali, M., 1995. Carbonate cement stratigraphy and timing of diagenesis in a Miocene mixed carbonate-clastic sequence, offshore Sabah, Malaysia - constraints from cathodoluminescence, geochemistry and isotope studies. Sedimentary Geology 99, 191-214.

Allan, J.R., and Matthews, R.K., 1982. Isotope signatures associated with early meteoric diagenesis. Sedimentology 29, 797-817.

Anderson, T.F., and Arthur, M.A., 1983. Stable isotopes of oxygen and carbon and their application to sedimentologic and paleoenvironmental problems. In: Arthur, M.A., Anderson, T.F., Kaplan, I.R., Veizer, J. and Land, L.S., (Eds.), Stable Isotopes in Sedimentary Geology, SEPM Short Course No. 10, 1-1 - 1-151.

Bathurst, R.G.C., 1966. Boring algae, micrite envelopes and lithification of molluscan biosparites. The Journal of Geology 5, 15-32.

Bowen, G.J., and Wilkinson, B., 2002. Spatial distribution of $\delta^{18}O$ in meteoric precipitation. Geology 30, 315-318.

Brachert, T.C., and Dullo, W.C., 2000. Shallow burial diagenesis of skeletal carbonates: selective loss of aragonite shell material (Miocene to Recent, Queensland Plateau and Queensland Trough, NE Australia) – implications for shallow cool-water carbonates. Sedimentary Geology 136, 169-187.

Budd, D.A., and Perkins, R.D., 1980. Bathymetric zonation and paleoecological significance of microborings in Puerto Rican shelf and slope sediments. Journal of Sedimentary Petrology 50, 881-904.

Camp, W.K., Guritno, E.E., Drajat, D., and Wilson, M.E.J., 2009. Middle-Lower Eocene turbidites: a new deepwater play concept, Kutei Basin, East

Kalimantan, Indonesia. Proceedings of the Indonesian Petroleum Association 33rd Annual Convention. 1-19 p.

Carnell, A.J.H., and Wilson, M.E.J., 2004. Dolomites in SE Asia - varied origins and implications for hydrocarbon exploration. In: Braithwaite, C.J.R., Rizzi, G., and Darke, G., (Eds.), The Geometry and Petrogenesis of Dolomite Hydrocarbon Reservoirs. Geological Society of London, Special Publication 235, 255-300.

Caron, V., and Nelson, C.S., 2009. Diversity of neomorphic fabrics in New Zealand Plio-Pleistocene cool-water limestones: Insights into aragonite alteration pathways and controls. Journal of Sedimentary Research 79, 226-246.

Cloke, I.R., Moss, S.J. and Craig, J., 1999. Structural controls on the evolution of the Kutai Basin, East Kalimantan. Journal of Asian Earth Science 17, 137-156.

Dickson, J.A.D., 1965, A modified staining technique for carbonates in thin section. Nature 205, 587.

Dickson, J.A.D., 1966. Carbonate identification and genesis as revealed by staining. Journal of Sedimentary Petrology 36, 491-505.

Dunham, R.J., 1962. Classification of carbonate rocks according to depositional texture. In*:* Ham, W.E. (Ed.), Classification of carbonate rocks. American Association of Petroleum Geologists, Memoir 1, 108-121.

Dunn, P.A., Kozar, M.G., and Budiyono, 1996. Application of geosciences technology in a geologic study of the Natuna gas field, Natuna Sea, offshore Indonesia. Proceedings of the Indonesian Petroleum Association 25th Annual Convention. 117-130.

Embry, A.F. and Klovan, J.E. 1971. A late Devonian reef tract on northeastern Banks Island, Northwest Territories. Canadian Petroleum Geologist, Bulletin 19, 730-781.

Epting, M., 1980. Sedimentology of Miocene carbonate buildups, central Luconia, offshore Sarawak. Bulletin of the Geological Society of Malaysia 12, 17-30.

Esteban, M., and Klappa, C.F., 1983. Subaerial exposure. In: Scholle, P.A., Bebout, D.G., and Moore, C.H., (Eds.), Carbonate Depositional Environments. American Association of Petroleum Geologists, Memoir 33, 1-55.

Finkel, E.A., and Wilkinson, B.H., 1990. Stylolitization as a source of cement in Mississippian Salem Limestone, west central Indiana. American Association of Petroleum Geologists, Bulletin 74, 174-186.

Flügel, E., 2004. Microfacies of carbonate rocks, Springer, Berlin Heidelberg New York, 976 p.

Fruth, L.S., Orme, G.R., and Donath, F.A., 1966. Experimental compaction effects in carbonate sediments. Journal of Sedimentary Petrology 36, 747-754.

Fulthorpe, C.S., and Schlanger, S.O., 1989. Paleo-Oceanographic and tectonic settings of Early Miocene reefs and associated carbonates of offshore Southeast-Asia. American Association of Petroleum Geologists, Bulletin 73, 729-756.

Golubic, S., Perkins, R.D., and Lukas, K.J., 1975. Boring microorganisms and microborings in carbonate substrates. In: Frey, R.W., (Ed.), The study of trace fossils, Springer, New York, p. 229-259.

Grötsch, J., and Mercadier, C., 1999. Integrated 3-D Reservoir Modeling Based on 3-D Seismic: The Tertiary Malampaya and Camago Buildups, Offshore Palawan, Philippines. American Association of Petroleum Geologists, Bulletin 83, 1703-1728.

Gunther, A., 1990. Distribution and bathymetric zonation of shell boring endoliths in recent reef and shelf environments: Cozumel, Yucatan (Mexico). Facies 22, 233-262.

Hall, R., 1996. Reconstructing Cenozoic SE Asia. In: Hall, R., and Blundell, D.J., (Eds.), Tectonic Evolution of Southeast Asia. Geological Society of London, Special Publication 106, 153-184.

Hall, R., 2002. SE Asian heat flow: Call for new data. Indonesian Petroleum Association, Newsletter 4, 20-21.

Halley, R.B. and Scholle, P.A. 1985. Radiaxial fibrous calcite as early-burial, open-system cement: isotopic evidence from the Permian of China. American Association of Petroleum Geologists, Bulletin 69, 261.

Harrison, R.S., 1977. Caliche profiles indicators of near-surface subaerial diagenesis, Barbados, West Indies. Canadian Petroleum Geologists, Bulletin 25, 123-173.

Hendry, J.P., Taberner, C., Marshall, J.D., Pierre, C., and Carey, P.F., 1999. Coral reef diagenesis records pore-fluid evolution and paleohydrology of a

siliciclastic basin margin succession (Eocene South Pyrenean foreland basin, northeastern Spain). Geological Society of America, Bulletin 111, 395-411.

Lind, I.L., 1993. Stylolites in chalk from Leg 130, Ontong Java Plateau. In: Berger, W.H., Kroenke, J.W., and Mayer, L.A., (Eds.). Proceedings of the Ocean Drilling Program, Scientific Results, 130. Ocean Drilling Program, College Station, TX, 445-451.

Machel, H.G., 2004. Concepts and models of dolomitization: A critical reappraisal. In: Braithwaite, C.J.R., Rizzi, G., and Darke, G., (Eds.). The Geometry and Petrogenesis of Dolomite Hydrocarbon Reservoirs. Geological Society of London, Special Publication 235, 7-63.

Madden, R.H.C., and Wilson, M.E.J., 2012. Diagenesis of Neogene delta-front patch reefs: Alteration of coastal, siliciclastic influenced carbonates from humid equatorial regions: Journal of Sedimentary Research 82, 871-888.

Mazzullo, J. and Graham, A.J., (Eds.), 1988. Handbook for Shipboard Sedimentologists. ODP Technical Notes 8.

Melim, L.A., Westphal, H., Swart, P.K., Eberli, G.P., and Munnecke, A., 2002. Questioning carbonate diagenetic paradigms: evidence from the Neogene of the Bahamas. Marine Geology 185, 27-53.

Moore, C.H., 2001. Carbonate reservoirs, porosity evolution and diagenesis in a sequence stratigraphic framework. Elsevier. Developments in Sedimentology 55, 444 p.

Morad, S., 1998. Carbonate cementation in sandstones: distribution patterns and geochemical evolution. In: Morad, S, (Ed.), Carbonate Cementation in Sandstones. International Association of Sedimentologists, Special Publication 26, 1-26.

Moss, S.J., and Chambers, J.L.C., 1999. Tertiary facies architecture in the Kutai Basin, Kalimantan, Indonesia. Journal of Asian Earth Sciences 17, 157-181.

Moss, S.J., Chambers, J., Cloke, I., Satria, D., Ali, J.R., Baker, S., Milsom, J., and Carter, A., 1997. New observations on the sedimentary and tectonic evolution of the Tertiary Kutai Basin, East Kalimantan. In: Fraser, A.J., Matthews, S.J. and Murphy, R.W., (Eds.), Petroleum Geology of Southeast Asia. Geological Society of London, Special Publication 126, 395-416.

Nelson, C.S., and Smith, A.M., 1996. Stable oxygen and carbon isotope compositional fields for skeletal and diagenetic components in New Zealand

Cenozoic nontropical carbonate sediments and limestones: a synthesis and review. New Zealand Journal of Geology and Geophysics 39, 93 - 107.

Nicolaides, S., and Wallace, M.W., 1997. Pressure dissolution and cementation in an Oligo-Miocene non-tropical limestone (Clifton Formation), Otway Basin, Australia. In: James, N.P. and Clarke, J.A.D., (Eds.), Cool Water Carbonates. SEPM, Special Publication 56, 249 - 261.

Park, R.K., Siemers, C.T., and Brown, A., 1992. Holocene carbonate sedimentation, Pulau Seribu, Java Sea: the third dimension. In: Siemers, C.T., Longman, L.W., Park, R.K., and Kaldi, J.G., (Eds.), Carbonate Rocks and Reservoirs of Indonesia, A Core Workshop. Indonesian Petroleum Association, Core Workshop Notes 2: 1-15.

Perry, C.T., 1998. Grain susceptibility to the effects of microboring: implications for the preservation of skeletal carbonates. Sedimentology 45, 39-51.

Perry, C.T., 1999. Biofilm-related calcification, sediment trapping and constructive micrite envelopes: a criterion for the recognition of ancient grass-bed environments? Sedimentology 46, 33-45.

Perry, C.T., and Bertling, M., 2000. Spatial temporal patterns of macroboring within Mesozoic and Cenozoic coral reef systems. In: Insalaco, E., Skeleton, P.W., and Palmer, T.J., (Eds.), Carbonate Platform Systems: Components and Interactions. Geological Society of London, Special Publication 178, 33-50.

Perry, C.T., and Macdonald, I.A., 2002. Impacts of light penetration on the bathymetry of reef microboring communities: implications for the development of microendolithic trace assemblages. Palaeogeography Palaeoclimatology Palaeoecology 186, 101-113.

Perry, C.T., and Larcombe, P., 2003. Marginal and non-reef-building coral environments. Coral Reefs 22, 427-432.

Perry, C.T., and Hepburn, L.J., 2008. Syn-depositional alteration of coral reef framework through bioerosion, encrustation and cementation: Taphonomic signatures of reef accretion and reef depositional events. Earth-Science Reviews 86, 106-144.

Railsback, L.B., 1993b. Lithologic controls on morphology of pressure-dissolution surfaces (stylolites and dissolution seams) in Paleozoic carbonate rocks from the Mideastern United States. Journal of Sedimentary Petrology 63, 513-522.

Rankey, E.C. and Reeder, S.L., 2010. Controls on platform-scale patterns of surface sediments, shallow Holocene platforms, Bahamas. Sedimentology 57, 1545-1565.

Saller, A.H., and Moore, C.H., 1991, Geochemistry of meteoric calcite cements in some Pleistocene limestones. Sedimentology 38, 601 - 622.

Saller, A.H., and Vijaya, S., 2002. Depositional and diagenetic history of the Kerendan Carbonate Platform, Oligocene, central Kalimantan, Indonesia. Journal of Petroleum Geology 25, 123-149.

Saller, A., Armin. R., Ichram, L.O., and Glenn-Sullivan, C., 1993. Sequence stratigraphy of aggrading and back stepping carbonate shelves, Central Kalimantan, Indonesia. In: Loucks, R.G. and Sarg, J.F., (Eds.), Carbonate sequence stratigraphy, recent developments and applications. American Association of Petroleum Geologists, Memoir 57, 267-290.

Sharaf, E., Simo, J.A., Carroll, A.R., and Shields, M., 2005. Stratigraphic evolution of Oligocene-Miocene carbonates and siliciclastics, East Java basin, Indonesia. American Association of Petroleum Geologists, Bulletin 89, 799-819.

Skryzypek G., and Paul, D., 2006. $\delta^{13}C$ analysis of calcium carbonate: comparison between the GasBench and elemental analyzer techniques. Rapid Communications in Mass Spectrometry 20, 2915–2920.

Steinen, R.P., 1974. Phreatic and vadose diagenetic modification of Pleistocene limestone; petrographic observations from subsurface of Barbados, West Indies. American Association of Petroleum Geologists, Bulletin 58, 1008-1024.

Swei, G.H., and Tucker, M.E., 2012. Impact of diagenesis on reservoir quality in ramp carbonates: Gialo Formation (middle Eocene), Sirt Basin, Libya. Journal of Petroleum Geology 35, 25-48.

Swinchatt, J.P., 1965. Significance of constituent composition, texture, and skeletal breakdown in some recent carbonate sediments. Journal of Sedimentary Petrology 35, 71-90.

Tomascik, T., Mah, A.J., Nontji, A. and Moosa, M.K., 1997. The Ecology of the Indonesian Seas. Oxford University Press, Singapore 1388 p.

Tucker, M.E., and Wright, V.P., 1990. Carbonate Sedimentology, Blackwell Scientific Publications, 482 p.

van der Kooij, B., Immenhauser, A., Steubers, T., Bahamonde Rionda, J.R., and Merino Tome, O., 2010. Controlling factors of volumetrically important marine carbonate cementation in deep slope settings. Sedimentology 57, 1491-1525.

van de Weerd, A.A., and Armin, R.A., 1992. Origin and evolution of the Tertiary hydrocarbon-bearing basin in Kalimantan (Borneo), Indonesia. American Association of Petroleum Geologists, Bulletin 76, 1778-1803.

Warrlich, G., Taberner, C., Asyee, W., Stephenson, B., Esteban, M., Boya-Ferrero, M., Dombrowski, A. and Van Konijnenburg, J.-H. 2010. The impact of postdepositional processes on reservoir properties: two case studies of Tertiary carbonate buildup gas fields in Southeast Asia (Malampaya and E11). In: Morgan, W.A., George, A.D, Harris, P.M., Kupecz, J.A. and Sarg, J.F. (Eds.). Cenozoic Carbonate Systems of Australasia. SEPM Special Publication 95, 99-127.

Wilson, M.E.J., 1996. Evolution and hydrocarbon potential of the Tertiary Tonasa Limestone Formation, Sulawesi, Indonesia. Proceedings of the Indonesian Petroleum Association 25th Annual Convention, 227-240.

Wilson, M.E.J., 2002. Cenozoic carbonates in Southeast Asia: implications for equatorial carbonate development. Sedimentary Geology 147, 295-428.

Wilson, M.E.J. 2008a. Global and regional influences on equatorial shallow marine carbonates during the Cenozoic. Palaeogeography, Palaeoclimatology, Palaeoecology, 265, 262-274.

Wilson, M.E.J., 2011. SE Asian carbonates: tools for evaluating environmental and climatic change in the equatorial tropics over the last 50 million years. In: Hall, R., Cottam, M.A., and Wilson, M.E.J., (Eds.), The SE Asian gateway: history and tectonics of Australia-Asia collision, Geological Society of London, Special Publication 355, 347-369.

Wilson, M.E.J., 2012. Equatorial carbonates: an earth systems approach. Sedimentology 59, 1-31.

Wilson, M.E.J., and Moss, S.J., 1999. Cenozoic palaeogeographic evolution of Sulawesi and Borneo. Palaeogeography Palaeoclimatology Palaeoecology 145, 303-337.

Wilson, M.E.J., and Evans, M.J., 2002. Sedimentology and diagenesis of Tertiary carbonates on the Mangkalihat Peninsula, Borneo: implications for subsurface reservoir quality. Marine and Petroleum Geology 19, 873-900.

Wilson, M.E.J., and Hall, R., 2010. Tectonic influences on SE Asian carbonate systems and their reservoir development. In: Morgan, W.A., George, A.D., Harris, P.M., Kupecz, J.A. and Sarg, J.F., (Eds.), Cenozoic Carbonates of Australasia. SEPM Special Publication 95, 122-149.

Wilson, M.E.J., Chambers, J.L.C., Evans, M.J., Moss, S.J., and Nas, D.S., 1999. Cenozoic carbonates in Borneo: case studies from northeast Kalimantan. Journal of Asian Earth Sciences 17, 183-201.

Wilson, M.E.J., Bosence, D.W.J., and Limbong, A., 2000. Tertiary syntectonic carbonate platform development in Indonesia. Sedimentology 47, 395-419.

Wilson, M.E.J., Chambers, J.L.C., Manning, C., and Nas, D.S. 2012. Spatio-temporal evolution of a Tertiary carbonate platform margin and adjacent basinal deposits. Sedimentary Geology 271-272, 1-27.

Witkowski, F.W., Blundell, D.J., Gutteridge, P., Horbury, A.D., Oxtoby, N.H., and Qing, H., 2000. Video cathodoluminescence microscopy of diagenetic cements and its applications. Marine and Petroleum Geology 17, 1085-1093.

Zampetti, V., Schlager, W., van Konijenburg, J.H., and Everts, A.J., 2003. Depositional history and origin of porosity in a Miocene carbonate platform of central Luconia, offshore Sarawak. Bulletin of the Geological Society of Malaysia 47, 139-152.

Chapter 5

DISCUSSION

MODERN AND NEOGENE ANALOGUES FOR PRODUCTIVE SUBSURFACE CARBONATE SYSTEMS IN SE ASIA

5.1 Introduction

Most modern analogues used to help evaluate carbonate development and their subsurface reservoir potentials are from regions like, Florida, the Bahamas, the Red Sea, or the Persian Gulf. However, within carbonate build-ups the world's most prolific hydrocarbon reserves are in Neogene subsurface deposits from SE Asia (Greenlee and Lehmann 1993) where models generated in other regions cannot easily be applied (Wilson 2002). This study has been based on the hypothesis that the study of a variety of modern and Neogene systems in SE Asia will allow evaluation of how depositional and diagenetic conditions unique to the equatorial tropics influence regional reservoir development. This discussion chapter indentifies the significane of each of the individual studies (chapters 2, 3 and 4) in terms of hydrocarbon reservoir characterisation, as well as placing the studies in a global context.

5.2 Reservoir Development of Humid Tropical Isolated Carbonates

During the Cenozoic large isolated carbonate platforms commonly developed on faulted highs throughout SE Asia where they developed: (1) protected from siliciclastic influx, (2) as pure carbonates and (3) commonly forming prolific hydrocarbon reservoirs in the subsurface (Wilson and Hall, 2010). Isolated carbonate platforms commonly built to sea level and experienced meteoric leaching due to subaerial exposure (Epting, 1980; Fulthorpe and Schlanger, 1989; Grötsch and Mercadier, 1999). A lack of siliciclastics reduced the potential for diagenetic alteration of feldspars and clays and related cementation (Hendry et al., 1999; Morad et al., 2000) There is the potential for preservation of vuggy porosity generated

through meteoric leaching, or its enhancement through later solution enhancement (Wilson and Hall, 2010). Furthermore, pure carbonates, especially if partially cemented, have a higher resistance to compaction processes, and subsequent cementation, under burial than admixed carbonate-siliciclastics (Purser, 1978; Hird and Tucker, 1988; Railsback, 1993a; Clari and Martire, 1996).

Over 75% of carbonate reservoirs in SE Asia are from isolated pure carbonate platforms (e.g. Luconia, Natuna, Luihua; Wilson and Hall, 2010). Despite the effects of widespread vadose aragonite dissolution there is also large-scale reprecipitation of carbonate cements in both the vadose and particularly the phreatic marine realm (Wilson, 2012). Meteoric cements typically show a soil-zone influenced carbon isotopic signature (Fournier et al., 2004). Many of the reservoirs have a layered development due to repeated subaerial exposure, leaching in the vadose zone and pervasive cementation in the phreatic zone (Epting, 1980; Dunn, 1996; Zampetti et al., 2003; Huebeck et al., 2004). Meteoric leaching of aragonitic components commonly results in porosities of up to 10-40% making such carbonate systems attractive hydrocarbon reservoirs.

5.3 Reservoir Potential of Humid Coastal Carbonates: The Samarinda Carbonates

The end products of diagenesis of coastal humid equatorial carbonates (as presented in chapter 3) are markedly different from those of their better studied isolated platform counterparts. Subaerial exposure and near surface meteoric diagenesis in the vadose and phreatic zones has led to the development of extensively leached carbonate units in isolated carbonate platforms, in comparison with sustained meteoric aquifer flow leading to pervasive stabilisation and cementation in humid coastal settings (cf. Samarinda carbonates).

The interpretation of the diagenetic history of the coastal Samarinda carbonates, as with that of other warm, humid tropical coastal examples (Hendry et al., 1999), suggests a model of continental aquifer flow driving early pervasive stabilisation (Fig. 3.10) without generating the relatively high porosity of many SE Asian humid isolated platforms and carbonates from arid settings. For the Samarinda carbonates,

the presence of siliciclastic units in association with the patch reefs, their early burial, location adjacent to a large landmass, and the humid equatorial climate are the factors resulting in their poor reservoir quality. It is likely that other carbonates developed in similar humid coastal settings with significant siliciclastic influx and sustained continental aquifer influence are also likely to include unattractive reservoir units (cf. Ali, 1995; Netherwood and Wright, 1992; Hook and Wilson, 2003; Wilson and Hall, 2010), due to the early stabilisation and cementation of reef components. Factors that help to mitigate against low reservoir quality in humid coastal carbonates are: (1) high original primary porosity linked to high depositional energy, (2) limited aragonitic components, (3) localised or limited aquifer flow and (4) subaerial exposure (Hood and Nelson, 1996; Nelson et al., 2003; Caron and Nelson, 2009).

The Samarinda carbonates from the Kutai Basin of eastern Kalimantan, Indonesia indicate that the diagenesis of these (and likely other) patch reefs from equatorial "ever-wet" climatic settings are strongly controlled by basin margin palaeohydrology. Notably, continental aquifer flow, which drove shallow subsurface flow and early pervasive stabilization of reef components, was driven by the humid 'ever-wet' climatic conditions associated with extensive Cenozoic tectonic uplift. Early stabilisation and cementation are developed in other carbonates in similar humid mixed carbonate-siliciclastic successions, with large adjacent landmasses, in which extensive meteoric phreatic to shallow burial fluid flow is the dominant diagenetic process (cf. Hendry et al,. 1999). Low reservoir quality with a porosity of <1-2% (Appendix C1) is commonly associated with this early stabilisation and cementation, but contrasts markedly with prolific reservoir development in many regional isolated carbonate platforms or arid sub-tropical systems. These findings are of particular relevance to SE Asia, with widespread mixed carbonate-siliciclastic systems developed in coastal settings with a humid equatorial climate, in which models generated in other regions cannot easily be applied.

5.4 Reservoir Potential of Humid Protected Isolated Carbonate Platforms: The Kedango Limestone

During periods of emergence, fresh water lenses commonly develop on carbonate platforms, leading to the pervasive dissolution of metastable calcite mineralogies. It is inferred that the Kedango Limestone was deposited in a largely subsiding area, although eustatic fluctuation may have caused localised shallowing and deepening of the platform top (Wilson et al., 2012). Despite eustatic variability, the continued post-rifting sag and subsidence of the Kedango Platform is the most likely reason for the apparent overall lack of subaerial exposure features and meteoric diagenetic effects. Also, an apparent lack of reefal framework, perhaps linked to the low-energy marine embayment setting, abundance of micrite and nutrient influx hindering reefal framework development may have reduced the potential for building to sea-level and subsequent exposure (cf. Wilson et al., 2012).

Overall the effects of diagenesis across the Kedango Platform have resulted in tight carbonates with very low porosities that are typically <1-2% (Appendix D1). The high abundance of low-energy, micrite-rich deposits in the Kedango Limestone resulted in low primary porosity. Where primary porosities may have been initially higher, particularly in the higher energy platform margin or lithoclastic facies deposits, porosity has been occluded partially by marine cementation together with neomorphic replacement of bioclasts and matrix and calcitisation into pore spaces, but also reduced via extensive mechanical and chemical compaction. In regional examples (Tonasa and Kerendan) higher primary porosities are also found in high energy deposits and lithoclastic facies deposits, however porosity has been nearly completely occluded by the effects of later cementation and compaction. In the case of the Kerendan Platform, acidic basinal waters expelled by the burial compaction of adjacent shales has caused late stage leaching and generated porosities of 5-13%. In the Kedango Limestone the generally low abundance of early marine cements has contributed little to mitigating against the effects of later compaction-related porosity reduction (cf. Purser, 1978; Bathurst, 1987; Hird and Tucker, 1988). Porosity and the potential for hydrocarbon reservoir development for the Kedango Limestone are best developed in the higher energy lithologies that show evidence of subaerial diagenesis and meteoric dissolution features, however the effects of sediment

infiltration localised nature of exposure, and later calcitisation of pore spaces still results in only minor porosity development (typically <1-2%). Furthermore, a low abundance of originally aragonitic components results in a low diagenetic potential (stabilisation versus dissolution and reprecipitation) and the effects of dissolution have not been pervasive. In similar high-energy deposits, if cementation has not been extensive it is possible that hydrocarbon reservoir potential could prove to be viable and perhaps laterally extensive.

In several dominantly low energy carbonate platforms within the SE Asian region diagenesis has resulted in limestones with comparable diagenetic properties to the Kedango Limestone (Wilson, 1996; Grötsch and Mercadier, 1999; Saller and Vijaya, 2000). In regional analogues to the Kedango Limestone there is a clear contrast in low energy platforms to the open oceanic carbonate platforms that are often the focus of hydrocarbon exploration. Low energy carbonate platforms are suggestive of diagenesis controlled by an interplay of factors: (1) subsidence versus uplift and exposure, (2) primary depositional facies, (3) local environmental settings, and (3) prevailing to local energy conditions.

5.5 Modern Isolated Carbonates as Models of Facies Attributes: Pulau Kaledupa and Hoga, Tukang Besi Archipelago

Despite a clear economic importance of Neogene carbonate build-ups as reservoir targets there are very few studies of analogous modern or Neogene outcrops in SE Asia (Wilson, 2008b). Detailed modern studies are largely restricted to those of the Pulau Seribu system, offshore Jakarta (Scrutton, 1978; Park et al., 1992; Jordan, 1998; O'Shea, 2005). These high-energy, small-scale build-ups do not fully encompass the inherent variability of carbonate depositional systems that have developed throughout the region (Wilson, 2008b). There has been a need for new evaluations of modern and Neogene carbonate systems to provide analogue data to aid in reservoir prediction of subsurface build-ups.

Results from the study of modern carbonate sediments from the Tukang Besi Archipelago, Indonesia were the quantification of facies characteristics, primary sedimentological properties and an index of early alteration features. The analysis of

modern environmental facies and associated sedimentological characteristics is of particular importance to the production of geologic models for isolated platform reservoirs. Modern analogues, such as the Kaledupa-Hoga system, provide conceptual facies predictions for characterising fickle hydrocarbon systems, whereby reservoir models may be created with realistic, heterogeneous environmental facies distributions, and more accurate predictions of likely sedimentary attributes and primary porosity characteristics.

The Kaledupa-Hoga systems detailed in chapter 2 are small-scale modern fringing reef systems around isolated, uplifted carbonate islands; just one of several modern carbonate systems from the wider Tukang Besi Archipelago. The archipelago consists of a wide range of coral reef systems and depositional settings including: large-scale atolls (>10 km across), small-scale atolls (<10 km across), small-scale build-ups lacking an (significant) interior lagoon, and barrier to fringing reefs encircling the uplifted carbonate islands. The primary sedimentological characteristics of Kaledupa-Hoga reveal that for the most part sediments throughout the system are grainstones, despite the significant development of sediment baffles (seagrass beds). More importantly the primary controls on grain size distribution are poorly developed windward-leeward settings, and strong tidal currents. What remains to be tested is whether or not similar sedimentological characteristics (grainstones with a high abundance of fragmented and abraded coral and shell material) persist throughout the remainder of the archipelago. Within carbonate systems grainstones are particularly attractive as possible reservoir units (cf. Kaczmarek et al., 2010). Not only are the distribution of modern carbonate sediments from SE Asia poorly understood but so are early diagenetic impacts. Although grainstones are attractive reservoir targets, modern carbonate sediments from the archipelago suggest that grainstones do not predominate in the rock record, instead packstones dominate (Wilson, 2008b). However, similar to the Kedango Platform, higher energy margins that undergo early marine cementation may prove to be effective reservoir units. Preliminary results from the uplifted carbonate islands of Tukang Besi reveal that high-energy cemented margins do occur (Wilson, 2008b).

Equatorial carbonate production was extensive and diverse throughout the SE Asian region during the Cenozoic (Wilson, 2002). The modern sedimentological study of

Kaledupa-Hoga may provide analogues within the SE Asian region for subsurface Cenozoic fringing or small-scale sand-cay-fringing systems that may be identifiable in the subsurface.

5.6 Summary

Modern and Neogene carbonate production is, and was extensive and diverse throughout the tropical waters of SE Asia. The studies presented within this thesis offer analogues to a variety of carbonate depositional systems seen in SE Asia, but may have applicability outside the region. Carbonate systems in SE Asia range from mixed carbonate clastic shelves, localised and ephemeral shoals or reefs, a variety of shallow-water platform top settings and deep water and/or reworked carbonates (Wilson et al., 1999; Wilson 2002; Wilson and Hall, 2010).

Almost half the world's oil production (Dickey, 1986) and a similar percentage of Indonesia's hydrocarbon production is from carbonate reservoirs (Park et al., 1995). The majority of SE Asia's hydrocarbon reserves are estimated to be contained in carbonate build-ups of Neogene age, with continuing major new discoveries (e.g. Kujung Formation; East Java Sea). Furthermore >45% of hydrocarbon reserves contained within Phanerozoic carbonate build-ups were in Neogene systems containing >16.5 BBOE, with most of these located in SE Asia (Greenlee and Lehmann, 1993). Despite the economic importance of Neogene carbonate systems as reservoir targets there are very few studies of analogous modern or Neogene outcrops from SE Asia.

This thesis presents data on three key carbonate systems: isolated fringing reefs, land-attached patch reefs and isolated platforms in semi-enclosed basins. The findings of each study have applicability within SE Asia, and perhaps elsewhere. Key reservoir-related findings are:

- Coastal mixed carbonate-siliciclastic deposits have low primary porosity and reservoir quality. These deposits are pervasively stabilised and cemented during early burial diagenesis due to the throughput of understaturated meteoric fluids. Diagenesis by meteoric fluids is promoted by the deposits

juxtaposition against uplifited contental islands in a humid equatorial climatic setting.

- Isolated carbonate platforms that developed in protected and/or subsiding settings possess low primary porosities and low reservoir qualities. Such carbonates developed in protected subsiding settings are subject to extensive burial compaction, stabilisation and cementation. However in high energy marginal settings it is likely that early marine cementation may be enhanced, with the potential to offset burial diagenetic effects and promote higher reservoir quality if primary porosity and pore throats are not occluded.

- In small-scale high energy fringing reef systems where grainstone textures predominate, if early partial cementation is promoted good quality reservoir units may be preserved. The ability to predict the location of primary sedimentological properties with the potential for good reservoir quality in Cenozoic examples may be enhanced through such models as the Kaledupa-Hoga system; however, it remains unclear as to how applicable this model is to the rest of the SE Asian region and forms part of an ongoing study to characterise the wider Tukang Besi Archipelago.

5.7 References

Ali, M., 1995. Carbonate cement stratigraphy and timing of diagenesis in a Miocene mixed carbonate-clastic sequence, offshore Sabah, Malaysia - constraints from cathodoluminescence, geochemistry and isotope studies. Sedimentary Geology 99, 191-214.

Bathurst, R.G.C., 1987. Diagenetically enhanced bedding in argillaceous platform limestones: stratified cementation and selective compaction. Sedimentology 34, 749-778.

Caron, V., and Nelson, C.S., 2009. Diversity of neomorphic fabrics in New Zealand Plio-Pleistocene cool-water limestones: Insights into aragonite alteration pathways and controls. Journal of Sedimentary Research 79, 226-246.

Clari, P.A., and Martire, L., 1996. Interplay of cementation, mechanical compaction, and chemical compaction in nodular limestones of the Rosso Ammonitico Veronese (Middle–Upper Jurassic, Northeastern Italy). Journal of Sedimentary Research 66, 447-458.

Dickey, P.A., 1985. Petroleum development geology. Penwell Publishing Company, 530 p.

Dunn, P.A., Kozar, M.G., and Budiyono, 1996. Application of geosciences technology in a geologic study of the Natuna gas field, Natuna Sea, offshore Indonesia. Proceedings of the Indonesian Petroleum Association 25th Annual Convention, 117-130.

Epting, M., 1980. Sedimentology of Miocene carbonate buildups, central Luconia, offshore Sarawak. Bulletin of the Geological Society of Malaysia 12, 17-30.

Fournier, F., Montaggioni, L. and Borgomano, J. 2004. Paleoenvironments and high-frequency cyclicity from Cenozoic South-East Asian shallow-water carbonates: a case study from the Oligo-Miocene buildups of Malampaya (Offshore Palawan, Philippines). Marine and Petroleum Geology 21, 1-21.

Fulthorpe, C.S., and Schlanger, S.O., 1989. Paleo-Oceanographic and tectonic settings of Early Miocene reefs and associated carbonates of offshore Southeast-Asia. American Association of Petroleum Geologists, Bulletin 73, 729-756.

Greenlee, S.M., and Lehmann, P.J., 1993. Stratigraphic framework of productive carbonate build-ups. In: R.G. Loucks, and J.F. Sarg (Eds.) Carbonate Sequence Stratigraphy, Recent Developments and Applications, American Association of Petroleum Geologists, Memoir 57, 267-290.

Grötsch, J., and Mercadier, C., 1999. Integrated 3-D Reservoir Modeling Based on 3-D Seismic: The Tertiary Malampaya and Camago Buildups, Offshore Palawan, Philippines. American Association of Petroleum Geologists, Bulletin 83, 1703-1728.

Hendry, J.P., Taberner, C., Marshall, J.D., Pierre, C., and Carey, P.F., 1999. Coral reef diagenesis records pore-fluid evolution and paleohydrology of a siliciclastic basin margin succession (Eocene South Pyrenean foreland basin, northeastern Spain). Geological Society of America, Bulletin 111, 395-411.

Hird, K., and Tucker, M.E., 1988. Contrasting diagenesis of two Carboniferous oolites from South Wales: a tale of climatic difference. Sedimentology 35, 587-602.

Hood, S.D., and Nelson, C.S., 1996. Cementation scenarios for New Zealand Cenozoic nontropical limestones. New Zealand Journal of Geology and Geophysics 39, 109-122.

Hook, J., and Wilson, M.E.J., 2003. Stratigraphic relationships of a Miocene mixed carbonate–siliciclastic interval in the Badak field, East Kalimantan, Indonesia. 29th Indonesian Petroleum Association, Annual Convention, Proceedings, 147-161.

Huebeck, C., Story, K., Peng, P., Sullivan, C., and Duff, S., 2004. An integrated reservoir study of the Liuhua 11-1 field using a high-resolution three-dimensional seismic data set. In: Eberli, G.P., Masafero, J.L., and Sarg, J.F., (Eds.) Seismic imaging of carbonate reservoirs and systems. American Association of Petroleum Geologists, Memoir 81, 149-168.

Jordan, C.J., 1998. The sedimentation of Kepuluan Seribu: A modern patch reef complex in the West Java Sea, Indonesia. Indonesian Petroleum Association Field Guide, Jakarta, Indonesia, 81 p.

Kaczmarek, S.E., Hicks, M.K., Fullmer, S.M., Steffen, K.L., Bachtel, S.L., 2010. Mapping facies distributions on modern carbonate platforms through integration of multispectral Landsat data, statistics-based unsupervised classifications, and surface sediment data. American Association of Petroleum Geologists, Bulletin 94, 1581-1606.

Morad, S., Ketzer, J.M., and Ros, L.F.D., 2000. Spatial and temporal distribution of diagenetic alterations in siliciclastic rocks: implications for mass transfer in sedimentary basins. Sedimentology, 47, 95-120.

Nelson, C.S., Winefield, P.R., Hood, S.D., Caron, V., Pallentin, A., and Kamp, P.J.J., 2003. Pliocene Te Aute limestones, New Zealand: expanding concepts for cool-water shelf carbonates. New Zealand Journal of Geology and Geophysics 46, 407-424.

Netherwood, R., and Wight, A., 1992. Structurally-controlled, linear reefs in a Pliocene delta-front setting, Tarakan Basin, Northeast Kalimantan. In: Siemers, C.T., Longman, M.W., Park, R.K., and Kaldi, J.G., (Eds.).

Carbonate Rocks and Reservoirs of Indonesia. Indonesian Petroleum Association, Core Workshop, Notes 1, Ch. 3, p. 3-1 – 3-37.

O'Shea, M. 2005. Evaluating shallow water variability in equatorial carbonates. Are deposit characteristics distinctive of local environments and water depths? Unpublished Masters Thesis, Durham University, UK, 149 p and Appendices.

Park, R.K., Siemers, C.T., Brown, A.A., 1992. Holocene Carbonate Sedimentation, Pulau Seribu, Java Sea, - The Third Dimension. In: Siemers, C.T., Longman, M.W., Park, R.K. and Kaldi, J.G. (Eds.) Carbonate Rocks and Reservoirs of Indonesia, a Core Workshop. Indonesian Petroleum Association, Jakarta, Indonesia, 2-1 - 2-15.

Park, R.K., Matter, A., and Tonkin, P.C., 1995. Porosity evolution in the Batu Raja Carbonates of the Sunda Basin – Windows of opportunity. Proceedings of the Indonesian Petroleum Association 24th Annual Convention, 63-184.

Purser, B.H., 1978. Early diagenesis and the preservation of porosity in Jurassic limestones. Journal of Petroleum Geology 50, 1149-1168.

Railsback, L.B., 1993a. Contrasting styles of chemical compaction in the Upper Pennsylvanian Dennis Limestone in the Midcontinent Region, U.S.A. Journal of Sedimentary Petrology 63, 61-72.

Saller, A.H., and Vijaya, S., 2002. Depositional and diagenetic history of the Kerendan Carbonate Platform, Oligocene, central Kalimantan, Indonesia. Journal of Petroleum Geology 25, 123-149.

Scrutton, M.E., 1978. Modern Reefs in the West Java Sea, Proceedings of the Indonesian Petroleum Association Carbonate Seminar (Special Volume), Jakarta, Indonesia, 14-41.

Wilson, M.E.J., 1996. Evolution and hydrocarbon potential of the Tertiary Tonasa Limestone Formation, Sulawesi, Indonesia. Proceedings of the Indonesian Petroleum Association 25th Annual Convention, 227-240.

Wilson, M.E.J., 2002. Cenozoic carbonates in SE Asia: Implications for equatorial carbonate development. Sedimentary Geology 147, 295-428.

Wilson, M.E.J., 2008b. Reservoir quality of Cenozoic carbonate buildups and coral reef terraces. Proceedings of the 32nd Indonesian Petroleum Association Annual Convention and Exhibition, 8 p.

Wilson, M.E.J., 2012. Equatorial carbonates: an earth systems approach. Sedimentology 59, 1-31.

Wilson, M.E.J., and Hall, R., 2010. Tectonic influences on SE Asian carbonate systems and their reservoir development. In: Morgan, W.A., George, A.D., Harris, P.M., Kupecz, J.A., and Sarg, J.F., (Eds.) Cenozoic Carbonates of Australasia. SEPM, Special Publication 95, 122-149.

Wilson, M.E.J., Chambers, J.L.C., Evans, M.J., Moss, S.J., and Nas, D.S., 1999. Cenozoic carbonates in Borneo: case studies from northeast Kalimantan. Journal of Asian Earth Sciences 17, 183-201.

Wilson, M.E.J., Chambers, J.L.C., Manning, C., and Nas, D.S. 2012. Spatio-temporal evolution of a Tertiary carbonate platform margin and adjacent basinal deposits. Sedimentary Geology 271-272, 1-27.

Zampetti, V., Schlager, W., van Konijenburg, J.H., and Everts, A.J., 2003. Depositional history and origin of porosity in a Miocene carbonate platform of central Luconia, offshore Sarawak. Bulletin of the Geological Society of Malaysia 47, 139-152.

Chapter 6

CONCLUSIONS AND FUTURE WORK

6.1 Conclusions

This study of modern and Neogene analogues for productive subsurface carbonate systems in SE Asia has provided an excellent opportunity to develop a better understanding of how depositional and diagenetic conditions unique to the equatorial tropics influence regional hydrocarbon development. The conclusions of this research and their implications for productive carbonate systems are given below.

6.2 Sedimentology of Modern Fringing Reef Carbonates

Fringing reefs of SE Asia may conservatively comprise ~30% of the world's coral reef area, but remain almost unstudied. The study of an isolated fringing reef system (Kaledupa-Hoga) from the Tukang Besi Archipelago, SE Asia has provided insights into the variability of primary sedimentological and early alteration characteristics from a range of shallow water carbonate environments. An environmental facies map generated from ground-truthed Landsat-7 satellite data accurately demonstrates the heterogeneous nature of the carbonate system. Although field and satellite imagery observations reveal ten environmental facies, sedimentological characterisation results in a lower number of distinctive categories due to similarities between some deposits. Sediment samples across all fringing reef environments from the Kaledupa-Hoga system are characterised almost exclusively by grain-rudstone textures, with <2-5% silt and clay size fractions, and minor baffling of fines in seagrass-associated settings. The paucity of fines across the fringing reef systems as a whole, and the degree of homogenisation of sediment characteristics across the different field- and satellite-identifiable environmental facies are attributed to: (1) high wave/current energies, (2) the small size of the islands rendering limited protection, (3) bidirectional monsoon winds and (4) the lack of reef-rimmed margins built to sea level. Absent from these deposits are well developed high energy windward and low energy leeward deposit characteristics and/or an overriding

cyclonic influence that may commonly be seen in fringing reef systems from other areas.

6.3 Diagenesis of Delta-Front Patch Reefs: Alteration of Siliciclastic Influenced Carbonates

Carbonate–siliciclastic mixing is common in both modern and ancient environments. In spite of their common occurrence, the diagenesis of siliciclastic-influenced coral reefs and carbonate platforms from equatorial to subtropical settings remains largely unstudied. Study of Neogene siliciclastic-influenced patch reefs from the Samarinda region, Mahakam Delta, Borneo reveals that both pervasive early stabilisation of reef components from aragonite to low-Mg calcite and calcite cementation are key diagenetic features of these coastal carbonates from the humid tropics. The early stabilisation of reef components and extensive cementation are attributed to the reefs being flushed by primarily undersaturated meteoric fluids. Stable-isotope data indicate a continental meteoric, upland source for the precipitating fluids with a lesser influence from trapped marine fluids expelled with increasing burial. The diagenesis of these patch reefs from equatorial "ever-wet" climatic settings are strongly controlled by basin-margin paleohydrology. Continental aquifer flow, which drove shallow subsurface flow and early pervasive stabilisation of reef components, was promoted by the humid "ever-wet" climatic conditions together with Neogene tectonic uplift of the adjacent landmass of Borneo. Early stabilisation and cementation are developed in other carbonates in similar humid mixed carbonate–siliciclastic successions, with large adjacent landmasses, in which extensive meteoric phreatic to shallow-burial fluid flow is the dominant diagenetic process. Furthermore these features of pervasive stabilisation and cementation are rare in arid or temperate counterparts from coastal settings. These findings are of particular relevance to SE Asia, with widespread mixed carbonate–siliciclastic systems developed in coastal settings with a humid equatorial climate, in which models generated in other regions cannot easily be applied.

6.4 Diagenesis of a Cenozoic Carbonate-Platform Margin and its Adjacent Basinal Deposits

The diagenesis and development of open marine Tertiary carbonate platforms from the humid equatorial tropics of SE Asia are relatively well documented, since many comprise hydrocarbon reservoirs in the subsurface. However the diagenetic variability across platform flank and contemporaneous bathyal deposits, particularly from low to moderate energy carbonate platforms is less well known. The diagenesis of the Eocene to Miocene Kedango platform from the semi-enclosed Kutai Basin of Borneo was strongly controlled by local environmental conditions, depositional facies variations and basin history. The low-energy, subsiding marine embayment setting of the Kedango Limestone had a pronounced impact on diagenesis with some cross-platform variability in components, lithological textures and hydrology also influential factors. These facies and environmental influences impact: (1) the degree of micritisation, (2) the location and prevalence of marine isopachous and bladed cements, (3) components and component-specific diagenesis including syntaxial overgrowth cements and the potential for mechanical breakage or compaction of grains, and (4) mineralogies, depositional textures and primary porosities that all influence the potential for burial-related stabilisation, cementation and chemical compaction. The basinal context and its history influenced the: (1) abundance of micrite; impacting primary porosity, (2) paucity of early cements and (3) prevalence of burial-related stabilisation, cementation and compaction. The variability in cross-platform facies and environments impacted upon early diagenesis, however the overall low energy setting of the platform in a semi-enclosed subsiding basin results in a similarity of many features across the whole system, and "masking" of features that are prevalent in many other carbonate systems in SE Asia. I.e. extensive micritisation, together with pervasive burial-related cements and compaction effects dominate in the Kedango Limestone versus volumetrically important marine cements and layered vadose zone leaching.

6.5 Modern and Neogene Analogues for Productive Subsurface Carbonate Systems

The studies presented within this thesis offer analogues to a variety of carbonate depositional systems seen in SE Asia, but may have applicability outside the region. Carbonate systems in SE Asia range from mixed carbonate clastic shelves, localised and ephemeral shoals or reefs, a variety of shallow-water platform top settings and deep water and/or reworked carbonates. With the extensive hydrocarbon production from SE Asian carbonate reservoirs the studies presented herein offer new data and models for SE Asian analogues. This thesis presents data on three key carbonate systems: isolated fringing reefs, land-attached patch reefs and isolated platforms in semi-enclosed basins. The findings of each study have implications for hydrocarbon exploration in other SE Asian carbonate systems.

6.6 Future Work

Cenozoic carbonates are extensively developed throughout SE Asia. This research assesess how depositional and diagenetic conditions unique to the equatorial tropics influence regional carbonate and hydrocarbon reservoir development. However, this research focuses on a fraction of the wide diversity of environmental, depositional and diagenetic conditions that are common to the equatorial tropics, and many carbonate systems in the region have not been adequately studied. Long term research needs to more fully evaluate the impact of regional versus global controls on the development and diagenesis of a whole remit of equatorial carbonate systems. Suggestions are made below as to how such goals may be better realised.

- Limited studies exist that examine the impact of the range of climatic, oceanographic and tectonic factors common to the equatorial tropics on the development, diagenesis and reservoir quality of large-scale Cenozoic carbonate platforms in SE Asia. Carbonate systems for potential further study include the isolated Melinau Limestone (N Borneo), the land-attached Berai Limestone (SE Borneo) the volcanically influenced shelf and isolated patch-reef systems of the Tacipi Formation (Sulawesi) and the cratonic-wide New Guinea Limestone. Further studies that examine major climatic shifts

(e.g. greenhouse to icehouse) and the development of biodiversity hotspots are also required on SE Asian and other systems to bring greater insight into cross platform variations in sedimentology and diagenesis, and increased understanding of the development of large-scale carbonate systems and their controlling influences.

- Isolated SE Asian Cenozoic carbonate build-ups are well known for their hydrocarbon reservoir potential; however, their clastic-dominated land-attached shelf counterparts are poorly studied and understood. An understanding of onshore to offshore trends in shelfal equatorial carbonate development and reservoir quality needs to be cultivated. In particular greater understanding is needed of the apparent paucity of reservoir development in nearshore versus offshore carbonate systems. Studies are needed that examine carbonate systems developed with a near-continuous influx of terrestrial sediments and nutrients and in the presence of meteoric aquifer flow together with the trends that occur across broad land-attached shelves.

- Throughout this study reference has been made to arid and sub-tropical carbonate systems that have proven to not be fully comparable with deposits from the humid equatorial tropics. To more fully test the variability of carbonate systems on global and regional scales further studies are needed. In particular, future studies comparing carbonate systems from arid-subtropical, temperate and the humid-equatorial tropics should further address the development and diagenesis of: (a) clastic-influenced coastal, (b) nutrient-impacted, (c) volcanogenically-influenced and (d) tectonically-affected systems.

- Understanding the past climatic and oceanographic conditions of marine carbonate systems or admixed siliciclastic-carbonates and their often complex diagenetic overprinting commonly relies on geochemical data, particularly $\delta^{18}O$ and $\delta^{13}C$ stable isotopes. There is a need for the collection and interpretation of further stable isotopic data (elucidated towards in chapter 4), as well as trace and major element studies, from modern SE Asian

components, marine and meteoric cements, and whole rock samples. This proposed geochemical study will allow for a better representation and understanding of the overall modern SE Asian isotopic signature, with implications for reconstructing past environmental change and understanding ancient diagenetic histories.

- The ability to predict the location of primary sedimentological properties with the potential for good reservoir quality in Cenozoic examples may be enhanced through more systematic and statistical studies of modern marine systems, such as those from the the Kaledupa-Hoga (chapter 2). However, it remains unclear as to how applicable the environmental, deposit and satellite characterisation study of fringing reefs from Kaledupa-Hoga is to other modern carbonate systems. There is a need to test the applicability of the model presented in chapter 2 to a wider range of systems, including large isolated atolls, small-scale build-ups and further land-attached fringing or barrier systems from both within and outside the equatorial tropics.

Chapter 7

REFERENCES

Ahmad, W., and Neil, D.T., 1994. An evaluation of Landsat Thematic Mapper (TM) digital data for discriminating coral reef zonation: Heron Reef (GBR). International Journal of Remote Sensing 15, 2583-2597.

Alam, H., Paterson, D.W., Syarifuddin, N., Busono, I., and Corbin, S.G., 1999. Reservoir potential of carbonate rocks in the Kutai Basin region, east Kalimantan, Indonesia. Journal of Asian Earth Sciences 17, 203-214.

Ali, M., 1995. Carbonate cement stratigraphy and timing of diagenesis in a Miocene mixed carbonate-clastic sequence, offshore Sabah, Malaysia - constraints from cathodoluminescence, geochemistry and isotope studies. Sedimentary Geology 99, 191-214.

Allan, J.R., and Matthews, R.K., 1982. Isotope signatures associated with early meteoric diagenesis. Sedimentology 29, 797-817.

Allen, G.P., and Chambers, J.L.C., 1998. Sedimentation in the Modern and Miocene Mahakam Delta. Indonesian Petroleum Association, Jakarta, Field Trip Guidebook, 236 p.

Almasi, M.N., Hoskin, C.M., Reed, J.K., and Milo, J., 1987. Effects of natural and artificial *Thalassia* on rates of sedimentation. Journal of Sedimentary Petrology 57, 901-906.

Anderson, T.F., and Arthur, M.A., 1983. Stable isotopes of oxygen and carbon and their application to sedimentologic and paleoenvironmental problems. In: Arthur, M.A., Anderson, T.F., Kaplan, I.R., Veizer, J. and Land, L.S., (Eds.) Stable Isotopes in Sedimentary Geology, SEPM Short Course No. 10, 1-1 - 1-151.

Andréfouët, S., Muller-Karger, F.E., Hochberg, E.J., Hu, C., and Carder, K.L., 2001. Change detection in shallow coral reef environments using Landsat 7 ETM+ data. Remote Sensing of Environment 78, 150-162.

Andréfouët, S., Kramer, P., Torres-Pulliza, D., Joyce, K.E., Hochberg, E.J., Garza-Pérez, R., Mumby, P.J., Riegl, B., Yamano, H., White, W.H., Zubia, M., Brock, J.C., Phinn, S.R., Naseer, A., Hatcher, B.G., and Muller-Karger, F.E.,

2003. Multi-site evaluation of IKONOS data for classification of tropical coral reef environments. Remote Sensing of Environment 88, 128-143.

Andrews, J.E., Christidis, S., and Dennis, P.F., 1997, Assessing mineralogical and geochemical heterogeneity in the sub 63 micron size fraction of Holocene lime muds. Journal of Sedimentary Research 67, 531-535.

Asriningrum, W. 2011. Reef morphology identification in Sikka, NTT using Landsat imagery. Journal of Indonesian Coral Reefs 1, 48-54.

Bathurst, R.G.C., 1966. Boring algae, micrite envelopes and lithification of molluscan biosparites. The Journal of Geology 5, 15-32.

Bathurst, R.G.C., 1987. Diagenetically enhanced bedding in argillaceous platform limestones: stratified cementation and selective compaction. Sedimentology 34, 749-778.

Beu, A.G., 1995. Pliocene limestones and their scallops: Lower Hutt, New Zealand. Institute of Geological and Nuclear Sciences Limited, Monograph 10, 243 p.

Beavington-Penney, S.J., 2004. Analysis of the effects of abrasion on the test of *Palaeonummulites venosus*: implications for the origin of nummulithoclastic sediments. PALAIOS 19 143–155.

Beavington-Penney, S.J. and Racey, A., 2004. Ecology of extant nummulitids and other larger benthic foraminifera: applications in palaeoenvironmental analysis. Earth Science Reviews 67, 219-265.Becking, L.E., Cleary, D.F.R., de Voogd, N.J., Renema, W., de Beer, M., van Soest, R.W.M., and Hoeksema, B.W., 2006. Beta diversity of tropical marine benthic assemblages in the Spermonde Archipelago, Indonesia. Marine Ecology 27, 76-88.

Bell, J.J., and Smith, D.J., 2004. Ecology of sponge assemblages (Porifera) in the Wakatobi region, south-east Sulawesi, Indonesia: richness and abundance. Journal of the Marine Biological Association of the United Kingdom 84, 581-591.

Bell, J.J., Berman, J., Powell, A., and Hepburn, L.J., 2010. The ecology of sponges in the Wakatobi National Park. In: Clifton, J., Unsworth, R.K.F. and Smith, D.J. (Eds.) Marine research and conservation in the Coral Triangle The Wakatobi National Park. Nova Science Publishers, New York, 85-109.

Bjørlykke, K., 1993. Fluid flow in sedimentary basins. Sedimentary Geology 86, 137-158.

Blanchon, P., and Jones, B., 1997. Hurricane control on shelf-edge-reef architecture around Grand Cayman. Sedimentology 44, 479-506.

Blanchon, P., Jones, B., and Kalbfleisch, W. 1997. Anatomy of a fringing reef around Grand Cayman: storm rubble not coral framework. Journal of Sedimentary Research 67, 1-16.

BouDagher-Fadel, M.K., and Wilson, M.E.J., 2000. A revision of some larger foraminifera of the Miocene of southeast Kalimantan. Micropaleontology 46, 153-165.

Bowen, G.J., and Wilkinson, B., 2002. Spatial distribution of $\delta^{18}O$ in meteoric precipitation. Geology 30, 315-318.

Brachert, T.C., and Dullo, W.C., 2000. Shallow burial diagenesis of skeletal carbonates: selective loss of aragonite shell material (Miocene to Recent, Queensland Plateau and Queensland Trough, NE Australia) – implications for shallow cool-water carbonates. Sedimentary Geology 136, 169-187.

Braithwaite, C.J.R., Montaggioni, L.F., Camoin, G.F., Dalmasso, H., Dullo,W.C., and Mangini, A., 2000. Origins and development of Holocene coral reefs: a revisited model based on reef boreholes in the Seychelles, Indian Ocean. International Journal of Earth Sciences 89, 431–445.

Brasier, M.D., 1975. An outline history of seagrass communities. Palaeontology 18, 681-702.

Budd, D.A., and Perkins, R.D., 1980. Bathymetric zonation and paleoecological significance of microborings in Puerto Rican shelf and slope sediments. Journal of Sedimentary Petrology 50, 881-904.

Budd, D.A., and Perkins, R.D., 1980. Bathymetric zonation and paleoecological significance of microborings in Puerto Rican shelf and slope sediments. Journal of Sedimentary Petrology 50, 881-904.

Burton, L.M., 2003. Carbonate-siliciclastic interactions: Tertiary examples from Spain. Unpublished Ph.D. thesis; The University of Durham, 396 p.

Cabioch, G., Montaggioni, L.F., and Faure, G., 1995. Holocene initiation and development of New Caledonian fringing reefs, SW Pacific. Coral Reefs 14, 131– 140.

Camp, W.K., Guritno, E.E., Drajat, D., and Wilson, M.E.J., 2009. Middle-Lower Eocene turbidites: a new deepwater play concept, Kutei Basin, East

Kalimantan, Indonesia. Proceedings of the Indonesian Petroleum Association 33rd Annual Convention. 19 p.

Carnell, A.J.H., and Wilson, M.E.J., 2004. Dolomites in SE Asia - varied origins and implications for hydrocarbon exploration. In: Braithwaite, C.J.R., Rizzi, G., and Darke, G., (Eds.), The Geometry and Petrogenesis of Dolomite Hydrocarbon Reservoirs. Geological Society of London, Special Publication 235, 255-300.

Caron, V., and Nelson, C.S., 2009. Diversity of neomorphic fabrics in New Zealand Plio-Pleistocene cool-water limestones: Insights into aragonite alteration pathways and controls. Journal of Sedimentary Research 79, 226-246.

Caron, V., Nelson, C.S., and Kamp, P.J.J., 2005. Sequence stratigraphic context of syndepositional diagenesis in cool-water shelf carbonates: Pliocene limestone, New Zealand. Journal of Sedimentary Research 75, 231-250.

Cavagnetto, C., and Anadón, P., 1996. Preliminary palynological data on floristic and climatic changes during the Middle Eocene-Early Oligocene of the eastern Ebro Basin, northeast Spain. Review of Palaeobotany and Palynology 92, 281-305.

Clari, P.A., and Martire, L., 1996. Interplay of cementation, mechanical compaction, and chemical compaction in nodular limestones of the Rosso Ammonitico Veronese (Middle–Upper Jurassic, Northeastern Italy). Journal of Sedimentary Research 66, 447-458.

Cleary, D.F.R., Becking, L.E., de Voogd, N.J., Renema, W., de Beer, M., van Soest, R.W.M., and Hoeksema, B.W., 2005. Variation in the diversity and composition of benthic taxa as a function of distance offshore, depth and exposure in the Spermonde Archipelago, Indonesia. Estuarine Coastal and Shelf Science 65, 557-570.

Cloke, I.R., Moss, S.J. and Craig, J., 1999. Structural controls on the evolution of the Kutai Basin, East Kalimantan. Journal of Asian Earth Science 17, 137-156.

Cordier, E., Poizot, E., and Méar, Y., 2012. Swell impact on reef sedimentary processes: a case study of the La Reunion fringing reef. Sedimentology 59, 2004-2023.

Crabbe, M.J.C., and Smith D.J. 2002. Comparison of two reef sites in the Wakatobi Marine National Park (SE Sulawesi, Indonesia) using digital image analysis. Coral Reefs 21, 242-244.

Dickey, P.A., 1985. Petroleum development geology. Penwell Publishing Company, 530 p.

Dickson, J.A.D., 1965. A modified staining technique for carbonates in thin section. Nature 205, 587.

Dickson, J.A.D., 1966. Carbonate identification and genesis as revealed by staining. Journal of Sedimentary Petrology 36, 491-505.

Dodd, J.R., and Nelson, C.S., 1998. Diagenetic comparisons between non-tropical Cenozoic limestones of New Zealand and tropical Mississippian limestones from Indiana, USA: Is the non-tropical model better than the tropical model? Sedimentary Geology 121, 1-21.

Doust, H., and Noble, R.A., 2008. Petroleum systems of Indonesia. Marine and Petroleum Geology 25, 103-129.

Dunham, R.J., 1962. Classification of carbonate rocks according to depositional texture. In*:* Ham, W.E. (Ed.) Classification of carbonate rocks. American Association of Petroleum Geologists, Memoir 1, 108-121.

Dunn, P.A., Kozar, M.G., and Budiyono, 1996. Application of geosciences technology in a geologic study of the Natuna gas field, Natuna Sea, offshore Indonesia. Proceedings of the Indonesian Petroleum Association 25th Annual Convention, 117-130.

Embry, A.F. and Klovan, J.E. 1971. A late Devonian reef tract on northeastern Banks Island, Northwest Territories. Canadian Petroleum Geologist, Bulletin 19, 730-781.

Epting, M., 1980. Sedimentology of Miocene carbonate buildups, central Luconia, offshore Sarawak. Bulletin of the Geological Society of Malaysia 12, 17-30.

Escher, M.G., 1920. Atollen in den Nederlandsch-Oost-Indischen Archipel: de riffen in de groep der Toekang Besi-Eilanden. Med Encyclopedisch Bureau, Weltevreden XXII, 17 p.

Esteban, M., 1996. An overview of Miocene reefs from Mediterranean areas: general trends and facies models. In: Franseen, E.K., Esteban, M., Ward, W., and Rouchy, J.M., (Eds.) Models for Carbonate Stratigraphy from Miocene

Reef Complexes of Mediterranean regions. SEPM, Concepts in Sedimentology and Paleontology 5, 3-53.

Esteban, M., and Klappa, C.F., 1983. Subaerial exposure. In: Scholle, P.A., Bebout, D.G., and Moore, C.H., (Eds.) Carbonate Depositional Environments. American Association of Petroleum Geologists, Memoir 33, 1-55.

Farzadi, P. 2006. The development of Middle Cretaceous carbonate platforms, Persian Gulf, Iran: Constraints from seismic stratigraphy, well and biostratigraphy. Petroleum Geoscience 12, 59-68.

Finkel, E.A., and Wilkinson, B.H., 1990. Stylolitization as a source of cement in Mississippian Salem Limestone, west central Indiana. American Association of Petroleum Geologists, Bulletin 74, 174-186.

Flügel, E., 2004. Microfacies of carbonate rocks, Springer, Berlin Heidelberg New York, 976 p.

Fournier, F., Montaggioni, L. and Borgomano, J. 2004. Paleoenvironments and high-frequency cyclicity from Cenozoic South-East Asian shallow-water carbonates: a case study from the Oligo-Miocene buildups of Malampaya (Offshore Palawan, Philippines). Marine and Petroleum Geology 21, 1-21.

Franks, P.C., 1969. Nature, origin, and significance of cone-in-cone structures in the Kiowa Formation (Early Cretaceous) North-Central Kansas. Journal of Sedimentary Petrology 39, 1438-1454.

Friedman, I., and O'Neil, J.R., 1977. Compilation of stable isotope fractionation factors of geochemical interest. In: Fleischer, M., (Ed.) Data of Geochemistry: U.S. Geological Survey, Professional Paper 440-K, 1-12.

Fruth, L.S., Orme, G.R., and Donath, F.A., 1966. Experimental compaction effects in carbonate sediments. Journal of Sedimentary Petrology 36, 747-754.

Fulthorpe, C.S., and Schlanger, S.O., 1989. Paleo-Oceanographic and tectonic settings of early Miocene reefs and associated carbonates of offshore Southeast-Asia. American Association of Petroleum Geologists, Bulletin 73, 729-756.

Gabrié, C., and Montaggioni, L.F., 1982. Sediments from fringing reefs of Réunion Island, Indian Ocean. Sedimentary Geology 31, 281– 301.

Galloway, W.E., 1984. Hydrogeologic regimes of sandstone diagenesis. In: McDonald, D.A., and Surdam, R.C., (Eds) Clastic Diagenesis. American Association of Petroleum Geologists, Memoir 37, 3-13.

Ginsburg, R.N., 1957. Early diagenesis and lithication of shallow-water carbonate sediments in South Florida. Regional Aspects of Carbonate Deposition 5, 80-100.

Ginsburg, R.N., and Lowenstam, H.A., 1958. The influence of marine bottom communities on the depositional environments of sediments. Geological Journal 66, 310-318.

Gischler, E., 2006. Sedimentation on Rasdhoo and Ari Atolls, Maldives, Indian Ocean. Facies 52, 341-360.

Gischler, E., 2011. Sedimentary facies of Bora Bora, Darwin's type barrier reef (Society Islands, South Pacific): The unexpected occurrence of non-skeletal grains. Journal of Sedimentary Research 81, 1-17.

Gischler, E. and Lomando, A.J., 1999. Recent sedimentary facies of isolated carbonate platforms, Belize-Yucatan system, Central America. Journal of Sedimentary Research 69, 747-763.

Gischler, E., Hausa, I., Heinrich, K., Scheitel, U., 2003. Characterization of Depositional Environments in Isolated Carbonate Platforms Based on Benthic Foraaminifera, Belize, Central America. Palaios 18, 236-255.

Gordon, A.L., 2005. Oceanography of the Indonesian Seas and their throughflow. Oceanography, 18, 14-27.

Golubic, S., Perkins, R.D., and Lukas, K.J., 1975. Boring microorganisms and microborings in carbonate substrates. n: Frey, R.W., (Ed.) The study of trace fossils, Springer, New York, p. 229-259.

Green, E.P., Mumby, P.J., and Edwards, A.J., 2000. Remote Sensing Handbook for Tropical Coastal Management Sourcebooks 3. UNESCO, Paris, 316 p and plates.

Greenlee, S.M., and Lehmann, P.J., 1993. Stratigraphic framework of productive carbonate build-ups. In: R.G. Loucks, and J.F. Sarg (Eds.) Carbonate Sequence Stratigraphy, Recent Developments and Applications, American Association of Petroleum Geologists, Memoir 57, 267-290.

Grötsch, J., and Mercadier, C., 1999. Integrated 3-D Reservoir Modeling Based on 3-D Seismic: The Tertiary Malampaya and Camago Buildups, Offshore Palawan, Philippines. American Association of Petroleum Geologists, Bulletin 83, 1703-1728.

Gunther, A., 1990. Distribution and bathymetric zonation of shell boring endoliths in recent reef and shelf environments: Cozumel, Yucatan (Mexico). Facies 22, 233-262.

Halford, A. 2003. Fish diversity and distribution. In: Pet-Soede, L., and Erdmann, M.V. (Eds.). Rapid ecological assessment Wakatobi National Park. WWF/TNC Joint Publication, Denpasar, Bali, 53-64.

Hall, R., 1996. Reconstructing Cenozic SE Asia. In: Hall, R., Blundell, D.J. (Eds.) Tectonic Evolution of Southeast Asia. Geological Society of London, Special Publication 106, 153-184.

Hall, R., 2002a. Cenozoic geological and plate tectonic evolution of SE Asia and the SW Pacific: computer-based reconstructions, model and animations. Journal of Asian Earth Sciences 20, 353-431.

Hall, R., 2002b. SE Asian heat flow: Call for new data: Indonesian Petroleum Association Newsletter 4, 20-21.

Hall, R., and Nichols, G., 2002. Cenozoic sedimentation and tectonics in Borneo: climatic influences on orogenesis. Geological Society, London, Special Publications 191, 5-22.

Halley, R.B. and Scholle, P.A. 1985. Radiaxial fibrous calcite as early-burial, open-system cement: isotopic evidence from the Permian of China. American Association of Petroleum Geologists, Bulletin 69, 261.

Hallock, P. and Glenn, E.C., 1986. Larger foraminifera: a tool for paleoenvironmental analysis of Cenozoic carbonate depositional facies. PALAIOS 1, 55-64.

Hammer,Ø., Harper, D.A.T., and Ryan, P.D., 2001. PAST: Paleontological statistics software package for education and data analysis. Palaeontologia Electronica 4, 9 p.

Harris, P.M., 1996. Reef styles of modern carbonate platforms: Bulletin of Canadian Petroleum Geology 44, 72-81.

Harris, P.M. 2010. Delineating and quantifying depositional facies patterns in carbonate reservoirs: Insight from modern analogs. American Association of Petroleum Geologists Bulletin 94, 61-86.

Harris, P. M., and Kowalik, W. S., (Eds.) 1994. Satellite images of carbonate depositional settings: Examples of reservoir- and exploration-scale geologic facies variation. AAPG Methods in Exploration Series No. 11, 147 p.

Harris, P.M., and Vlaswinkel, B., 2008. Modern isolated carbonate platforms: Templates for quantifying facies attributes of hydrocarbon reservoirs. In: J. Lukasik and T. Simo, (Eds.) Controls on carbonate platform and reef development: SEPM Special Publication 89, p. 323–341.

Harris, P.M., Ellis, J., and Purkis, S., 2010. Delineating and quantifying depositional facies patterns in modern carbonate sand deposits on Great Bahama Bank; SEPM Short Course Notes No. 54, p, paper p. 1-51, appendix p. 1-31, and 2 DVDs.

Harris, P.M., Purkis, S.J., and Ellis, J., 2011. Analyzing spatial patterns in modern carbonate bodies from Great Bahama Bank: Journal of Sedimentary Research 81, 185-206.

Harrison, R.S., 1977. Caliche profiles indicators of near-surface subaerial diagenesis, Barbados, West Indies. Canadian Petroleum Geologists, Bulletin 25, 123-173.

Hamilton, W., 1979. Tectonics of the Indonesian region. U.S. Geological Survey, Professional Papers 1078.

Hayward, A.B., 1982. Coral reefs in a clastic sedimentary environment: Fossil (Miocene, S.W. Turkey) and Modern (Recent, Red Sea) analogues. Coral Reefs 1, 109-114.

Hendry, J.P., Taberner, C., Marshall, J.D., Pierre, C., and Carey, P.F., 1999. Coral reef diagenesis records pore-fluid evolution and paleohydrology of a siliciclastic basin margin succession (Eocene South Pyrenean foreland basin, northeastern Spain). Geological Society of America, Bulletin 111, 395-411.

Hetzel, W.H., 1930. Over de Geologie Der Toekang-Besi Eilanden. De Mijningenieur, 11, 51-53.

Hewins, H.R. and Perry, C.T. 2006. Bathymetric and Environmentally influenced patterns of carbonate sediment accummulation in three contrasting reef settings, Danjugan Island, Philippines. Journal of Coastal Research 22, 812-824.

Hird, K., and Tucker, M.E., 1988. Contrasting diagenesis of two Carboniferous oolites from South Wales: a tale of climatic difference. Sedimentology 35, 587-602.

Hood, S.D., and Nelson, C.S., 1996. Cementation scenarios for New Zealand Cenozoic nontropical limestones. New Zealand Journal of Geology and Geophysics 39, 109-122.

Hook, J., and Wilson, M.E.J., 2003. Stratigraphic relationships of a Miocene mixed carbonate–siliciclastic interval in the Badak field, East Kalimantan, Indonesia. 29th Indonesian Petroleum Association, Annual Convention, Proceedings, 147-161.

Hopley, D. and Partain, B. 1987. The structure and development of fringing reefs off the Great Barrier Reef Province. In : Baldwin, C.L. (ed.). Fringing Reef Workshop. Great Barrier Reef Marine Park Authority, Townsville. Science, Industry and Management Workshop Series 9, 32 p.

Hoskin, C.M., 1968. Magnesium and strontium in mud fraction of recent carbonate sediment, Alacran Reef, Mexico. American Association of Petroleum Geologists, Bulletin 52, 2170-2177.

Huebeck, C., Story, K., Peng, P., Sullivan, C., and Duff, S., 2004. An integrated reservoir study of the Liuhua 11-1 field using a high-resolution three-dimensional seismic data set. In: Eberli, G.P., Masafero, J.L., and Sarg, J.F., (Eds.) Seismic imaging of carbonate reservoirs and systems. American Association of Petroleum Geologists, Memoir 81, 149-168.

Husseini, S.I., and Matthews, R.K., 1972. Distribution of high-magnesium calcite in lime muds of the Great Bahama Bank: diagenetic implications. Journal of Sedimentary Petrology 42, 179-182.

Insalaco, E., 1998. The descriptive nomenclature and classification of growth fabrics in fossil scleractinian reefs. Sedimentary Geology 118, 159-186.

James, N.P., 1997. The cool-water carbonate depositional realm. In: James, N.P., and Clarke, J.D.A., (Eds.) Cool-Water Carbonates. SEPM, Special Publication 56, 1–22.

James, N.P., and Choquette, P.W., 1990. Limestones: The meteoric diagenetic environment. In: McIlreath, I.A., and Morrow, D.W., (Eds.) Diagenesis. Geoscience Canada Reprint Series 4: Toronto, Geological Association of Canada, 35-74.

Jordan, C.J., 1998. The sedimentation of Kepuluan Seribu: A modern patch reef complex in the West Java Sea, Indonesia. Indonesian Petroleum Association Field Guide, Jakarta, Indonesia, 81 p.

Kaczmarek, S.E., Hicks, M.K., Fullmer, S.M., Steffen, K.L., and Bachtel, S.L., 2010. Mapping facies distributions on modern carbonate platforms through integration of multispectral Landsat data, statistics-based unsupervised classifications, and surface sediment data. American Association of Petroleum Geologists, Bulletin 94, 1581-1606.

Kamp, P.J.J., and Nelson, C.S., 1988. Nature and occurrence of modern and Neogene active margin limestones in New Zealand. New Zealand Journal of Geology and Geophysics 31, 1-20.

Kuenen, P.H., 1933. Geology of Coral Reefs: The Snellius Expedition in the Eastern part of the Netherlands East Indies 1929-1930. Volume 5: Geological Results, part 2. Kemink en Zoon N.V., 125 p and plates.

Insalaco, E., 1998, The descriptive nomenclature and classification of growth fabrics in fossil scleractinian reefs. Sedimentary Geology 118, 159-186.

Jordan, C.J., 1998. The sedimentation of Kepuluan Seribu: A modern patch reef complex in the West Java Sea, Indonesia. Indonesian Petroleum Association Field Guide, Jakarta, Indonesia, 81 p.

Joyce, K.E., and Phinn, S.R., 2001. Optimal spatial resolution for coral reef mapping. Proceedings of the International Geoscience and Remote Sensing Symposium volume 2, 619-621.

Kaczmarek, S.E., Hicks, M.K., Fullmer, S.M., Steffen, K.L., Bachtel, S.L., 2010. Mapping facies distributions on modern carbonate platforms through integration of multispectral Landsat data, statistics-based unsupervised classifications, and surface sediment data. American Association of Petroleum Geologists Bulletin 94, 1581-1606.

Kennedy, D.M. and Woodroffe, C.D. 2002. Fringing reef growth and morphology: a review. Earth-Science Reviews 57, 255-277.

Koswara, A. and Sukarna, D., 1994. Geology of the Tukang Besi Sheet, Sulawesi. Geological Research and Development Centre, Bandung, Indonesia, 14 p and map.

Kuenen, Ph.H. 1933a. The Geology of Coral reefs. The Snellius Expedition in the eastern part of the Netherlands East Indies 1929-1930. Geological Results. Proc. Kon. Akad. V. Wetensch., Amsterdam 36, 125 p.

Kuenen, Ph.H. 1933b. The formation of the atolls in the Toekang-Besi-group by subsidence. Proc. Kon. Akad. V. Wetensch., Amsterdam 36, 331-336.

Land, L.S., 1983. The applications of stable isotopes to studies of the origin of dolomite and to problems of diagenesis of clastic sediments. In: Arthur, M.A., Anderson, T.F., Kaplan, I.R., Veizer, J., and Land, L.S., (Eds.) Stable Isotopes in Sedimentary Geology. SEPM, Short Course no. 10, 4-1 – 4-22.

Larcombe, P., and Woolfe, K.J., 1999. Terrigenous sediments as influences upon Holocene near shore coral reefs, central Great Barrier Reef, Australia. Australian Journal of Earth Sciences 46, 141-154.

Lees, A. and Buller, A.T., 1972. Modern temperate-water and warm-water shelf carbonate sediments contrasted. Marine Geology 13, 67-73.

Lewis, M.S., 1969. Sedimentary environments and unconsolidated carbonate sediments of the fringing coral reefs of Mahé, Seychelles. Marine Geology 7, 95-127.

Lind, I.L., 1993. Stylolites in chalk from Leg 130, Ontong Java Plateau. In: Berger, W.H., Kroenke, J.W., and Mayer, L.A., (Eds.) Proceedings of the Ocean Drilling Program, Scientific Results, 130. Ocean Drilling Program, College Station, TX, 445-451.

Lokier, S.W., Wilson, M.E.J., and Burton, L.M., 2009. Marine biota response to clastic sediment influx: A quantitative approach. Palaeogeography Palaeoclimatology Palaeoecology 281, 25-42.

Lyzenga, D.R., 1981. Remote sensing of bottom reflectance and water attenuation parameters in shallow water using aircraft and Landsat data. International Journal of Remote Sensing 2, 71-82.

Machel, H.G., 2004. Concepts and models of dolomitization: A critical reappraisal. In: Braithwaite, C.J.R., Rizzi, G., and Darke, G., (Eds.) The Geometry and Petrogenesis of Dolomite Hydrocarbon Reservoirs. Geological Society of London, Special Publication 235, 7-63.

Madden, R.H.C., 2008. The effect of diagenesis on the reservoir quality of mixed carbonate–siliciclastics from Sabah, Borneo. Unpublished MSCi. Thesis, The University of Durham, 78 p.

Madden, R.H.C., and Wilson, M.E.J., 2012. Diagenesis of Neogene delta-front patch reefs: Alteration of coastal, siliciclastic influenced carbonates from humid equatorial regions. Journal of Sedimentary Research 82, 871-888.

Madden, R.H.C., and Wilson, M.E.J., 2013. Diagenesis of a SE Asian Cenozoic carbonate-platform margin and its adjacent basinal deposits. Sedimentary Geology 286-287, 20-38.

Mazzullo, J. and Graham, A.J., (Eds.), 1988. Handbook for Shipboard Sedimentologists. ODP Technical Notes 8.

McBride, E.F., Picard, M.D., and Milliken, K.L., 2003. Calcite-cemented concretions in Cretaceous sandstone, Wyoming and Utah, U.S.A. Journal of Sedimentary Research 73, 462-483.

McMellor, S. and Smith, D.J. 2010. Coral reefs of the Wakatobi: abundance and biodiversity. In: Clifton, J., Unsworth, R.K.F. and Smith, D.J. (Eds.) Marine research and conservation in the Coral Triangle The Wakatobi National Park. Nova Science Publishers, New York, 11-26.

Melim, L.A., Westphal, H., Swart, P.K., Eberli, G.P., and Munnecke, A., 2002. Questioning carbonate diagenetic paradigms: evidence from the Neogene of the Bahamas. Marine Geology 185, 27-53.

Milliman, J.D., 1974. Marine Carbonates: Berlin, Springer-Verlag, 375 p.

Milsom, J., Ali, J., and Sudarwono, 1999. Structure and collision history of the Buton continental fragment, Eastern Indonesia. American Association of Petroleum Geologists Bulletin 83, 1666-1689.

Moore, C.H., 2001. Carbonate reservoirs, porosity evolution and diagenesis in a sequence stratigraphic framework. Elsevier. Developments in Sedimentology 55, 444 p.

Montaggioni, L.F. 2005. History of Indo-Pacific coral reef systems since the last glaciation: Development patterns and controlling factors. Earth Science Reviews 71, 1-75.

Morad, S., 1998. Carbonate cementation in sandstones: distribution patterns and geochemical evolution. In: Morad, S, (Ed.) Carbonate Cementation in Sandstones. International Association of Sedimentologists, Special Publication 26, 1-26.

Morad, S., Ketzer, J.M., and Ros, L.F.D., 2000. Spatial and temporal distribution of diagenetic alterations in siliciclastic rocks: implications for mass transfer in sedimentary basins. Sedimentology, 47, 95-120.

Morrison, J.O., and Brand, U., 1986. Geochemistry of recent marine invertebrates. Geoscience Canada 13, 237-254.

Moss, S.J., and Chambers, J.L.C., 1999. Tertiary facies architecture in the Kutai Basin, Kalimantan, Indonesia. Journal of Asian Earth Sciences 17, 157-181.

Moss, S.J., Chambers, J., Cloke, I., Satria, D., Ali, J.R., Baker, S., Milsom, J., and Carter, A., 1997. New observations on the sedimentary and tectonic evolution of the Tertiary Kutai Basin, East Kalimantan. In: Fraser, A.J., Matthews, S.J. and Murphy, R.W., (Eds.) Petroleum Geology of Southeast Asia. Geological Society of London, Special Publication 126, 395-416.

Mount, J.F., 1984. Mixing of siliciclastic and carbonate sediments in shallow shelf environments. Geology 12, 432-435.

Mumby, P.J., Green, E.P., Clark, C.D., and Edwards, A.J., 1998. Digital analysis of multispectral airborne imagery of coral reefs. Coral Reefs 17, 59-69.

Nelson, C.S., and Smith, A.M., 1996. Stable oxygen and carbon isotope compositional fields for skeletal and diagenetic components in New Zealand Cenozoic nontropical carbonate sediments and limestones: a synthesis and review. New Zealand Journal of Geology and Geophysics 39, 93-107.

Nelson, C.S., Winefield, P.R., Hood, S.D., Caron, V., Pallentin, A., and Kamp, P.J.J., 2003. Pliocene Te Aute limestones, New Zealand: expanding concepts for cool-water shelf carbonates. New Zealand Journal of Geology and Geophysics 46, 407-424.

Netherwood, R., and Wight, A., 1992. Structurally-controlled, linear reefs in a Pliocene delta-front setting, Tarakan Basin, Northeast Kalimantan. In: Siemers, C.T., Longman, M.W., Park, R.K., and Kaldi, J.G., (Eds.). Carbonate Rocks and Reservoirs of Indonesia. Indonesian Petroleum Association, Core Workshop, Notes 1, Ch. 3, p. 3-1 – 3-37.

Nicolaides, S., and Wallace, M.W., 1997. Pressure dissolution and cementation in an Oligo-Miocene non-tropical limestone (Clifton Formation), Otway Basin, Australia. In: James, N.P. and Clarke, J.A.D., (Eds.) Cool Water Carbonates. SEPM, Special Publication 56, 249 - 261.

O'Shea, M. 2005. Evaluating shallow water variability in equatorial carbonates. Are deposit characteristics distinctive of local environments and water depths? Unpublished Masters Thesis, Durham University, UK, 149 p and Appendices.

Ouillon, S., Douillet, P. and Andréfouët, S. 2004. Coupling satellite data with in situ measurements and numerical modeling to study fine suspended-sediment transport: a study for the lagoon of New Caledonia. Coral Reefs 23, 109-122.

Park, R.K., Siemers, C.T., and Brown, A.A., 1992. Holocene Carbonate Sedimentation, Pulau Seribu, Java Sea, - The Third Dimension. In: Siemers, C.T., Longman, M.W., Park, R.K. and Kaldi, J.G. (Eds.) Carbonate Rocks and Reservoirs of Indonesia, a Core Workshop. Indonesian Petroleum Association, Jakarta, Indonesia, 2-1 - 2-15.

Park, R.K., Matter, A., and Tonkin, P.C., 1995. Porosity evolution in the Batu Raja Carbonates of the Sunda Basin – Windows of opportunity. Proceedings of the Indonesian Petroleum Association 24th Annual Convention, 63-184.

Perry, C.T., 1998. Grain susceptibility to the effects of microboring: implications for the preservation of skeletal carbonates. Sedimentology 45, 39-51.

Perry, C.T., 1999. Biofilm-related calcification, sediment trapping and constructive micrite envelopes: a criterion for the recognition of ancient grass-bed environments? Sedimentology 46, 33-45.

Perry, C.T., and Bertling, M., 2000. Spatial temporal patterns of macroboring within Mesozoic and Cenozoic coral reef systems. In: Insalaco, E., Skeleton, P.W., and Palmer, T.J., (Eds.) Carbonate Platform Systems: Components and Interactions. Geological Society of London, Special Publication 178, 33-50.

Perry, C.T., and Macdonald, I.A., 2002. Impacts of light penetration on the bathymetry of reef microboring communities: implications for the development of microendolithic trace assemblages. Palaeogeography Palaeoclimatology Palaeoecology 186, 101-113.

Perry, C.T., and Larcombe, P., 2003. Marginal and non-reef-building coral environments. Coral Reefs 22, 427-432.

Perry, C.T., and Hepburn, L.J., 2008. Syn-depositional alteration of coral reef framework through bioerosion, encrustation and cementation: Taphonomic signatures of reef accretion and reef depositional events. Earth-Science Reviews 86, 106-144.

Pet-Soede, L., and Erdmann, M.V. (Eds.). 2003. Rapid ecological assessment Wakatobi National Park. WWF/TNC Joint Publication, Denpasar, Bali, 187 pp.

Pettijohn, F.J., Potter, P.E., and Siever, R. 1973. Sand and sandstone. Springer, Berlin, 618 p.

Philip, J., Bogomano, J. and Al-Maskiry, S., 1995. Cenomanian-Early Turonian carbonate platform of northern Oman: Stratigraphy and Palaeo-environments. Palaeogeography, Palaeoclimatology, Palaeoceology 119, 77-92.

Purkis, S.J., and Pasterkamp, R., 2004. Integrating in situ reef-top reflectance spectra with Landsat TM imagery to aid shallow-tropical benthic habitat mapping. Coral Reefs 23, 5-20.

Purkis, S.J., Harris, P.M., and Ellis, J., 2012. Patterns of sedimentation in the contemporary Red Sea as an analog for ancient carbonates in rift settings. Journal of Sedimentary Research 82, 859-870.

Purkis, S.J., Riegl, B.M., and Andréfouët, S., 2005. Remote sensing of geomorphology and facies on a modern carbonate ramp (Arabian Gulf, Dubai, U.A.E.). Journal of Sedimentary Research 75, 861-876.

Purser, B.H., 1978. Early diagenesis and the preservation of porosity in Jurassic limestones. Journal of Petroleum Geology 50, 1149-1168.

Railsback, L.B., 1993a. Contrasting styles of chemical compaction in the Upper Pennsylvanian Dennis Limestone in the Midcontinent Region, U.S.A. Journal of Sedimentary Petrology 63, 61-72.

Railsback, L.B., 1993b. Lithologic controls on morphology of pressure-dissolution surfaces (stylolites and dissolution seams) in Paleozoic carbonate rocks from the Mideastern United States. Journal of Sedimentary Petrology 63, 513-522.

Rankey, E.C., 2002. Spatial patterns of sediment accumulation on a Holocene carbonate tidal flat, northwest Andros Island, Bahamas. Journal of Sedimentary Research 72, 591-601.

Rankey, E.C., and Harris, P.M., 2008. Remote sensing and comparative geomorphology of Holocene carbonate depositional systems. In Lukasik, J. and Simo, T. (Eds.). Controls on carbonate platform and reef development, SEPM Special Publication No. 89, 317-322 and CD.

Rankey, E. C. and Reeder, S. L., 2010. Controls on platform-scale patterns of surface sediments, shallow Holocene platforms, Bahamas. Sedimentology 57, 1545–1565.

Renema, W., 2006a. Habitat variables determining the occurrence of large benthic foraminifera in the Berau area (East Kalimantan, Indonesia). Coral Reefs 25, 351-359.

Renema, W., 2006b. Large benthic foraminifera from the deep photic zone of a mixed siliciclastic-carbonate shelf off East Kalimantan, Indonesia. Marine Micropaleontology 58, 73-82.

Renema W, and Hohenegger J., 2005. On the identity of *Calcarina spengleri* (Gmelin, 1791). Journal of Foraminiferal Research 35:15–21.

Ricketts, B.D., Caron, V., and Nelson, C.S., 2004. A fluid flow perspective on the diagenesis of Te Aute limestones. New Zealand Journal of Geology and Geophysics 47, 823-838.

Riegl, B.M., Halfar, J., Purkis, S.J., and Godinez-Ort, L., 2007. Sedimentary facies of the Eastern Pacific's northernmost reef-like setting (Cabo Pulmo, Mexico). Marine Geology 236, 61-77.

Roberts, H.H., and Murray, S.P., 1984. Developing carbonate platforms: southern Gulf of Suez, northern Red Sea. Marine Geology 59, 165-185.

Roberts, H.H., and Sydow, J., 1996. The offshore Mahakam Delta: Stratigraphic response of Late Pleistocene-to-Modern sea level cycle. Proceedings of the 25th Indonesian Petroleum Association, Annual Convenetion, 147-161

Roberts, H.H., Amaron, P., and Phipps, C.V., 1988. Morphology and sedimentology of *Halimeda* bioherms from Eastern Java Sea (Indonesia). Coral Reefs 6, 61-172.

Salinas de León, P., Unsworth, R.K.F. and Bell, J.J. 2010. Marine habitat connectivity in the Wakatobi National Park. In: Clifton, J., Unsworth, R.K.F. and Smith, D.J. (Eds.) Marine research and conservation in the Coral Triangle The Wakatobi National Park. Nova Science Publishers, New York, 129-148.

Saller, A.H., and Moore, C.H., 1991, Geochemistry of meteoric calcite cements in some Pleistocene limestones. Sedimentology 38, 601 - 622.

Saller, A.H., and Vijaya, S., 2002. Depositional and diagenetic history of the Kerendan Carbonate Platform, Oligocene, central Kalimantan, Indonesia. Journal of Petroleum Geology 25, 123-149.

Saller, A., Armin. R., Ichram, L.O., and Glenn-Sullivan, C., 1993. Sequence stratigraphy of aggrading and back stepping carbonate shelves, Central

Kalimantan, Indonesia. In: Loucks, R.G. and Sarg, J.F., (Eds.) Carbonate sequence stratigraphy, recent developments and applications. American Association of Petroleum Geologists, Memoir 57, 267-290.

Saller, A.H., Reksalegora, S., and Bassant, P., 2010. Sequence stratigraphy and growth of shelf margin and middle shelf carbonates. In: Morgan, W.A., George, A.D., Harris, P.M., Kupecz, J.A. and Sarg, J.F., (Eds.) Cenozoic Carbonates of Australasia. SEPM, Special Publication 95, 147–174.

Santisteban, C., and Taberner, C., 1988. Sedimentary models of siliciclastic deposits and coral reef interrelation. In: Doyle, J.L., and Roberts, H.H., (Eds.) Carbonate–Clastic Transitions. Amsterdam, Elsevier, Developments in Sedimentology 42, 35–76.

Scoffin, T.P., 1970. The trapping and binding of subtidal carbonate sediments by marine vegetation in Bimini lagoon, Bahamas. Journal of Sedimentary Petrology 40, 249-273.

Scrutton, M.E., 1976. Aspects of Carbonate Sedimentation in Indonesia. Fifth Annual Convention of the Indonesian Petroleum Association 1, 179-194.

Scrutton, M.E., 1978. Modern Reefs in the West Java Sea, Proceedings of the Indonesian Petroleum Association Carbonate Seminar (Special Volume), Jakarta, Indonesia, 14-41.

Sharaf, E., Simo, J.A., Carroll, A.R., and Shields, M., 2005. Stratigraphic evolution of Oligocene-Miocene carbonates and siliciclastics, East Java basin, Indonesia. American Association of Petroleum Geologists, Bulletin 89, 799-819.

Skryzypek G., and Paul, D., 2006. $\delta^{13}C$ analysis of calcium carbonate: comparison between the GasBench and elemental analyzer techniques. Rapid Communications in Mass Spectrometry 20, 2915–2920.

Smith, R.B., and Silver, E.A., 1991. Geology of a Miocene collision complex, Buton, eastern Indonesia. Geological Society of America Bulletin 103, 660-678.

Steinen, R.P., 1974. Phreatic and vadose diagenetic modification of Pleistocene limestone; petrographic observations from subsurface of Barbados, West Indies. American Association of Petroleum Geologists, Bulletin 58, 1008-1024.

Suharsono, Giyanto, Budiyanto, A., and Dehwani, N., 2006. Status and Monitoring of Coral Reefs in Kaledupa Islands, South East Sulawesi, Indonesia. Proceedings of the tenth International Coral Reef Symposium, Japanese Coral Reef Society, Okinawa, 1033-1038.

Sun, S.Q., 1992. Skeletal aragonite dissolution from hypersaline seawater: a hypothesis. Sedimentary Geology 77, 249–257.

Sun, S.Q., and Esteban, M., 1994. Paleoclimatic controls on sedimentation, diagenesis, and reservoir quality: Lessons from Miocene carbonates. American Association of Petroleum Geologists, Bulletin, 78, 519 - 543.

Swei, G.H., and Tucker, M.E., 2012. Impact of diagenesis on reservoir quality in ramp carbonates: Gialo Formation (middle Eocene), Sirt Basin, Libya. Journal of Petroleum Geology 35, 25-48.

Swinchatt, J.P., 1965. Significance of constituent composition, texture, and skeletal breakdown in some recent carbonate sediments. Journal of Sedimentary Petrology 35, 71-90.

Taberner, C., Marshall, J.D., Hendry, J.P., Pierre, C., and Thirlwall, M.F., 2002. Celestite formation, bacterial sulphate reduction and carbonate cementation of Eocene reefs and basinal sediments (Igualada, NE Spain). Sedimentology 49, 171-190.

Tomascik, T., Mah, A.J., Nontji, A., and Moosa, M.K., 1997. The Ecology of the Indonesian Seas. Oxford University Press, Singapore, 1388 p.

Tucker, M.E., and Wright, V.P., 1990. Carbonate Sedimentology, Blackwell Scientific Publications, 482 p.

Turak, E., 2003. Coral reef surveys during TNC SEACMPA RAP of Wakatobi National Park, Southeast Sulawesi. Final Report to the Nature Conservancy, Bali. In: Pet-Soede, L., and Erdmann, M.V. (Eds.). Rapid ecological assessment Wakatobi National Park. WWF/TNC Joint Publication, Denpasar, Bali, 33-52.

Udden, J.A. 1914. Mechanical composition of clastic sediments. Geological Society of America Bulletin 25, 655-744.

Umbgrove, J.H.F., 1946. Evolution of reef corals in East Indies since Miocene times. American Association of Petroleum Geologists, Bulletin 30, 23-31.

Umbgrove, J.H.F., 1947. Coral Reefs of the East Indies. Bulletin of the Geographic Society of America 58, 729-778.

Unsworth, R.K.F. 2010. Seagrass meadows of the Wakatobi National Park. In: Clifton, J., Unsworth, R.K.F. and Smith, D.J. (Eds.) Marine research and conservation in the Coral Triangle The Wakatobi National Park. Nova Science Publishers, New York, 45-65.

van Bemmelen, R.W., 1949. The Geology of Indonesia. Vol. 1a. Government Printing Office, The Hague, 2nd Edition, 732 p.

van der Kooij, B., Immenhauser, A., Steubers, T., Bahamonde Rionda, J.R., and Merino Tome, O., 2010. Controlling factors of volumetrically important marine carbonate cementation in deep slope settings. Sedimentology 57, 1491-1525.

van de Weerd, A.A., and Armin, R.A., 1992. Origin and evolution of the Tertiary hydrocarbon-bearing basin in Kalimantan (Borneo), Indonesia. American Association of Petroleum Geologists, Bulletin 76, 1778-1803.

Veizer, J., 1983. Chemical diagenesis of carbonates: Theory and application of trace element techniques. In: Arthur, M.A., Anderson, T.F., Kaplan, I.R., Veizer, J., and Land, L.S., (Eds.) Stable Isotopes in Sedimentary Geology. SEPM, Short Course no. 10, 3-1 - 3-100.

Wanless, H.R., 1979. Limestone response to stress: pressure solution and dolomitization. Journal of Sedimentary Petrology 49, 437-462.

Warren, J., 2000, Dolomite: Occurrence, evolution and economically important associations: Earth-Science Reviews, v. 52, p. 1 - 81.

Warrlich, G., Taberner, C., Asyee, W., Stephenson, B., Esteban, M., Boya-Ferrero, M., Dombrowski, A. and Van Konijnenburg, J.-H. 2010. The impact of postdepositional processes on reservoir properties: two case studies of Tertiary carbonate buildup gas fields in Southeast Asia (Malampaya and E11). In: Morgan, W.A., George, A.D, Harris, P.M., Kupecz, J.A. and Sarg, J.F. (Eds.) Cenozoic Carbonate Systems of Australasia. SEPM Special Publication 95, 99-127.

Wentworth, C.K., 1922. A scale of grade and class terms for clastic sediments. Journal of Geology 30, 377-394.

White, T.L. 1987. Coral reefs: valuable resources of SE Asia. Volume 1 of ICLARM education series, Issue 1 of Education Series. Issue 386 of ICLARM contribution. International Center for Living Aquatic Resources Management

on behalf of the Association of Southeast Asian Nations/United States Coastal Resources Management Project, 1987, 36 p.

Wilkinson, C.R., 2000. Status of the coral reefs of the world: 2000. Australian Institute of Marine Science, 363 p.

Wilson, M.E.J., 1996. Evolution and hydrocarbon potential of the Tertiary Tonasa Limestone Formation, Sulawesi, Indonesia. Proceedings of the Indonesian Petroleum Association 25th Annual Convention, 227-240.

Wilson, M.E.J., 2002. Cenozoic carbonates in Southeast Asia: implications for equatorial carbonate development. Sedimentary Geology 147, 295-428.

Wilson, M.E.J., 2005. Development of equatorial delta-front patch reefs during the Neogene, Borneo. Journal of Sedimentary Research 75, 114-133.

Wilson, M.E.J., 2008a. Global and regional influences on equatorial shallow-marine carbonates during the Cenozoic. Palaeogeography, Palaeoclimatology, Palaeoecology 265, 262-274.

Wilson, M.E.J., 2008b. Reservoir quality of Cenozoic carbonate buildups and coral reef terraces. Proceedings of the 32nd Indonesian Petroleum Association Annual Convention and Exhibition, 8 p.

Wilson, M.E.J., 2011. SE Asian carbonates: tools for evaluating environmental and climatic change in the equatorial tropics over the last 50 million years. In: Hall, R., Cottam, M.A., and Wilson, M.E.J., (Eds.) The SE Asian Gateway: History and Tectonics of the Australia-Asia Collision. Geological Society of London, Special Publication 355, 347-369.

Wilson, M.E.J., 2012. Equatorial carbonates: an earth systems approach. Sedimentology 59, 1-31.

Wilson, M.E.J., and Moss, S.J., 1999. Cenozoic palaeogeographic evolution of Sulawesi and Borneo. Palaeogeography, Palaeoclimatology, Palaeoecology 145, 303-337.

Wilson, M.E.J., and Evans, M.J., 2002. Sedimentology and diagenesis of Tertiary carbonates on the Mangkalihat Peninsula, Borneo: implications for subsurface reservoir quality. Marine and Petroleum Geology 19, 873-900.

Wilson, M.E.J., and Lokier, S.W., 2002. Siliciclastic and volcaniclastic influences on equatorial carbonates: insights from the Neogene of Indonesia. Sedimentology 49, 583-601.

Wilson, M.E.J., and Hall, R., 2010. Tectonic influences on SE Asian carbonate systems and their reservoir development. In: Morgan, W.A., George, A.D., Harris, P.M., Kupecz, J.A., and Sarg, J.F., (Eds.) Cenozoic Carbonates of Australasia. SEPM, Special Publication 95, 122-149.

Wilson, M.E.J., Bosence, D.W.J., and Limbong, A., 2000. Tertiary syntectonic carbonate platform development in Indonesia. Sedimentology 47, 395-419.

Wilson, M.E.J., Chambers, J.L.C., Evans, M.J., Moss, S.J., and Nas, D.S., 1999. Cenozoic carbonates in Borneo: case studies from northeast Kalimantan. Journal of Asian Earth Sciences 17, 183-201.

Wilson, M.E.J, Al Aghbari, A.A.S., Deeks, N.R., Kananan, P., Madden, R.H.C., and Zafir, A., 2013. Modern reef-associated sediments and environments from SE Asia. 30th International Association of Sedimentologists, (Abstract) Manchester, UK.

Witkowski, F.W., Blundell, D.J., Gutteridge, P., Horbury, A.D., Oxtoby, N.H., and Qing, H., 2000. Video cathodoluminescence microscopy of diagenetic cements and its applications. Marine and Petroleum Geology 17, 1085-1093.

Woolfe, K.J., and Larcombe, P., 1999. Terrigenous sedimentation and coral reef growth: a conceptual framework. Marine Geology 155, 331-345.

Zampetti, V., Schlager, W., van Konijenburg, J.H., and Everts, A.J., 2003. Depositional history and origin of porosity in a Miocene carbonate platform of central Luconia, offshore Sarawak. Bulletin of the Geological Society of Malaysia 47, 139-152.

APPENDICES

APPENDIX A

CLASSIFICATION SCHEMES

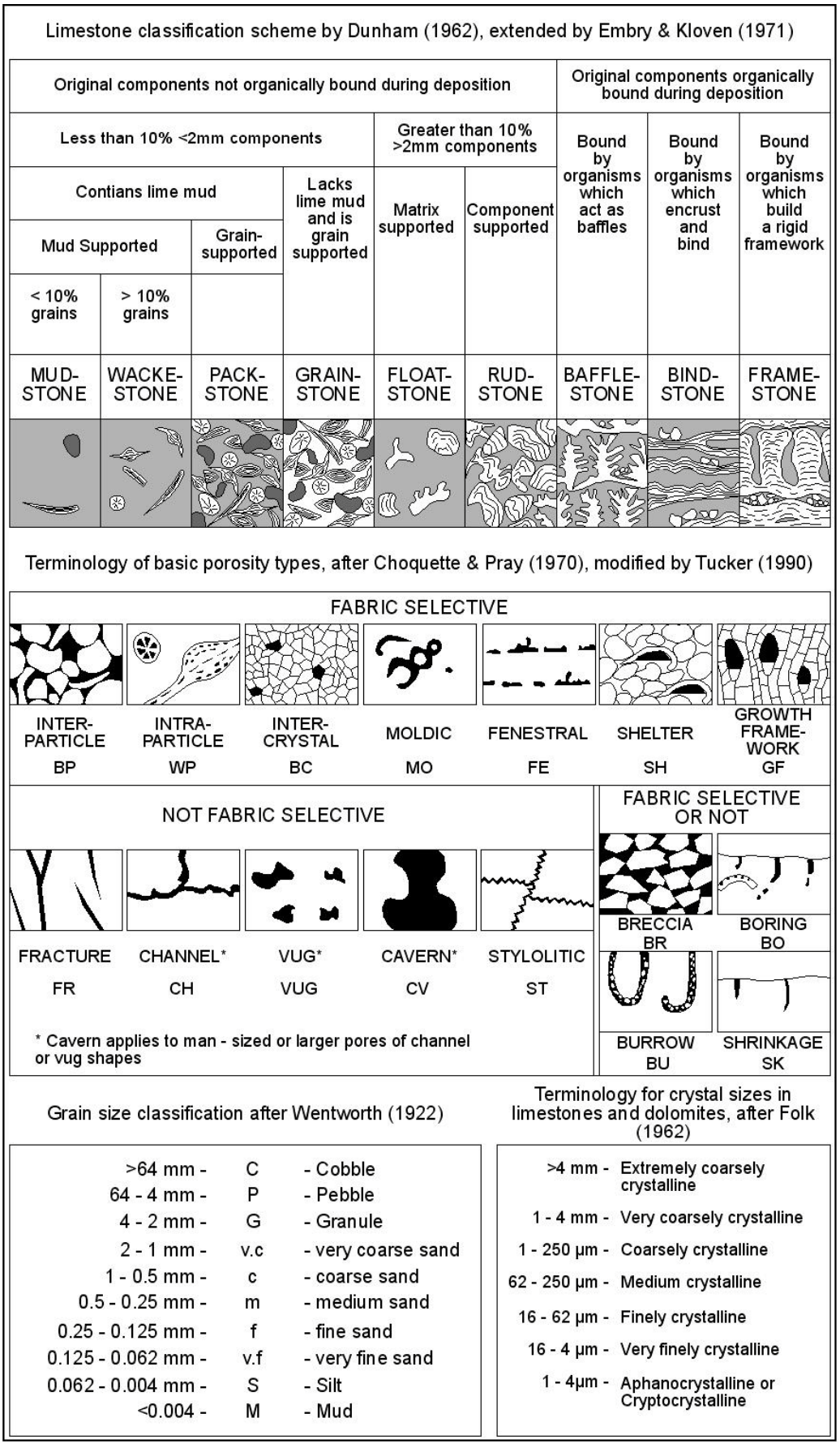

A1. Fabric descriptive terminology.

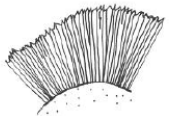

Acicular: Needle-like crystals, growing normal to the substrate. Crystals elongated parallel to the c-axis, exhibiting straight extinction. Terminations are pointed or chisel-shaped, twinning is common. Width < 10 μm, length about 100 μm and more. Often forming isopachous crusts. Predominantly aragonite, but also Mg-calcite. Marine phreatic. Pl. 31/2, Pl. 34/1.

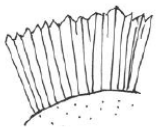

Fibrous: Fibrous crystals, growing normal to the substrate. Crystals show a significant length elongation, usually parallel to the c-axis. Crystal shape is needle-like or columnar (length to width ratio > 6:1, width > 10 μm). Size commonly fine to medium crystalline. Often forming isopachous crusts; common in inter- and intraparticle pores. Aragonite or High-Mg calcite. Mostly marine-phreatic, but also meteoric-vadose and marine-vadose (columnar crystal shape). Syn.: Radial fibrous. Pl. 2/4, Pl. 31/1-2, Pl. 32/1-4, Pl. 50/6.

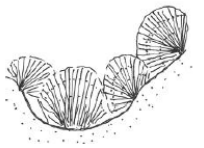

Botryoidal: Pore-filling cement made of individual and coalescent mamelons exhibiting discontinuous horizons, e.g. dust lines ranging in size from tens of microns to several centimeters. The cement consists of individual and compound fans, which in turn are composed of elongated euhedral fibers with a characteristic sweeping extinction in cross-polarized light. Aragonite. Usually marine (common in cavities of reefs and steep seaward slopes), but also known from burial environments. Syn.: Spherulitic. Pl. 145/1-3.

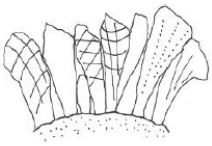

Radiaxial fibrous: Large, often cloudy and turbid, inclusion-rich calcite crystals with undulose extinction. Size medium to coarse crystalline. Sometimes extending several millimeters in length, usually about 30 to 300 μm. Crystal length/width ratio 1:3 to 1:10. Crystals show a pattern of subcrystal units. Within each subcrystal that diverges away from the substrate an opposing pattern of distally-convergent optic axes occurs, caused by a curvature of cleavage and twin lamellae. Undulose extinction of subcrystals or subcrystal units are used in distinguishing three radiaxial subtypes (see text). Often forming isopachous crusts. Phreatic-marine and burial. Pl. 27/2, Pl. 34/2; Fig. 7.9.

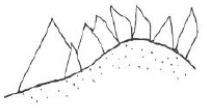

Dog tooth: Sharply pointed acute calcite crystals of elongated scalenohedral or rhombohedral form, growing normal and subnormal to the substrate (grain surfaces, atop earlier cements). Crystals are a few tens to a few hundred micrometers long and have acute and sometimes blunted terminations. Often meteoric and shallow-burial but also marine-phreatic and hydrothermal. Syn.: Bladed scalenohedral cement, bladed prismatic calcite cement, dentate cement, scalenohedral calcite cement. Pl. 2/3, Pl. 31/5-6, Pl. 34/8.

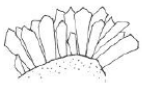

Bladed: Crystals that are not equidimensional and not fibrous. They correspond to elongate crystals somewhat wider than fibrous crystals (length/width ratio between 1.5:1 to 6:1) and exhibiting broad flattened and pyramid-like terminations. Crystal size up to 10 μm in width and between less than 20 and more than 100 μm in length. Crystals increase in width along their length. Commonly forming thin isopachous fringes on grains. Usually High-Mg calcite but also aragonite. Marine-phreatic (abundant in shallow-marine settings) and marine-vadose. Pl. 33/1, 3, 5, 8; Pl, 34/7.

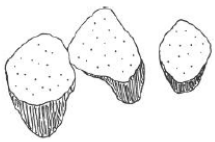

Dripstone: Pendant cement characterized by distinct thickening of cement crusts beneath grains or under the roofs of intergranular and solution voids. The cement forms on droplets beneath grains after the bulk of the mobile water has drained out of the pores, leaving a thicker water film at the lower surface of the grains. Forms typically gravitational, beard-like patterns. Predominantly calcite. Formed below the zone of capillarity and above the water table within the meteoric-vadose zone (often associated with meniscus cement), but also in the meteoric-phreatic and sporadically in marine-vadose diagenetic environments (e.g. inter- and supratidal, and beachrocks: aragonitic dripstone cement). Syn.: Gravitational cement, microstalactitic cement, microstalactitic druse cement, stalactitic cement. Pl. 34/6, Pl. 126/1.

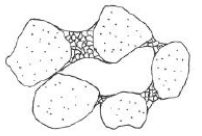

Meniscus: Calcite cement precipitated in meniscus style at or near grain-to-grain contacts in pores containing both air and water. Exhibits a curved surface below grains. Resulting intergranular pores have a rounded appearance due to the meniscus effect. Characteristically formed in the meteoric-vadose zone but may also occur in the phreatic-meteoric and the vadose-marine environment (beachrock). Pl. 14/1, Pl. 32/5-6, Pl. 33/4, Pl. 126/1.

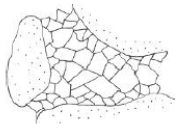

Drusy: Void-filling and pore-lining cement in intergranular and intraskeletal pores, molds and fractures, characterized by equant to elongated, anhedral to subhedral non-ferroan calcite crystals. Size usually >10 μm. Size increases toward the center of the void. Displays a characteristic fabric (see Fig. 7.12). Near-surface meteoric as well as burial environments. Syn.: Drusy calcite spar mosaic, drusy equant calcite mosaic. Pl. 10/2.

A2. Cement morphologies part 1 (from Flügel, 2004).

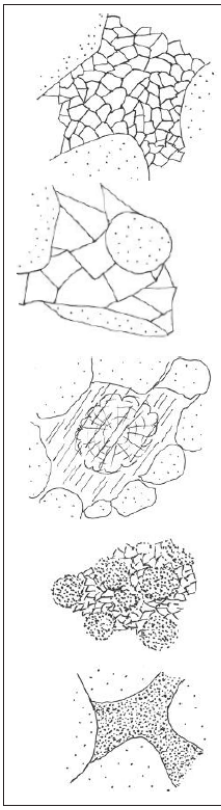

Granular: Calcite cement consisting of relatively equidimensional pore-filling small crystals. Common in interparticle pores, generally without distinct substrate control. Formed in meteoric-vadose, meteoric-phreatic and burial environments. Can also originate from recrystallization of pre-existing cements. Pl. 10/2.

Blocky: Calcite cement consisting of medium to coarse-grained crystals without a preferred orientation. Characterized by variously sized crystals (tens of microns to several millimeters), often showing distinct crystal boundaries. Xenotopic and hypidiotopic crystal fabrics common. High-Mg calcite or Low-Mg calcite. Typically in meteoric (meteoric phreatic and vadose) and burial environments; rare in marine hardgrounds and reefs. Precipitated after the dissolution of aragonite cements or grains or as late diagenetic cement filling remaining pore space. Blocky textures can also originate from recrystallization of pre-existing cements. Pl. 20/1, Pl. 28/2, Pl. 34/1.

Syntaxial calcite overgrowth cement: Substrate-controlled overgrowth around a host grain made by a single crystal (usually High-Mg calcitic echinoderm fragments). Overgrowth often in crystallographic lattice continuity with the host grain. Echinoderm overgrowth is often zoned. Color differences between the skeletal grain and the overgrowth cement can be conspicuous. Overgrowth cements from near-surface marine, vadose-marine and meteoric-phreatic environments are inclusion-rich and cloudy, in contrast to clear overgrowth from deep burial environments Syn.: Grain overgrowth cement, syntaxial echinoderm cement, syntaxial cement rim, syntaxial overgrowth rim cement. Pl. 31/3-4, Pl. 34/3-4, Pl.144/5; Fig. 7.10.

Peloidal microcrystalline cement: Characterized by a peloidal (or pelleted) fabric composed of tiny peloids (size <100 μm) within a microcrystalline calcite matrix. The peloids consist of micrite-sized crystals bearing a radiating halo. Shallow-marine. Common in modern and ancient reefs. Possible interpretations: Chemical and/or microbially induced precipitation (Sect. 4.2.2). Pl. 8/5.

Microcrystalline or micrite cement: Micron-sized curved rhombic crystals. Forms thin coatings around grains, lines intraskeletal pores, fills pores completely or constructs bridges between grains (contributing to meniscus cement). Mg-calcite. Micritic cement fringes should be distinguished from micrite envelopes (Sect. 4.2.3). Often associated with peloidal cements. Pl. 31/3-4, Pl. 32/1-4, Pl. 33/2.

A2 (cont.). Cement morphologies part 2 (from Flügel, 2004).

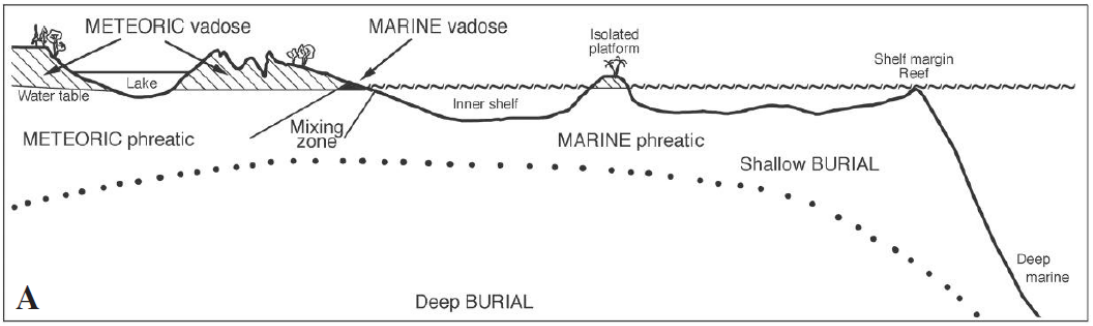

Diagenetic environment	Location	Pore Filling	Processes	~ Time needed
Meteoric vadose environment	Above water table, between land surface and meteoric phreatic zone	Pores filled with freshwater and/ or air	*Solution zone* (soil): Extensive solution; removal of aragonite; formation of vugs. *Precipitation zone* (near surface): Minor cementation	10^3 - 10^5 years
Meteoric phreatic environment	Below water table, may tend downwards 100s of meters	Pores filled with freshwater	*Solution zone* (e.g. sinkholes, caves): Solution; formation of molds and/or vugs. *Active zone* (upper part of meteoric phreatic environment): Dissolution of aragonite and Mg-calcite; rapid and diverse cementation; precipitation of calcite; creation of molds and vugs. *Stagnant zone* (deeper part and in arid climates): Little cementation; stabilization of aragonite and Mg-calcite	10^3 -10^5 up to 10^6 - 10^7 years
Marine phreatic environment	On the shallow or deep sea floor or just below	Pores filled with marine water	*Shallow-marine environment:* Waters oversaturated with respect to $CaCO_3$; rapid cementation by aragonite and Mg-calcite; diverse cement types. *Deep-marine and cold-water environments:* Waters undersaturated with respect to $CaCO_3$; strong dissolution of aragonite and calcite at two dissolution levels	10^1 - 10^4 years
Burial environment **B**	Subsurface beneath reach of surface-related processes, down to realm of low-grade metamorphism. May tend downwards 1000s of meters	Pores filled with brines of varying salinity, from brackish to highly saline	*Shallow burial* (first few meters fo tens of meters) and *deeper burial* (sediment overburden of hundreds to thousands of meters): Physical compaction; chemical compaction (pressure solution); cementation; porosity reduction	10^6 -10^8 years

Fig. 7.2. *Major diagenetic environments.* **A** – Simplified scheme. Many of the studies dealing with the diagenesis of carbonate rocks are environment-specific and concentrate on processes affecting particular hydrogeochemically defined diagenetic environments. Carbonate diagenesis operates in the *meteoric environment*, the *marine environment* and the *burial environment*. In the *meteoric environment* pore space is occupied by freshwater and air (*meteoric vadose zone* above water table; hatched) or by freshwater (*meteoric phreatic zone*). The *marine-vadose zone* at the land-sea boundary and the *mixing zone* in coastal areas and shallow near-coastal subsurface exhibits meteoric and marine criteria. In the *marine phreatic environment* water is supersaturated with respect to $CaCO_3$ in shallow seas and undersaturated in cold and deep seas. The subsurface *burial environment* comprises the subsurface beneath the reach of surface-related processes down to the realm of low-grade metamorphism. Conventionally *shallow burial* and *deep burial* are differentiated. The term *near-surface diagenesis* refers to processes at or close to the sea floor and in the meteoric environment within the reach of surface-related processes related to depositional or weathering interfaces. Here, cementation is highly facies-specific. The terms eogenic, mesogenic and telegenic, introduced by Choquette and Pray (1970), refer to early near-surface, burial and uplift/unconformity-related processes (Sect. 7.3.2).

B – Major processes occurring in different diagenetic environments. The time involved in diagenetic processes varies significantly in different diagenetic zones. Early diagenetic solution/precipitation processes in meteoric vadose and shallow marine phreatic environments need far less time than late diagenetic deeper burial diagenesis, which can last millions of years. Similarly, unconformity-related meteoric phreatic processes may continue over very long time intervals. Early cementation in intertidal and shallow subtidal environments occurs within a range of almost recent to several tens to a few thousand years. Synsedimentary botryoidal cements on marginal slopes of platforms may grow over several tens of years, resulting in synsedimentary stabilization of steep carbonate slope deposits at or above angles of repose (Grammer et al. 1993).

A3. Diagenetic environments and processes (from Flügel, 2004).

ALLOCHTHONOUS		AUTOCHTHONOUS					
Depositional fabric dominated by bio- and lithoclastic reefal material. More than 10% of the fragments are greater than 1 cm in size.		Facies dominated by a growth fabric of *in situ* and *in growth position* skeletons of calcifying organisms.					
Matrix supported.	Supported by the greater than 1 cm component.	Growth fabric dominated by platy to tabular colonies where calcification in the horizontal plane dominates over that of the vertical plane (width to height ratio of dominant organisms: 30:1 - 5:1). These growth forms constitute more than 60% of the total CSV.	Growth fabric dominated by sheet-like & lamellar colonies where calcification in the horizontal plane greatly dominates over that of the vertical plane (width to height ratio: >30:1). These growth forms constitute more than 60% of the total CSV.	Growth fabric dominated by domal & irregular massive colonies which have the same calcification potential in all free directions. These growth forms constitute more than 60% of the total CSV.	Growth fabric dominated by organisms which have a dominant vertical component of growth and relatively restricted lateral growth (for example all types of branching colonies and rod and tubular solitary forms). These growth forms constitute more than 60% of the total CSV.		No one growth form dominate in terms of CSV.
					PILLARSTONE		
FLOATSTONE	RUDSTONE	PLATESTONE	SHEETSTONE	DOMESTONE	*Sparse*	*Dense*	MIXSTONE
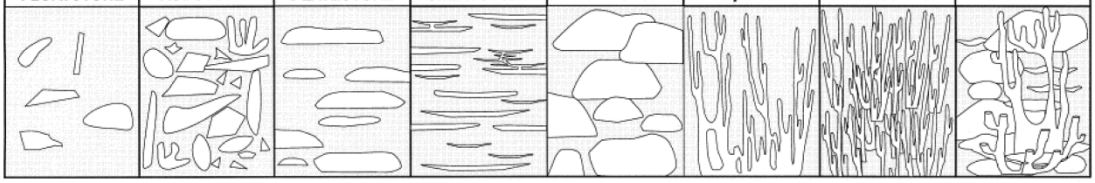							

A4. Modified descriptive classification for styles of scleractinian growth fabric. *CSV* = coral skeletal volume.. After Insalaco (1978).

APPENDIX B

WORK BOOKS, PETROGRAPHIC OBSERVATIONS AND PHOTOMICROGRAPHS RELATING TO CHAPTER 2

Appendix B1

ERDAS IMAGINE Area of Interest Cropping Work Book

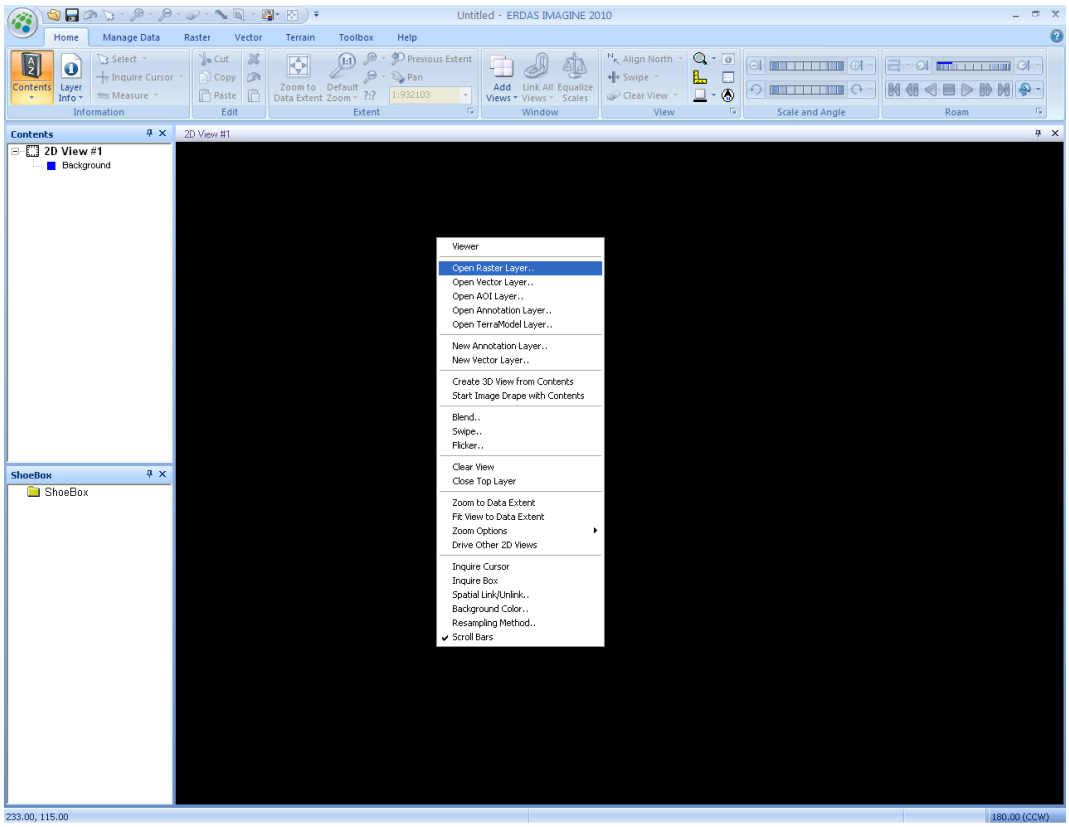

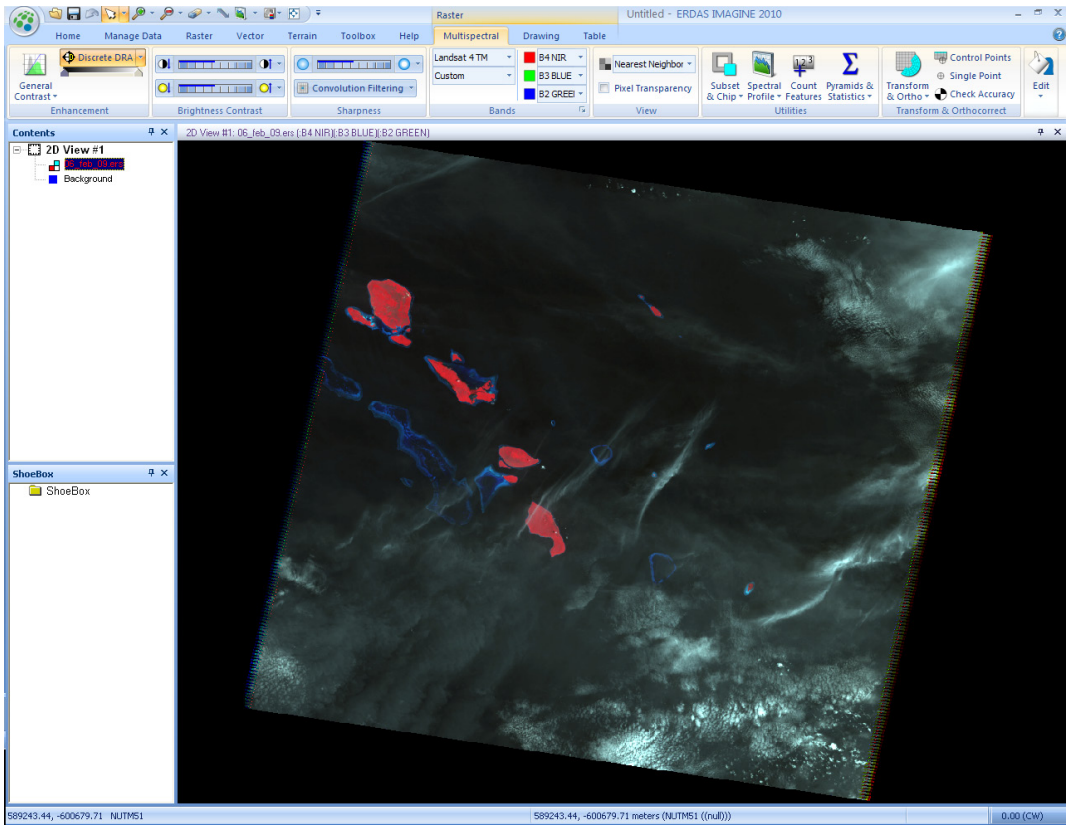

1. Open viewer window
2. In first viewer window choose Open Raster Layer.

.

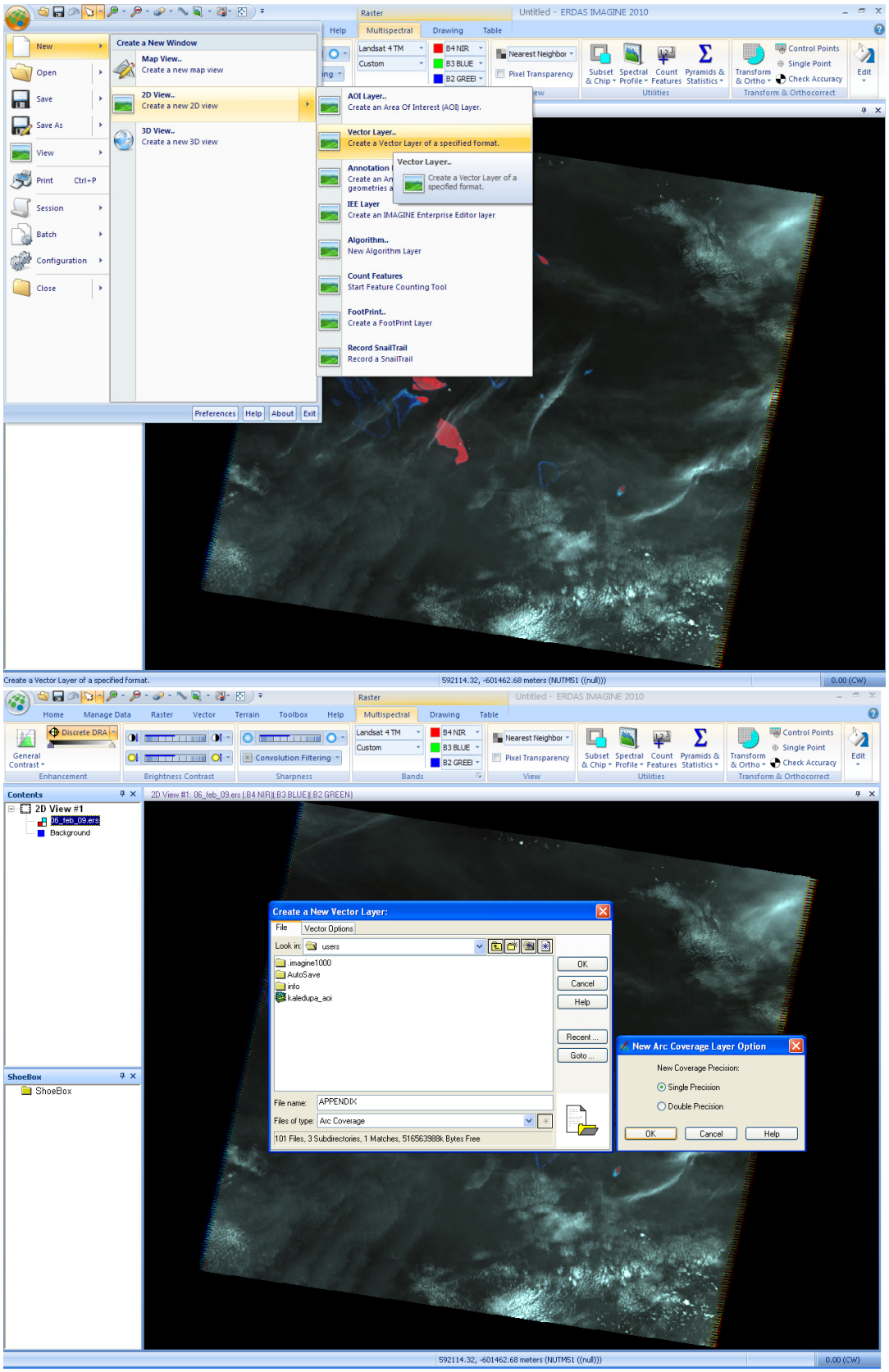

3. In first viewer File menu bar create New Vector Layer.
4. Save file type in arc coverage. Click OK. Choose Single Precision. Click OK.

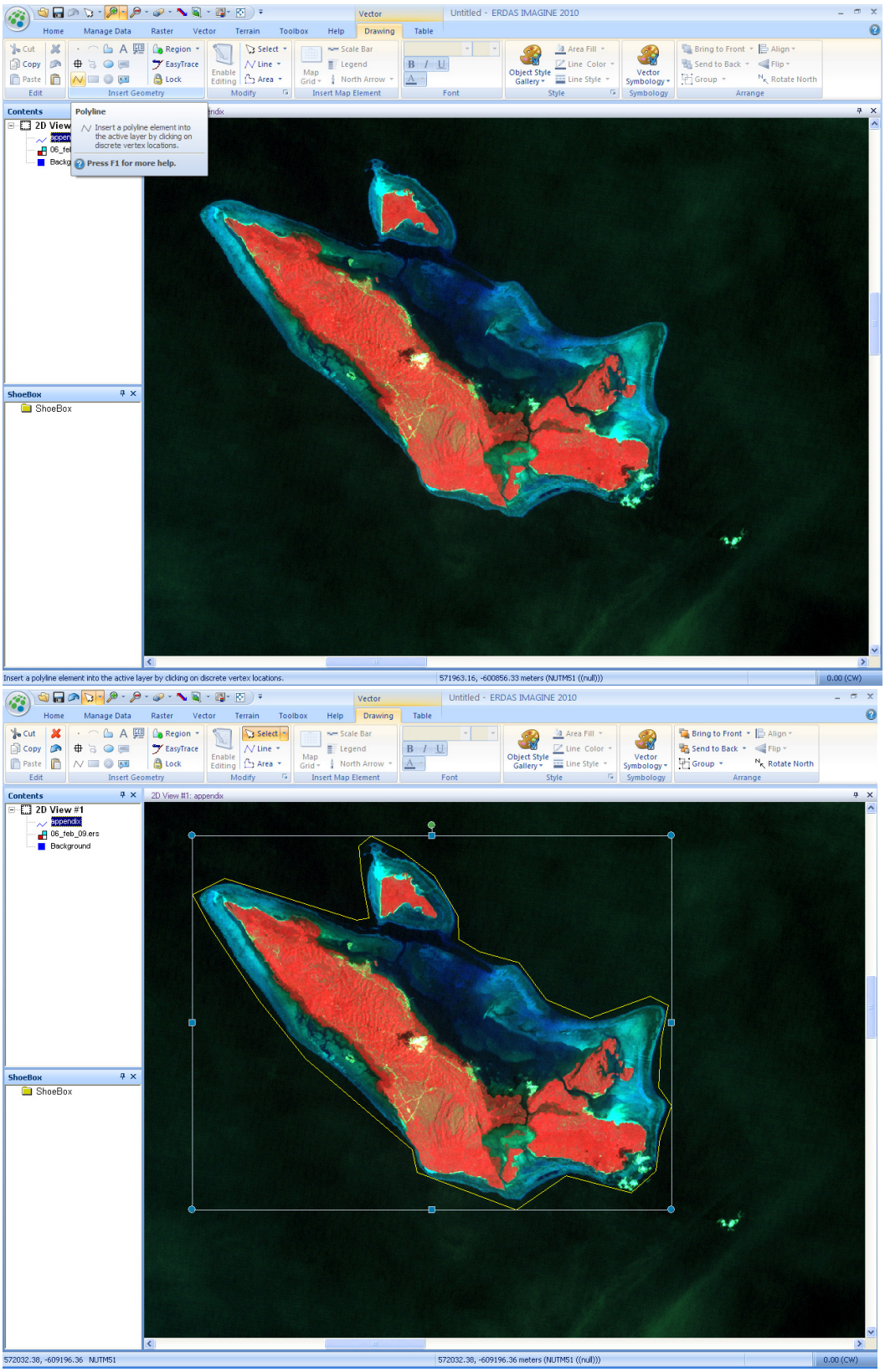

5. Vector Tool Box Display. Click on Draw Polygon.
6. Draw a polygon on the image where you wish to crop to.

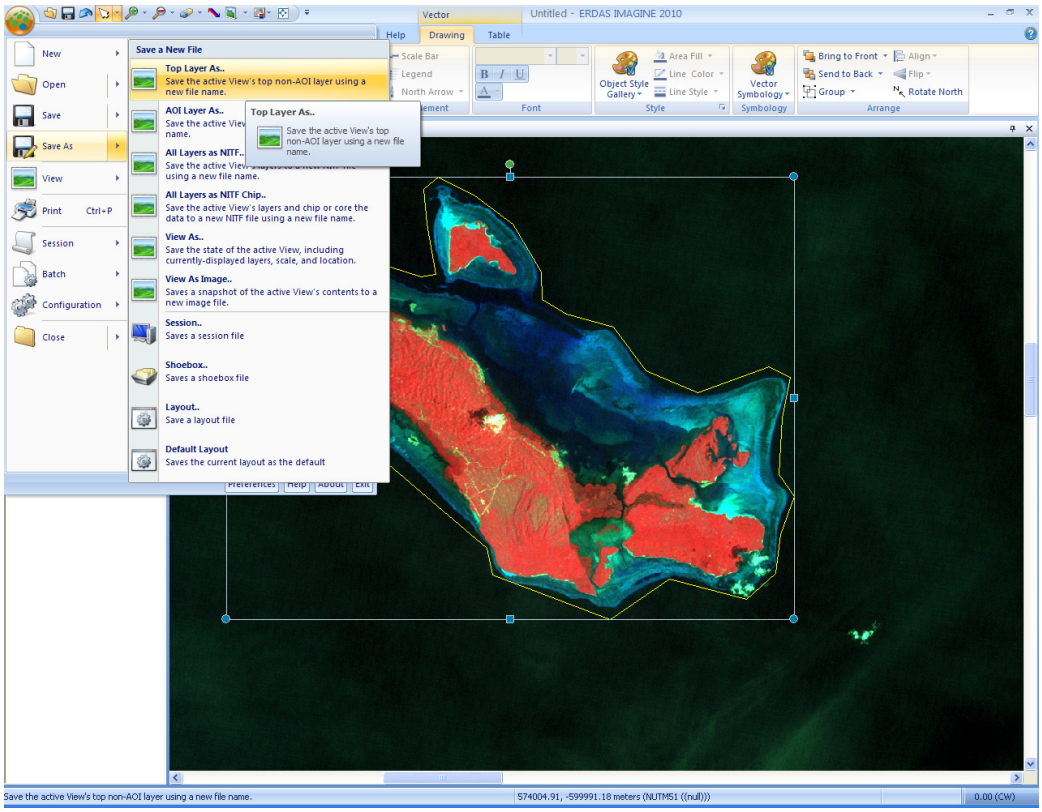

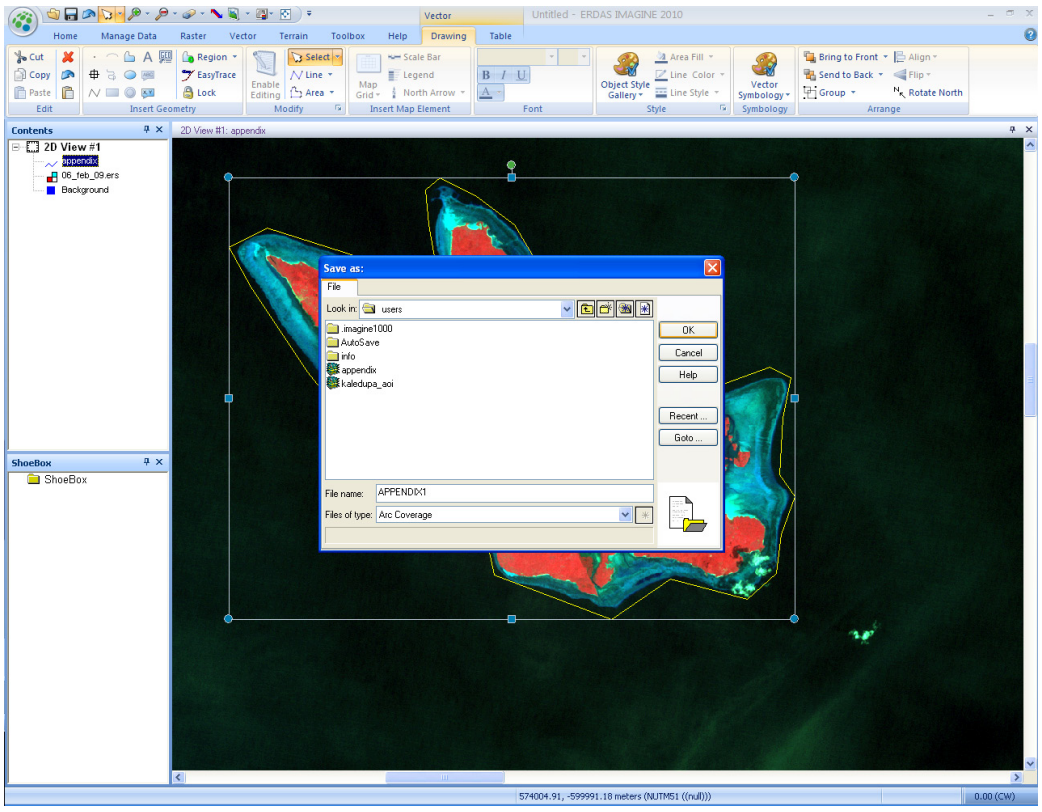

7. First viewer window File menu bar Save Top Layer As.
8. Select arc file saved previously. Click yes to delete file. Click OK again to save.

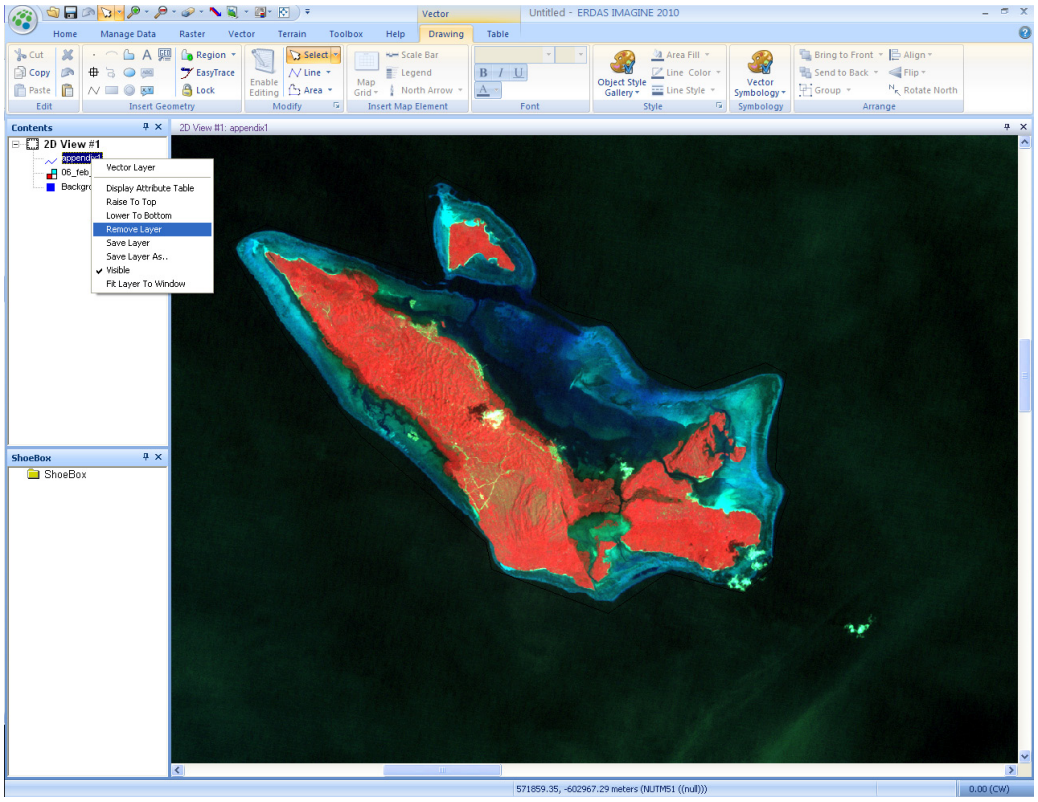

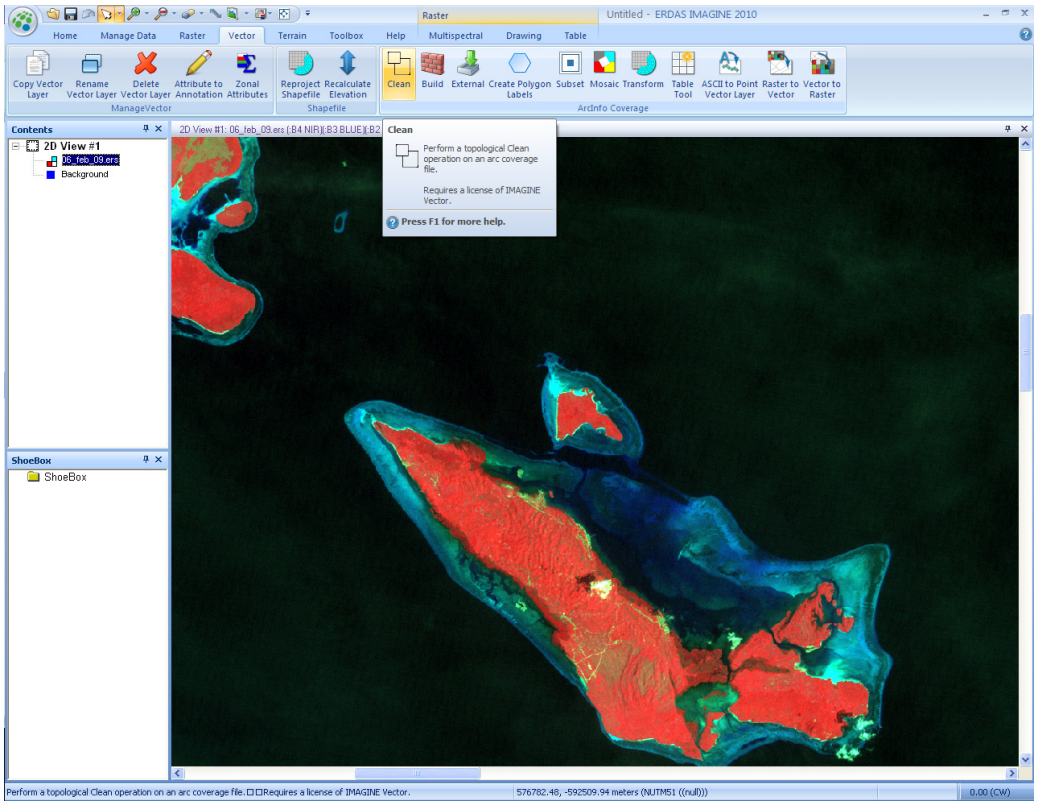

9. In contents pane right click the vector layer. Remove layer.
10. On Vector menu select Clean.

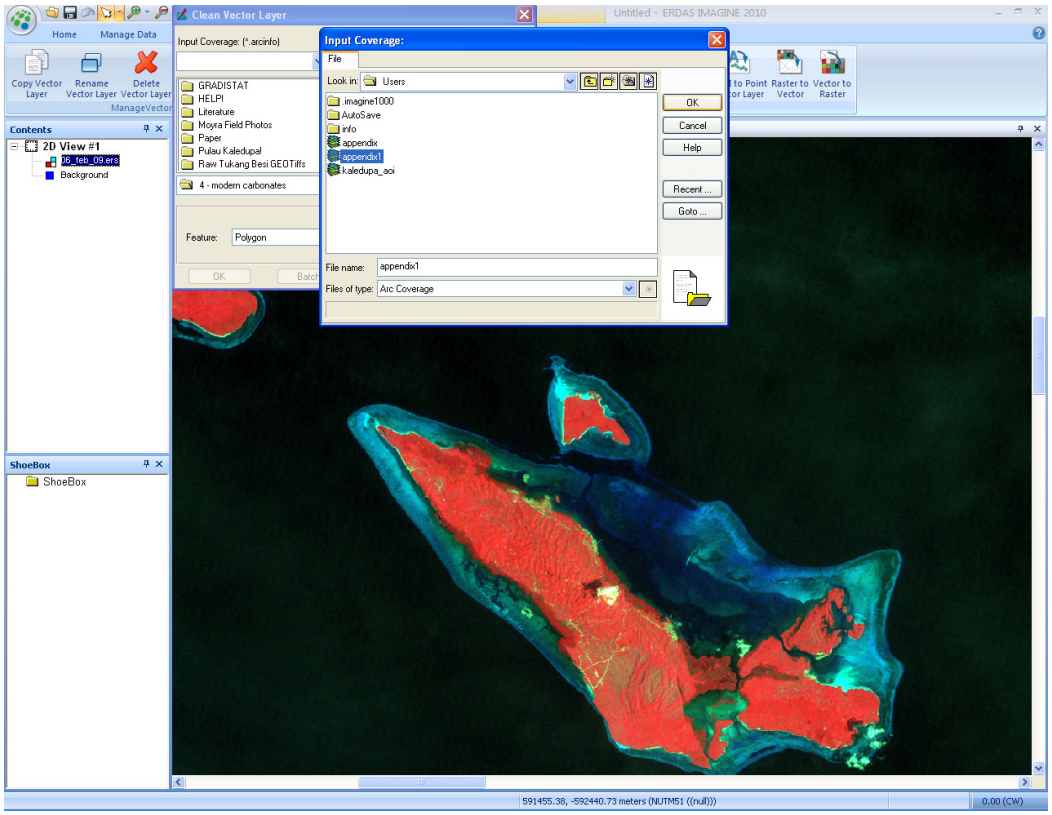

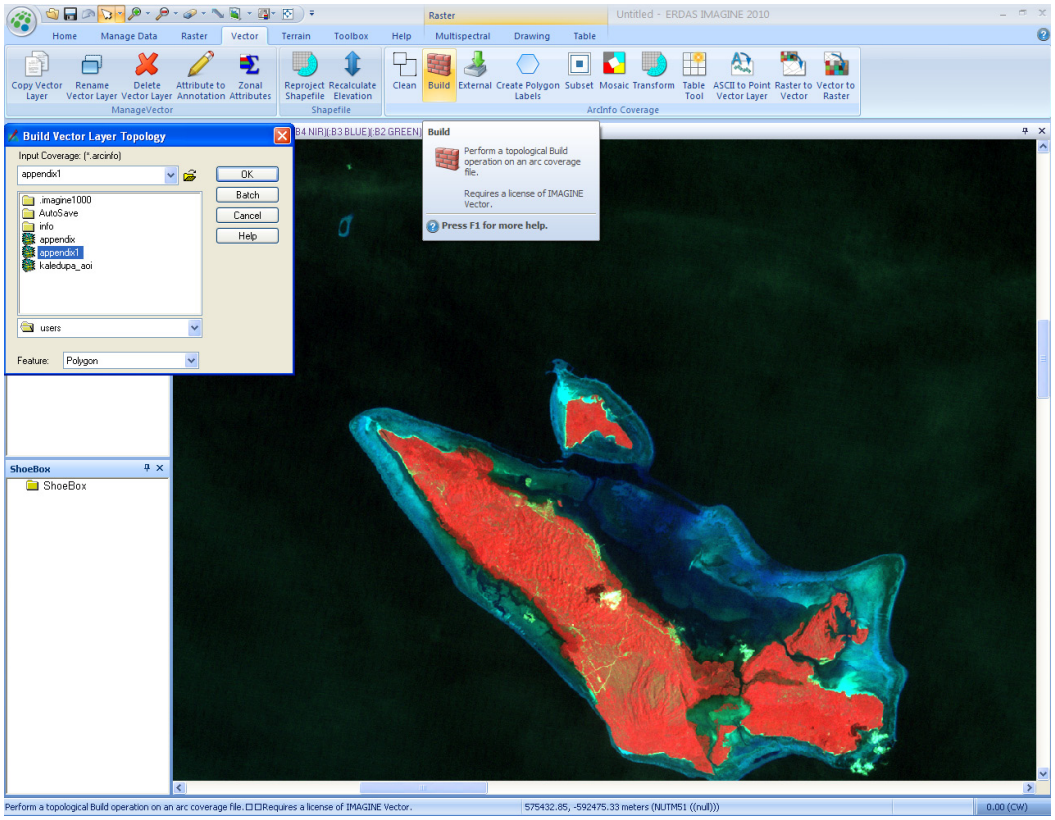

11. Select the vector file saved previously. Click OK.

12. In Vector Menu select Build. Select previously saved file. Clcik OK.

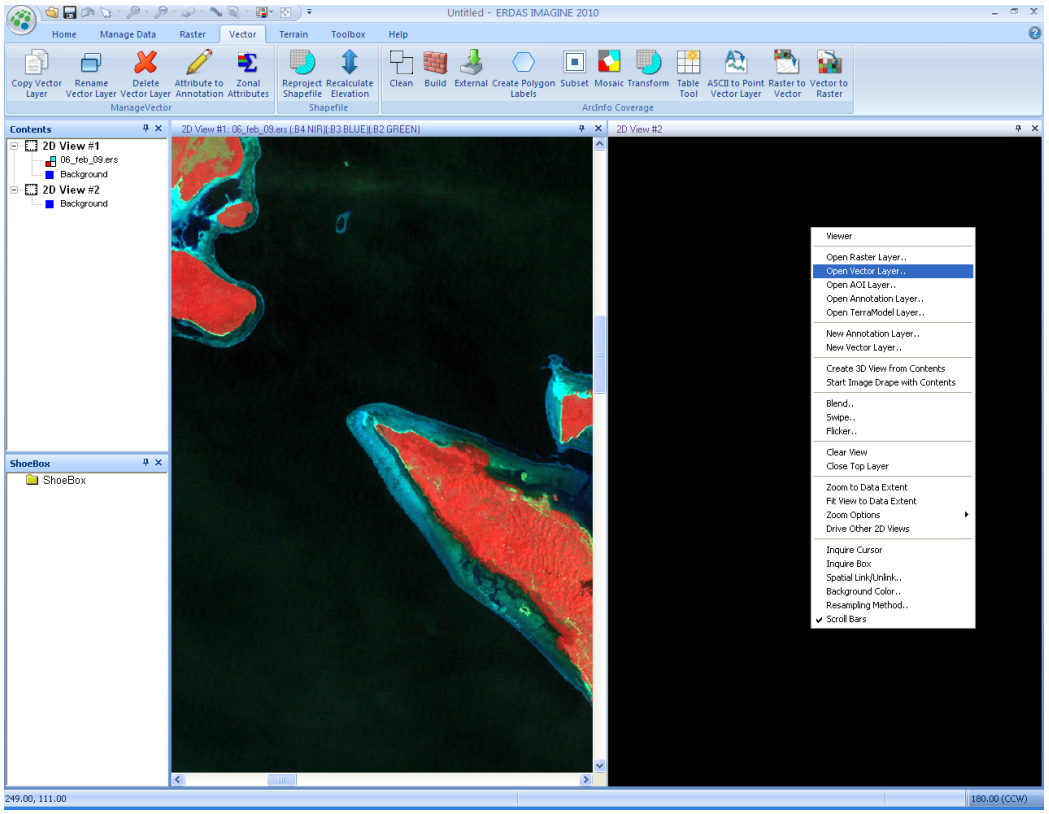

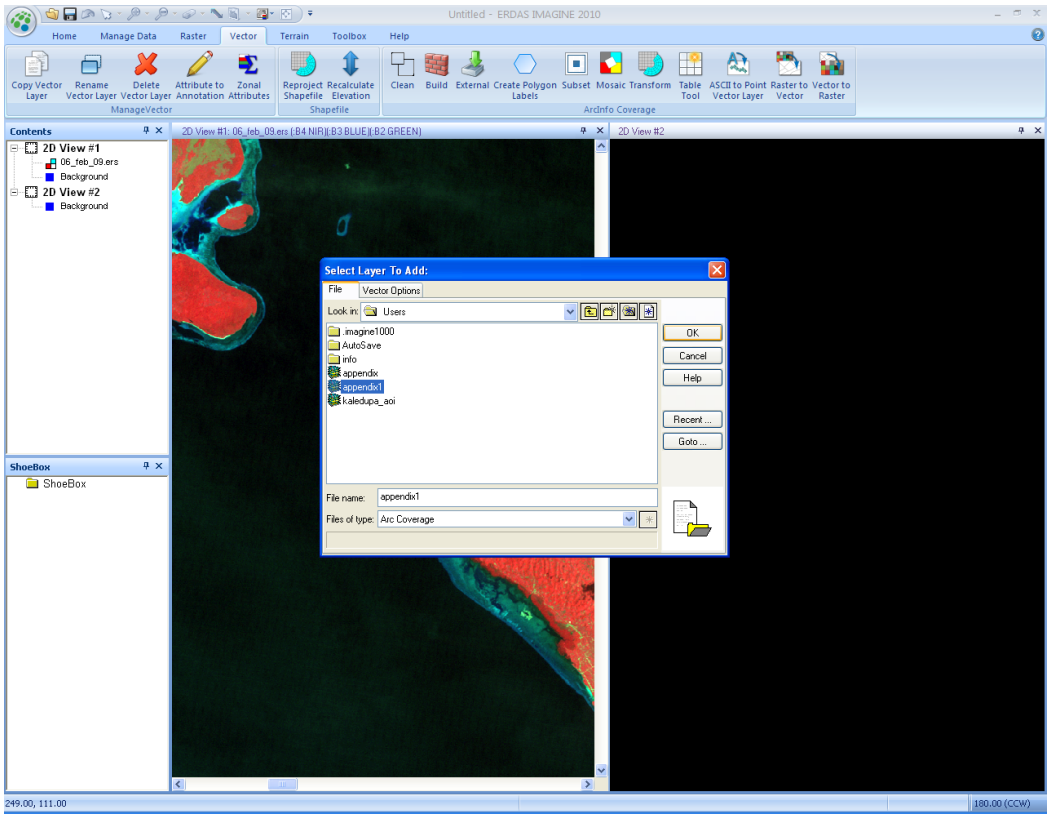

13. Add a new viewer.
14. Open vector layer previously saved.

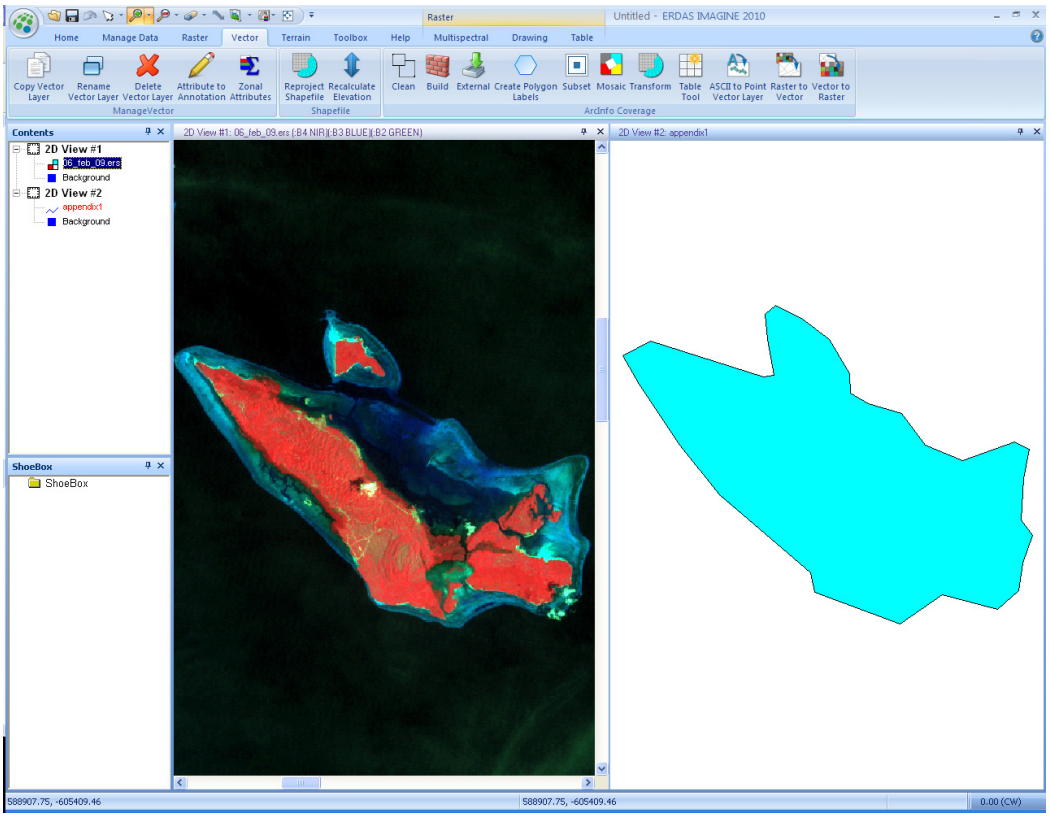

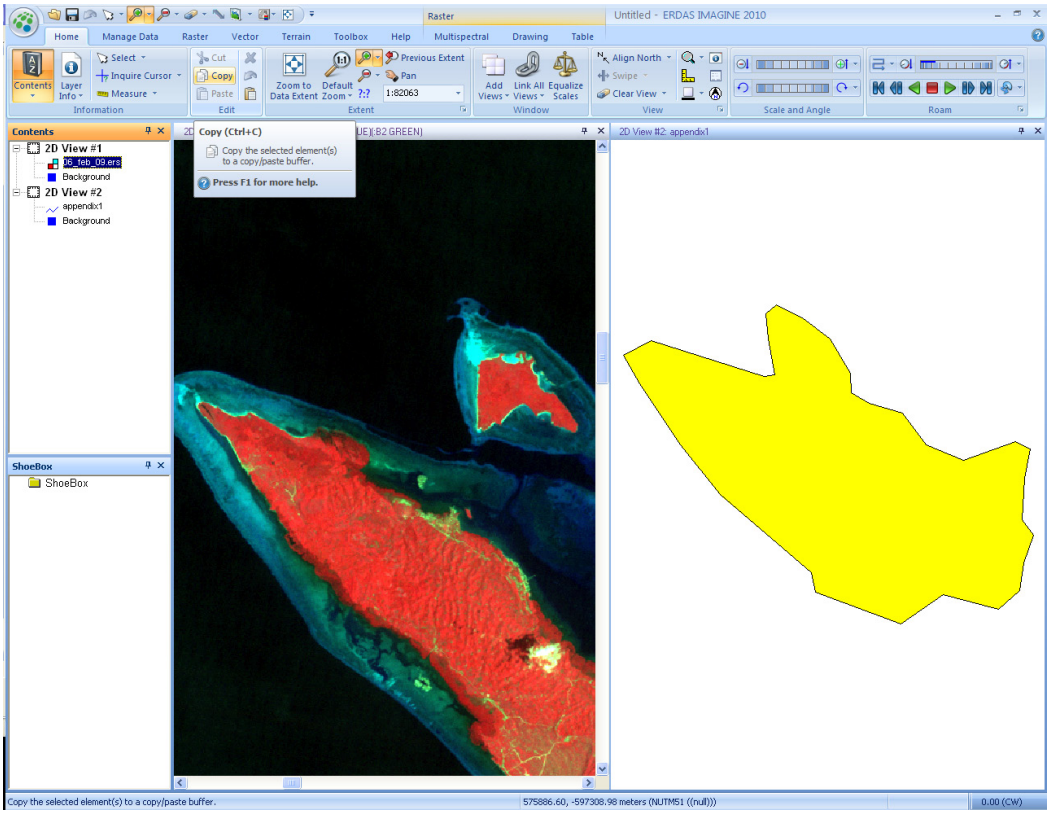

15. In second viewer window click inside polygon (blue – turns yellow).
16. In first viewer window on the Home Menu select Copy.

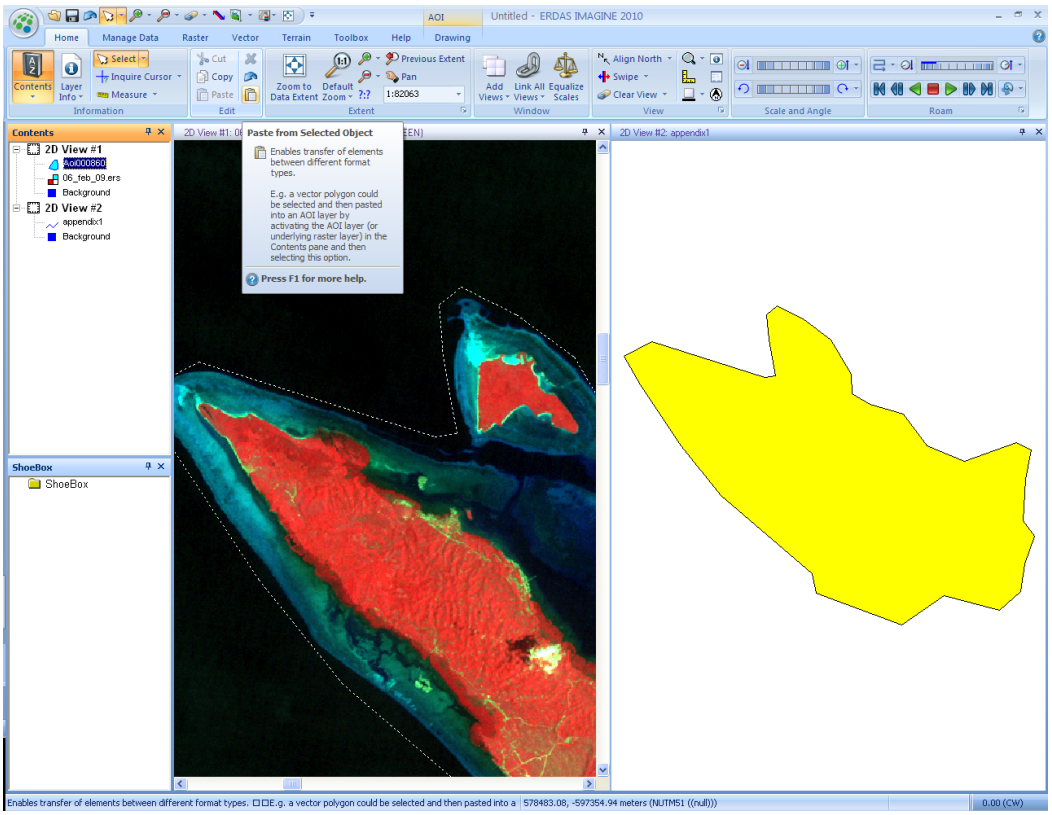

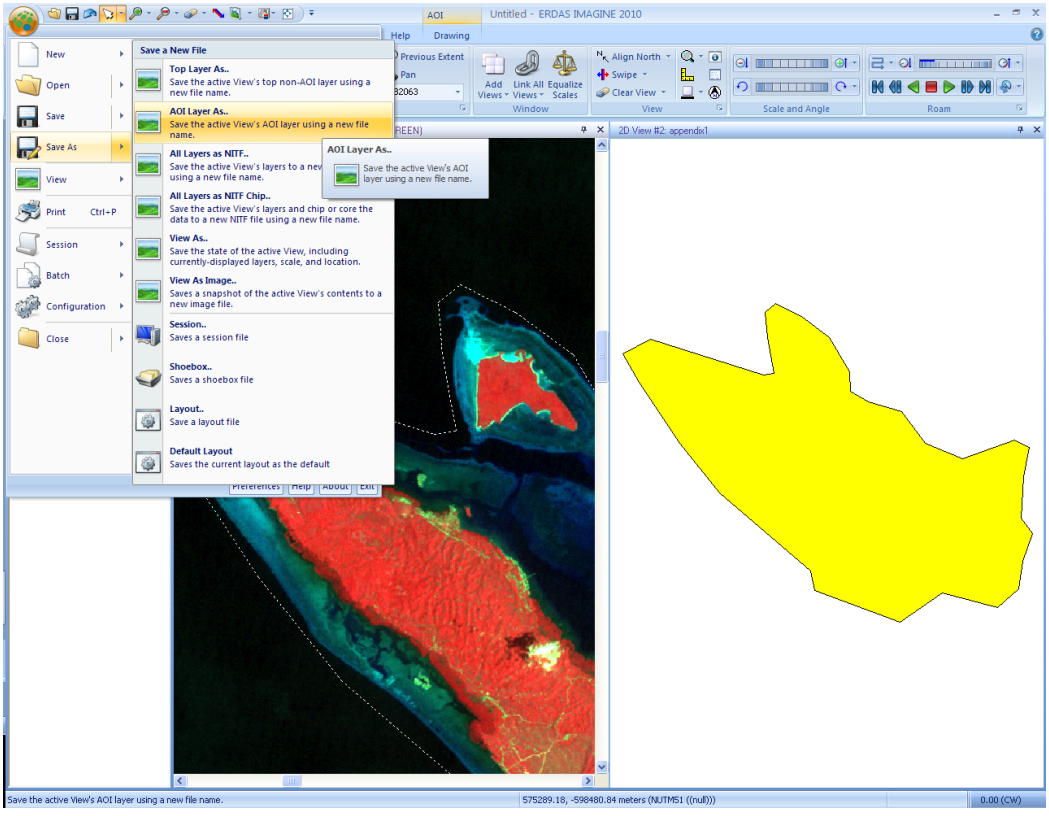

17. In first viewer window on the Home Menu select Paste.
18. In first viewer window on the File Menu bar choose save AOI Layer As.

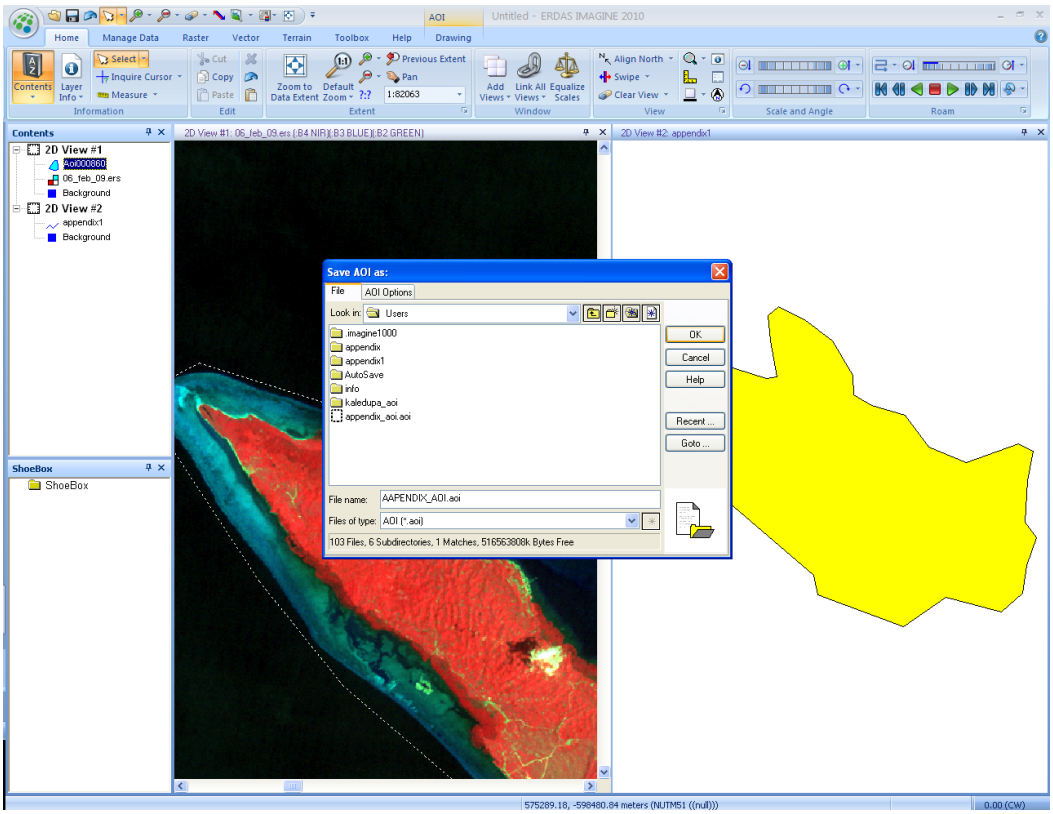

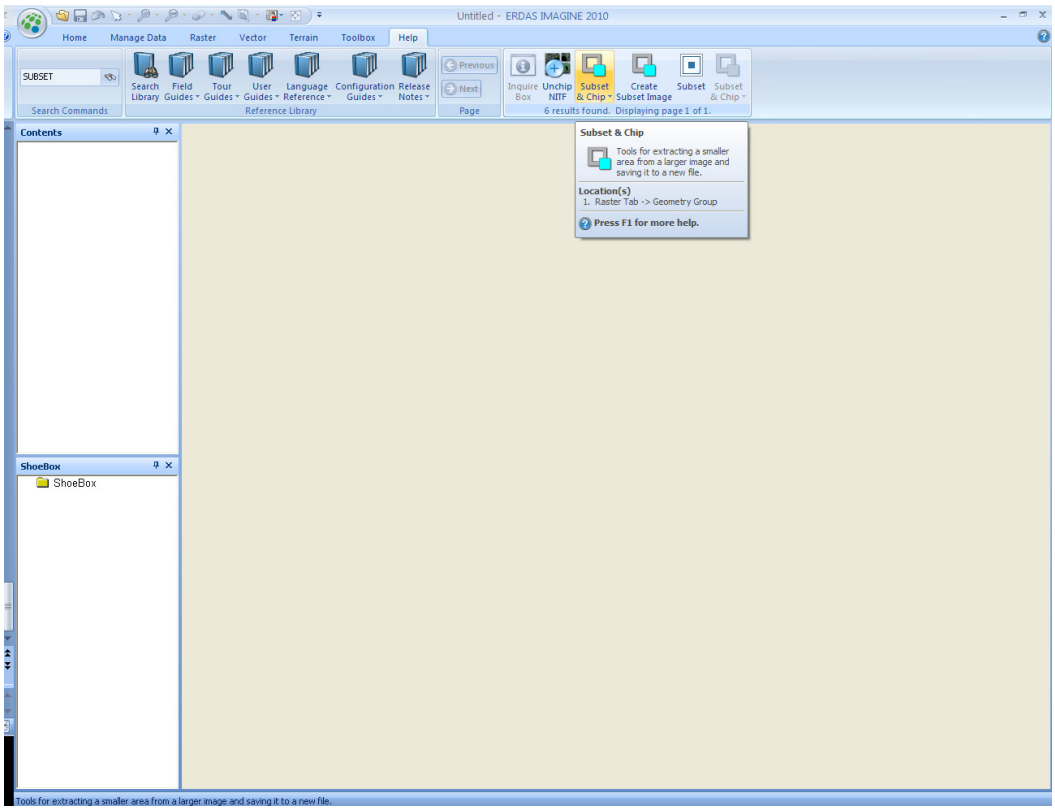

19. Save as an .AOI layer file.
20. Close all viewers. Selct Subset Image in Menu Bar.

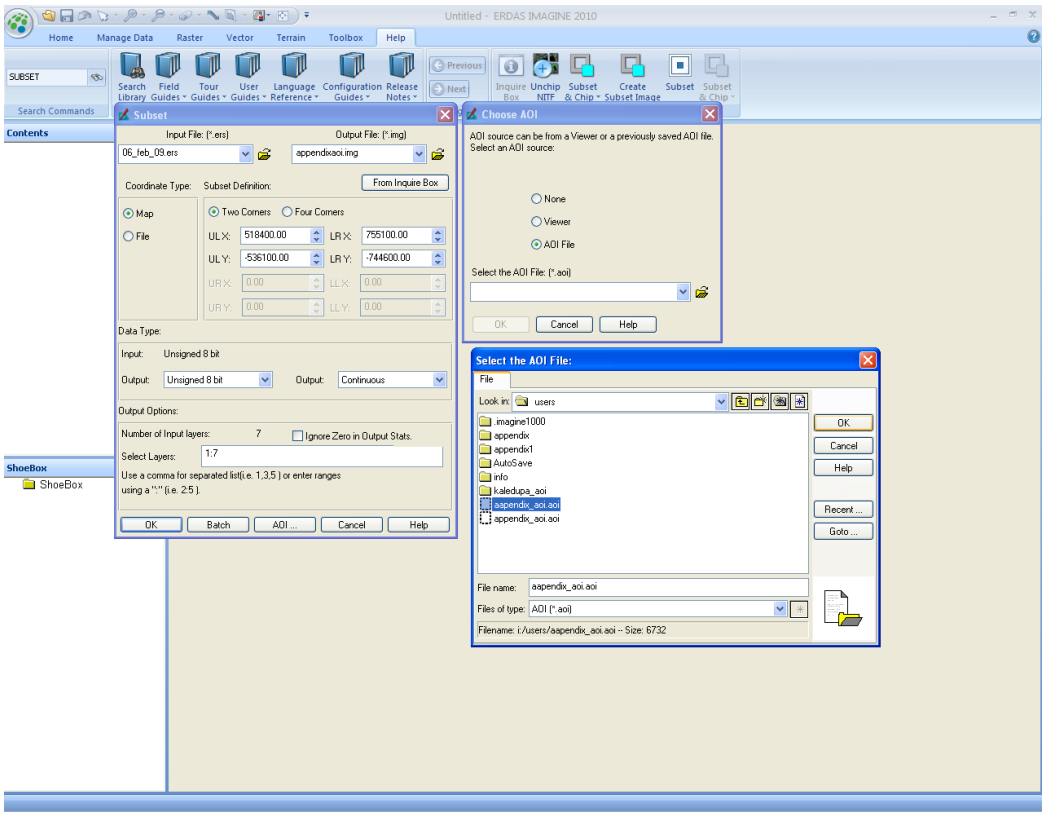

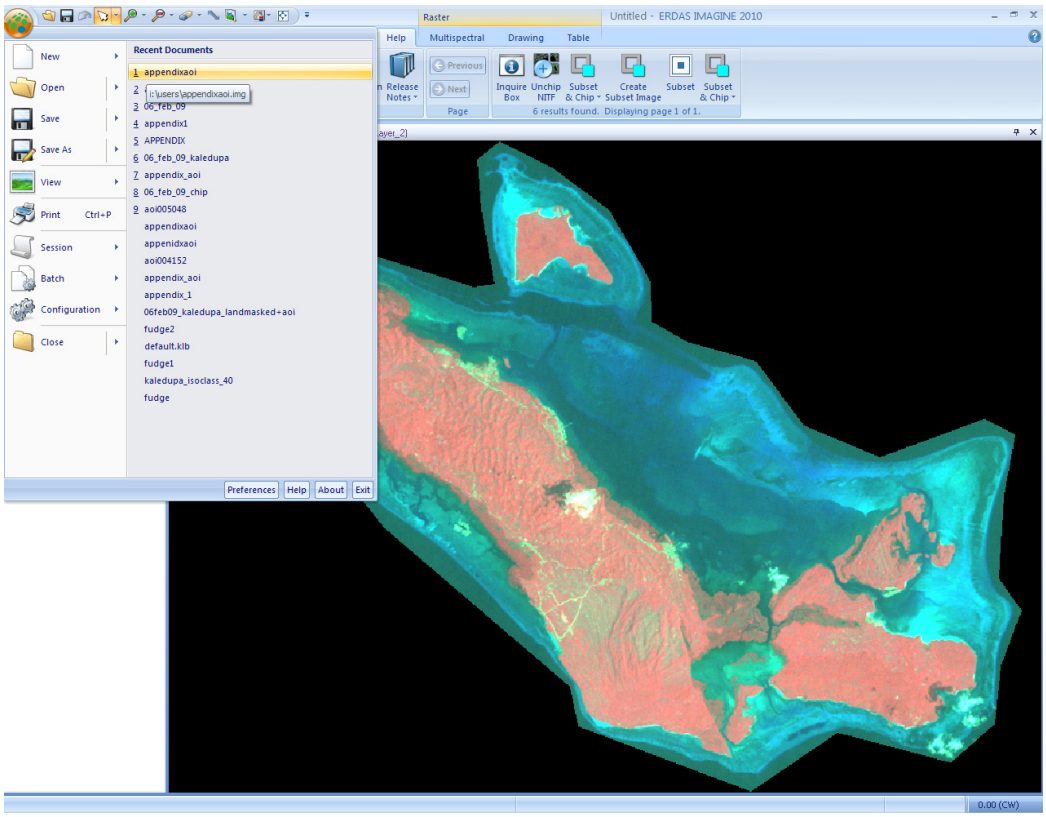

21. Select input file (original landsat image), then give an output file name.
22. Select the AOI button. Select file (last saved .AOI file). Click OK.
23. Open new viewer. Open raster layer. Selct newly created subset file

Appendix B2

ER Mapper Cloud Masking Work Book

.

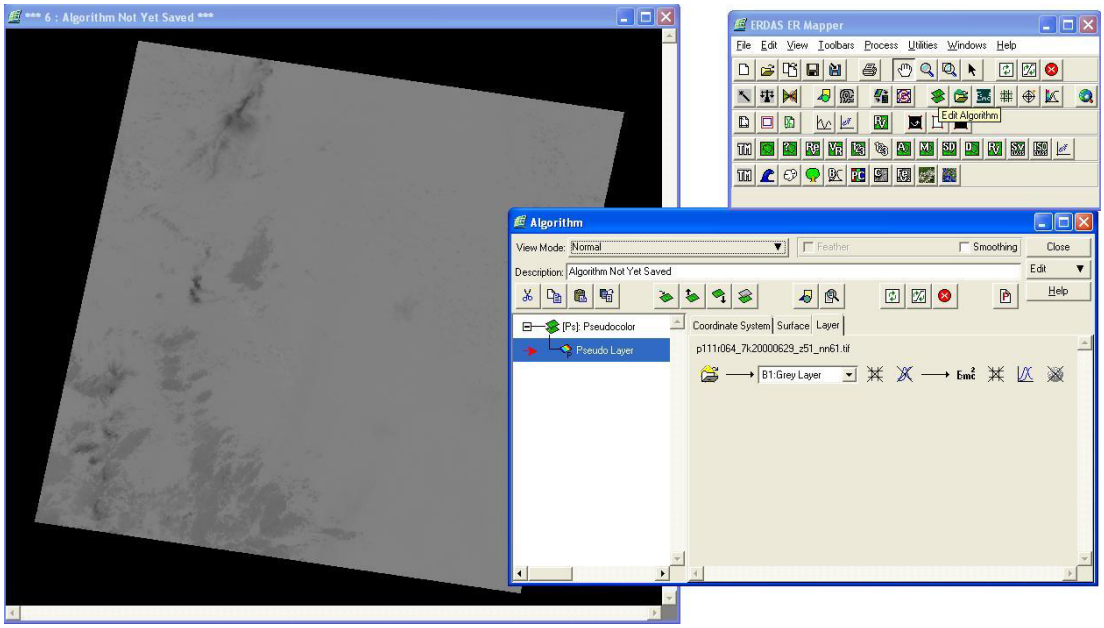

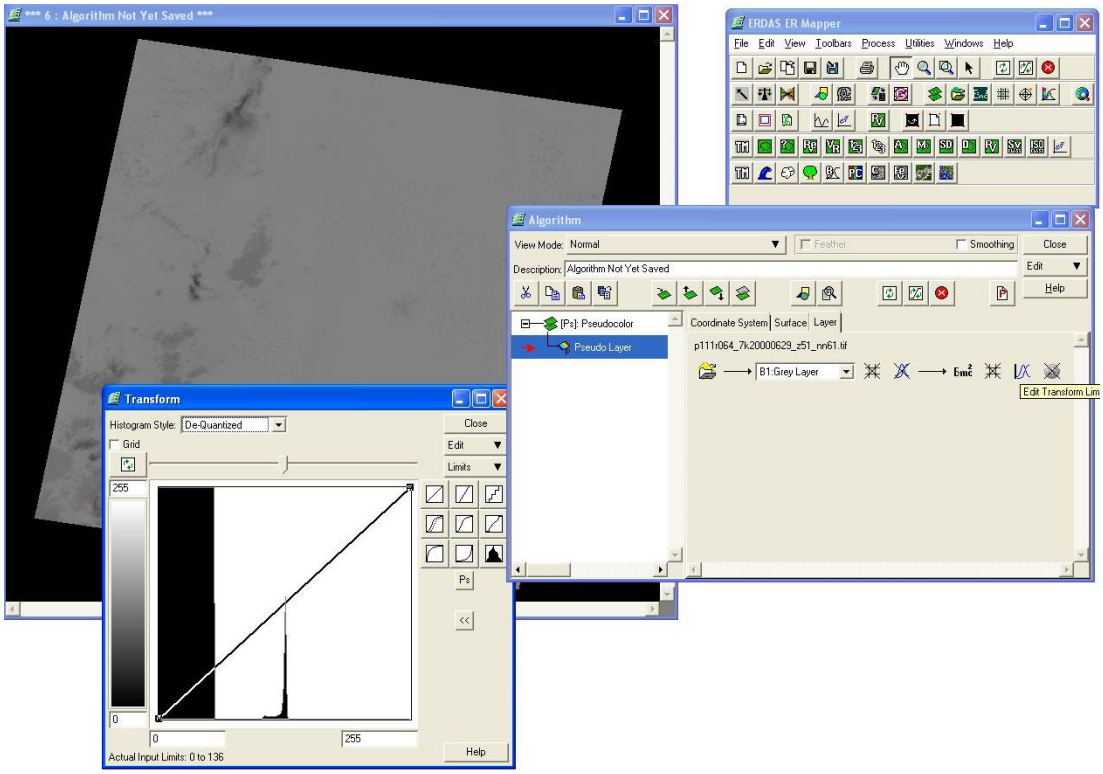

1. Open ER MAPPER. File, Open, Thermal Band 6.
2. File opens in algorithm window. This should show a pseudo colour layer. B1: Grey Layer.
3. Open algorithm window. Edit transform limits. Default linear transformation.

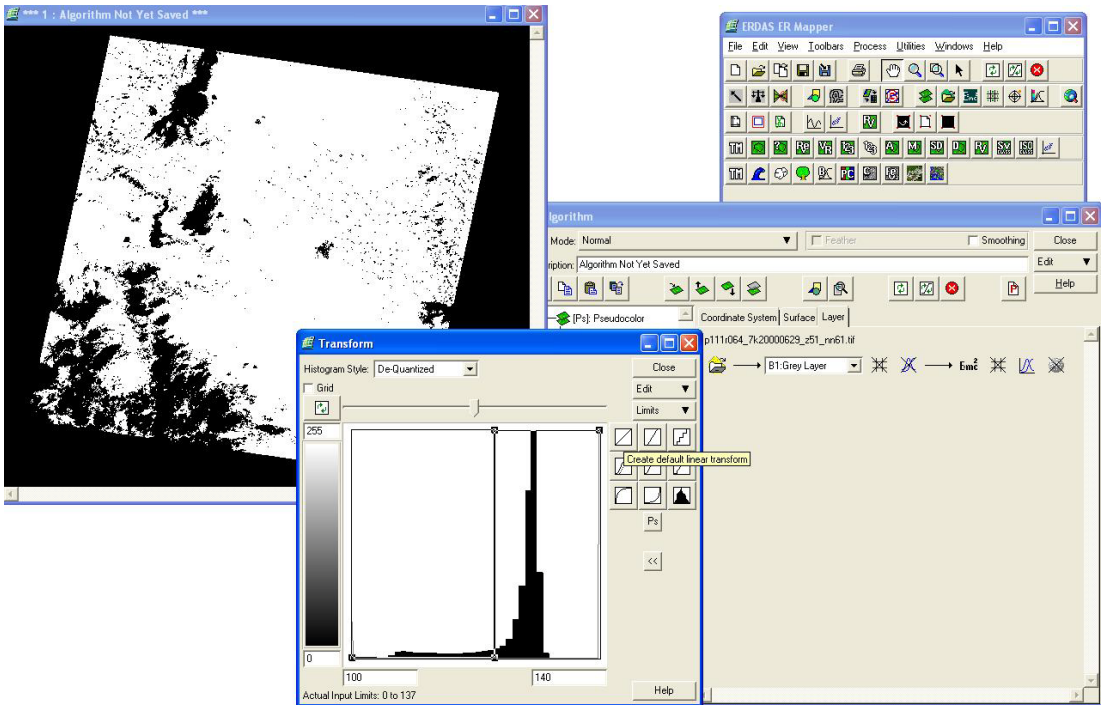

4. Apply contrast stretch consistent with actual display values; e.g. 100:140.

5. Set cut off point with vertical line where histogram spikes, consistent with lower end member cloud values; e.g. 123.

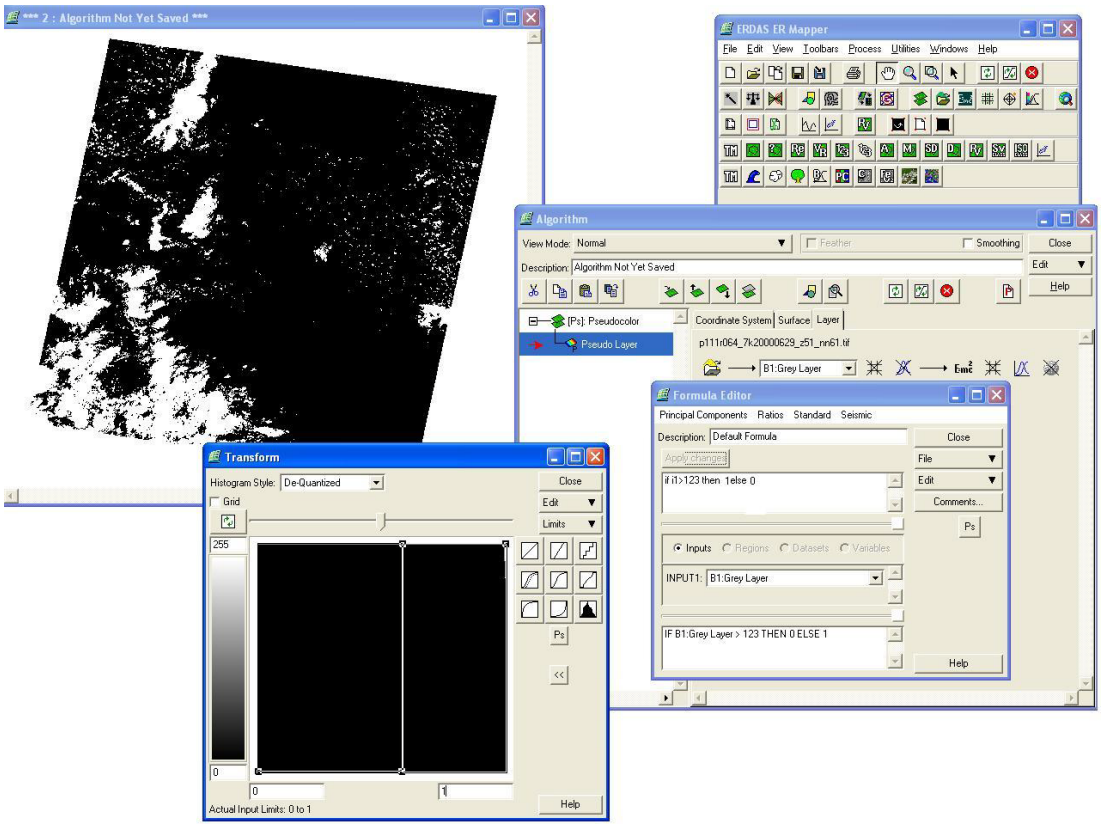

6. Open formula editor.
7. Enter formula " if i1>123 then 1 else 0".
8. Set input limits on transform window to 0:1.
9. Save as .ers file.

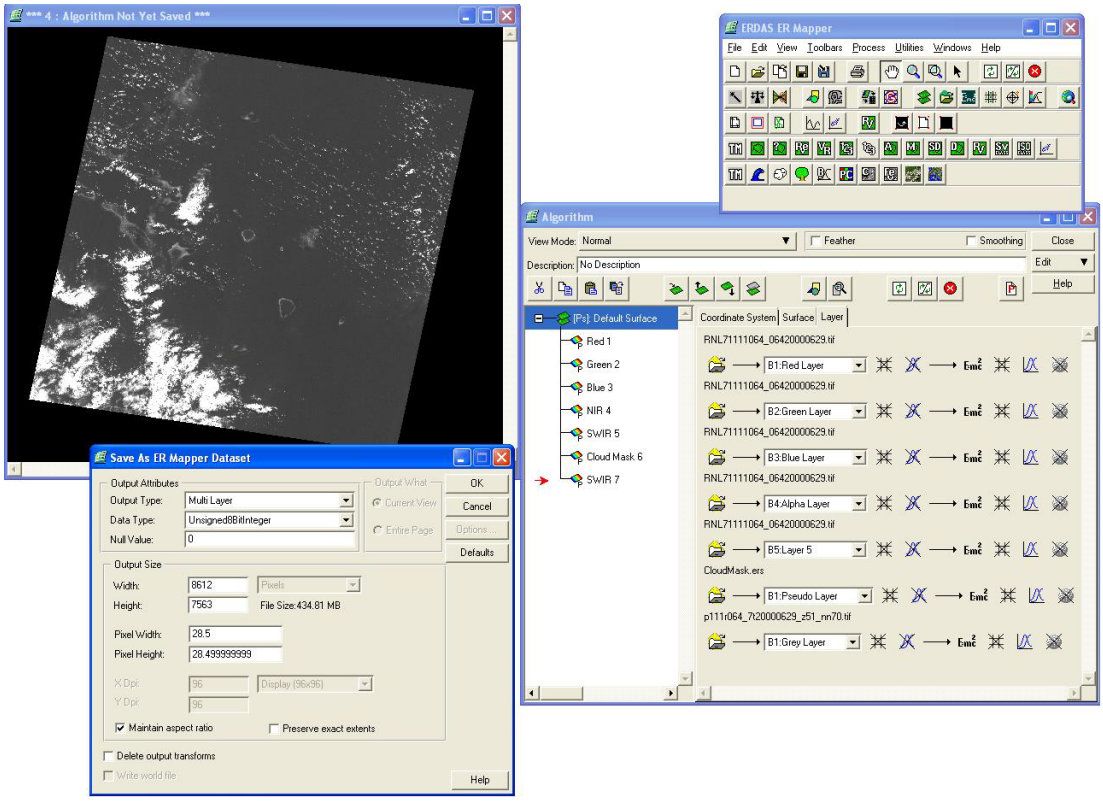

10. Combine .ers files; open raster file as individual pseudo layers 1-5 and 7, layer 6 is cloud mask .ers file.
11. Rename layers appropriate to bands.
12. Save as a multilayer .ers file.

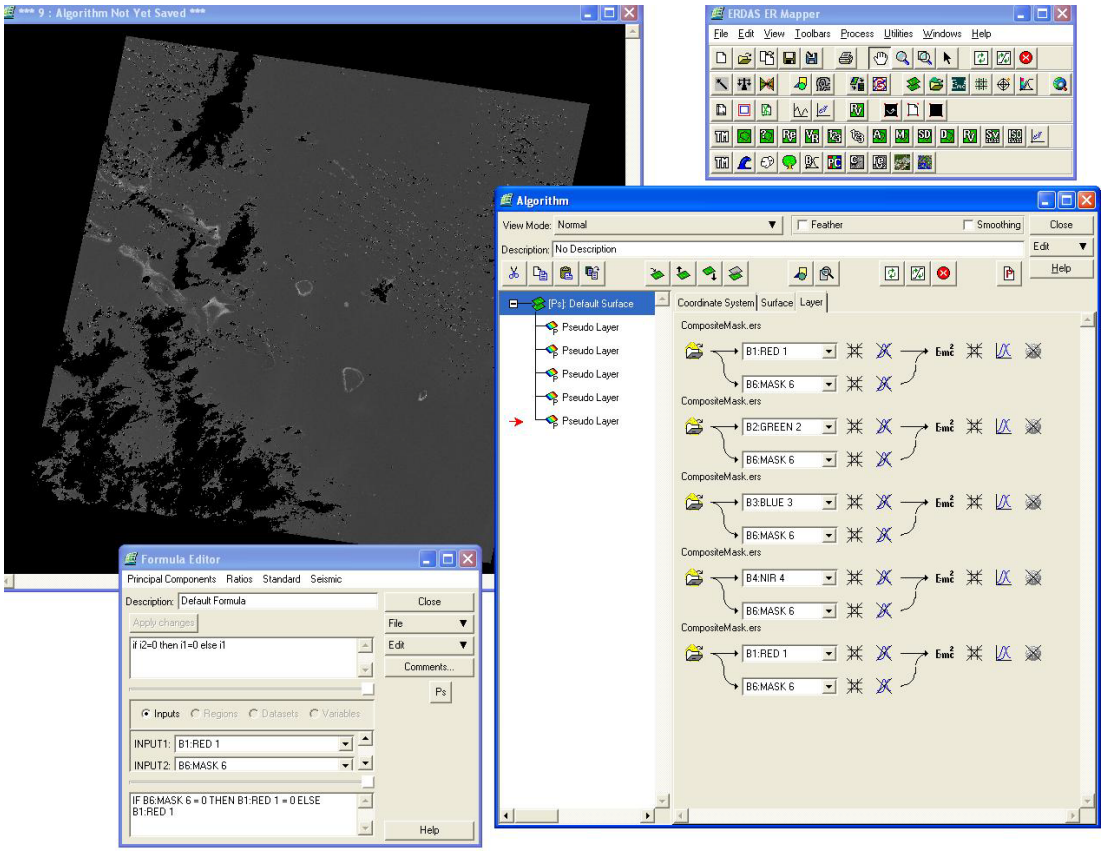

13. Open composite .ers file as individual pseudo layers.
14. Formula editor input equation " if i2=0 then i1=0 else i1" for each individual band/pseudo layer expect for cloud mask layer. INPUT 2/ i2 = Cloud mask layer 6.
15. (Open each pseudo layer and perform equation entry one after the other)
16. Save as .ers file.

NB: Colours may appear to have altered in display following either the cloud mask or the area of interest subsetting processes. This is a display algorithm variation, the data points in each pixel are however unaffected and may have classficiations and/or other techniques performed with no data loss.

Appendix B3

Petrographic Observations of Samples Relating to Chapter 2

	(Mostly) >2 mm Bioclasts (approximate percentage breakdowns from sediment samples)																(Mostly) <2 mm Bioclasts (approximate percentage breakdowns from grain mounts)															Early Grain Alteration					
Sample	**Coral**	**Shells**	***Halimeda***	**Imperforate**	**Miliolids**	**Perforate**	**Calcarinids**	**Smaller Benthics**	**Planktonics**	**Coralline Algae**	**Echinodermata**	**Alcyonarian sclerites**	**Seagrass**	**Lithics**	**Other/Unknown**	**Total**	**Coral**	**Shells**	***Halimeda***	**Imperforate**	**Miliolids**	**Perforate**	**Calcarinids**	**Smaller Benthics**	**Planktonics**	**Coralline Algae**	**Echinodermata**	**Alcyonarian sclerites S**	**eagrass**	**Lithics**	**Other/Unknown**	**Total**	**Abrasion**	**Fragmentation**	**Encrustation**	**Bioerosion**	**Cementation**	**Notes**
HSB41	60	9	12	12	0	2	1	0	0	2	1	1	0	0	0	100	30	20	2	3	2	10	10	4	1	8	3	7	0	0	0	100	1	2	0	1	0	
HSB42	70	6	11	1	0	1	0	1	0	5	0	0	0	0	5	100	25	15	5	10	2	10	5	2	1	5	10	10	0	0	0	100	2	2	0	1	0	
HGG1	60	20	5	4	0	0	4	0	0	1	1	0	5	0	0	100	15	15	1	0	0	4	20	0	0	40	4	0	0	0	1	100	1	1	2	1	0	
HGG2	20	15	13	6	0	0	0	0	0	1	4	0	40	0	1	100	35	15	15	1	0	5	20	0	0	7	2	0	0	0	0	100	1	2	1	1	0	
HGG3	50	13	7	25	1	2	0	0	0	2	0	0	0	0	0	100	15	15	5	5	0	5	25	10	0	15	5	0	0	0	0	100	2	3	1	2	0	
HGG4	70	13	1	13	0	0	1	0	0	1	0	0	1	0	0	100	25	15	10	5	0	7	15	3	0	15	5	0	0	0		100	2	2	0	3	0	
HGG5	20	7	2	60	0	0	1	0	0	0	0	0	10	0	0	100	15	20	6	10	0	6	25	1	0	15	2	0	0	0	0	100	2	2	0	3	0	
HGG6	4	50	10	18	0	1	0	0	0	1	1	0	15	0	0	100	5	20	55	4	3	2	4	1	0	4	1	0	0	1	0	100	2	3	0	3	0	
HGG7	4	3	50	25	1	0	0	0	0	1	1	0	15	0	0	100	5	20	30	15	4	10	3	2	3	5	2	0	0	1	0	100	3	3	1	2	0	
HGG8	25	20	40	0	0	15	0	0	0	0	0	0	0	0	0	100	4	20	10	5	3	5	4	1	0	5	1	0	0	2	40	100	2	2	1	3	0	
HGG9	50	10	25	10	0	5	0	0	0	0	0	0	0	0	0	100	10	20	5	2	4	3	2	2	1	5	0	0	0	1	45	100	2	3	0	3	0	
HGG10	5	65	2	3	0	0	0	0	0	0	0	0	25	0	0	100	10	20	10	2	0	2	5	1	1	5	2	2	0	0	40	100	2	3	0	3	0	
PK5	60	15	12	9	0	0	0	0	0	3	1	0	0	0	0	100	35	25	5	2	1	5	1	3	1	10	8	4	0	0	0	100	2	2	1	1	0	
PK10	71	15	4	3	0	0	0	0	0	2	4	0	0	0	1	100	45	7	4	1	1	9	0	7	0	11	7	8	0	0	0	100	2	2	0	1	0	
PK11	**60**	**28**	**3**	**2**	**0**	**0**	**0**	**0**	**0**	**1**	**4**	**0**	**0**	**0**	**2**	**100**	**45**	**11**	**3**	**2**	**1**	**12**	**0**	**4**	**0**	**6**	**5**	**11**	**0**	**0**	**0**	**100**	**2**	**2**	**0**	**1**	**0**	
PK12	40	17	40	0	0	0	1	0	0	0	0	0	0	0	2	100	53	7	7	4	1	8	0	3	0	6	4	7	0	0	0	100	2	3	0	2	0	
PK13	70	13	6	8	0	1	0	0	0	2	0	0	0	0	0	100	40	10	10	5	1	10	5	1	1	5	5	7	0	0	0	100	1	2	1	2	0	
PK14	75	10	2	5	0	1	0	0	0	4	1	0	0	0	2	100	55	11	7	6	1	5	0	2	0	10	0	3	0	0	0	100	2	2	1	3	0	
PK15	10	15	32	7	0	0	0	1	0	0	0	0	35	0	0	100	52	11	7	8	2	3	0	7	0	5	5	0	0	0	0	100	3	3	0	2	0	
PK16	65	32	0	3	0	0	0	0	0	0	0	0	0	0	0	100	49	15	11	3	0	4	3	2	0	7	2	4	0	0	0	100	2	3	0	3	0	
PK17	52	40	0	8	0	0	0	0	0	0	0	0	0	0	0	100	55	12	7	1	4	2	0	5	2	5	3	4	0	0	0	100	3	3	0	3	0	
PK18	39	39	5	12	0	3	0	1	0	1	0	0	0	0	0	100	45	15	15	4	2	0	1	4	1	8	1	4	0	0	0	100	3	3	0	3	0	
PK19	**15**	**51**	**17**	**17**	**0**	**0**	**0**	**0**	**0**	**0**	**0**	**0**	**0**	**0**	**0**	**100**	**30**	**15**	**8**	**6**	**2**	**2**	**1**	**5**	**4**	**2**	**0**	**2**	**0**	**0**	**23**	**100**	**2**	**2**	**0**	**3**	**0**	
PK20	62	30	2	0	0	0	1	1	0	1	1	0	2	0	0	100	36	23	7	2	6	2	0	1	1	7	2	2	0	8	3	100	3	3	0	3	0	
PK21	7	92	0	0	0	0	0	1	0	0	0	0	0	0	0	100	33	25	7	4	2	3	12	8	1	3	2	0	0	0	0	100	3	3	0	2	0	
HB3-6	65	20	12	0	0	0	0	1	0	1	1	0	0	0	0	100	40	15	10	0	0	10	0	5	2	7	5	5	0	1	0	100	1	2	0	2	0	
HB3-7	90	2	2	0	0	1	0	1	0	1	1	1	0	0	1	100	35	15	6	1	0	10	0	7	2	10	2	7	0	0	5	100	2	1	0	1	0	
HSB2S-1	90	7	0	0	0	0	0	0	0	1	0	2	0	0	0	100	40	25	10	4	2	2	0	1	1	12	1	2	0	0	0	100	2	3	1	1	0	
HSB2S-2	65	30	2	0	0	0	0	0	0	1	2	0	0	0	0	100	45	20	10	0	3	8	0	0	1	6	2	4	0	0	1	100	3	3	1	1	0	
HSB2S-3	63	35	0	1	0	0	0	0	0	1	0	0	0	0	0	100	35	29	5	4	6	3	0	1	1	8	2	5	0	1	0	100	2	3	1	2	0	
HSB2S-4	**60**	**35**	**2**	**0**	**0**	**0**	**0**	**0**	**0**	**1**	**0**	**0**	**2**	**0**	**0**	**100**	**40**	**20**	**4**	**2**	**2**	**5**	**0**	**3**	**2**	**10**	**5**	**5**	**0**	**2**	**0**	**100**	**2**	**2**	**0**	**2**	**0**	
HSB2S-5	30	17	13	33	1	0	0	0	0	0	1	0	5	0	0	100	15	25	15	5	6	1	1	3	2	10	2	3	0	0	12	100	3	2	0	3	0	
HSB2S-6	60	20	4	15	0	0	0	1	0	0	0	0	0	0	0	100	25	20	10	5	5	7	0	2	2	10	3	6	0	5	0	100	1	2	1	3	0	
HSB2S-7	20	60	1	15	1	0	0	1	0	0	2	0	0	0	0	100	45	18	7	8	4	3	1	2	1	6	1	2	0	2	0	100	3	2	0	2	0	
HSB2S-8	40	45	5	7	0	0	0	1	0	2	0	0	0	0	0	100	30	20	15	4	1	2	15	2	1	5	3	2	0	0	0	100	2	2	0	3	0	
HSB2S-9	40	43	3	10	0	0	0	2	0	0	0	0	0	1	1	100	33	15	10	6	5	7	12	1	0	6	2	2	0	1	0	100	3	2	0	2	0	
HSB2S-10	40	40	2	16	0	0	0	0	0	0	0	1	0	1	0	100	35	20	10	4	2	5	10	2	1	5	5	1	0	0	0	100	2	3	1	1	0	
S2-3 8m	70	13	1	3	0	2	0	1	0	4	1	2	0	0	3	100	59	10	4	0	0	3	2	0	0	15	2	5	0	0	0	100	1	2	2	1	0	
S2-3 5m	60	17	0	16	0	1	0	0	0	2	1	1	0	1	1	100	44	12	10	3	3	5	1	0	0	10	1	4	8	0	0	100	1	3	2	1	0	
S2-3 3m	64	20	0	4	0	1	0	0	0	1	2	2	0	1	5	100	45	20	4	0	1	4	0	0	1	12	3	10	0	0	0	100	2	2	1	1	0	
SS1	75	20	0	0	0	0	0	0	0	1	2	2	0	0	0	100	48	15	7	4	2	1	0	0	0	12	1	9	0	1	0	100	2	3	0	2	0	
SS2	20	75	0	0	0	0	0	0	0	0	0	0	0	0	5	100	45	15	10	0	2	5	0	2	1	10	3	7	0	0	0	100	2	3	0	1	0	
SS3	70	28	0	1	0	0	0	0	0	1	0	0	0	0	0	100	17	20	10	5	6	0	1	4	2	15	8	10	0	2	0	100	2	3	0	2	0	
SS4	90	4	0	0	0	0	0	0	0	6	0	0	0	0	0	100	32	20	8	1	2	10	2	1	0	10	6	8	0	0	0	100	2	3	0	2	0	
SS5	23	30	45	1	0	0	0	0	0	1	1	0	0	0	0	100	25	25	15	0	3	10	3	1	0	10	3	5	0	0	0	100	2	2	2	2	0	
SS6	40	50	4	0	0	0	0	0	0	0	2	0	0	4	0	100	34	15	15	4	2	12	1	1	1	8	2	5	0	0	0	100	2	2	1	2	0	
SS7	35	25	33	5	0	0	0	1	0	1	1	0	0	0	0	100	5	10	30	2	5	10	10	5	0	10	10	3	0	0	0	100	1	3	1	1	0	
WSUM2	75	18	0	2	0	0	1	0	0	1	2	1	0	0	0	100	45	10	0	10	1	5	4	4	2	10	5	3	0	0	1	100	3	3	1	1	0	
KAL1	88	4	1	2	0	1	0	0	0	2	1	0	0	0	1	100	43	5	0	10	5	10	10	0	1	10	5	0	0	0	1	100	3	3	0	1	0	
KAL2	70	9	20	0	0	0	0	0	0	1	0	0	0	0	0	100	48	5	1	5	0	15	8	0	1	10	5	2	0	0	0	100	2	3	1	1	0	
KAL3	80	4	0	13	0	0	0	0	0	1	1	0	0	0	1	100	42	5	1	5	2	10	15	1	0	10	3	3	0	0	3	100	3	3	0	1	0	
KAL4	82	5	0	0	0	4	3	0	0	3	0	1	0	0	2	100	47	10	7	3	1	12	10	1	0	5	1	3	0	0	0	100	2	3	0	1		
KAL5	80	5	5	4	1	0	1	0	0	1	0	0	0	0	3	100	25	15	0	5	4	10	15	5	0	15	3	1	0	1	1	100	3	3	1	1	0	
KAL7	15	8	0	4	0	0	2	0	0	1	0	0	70	0	0	100	20	20	5	10	1	5	15	1	5	10	7	1	0	0	0	100	2	3	0	2	0	
KAL9	55	30	1	4	0	0	0	0	0	0	0	0	10	0	0	100	25	20	12	13	0	3	12	3	0	6	6	0	0	0	0	100	1	2	1	2	0	
KAL11	13	0	1	6	0	0	0	0	0	0	0	0	80	0	0	100	15	8	10	10	8	3	10	3	3	10	10	0	0	0	10	100	2	2	0	3	0	
KAL13	6	30	11	35	1	2	1	1	0	0	2	0	10	0	1	100	5	20	30	15	3	2	3	1	1	5	5	0	0	0	10	100	1	1	0	3	0	
KAL15	10	75	4	10	0	1	0	0	0	0	0	0	0	0	0	100	0	5	55	7	7	3	7	4	0	5	4	1	0	0	2	100	2	3	0	3	0	
KAL16	8	10	44	30	0	1	0	0	0	0	2	0	5	0	0	100	3	6	53	9	10	6	6	2	1	2	1	1	0	0	0	100	2	3	0	3	0	
KAL17	16	15	35	25	1	2	0	0	0	0	0	1	5	0	0	100	1	5	50	8	10	2	7	1	1	8	1	0	0	1	5	100	2	1	0	1	0	
KAL18	10	45	20	23	0	0	0	0	0	1	0	0	0	1	0	100	10	10	25	8	8	6	12	3	1	10	4	1	1	1	0	100	2	2	0	2	0	
KAL19	25	50	2	17	0	1	0	0	0	0	0	0	0	4	1	100	45	15	0	7	0	4	17	0	1	8	2	1	0	0	0	100	3	3	1	3	0	
KAL20	25	35	0	0	0	0	0	0	0	0	40	0	0	0	0	100	35	20	5	3	1	2	16	1	0	10	4	1	0	0	2	100	3	3	0	2	0	
KAL21	15	55	15	15	0	0	0	0	0	0	0	0	0	0	0	100	40	5	2	3	1	5	7	1	0	30	3	2	1	0	0	100	3	3	1	3	0	
KAL6	60	12	0	4	0	0	2	0	0	0	1	0	20	0	1	100																						
KAL8	33	20	10	15	0	1	0	0	0	0	1	0	20	0	0	100																						
KAL10	15	30	33	20	1	0	0	0	0	0	0	1	0	0	0	100																						
KAL12	17	80	0	3	0	0	0	0	0	0	0	0	0	0	0	100																						
KAL14	10	80	0	10	0	0	0	0	0	0	0	0	0	0	0	100																						
WHB1-2	45	48	0	0	0	0	0	1	0	0	1	2	0	0	3	100	40	25	5	2	0	2	0	3	0	8	5	10	0	0	0	100	3	3	0	2	0	
KAL41	66	20	0	1	0	0	0	0	0	3	0	0	0	0	10	100	50	30	0	0	0	0	0	5	4	10	1	0	0	0	0	100	1	2	2	1	0	
KAL40	**18**	**65**	**3**	**1**	**4**	**3**	**2**	**0**	**0**	**0**	**3**	**0**	**0**	**1**	**0**	**100**	**5**	**30**	**0**	**10**	**10**	**5**	**0**	**10**	**4**	**4**	**20**	**0**	**0**	**1**	**1**	**100**	**2**	**2**	**0**	**1**	**0**	
KAL39	88	4	0	1	0	1	1	0	0	2	0	2	1	0	0	100																						
KAL38	7	60	2	22	0	2	0	2	0	0	4	0	0	1	0	100	5	25	5	10	4	3	0	6	1	15	20	5	0	1	0	100	2	2	2	2	0	
KAL37	14	60	10	10	0	0	0	0	0	0	1	2	0	2	1	100	15	40	0	10	5	5	0	7	1	5	6	1	0	0	5	100	2	2	1	3	0	
KAL36	0	0	0	0	0	0	0	0	0	0	0	0	0	100	0	100	0	2	0	0	0	0	0	0	0	0	0	1	0	97	0	100						
KAL35	0	0	0	0	0	0	0	0	0	0	0	1	0	99	0	100	1	3	0	0	0	0	0	0	0	0	0	1	0	95	0	100						
KAL34	0	0	0	0	0	0	0	0	0	0	0	0	0	100	0	100	10	10	3	1	4	1	0	4	2	5	8	2	1	47	2	100	3	3	1	3	0	

Notes on grain alteration index.

Abrasion:
0 = No visible effects of abrasion, clasts entact and well preserved
1 = Some evidence of abrasion. Minor truncations to clasts, fragile spines may be removed, elongate clasts showing a slight degree of rounding.
2 = Moderate abrasion. Elongate clasts with moderate rounding, many long axes truncated, many spines removed.
3 = Major abrasion. Elongate clasts truncated and rounded, all spines removed .

Fragmentation:
0 = No visibly fractured or broken grains
1 = Long and delicate clasts may be fractured into smaller pieces, common on fine shell material and spicules.
2 = Moderate fragmentation. More robust clasts clearly broken into smaller sizes, along multiple breakage surfaces.
3 = Major fragmentation,. All clasts fragmented into smaller sizes. Robust corals and foraminifera commonly brokenn.

Encrustation:
0 = No eveidence of encrustation.
1 = Some fine development of encrusting alage or foraminifera, occurs rarely on few clasts.
2 = Common occurence of encrusting forams or algae, or thick development.
3 = Abundance of pervasively encrusted grains.

Bioerosion:
0 = No evidence of micritised grain margins
1 = Rare occurence or minor (<10 um) thick rims
2 = Common occurence or moderate (10-30 um) thickness to rims
3 = Abundance of micrititised margins ,with thick (.30 um) rims.

Appendix B4

Modern Sediment Photographs and Thin Section Photomicrographs of Samples Relating to Chapter 2

HGG1 +2MM 8X.jpg

HGG1 UNSORTED 8X.jpg

HGG2 +2MM 8X.jpg

HGG2 UNSORTED 8X.jpg

HGG3 +2MM 8X.jpg

HGG3 UNSORTED 8X.jpg

HGG4 +2MM 8X.jpg

HGG4 UNSORTED 8X.jpg

HGG5 +2MM 8X.jpg

HGG5 UNSORTED 8X.jpg

HGG6 +2MM 8X(2).jpg

HGG6 +2MM 8X.jpg

HGG6 UNSORTED 8X.jpg

HGG7 +2MM 8X.jpg

HGG7 UNSORTED 8X.jpg

HGG8 +2MM 8X.jpg

HGG8 UNSORTED 8X.jpg

HGG9 +2MM 8X.jpg

HGG9 UNSORTED 8X.jpg

HGG10 +2MM 8X.jpg

HGG10 UNSORTED 8X.jpg

HSB41 +2MM 8X.jpg

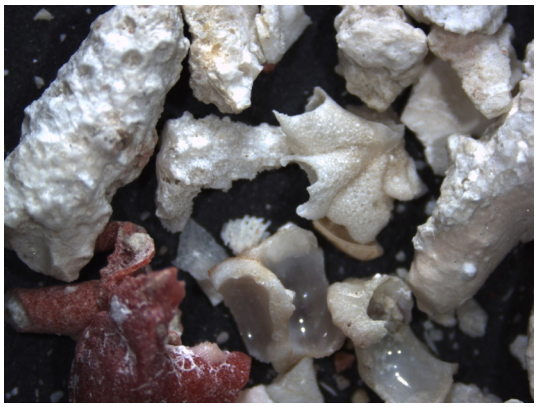

HSB42 +2MM 8X.jpg

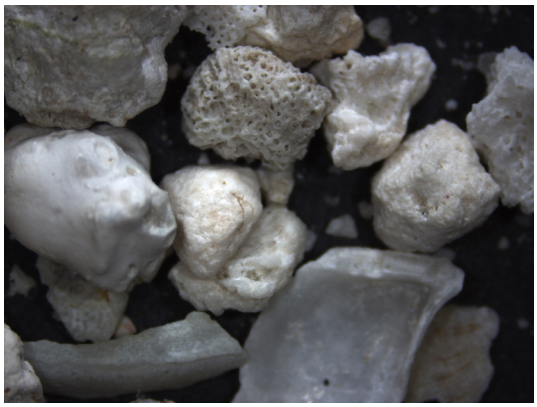

KAL1 +2MM 8X.jpg

KAL1 UNSORTED 8X.jpg

KAL2 +2MM 8X.jpg

KAL2 UNSORTED 8X.jpg

KAL3 +2MM 8X.jpg

KAL3 UNSORTED 8X.jpg

KAL4 UNSORTED 8X(2).jpg

KAL4 UNSORTED 8X.jpg

KAL5 +2MM 8X.jpg

KAL5 UNSORTED 8X.jpg

KAL6 +2MM 8X.jpg

KAL6 UNSORTED 8X.jpg

KAL7 +2MM 8X.jpg

KAL7 UNSORTED 8X.jpg

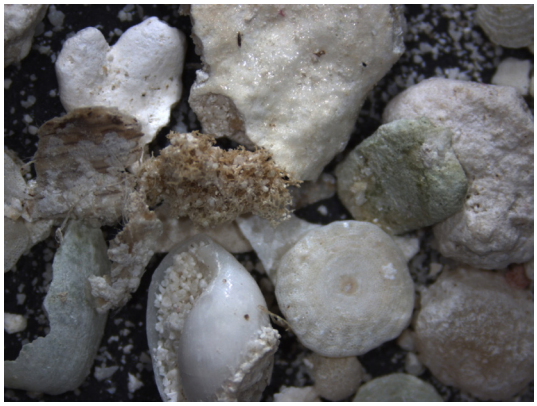

KAL8 +2MM 8X.jpg

KAL8 UNSORTED 8X.jpg

KAL9 +2MM 8X.jpg

KAL9 UNSORTED 8X.jpg

KAL10 +2MM 8X.jpg

KAL10 UNSORTED 8X.jpg

KAL11 +2MM 8X.jpg

KAL11 UNSORTED 8X.jpg

KAL12 +2MM 8X.jpg

KAL12 UNSORTED 8X.jpg

KAL13 +2MM 8X.jpg

KAL13 UNSORTED 8X.jpg

KAL14 +2MM 8X.jpg

KAL14 UNSORTED 8X.jpg

KAL15 +2MM 8X.jpg

KAL15 UNSORTED 8X.jpg

KAL16 +2MM 8X.jpg

KAL16 UNSORTED 8X.jpg

KAL17 +2MM 8X.jpg

KAL17 +2MM 35X MILLIOLID.jpg

KAL17 UNSORTED 8X.jpg

KAL18 +2MM 8X.jpg

KAL18 UNSORTED 8X.jpg

KAL19 +2MM 8X.jpg

KAL19 UNSORTED 8X.jpg

KAL20 +2MM 8X.jpg

KAL20 UNSORTED 8X.jpg

KAL21 +2MM 8X.jpg

KAL21 UNSORTED 8X.jpg

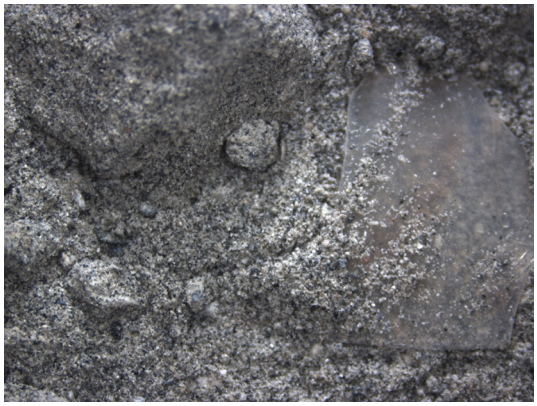

KAL34 UNSORTED 8X.jpg

KAL35 UNSORTED 8X.jpg

KAL36 UNSORTED 8X.jpg

KAL37 +2MM 8X.jpg

KAL37 UNSORTED 8X.jpg

KAL38 +2MM 8X.jpg

KAL38 UNSORTED 8X.jpg

KAL39 +2MM 8X.jpg

KAL39 UNSORTED 8X.jpg

KAL40 +2MM 8X.jpg

KAL40 UNSORTED 8X.jpg

KAL41 +2MM 8X.jpg

KAL41 UNSORTED 8X.jpg

PK5 +2MM 8X.jpg

PK10 +2MM 8X.jpg

PK11 +2MM 8X.jpg

PK12 +2MM 8X.jpg

PK13 +2MM 8X.jpg

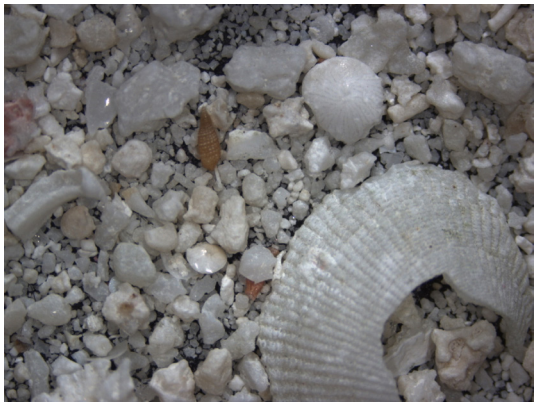

PK13 UNSORTED 8X.jpg

PK14 +2MM 8X.jpg

PK15 +2MM 8X.jpg

PK16 +2MM 8X.jpg

PK17 +2MM 8X.jpg

PK18 +2MM 8X.jpg

PK19 +2MM 8X.jpg

PK20 +2MM 8X.jpg

PK21 +2MM 8X.jpg

S2-3 3m UNSORTED 8X.jpg

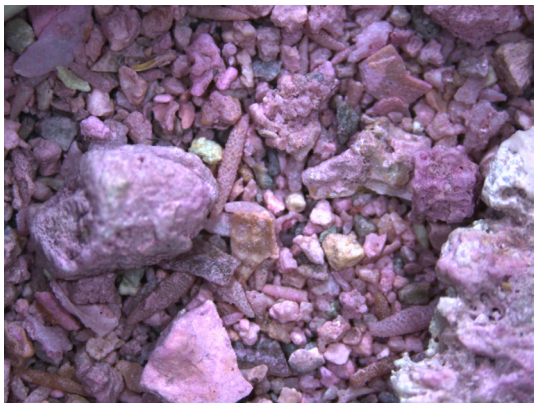

S2-3 5m UNSORTED 8X.jpg

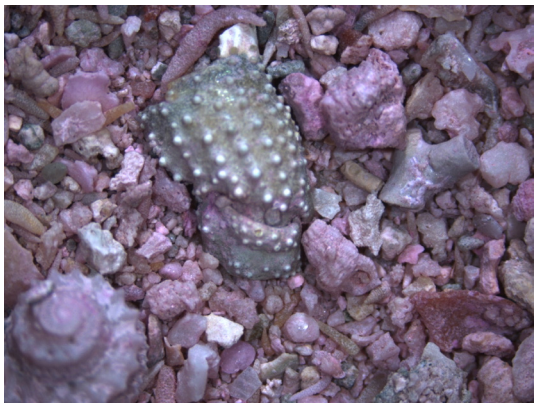

S2-3 8m UNSORTED 8X.jpg

SS1 +2MM 8X.jpg

SS1 UNSORTED 8X.jpg

SS2 +2MM 8X.jpg

SS2 UNSORTED 8X.jpg

SS3 +2MM 8X.jpg

SS3 UNSORTED 8X.jpg

SS4 +2MM 8X.jpg

SS4 UNSORTED 8X.jpg

SS5 +2MM 8X.jpg

SS5 UNSORTED 8X.jpg

SS6 +2MM 8X.jpg

SS6 UNSORTED 8X.jpg

SS7 +2MM 8X.jpg

SS7 UNSORTED 8X.jpg

WHB1-2 +2MM 8X.jpg

WHB1-2 UNSORTED 8X.jpg

WHB3-6 +2MM 8X.jpg

WHB3-6 UNSORTED 8X.jpg

WHB3-7 +2MM 8X.jpg

WHB3-7 UNSORTED 8X.jpg

WHBS2-1 +2MM 8X.jpg

WHBS2-1 UNSORTED 8X.jpg

WHBS2-2 +2MM 8X.jpg

WHBS2-2 UNSORTED 8X.jpg

WHBS2-3 +2MM 8X.jpg

WHBS2-3 UNSORTED 8X.jpg

WHBS2-4 +2MM 8X.jpg

WHBS2-4 UNSORTED 8X.jpg

WHBS2-5 +2MM 8X.jpg

WHBS2-5 UNSORTED 8X.jpg

WHBS2-6 +2MM 8X.jpg

WHBS2-6 UNSORTED 8X.jpg

WHB2S-6 UNSORTED 8X.jpg

WHB2S-7 +2MM 8X.jpg

WHBS2-7 UNSORTED 8X.jpg

WHBS2-8 +2MM 8X.jpg

WHBS2-8 UNSORTED 8X.jpg

WHBS2-9 +2MM 8X.jpg

WHBS2-9 UNSORTED 8X.jpg

WHBS2-10 +2MM 8X.jpg

WHBS2-10 UNSORTED 8X.jpg

WSUM2 +2MM 8X.jpg

WSUM2 UNSORTED 8X.jpg

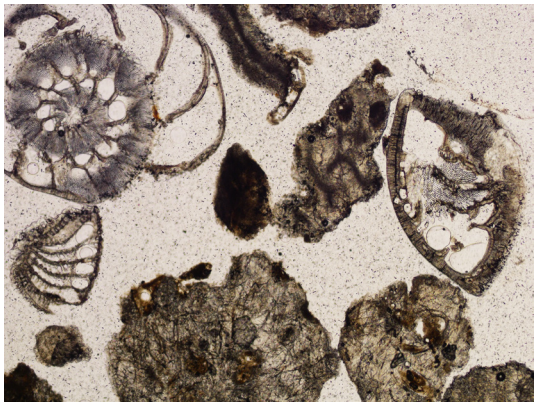

HGG2 5x.tif

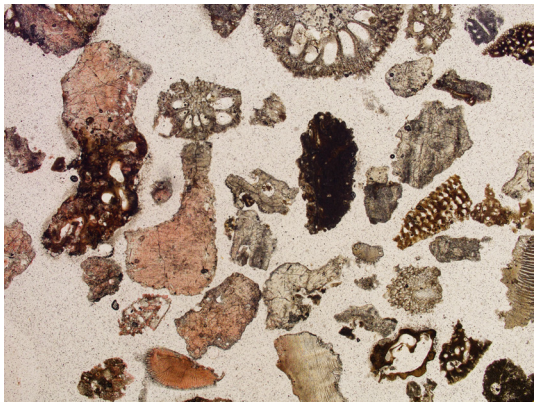

HGG4 2.5x.tif

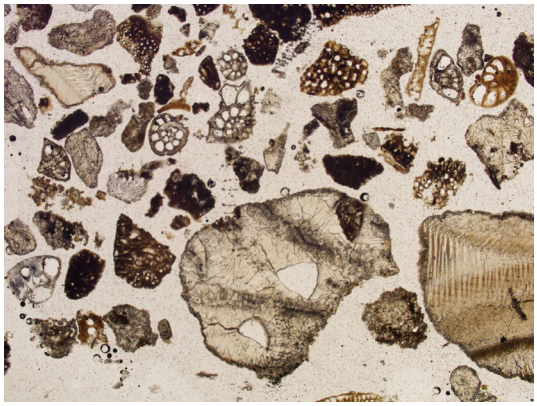

HGG7 2.5x.tif

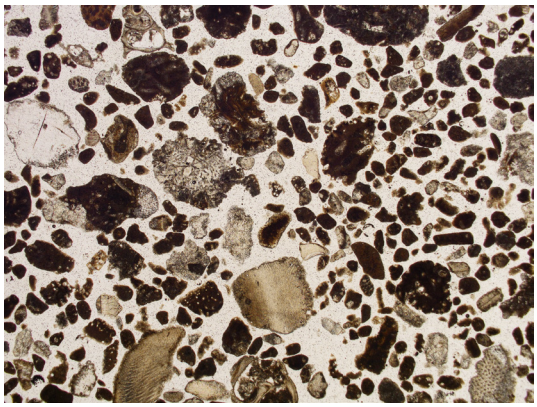

HGG10 2.5x.tif

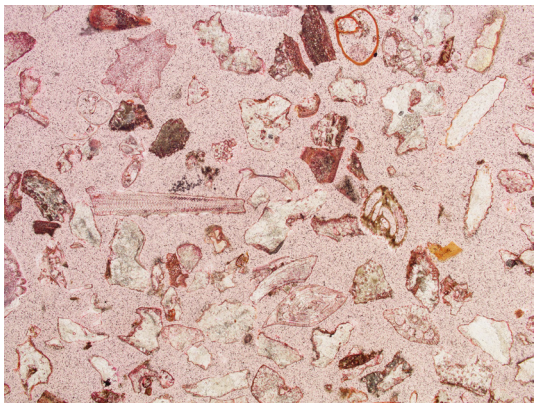

HSB42 2.5x unused.tif

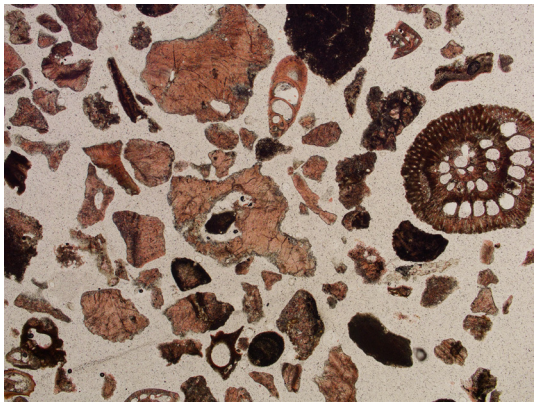

KAL3 2.5x.tif

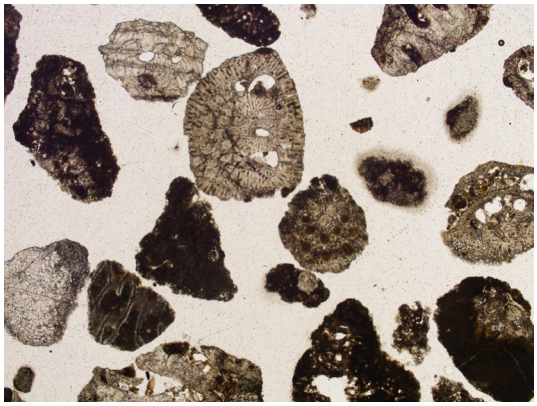

KAL19 2.5x.tif

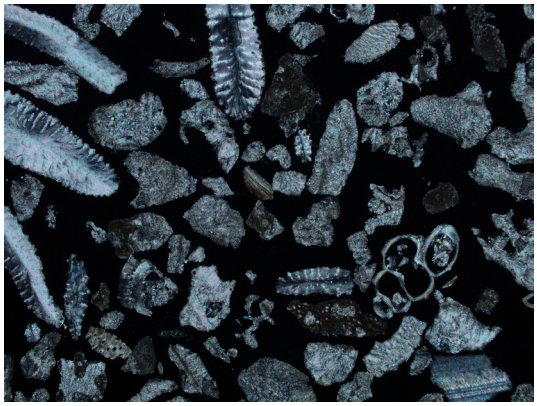

PK10 2.5x XPL unused.tif

PK10 2.5x.tif

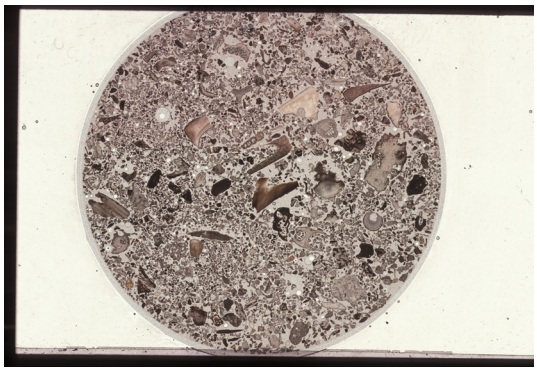

HBS2S-1.tif

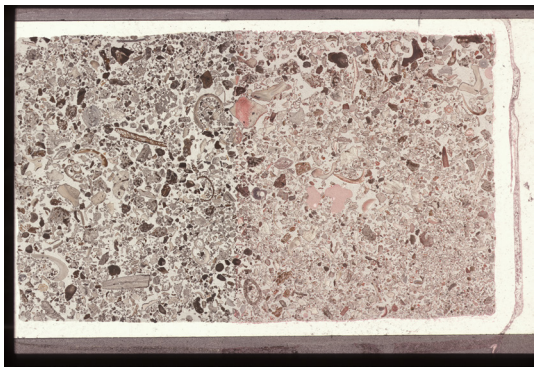

HBS2S-2.tif

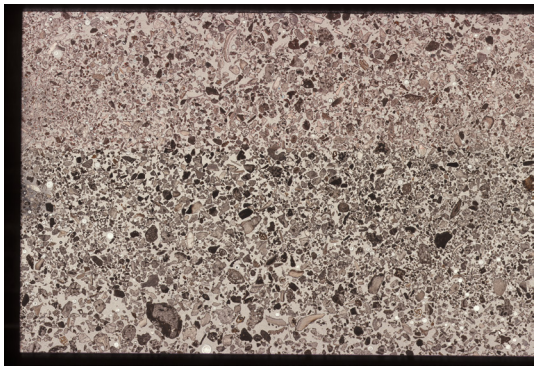

HBS2S-3.tif

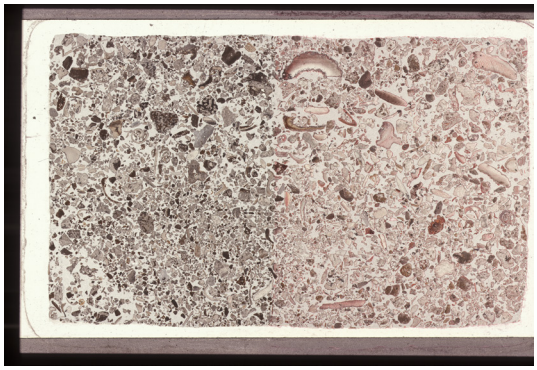

HBS2S-4.tif

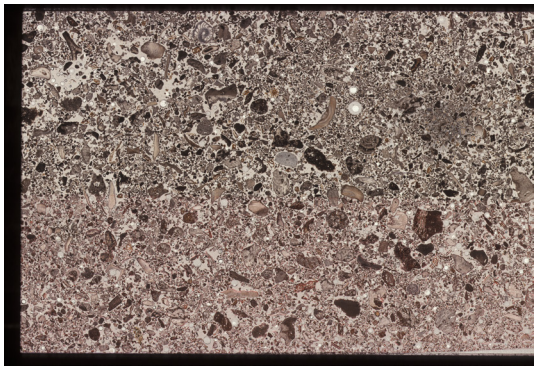

HBS2S-5.tif

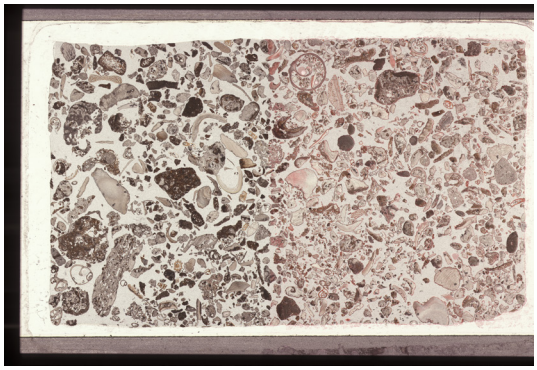

HBS2S-6.tif

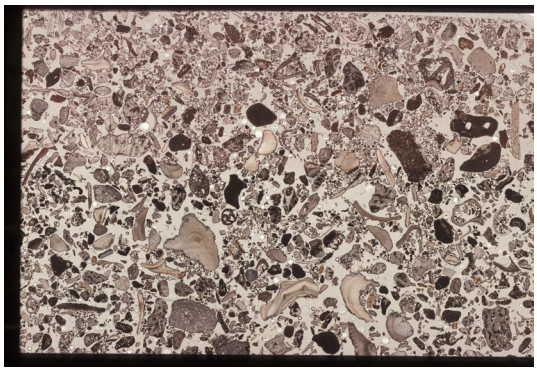

HBS2S-7.tif

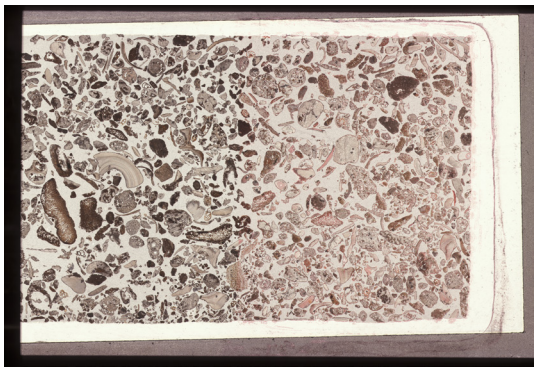

HBS2S-8.tif

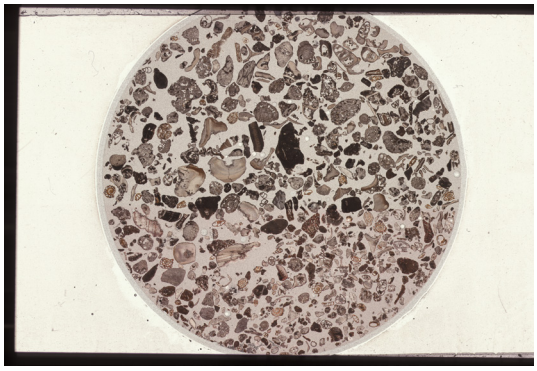

HBS2S-9.tif

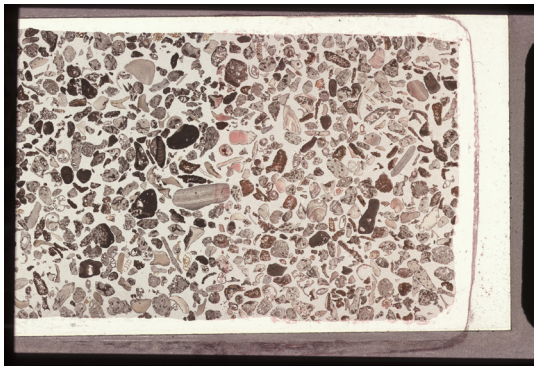

HBS2S-10.tif

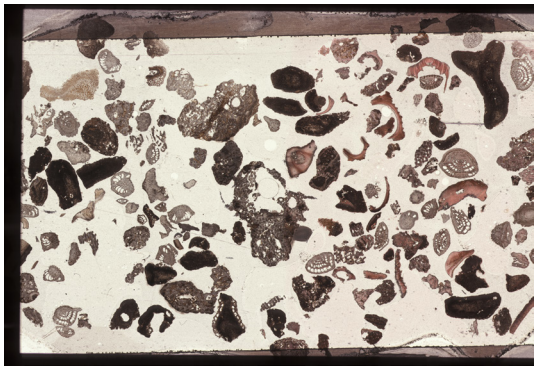

HGG1.tif

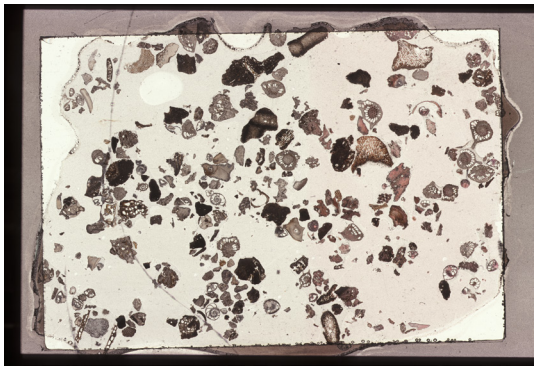

HGG2.tif

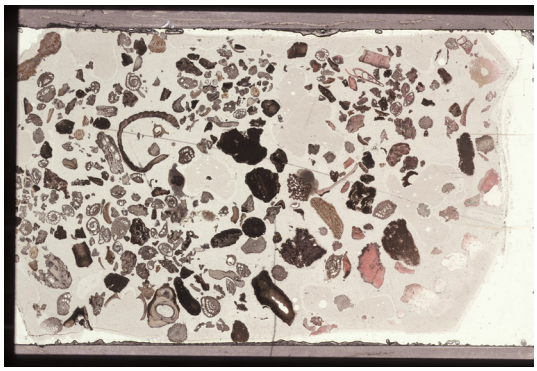

HGG3.tif

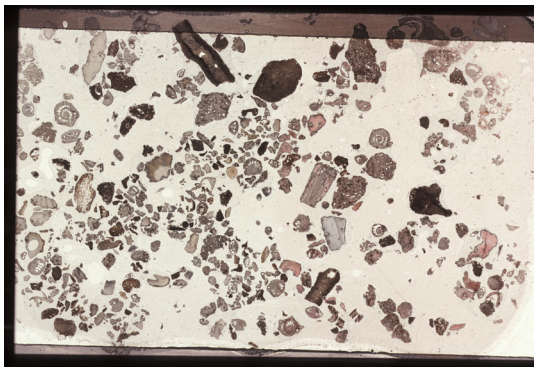

HGG4.tif

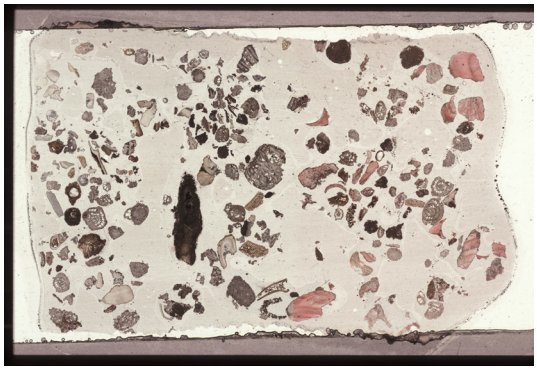

HGG5.tif

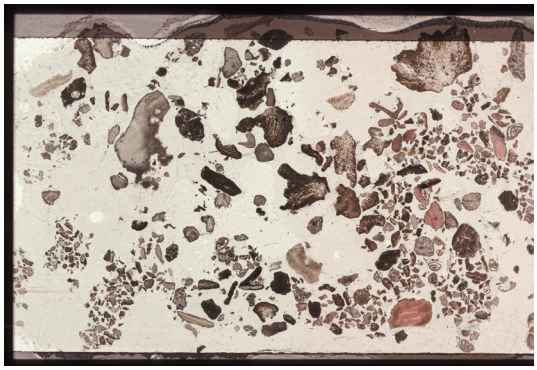

HGG6.tif

HGG7.tif

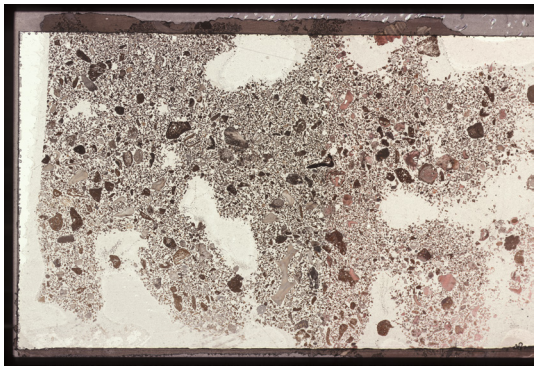

HGG8.tif

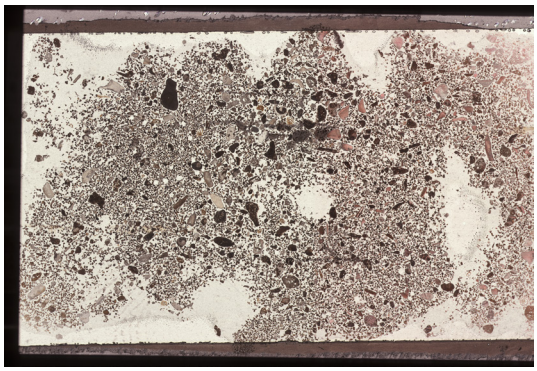

HGG9.tif

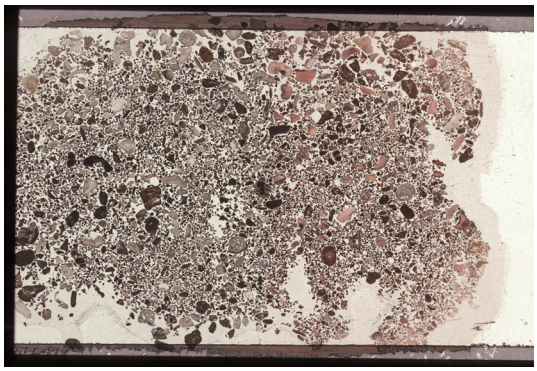

HGG10.tif

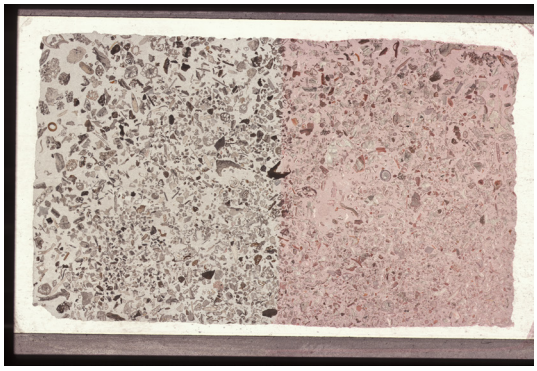

HSB41.tif

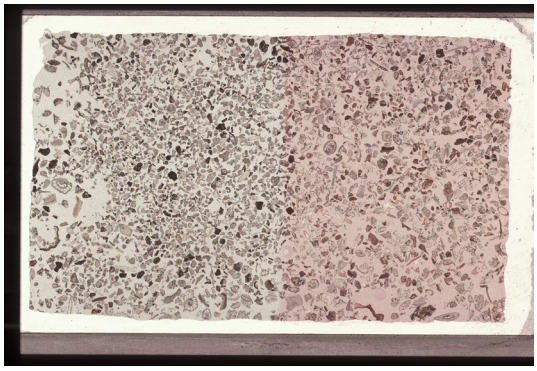

HSB42.tif

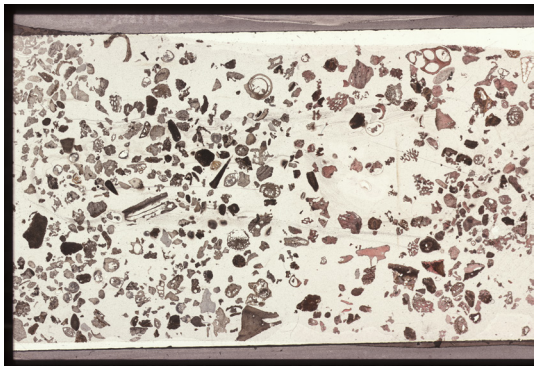

KAL1.tif

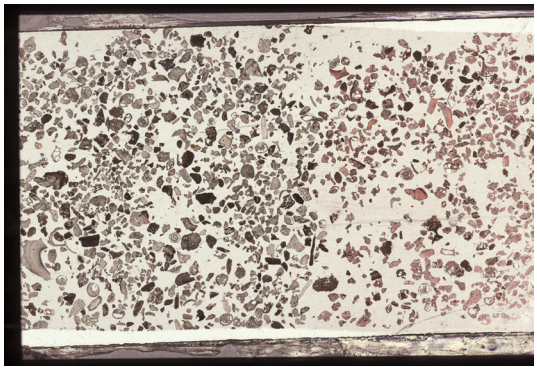

KAL2.tif

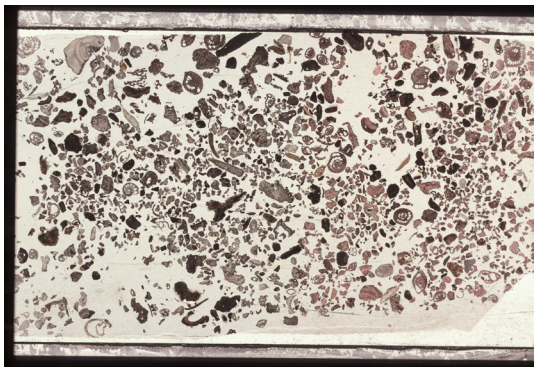

KAL3.tif

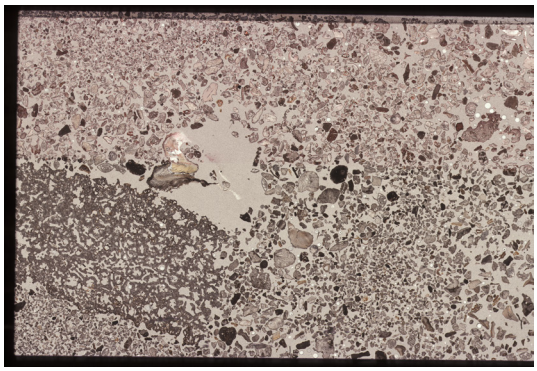

KAL4.tif

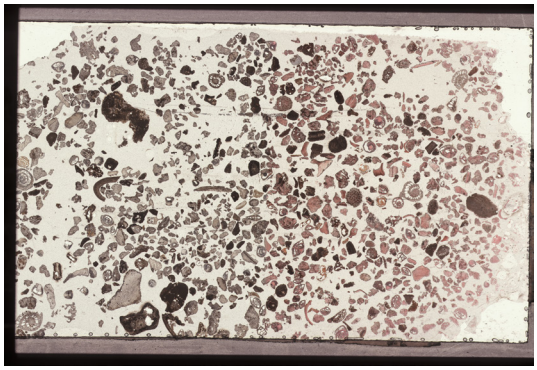

KAL5.tif

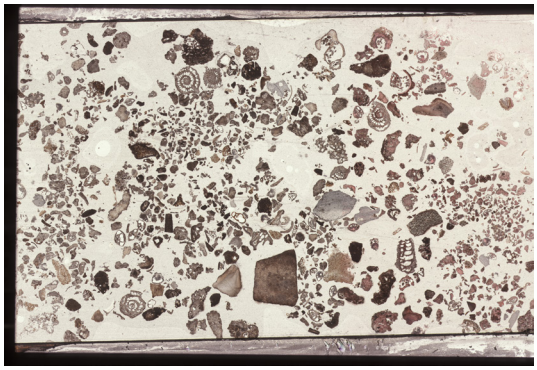

KAL7.tif

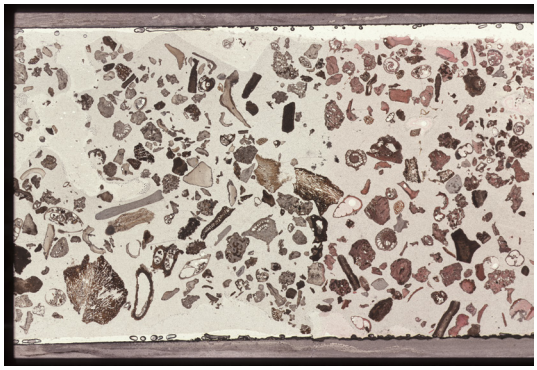

KAL9.tif

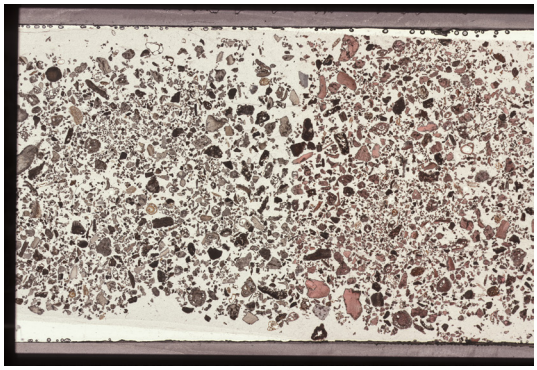

KAL11.tif

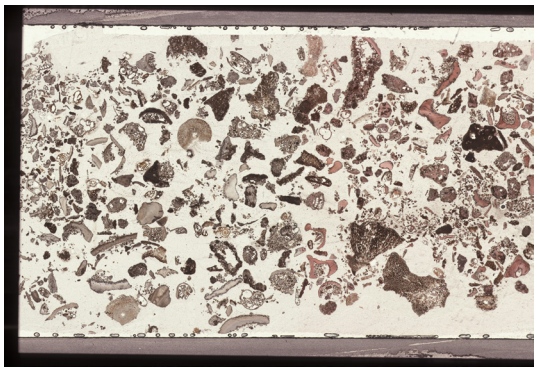

KAL13.tif

KAL15.tif

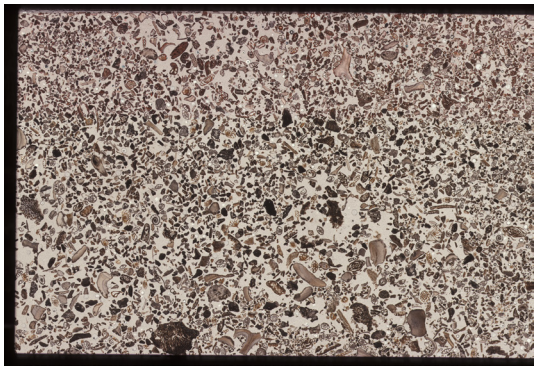

KAL16.tif

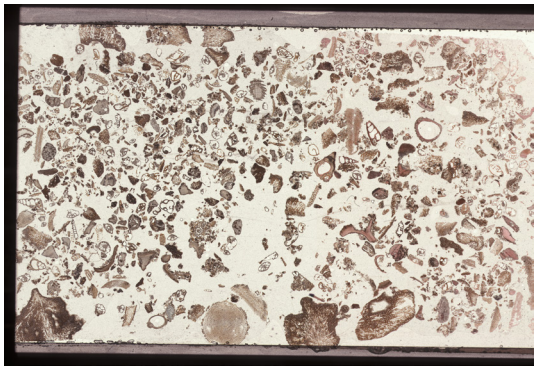

KAL17.tif

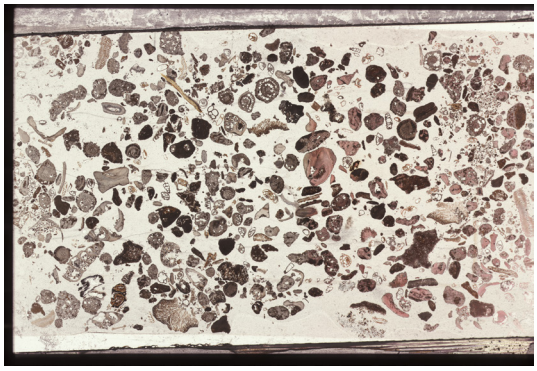

KAL18.tif

KAL19.tif

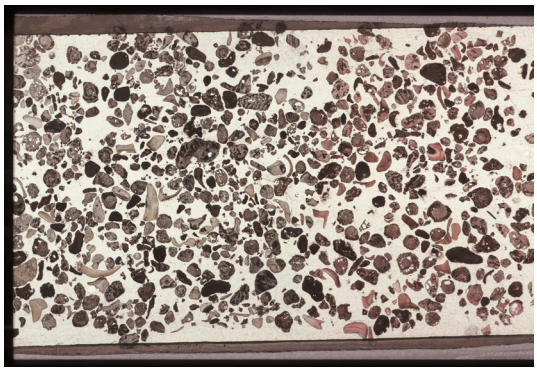

KAL20.tif

KAL21.tif

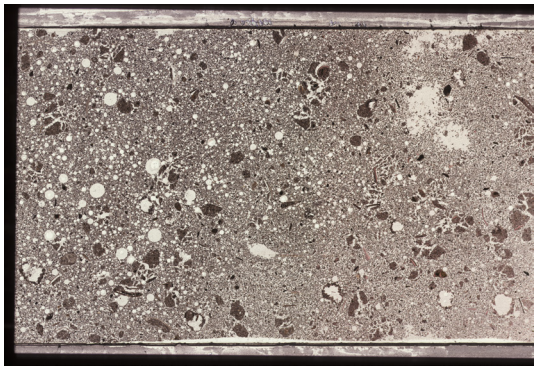

KAL34.tif

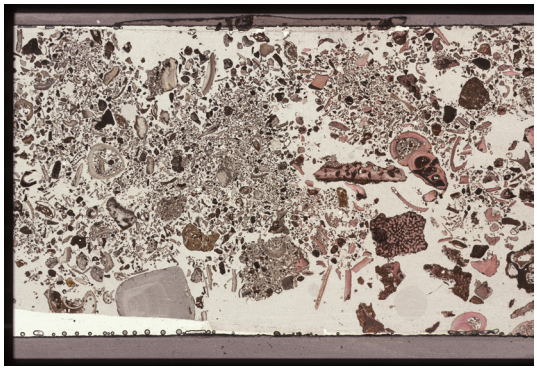

KAL37.tif

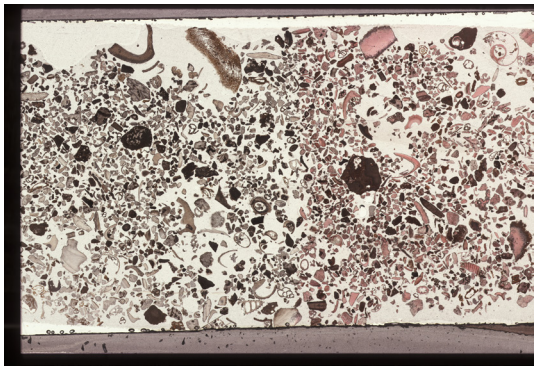

KAL38.tif

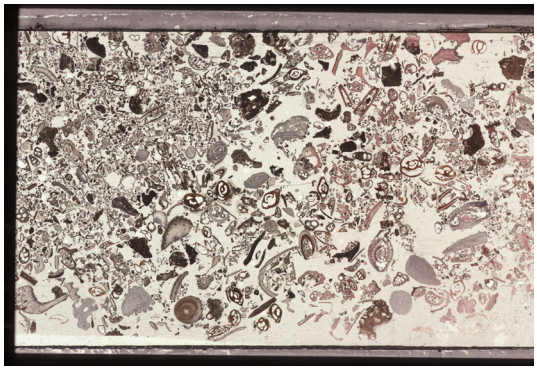

KAL40.tif

KAL41.tif

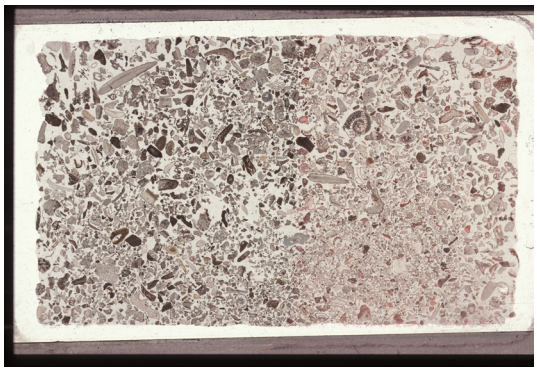

PK5.tif

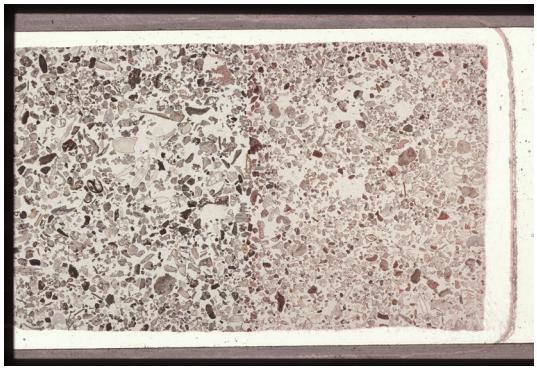

PK10.tif

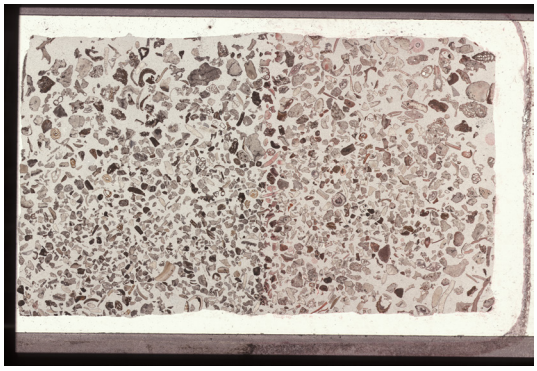

PK11.tif

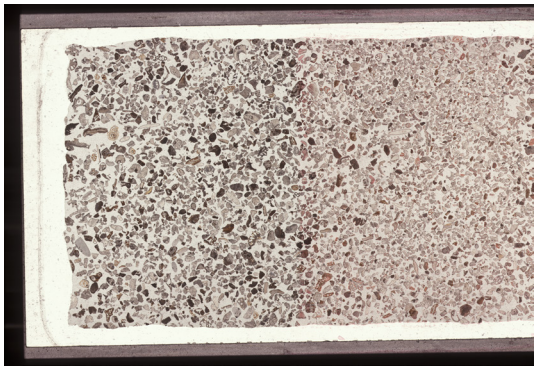

PK12.tif

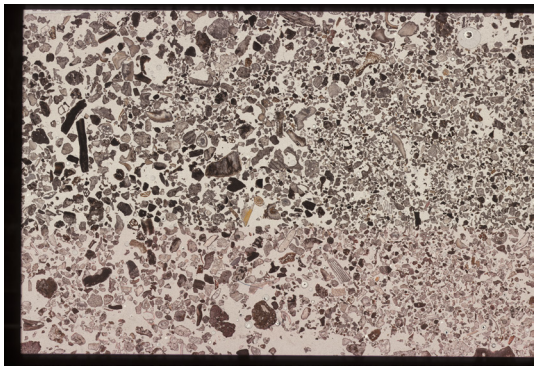

PK13.tif

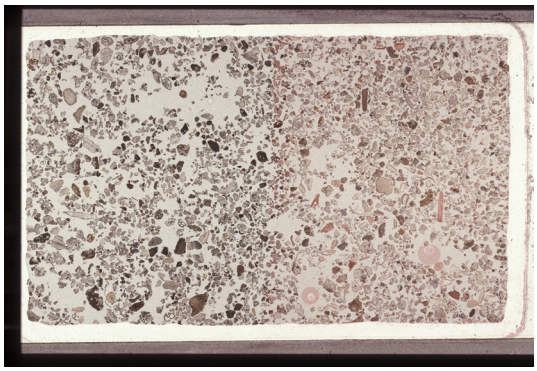

PK14.tif

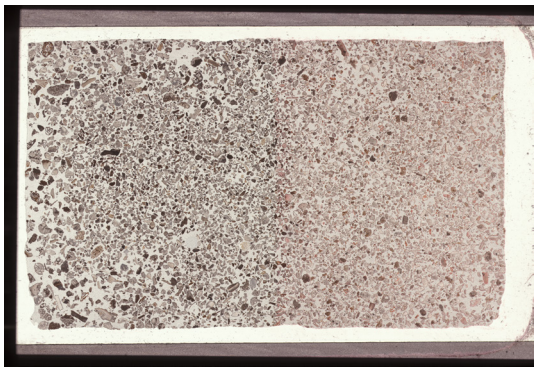

PK15.tif

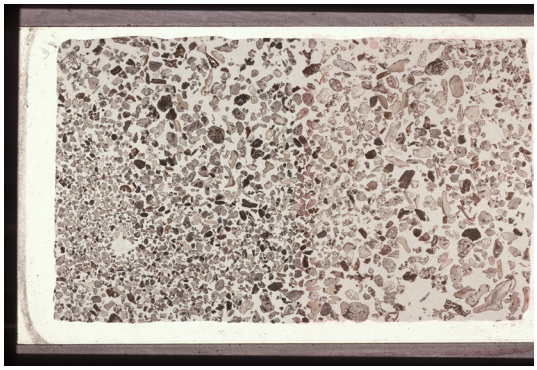

PK16.tif

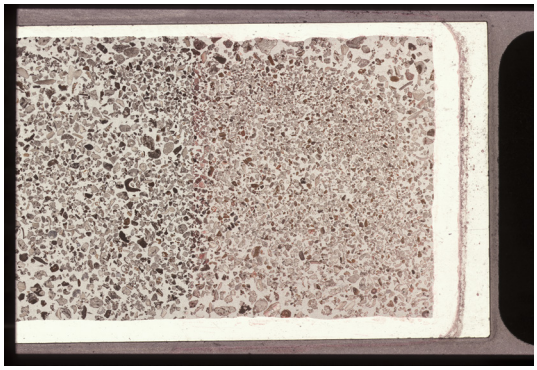

PK17.tif

PK18.tif

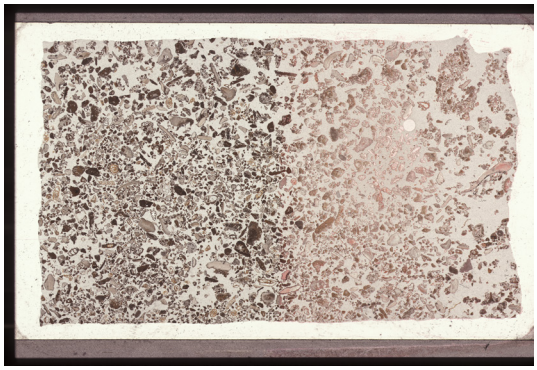

PK19.tif

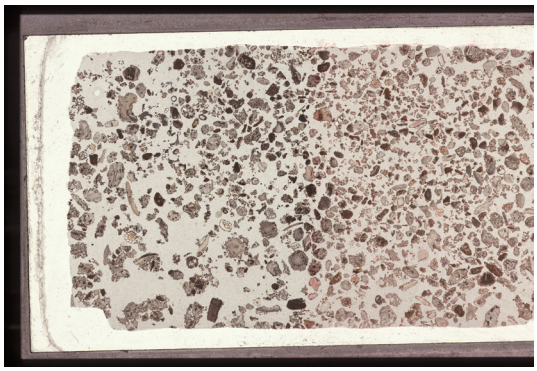

PK20.tif

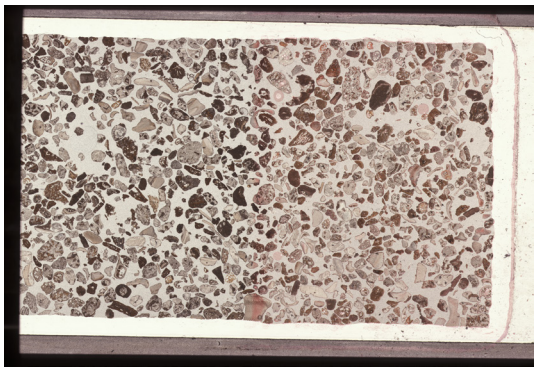

PK21.tif

S2-3 3m.tif

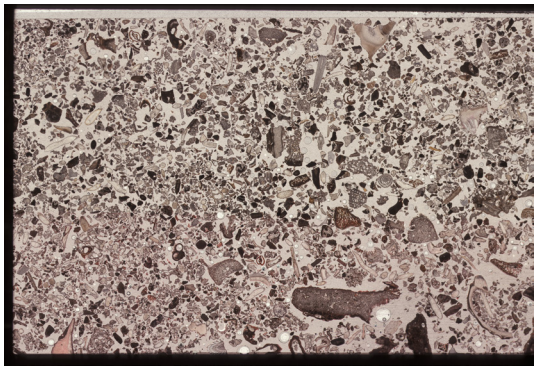

S2-3 5m.tif

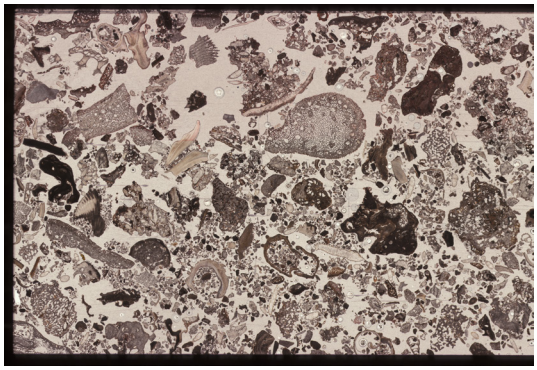

S2-3 8m.tif

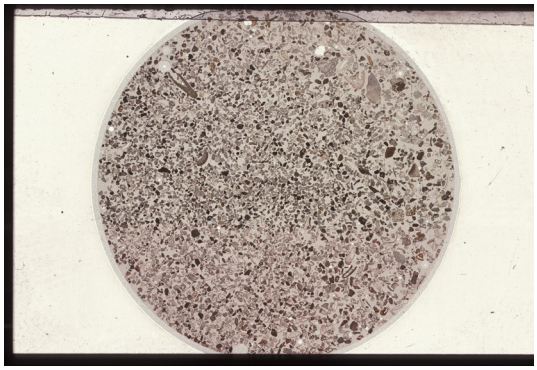

SS1.tif

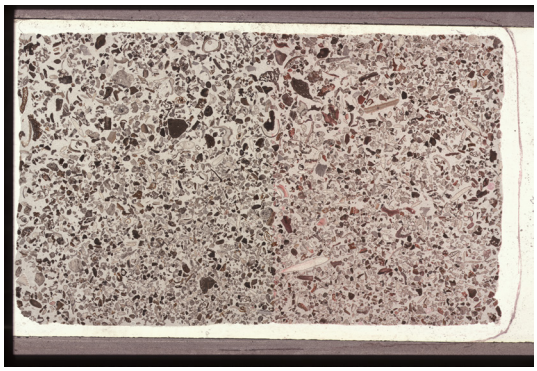

SS2.tif

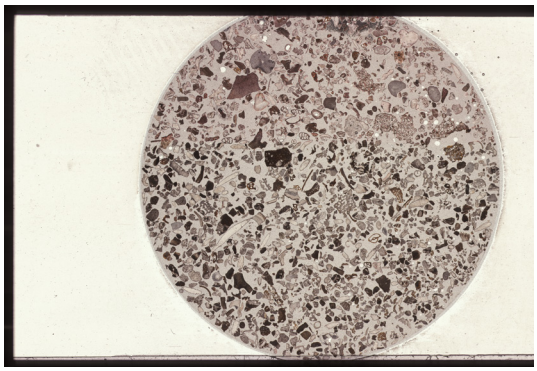

SS3.tif

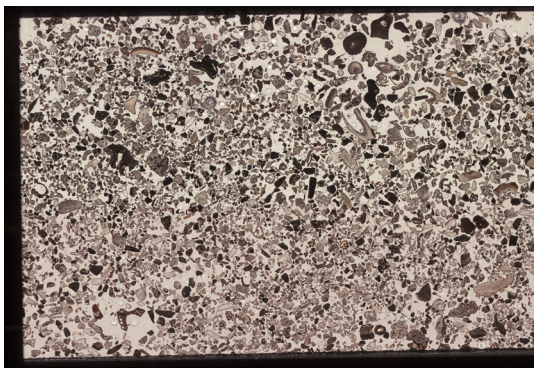

SS4.tif

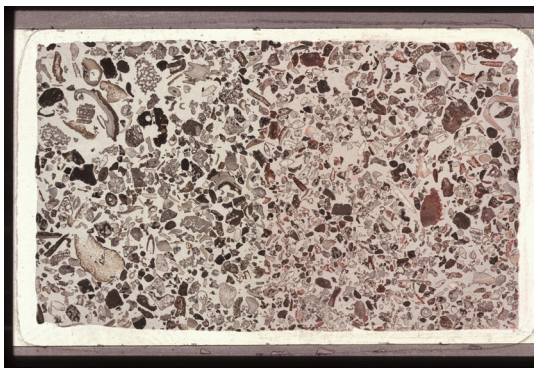

SS5.tif

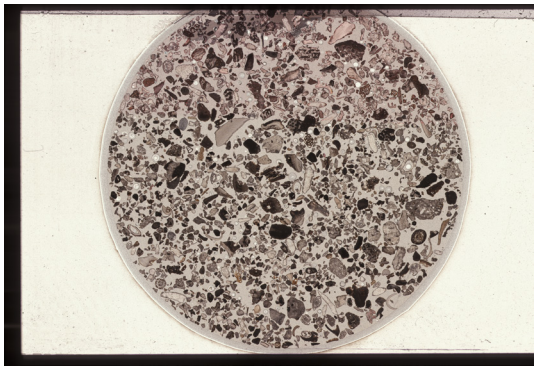

SS6.tif

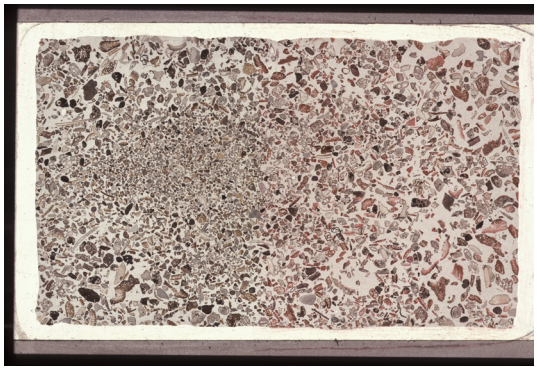

SS7.tif

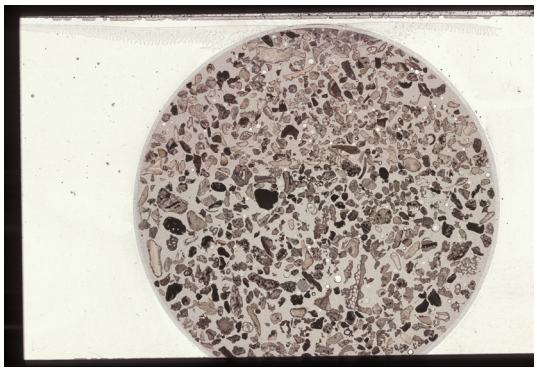

WHB1-2a.tif

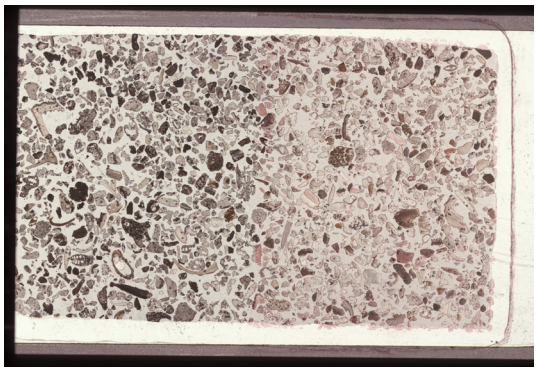

WHB1-2B.tif

WHB3-6.tif

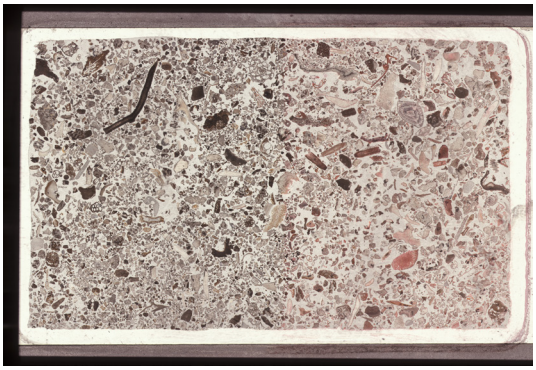

WHB3-7.tif

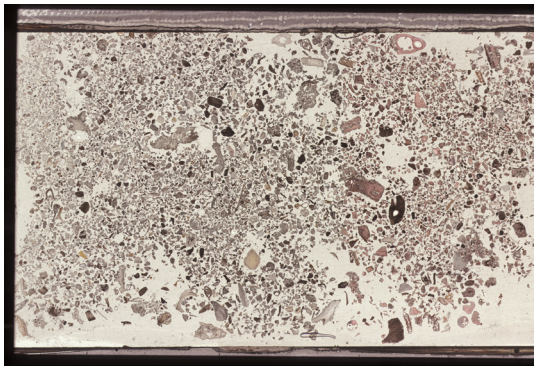

WSUM2.tif

APPENDIX C

PETROGRAPHIC OBSERVATIONS AND PHOTOMICROGRAPHS RELATING TO CHAPTER 3

Appendix C1

Petrographic Observations Relating to Chapter 3

Facies (based on petrology, and outcrop data of Wilson 2005)

Section	Sample	Lithology	Age Notes	Shale-Clay Facies	Silty Sand & Clay Facies	Platy Coral Sheetstone Facies	Clayey Wackestone Facies	Sandy Packstone Facies	Larger Benthic Foraminifera Packstone Facies	Branching Coral Pillarstone Facies	Coral Rud-Floatstone Facies	Coralline Algal & Coral Floatstone Facies	Bioclastic Wacke-Pack-Floatstone Facies	Halimeda & Foraminifera-Coral Wackestone Facie	Head Coral Mix-Domestone Facies
Airputih A	AA04	Dolomitized bioclastic Wackestone											■		
Airputih A	AA08	Coral bioclastic pack/floatstone											■		
Airputih A	AA11	Coral bioclastic pack/floatstone (predominantly coral)				■									
Airputih A	AA13	Larger benthic foraminifera bioclastic packstone									■				
Airputih A	AA16	Branching coral bioclastic pack/floatstone									■				
Airputih A	AA20	Branching coral bioclastic pack/floatstone								■					
Airputih A	AA21a	Branching coral bioclastic pack/float/rudstone										■			
Airputih A	AA24	Platy coral bioclastic pack/float/sheetstone				■									
Airputih A	AA26	Larger benthic foraminifera packstone							■						
Airputih B	AB01	Coral rudstone									■				
Airputih B	AB03	Sandy coral bioclastic rudstone											■		
Airputih B	AB05	Platy coral sheetstone (predominantly coral)				■									
Airputih B	AB07	Coral & coralline algae/encrusting larger foraminifera float/packstone										■			
Airputih B	AB08	Bioclastic wacke/packstone					■								
Airputih B	AB09	Bioclastic wackestone										■			
Airputih B	AB12	Branching coral floatstone								■					
Airputih B	AB13	Coral floatstone													■
Airputih B	AB17	Recrystalised coral bioclastic float/packstone										■			
Airputih B	AB24	Branching coral bioclastic pack/rudstone								■					
Airputih B	AB29	Larger benthic foraminifera packstone							■						
Airputih C	AC03	Coral bioclastic wacke/floatstone											■		
Airputih C	AC04	Bioclastic packstone											■		
Airputih C	AC08	Larger benthic Foraminifera packstone							■						
Airputih D	AD02	Recrystalised coral				■									
Airputih D	AD04	Bioclastic packstone				■									
Airputih D	AD05	Recrystallised massive coral													■
Airputih D	AD08	Recrystallised branching coral float/pillarstone								■					
Airputih D	AD13	Branching coral float/rudstone									■				
Airputih D	AD15	Branching coral rudstone									■				
Airputih E	AE02	Sandy coral bioclastic rudstone									■				
Airputih E	AE05	Recrystallised massive coral bioclastic rud/domestone													■
Airputih E	AE06	Bioclastic packstone									■				
Airputih E	AE08	Branching coral pillar/floatstone								■					
Airputih E	AE09	Coral rudstone									■				
Airputih E	AE11	Coral & coralline algae bioclastic float/packstone										■			
Airputih E	AE13	Larger benthic foraminifera packstone								■					
Airputih F	AF02	Platy coral sheetstone				■									
Airputih F	AF06	Coral floatstone									■				
Airputih F	AF08	Larger benthic foraminifera bioclastic packstone							■						
Airputih F	AF10	Larger benthic foraminifera bioclastic packstone							■						
Airputih G	AG01	Bioclastic wackestone									■				
Airputih G	AG03	Recrystalised coral rud/domestone													■
Airputih G	AG04	Coral bioclastic wacke/floatstone									■				
Airputih G	AG06	Bioclastic wackestone									■				
Airputih H	AH01	Bioclastic packstone											■		
Airputih H	AH02	Branching coral pillar/floatstone								■					
Airputih H	AH03	Branching coral bioclastic pillar/floatstone													■
Airputih H	AH07	Branching coral pillar/rudstone								■					
Airputih H	AH08	Branching coral & coralline algal bioclastic pack/rudstone											■		

Components

Sample	Coral	Mollusc / Shell (G - Gastropod)	Echinoderm	Coralline Algae (Articulating)	Coralline Algae (B - Branching, E - Encrusting)	Green Algae (H - Halimeda, D - Dasycladacean)	Encrusting Foraminifera	Larger Benthic Foraminifera	Lepidocyclinids	Myogypsinids (Mo - Miogypsinoides, Mg - Miogyp	Heterostegnia / Cycloclypeus	Amphistegnia	Imperforate Foraminifera (Larger Benthic)	Imperforate Foraminifera (Miliolids)	Small Benthic Foraminifera (Rotallids)	Planktonic Foraminifera	Bryozoa	Peloids (Commonly Micritized Coralline Algae)	Lithified Carbonate Clasts	Other Lithic Clasts	Siliciclastics (* - Clay Shrinkage Features)	Dolomite	Calcite Cement	Micrite	Phosphate/Iron	Porosity
AA04		P	R					P				P			R						P	A	C	P		R
AA08	A	PG	R		CE	RH	P	R							R	P					C		A	C		P
AA11	A	P		P			R	P	P	P					R						A		A	C		P
AA13	C		P		CE	PH	R	A	C	R				R	P						C		C	C		P
AA16	C	R	R		C	CH	C	P		P					R		R				C		C	A		C
AA20	A	R	R		C		C								P						C		A	C		P
AA21a	A	P	R		C	P	C		R					R	R						P	R	A	C		P
AA24	A	PG	P		C		P	P	R	PMg					R						C	P	A	A		P
AA26	R	PG	P		CE	PH	P	A	C	CMg		P			R		R				A	P	P	P		P
AB01	A	R			PE		C														C	A	A	P		C
AB03	A				CE		C	P		PMg					P	R					C		A	C		P
AB05	A							R		RMg											C		A	R		P
AB07	A	PG	R		AE		A	R		RMg					P	R		P			C		A	C		P
AB08	R	P	P		CBE		R	C	P	PMg		R			P	P		P			R		C	C		R
AB09		C	P			PH	P	P		PMg		P			P	P					P		A	P		R
AB12	C	R			P										P						P		A	P		P
AB13	A					CH	P								P						C		A	A		P
AB17	A		P					R				R			P						A		A	P		C
AB24	A	P	R				R	C		CMg					P	R					C	P	A	C		R
AB29		R	P				P	A	A	CMo	P	P			P	R	P				C		P	C		P
AC03	A	R			CE			R				R			P	R					C		C	C		P
AC04	P	P			CE		P	C	C	PMoMg		P			P	R	R	P			A		C	A		P
AC08	C	R	R		PE		P	A	P	AMg						T		R			A		C	P		C
AD02	A																				P		A	P		R
AD04	P	P	P		CE	RH	P	A	P	CMg	P	R				R		R			A	C	C	P		R
AD05	D				PE																P		A	C		P
AD08	D	P			PE		P	R				R						P			P		A	C		C
AD13	A	PG			CE		P	R				R				R		R			C		A	P		P
AD15	A	RG	R		PE		C	R				R			T	T					C		A	P		C
AE02	A		R		CE		C	C		CMg					P			P			A		A	P		P
AE05	D	R			CE		C											P			P*		A	C		P
AE06		C	R		RE		R	R				R			C	P					P		A	P		R
AE08	A	R	R		RE		R			RMg						T							A	C		P
AE09	A	R	P		PE	PH	C								P	R		P			P		A	A		P
AE11	A	R	R		CE		P	R		RMg					R	R		R			R		A	P		P
AE13							R	A	C	PMg	C	C				R	R				A		P	P		C
AF02	C		P		C	PH	P	R	R					R	R	R					C		C	A		C
AF06	A	P	R		P	RH		P	P					C	P	R					A	A	A	C		P
AF08	C	R	P		CE	RH	R	C	P	CMg		P		P	P	P		R			A		C	C		P
AF10	P	P	P		PE	PH		C	P	CMg				P	R	R					C		A	A		C
AG01		R	P		PE	RH	C	C		PMg		P			P	P		P			C	A	A	C		P
AG03	A	R	P		PE		C	R				R			R			R			C		A	C		R
AG04	C	P	P				R	P		PMg		P			R	R		P			C		A	P		P
AG06	P		C		RE		P	P		RMg		P		T	R			R			A		P	A		P
AH01	C	C	P		PE		R	P		RMg	P	P		R	R	R		R			P		C	A		R
AH02	C	P			CE	RH		R				R		R	R	R		R			C	A	C	P		P
AH03	C	P			CE		P	R			R			R	R						A		C	A		P
AH07	A	PG	P		CE		C	R		RMg		R			P						C		A	A		P
AH08	C	PG			CE	RH	C	C		CMg	R				P						C		A	C		P

Reservoir Quality

Sample	Fragmentation / Abrasion	Encrustation	Bioerosion	Grain Size	Sorting (U - Unimodal, B - Bimodal, T - Trimodal)	Fabric (A - Alignment, CE - Compaction Enhanced)	Low	Moderate	Good	Excellent	Visible Porosity (Based On Petrographic & Hand Specimin Observations)		C- Connected, PC - Partially Connected, NC - Non	Micropores	Rounded	Irregular (Often Intergranular)	Linear (Includes Fractures)	Porosity Type
AA04	0 or 1	0	1 or 2	C > f	m > w (B)		■				Minor	<1%	NC	<1%				Matrix microporosity,
AA08	2 or 3	2 or 3	1 or 2	C > c	p > m (T)		■				Minor	<2%	NC	<1%		<100 µm <1 %		Matrix microporosity, interparticle
AA11	0 or 1	0 or 1	0 or 1	C > f	m > p (T)		■				Minor	<5%	NC	<1%		<750 µm <5 %		Matrix microporosity, intercrystalline
AA13	0 or 1	0 or 1	0 or 1	c > G	m > p (B)		■				Minor	5%	NC	<1%		<200 µm <4 %	<1 mm <1 %	Matrix microporosity, interparticle & fracture
AA16	1 or 2	1 or 2	0 or 1	C > G	m > w (B)			■			Moderate (some artefact)	10%	PC	<2 %		<200 µm <3%	<5 mm <4 %	Matrix microporosity, intercrystalline, solution enhanced fracture
AA20	1 or 2	1 or 2	0 or 1	C > G	m > p (T)		■				Minor	5%	NC	<1 %		<200 µm <5 %		Matrix microporosity, intercrystalline, intraparticle, solution enhanced interparticle
AA21a	0 or 1	1 or 2	0 or 1	C > c	m > w (B)		■				Minor	<5%	PC	<1 %	<2 % <100 µm	<4 % <1 mm	<2 % <1 mm	Matrix microporosity, interparticle, intercrystalline, fracture porosity
AA24	0 or 1	2 or 3	0 or 1	C > G	m > w (B)		■				Minor	2%	NC	<1 %		<2 % <100 µm		Matrix microporoisty, interparticle
AA26	1 or 2	0 or 1	0 or 1	C > G	m > w (B)	ACE	■				Minor	5%	NC	<1 %		<2 % <1 mm	<2 % <1 mm	Matrix microporosity, interpartice, fracture porosity
AB01	0 or 1	1 or 2	0 or 1	C > G	m > w (T)			■			Moderate (some artefact)	<15%	PC	<2%	<5% <1 mm	<8% <1mm	<2% <750 µm	Matrix microporosity, solution enhanced intercrystalline, fracture porosity
AB03	0 or 1	1 or 2	0 or 1	C > G	p (B)		■				Minor	5%	NC	<1%		<3% <500µm	<1% <750µm	Matrix microporosity, solution enhanced intercrystalline, fracture porosity
AB05	0	0	0 or 1	f > c	w > m (U)		■				Minor	<2%	NC			<2% <500µm		Interparticle
AB07	2 or 3	3	0 or 1	f > G	p (B)	ACE	■				Minor	<2%	C				<2% <4 mm	Fracture/Channel pososity
AB08	1 or 2	1 or 2	0 or 1	f > G	m > w (B)		■				Minor	1%	NC	1%				Matrix microporosity
AB09	0 or 1	0 or 1	0 or 1	f > G	w > m (B)		■				Minor	1%	NC	1%				Matrix microporosity
AB12	0 or 1	0	0	f > c	w (U)		■				Minor	<5%	PC			<2 mm <5%	<3 mm <2%	intercrystalline vuggy, solution enhanced fracture porosity
AB13	0 or 1	0 or 1	0	C > c	m > w (B)		■				Minor	5%	PC				<5% <2 mm	Solution enhanced fracture porosity
AB17	0 or 1	0	0	f > c	w (U)			■			Moderate (some artefact)	15%	PC	<1%		<1.5 mm <13 %	<1 mm <2%	Matrix microporosity, intercrystalline vuggy porosity, solution enhanced fracture porosity
AB24	1 or 2	0 or 1	0 or 1	f > P	m > p (B)	ACE	■				Minor	<1%	NC	<1%				Matrix microporosity
AB29	2 or 3	1 or 2	0 or 1	C > G	p (B)		■				Minor	5%	NC			<500 µm <3%	<1 mm <2%	Intercrystalline porosity, fracture porosity
AC03	1 or 2	2 or 3	0 or 1	C >c	m > w (B)		■				Minor	5%	PC	<1%		<250 µm <5%		Matrix microporosity, intercrystalline porosity
AC04	2	1 or 2	0 or 1	C > G	m > p (T)		■				Minor	5%	NC	<1%		<750 µm <4%	<250 µm <1%	Matrix microporosity, intraparticle, interparticle
AC08	1 or 2	1 or 2	0 or 1	C > G	p (T)			■			Moderate (some artefact)	15%	PC	<1%	<1 mm <5%	< 2 mm <10%		Matrix microporosity, solution enhanced intercrystalline, minor vuggy porosity
AD02	0 or 1	0	0	f > c	w (U)		■				Minor	<1%	NC	<1%				Matrix microporosity
AD04	2 or 3	1 or 2	0 or 1	C > G	m > p (B)		■				Minor	<1%	NC	<1%				Matrix Microporosity
AD05	0 or 1	0 or 1	0	C > G	m > w (B)		■				Minor	5%	NC			<500 µm 5%		Solution enhanced intercrystalline porosity
AD08	1 or 2	0 or 1	0	C > G	m > w (B)		■				Moderate	10%	NC			<500 µm 10%		Interparticle, solution enhanced intraparticle and intercrystalline porosity
AD13	2 or 3	2 or3	0 or 1	f > G	m > p (T)		■				Minor	5%	NC			<500 µm <5%	<1 mm <1%	Solution enhanced intercrystalline and fracture porosity
AD15	1 or 2	2 or 3	0 or 1	C > G	m > p (T)		■				Moderate (some artefact)	<8%	NC			<1 mm <5%	<1 mm <5%	Solution enhanced intercrystalline and fracture
AE02	1 or 2	2 or 3	0 or 1	C > G	m > p (B)		■				Minor	5%	NC		<100 µm <2%	<500 µm <3%		Interparticle, intercrystalline
AE05	1 or 2	2 or 3	0 or 1	C > G	m > w (B)		■				Minor	5%	NC	<1%		<250 µm <2%	<2 mm <2%	Matrix microporosity, intercrystalline and fracture porosity
AE06	2 or 3	0 or 1	0 or 1	C > c	m > w (B)		■				Minor	<1%	NC	<1%				Matrix microporosity
AE08	0 or 1	0 or 1	0 or 1	C > P	m > w (B)		■				Minor	5%	NC	<3%		<1 mm <2%		Matrix microporosity, intercrystalline
AE09	0 or 1	2 or 3	0 or 1	C > P	m > w (B)		■				Minor	<2%	NC	<1%		<100 µm <2%		Matrix microporosity, intraparticle, intercrystalline
AE11	1 or 2	2 or 3	0 or 1	C > G	m > w (B)		■				Minor	5%	NC	<1%		<750 µm <2%	<750 µm <2%	Matrix microporosity, intercrystalline and fracture
AE13	2 or 3	0 or 1	1 or 2	C > G	p (B)			■			Moderate (some artefact)	15%	C			<1 mm <15%		Intraparticle, interparticle, shelter
AF02	0 or 1	1 or 2	0 or 1	C > c	w > m (B)			■			Moderate	<6%	PC	<1%		<500 µm <6%		Matrix microporosity, interparticle, solution enhanced intercrystalline
AF06	0 or 1	0 or 1	0 or 1	C > G	m > w (B)		■				Minor	5%	NC	<1%		<250 µm <5%		Matrix microporosity, intercrystalline
AF08	2 or 3	1 or 2	0 or 1	C > G	m > p (B)		■				Minor	5%	NC			<200 µm <3%	<5 mm <2%	intercrystalline and fracture
AF10	1 or 2	1 or 2	0 or 1	C > c	m > p (B)			■			Moderate (some artefact)	<10%	PC	<1%		<2 mm <8%	<1 mm <1%	Matrix microporosity, intercrystalline and fracture
AG01	1 or 2	1 or 2	0 or 1	C > G	m > w (T)		■				Minor	<2%	NC	<1%		<100 µm <1%		Matrix microporosity, intercrystalline
AG03	1 or 2	2 or 3	1 or 2	C > c	m > w (B)		■				Minor	<1%	NC	<1%		<100 µm <1%		Matrix microporosity, intercrytalline
AG04	2 or 3	0 or 1	0 or 1	C > G	m > p (T)		■				Minor	5%	NC	<1%		<200 µm <3%	<500 µm <2%	Matrix microporosity, intercrystalline and fracture
AG06	2 or 3	1 or 2	0 or 1	C > G	m > w (B)		■				Minor	<2%	NC	<1%		<100 µm <1%		Matrix microporosity, intercrystalline
AH01	2 or 3	1 or 2	0 or 1	C > c	w > m (B)		■				Minor	<1%	NC	<1%				Matrix microporosity
AH02	2 or 3	2 or 3	1 or 2	C > G	m > w (B)		■				Minor	<2%	NC	<1%		<100 µm <1%		Matrix microporosity, intercrystalline
AH03	2 or 3	2 or 3	1 or 2	C > G	m > w (B)		■				Minor	<2%	NC	<1%		<100 µm <1%		Matrix microporosity, intercrystalline
AH07	2 or 3	2 or 3	1 or 2	C > P	m > p (B)		■				Minor	<4%	C	<1%		<200 µm <1%	<2 mm <4%	Matrix microporosity, intercrystalline, fracture
AH08	2 or 3	2 or 3	1 or 2	C > P	p > m (B)		■				Minor	5%	NC	<1%		<300 µm <1%	<2 mm <3%	Matrix microporosity, intercrystalline, solution enhanced fracture

Sample	1 Micritization	Isopachous Fringing Cements (SB - Selected Bioclasts, F - Ferroan, X - Non Ferroan)	Non Continuous Fractures, Silt Infiltration	2 Cone In Cone Calcite (F - Ferroan, X - Non Ferroan)	3 Granular Mosaic Neomorphic Calcite (D - Drusy, F - Ferroan, X - Non Ferroan)	4 Mechanical Compaction / Fracturing	5 Blocky/Equant Calcite (D - Drusy, F - Ferroan, X - Non Ferroan)	6 Mechanical Compaction / Fracturing	Syntaxial Overgrowths	7 Mechanical Compaction / Fracturing	8 Blocky/Equant Calcite (D - Drusy, F - Ferroan, X - Non Ferroan)	Compaction (Mostly Mechanical)	(9) Fracturing	10 Chemical Compaction Suturing	10 Dissolution Seams	11 Dolomite (M - Microdolomite Rhombs, R - Replacive)
AA04	1				2FX	3	4F							5		6MR
AA08	1				2X	3	4X								5	
AA11	1				2X					3	4(F)X				5	
AA13	1				2X	3	4X									
AA16	1				2X	3			4	5	6X				7	
AA20	1				2X			3			4(F)X				6	
AA21a	1			2X	3X	4	5X			6	7FX			8		9MR
AA24	1				2X	3	4F			5	6X				7	7MR
AA26	1				2F(X)	3	4F						5	6	6	7MR
AB01	1			2X	3X			4		5					6	7MR
AB03	1				2X	3	4(F)X						5	6	6	
AB05	1				2(F)X			3			4X				5	
AB07	1				2X	4	4FX							5	5	
AB08	1				2X	3	4X							5	5	
AB09	1						2(F)X	3						4		
AB12	1				2X	3	4X								5	
AB13	1				2X	3	4(F)X							5		
AB17	1				2X		3(F)X		4	5					6	
AB24	1				2X	3	4X							5	5	6MR
AB29	1				2F(X)	3	4F		5	6	7FX				8	
AC03	1				2X			3		4	5X	6			7	
AC04	1				2X	3	4FX		5	6					7	
AC08	1			2X	2X			3			4(F)X				5	
AD02	1				2(F)	3	4X			5	6(F)X				7	
AD04	1				2X				3	4	5X				6	7MR
AD05	1				2X		3FX									
AD08	1				2X					3	4FX				5	
AD13	1	2SBX			3X			4			5(F)X				6	
AD15	1			2X	3X		4(F)X	5			6X				7	
AE02	1				2X			3			4FX		5	6	6	
AE05	1				2X	3	4FX			5					6	
AE06	1				2X	3	4X							5		
AE08	1				2X	3	4(F)X				5X				6	
AE09	1				2X			3			4X				5	
AE11	1				2X			3			4F(X)		5		6	
AE13	1				2X			3		4	5X		6		7	
AF02	1				2X			3			4X				5	
AF06	1				2X			3			4FX		5		6	7MR
AF08	1				2FX	3	4FX								5	
AF10	1				2X			3			4FX				5	
AG01	1				2X			3			4X				5	6MR
AG03	1				2X	3	4FX			5	6X				7	
AG04	1				2X	3	4FX			5	6X				7	
AG06	1				2X	3	4X			5	6X				7	
AH01	1				2X	3				4	5(F)X				6	
AH02	1				2X			3		4	5X				6	7MR
AH03	1				2X	3				4	5(F)X				6	
AH07	1				2X	3	4F			5	6X				7	
AH08	1				2X			3		4	5(F)X				6	

Airputih H	AH09	Coral bioclastic rudstone
Airputih K	AK03	Platy coral sheetstone
Airputih K	AK07	Coral bioclastic rudstone
Airputih K	AK09	Sandy coral bioclastic packstone
Airputih K	AK11	Bioclastic packstone
Airputih K	AK12	Coral bioclastic wacke/pack/floatstone
Airputih L	AL02	Platy coral sheetstone
Airputih L	AL03	Platy coral sheetstone
Dibelakan Parliament	DPR02	Platy coral sheetstone
Dibelakan Parliament	DPR04	Dolomitized, coral & Halimeda domestone/packstone
Dibelakan Parliament	DPR05	Foraminiferal & Coralline Algal floatstone/packstone
Dibelakan Parliament	DPR09	Sandy, Coral & Coralline Algal pillarstone/packstone
Dibelakan Parliament	DPR10	Sandy, foraminiferal & coralline algal floatstone/packstone
Kota Bangun	KB01	Coral bioclastic sheetstone/packstone
Kota Bangun	KB02	Foraminiferal, Coralline Algal floatstone/wackestone
Kota Bangun	KB03	Coral, Foraminiferal floatstone/wackestone
Kota Bangun	KB05	Coralline algal bioclastic floatstone/wackestone
Kota Bangun	KB07	Foraminiferal Mudstone
Kota Bangun	KB08	Coralline bioclastic floatstone/packstone
Kota Bangun	KB09	Coraline algal bioclastic floatstone/packstone
Kota Bangun	KB10	Coralline & coralline algal domestone/packstone
Kota Bangun	KB11	Coral,bioclastic floatstone/wackestone
Kota Bangun	KB12	Coral bioclastic rudstone/packstone
Permasip A	PA01	Coral domestone/wackestone
Permasip A	PA02	Coral bioclastic floatstone/wackestone
Permasip A	PA04	Coral & Foraminiferal floatstone/grainstone
Permasip A	PA05	Sandy, bioclastic mudstone
Permasip A	PA07	Sandy coralline algal & foraminiferal floatstone/bindstone/packstone
Permasip B	PB02	Foraminiferal & Halimeda floatstone/wackestone
Permasip C	PC04	Coral, coralline algal & foraminiferal floatstone/wackestone
Permasip C	PC06	Sandy, foraminiferal & coralline algal floatstone/packstone
Permasip C	PC08	Dolomitized, coralline algal & foraminiferal floatstone/rudstone/grainstone
Permasip C	PC09	Coral, bioclastic domestone/grainstone
Permasip C	PC11	Coralline algal floattone/bindstone/mudstone
Permasip C	PC16	Coral bioclastic floatstone/packstone
Permasip C	PC17	Bioclastic floatstone/rudstone/packstone
Permasip C	PC18	Coral bioclastic floatstone/packstone
Permasip D	PD01	Coralline algal bioclastic floatstone/wackestone
Permasip D	PD04	Sandy, coral bioclastic pillarstone/rudstone/grainstone
Permasip D	PD05	Sandy, foraminiferal bioclastic grainstone
Permasip D	PD06	Sandy, foraminiferal bioclastic wackestone
Permasip D	PD08	Foraminiferal bioclastic mudstone
Permasip E	PE02	Coral, (crystalline carbonate) pillarstone
Permasip E	PE04	Coral bioclastic sheetstone/packstone
Permasip E	PE06	Dolomitized, coral pillarstone/grainstone
Permasip E	PE07	Coralline bioclastic bindstone/rudstone/grainstone
Badak	BA01	Coral bioclastic sheetstone/grainstone
Badak	BA03	Sandy, coral bioclastic sheetstone/grainstone
Bontang	BB02	Coral bioclastic sheetstone/wackestone
Bontang	BB03	Coral bioclastic sheetstone/packstone
Bontang	BB04	Coral bindstone/sheetstone/grainstone
Bontang	BB05	Coral bioclastic sheetstone/packstone
Bontang	BB06	Sandy, coral, bioclastic sheetstone/bindstone/grainstone
Bontang	BB09	Sandy, coral bioclastic floatstone/grainstone
Bontang	BB11	Foraminiferal & Halimeda bioclastic packstone
Bontang	BB13	Coral & foraminiferal bioclastic floatstone/grainstone
Bontang	BB14	Coral bioclastic floatstone/sheetstone/wackestone
Senoni A	SA02	Sandy, Coral, bioclastic sheetstone/wackestone
Senoni A	SA03	Coral sheetstone/grainstone
Senoni A	SA04	Coral bioclastic floatstone/sheetstone/wackestone
Senoni A	SA06b	Bioclastic floatstone/wackestone

Senoni B	SB04	Sandy, coral bioclastic sheetstone/packstone	C	R	R	CBI	RH		P	P	PMg		R	R	R		A	A	P	P	2 or 3	1 or 2	1 or 2	C > G	p > m (T)		Minor	<2%	NC		<150 µm <2%		Intercrystalline	1	2	3X	4	5X		6	7X			8
Senoni B	SB05	Coral bioclastic sheetstone/pillarstone/packstone	D	R		PBI	RH		C	C		P	R	R	R		C	A	P	P	1 or 2	1 or 2	1 or 2	C > G	m > p (T)		Minor	<2%	NC	<1%	<200 µm <1%		Matrix microporosity, intercrystalline	1		2X			3		4(F)X			6
Senoni B	SB10	Sandy, foraminiferal bioclastic floatstone/rudstone/packstone		R	P	CBE			A	C	PMg		C	R	T	P	A	A	A	P	2 or 3	2 or 3	1 or 2	C > G	p > m (T)		Minor	<5%	NC	<1%	<200 µm <2%	<2 mm <1%	Matrix microporosity, intercrystalline, fracture	1		2X			3		4X	5	6	6
Senoni B	SB11	Sandy, coralline bioclastic floatstone/rudstone/packstone	A		R	PB	RH	P	P		PMo		P	P	R		A	A	A	P	1 or 2	1 or 2	1 or 2	C > G	m > p (T)		Minor	<5%	NC	<1%	<1 mm <4%		Matrix microporosity, intercrystalline	1		2X			3		4X	5		6
Senoni C	SC01	Sandy, coral bioclastic sheetsone/packstone	A		P	PE	RH		P	P		P		R	R		A	C	C	C	1 or 2	1 or 2	1 or 2	C > P	m > w (T)	ACE	Moderate (Artefact)	<15%	C	<1%	<200 µm <10%	<10 mm <5%	Matrix microporosity, solution enhanced intercrystalline/channel porosity	1		2X			3		4F(X)	5		6
Senoni C	SC02	Coral bioclastic sheetstone/packstone	D	R		PE	PH	P	C	P	PMg	R	R	R		R	C	A	A	P	1 or 2	0 or 1	1 or 2	C > c	p > m (B)		Moderate (Artefact)	<10%	C	<1%	<2000 µm <10%		Matrix microporosity, channel porosity	1		2(F)X			3		4F(X)	5		6
Senoni C	SC04	Bioclastic wackestone/packstone	P	C		R	PH	P	C	P	RMg		R	R	R		P	A	P	P	2 or 3	1 or 2	1 or 2	C > c	m > w (B)		Minor (Artefact)	<5%	PC		<250 µm <5%		Intercrystaline porosity	1		2X			3		4X			5

Abbreviation	(% of total volume)
T	0-0.1%
R	0.1-1%
P	1-5%
C	5-25%
A	25-50%
D	>50%

Appendix C2

Thin Section Photomicrographs of Samples Relating to Chapter 3

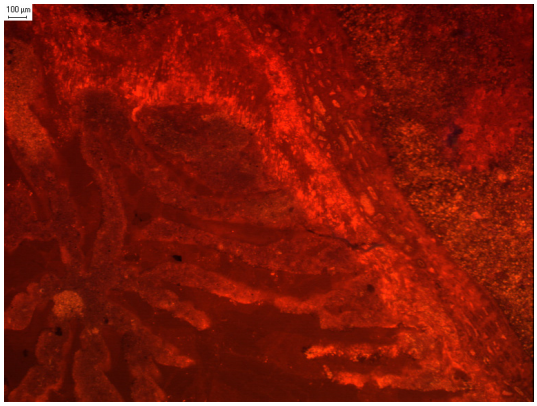

aa16a4c.TIF

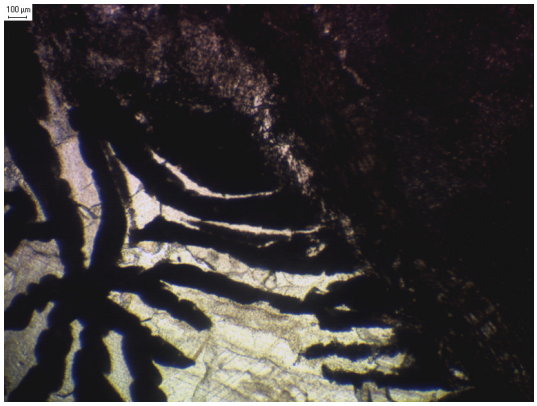

aa16a4p.TIF

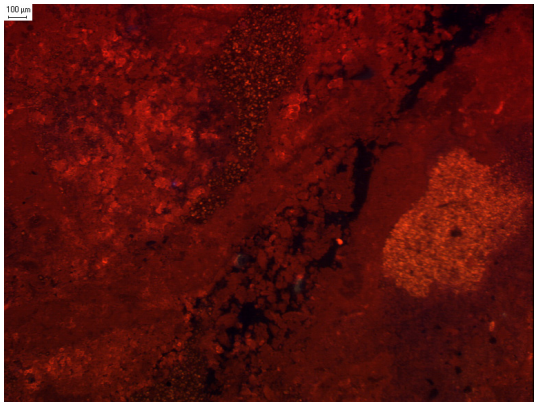

aa16b4c.TIF

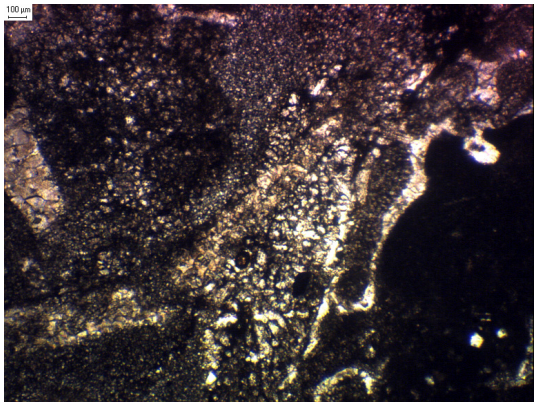

aa16b4p.TIF

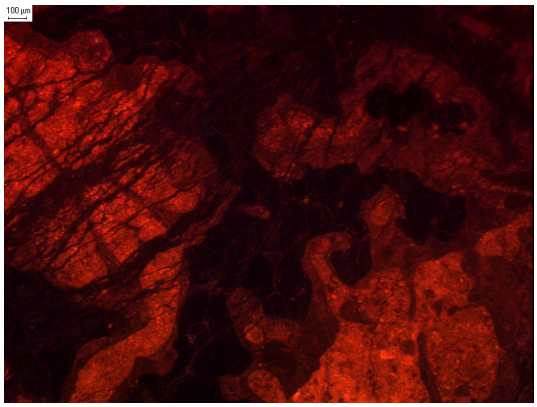

aa21aa4c.TIF

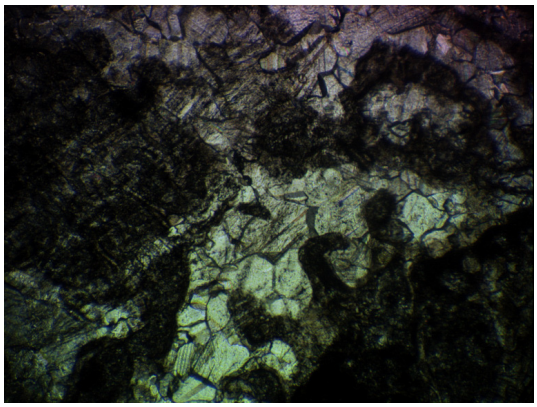

aa21aa4p.TIF

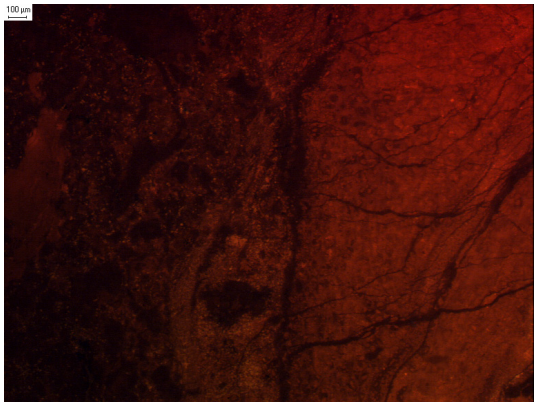

aa21ab4c.TIF

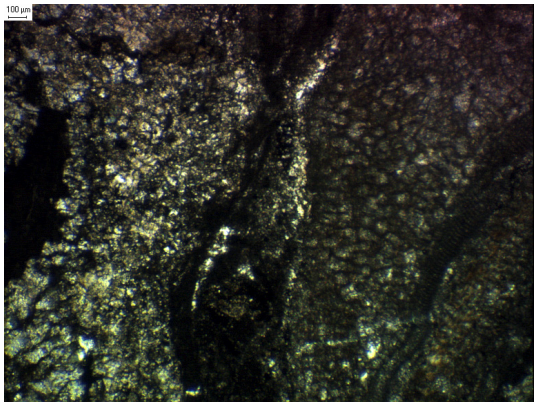

aa21ab4p.TIF

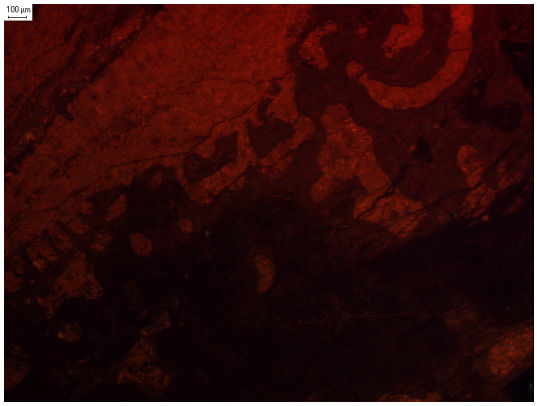

aa21ac4c.TIF

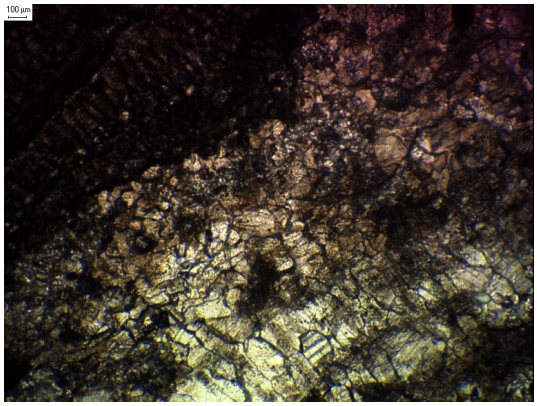

aa21ac4p.TIF

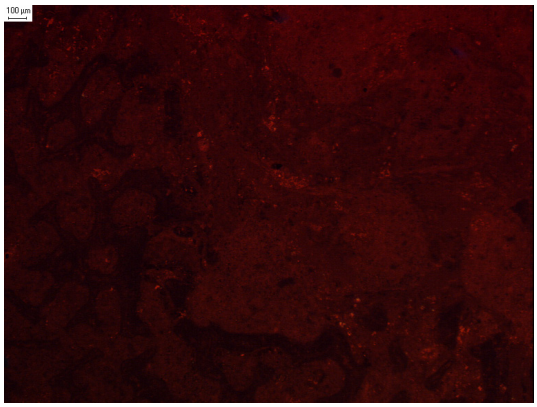

aa24a4c.TIF

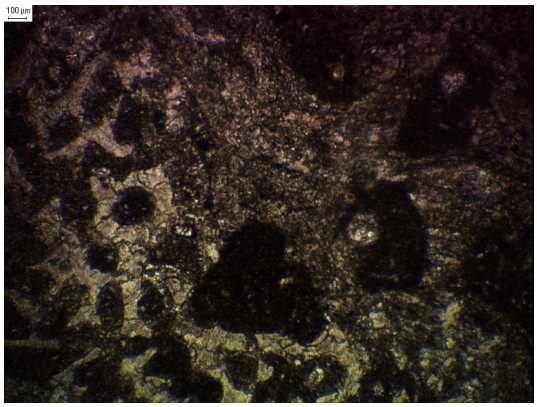

aa24a4p.TIF

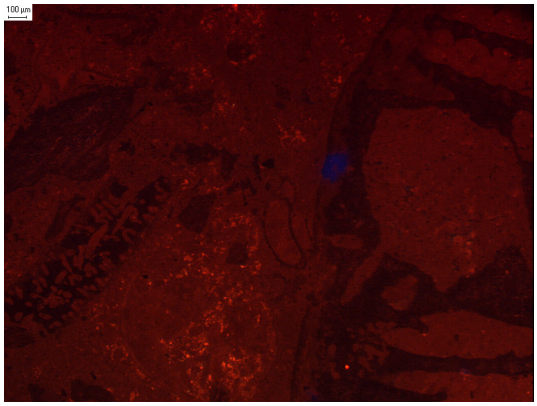

aa24b4c.TIF

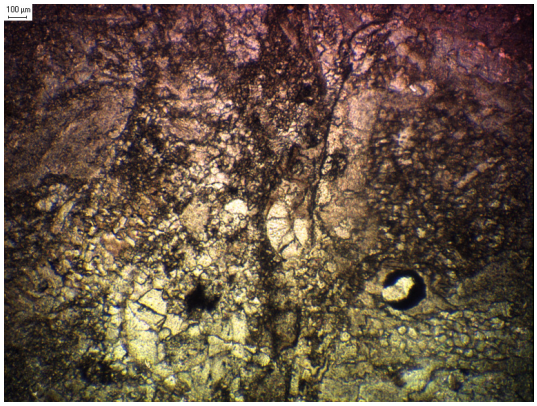

aa24b4p.TIF

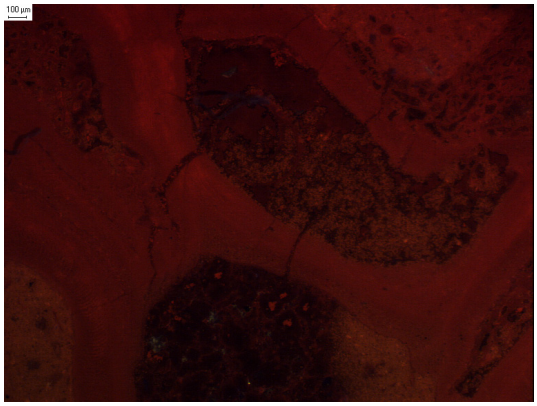

ab7a4c.TIF

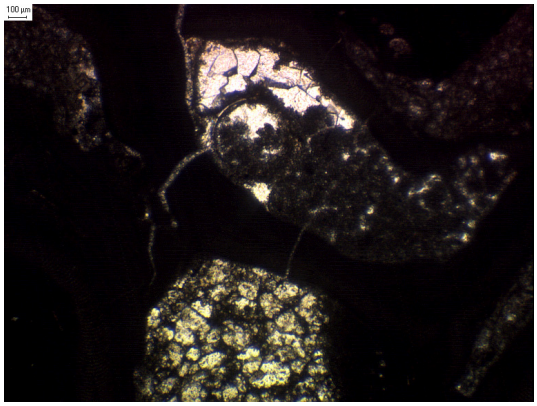

ab7a4p.TIF

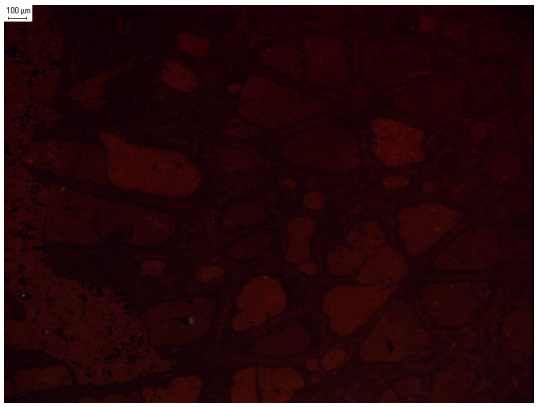

ab24a4c.TIF

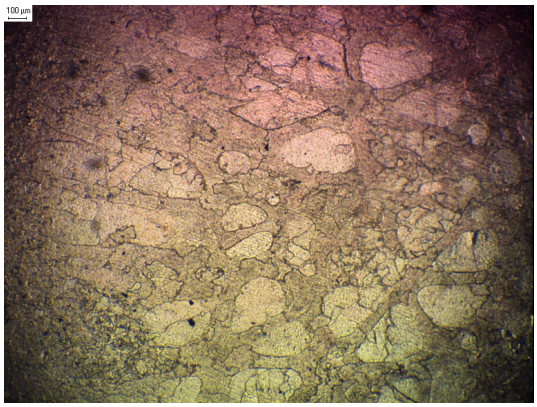

ab24a4p.TIF

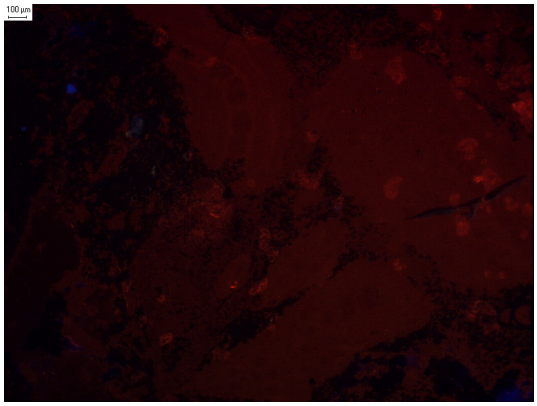

ac7a4c.TIF

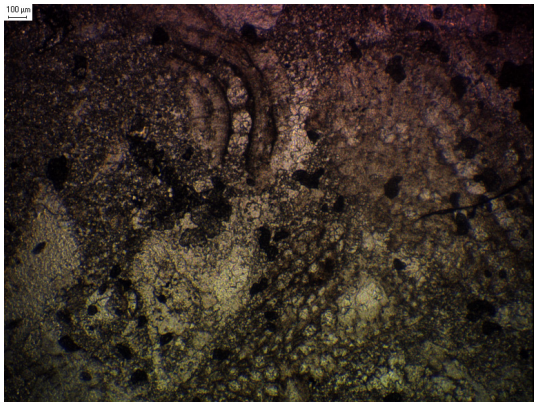

ac7a4p.TIF

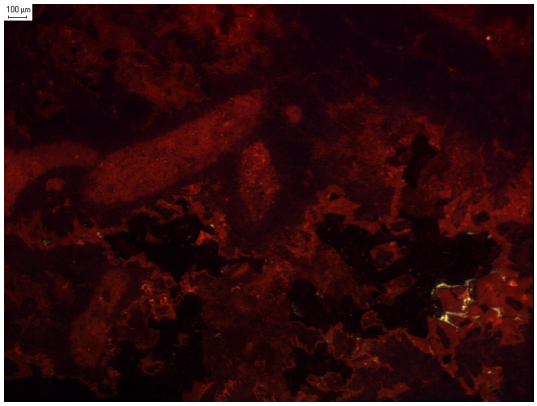

ad2a4c.TIF

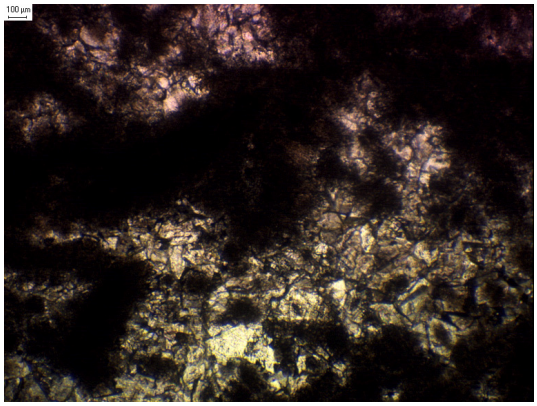

ad2a4p.TIF

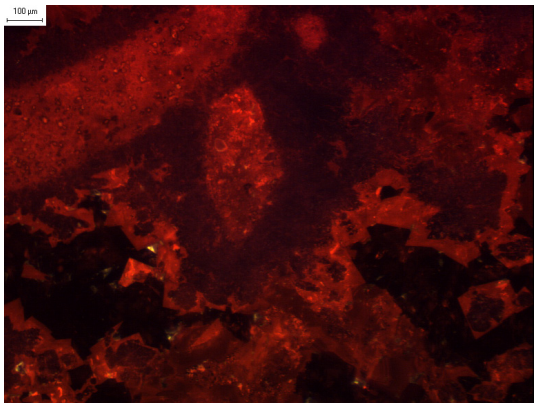

ad2a10c.TIF

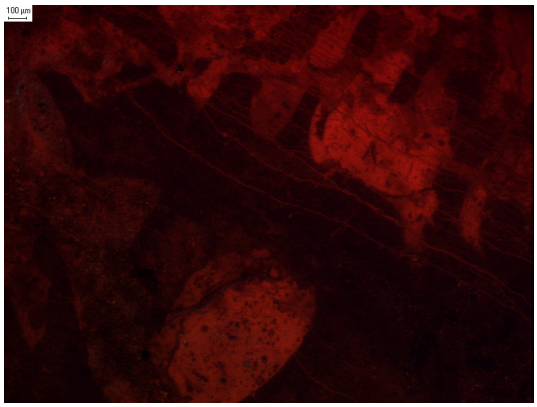

ad2b4c.TIF

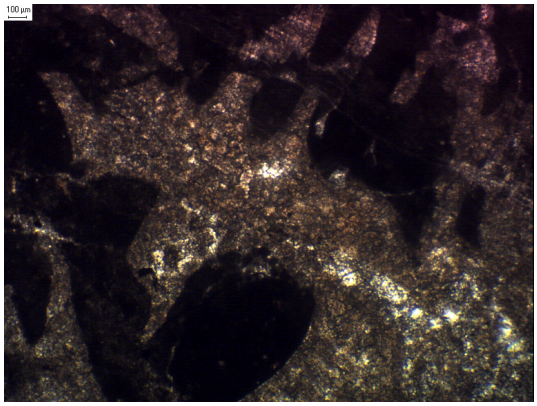

ad2b4p.TIF

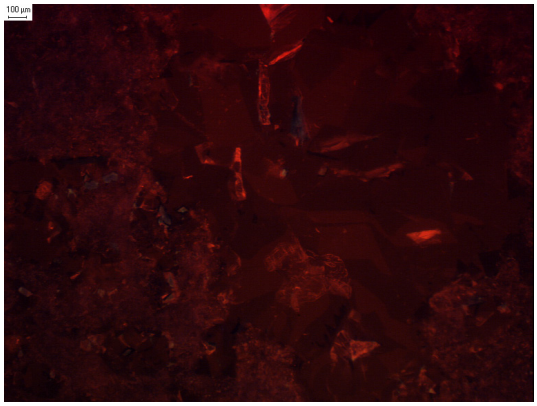

ad5a4c.TIF

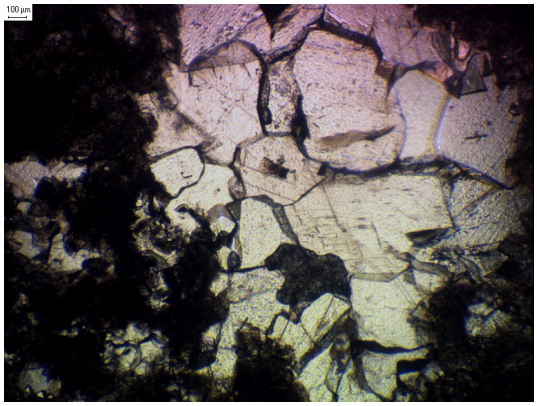

ad5a4p.TIF

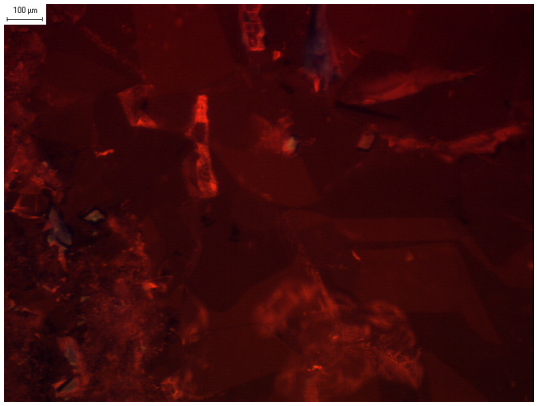

ad5a10c.TIF

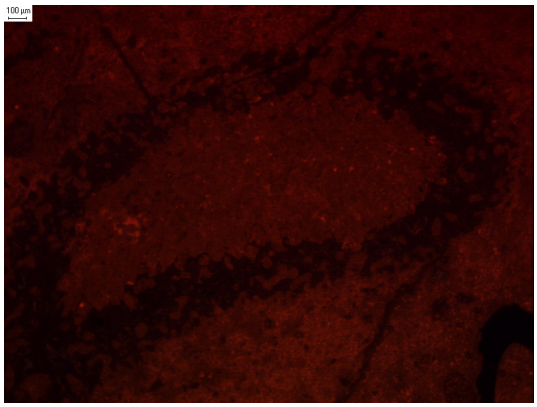

ad8a4c.TIF

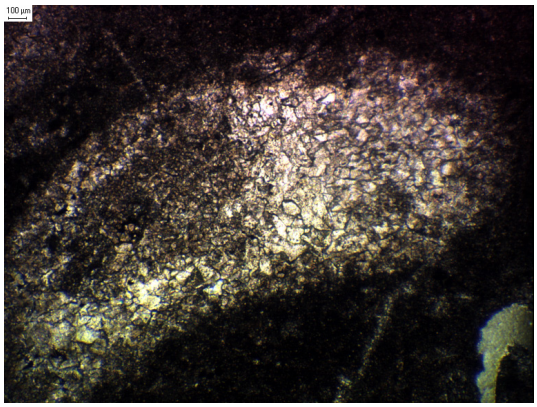

ad8a4p.TIF

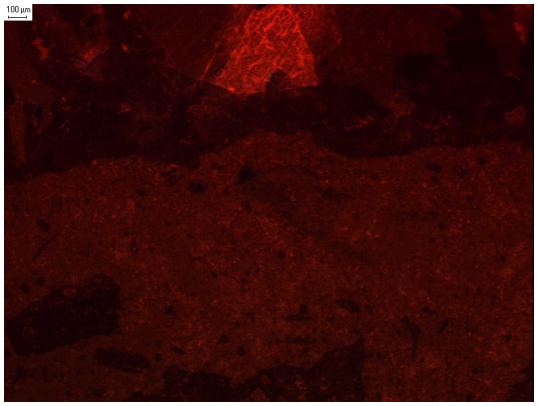

ad8b4c.TIF

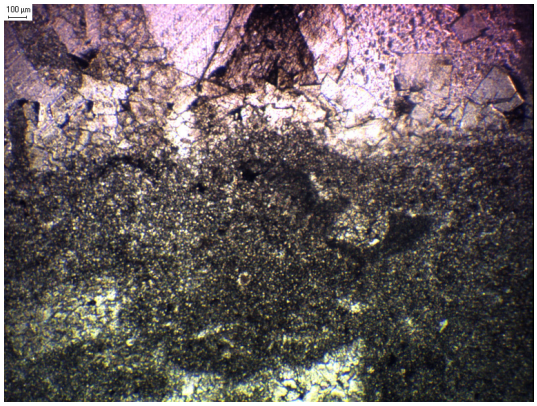

ad8b4p.TIF

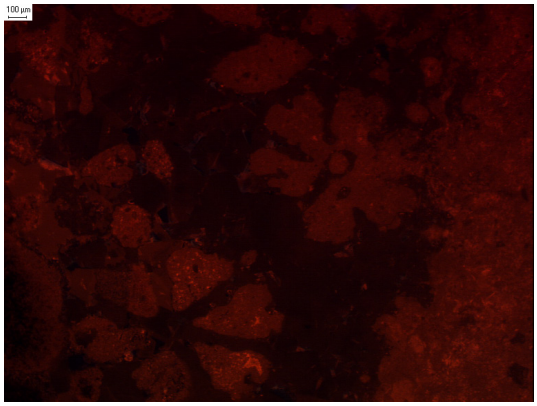

ad8c4c.TIF

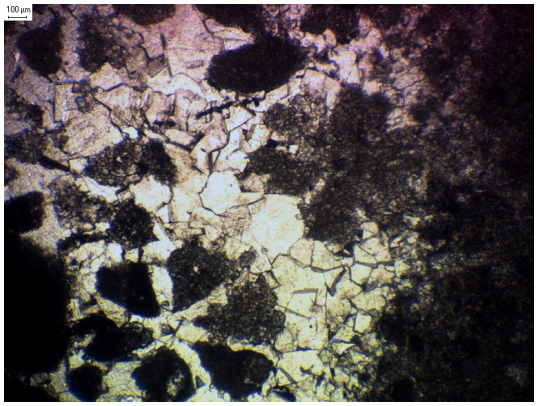

ad8c4p.TIF

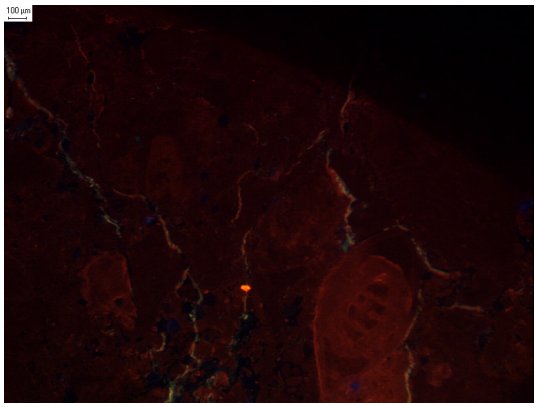

af8a4c.TIF

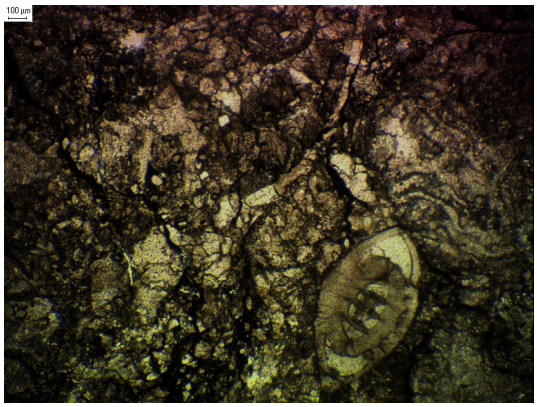

af8a4p.TIF

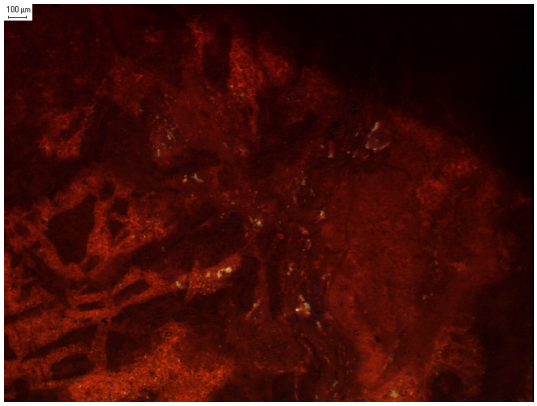

ag3a4c.TIF

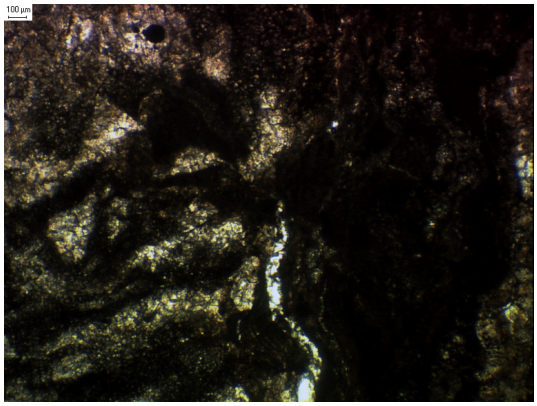

ag3a4p.TIF

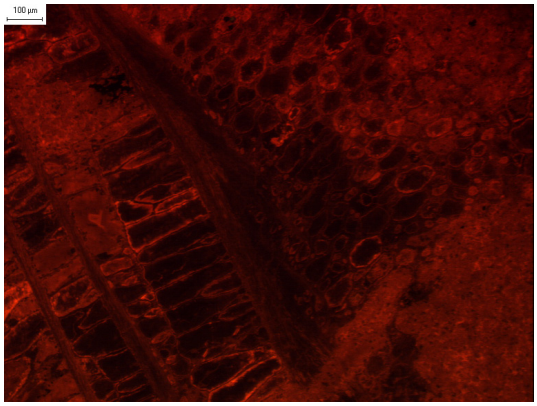

ag4a10c.TIF

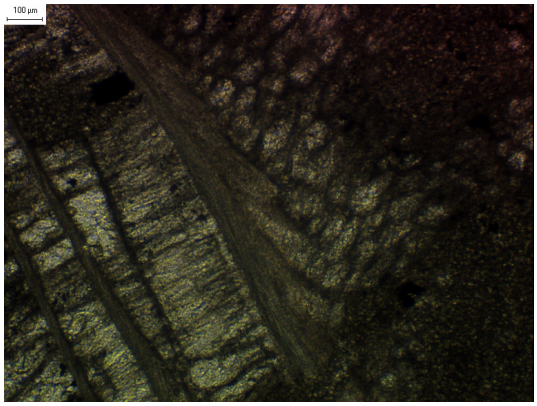

ag4a10p.TIF

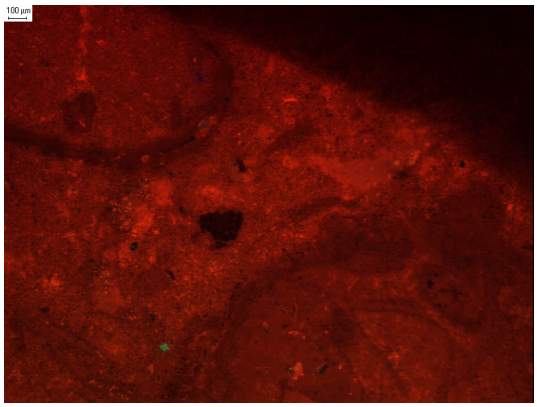

ag4b4c.TIF

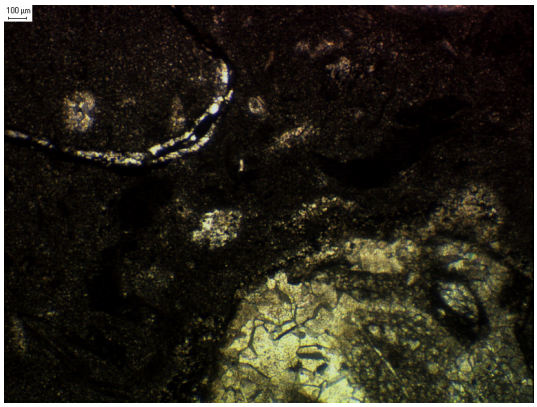

ag4b4p.TIF

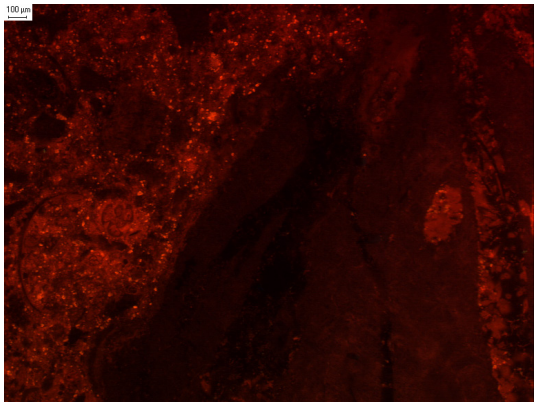

ah3a4c.TIF

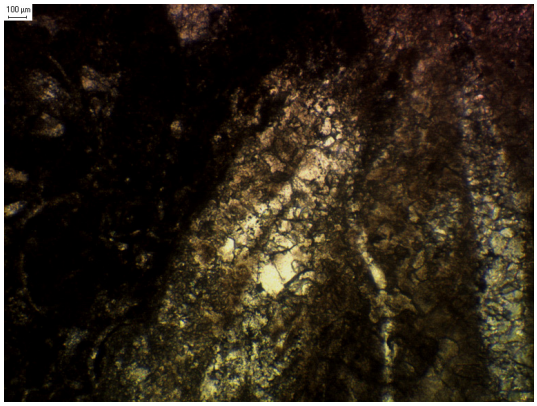

ah3a4p.TIF

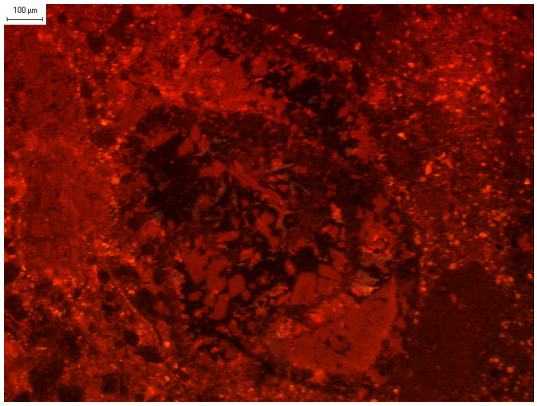

ah3b10c.TIF

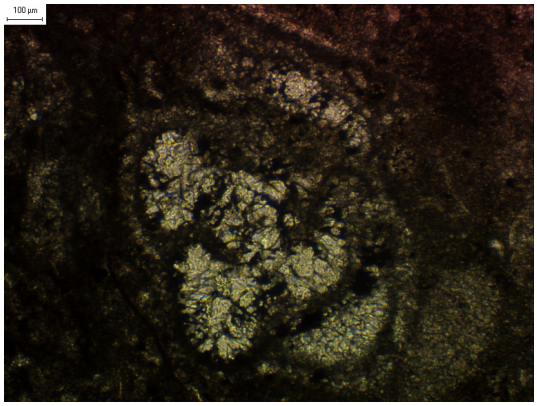

ah3b10p.TIF

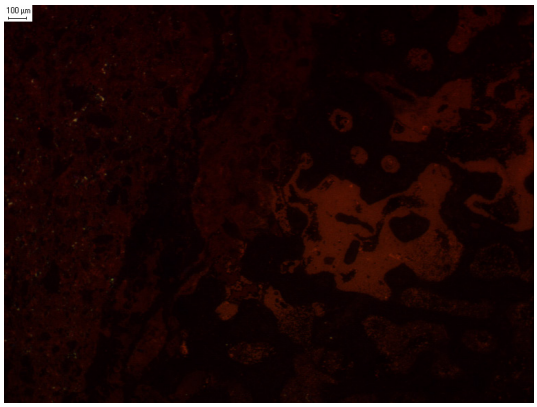

ah7a4c.TIF

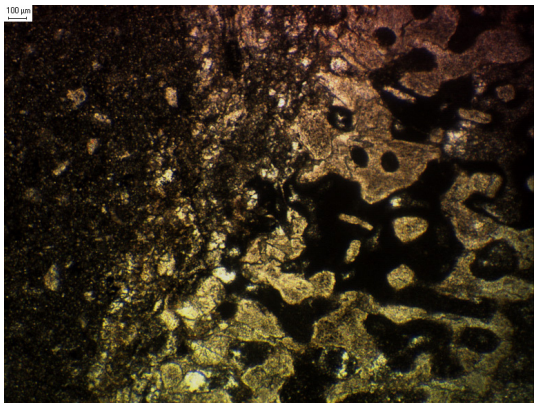

ah7a4p.TIF

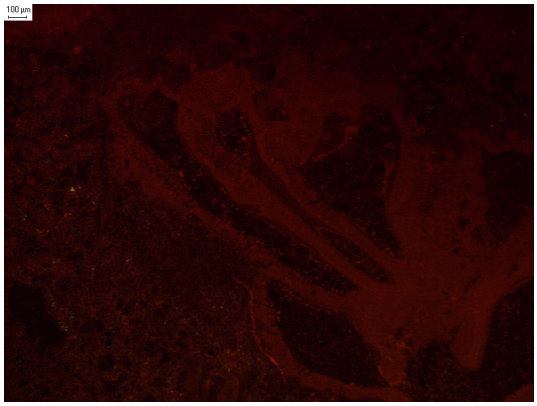

ah7b4c.TIF

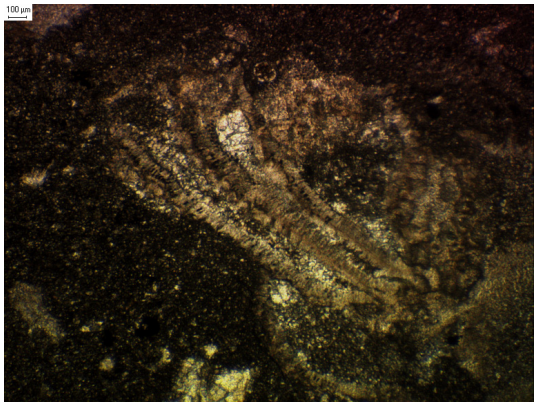

ah7b4p.TIF

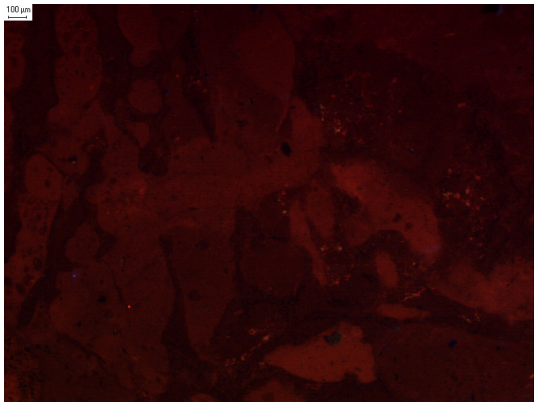

al3a4c.TIF

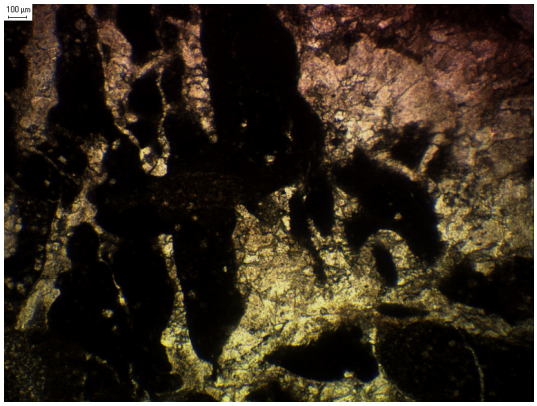

al3a4p.TIF

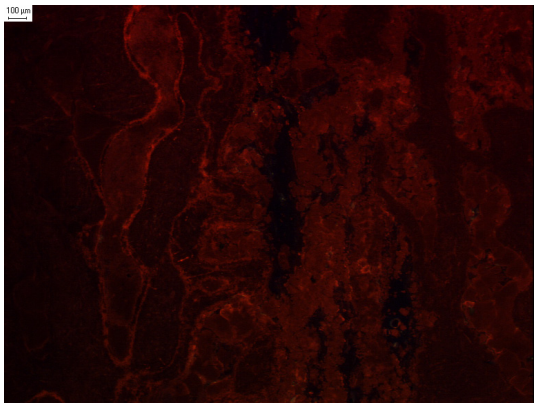

ba1a4c.TIF

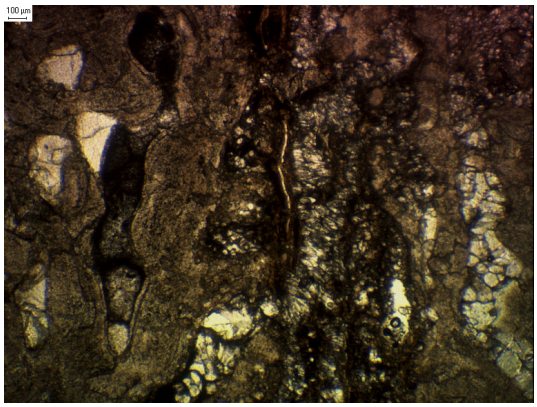

ba1a4p.TIF

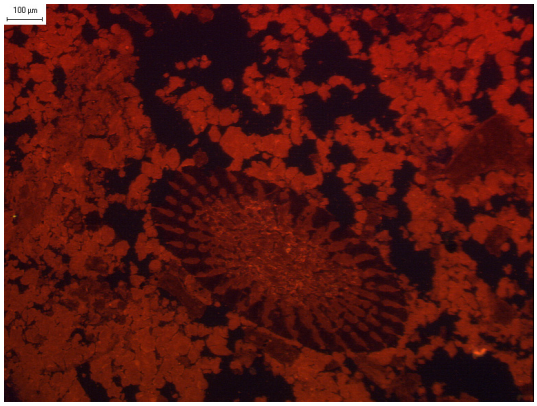

ba1b10c.TIF

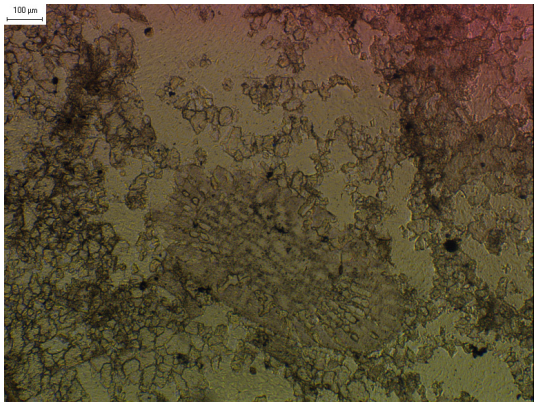

ba1b10p.TIF

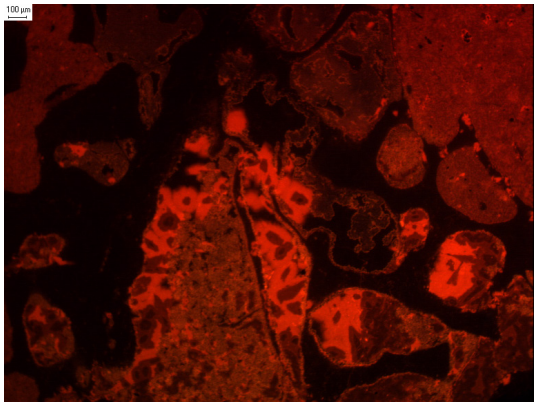

bb5a4c.TIF

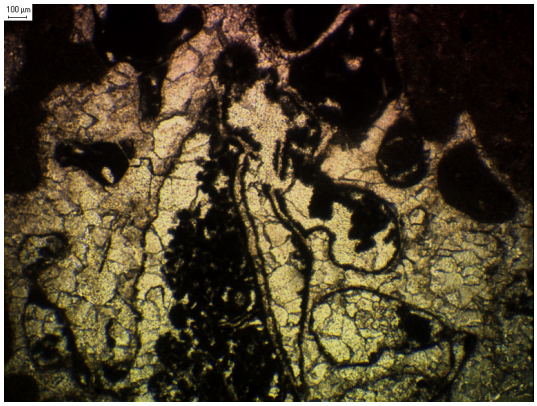

bb5a4p.TIF

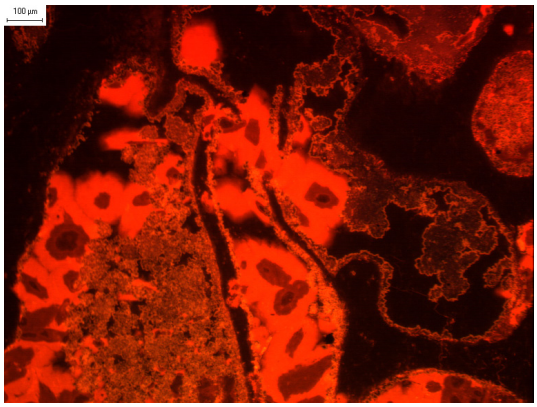

bb5a10c.TIF

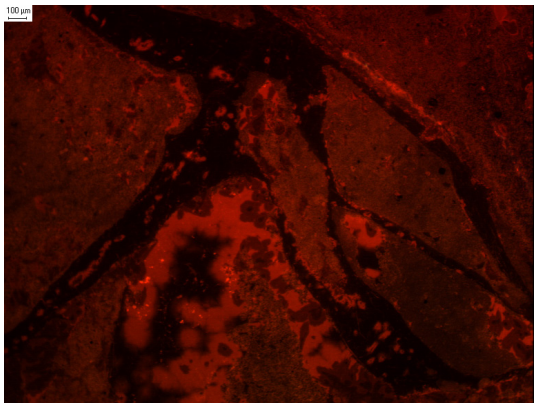

bb5b4c.TIF

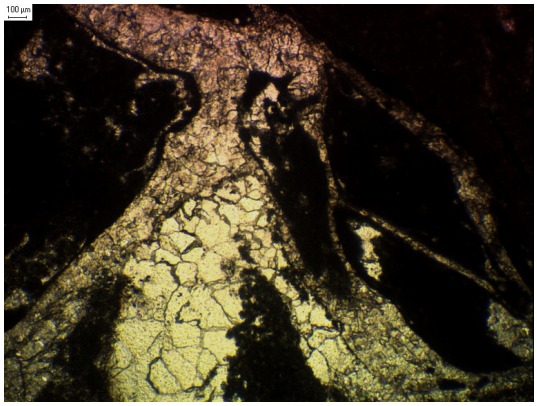

bb5b4p.TIF

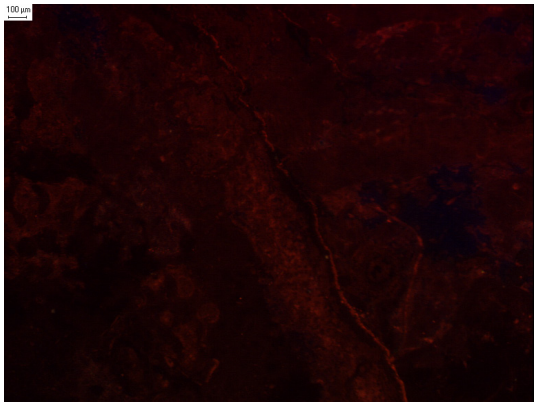

bb6a4c.TIF

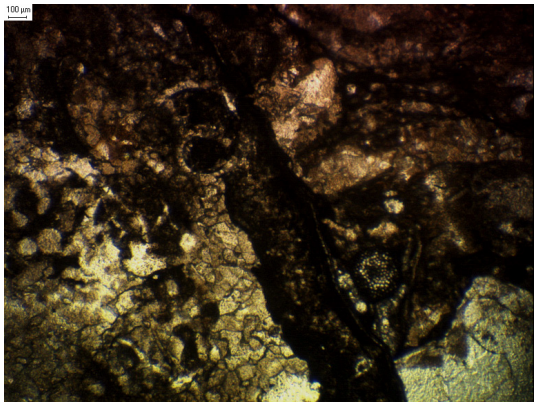

bb6a4p.TIF

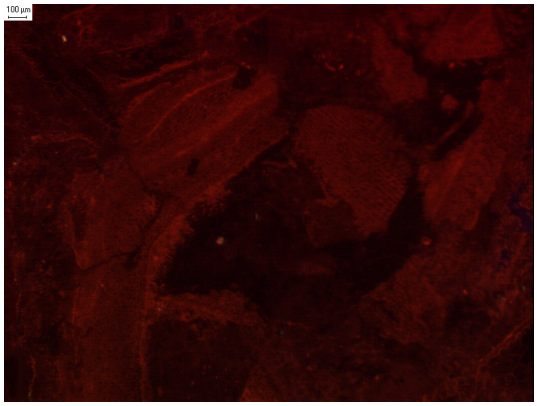

bb6b4c.TIF

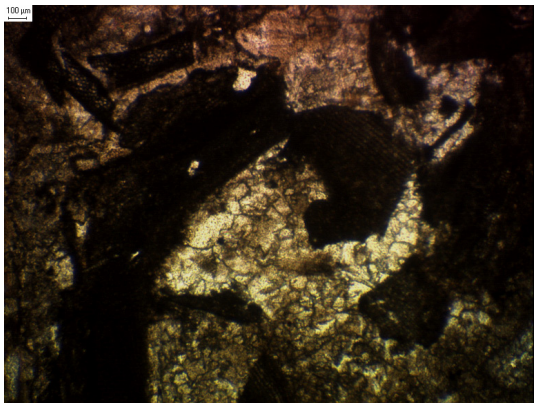

bb6b4p.TIF

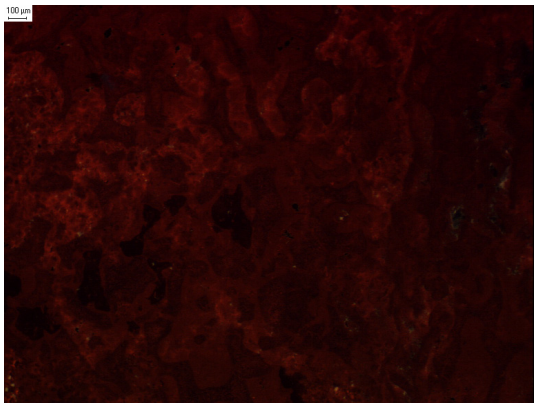

dpr2a4c.TIF

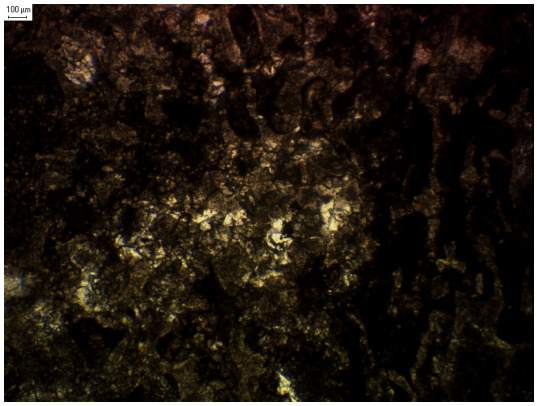

dpr2a4p.TIF

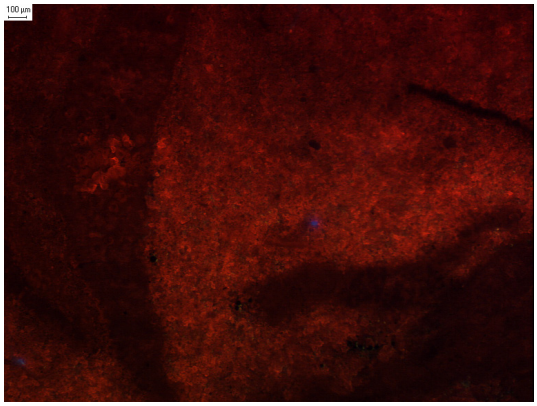

dpr4a4c.TIF

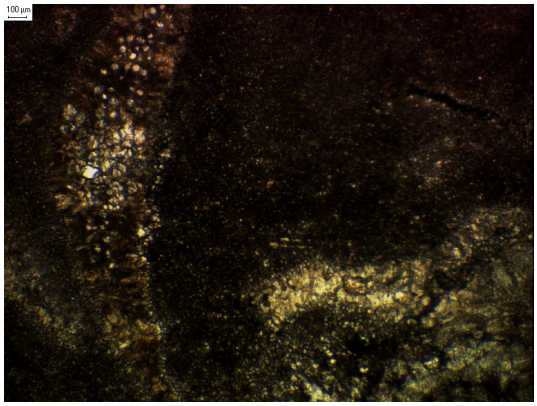

dpr4a4p.TIF

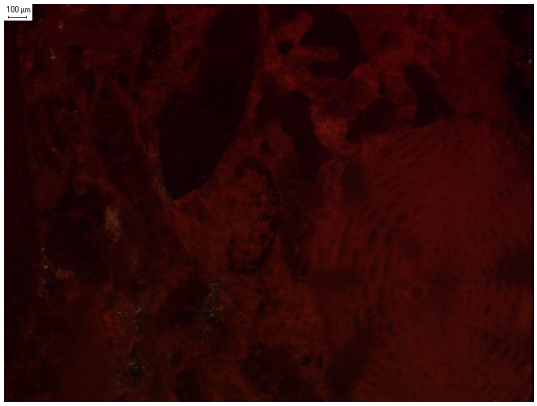

dpr10a4c.TIF

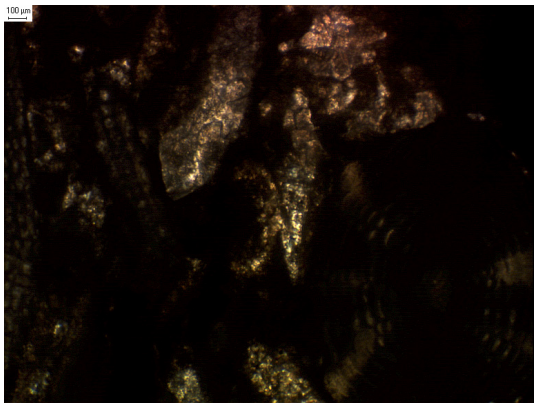

dpr10a4p.TIF

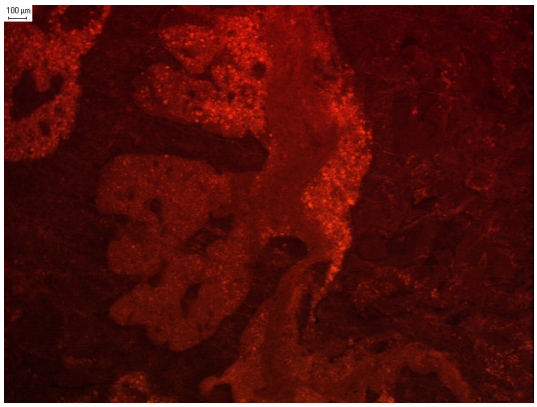

pa2a4c.TIF

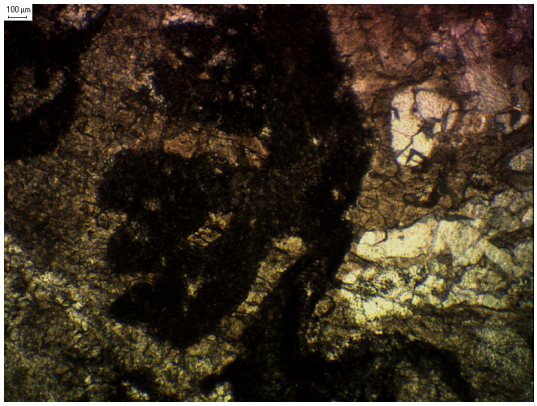

pa2a4p.TIF

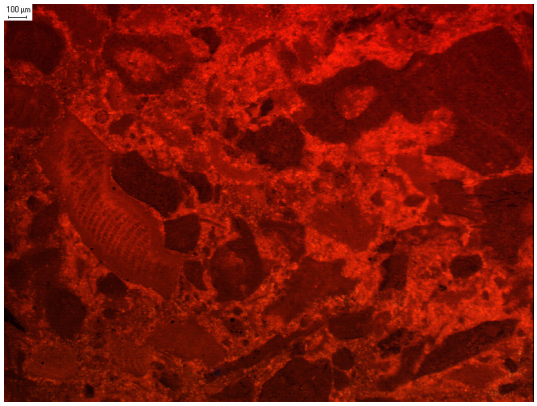

pa2b4c.TIF

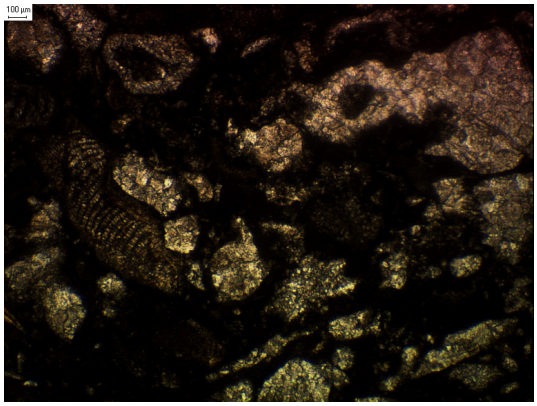

pa2b4p.TIF

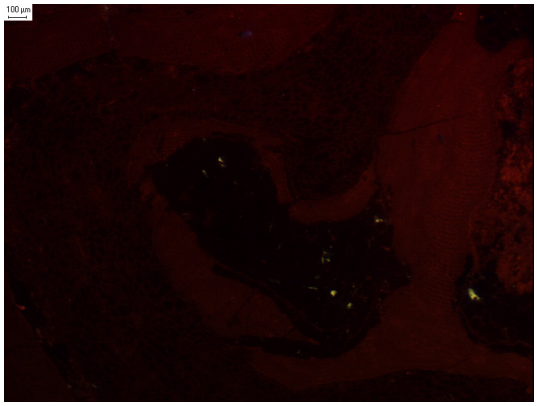

pa7a4c.TIF

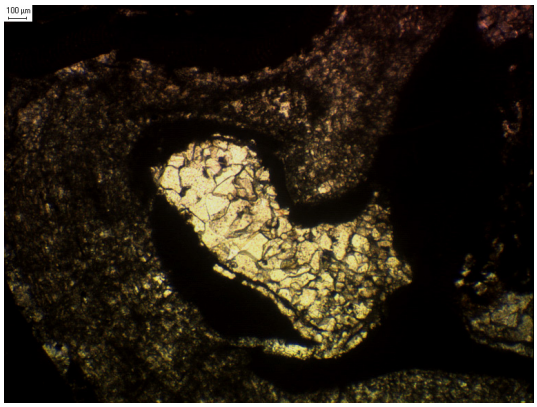

pa7a4p.TIF

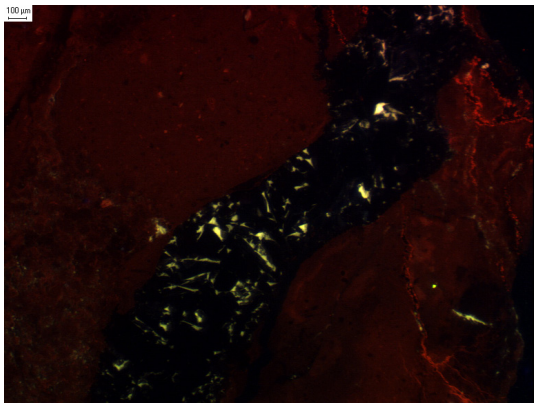

pa7b4c.TIF

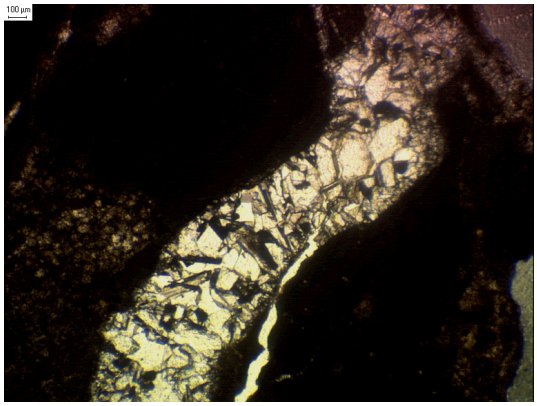

pa7b4p.TIF

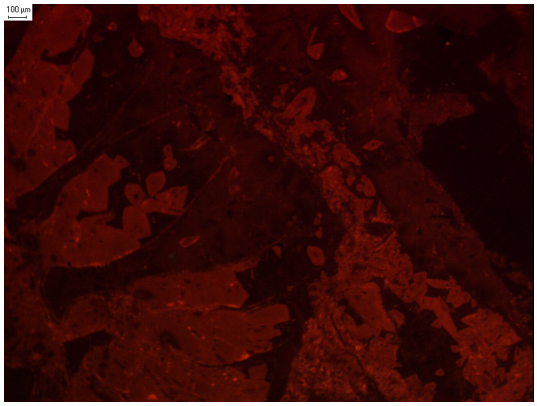

pc9a4c.TIF

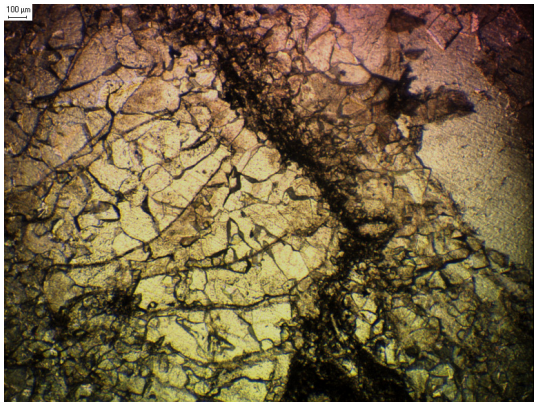

pc9a4p.TIF

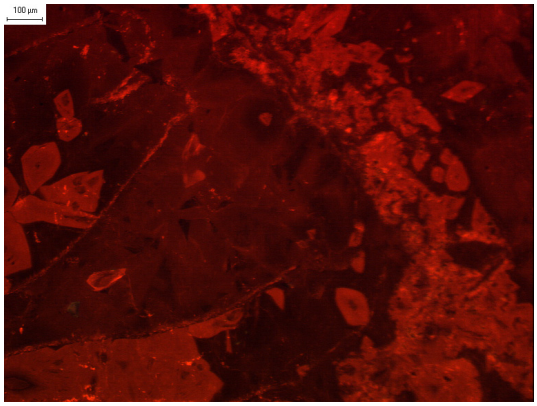

pc9a10c.TIF

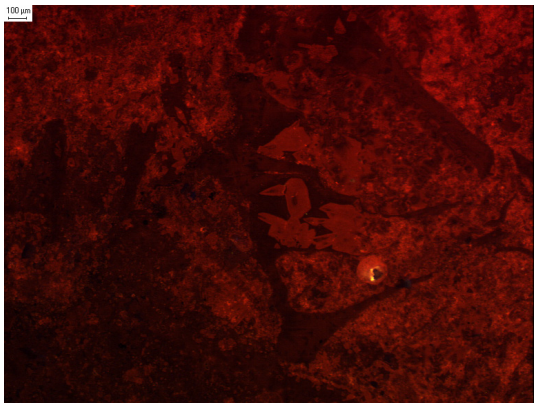

pc9b4c.TIF

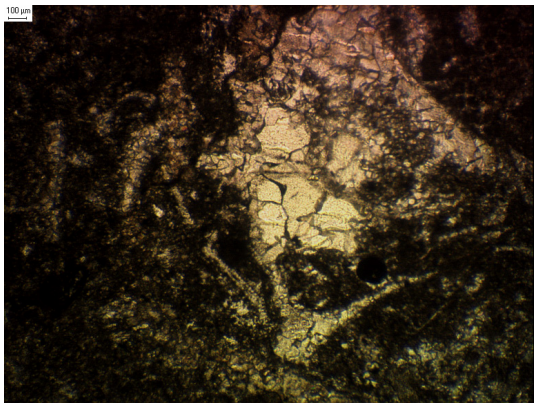

pc9b4p.TIF

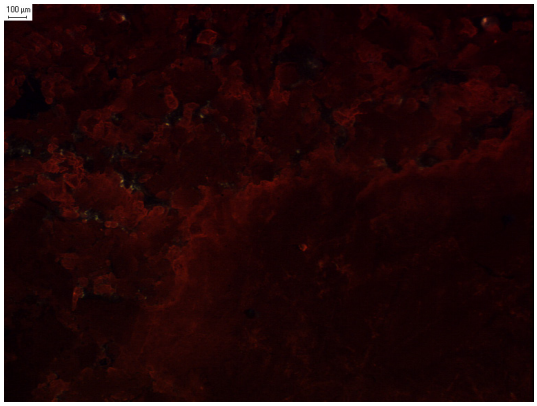

pe2a4c.TIF

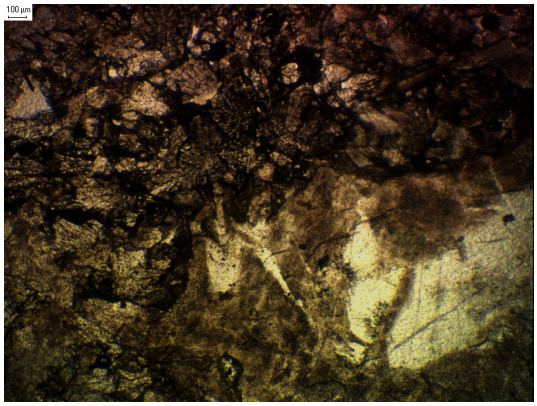

pe2a4p.TIF

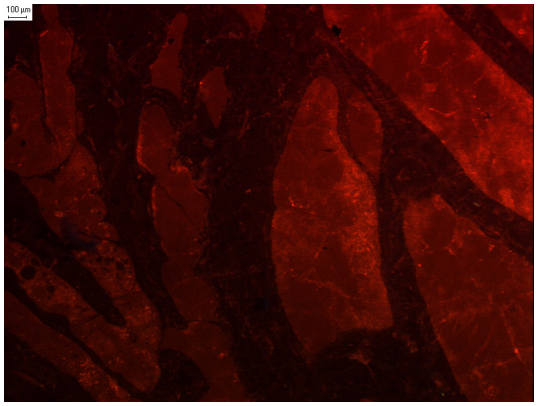

pe6a4c.TIF

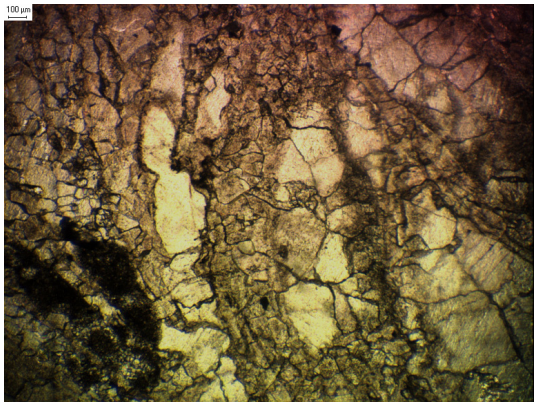

pe6a4p.TIF

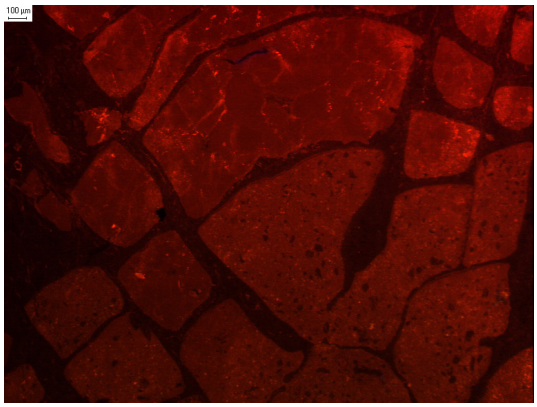

pe6b4c.TIF

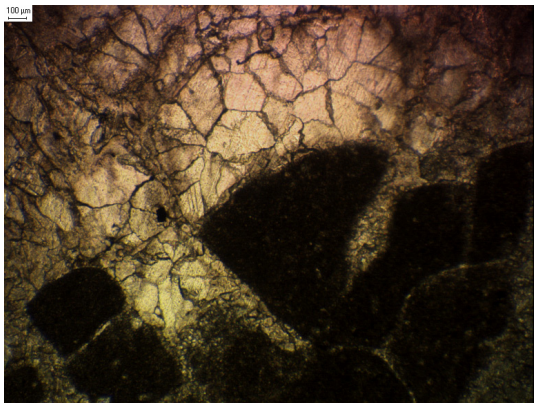

pe6b4p.TIF

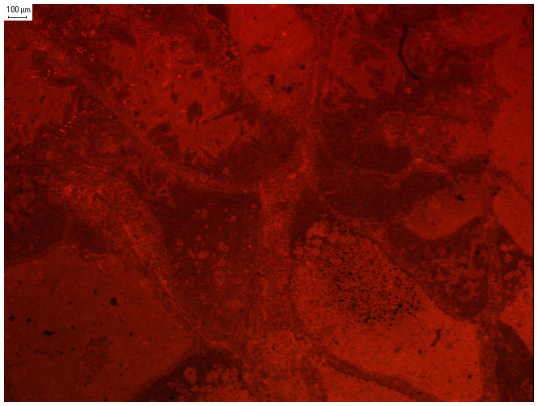

sa2a4c.TIF

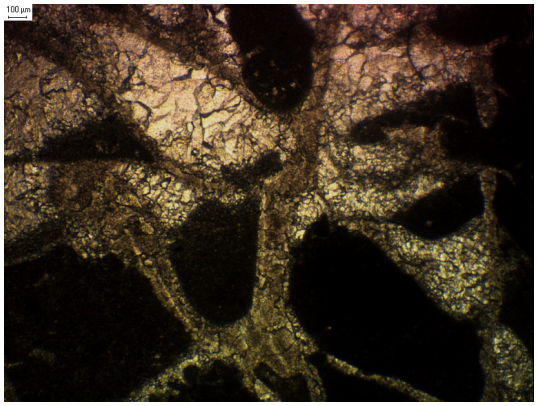

sa2a4p.TIF

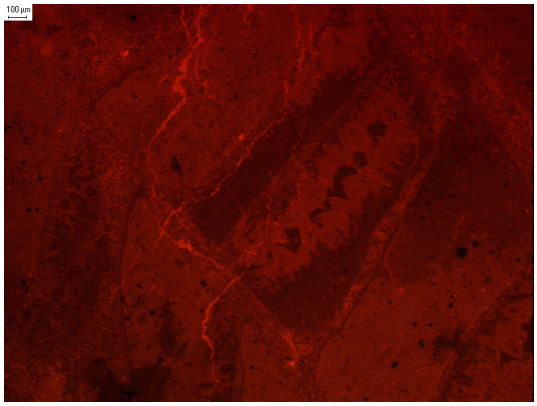

sa2b4c.TIF

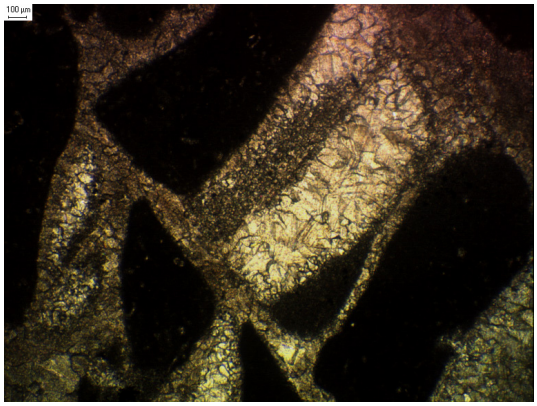

sa2b4p.TIF

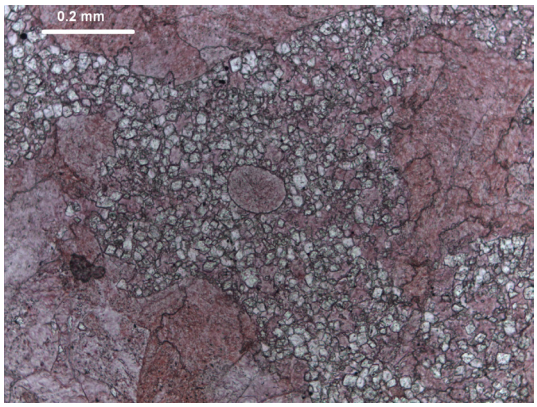

AB01 10X .tif

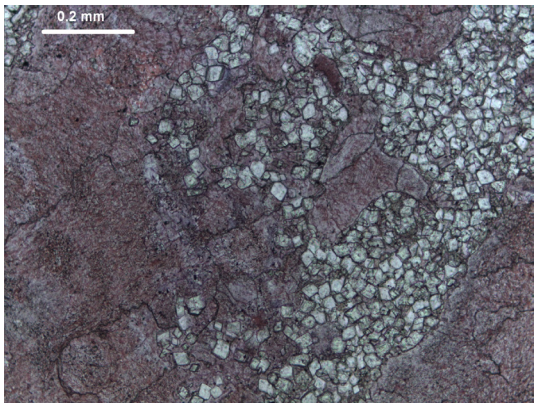

AB01 10X 1.tif

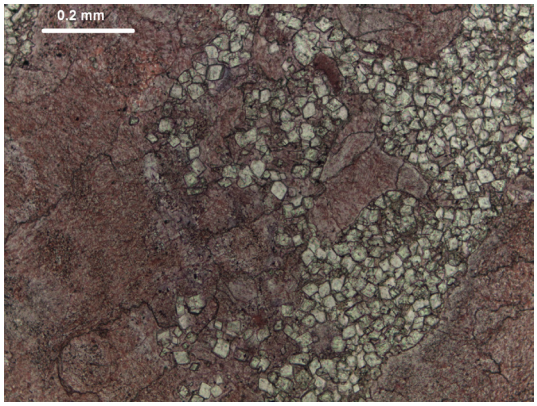

AB01 10X 2.tif

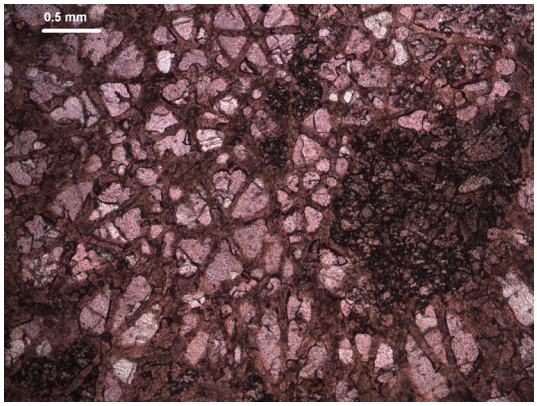

AB24 1.tif

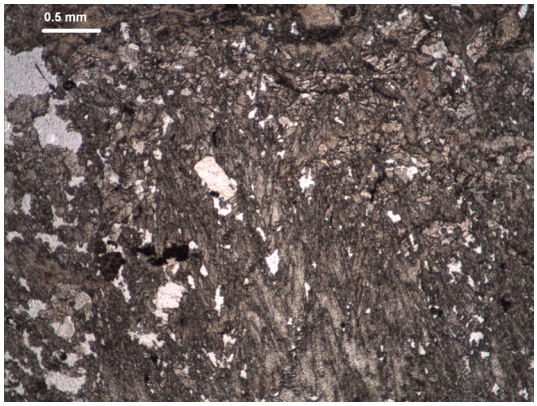

ABO1 1.tif

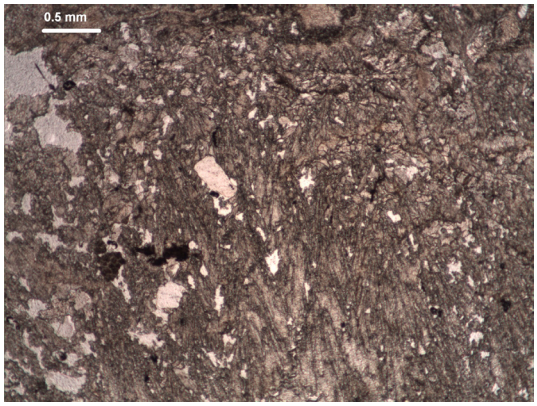

ABO1 2.tif

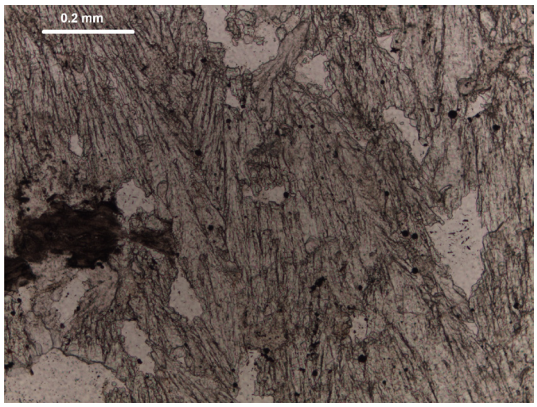

ABO1 10X PPL .tif

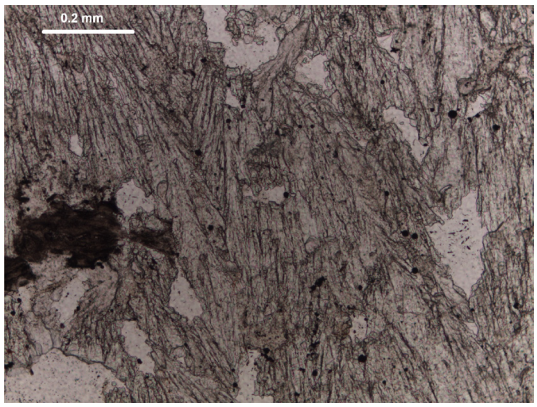

ABO1 10X PPL 1.tif

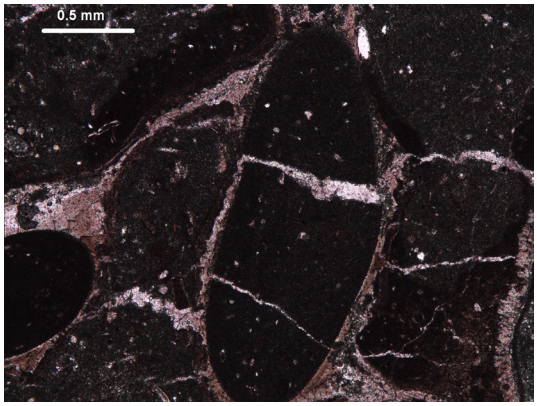

AC03 4X 1.tif

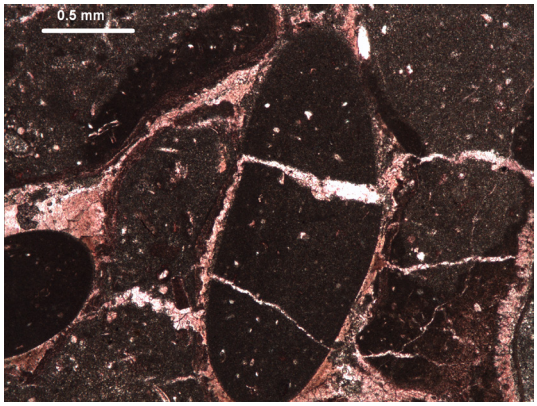

AC03 4X.tif

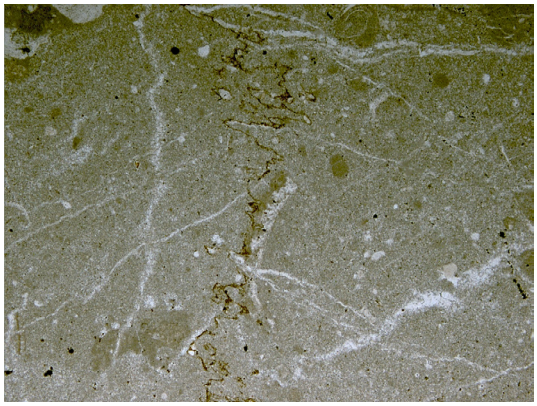

AC03-03-5XPPL.tif

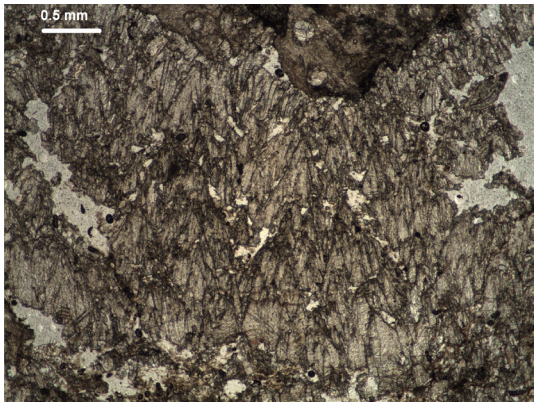

AK03 1.tif

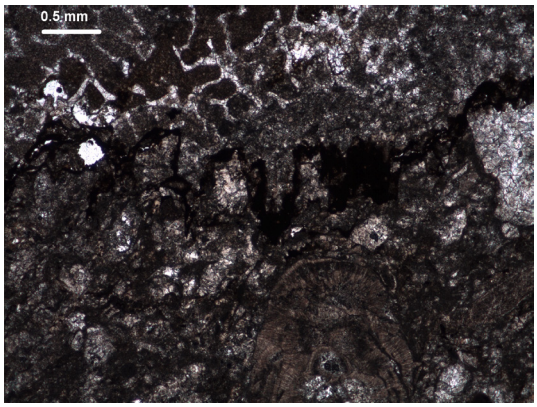

BB09 1.tif

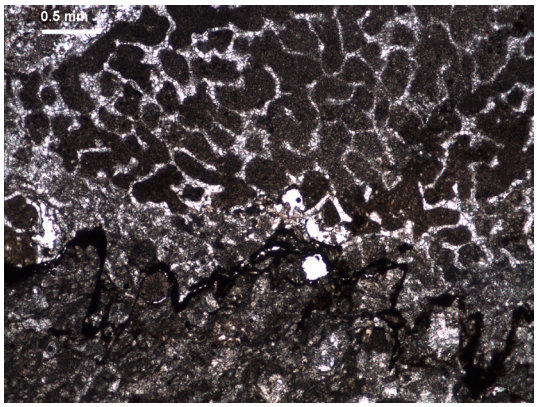

BB09 2.tif

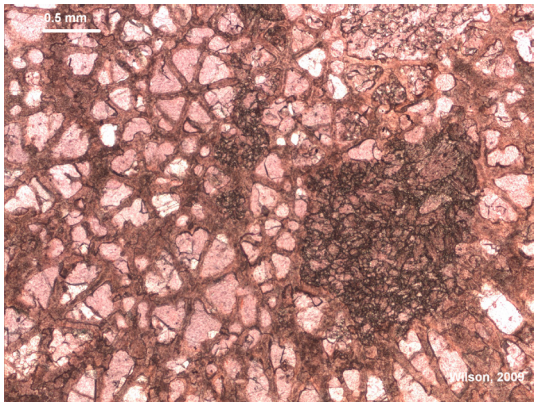

Samcar-AB24-ppl-x2.jpg

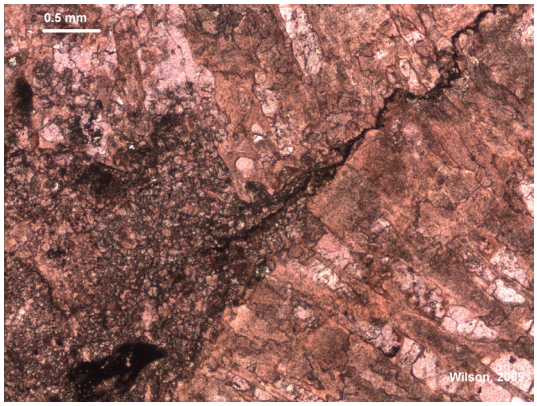

Samcar-AB24-ppl-x21.jpg

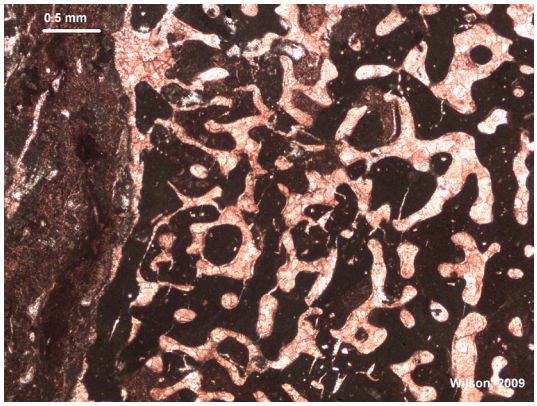

Samcar-AC3-ppl-x2.jpg

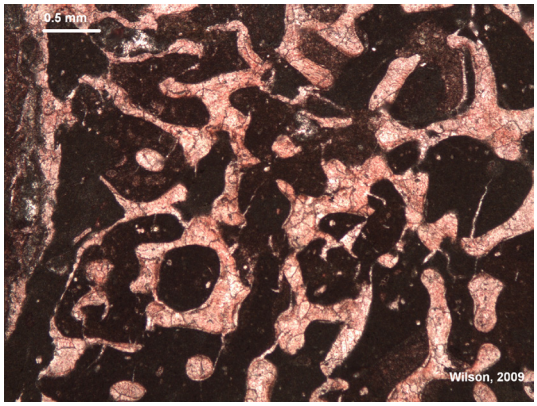

Samcar-AC3-ppl-x4.jpg

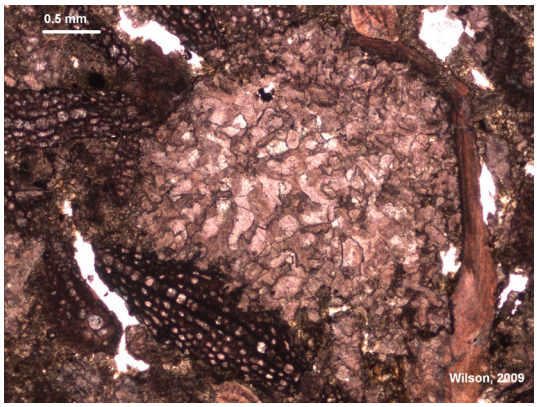

Samcar-AC8-ppl-x2.jpg

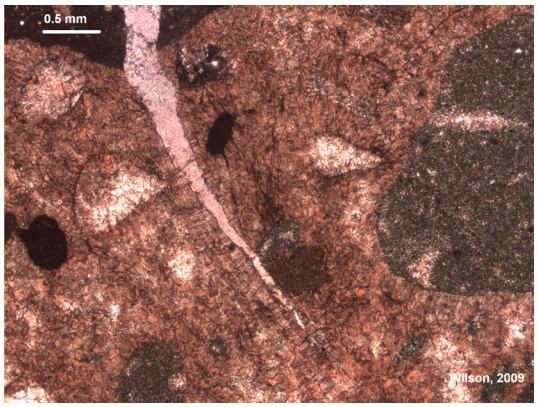

Samcar-AD2-ppl-x2.jpg

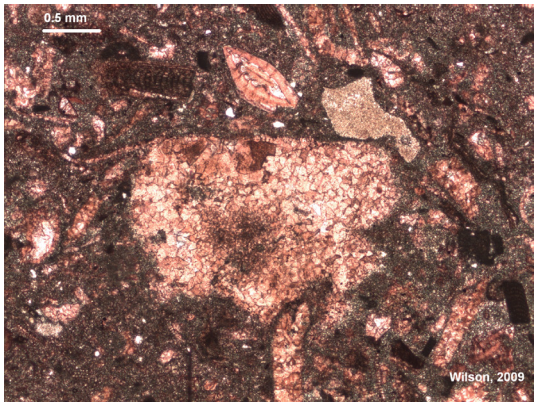

Samcar-AD4-ppl-x2.jpg

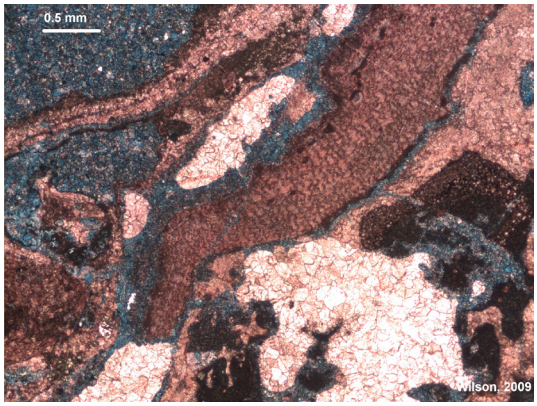

Samcar-AE5-ppl-x2.jpg

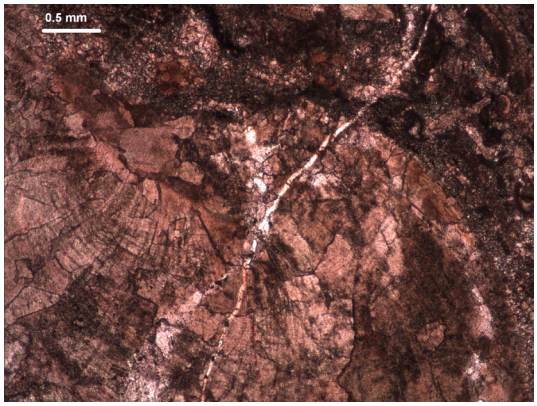

Samcar-AE6-frac&recryx2.jpg

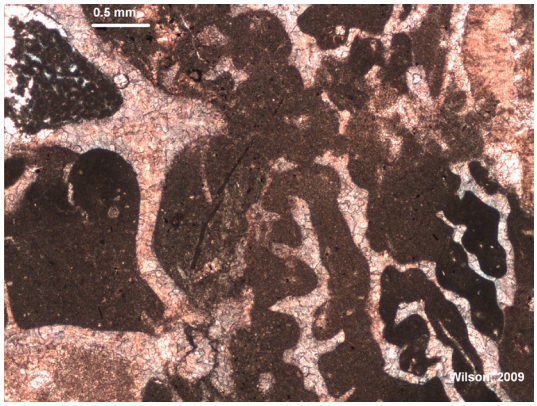

Samcar-BB5-ppl-x2.jpg

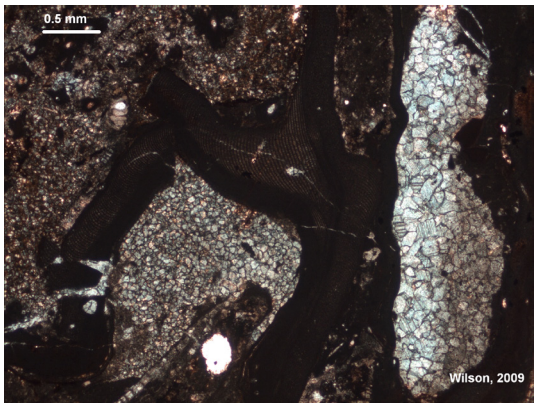

Samcar-PA7-ppl-x2.jpg

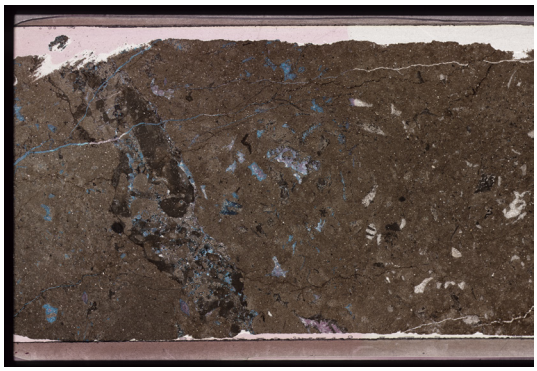

AA04.tif

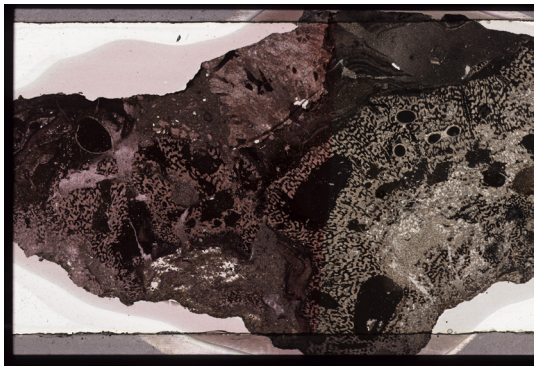

AA08.tif

AA11.tif

AA13.tif

AA16.tif

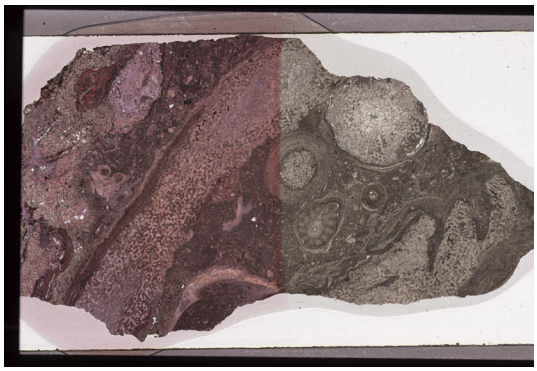

AA20.tif

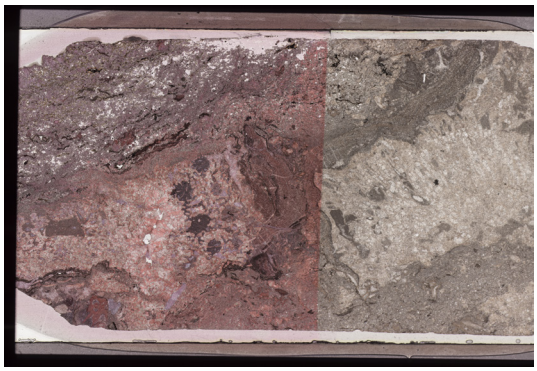

AA21a.tif

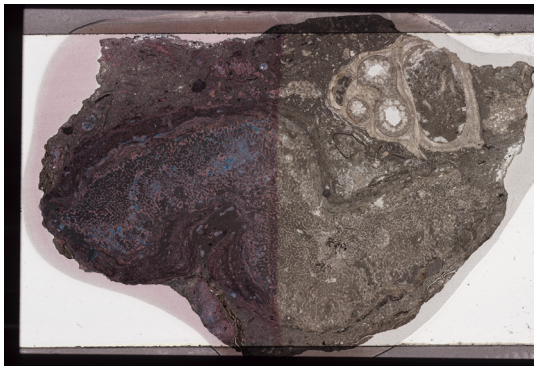

AA24.tif

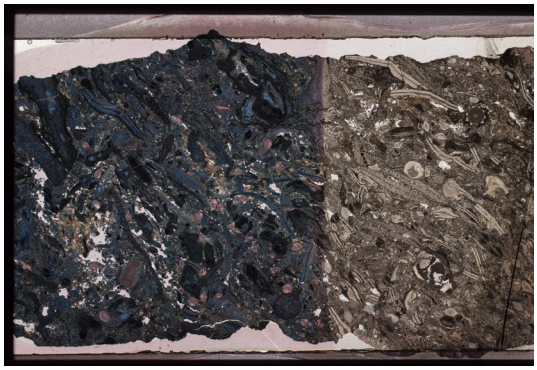

AA26.tif

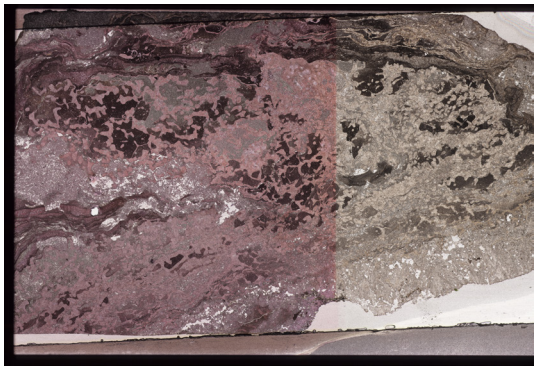

AB01.tif

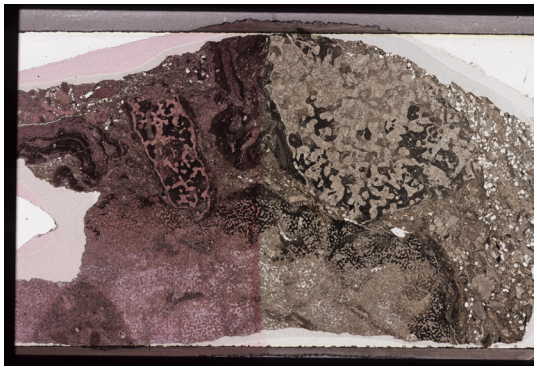

AB03.tif

AB05.tif

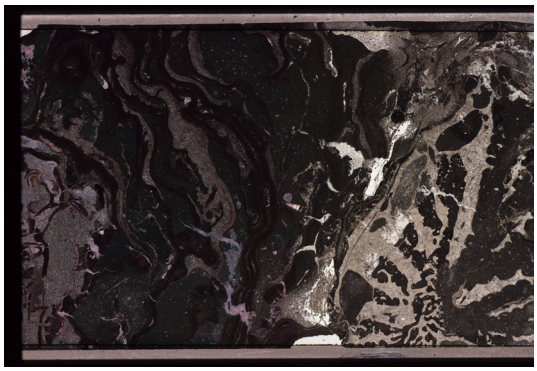

AB07.tif

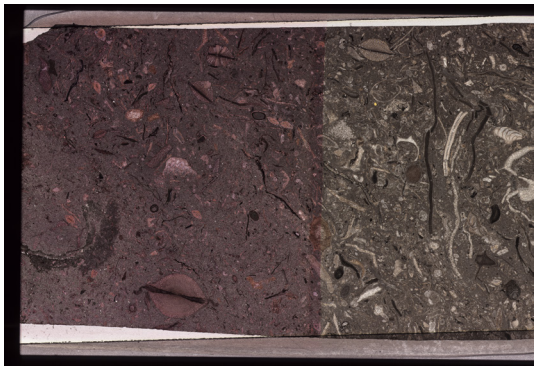

AB08.tif

AB09.tif

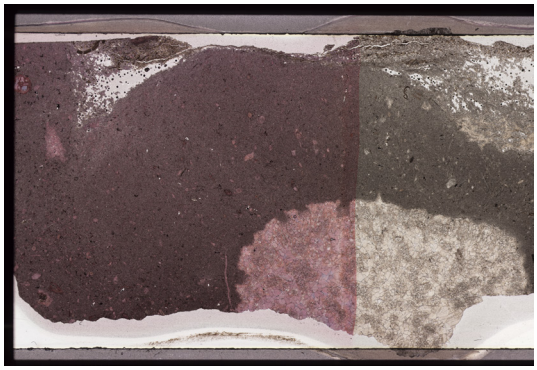

AB12.tif

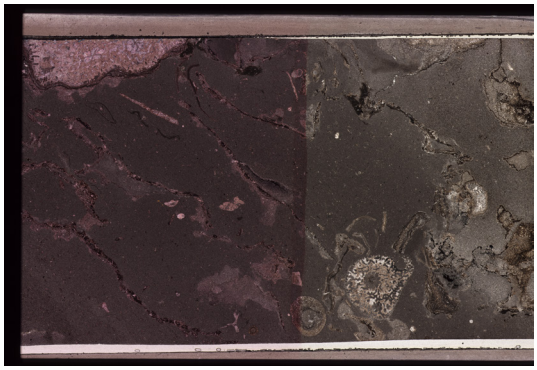

AB13.tif

AB17.tif

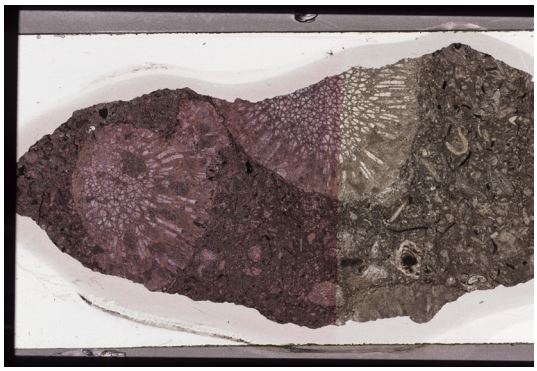

AB24.tif

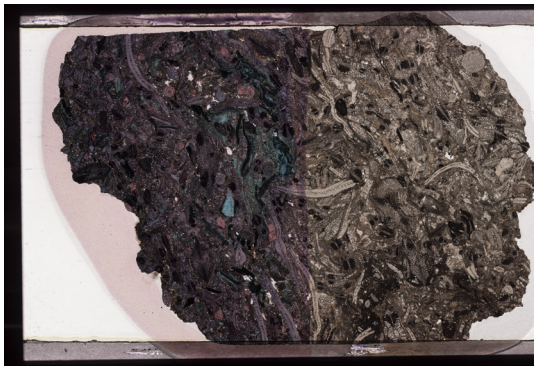

AB29.tif

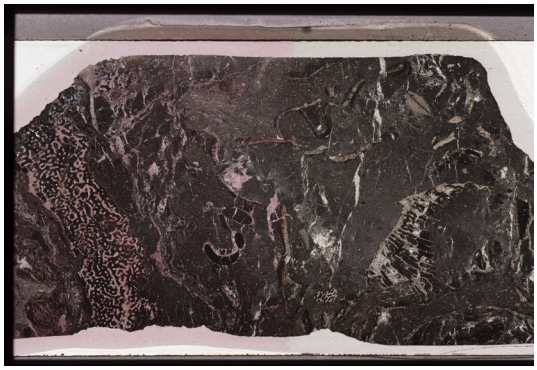

AC03.tif

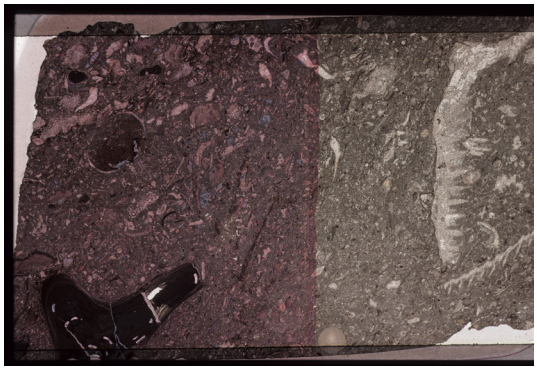

AC04.tif

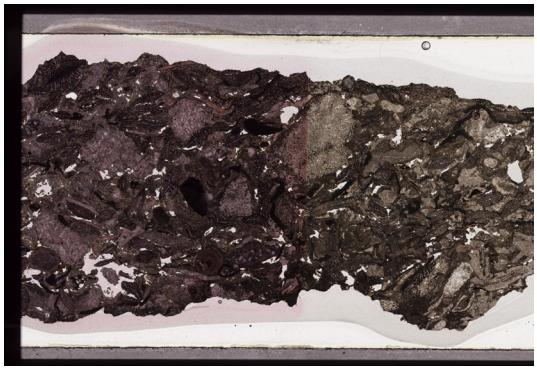

AC08.tif

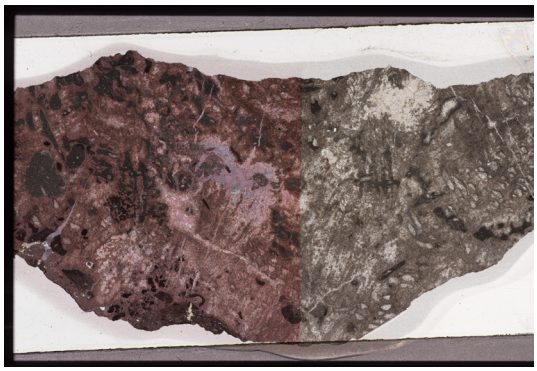

AD02.tif

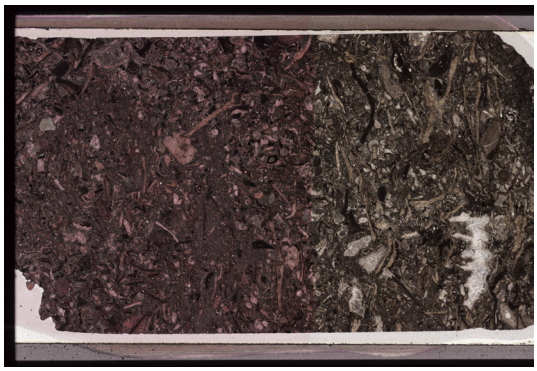

AD04.tif

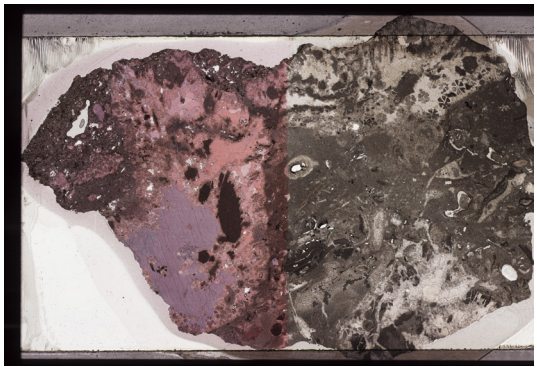

AD08.tif

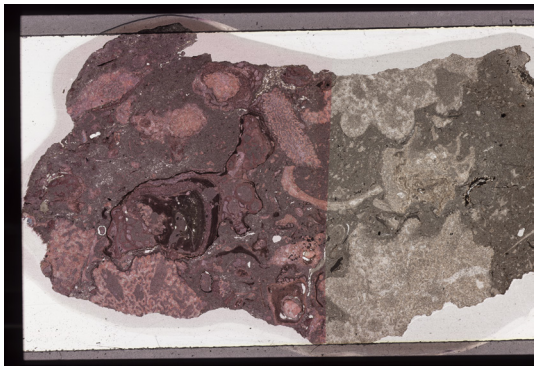

AD13.tif

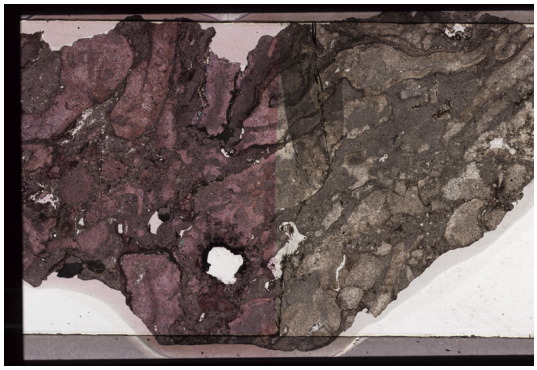

AD15.tif

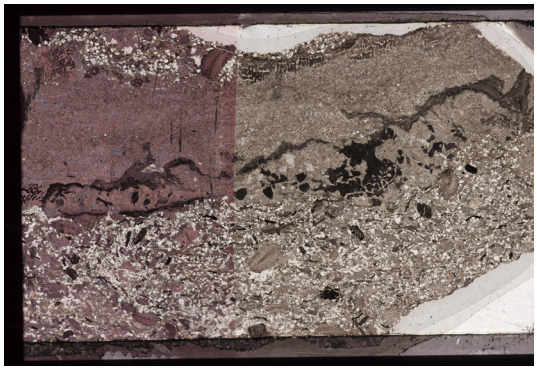

AE02.tif

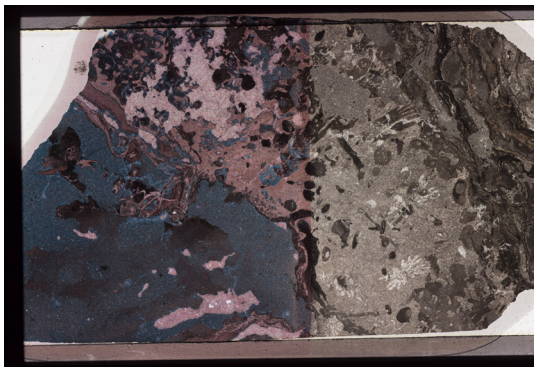

AE05.tif

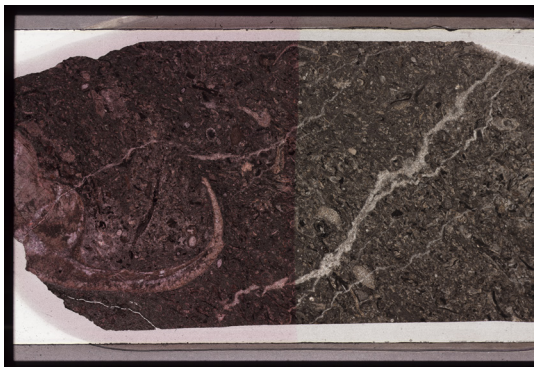

AE06.tif

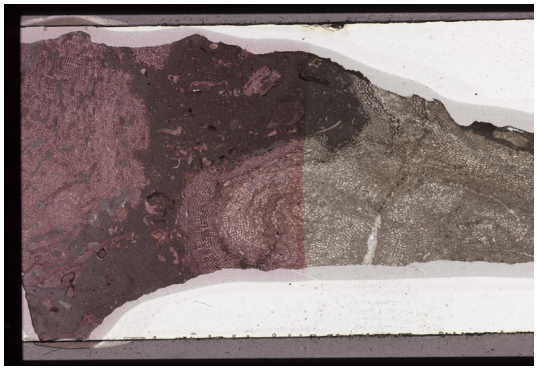

AE08.tif

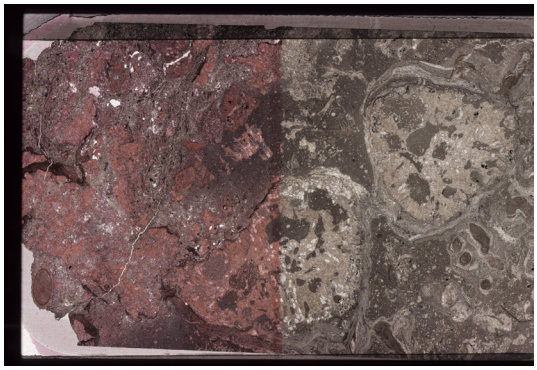

AE09.tif

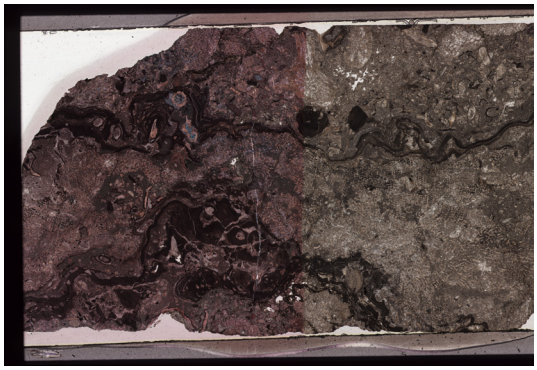

AE11.tif

AE13.tif

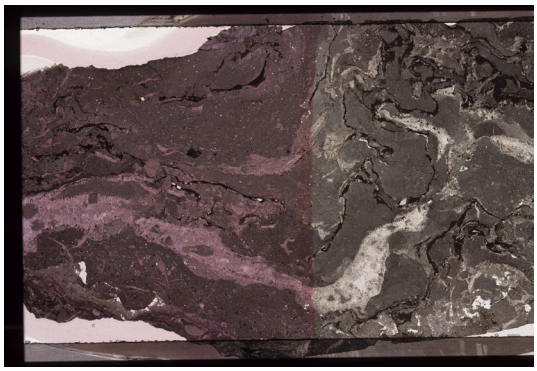

AF02.tif

AF06.tif

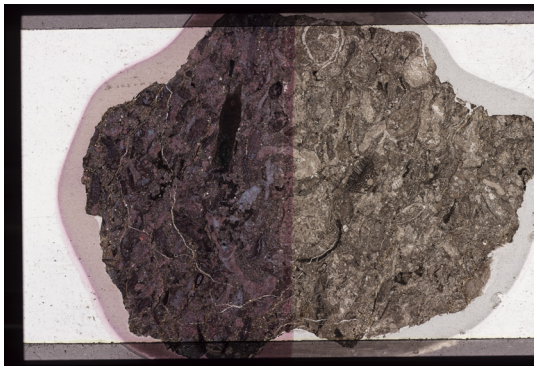

AF08.tif

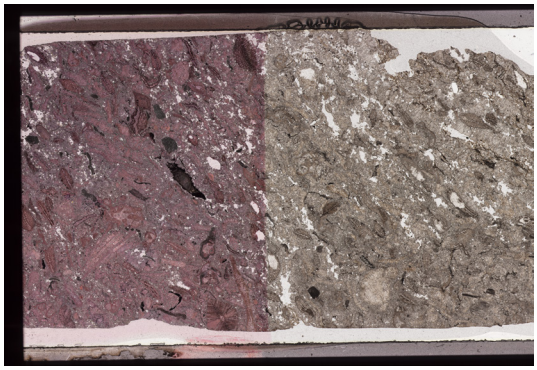

AF10.tif

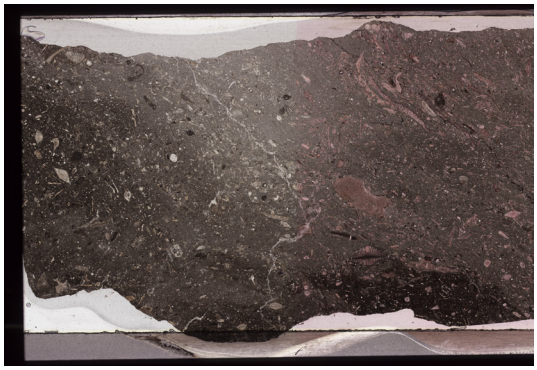

AG01.tif

AG03.tif

AG04.tif

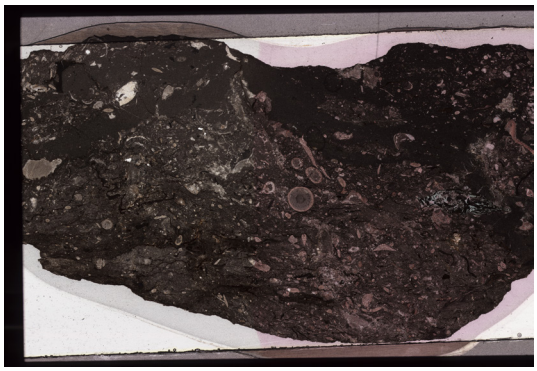

AG06.tif

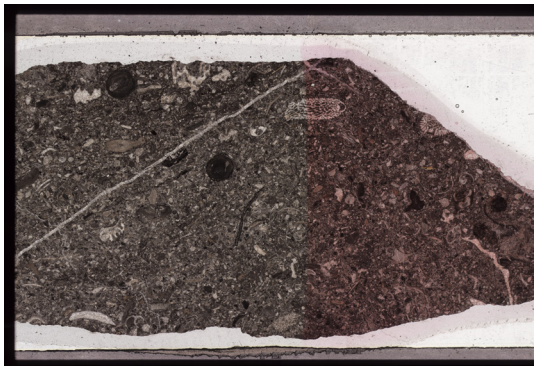

AH01.tif

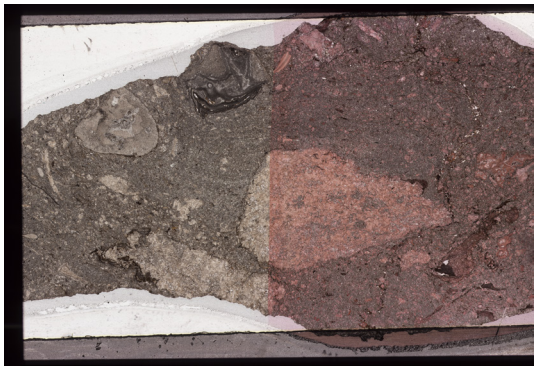

AH02.tif

AH03.tif

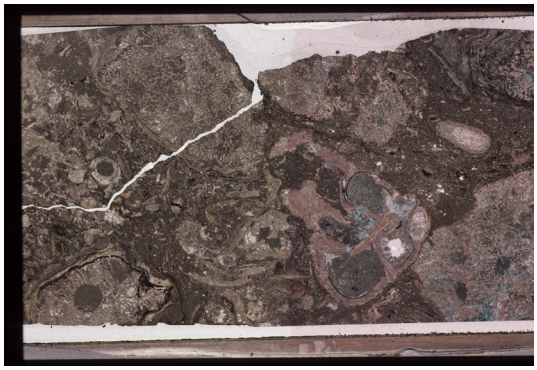

AH07.tif

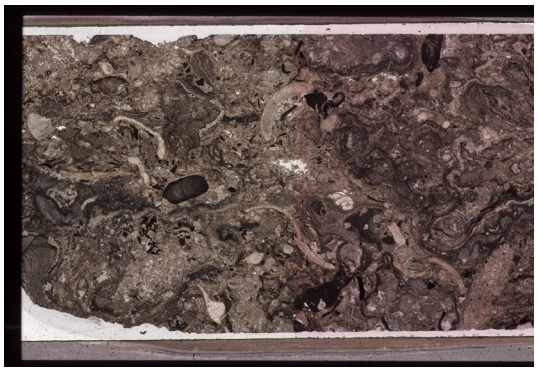

AH08.tif

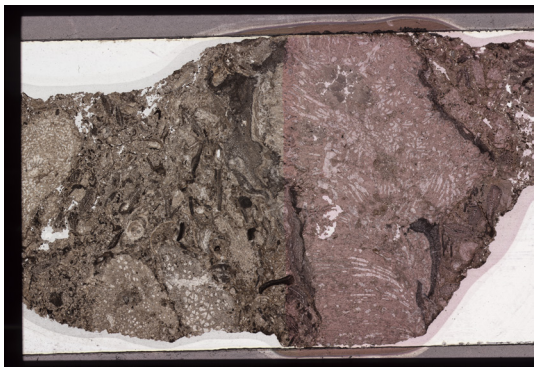

AH09.tif

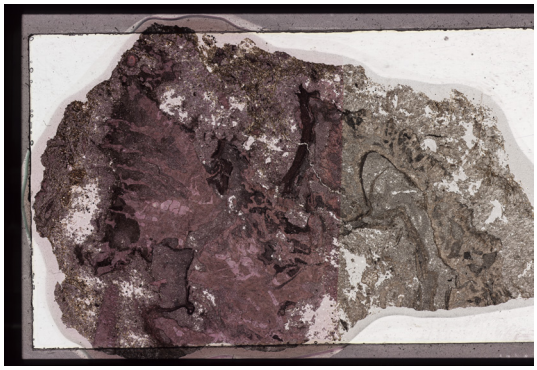

AK03.tif

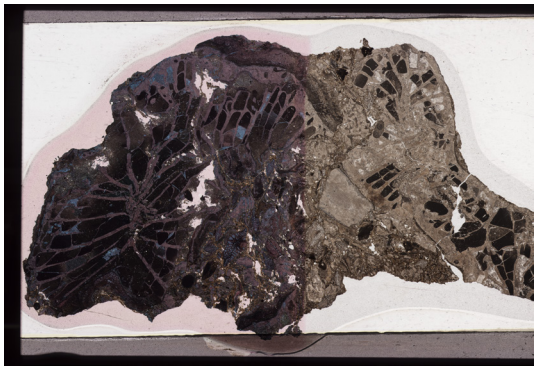

AK07.tif

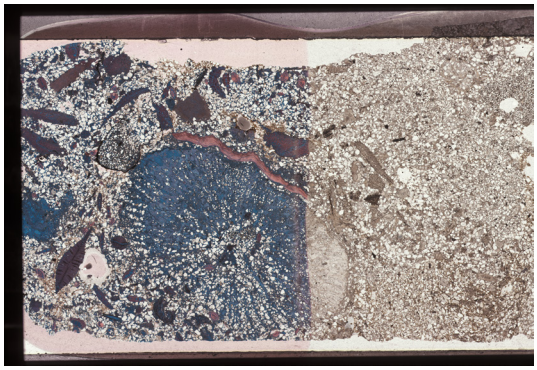

AK09.tif

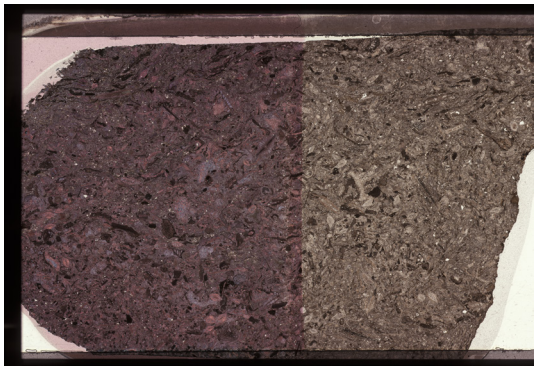

AK11.tif

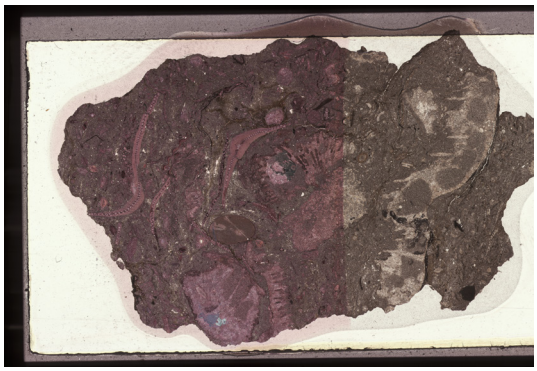

AK12.tif

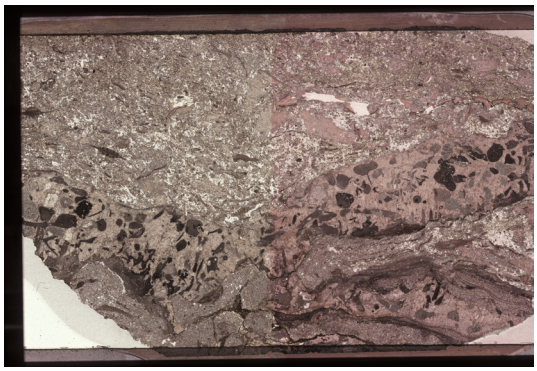

AL02.tif

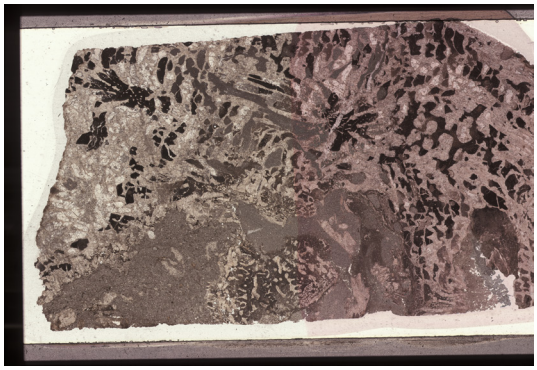

AL03.tif

BA01.tif

BA03.tif

BB02.tif

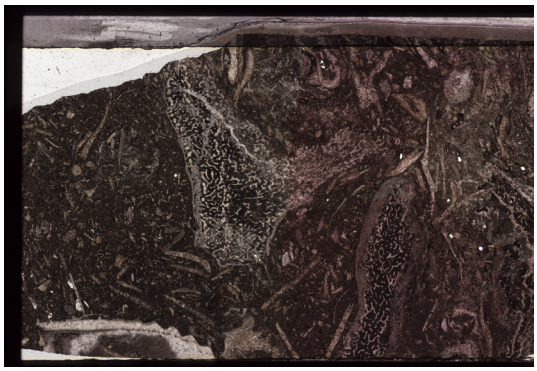

BB03.tif

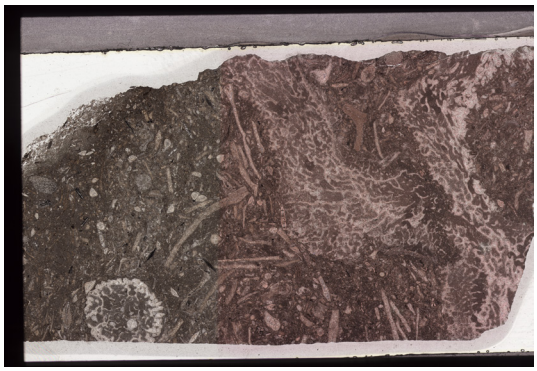

BB04.tif

BB05.tif

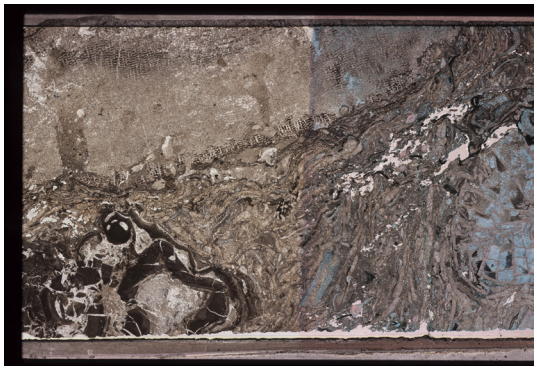

BB06.tif

BB09.tif

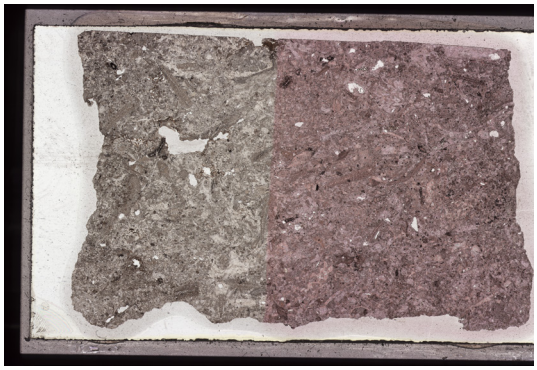

BB11.tif

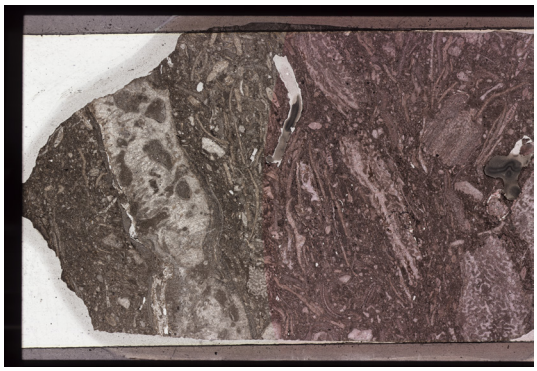

BB13.tif

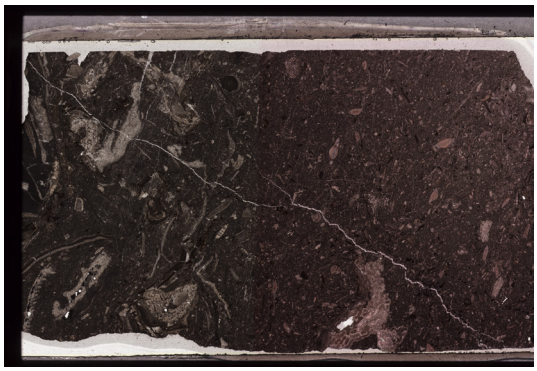

BB14.tif

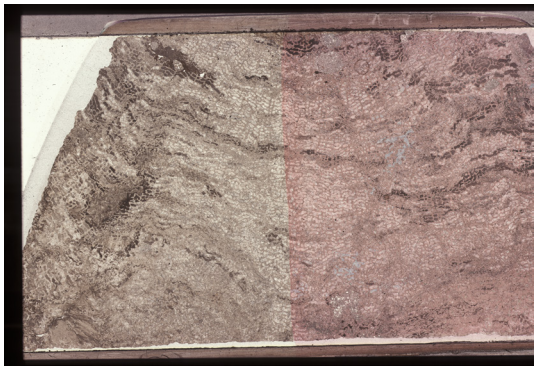

DPR02.tif

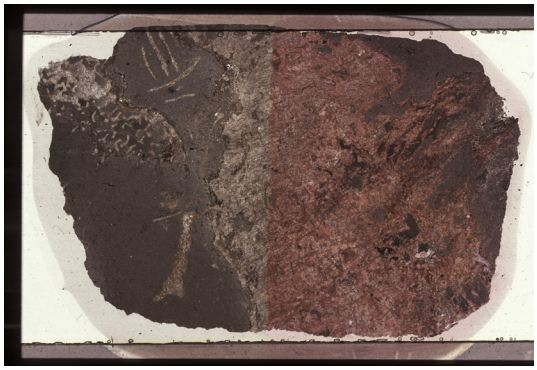

DPR04.tif

DPR05.tif

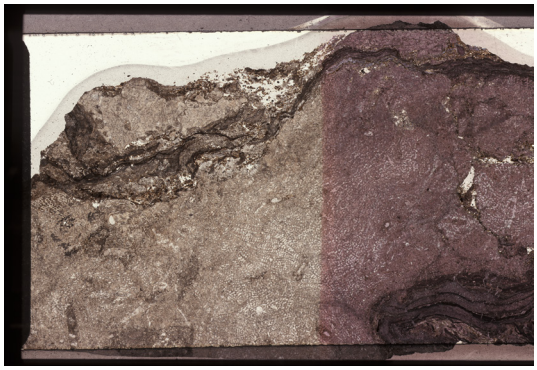

DPR09.tif

DPR10.tif

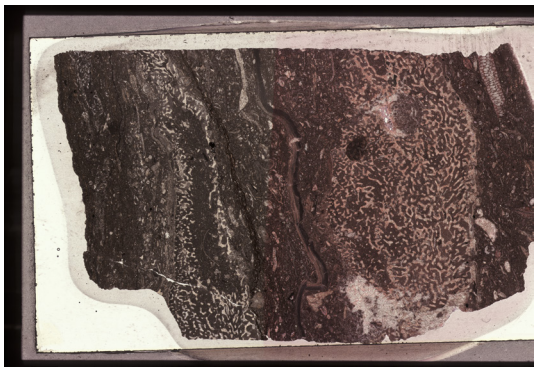

KB01.tif

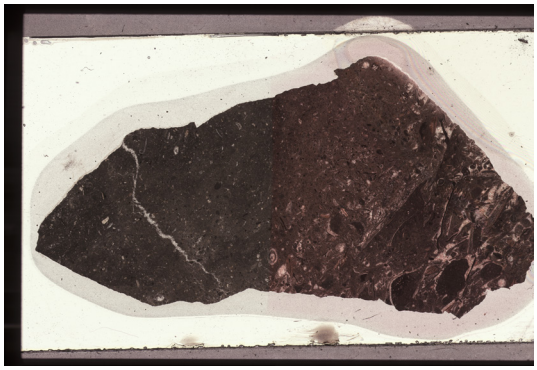

KB02.tif

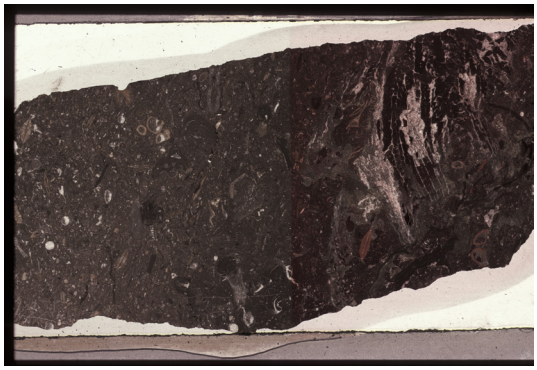

KB03.tif

KB05.tif

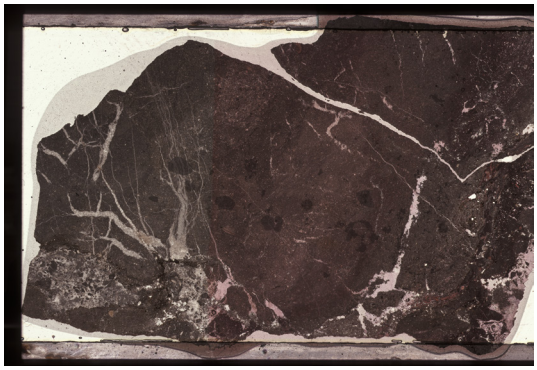

KB07.tif

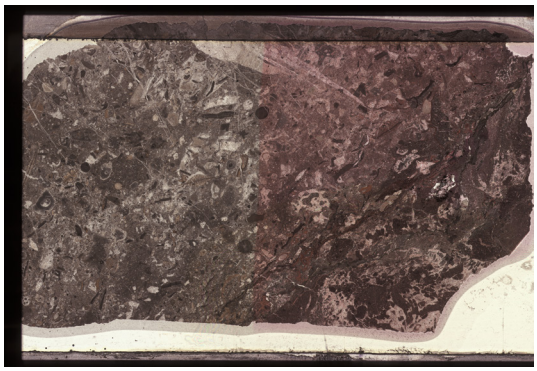

KB08.tif

KB09.tif

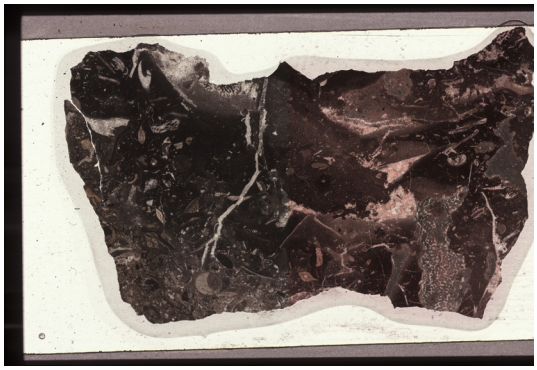

KB11.tif

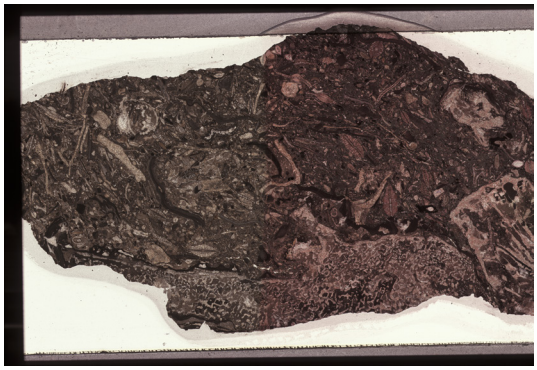

KB12.tif

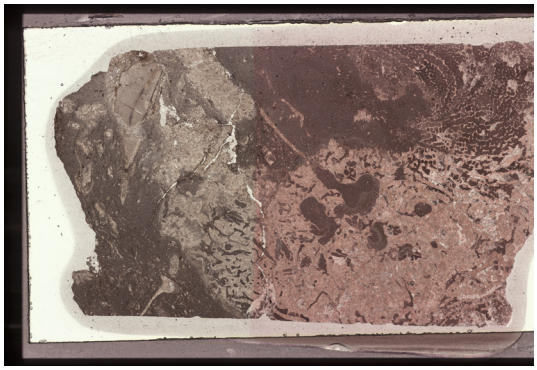

PA01.tif

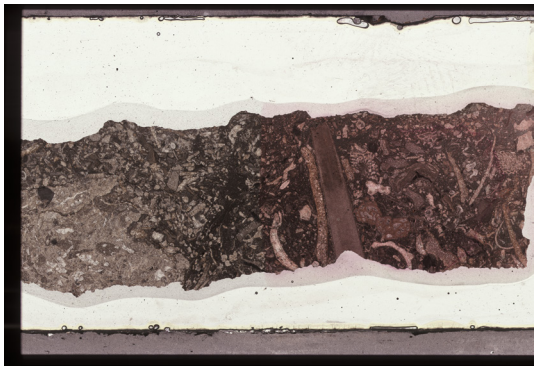

PA02.tif

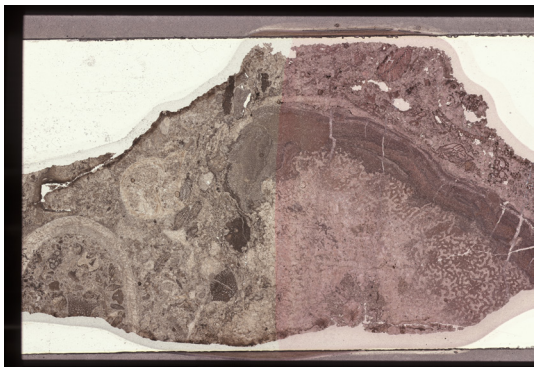

PA04.tif

PA05.tif

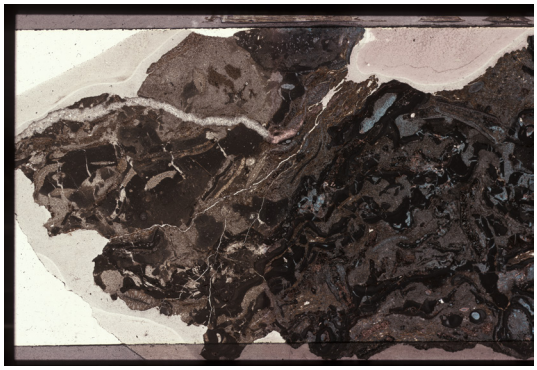

PA07.tif

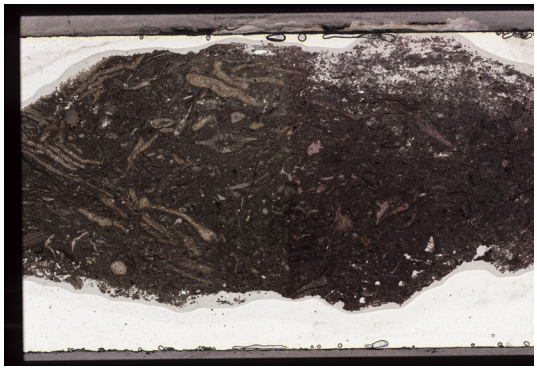

PB02.tif

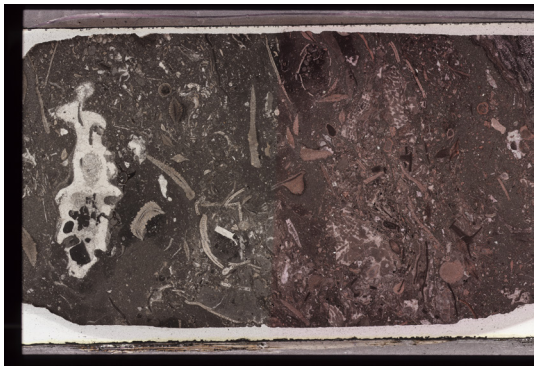

PC04.tif

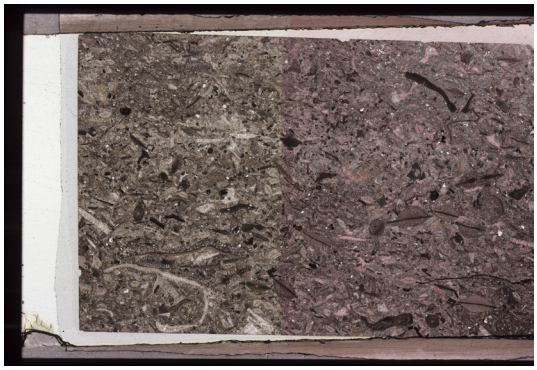

PC06.tif

PC08.tif

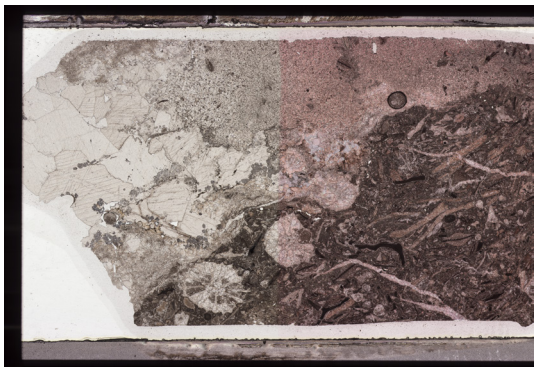

PC09.tif

PC11.tif

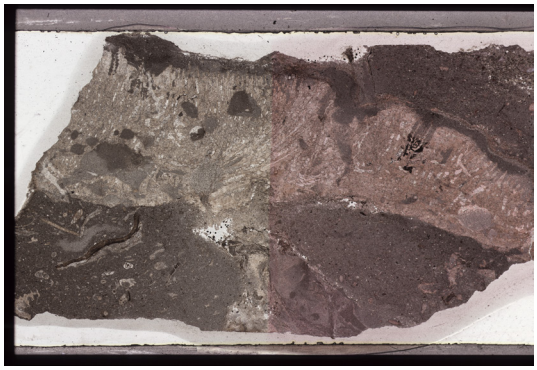

PC16.tif

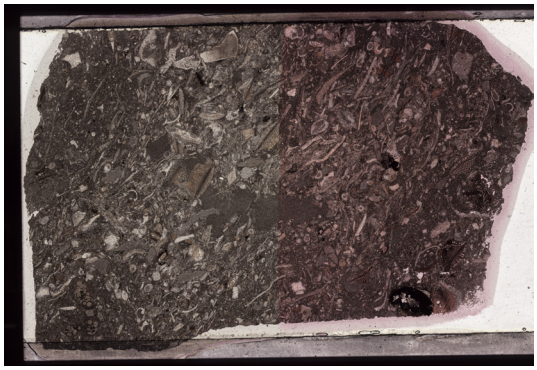

PC17.tif

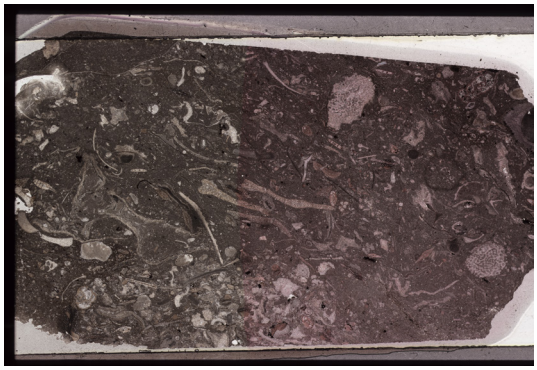

PC18.tif

PD01.tif

PD04.tif

PD05.tif

PD06.tif

PD08.tif

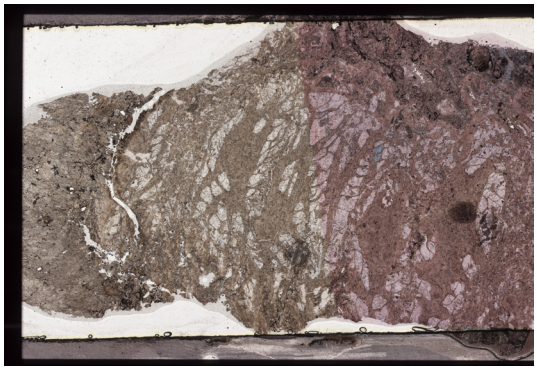

PE02.tif

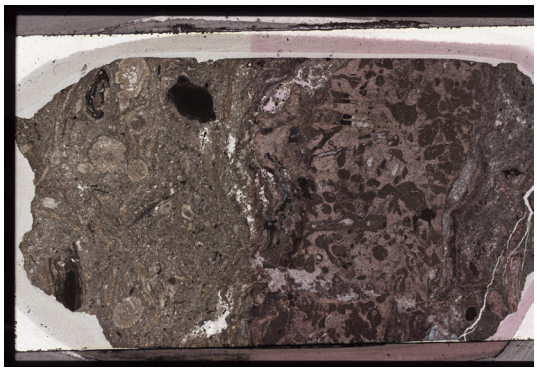

PE04.tif

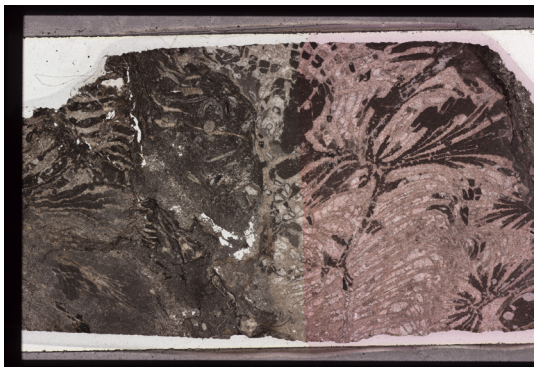

PE06.tif

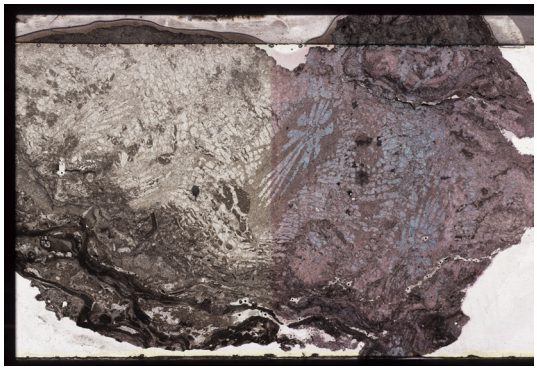

PE07.tif

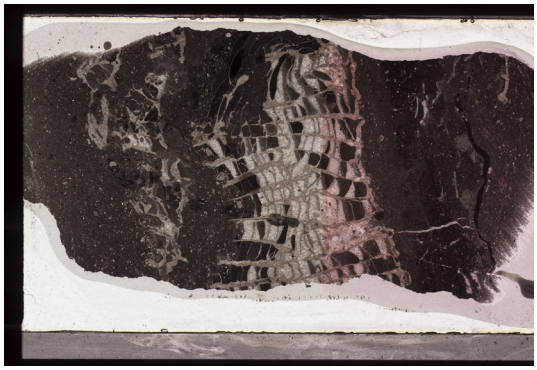

SA02.tif

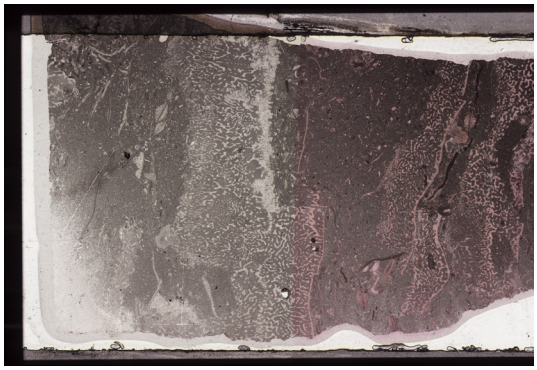

SA03.tif

SA04.tif

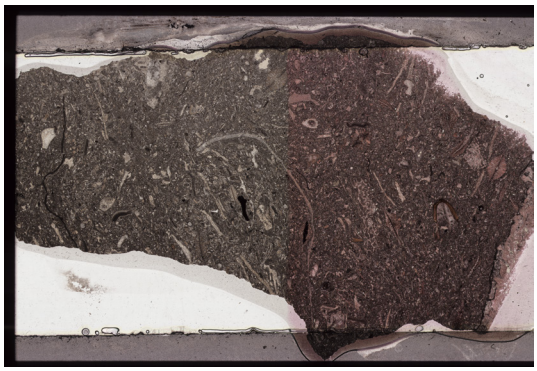

SA06b.tif

SB04.tif

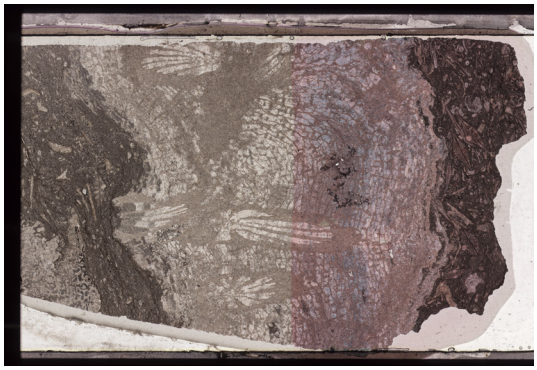

SB05.tif

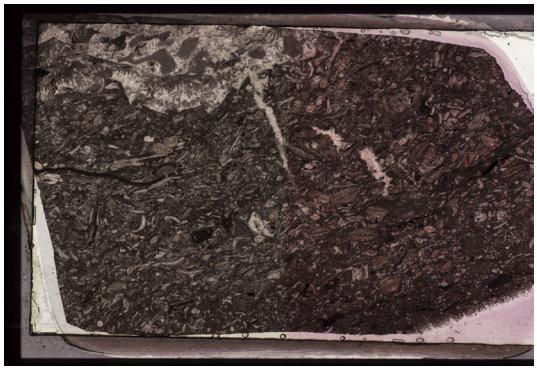

SB10.tif

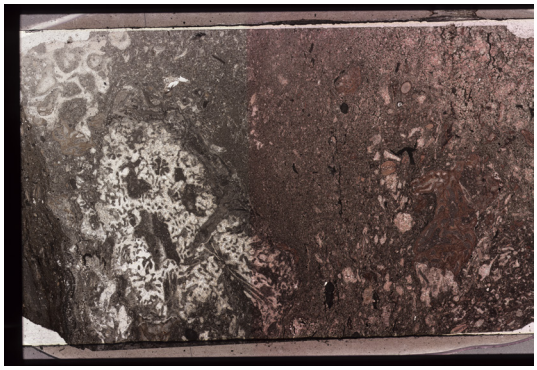

SB11.tif

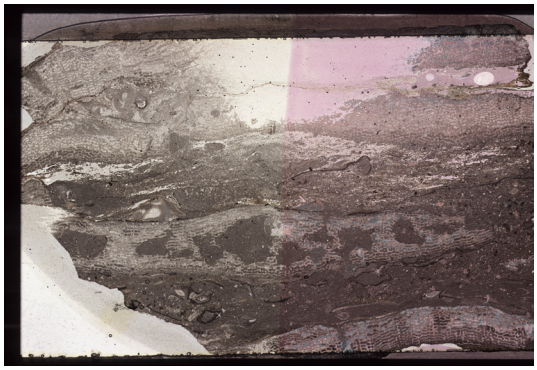

SC01.tif

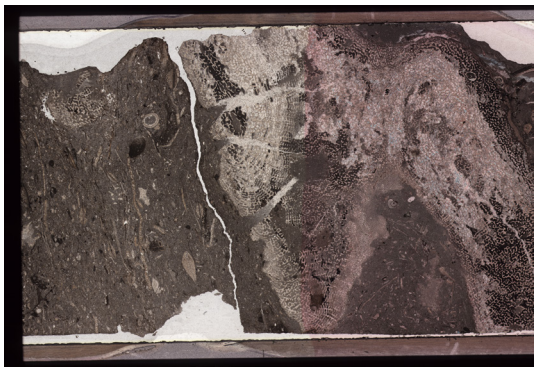

SC02.tif

SC04.tif

APPENDIX D

PETROGRAPHIC OBSERVATIONS AND PHOTOMICROGRAPHS RELATING TO CHAPTER 4

Appendix D1

Petrographic Observations Relating to Chapter 4

Section	Setting	Sample	Age Notes	Lithology (based on outcrop and thin section observations)
Gunung Pengabun Karstic	Shallow water platform deposits	BR80	Upper Eocene - Tb	Coarse/gravel coralline alage bioclastic pack/grain/rudstone
Gunung Pengabun Karstic	Shallow water platform deposits	BR81	Upper Eocene - Tb	Coarse/gravel *Discocyclina* and *Biplanispira* bioclastic pack/rudstone
Gunung Pengabun Karstic	Shallow water platform deposits	BR84	Upper Eocene - Tb	Medium *Discocyclina* bioclastic packstone
Gunung Pengabun Karstic	Shallow water platform deposits	BR86	Upper Eocene - Tb	Medium bioclastic packstone
Gunung Pengabun Karstic	Shallow water platform deposits	BR87	Upper Eocene - Tb	Medium coralline algae and *Pellatispira* bioclastic packstone
Western Bengalon	Shallow water platform deposits	BR110	Upper Eocene - Tb	Coarse bioclastic pack/grainstone
Gunung Pengabun Karstic	Shallow water platform deposits	GP1	Lower Oligocene - Tc	Branching coral wacke/floatstone
Gunung Pengabun Karstic	Shallow water platform deposits	GP3	Lower Oligocene - Tc	Coral bioclastic grain/rudstone
Gunung Pengabun Karstic	Shallow water platform deposits	GP6	Lower Oligocene - Tc	Coral and coralline algae bioclastic pack/rudstone
Gunung Pengabun Karstic	Shallow water platform deposits	GP8	Lower Oligocene - Tc	Coarse bioclastic packstone
Gunung Pengabun Karstic	Shallow water platform deposits	GP12b	Lower Oligocene - Tc	Coarse/gravel bioclastic pack/rudstone
Gunung Pengabun Karstic	Shallow water platform deposits	GP15	Lower Oligocene - Tc	Coarse/gravel bioclastic pack/rudstone
Gunung Pengabun Karstic	Shallow water platform deposits	GP22	Lower Oligocene - Tc	Medium/coarse bioclastic pack/grainstone
Gunung Pengabun Karstic	Shallow water platform deposits	GU1b	Lower Oligocene - Tc	Coarse imperforate foraminifera bioclastic pack/grainstone
Gunung Pengabun Karstic	Shallow water platform deposits	GU3	Lower Oligocene - Tc	Fine bioclastic pack/floatstone
Gunung Pengabun Karstic	Shallow water platform deposits	GU6	Lower Oligocene - Tc	Medium/coarse bioclastic pack/grainstone
Gunung Pengabun Karstic	Shallow water platform deposits	GU8c	Lower Oligocene - Tc	Medium bioclastic packstone
Gunung Pengabun Karstic	Shallow water platform deposits	GU12	Lower Oligocene - Tc	Medium/coarse bioclastic packstone
Gunung Pengabun Karstic	Shallow water platform deposits	GU13	Lower Oligocene - Tc	Medium bioclastic packstone
Gunung Pengabun Karstic	Shallow water platform deposits	GU17	Lower Oligocene - Tc	Fine branching coral wacke/floatstone
Gunung Pengabun Karstic	Shallow water platform deposits	GU23	Lower Oligocene - Tc	Medium bioclastic packstone
Gunung Pengabun Karstic	Shallow water platform deposits	GU29	Lower Oligocene	Medium bioclastic pack/grainstone
Gunung Pengabun Karstic	Shallow water platform deposits	GU40	Lower Oligocene - Tc	Medium/coarse imperforate foraminifera bioclastic pack/grainstone
Gunung Pengabun Karstic	Shallow water platform deposits	GB1a	Lower Oligocene - Tc	Coarse bioclastic pack/grainstone
Gunung Pengabun Karstic	Shallow water platform deposits	GB4b	Lower Oligocene - Tc	Fine/medium bioclastic pack/grainstone
Gunung Pengabun Karstic	Shallow water platform deposits	GB7a	Lower Oligocene - Tc	Medium/coarse bioclastic packstone
Gunung Pengabun Karstic	Shallow water platform deposits	GB10	Lower Oligocene - Tc	Fine bioclastic packstone
Gunung Pengabun Karstic	Shallow water platform deposits	GB20	Lower Oligocene - Tc	Fine/medium bioclastic pack/floatstone
Gunung Pengabun Karstic	Shallow water platform deposits	GB23a	Lower Oligocene - Tc	Medium bioclastic packstone
Gunung Pengabun Karstic	Shallow water platform deposits	GB23c	Lower Oligocene - Tc	Coarse imperforate foraminifera bioclastic pack/grainstone
Gunung Pengabun Karstic	Shallow water platform deposits	GB24	Lower Oligocene - Tc	Medium/coarse bioclastic pack/grainstone
Gunung Pengabun Karstic	Shallow water platform deposits	GB28	Lower Oligocene - Tc	Medium bioclastic packstone
Gunung Pengabun Karstic	Shallow water platform deposits	GB31	Lower Oligocene - Tc	Medium/coarse imperforate foraminifera bioclastic pack/grainstone
Gunung Pengabun Karstic	Shallow water platform deposits	GB34	Lower Oligocene - Tc	Coarse bioclastic packstone
Gunung Pengabun Karstic	Shallow water platform deposits	GB36	Lower Oligocene - Tc	Fine/medium imperforate foraminifera bioclastic grain/floatstone
Gunung Pengabun Karstic	Shallow water platform deposits	GB41	Lower Oligocene - Tc	Medium bioclastic pack/floatstone
Gunung Pengabun Karstic	Shallow water platform deposits	GB43	Lower Oligocene - Tc	*Nummulites* and *Heterostegina* coarse/gravel bioclastic pack/rudstone
Gunung Pengabun Karstic	Shallow water platform deposits	GB45	Lower Oligocene - Tc	*Nummulites* medium/coarse bioclastic packstone
Gunung Pengabun Karstic	Shallow water platform deposits	GB47	Lower Oligocene - Tc	*Nummulites* and *Heterostegina* coarse/gravel bioclastic pack/rudstone
Gunung Pengabun Karstic	Shallow water platform deposits	GB48	Lower Oligocene - Tc	Fine bioclastic pack/floatstone
Gunung Haji Karstic	Shallow water platform deposits	GKM1	Lower Miocene - Te5	Medium imperforate foraminifera bioclastic packstone
Gunung Haji Karstic	Shallow water platform deposits	GKM4	Lower Miocene - Te5	Coral and imperforate foraminifera bioclastic packstone
Gunung Haji Karstic	Shallow water platform deposits	GKM5	Lower Miocene - Te5	Coral and imperforate foraminifera wacke/floatstone
Gunung Haji Karstic	Shallow water platform deposits	GKM8	Lower Miocene - Te5	Branching coral bioclastic wacke/floatstone
Gunung Haji Karstic	Shallow water platform deposits	GKM9	Lower Miocene - Te5	Coarse/gravel bioclastic pack/rudstone
Gunung Haji Karstic	Shallow water platform deposits	GKM11	Lower Miocene - Te5	Coral wacke/floatstone
Gunung Haji Karstic	Shallow water platform deposits	GKM17	Lower Miocene - Te5	Coral bioclastic pack/floatstone
Gunung Haji Karstic	Shallow water platform deposits	GKM18b	Lower Miocene - Te5	Medium bioclastic wacke/pack/floatstone
Gunung Haji Karstic	Shallow water platform deposits	GKM20	Lower Miocene - Te5	Fine bioclastic wacke/packstone
Gunung Haji Karstic	Shallow water platform deposits	GS1	Lower Miocene - Te5-Tf1	Gravel grade bioclastic pack/grain/rudstone
Gunung Haji Karstic	Shallow water platform deposits	GS2	Lower Miocene - Te5-Tf1	Medium/coarse imperforate foraminifera bioclastic pack/grainstone
Gunung Haji Karstic	Shallow water platform deposits	GS5	Lower Miocene - Te5-Tf	Coarse/gravel bioclastic grain/rudstone
Gunung Haji Karstic	Shallow water platform deposits	GS7	Lower Miocene - Te5-Tf	Fine bioclastic packstone
Gunung Haji Karstic	Shallow water platform deposits	GS10	(Prob.) Lower Miocene - Te5-Tf	Fine/medium bioclastic packstone
Gunung Haji Karstic	Shallow water platform deposits	GS11	(Prob.) Lower Miocene - Te5-Tf	Fine/medium bioclastic wacke/packstone
Gunung Haji Karstic	Shallow water platform deposits	GS12	(Prob.) Lower Miocene - Te5-Tf	Fine/medium bioclastic wacke/packstone
Gunung Haji Karstic	Shallow water platform deposits	GS13	(Prob.) Lower Miocene - Te5-Tf	Fine/medium bioclastic packstone
Gunung Haji Karstic	Shallow water platform deposits	GH2	Lower Miocene - Te5-Tf	Medium bioclastic pack/grainstone
Gunung Haji Karstic	Shallow water platform deposits	GH6	Lower Miocene - Te5-Tf	Fine bioclastic wacke/packstone
Gunung Haji Karstic	Shallow water platform deposits	GH7	Lower Miocene - Te5-Tf	Medium/coarse bioclastic packstone
Gunung Haji Karstic	Shallow water platform deposits	GH10	(Prob.) Lower Miocene - Te5-Tf	Fine bioclastic wacke/packstone
Northern Bengalon	Steep platform margin deposits	HP1	Upper Oligocene - Te1-4	Medium/coarse bioclastic pack/rudstone
Northern Bengalon	Steep platform margin deposits	HP2	(Prob.) Upper Oligocene - Te1-4	Fine carbonate mud/wacke/floatstone containing coral clasts
Northern Bengalon	Steep platform margin deposits	HP3	(Prob.) Upper Oligocene - Te1-4	Medium/coarse bioclastic pack/grainstone
Northern Bengalon	Steep platform margin deposits	HP4	(Prob.) Upper Oligocene - Te1-4	Medium/coarse bioclastic pack/rudstone
Northern Bengalon	Steep platform margin deposits	HP5	Lower Miocene - Te5	Coarse/gravel bioclastic grain/rudstone
Northern Bengalon	Steep platform margin deposits	HP6	Lower Miocene - N5/Te5	Clast-supported limestone breccia
Northern Bengalon	Steep platform margin deposits	HP7	(Prob.) Lower Miocene - N5/Te5	Clast-supported limestone breccia
? Western Bengalon	? Steep platform margin deposits	BR39	Lower Miocene - Te5	Fine/medium bioclastic packstone
Western Bengalon	Steep platform margin deposits	BR41	Lower Miocene - Te5	Medium/coarse imperforate foraminifera bioclastic packstone
Western Bengalon	Steep platform margin deposits	BR43b	Lower Miocene - Te5	Recrystallized branching coral bioclastic pack/floatstone
Western Bengalon	Shallow water platform deposits	BR46	Lower Miocene - Te5	Medium bioclastic packstone
Western Bengalon	Shallow water platform deposits	BR48	Lower Miocene - Te5	Medium/coarse bioclastic packstone
Western Bengalon	Shallow water platform deposits	BR49	Lower Miocene - Te5	Medium bioclastic packstone
Western Bengalon	Shallow water platform deposits	BR53	Lower Miocene - Te6	Recrystalised and replaced mud/wacke/floatstone
Western Bengalon	Shallow water platform deposits	BR55	Lower Miocene - Te5	Medium/coarse bioclastic packstone
Western Bengalon	Shallow water platform deposits	BR56	Lower Miocene - Te5	Medium imperforate foraminifera bioclastic pack/floatstone
Western Bengalon	Steep platform margin deposits	BR61	Upper Oligocene - P22	Medium bioclastic packstone
Western Bengalon	Steep platform margin deposits	BR63	Upper Oligocene - P22	Fine grained coralline algae bioclastic pack/grainstone
Western Bengalon	Steep platform margin deposits	BR65	Upper Oligocene - P22	Coarsening upward coarse bioclastic packstone to pack/rudstone
Western Bengalon	Steep platform margin deposits	BR68	Upper Oligocene - P22	Medium/coarse bioclastic pack/grainstone
Western Bengalon	Steep platform margin deposits	BR73	Upper Oligocene - P22	Coarsening then fining upwards coarse bioclastic pack/grainstone to rudstone
Western Bengalon	Steep platform margin deposits	BR75a	Upper Oligocene - P22	Clast-supported limestone breccia
Western Bengalon	Steep platform margin deposits	BR75b	Upper Oligocene - P22	Clast-supported limestone breccia
Western Bengalon	Steep platform margin deposits	BR75d	Upper Oligocene - P22	Clast-supported limestone breccia
Western Bengalon	Steep platform margin deposits	BR76	Upper Oligocene - P22	Clast-supported limestone breccia
Northern Bengalon	Northern ramp-type margin deposits	HP8	Oligocene - (indet.) - ? P18-22	Fine planktonic foraminifera bioclastic wacke/packstone
Northern Bengalon	Northern ramp-type margin deposits	HP13	Upper Oligocene - P21-22	Fine/medium lithic planktonic foraminifera bioclastic packstone
Northern Bengalon	Northern ramp-type margin deposits	HP14	Upper Oligocene - P21-22	Fine lithic planktonic foraminifera bioclastic wacke/packstone

Components

Sample	Coral	Mollusc / Shell (G - Gastropod O - Ostracod)	Echinoderm / Sponge	Coralline Algae (Articulating)	Coralline Algae (B - Branching, E - Encrusting)	Green Algae (H - *Halimeda*, D - Dasycladacean)	Encrusting Foraminifera	Lepidocyclinids / *Nummulites* / Discocyclinids	*Pellatispira* / *Biplanispira*	Myogypsinids (Mo - Miogypsinoides, Mg - Miogypsina)	*Heterostegina* / *Cycloclypeus* / *Operculina*	Alveolinid	*Amphistegina*	Imperforate Foraminifera (inc. Miliolids, Austrotrillina)	Small Benthic Foraminifera (Rotalids)	Planktonic Foraminifera	Bryozoa	Peloids (Commonly Micritised Coralline Algae)	Lithified Carbonate Clasts	Other Lithic Clasts	Siliciclastics	Dolomite	Calcite Cement	Micrite	Phosphate/Iron	Porosity
BR80	P		P	D				P	P						P			P					C	C		P
BR81	P	P		C				A	P		C				P						C	C	P	A		
BR84		P	P					D	P						P			P					C	C		P
BR86	C	P	P	P			P	P	C					P	P				P				C	A		C
BR87			P	C	PB			P	C						R			C					P	A		
BR110		P	P	P	CE			A	C		P											P	P	A		
GP1	A	PG	P	P	PBE	PH	P	P							P	P	R	P					C	D		
GP3	A		P	C	CBE	PH		P			P	P			P			P					C	A		C
GP6	A		P	P	CE		P	P			P	P			P			P					A	A		C
GP8	C	P	P	A	PE			P			P	P			P	P		P			R		C	A		C
GP12b			C	A	CB		P	R			P	R			R								C	A		C
GP15	P	P	P	AE	PE			P			P	P			P	R			P				C	A		P
GP22	A		R	C	PE			R			R	P		P	P			P			P		A	A		C
GU1b		C	P	P				P?				C		C	P						P		A	C		P
GU3	P		P	P	RB			P						P	R			P					A	A		P
GU6	P	P	P	C	PBE	PH		P			R	R		P	P			R					A	A		C
GU8c		P	P	C	PE	PH		P			P	P		P				R					C	A		C
GU12	C		P	P			P	P			P	R			P			P					C	D		P
GU13		P	C	P				C			C	R		P	P								C	A		P
GU17	C	P	R		CE		C	P				R			R	R		P					C	A		P
GU23	C	P	P	P	CE		P	C			C	P		C	P			P					C	A		P
GU29			P	P	PB			P				C		C	P	P		P					D	C		R
GU40		P	P	C				R?				C		C	P			P					A	C		P
GB1a		P	P	P	PB			P			P	P		R	R								A	A		P
GB4b			P	C	PB							P		C	P			P			R		A	C		P
GB7a			P	C	PB			P			P	C		C	C			P					C	D		P
GB10			C	C		RH						P		A	C			P					C	C		P
GB20	C	P	P	PB		RH		C			P	P		P	P						P		C	D	P?	P
GB23a			P	C			P	C			P	P		P	P								C	A		P
GB23c			C	C	PB			P?				P		C	R			P					A	C		P
GB24	A	R	P	C	P			P			P	R		R									C	A		P
GB28		PG	P	P	CE			C			P		P	P	P						P		C	A		P
GB31	P		P	C				P			P	C		C	R								A	C		P
GB34	P	C	P	P	PB		R	C			C	P		P	R						P		C	A		P
GB36		R	P	C								C		C	P	R		R					A	C		P
GB41	P		P	C				P			P	P		P	P						C		C	A		P
GB43		P	P	P	CB		P	A			C				R						A		R	C		P
GB45			P	C	PE	RH	R	A			C	C			P			P					A	C		P
GB47			R	P	CBE			A			A				P						A		P	C		P
GB48	C	PG	P	P	PBE			P							P	R							C	A		P
GKM1		PG	P		RE	PH						P	R	C				R					A	A		P
GKM4	C	P					R	R				P		C		R		R					C	D		C
GKM5	C	P	R									P		C	R								C	D		C
GKM8	C	CG	P	P	PE	PH		C			P			P									C	D		R
GKM9	C	PG	P	P	PE	PH		C			P			P				R					A	A		P
GKM11	A			R										R									A	A		
GKM17	C	CG	R	P	PE	CH	P					T		P									A	D		C
GKM18b	C	P	P	R		CH		P			R	P	R	P	R	C					R		A	A		P
GKM20	C	P	P			CH		R			R	P	R	P	P			R					C	D		P
GS1	P	P	P	C	PE			C		PMg			R	R	P								D	P		C
GS2		P	C	P	PBE			P		PMg	P		R	C									A	A		P
GS5		C	P		CB			C		CMg	P		P	R	P			P					A	C		P
GS7	A	R	R	R	RB					RMg	P		R	R	R								A	A		P
GS10		P	P	P	CB			P		RMg	C		R	R	R	R		R					A	A		P
GS11		PG	P	P	CBE	CH	P	C		RMg	P				P	P							C	D		
GS12	R	PG	P	P	CBE	CH		C		RMg	P				P								C	D		
GS13	P		R	P				P						P	P	P							C	D		P
GH2	P	P	P	C	CBE	PH		P		PMg	P			P	P			C					D	P		P
GH6			P	P	CE		P	P		PMg				P	R								C	D		C
GH7		R	P	P				C		PMg				P	P	P							C	D		P
GH10		PG	P	P	PE			R						R	R			P					A	C		C
HP1	A	P	R	C	CE	RH	P	C					R		C	C					T		A	A		P
HP2	C		R	R											P	R							C	D		P
HP3	C	P	P	C	PB	RH	R	P			P				P	R					T		D	C		P
HP4	A		P	C	PB	RH		C			R			R	P	R					T		A	A		P
HP5		P	P	C	CB			C		RMgMo	R			R				C	C		R		D	P		R
HP6	C	R	P	P	PE	PH	P	P	P		R			P	P				C				A	A		C
HP7	C	P	R	P	PBE			C			R				P				C				C	A		P
BR39	C	P	P	P				R		PMg			P	P	P								D	C		R
BR41	P	CG	P	R		PH				RMg		C			P								A	C	R?	P
BR43b	C	P		P	PE	PH	C					C	R	P	P								A	A		
BR46		PG	P	P	PE	PH		P		PMg	P	C	P	R	P	P			P				A	C		P
BR48	C	PG	P		RE	CH	C	C		PMgMo		P		P					R		C		A	C		C
BR49		R	R		PB	PH		C		RMg	P	R			P	P							A	A	R?	P
BR53		CO		R										R									A	A		P
BR55	P	R	R	R			P	C		PMg	P	R	R	R	P	P							A	A		R
BR56	C	PG		R				P			C	C		P	P								C	A		R
BR61	C	P	P	P	PB			P?						P	R			C					A	A		P
BR63	C	PG	C	P	CBE			P			R	R		P	P	R		C					A	C		P
BR65	A	P	P	P	CBE			P			R			R	R								A	A		C
BR68		PG	P	P	CBE		P	P			R			P				R					D	C		P
BR73	C	R	P	P	CBE			P			R			P	R			P	P				A	A		R
BR75a	A	P	C	P	PE			P			P			R	R	P		P	C				A	A		P
BR75b	A	PG		P	CB			P			P			R	P			R					D	P		
BR75d	A	PG	P	C	CBE			R			P			R	R								A	A		R
BR76	C	R		P	CE						T			P	P			P					A	A		P
HP8								R							P	A					R		A	A		
HP13			R												P	A					C		A	A		P
HP14			R	T											P	P					P		A	A	R?	

Texture, Reservoir Quality and Porosity

Sample	Fragmentation / Abrasion	Encrustation	Bioerosion	Grain Size	Sorting	Fabric (A - Alignment, CE - Compaction Enhanced)	Reservoir Quality: Low	Moderate	Good	Excellent	Visible Porosity (Based On Petrographic & Hand Specimin Observations)		C- Connected, PC - Partially Connected, NC - Non Connected	Micropores	Rounded	Irregular	Linear (Includes Fractures)	Porosity Type
BR80	1 or 2	0	1 or 2	M-G	Moderate						Minor	<5%	NC	<1%		<5% <250 µm		Matrix microporosity, intercrystalline
BR81	1 or2	0	3	M-G	Poor						N/A							N/A
BR84	2 or 3	0	3	M-G	Moderate						Minor	<5%	NC			<5% <100 µm		Intercrystalline/Interparticle
BR86	1	0	2	M-P	Poor						Moderate	<10%	PC			<10% <1 mm	<1% <20 mm	Intercrystalline, Fracture porosity - ARTIFACT?
BR87	3	0 or 1	2 or 3	M-G	Poor						N/A							N/A
BR110	2	0 or 1	0 or 1	M-P	Moderate						N/A							N/A
GP1	1	1	3	M-P	Poor						N/A							N/A
GP3	1	1	2 or 3	M-P	Poor						Moderate	<10%	C				<10% <25 mm	Solution enhanced channel porosity
GP6	1	1 or 2	2 or 3	M-P	Poor						Moderate	<15%	PC			<5% <250 µm	<10% <25 mm	Intercrystalline/Interparticle porosity, Solution enhanced channel porosity
GP8	0 or 1	1	2 or 3	M-P	Poor						Minor	<5%	NC			<5% <250 µm		Intercrystalline/interparticle porosity
GP12b	0 or 1	3	0 or 1	M-P	Moderate						Moderate	<10%	NC			<10% <100 µm		Intercrystalline/interparticle porosity
GP15	1	3	1 or 2	M-P	Poor						Minor	<5%	PC			<5% <100 µm	<1% <30 mm	Intercrystalline, solution enhanced channel porosity
GP22	0 or 1	0 or 1	3	M-P	Poor						Moderate	<15%	NC			<10% <100 µm	<10% <25 mm	Intercrystalline/Interparticle porosity, Solution enhanced channel porosity
GU1b	1 or 2	0 or 1	1	M-G(P)	Moderate						Minor	<5%	NC			<5% <250 µm		Intercrystalline - ARTIFACT?
GU3	1	0 or 1	2	M-P	Poor						Minor	<5%	NC			<5% <100 µm		Intercrystalline/Interparticle
GU6	1 or 2	1	1 or 2	M-vc	Moderate						Moderate	<10%	C			<1% <100 µm	<10% <30 mm	Intercrystalline/Interparticle, fracture porosity
GU8c	1	1	2	M-G	Moderate						Moderate	<10%	PC			<5% <250 µm	<5% <20 mm	Intercrystalline/interparticle, solution enhanced channel porosity
GU12	1	1	1	M-P	Poor						Minor	<5%	NC	<1%		<5% < 200 µm		Matrix microporosity, solution enhanced Intercrystalline/interparticle porosity
GU13	1	0	2	M-P	Poor						Minor	<5%	PC			<5% < 200 µm		Intercrystalline/interparticle
GU17	1	3	1	M-P	Poor						Poor	<5%	PC			<1% <250 µm	<5% <30 mm	Intercrystalline, solution enhanced channel porosity
GU23	1	3	1 or 2	M-P	Poor						Minor	<5%	NC	<1%			<5% <10 mm	Matrix microporosity, channel porosity
GU29	2	0	1 or 2	M-G	Poor						Minor	<1%	NC			<1% <100 µm		Intercrystalline/interparticle
GU40	2	0	1 or 2	M-vc	Moderate						Minor	<5%				<5% < 200 µm		Intercrystalline
GB1a	2	0	1	M-G	Poor						Moderate	<10%	PC			<10% <250 µm	<1% <1 mm	Intercrystalline/Interparticle, Fracture porosity
GB4b	1 or 2	0	2	M-vc	Poor						Minor	<5%	NC			<5% <250 µm		Intercrystalline/Interparticle, Mouldic porosity
GB7a	1 or 2	0	2	M-c	Poor						Minor	<5%	NC			<5% <250 µm		Intercrystalline/Interparticle
GB10	1 or 2	1	1 or 2	M-m	Poor						Minor	<5%	PC			<5% <150 µm	<1% <10mm	Intercrystalline//interparticle, solution enhanced channel
GB20	1	0	2	M-P	Poor						Moderate	<20%	PC	<10%		<5% <250 µm	<5% <25 mm	Matrix microporosity, intercrystalline/interparticle, solution enhanced channel
GB23a	2	0 or 1	2	M-vc	Poor						Minor	<5%	NC			<5% <250 µm		Intercrystalline/Interparticle
GB23c	1	0	2	M-vc	Poor						Minor	<5%	NC			<5% <250 µm		solution enhanced?? - Intercrystalline/Interparticle
GB24	0 or 1	3	1	M-P	Poor						Minor	<1%	NC	<1%				Matrix microporosity
GB28	1	2	1 or 2	M-G	Moderate						Minor	<5%	NC			<5% <100 µm	<1% <5 mm	Interparticle, fracture porosity
GB31	1 or 2	0	2 or 3	M-vc	Moderate						Minor	<5%	PC			<5% <100 µm		interparticle/intercrystalline
GB34	2	0 or 1	3	M-G	Poor						Moderate	<10%	PC			<10% <250 µm	<1% <10 mm	Interparticle, solution enhanced channel porosity
GB36	0 or 1	0	3	M-vc	Poor						Moderate	<20%						ARTIFACT
GB41	0 or 1	0	1 or 2	M-c(G)	Poor						Major	<25%						ARTIFACT
GB43	2 or 3	2 or 3	1	M-G	Poor						Minor	<5%	PC			<5% <100 µm		Interparticle
GB45	1 or 2	1	1	M-P	Poor						Moderate	<10%	PC	<5%		<5% <100 µm		Matrix microporosity, interparticle/intercrystalline
GB47	0 or 1	2	1	M-P	Poor						Minor	<1%	NC	<1%				Matrix microporosity
GB48	1	1	3	M-P	Poor						Minor	<5%	PC	<1%		<5% <250 µm	<1% <10 mm	Matrix microporosity, intercrystalline/interparticle, crystalisation reduced fracture
GKM1	0 or 1	0	3	M-G	Moderate						Minor	<5%	NC	<1%		<5% <300 µm		Matrix microporosity, intercrystalline
GKM4	1	0 or 1	3	M-P	Moderate						Moderate	<15%	NC	<10%		<5% <100 µm		Matrix microporosity, intercrystalline
GKM5	0 or 1	0 or 1	2 or 3	M-P	Moderate						Moderate	<10%	NC	<1%		<10% <100 µm		Matrix microporosity, intercrystalline
GKM8	1 or 2	1 or 2	2 or 3	M-P	Poor						Minor	<1%	NC			<1% <1 mm		Intraparticle
GKM9	1 or 2	1	3	M-P	Poor						Minor	<1%	NC	<1%		<1% <250 µm		Matrix microporosity, mouldic -ARTIFACT
GKM11	0	0	3	M-P	N/A						N/A							N/A
GKM17	0 or 1	0 or 1	2	M-P	Poor						Moderate	<10%	PC	<10%		<1% <250 µm	<1% <5 mm	Matrix microporosity, intercrystalline, fracture/(dissolution) channel porosity
GKM18b	1 or 2	0	2 or 3	M-P	Poor						Minor	<1%	NC	<1%		<1% <250 µm		Matrix Microporosity
GKM20	1 or 2	0	1 or 2	M-P	Moderate						Minor	<5%	NC	<5%				Matrix microporosity
GS1	1	1	2 or 3	M-P	Poor						Moderate	<10%	NC	<1%		<10% <300 µm		Matrix microporosity, intercrystalline (solution enhanced?) to vuggy porsoity
GS2	2	1 or 2	3	M-P	Poor						Minor	<5%	C				<5% <25 mm	Solution enhanced channel porosity
GS5	2	0 or 1	3	M-G	Poor						Minor	<5%	NC				<5% <300 µm	Solution enhanced? Intercrystalline porosity
GS7	0 or 1	0 or 1	2 or 3	M-C	Poor						Minor	<5%	C	<1%			<5% <25 mm	Solution enhanced channel porosity
GS10	1 or 1	0	2 or 3	M-P	Poor						Minor	<5%	NC	<1%			<5% <25 mm	Matrix microporosity, solution enhanced channel porosity
GS11	0 or 1	2	2	M-P	Poor						N/A							N/A
GS12	0 or 1	2	2 or 3	M-P	Poor						N/A							N/A - ARTIFACT
GS13	1	0 or 1	1	M-P	Poor						Minor	<5%	PC			<3% <750 µm	<2% <50 mm	Interparticle, intraparticle, minor stylolitic/fracture, minor coralline biomouldic
GH2	1 or 2	1	2 or 3	M-P	Poor						Minor	<1%	NC	<1%			<1% <2 mm	Intercrystalline microporosity, fracture porosity
GH6	1 or 2	2	1	M-P	Poor						Moderate	<15%	PC	<5%		<5% <250 µm	<5% <25 mm	Matrix microporosity, intercrystalline, crystalisation reduced/solution enhanced channel porosity
GH7	2	0	2	M-vc	Moderate						Minor	<5%	NC			<5% <250 µm		Interparticle, intraparticle, stylolitic
GH10	1 or 2	0 or 1	1	M-G	Poor						Moderate	<10%	PC	<5%			<5% <50 mm	Matrix microporosity, intercrystalline, crystalisation reduced/solution enhanced fracture porosity
HP1	2	0 to 1	2 to 3	M-G(P)	Poor						Minor	<5%	PC	<5%		<1% <500 µm		Intergranular, matrix microporosity (solution related?)
HP2	2 or 3	0	3	M-P	Moderate						Minor	<5%	PC				<5% <300 µm	Non-cemented fracture porosity
HP3	2 to 3	0 to 1	2	M-G(P)	Poor						Minor	<5%	C			<5% <1 mm		Intercrystalline
HP4	1 or 2	0	2	M-P	Poor						Minor	<5%	NC			<5% <300 µm		Intercrystalline and intergranular
HP5	0 or 1	0	3	M-G(P)	Moderate						Minor	<1%	NC			<1% <100 µm		Intercrystalline
HP6	1	1 to 2	2 to 3	M-P	Poor						Moderate	<10%	PC	<5%		<5% <400 µm	<1% <500 µm	Intergranular matrix microporosity, Linear dissolution, (Intercrystalline- ARTIFACT)
HP7	1	2	2 to 3	M-P	Poor						Minor	<5%	PC	<5%			<1% <2 mm	Linear dissolution, intercrystalline (incl. matrix) microporosity
BR39	2 or 3	0	1	M-P	Moderate						Minor	<1%	NC			<1% <100 µm		Intercrystalline
BR41	2 or 3	0	1 or 2	M-P	Poor						Minor	<5%	NC			<5% <1 mm		Intercrystalline/Interparticle
BR43b	0 or 1	2	1	M-P	Poor						N/A							N/A
BR46	1	1	2	M-vc(G)	Moderate						Minor	<5%	NC			<5% <300 µm		Intercrystalline
BR48	1 or 2	2	1 or 2	M-P	Poor						Moderate	<10%	PC			<10% <300 µm	<1% <10 mm	Solution enhanced intercrystalline and channel porosity
BR49	2	0	2 or 3	M-vc(G)	Poor						Minor	<5%	NC			<5% <250 µm		Intercrystalline/interparticle
BR53	0 or 1	0	1	M-vc	Moderate						Minor	<1%	PC			1% <250 µm	<1% <10 mm	Vuggy, fracture
BR55	1 or 2	0 or 1	1 or 2	M-P	Poor						Minor	<1%	NC			1% <250 µm	<1% <20 mm	Intercrystalline/interparticle, solution enchanced channel
BR56	1	0	0 or 1	M-P	Moderate						Minor	<1%	NC	<1%				Matrix microporosity
BR61	0 or 1	0	1 or 2	M-P	Moderate						Minor	<5%	NC			<5% <300 µm		Intercrystalline
BR63	1 or 2	3	2	M-P	Poor						Minor	<5%						ARTIFACT
BR65	1 or 2	2 or 3	2	M-P	Poor						Moderate	<10%	PC			<5% <250 µm	<5% <25 mm	Intercrystalline/Interparticle, Solution enchanced channel porosity
BR68	2	0	2 or 3	M- G	Poor						Minor	<5%				<5% <250 µm	<1% <15 mm	Intergranular/Interparticle, Fracture porosity
BR73	1 or 2	0 or 1	2 or 3	M-P	Poor						Minor	<1%	NC	<1%				Matrix microporosity
BR75a	2	0 or 1	2 or 3	M-P	Poor						Minor	<5%	NC	<1%		<5% <250 µm		Matrix microporosity, Intercrystalline-ARTIFACT
BR75b	1 or 2	2 or 3	3	M-P	Poor						N/A							N/A
BR75d	2 or 3	0 or 1	3	M-P	Poor						Minor	<1%	NC	<1%				Matrix microporosity
BR76	2 or 3	2 or 3	3	M-P	Poor						Minor	<5%	NC	<5%				Matrix microporosity
HP8	0	0	0 to 1	M-(vf)	Very Well						Minor	<1%	NC	<1%				Matrix microporosity
HP13	1	0	1 to 2	M-f	Moderate						Minor		NC			<5% <100 µm		Intercrystalline
HP14	0	0	0 to 1	M-vf	Very Well						N/A							N/A

Diagenesis

Sample	Micritisation	Isopachous Fringing Cement (Fb - Fibrous, F - Ferroan, X - Non Ferroan)	Syntaxial Overgrowth (Selected Bioclasts - SB)	Bladed (B) to Radiaxial (R) Calcite (F- Ferroan, X - Non Ferroan) (W - cement within clast, B - cement between clasts)	Botryoidal Calcite (F - Ferroan, X - Non Ferroan)	Alveolar Textures	Karstic(?) Dissolution (prior to reworking and redeposition of clasts)	Early Fracturing/Brecciation	Banded Bladed Spary Calcite (F - Ferroan, X - Non Ferroan) (W - cement within clast, B - cement between clasts)	Fine crystal silt -C / Nonlaminated Sediment Infiltration - S (within clasts)	Mechanical Bioclast / Grain Compaction	Mechanical Fracturing	Dissolution (SB - Selected Bioclasts)	Granular Mosaic Neomorphic Calcite (D - Drusy, F - Ferroan, X - Non Ferroan)	Dog Tooth Calcite (F - Ferroan, X - Non Ferroan)	Equant Calcite (D - Drusy, G - Granular, B - Blocky, F - Ferroan, X - Non Ferroan)	Mechanical Fracturing	Grain suturing	Dissolution Seams	Stylolites	Dolomite (M - Microdolomite Rhombs, R - Replacive)	Radiaxial Fibrous Calcite (F - Ferroan, X - Non Ferroan)	Mechanical Fracturing
BR80	1		1SB								2	2		3X		3GX							
BR81	1		1SB								2	2		3X		3GX			4		5MR		
BR84	1		1SB								2	2		3X		3GX							
BR86	1		1SB									2		3X	3X	3GX							
BR87	1		1SB									2		3X		3GX							
BR110	1		1SB									2		3X		3GX			4		4MR		
GP1	1	1FbX												2X		2BGX	3						
GP3	1	1FbX									2	2		3X		3GX		4	4				
GP6	1	1X									2	2		3X		3GBX		4	4	4			
GP8	1											2	3SB	4X		4G(B)X							
GP12b	1										2	2		3X		3GBX		4	4				
GP15	1										2	2		3X		3GX		4	4				
GP22	1										2	2		3X		3G(B)X			4				
GU1b	1											2		3X		3GBX			4				
GU3	1											2		3X		3(D)BX	4		4				
GU6	1										2			3X		3BX			5	5			
GU8c	1										2	2		3X		3GX		4	4	4			
GU12	1													2X		2GBX		3	3				
GU13	1													2X		2GBX		3	3				
GU17	1											2		3X		3GBX		4	4				
GU23	1											2		3X		3GBX		4	4				
GU29	1											2		3X		3GBX							
GU40	1													2X		2GX							
GB1a	1											2		3X		3GX	4						
GB4b	1		1SB								2	2		3X		3GBX							
GB7a	1	1FbX	1SB								2	2		3X		3GX							
GB10	1											2		3X		3GX		4	4				
GB20	1										2			2X		2GX		3	3				
GB23a	1											2		3X		3GX		4	4				
GB23c	1		1SB								2	2		3X		3GX							
GB24	1											2		3X		3GX							
GB28	1		1SB								2	2		3X		3GX			4				
GB31	1		1SB								2	2		3X		3GX							
GB34	1		1SB								2	2		3X		3GX		4	4				
GB36	1											2		3X		3GBX			4				
GB41	1	1FbX									2	2		3X		3GX			4	4			
GB43	1										2	2		3X		3GX			4				
GB45	1										2			3X		3GX			4				
GB47	1										2			3X		3GX			4				
GB48	1											2		3X		3GX							
GKM1	1													2X		2G(B)X							
GKM4	1											2		3X		3GBX							
GKM5	1											2		3X		3GBX							
GKM8	1											2		3X		4GBX			5				
GKM9	1												2SB	3X		3GBX							
GKM11	1													2X					3				
GKM17	1											2		3X		3GBX			4				
GKM18b	1													2X		2GBX			3				
GKM20	1											2		3X		3GBX							
GS1	1			2BRX							3	3		4X		4(G)BX		5	5				
GS2	1													2X		2GBX		3	3				
GS5	1	1FbX	1SB								2	2		3X		3GBX							
GS7	1										2	2		3X		3GBX		4	4				
GS10	1											2		3X		3GX		4		4			
GS11	1											2		3X		3GX							
GS12	1											2		3X		3GX							
GS13	1											2	3SB	3X		3BX		4					
GH2	1										2	2		3X		3GBX							
GH6	1											2		3X		3GX		4	4				
GH7	1	1FbX										2		3X		3BX		4					
GH10	1										2	2		3X		3G(B)X							
HP1	1										2		2SB	3X		3GBX			4				
HP2	1										2	2	3SB	4X		4DGBX							
HP3	1		1SB								2	2	3SB	4X		4(D)GBX							
HP4	1										2			3X		3GBX							
HP5	1	2FbX	2SB								2			3X		3G(B)X	4						
HP6	1										2	2		3X		3GX		4	4	4			
HP7	1										2			3X		3GX		4	4	4			
BR39	1	2FbX												3X	3X	3GBX							
BR41	1			2BX							3			4X	4X	4GBX			5	5			
BR43b	1													3X		3GBX			4				
BR46	1											2		3X		3GBX							
BR48	1												2SB	3X		3GBX		4	4				
BR49	1													2X		2(D)GBX			3				
BR53	1					2		2Br		2C				3X		3D(B)X	4						
BR55	1											2		3X	3X	3(D)GBX		4	4				
BR56	1											2		3X		3GBX			4				
BR61	1		1SB									2		3X		3GBX							
BR63	1		1SB								2	2		3X		3GBX			4				
BR65	1		1SB								2	2		3X		3DGBX		4	4				
BR68	1		1SB									2		3X		3GBX							
BR73	1		1SB									2		3X		3GBX							
BR75a	1			2BRX										3X		3GBX							
BR75b	1			2XB										3X	3X	3(G)BX							
BR75d	1											2		3X	3X	3GBX							
BR76	1			2BRX								3		4X		4GBX							
HP8												1		2X		2GX							
HP13											1			2X		2GX			3				
HP14												1		2X		2GX							

Northern Bengalon	Northern ramp-type margin deposits	HP17	Upper Oligocene - P21-21	Clast-supported limestone breccia
Northern Bengalon	Northern ramp-type margin deposits	HP18	Upper Oligocene - P21-22	Medium/coarse bioclastic pack/grainstone
Northern Bengalon	Northern ramp-type margin deposits	HP19	Upper Oligocene - P21-22	Fine, recrystalised planktonic foraminifera bioclastic pack/grainstone
Northern Bengalon	? Bathyl to upper bathyl deposits	HP24	Lower Miocene - N4	Medium lithic bioclastic packstone
Western Bengalon	Bathyl to upper bathyl deposits	BR1d	? Lower Miocene - N4	Coarse/gravel bioclastic pack/grain/rudstone
Western Bengalon	Bathyl to upper bathyl deposits	BR2	Lower Miocene - N4	Coarse/gravel bioclastic pack/grain/rudstone
Western Bengalon	Bathyl to upper bathyl deposits	BR7a	Lower Miocene - N4	Carbonate clasts from limestone breccia
Western Bengalon	Bathyl to upper bathyl deposits	BR7b	Lower Miocene - N4	Coarse/gravel bioclastic pack/grain/rudstone
Western Bengalon	Bathyl to upper bathyl deposits	BR8a	?	Clast-supported limestone breccia
Western Bengalon	Bathyl to upper bathyl deposits	BR8b	?	Clast-supported limestone breccia
Western Bengalon	Bathyl to upper bathyl deposits	BR8c	?	Clast-supported limestone breccia
Western Bengalon	Bathyl to upper bathyl deposits	BR9a	?	Clast-supported limestone breccia dominated by coral clasts
Western Bengalon	Bathyl to upper bathyl deposits	BR9b	?	Clast-supported limestone breccia dominated by coral clasts
Western Bengalon	Bathyl to upper bathyl deposits	BR10a	Lower Miocene - N4	Clast-supported limestone breccia fining up to a bioclastic pack/grainstone
Western Bengalon	Bathyl to upper bathyl deposits	BR10b	Lower Miocene - N4	Clast-supported limestone breccia fining up to a bioclastic pack/grainstone
Western Bengalon	Bathyl to upper bathyl deposits	BR14	Lower Miocene - N4	Laminated planktonic foraminifera bioclastic packstone
Western Bengalon	Bathyl to upper bathyl deposits	BR16a	Lower Miocene - N4	Clasts from clast supported limestone breccia
Western Bengalon	Bathyl to upper bathyl deposits	BR16b	Lower Miocene - N4	Clasts from clast supported limestone breccia
Western Bengalon	Bathyl to upper bathyl deposits	BR18	Lower Miocene - N5	Clast-supported limestone breccia
Western Bengalon	Bathyl to upper bathyl deposits	BR25	Lower Miocene - N4	Coarse/gravel bioclastic pack/grainstone
Western Bengalon	Bathyl to upper bathyl deposits	BR28	Lower Miocene - N4	Clast-supported limestone breccia
Western Bengalon	Bathyl to upper bathyl deposits	BR92a	Probably Upper Oligocene - P21	Clasts from clast supported limestone breccia
Western Bengalon	Bathyl to upper bathyl deposits	BR92b	Probably Upper Oligocene - P21	Clast-supported limestone breccia
Western Bengalon	Bathyl to upper bathyl deposits	BR93	Probably Upper Oligocene - P21	Gravel grade bioclastic pack/rudstone from fining upwards top to limestone breccia
Western Bengalon	Bathyl to upper bathyl deposits	BR95	Probably Upper Oligocene - P21	Medium/coarse quartzose bioclastic pack/grainstone
Western Bengalon	Bathyl to upper bathyl deposits	BR97	Probably Upper Oligocene - P21	Fining upwards coarse to fine/medium bioclastic packstone
Western Bengalon	Bathyl to upper bathyl deposits	BR99	Probably Upper Oligocene - P21	Fine planktonic foraminifera wackestone
Western Bengalon	Bathyl to upper bathyl deposits	BR102	Probably Upper Oligocene - P21	Fining upwards gravel to fine/medium bioclastic pack/rudstone
Western Bengalon	Bathyl to upper bathyl deposits	BR104	Probably Upper Oligocene - P21	Fining upwards gravel to medium bioclastic pack/rudstone
Western Bengalon	Bathyl to upper bathyl deposits	PR5	Oldest Poss. Lower Miocene - Te5-Tf	Clast-supported limestone breccia
Western Bengalon	Bathyl to upper bathyl deposits	QB1	Probably Lower Miocene - N4	Fining upwards gravel to medium limestone breccia/bioclastic packstone
Western Bengalon	Bathyl to upper bathyl deposits	QB7	Probably Lower Miocene - N4	Clast-supported limestone breccia
Western Bengalon	Bathyl to upper bathyl deposits	QB11a	Probably Upper Oligocene - P21	Clasts of clast supported llimestone breccia (QB10)
Western Bengalon	Bathyl to upper bathyl deposits	QB11b	Probably Upper Oligocene - P21	Clasts of clast supported llimestone breccia (QB10)
Western Bengalon	Bathyl to upper bathyl deposits	QB12	Probably Upper Oligocene - P21	Fining upwards bioclastic pack/grainstone

HP17	C			P				P		P				P	P		C	P	C	C			1 or 2	0	1 or 2	M-P	Poor
HP18			C	P	CBE			C		C		P		P	A			P	A	C			0 to 1	0 to 1	2 to 3	M - G	Poor
HP19			P	R										C		P		R	A	C			0 to 1	0	2 to 3	M - vf	Well
HP24		P	P	C	PBE			C		P				R	R			P	C	A		C	2	0 or 1	2 or 3	M-vc	Moderate
BR1d			P	C	CB	RH		R				R	P		P	P		P	A	C		C	2	0	2	M-c	Moderate
BR2	P			P	PB			P	PMg				P	P	R		P	P	A	C	P	C	2 or 3	0	1 or 2	M-vc	Poor
BR7a	C	RG	P	P	CBE			C		P				P			P	P	A	C		P	2	2	2 or 3	M-P	Poor
BR7b		P	P	C				C	RMg	P				P	R		P	P	A	P		C	2	0	2	M-vc	Poor
BR8a	P	P	P					C		C			P	P			P	P	C	A		P	1 or 2	0	2	M-P	Poor
BR8b			P	C	CBE		P			P							C		A	A			2	2	1	M-vc	Poor
BR8c			T												P			D	C	P							
BR9a	P		P	P			P	C		C				P	R	P			C	D		C	2	0 or 1	1 or 2	M-P	Poor
BR9b	A			R									R	R			C		A	C			0	0	3	M-P	Poor
BR10a	C			C	PB			C	RMg	P				P	P		C	P	A	P		P	2	0	3	M-P	Poor
BR10b		P	P	C	CB			C					P		C			C	A	P		C	2	0	1	M-vc	Moderate
BR14				P				R	RMg	R				P	A		P	C	A	C	P?	P	1	0	0	M-m(P)	Well
BR16a															P		P	D	A		P?						
BR16b		P		P	PE			C						P	C			C	A	A		P	2 or 3	1 or 2	2	M-vc(P)	Poor
BR18	C		P	P	CE			P						P	P		C	P	C	A		R	2	2 or 3	2	M-P	Poor
BR25		P	P	C	PB			C	RMg					R	P		C	P	C	C	P	P	2 or 3	0	3	M-G	Poor
BR28	C		P	P	PE			C						P	P		C	C	A	A		C	2	1	2 or 3	M-P	Poor
BR92a															P			D	A				0	0	0	M-vc	Well
BR92b	C		P	P				P			P		P				A	P	C	C		R	3	0	1 or 2	M-P	Poor
BR93			P	P	PE			P		P			P	P			C		A	A		P	2	0 or 1	1 or 2	M-vc(G)	Poor
BR95			P	R	PB			R		R			R	P				D	C	C		A	3	0	0	M-vc	Well
BR97		P	PG	P	PBE			C		P				C	C	P		C	C	A		P	2 or 3	0 or 1	1	M-vc	Poor
BR99			T											P	A			C	P	A			0	0	0	M-f(m)	Well
BR102		R	R	P				C		P				P	R	R	P	C	C	A		C	2	0 or 1	2	M-P	Poor
BR104	P		P	C	PE			C		C				P	P		P	P	P	A		P	2	1	2 or 3	M-P	Poor
PR5		C	P				R		RMg		R		P		P	P		C	A	A	R?		0 or 1	3	2	M-P	Poor
QB1		P	P	P	CBE			C						P	P		P	P	A	A		C	2 or 3	1 or 2	2 or 3	M-P	Poor
QB7	C		C	C	PBE			P?		P?					P		P	P	A	A		P	2	1 or 2	2	M-P	Poor
QB11a	P		P	C	CBE			P		P			P	R			C		C	A	P	P	2	0 or 1	2 or 3	M-G	Moderate
QB11b															P			D	A	C							
QB12	P		P	C	PB		T	C		P				P	P	P	P	P	D	C		C	2 or 3	0	2 or 3	M-G	Poor

HP17	N/A							1						2		3X		3BX						
HP18	N/A						N/A	1						2		3X		3GX			4			
HP19	N/A						N/A	1		1SB				2		3X		3GX				4		
HP24	Moderate	<15%	PC	<5%	<10% <1 mm		Matrix microporosity, solution enhanced vuggy intergranular	1		2SB				3		4X		4GX		5	5			
BR1d	Moderate	<10%	NC		<10% <250 µm		Intercrystalline/Interparticle	1							2	3X		3GBX			4			
BR2	Moderate	<15%	NC		<15% <25 mm		Intercrystalline/Interparticle	1								3X	3X	3GX		4	4			
BR7a	Minor	<5%					ARTIFACT	1	2FbX		4	5XW (Pendant?)	5S			3X	3X	3GBX						
BR7b	Minor	<5%	NC		<5% <1 mm		Intercrystalline/Interparticle	1							2	3X		3GBX		4	4			
BR8a	Minor	<5%	NC	<5%		<1% <5 mm	Matrix microporosity, solution enhanced channel porosity	1						2		3X		3GX		4	4			
BR8b	N/A						N/A	1							2	3X		3GX						
BR8c																1X								
BR9a	Moderate	<10%					ARTIFACT	1							2	3X		3GBX						
BR9b	N/A						N/A	1								2X	2X	2GBX						
BR10a	Minor	<5%	NC		<5% <250 µm		Intercrystalline	1						2	2	3X		3GBX			4			
BR10b	Moderate	<10%					ARTIFACT	1								2X		3G(B)X						
BR14	Minor	<5%	NC		<5% <100 µm		Intercrystalline/interparticle								2	3X		3GX			4			
BR16a															1			2GX						
BR16b	Minor	<5%	C			<5% <40 mm	Fracture porosity	1	2X						3	4X		4GBX	4					
BR18	Minor	<1%	NC		<1% <100 µm	<1% <100 µm	Intergranular and fracture	1						2	2	3X		3BX	4					
BR25	Minor	<5%	C			<5% <40 mm	Fracture porosity	1						2		3X		3GX			4			
BR28	Moderate	<20%	PC		<15% <2 mm	<5% <20 mm	Intergranular/Interpaticle, solution enhanced? Channel porosity ARTIFACT?	1						2	2	3X		3GBX			4	4		
BR92a	N/A						N/A											1GX	2				3X	4
BR92b	Minor	<1%			<1% <300 µm		Intergranular, intragranular	1							2	3X		3BX			4	4		
BR93	Minor	<5%				<5% <30 mm	Solution enhanced channeL porosity	1						2	2	3X		3GX		4	4	4		
BR95	Major	<30%			<30% <5 mm		Interpartcile - ARTIFACT							1	1			2GBX			3			
BR97	Minor	<5%	NC		<5% <300 µm		Intercrystalline and mouldic	1						2	2	3X		3GX			4			
BR99	N/A						N/A								1	2X		2GX			3			
BR102	Moderate	<10%	NC		<10% <300 µm		Interparticle	1						2	2	3X		3GX			4	4		
BR104	Minor	<5%	NC		<1% <100 µm	<5% <45 mm	Intercrystalline, Fracture Porosity	1						2	2	3X		3GX	4					
PR5	N/A						N/A	1			3	4XW	4S				2X	2GBX						
QB1	Minor	<5%	NC		<5% <1 mm		Intercrystalline (soulution enhanced) - ARTIFACT?	1						2	2	3X		3BX			4	4		
QB7	Minor	<5%	NC		<5% <1 mm	<1% <5 mm	Intercrystalline, Intraparticle, Fracture - ARTIFACT?	1							2	3X		3(D)GBX			4			
QB11a	Minor	<5%	NC		<5% <1 mm		Vuggy (Solution enchanced? Cyrstallisation reduced? ARTIFACT?)	1		1SB				2	2	3X		4G(B)X			6			
QB11b																		1X						
QB12	Moderate	<10%	NC		<10% <1 mm		Intercrystalline, solution enhanced? Vuggy - ARTIFACT?	1						2	2	3X		3GX		4	4			

Key to Appendix 1	
Process/feature abundance	Percentage Range
Trace (T)	0-0.1
Rare (R)	0.1-1
Present (P)	1-5
Common (C)	5-25
Abundant (A)	25-50
Dominant (D)	50-100

Appendix D2

Thin Section Photomicrographs of Samples Relating to Chapter 4

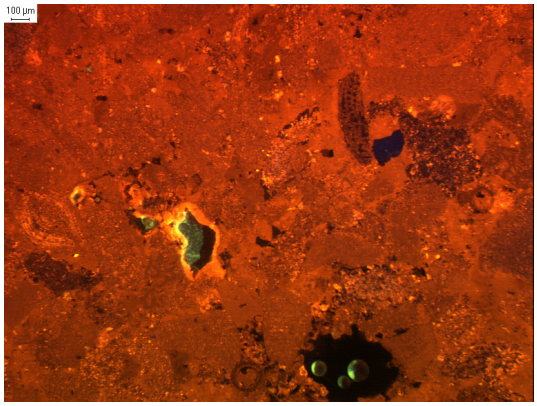

BR1d-a-4x-cl.TIF

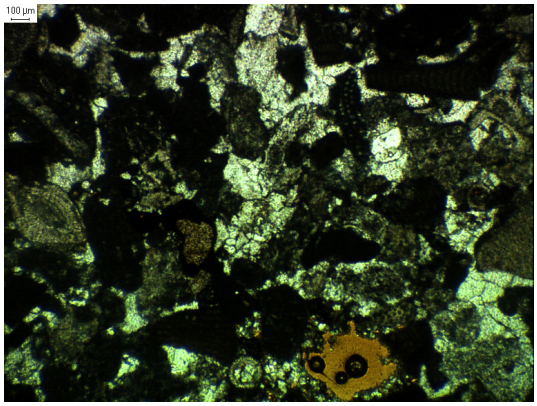

BR1d-a-4x-pl.TIF

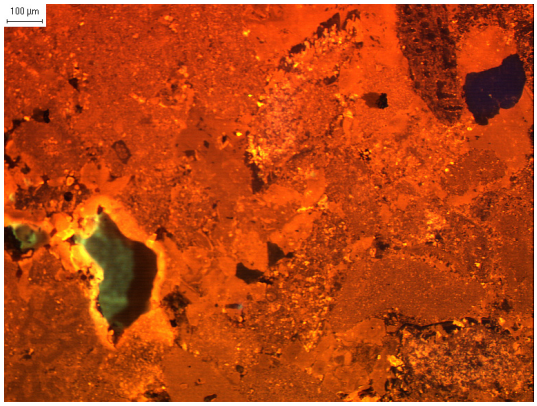

BR1d-a-10x-cl.TIF

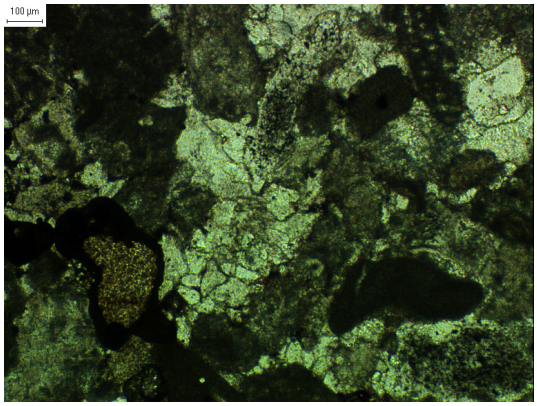

BR1d-a-10x-pl.TIF

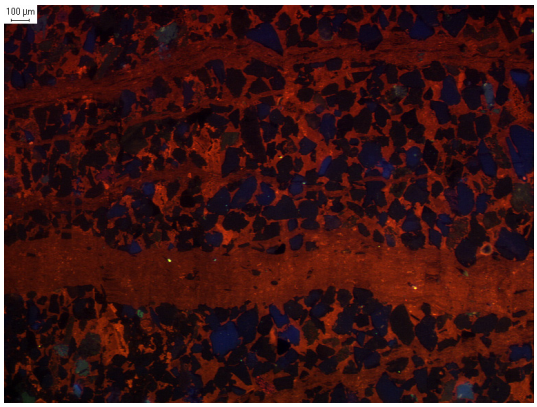

BR16a-a-4x-cl.TIF

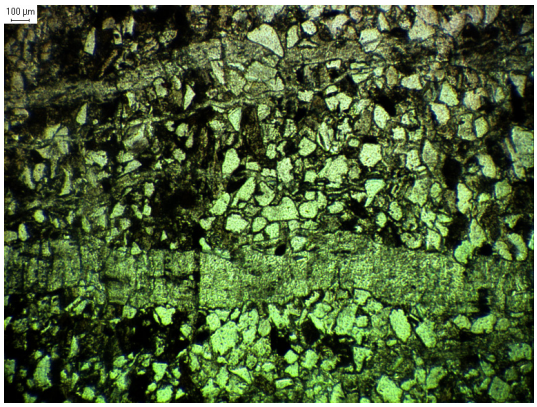

BR16a-a-4x-pl.TIF

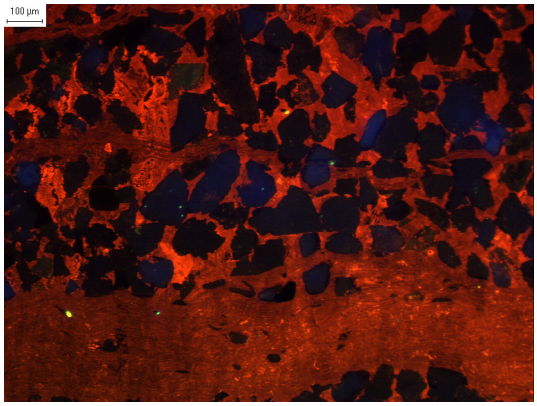

BR16a-a-10x-cl.TIF

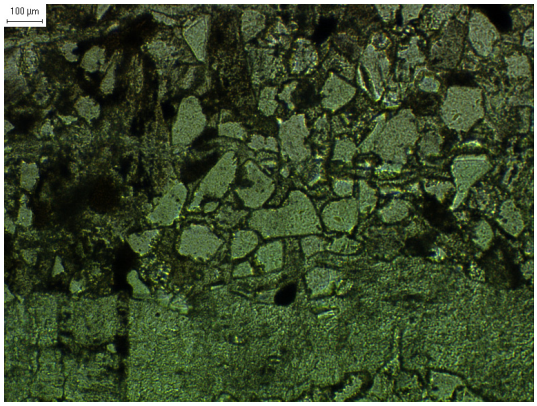

BR16a-a-10x-pl.TIF

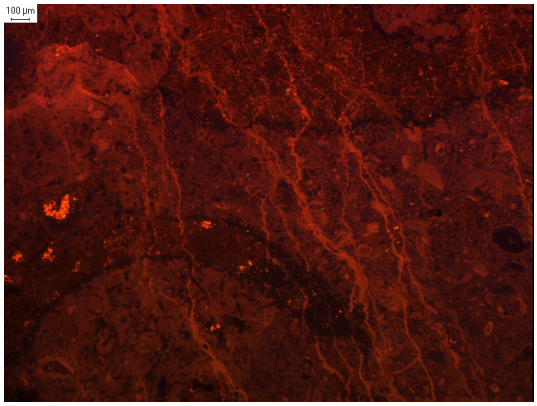

BR16b-a-4x-cl.TIF

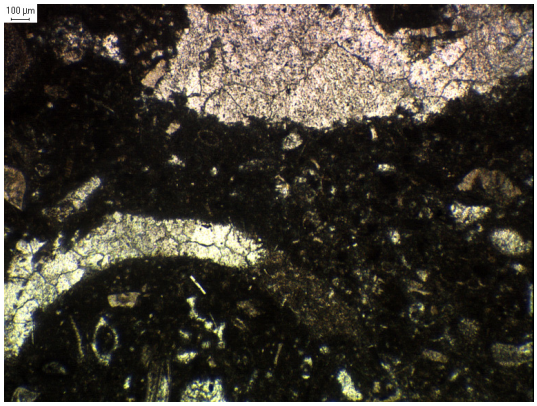

BR16b-a-4x-pl.TIF

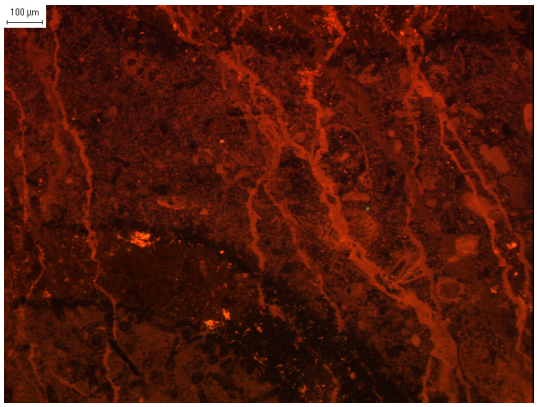

BR16b-a-10x-cl.TIF

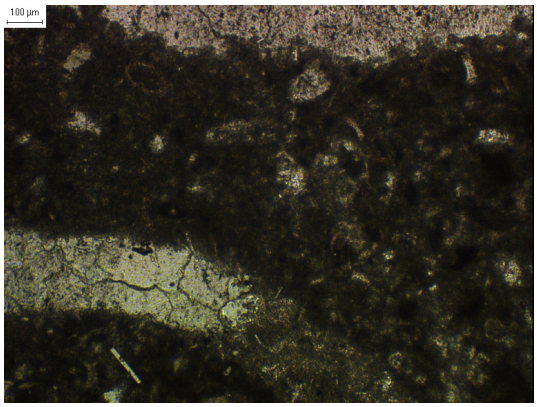

BR16b-a-10x-pl.TIF

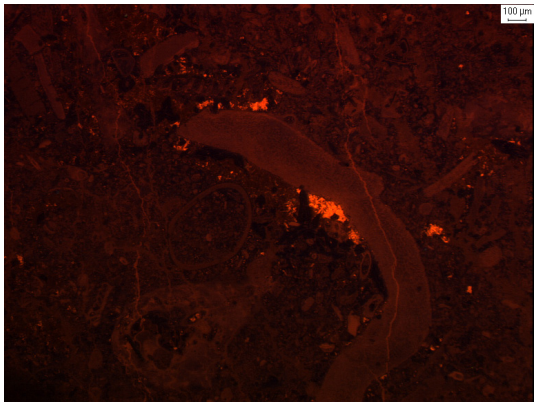

BR16b-b-4x-cl.TIF

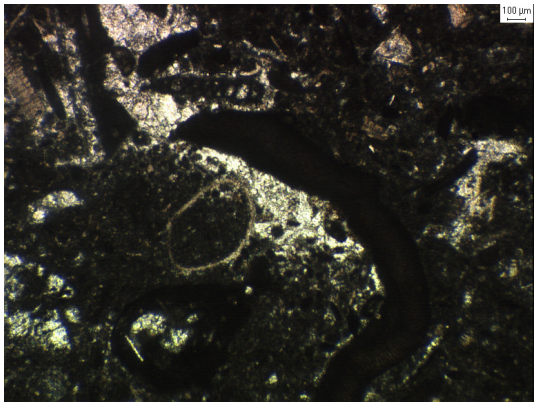

BR16b-b-4x-pl.TIF

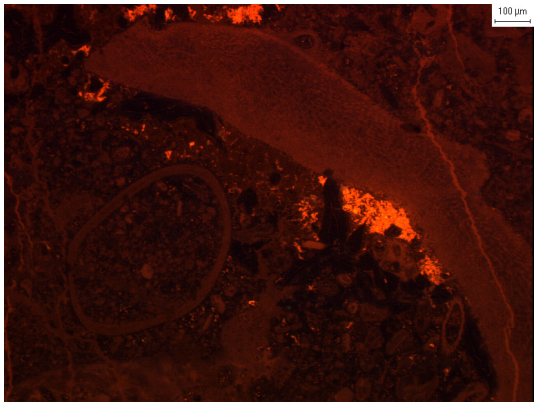

BR16b-b-10x-cl.TIF

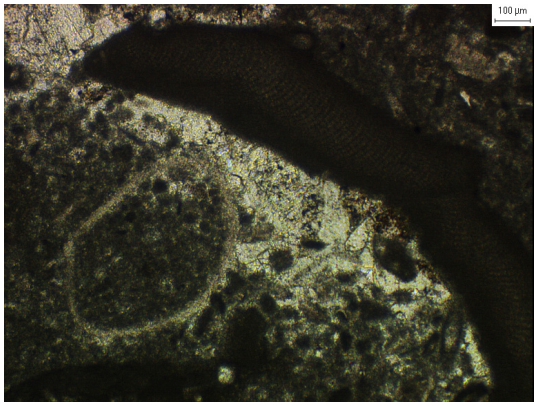

BR16b-b-10x-pl.TIF

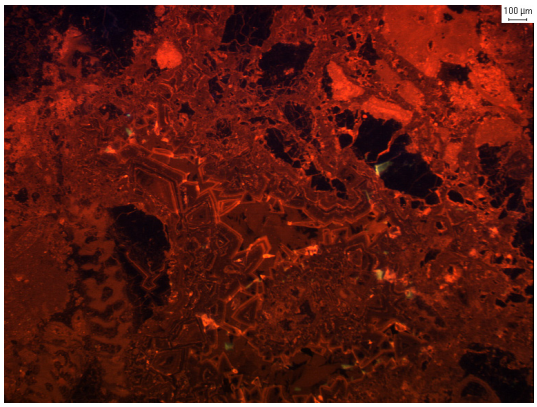

BR55-a-4x-cl.TIF

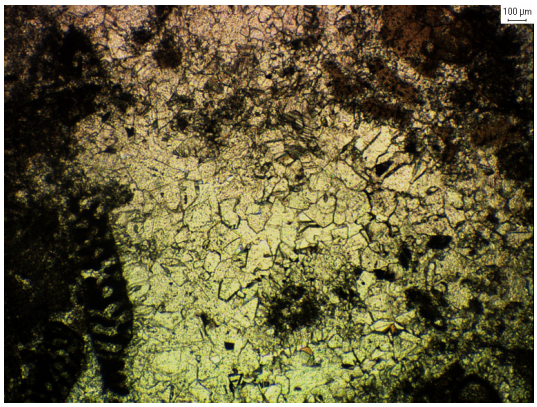

BR55-a-4x-pl.TIF

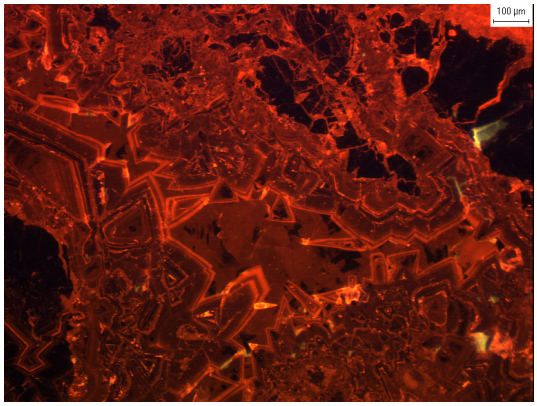

BR55-a-10x-cl.TIF

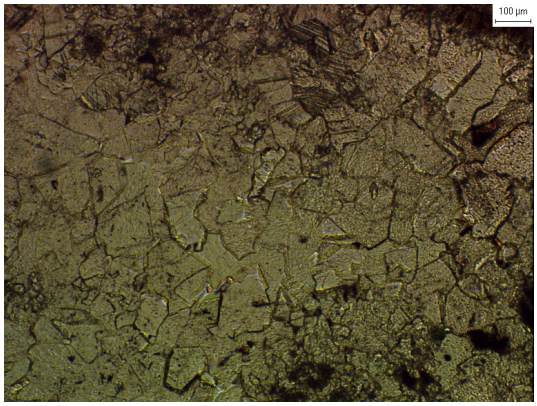

BR55-a-10x-pl.TIF

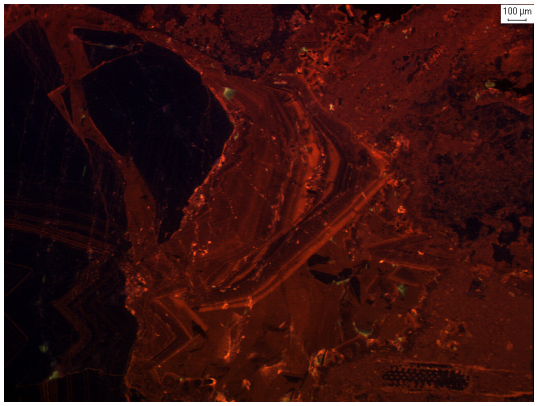

BR55-b-4x-cl.TIF

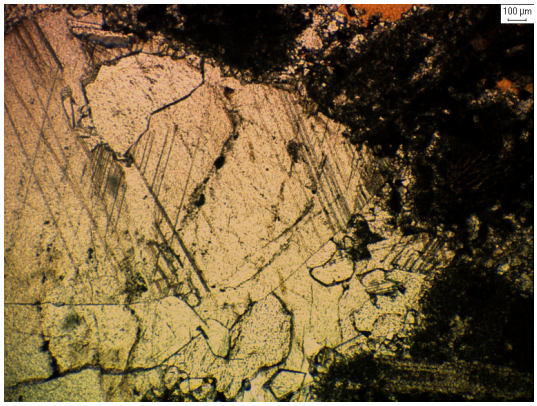

BR55-b-4x-pl.TIF

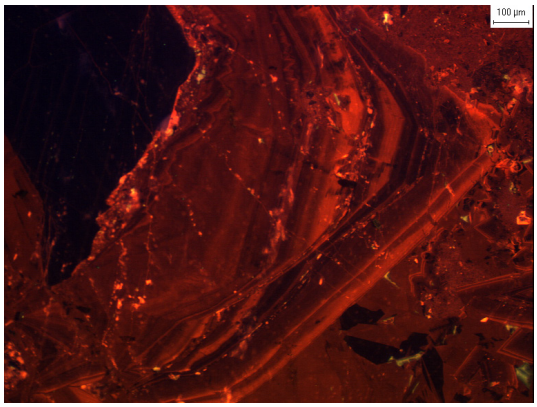

BR55-b-10x-cl.TIF

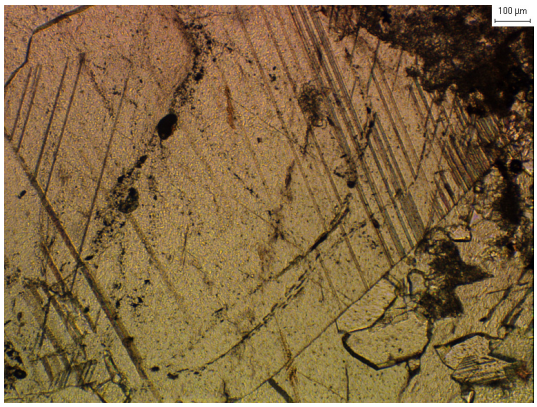

BR55-b-10x-pl.TIF

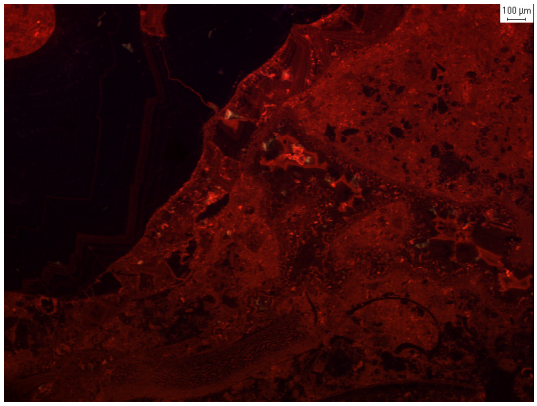

BR55-c-4x-cl.TIF

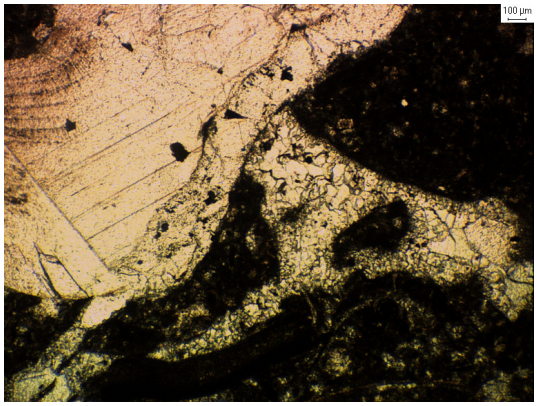

BR55-c-4x-pl.TIF

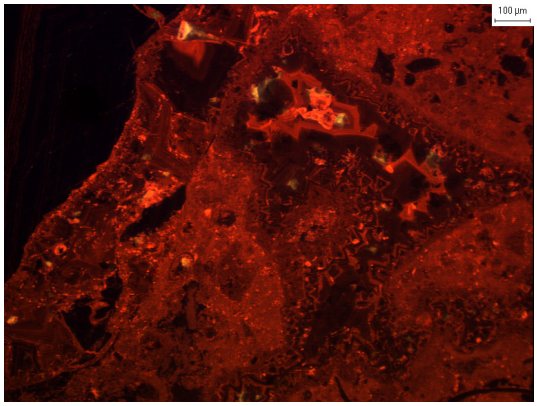

BR55-c-10x-cl.TIF

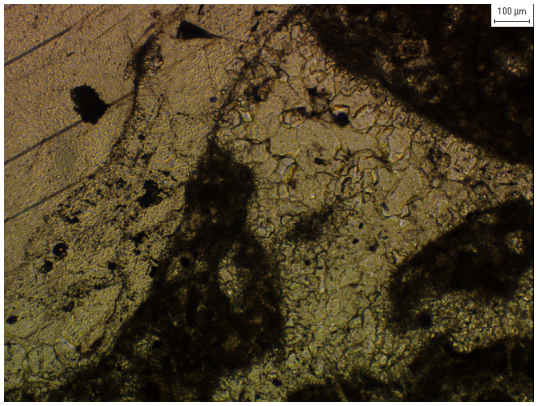

BR55-c-10x-pl.TIF

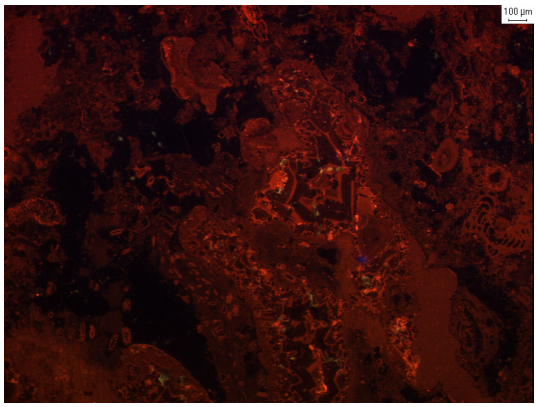

BR55-d-4x-cl.TIF

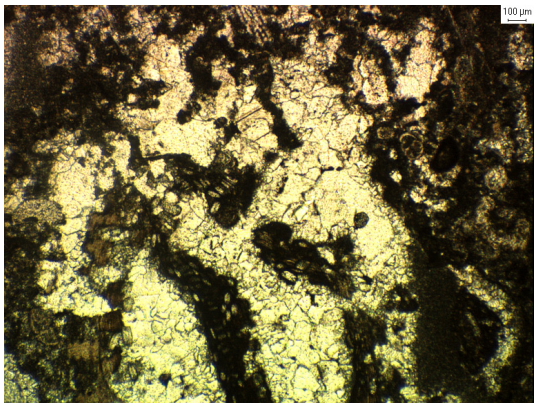

BR55-d-4x-pl.TIF

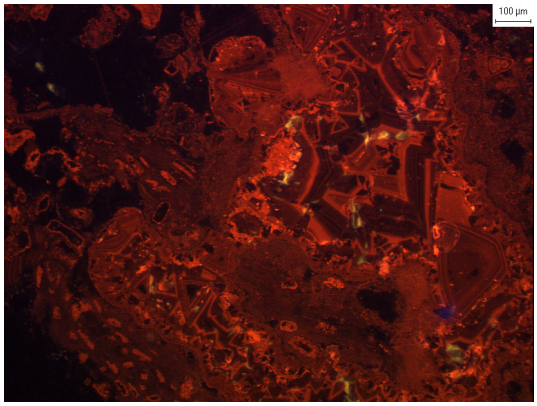

BR55-d-10x-cl.TIF

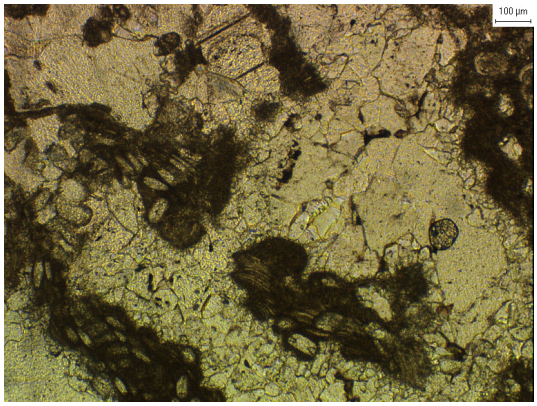

BR55-d-10x-pl.TIF

BR76-a-4x-cl.TIF

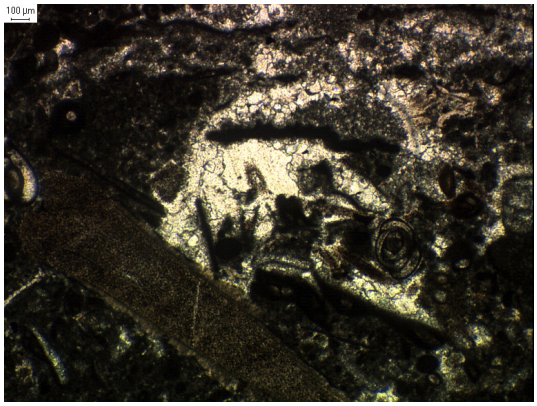

BR76-a-4x-pl.TIF

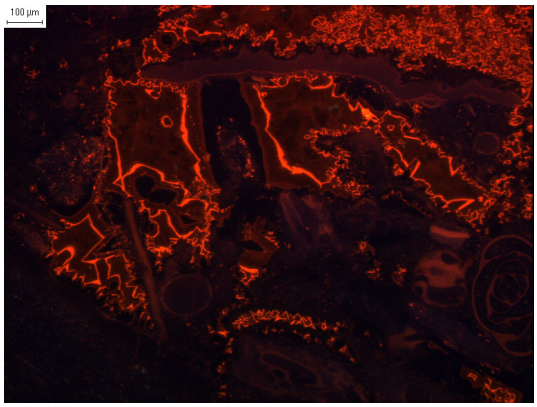

BR76-a-10x-cl.TIF

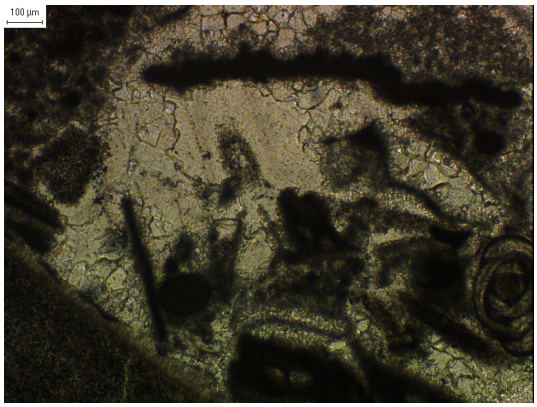

BR76-a-10x-pl.TIF

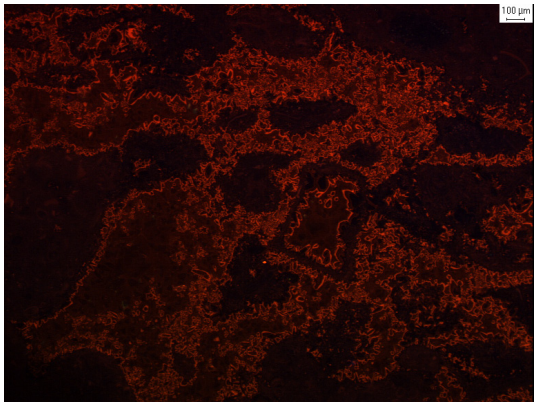

BR76-b-4x-cl.TIF

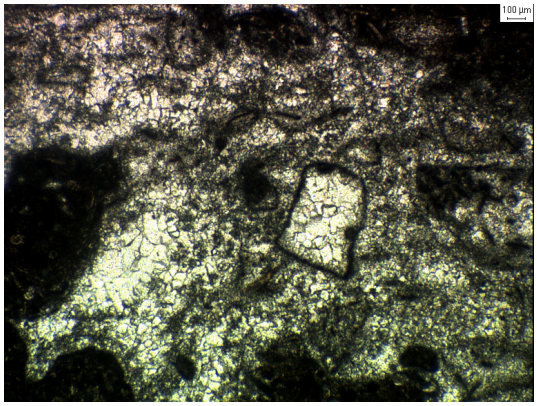

BR76-b-4x-pl.TIF

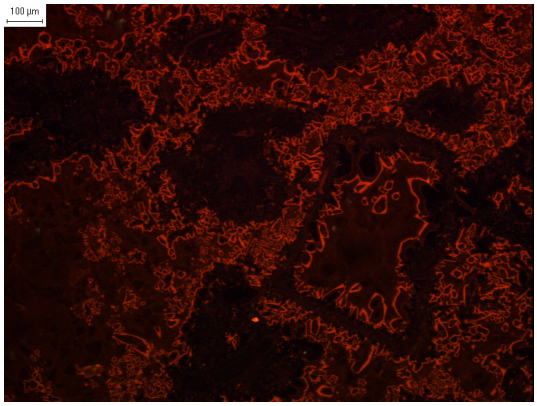

BR76-b-10x-cl.TIF

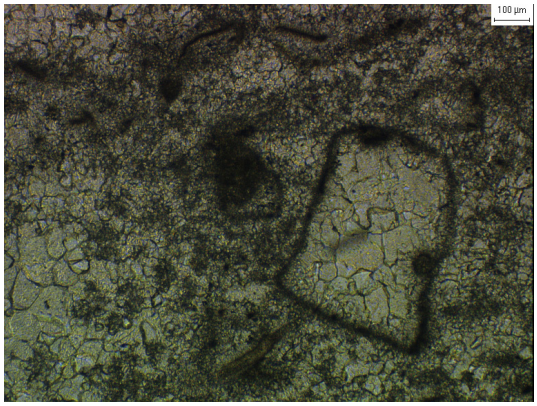

BR76-b-10x-pl.TIF

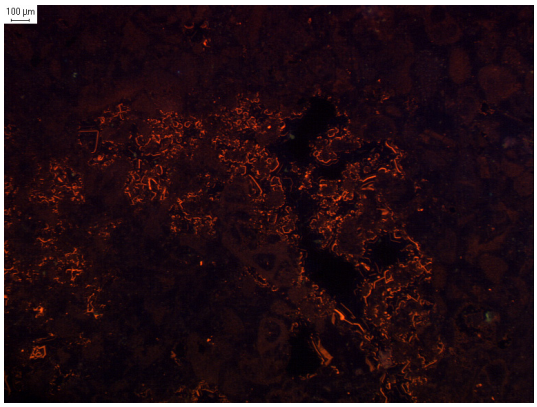

GB4b-a-4x-cl.TIF

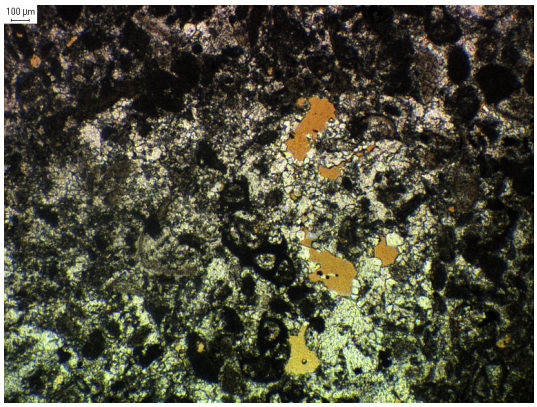

GB4b-a-4x-pl.TIF

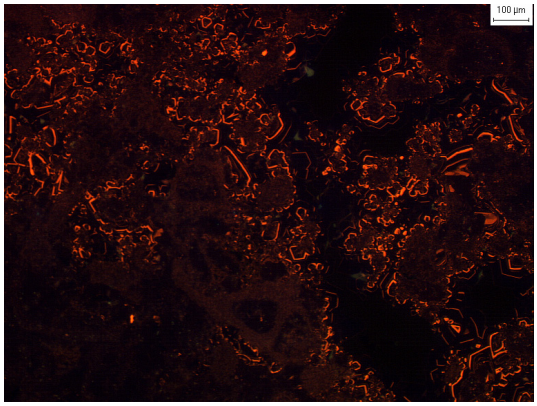

GB4b-a-10x-cl.TIF

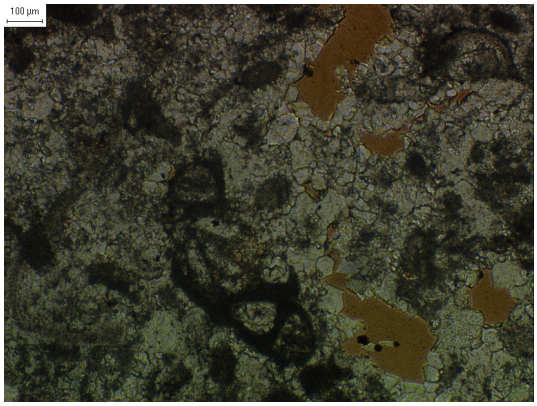

GB4b-a-10x-pl.TIF

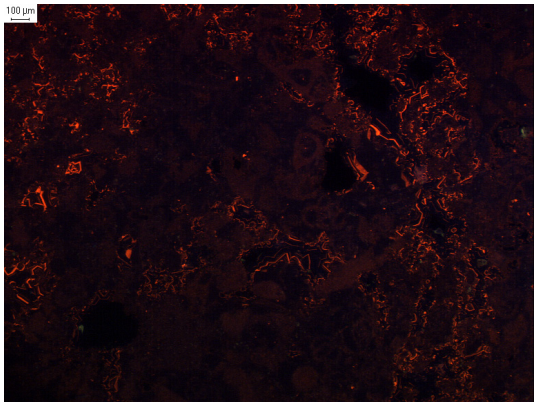

GB4b-b-4x-cl.TIF

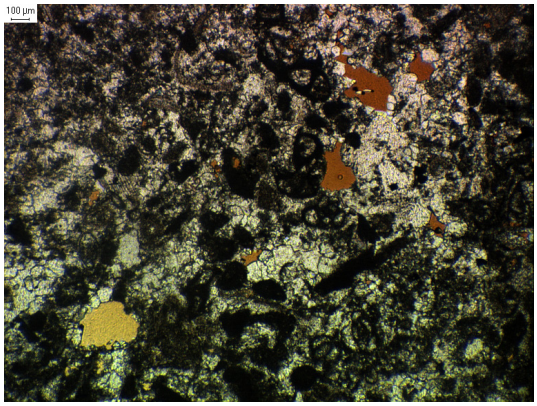

GB4b-b-4x-pl.TIF

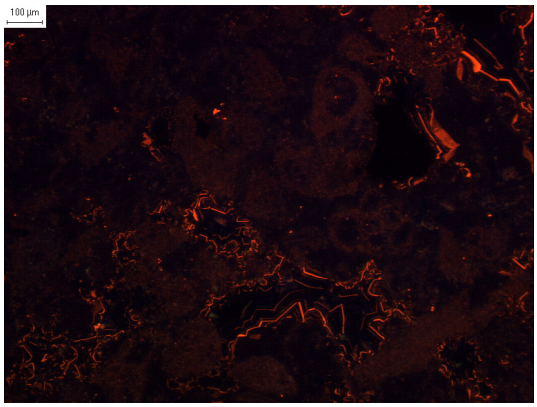

GB4b-b-10x-cl.TIF

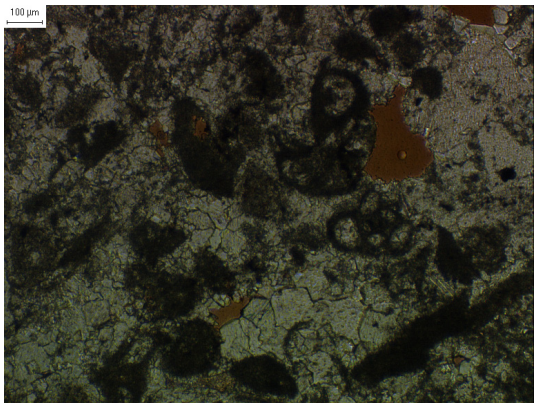

GB4b-b-10x-pl.TIF

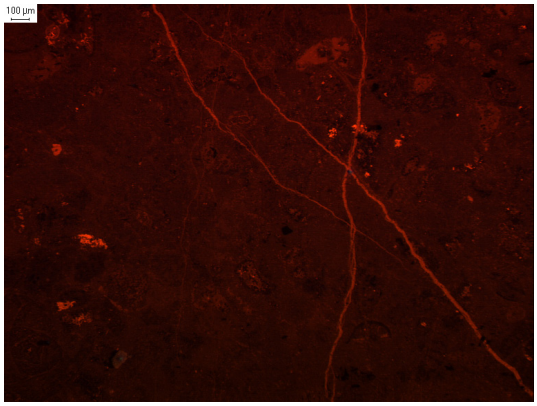

GH2-a-4x-cl.TIF

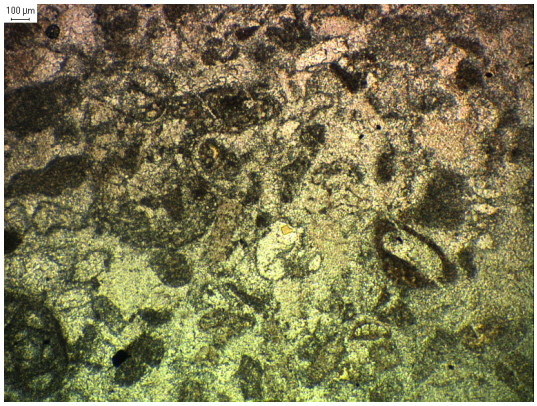

GH2-a-4x-pl.TIF

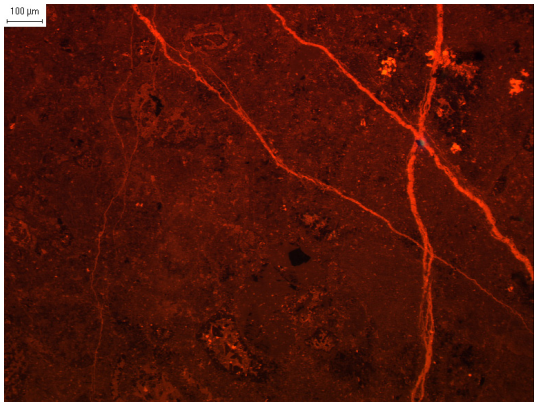

GH2-a-10x-cl.TIF

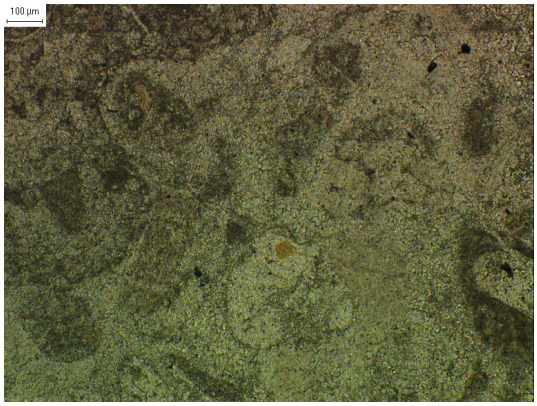

GH2-a-10x-pl.TIF

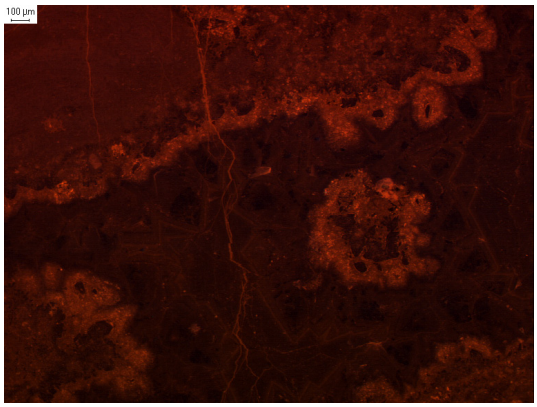

GH2-b-4x-cl.TIF

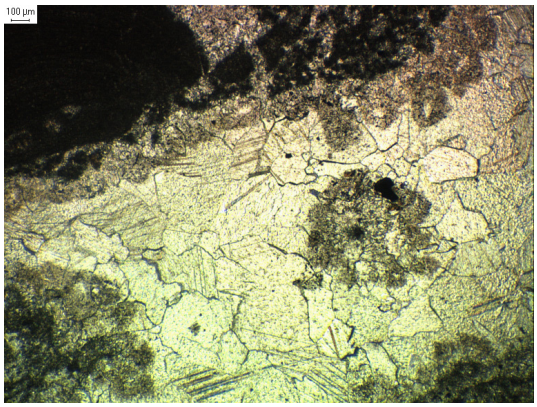

GH2-b-4x-pl.TIF

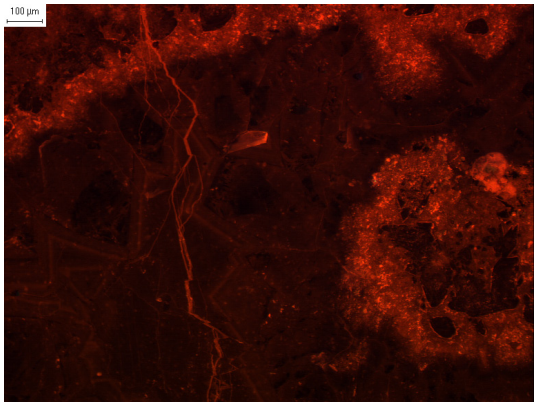

GH2-b-10x-cl.TIF

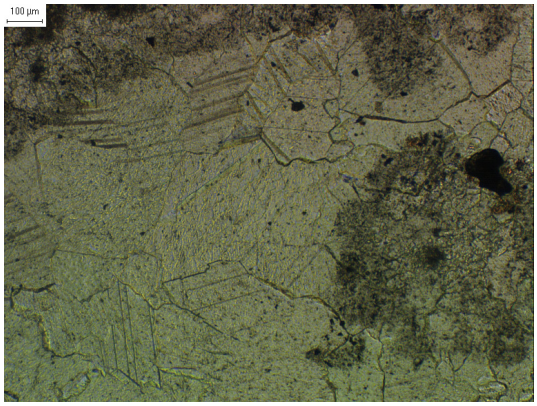

GH2-b-10x-pl.TIF

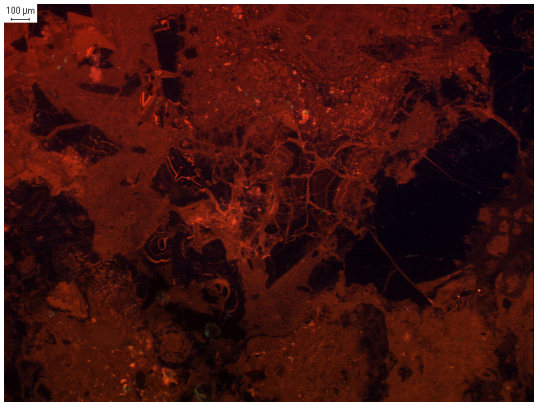

GS1-a-4x-cl.TIF

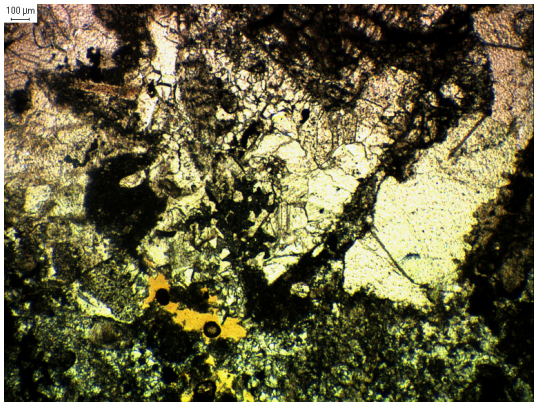

GS1-a-4x-pl.TIF

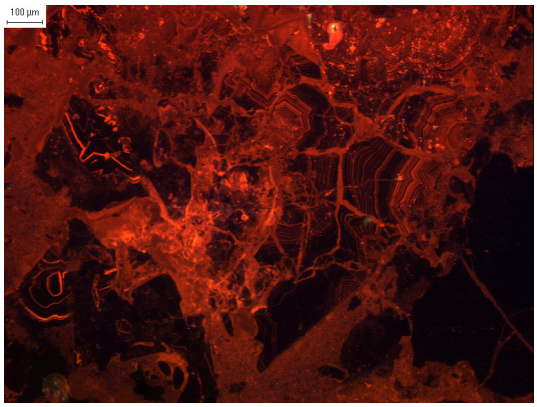

GS1-a-10x-cl.TIF

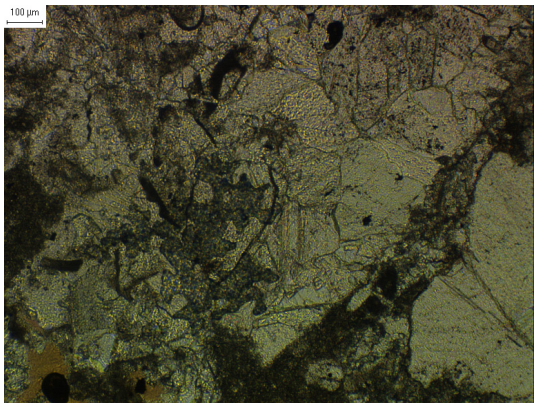

GS1-a-10x-pl.TIF

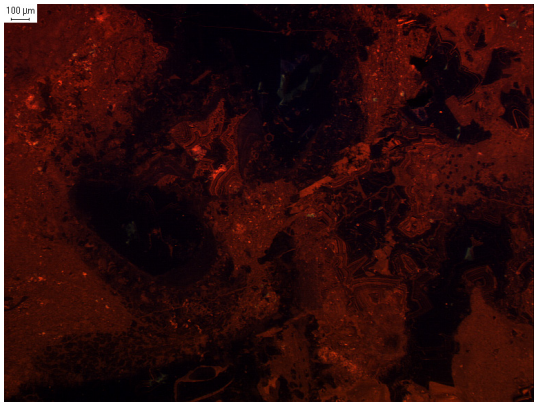

GS1-b-4x-cl.TIF

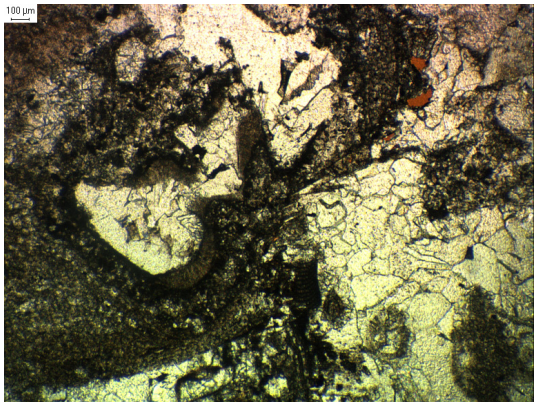

GS1-b-4x-pl.TIF

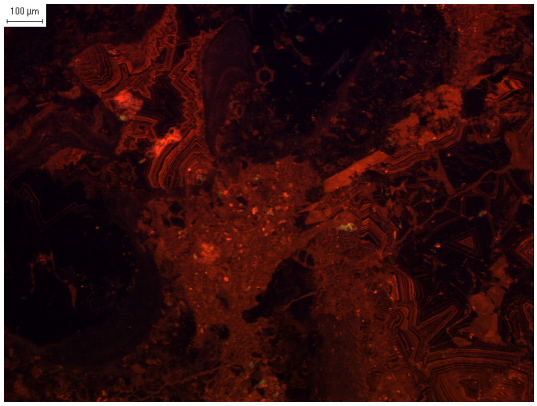

GS1-b-10x-cl.TIF

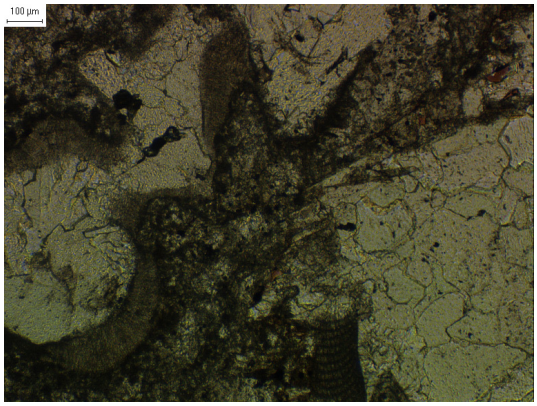

GS1-b-10x-pl.TIF

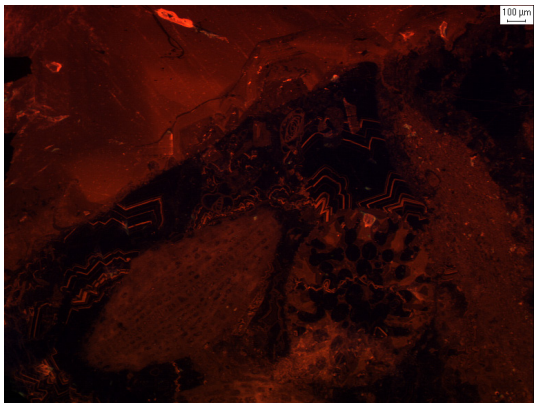

GS1-c-4x-cl.TIF

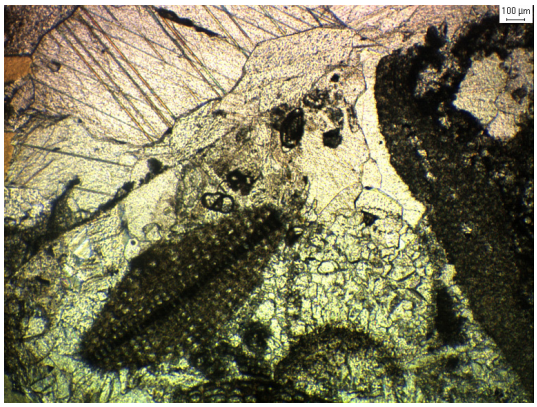

GS1-c-4x-pl.TIF

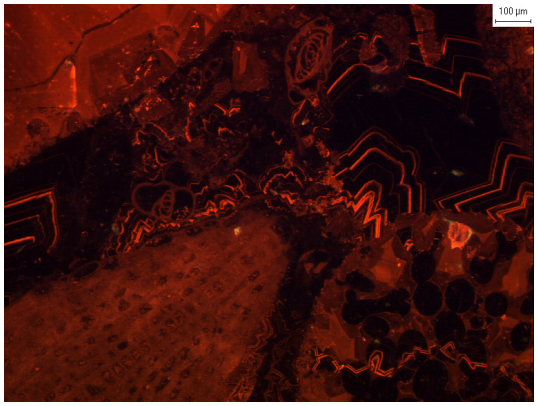

GS1-c-10x-cl.TIF

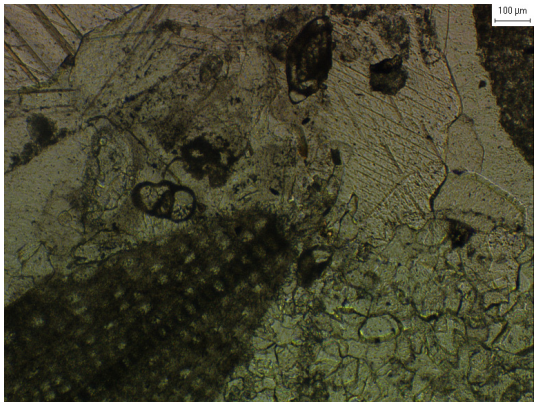

GS1-c-10x-pl.TIF

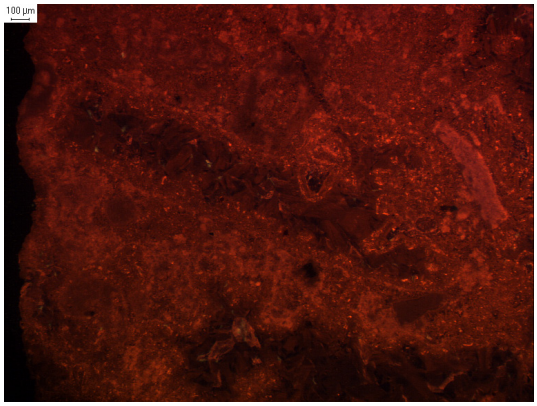

GS5-a-4x-cl.TIF

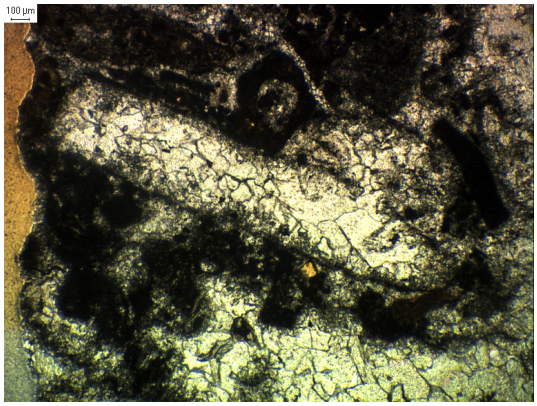

GS5-a-4x-pl.TIF

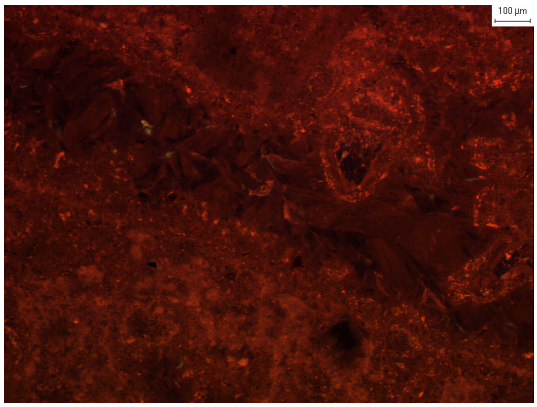

GS5-a-10x-cl.TIF

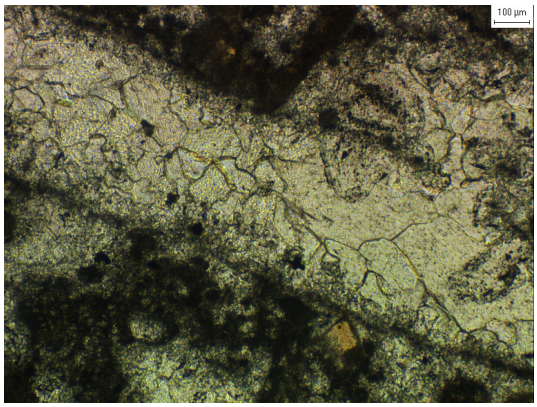

GS5-a-10x-pl.TIF

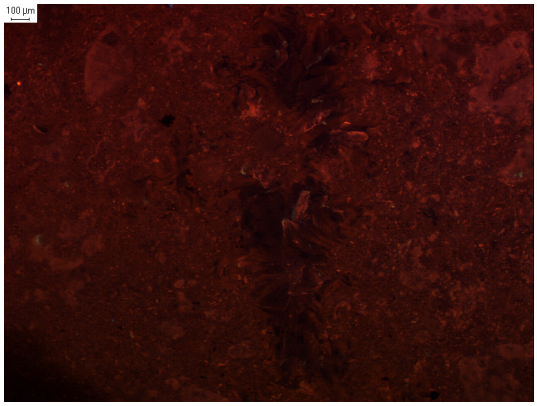

GS5-b-4x-cl.TIF

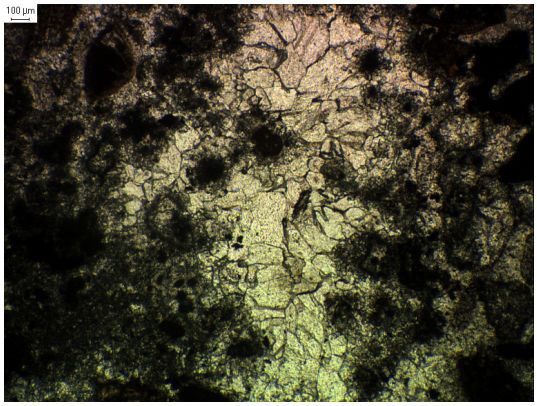

GS5-b-4x-pl.TIF

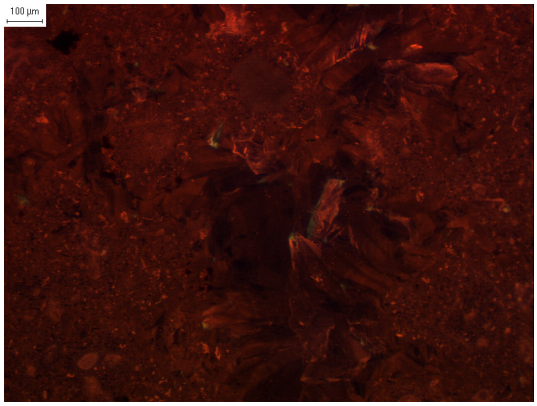

GS5-b-10x-cl.TIF

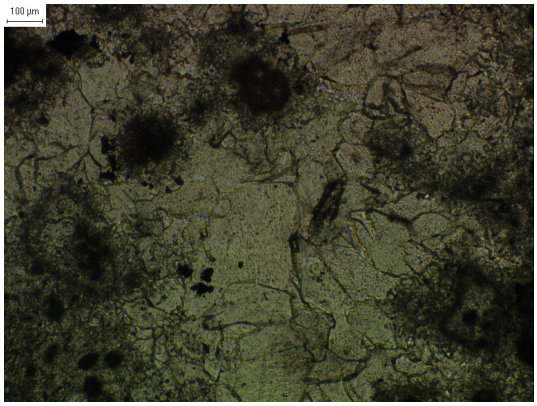

GS5-b-10x-pl.TIF

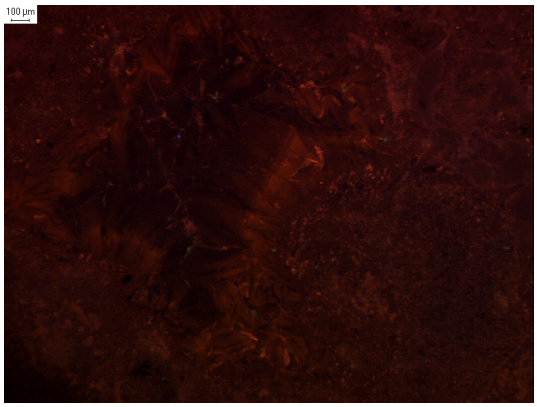

GS5-c-4x-cl.TIF

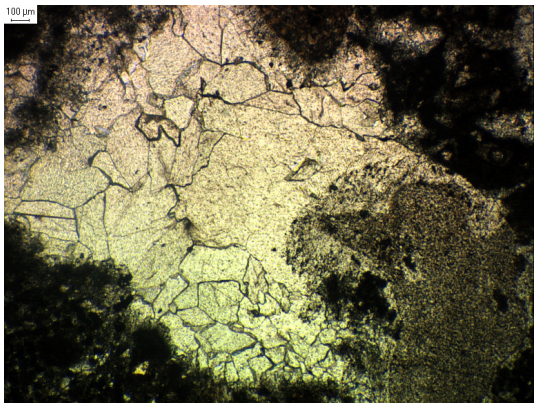

GS5-c-4x-pl.TIF

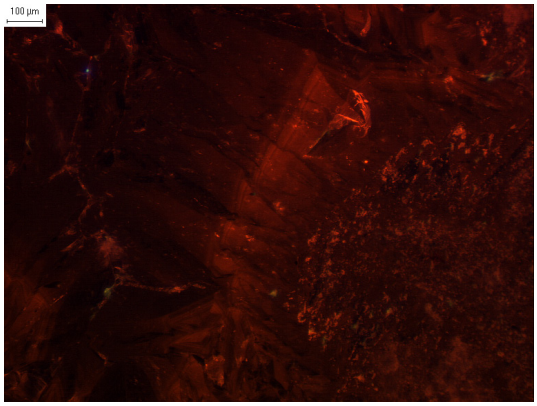

GS5-c-10x-cl.TIF

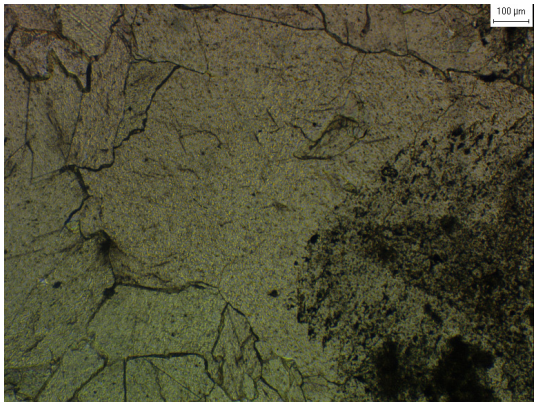

GS5-c-10x-pl.TIF

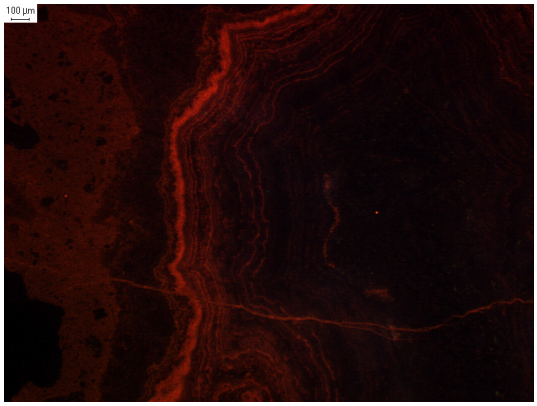

PR5-a-4x-cl.TIF

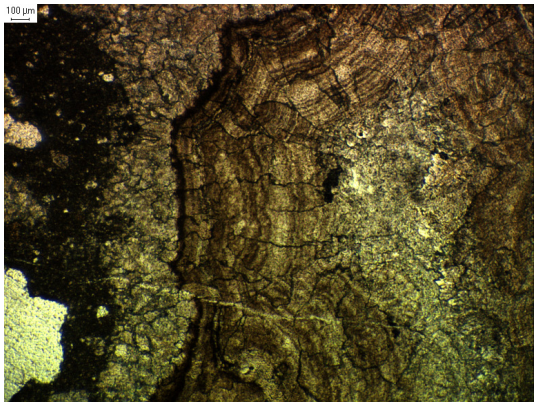

PR5-a-4x-pl.TIF

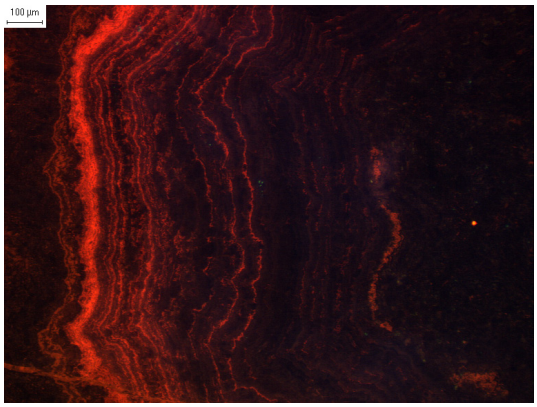

PR5-a-10x-cl.TIF

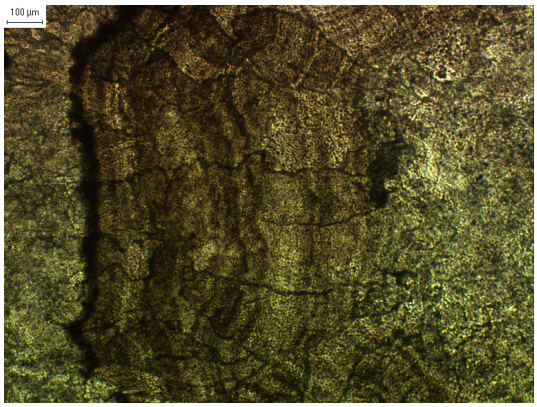

PR5-a-10x-pl.TIF

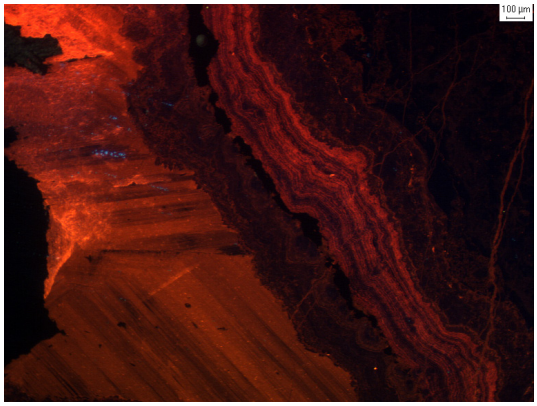

PR5-b-4x-cl.TIF

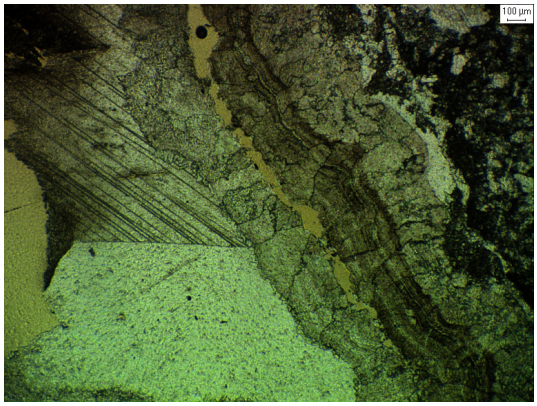

PR5-b-4x-pl.TIF

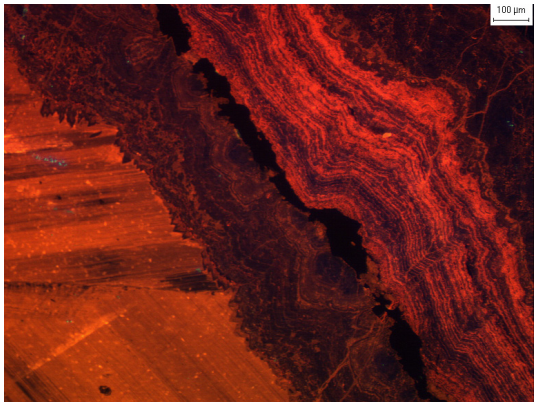

PR5-b-10x-cl.TIF

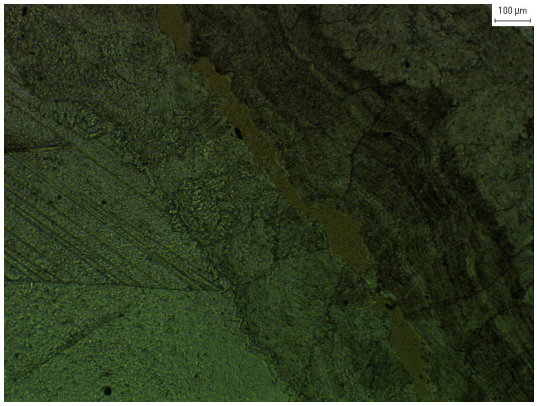

PR5-b-10x-pl.TIF

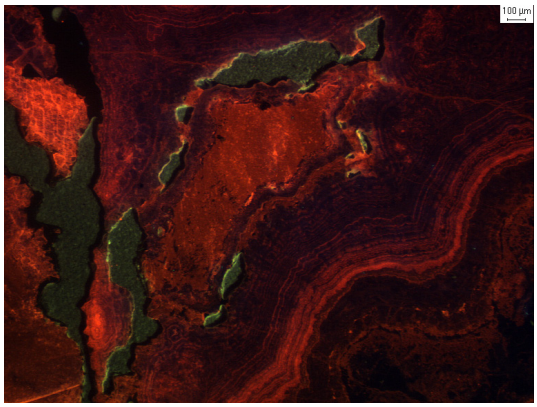

PR5-c-4x-cl.TIF

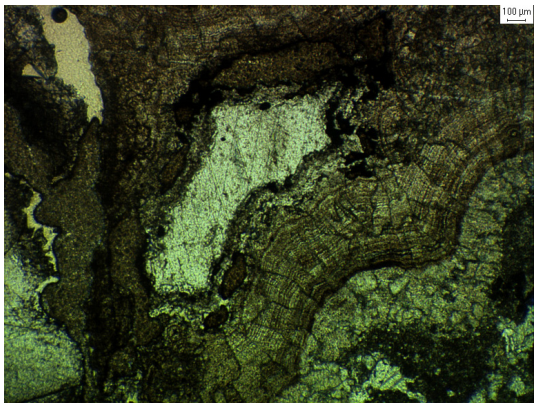

PR5-c-4x-pl.TIF

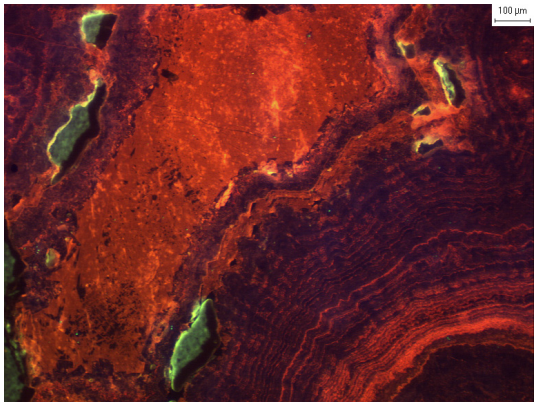

PR5-c-10x-cl.TIF

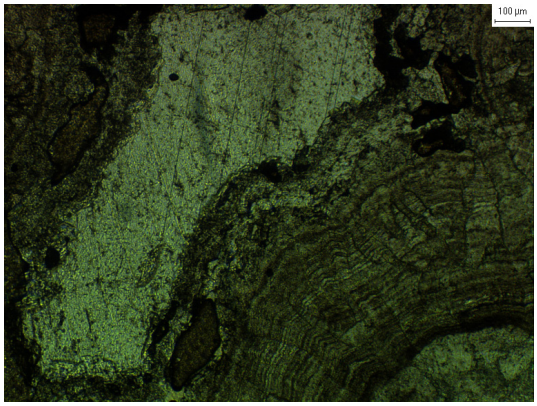

PR5-c-10x-pl.TIF

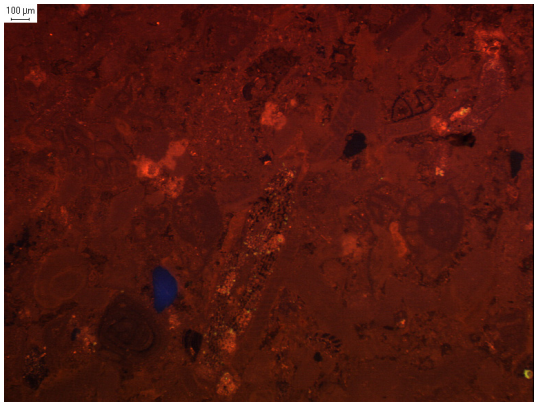

Q5-a-4x-cl.TIF

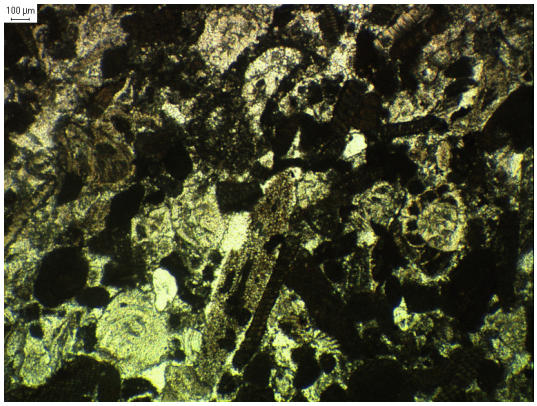

Q5-a-4x-pl.TIF

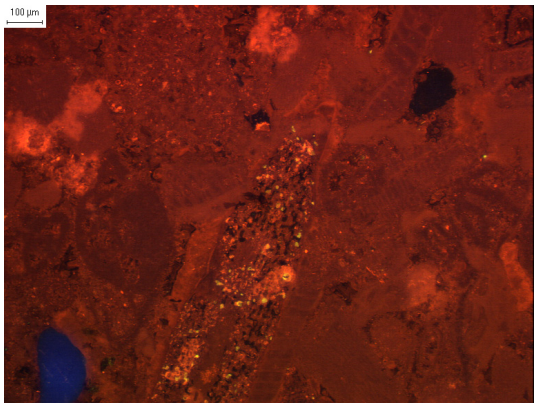

Q5-a-10x-cl.TIF

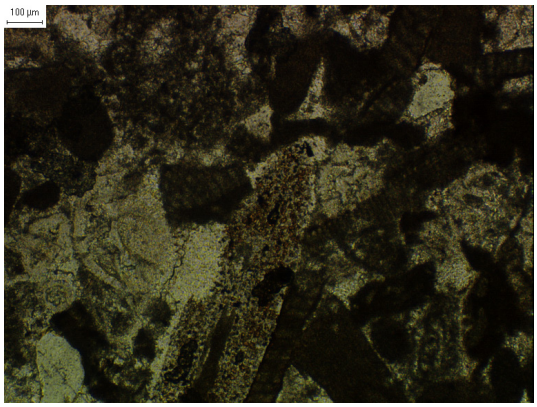

Q5-a-10x-pl.TIF

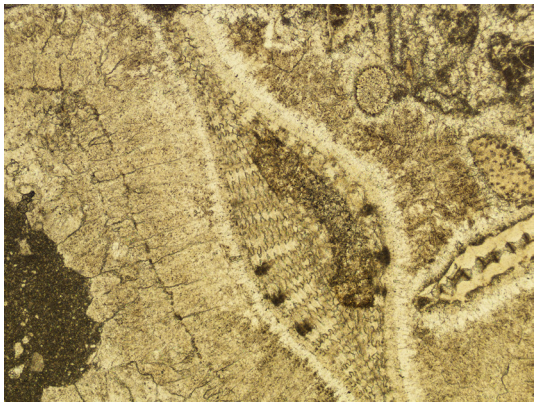

BR07a-IsopachousFringing to BandedBladed 5xPPL.tif

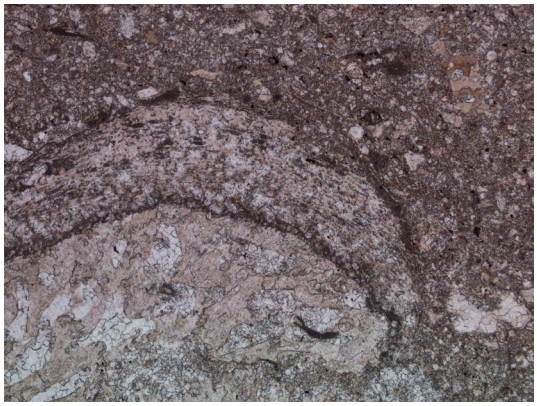

BR43b 5xPPL.tif

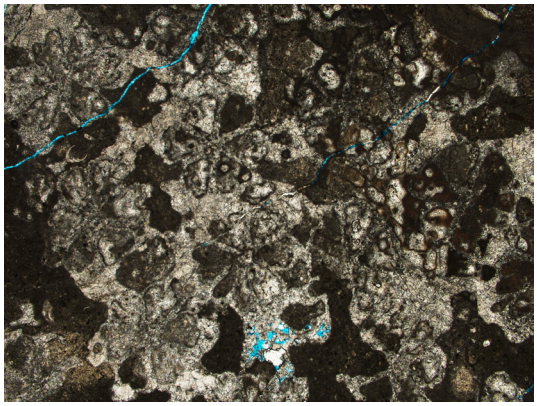

BR53 2.5xPPL Microcodium.tif

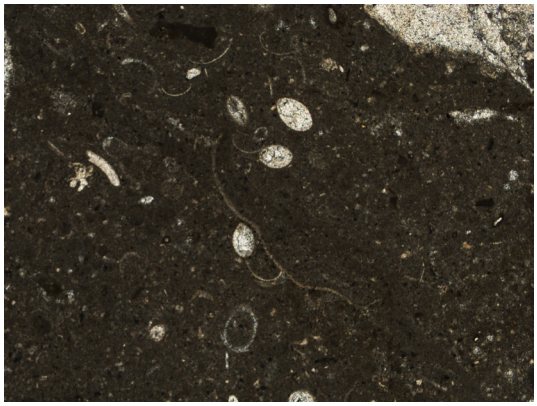

BR53 5xPPL Ostracods.tif

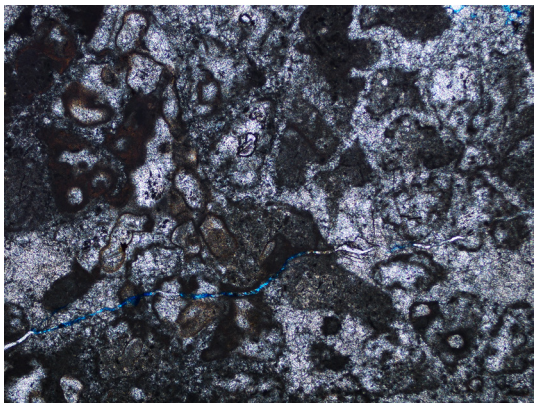

BR53 Alveolar and Corals 5x (2).tif

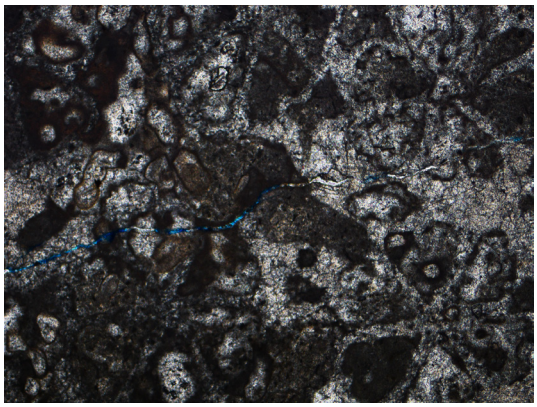

BR53 Alveolar and Corals 5x (3).tif

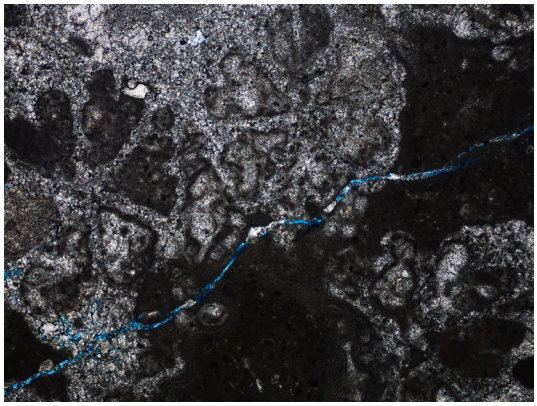

BR53 Alveolar and Corals 5x.tif

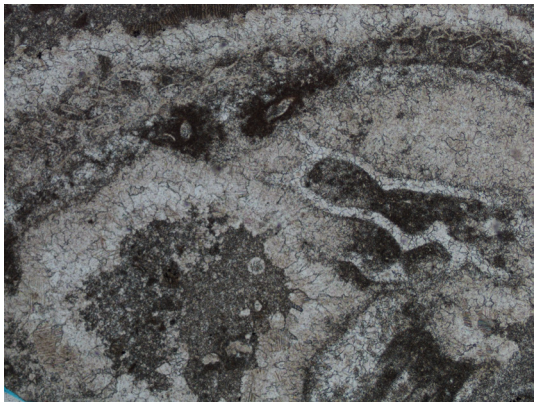

BR75a 5xPPL.tif

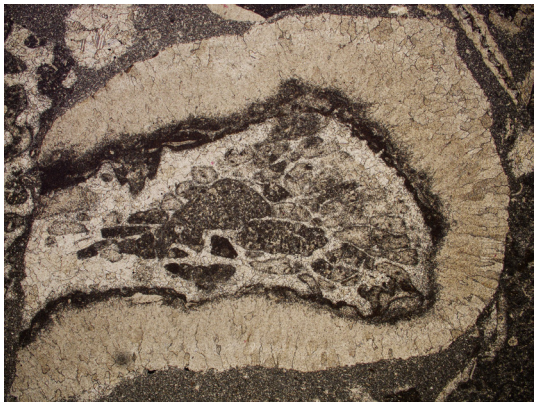

BR75a Reworked coral bladed 2.5ppl.tif

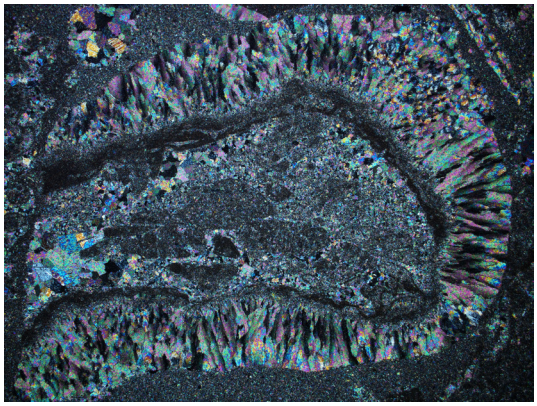

BR75a Reworked coral bladed 2.5xpl.tif

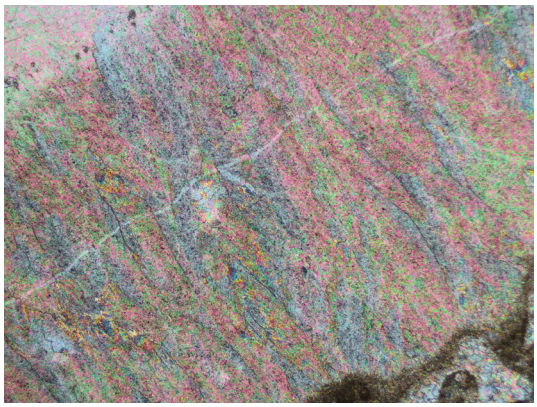

BR76-BladedCalcite,BottomRightCalcitizedCoral,Fracture 5xXPL.tif

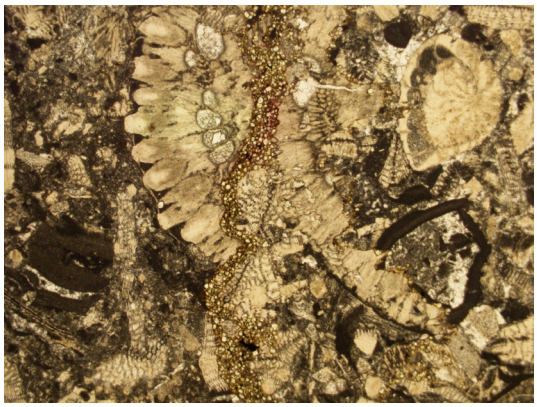

BR81-DissolutionSeam,DolomiteRhombs 2.5xPPL.tif

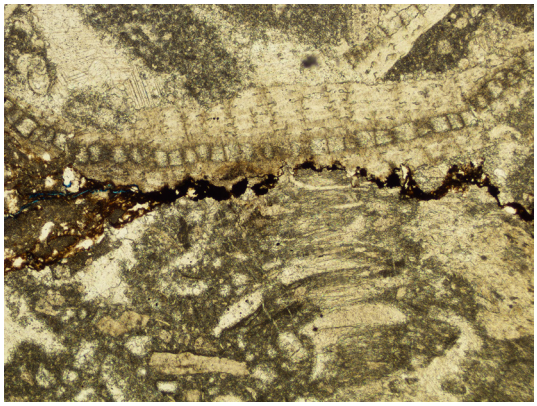

BR93-DissolutionSeam 5xPPL.tif

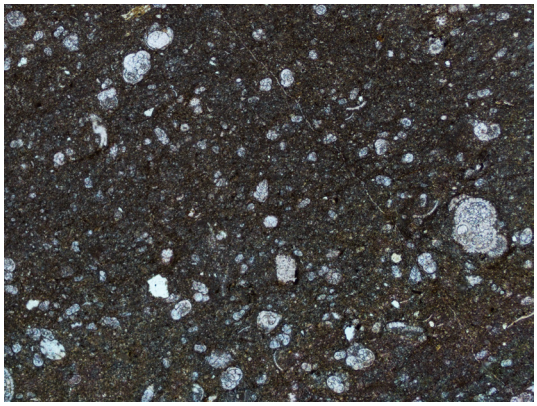

BR99 5xPPL.tif

GB04b 5xPPL micritised bioclasts.tif

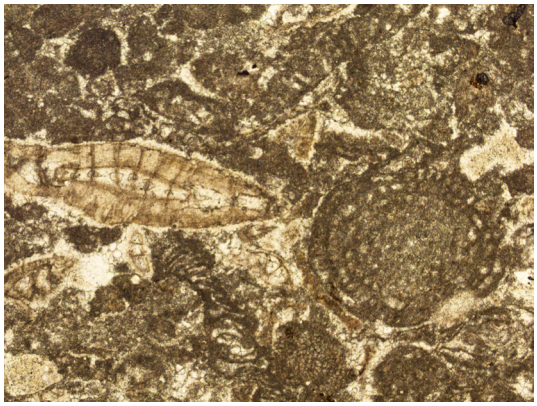

GB7a-IsopachousFringinG 5xPPL.tif

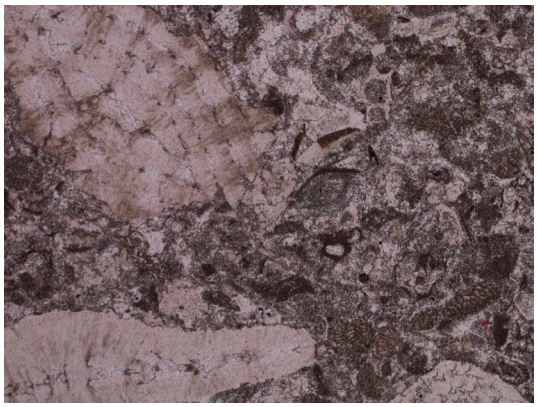

GB23a 5xPPL Minorly micritised foram.tif

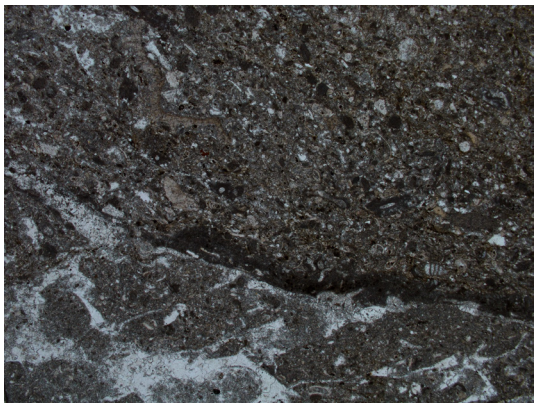

GB41 2.5xPPL.tif

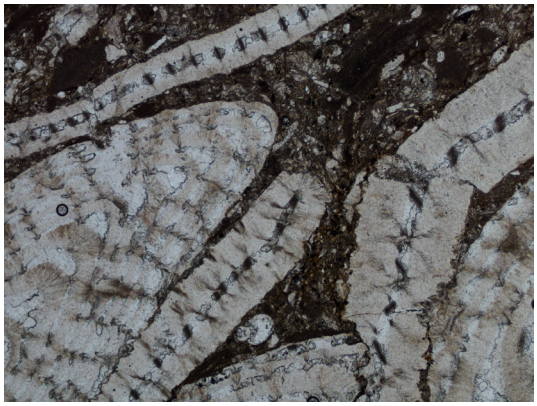

GB43 5xPPL.tif

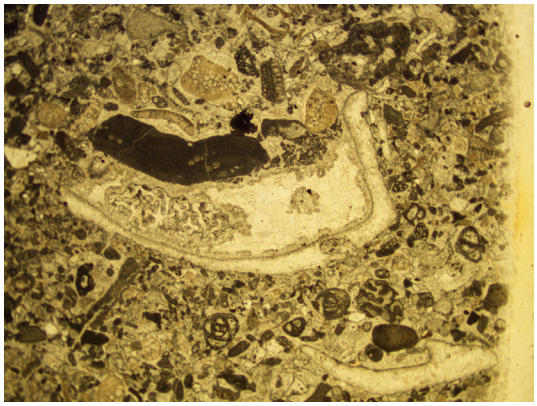

GH2-Polished-CL View Overview.tif

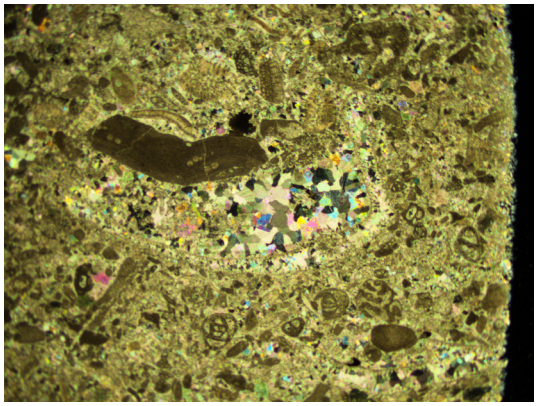

GH2-Polished-CL View OverviewXPL.tif

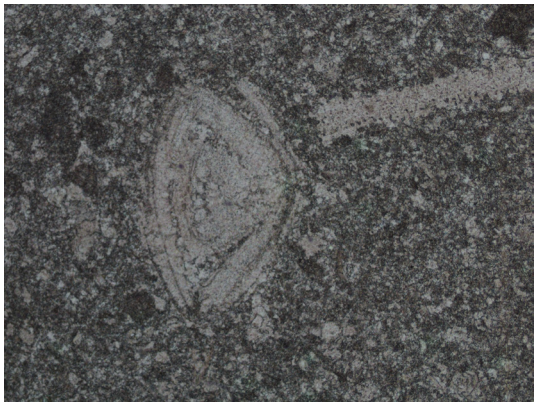

GH10 5xPPL.tif

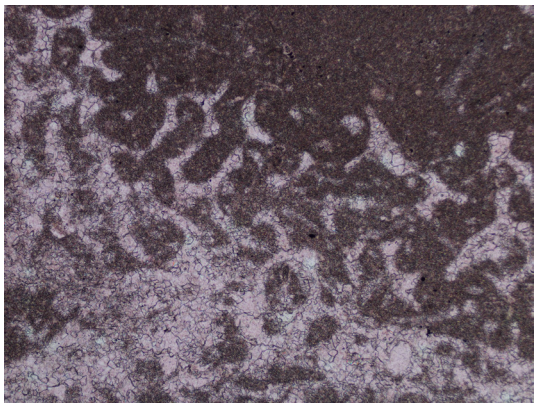

GKM11 5xPPL.tif

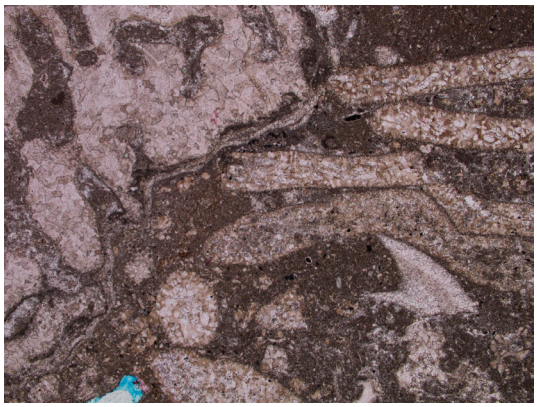

GKM17 2.5xPPL Micritization.tif

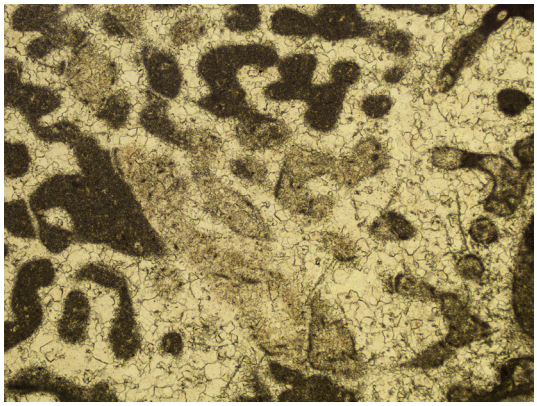

GP01-Neomorphic + ContemporaneousCalcitization_of_chamber+neomorphism_of_micrite_fill 5xPPL.tif

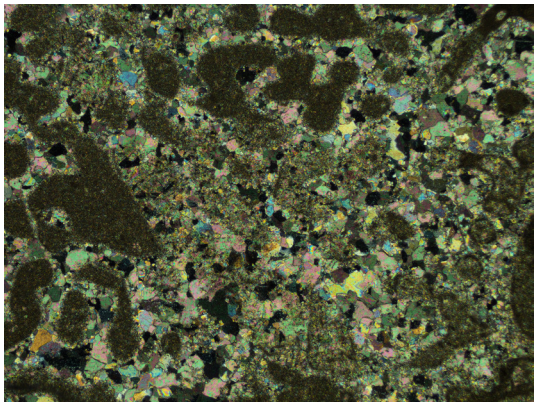

GP01-Neomorphic + ContemporaneousCalcitization_of_chamber+neomorphism_of_micrite_fill 5xXPL.tif

GP3 imperforate compaction 2.tif

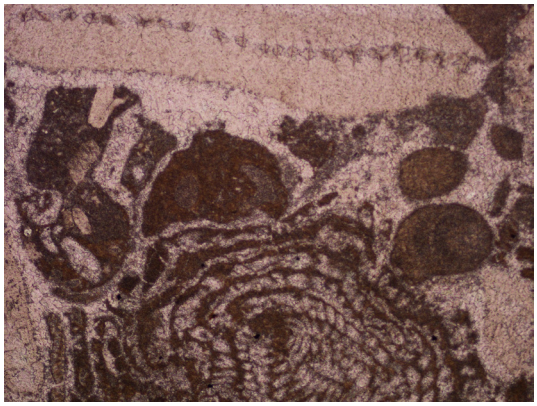

GP3 imperforate compaction 5x.tif

GS11 2.5xPPL.tif

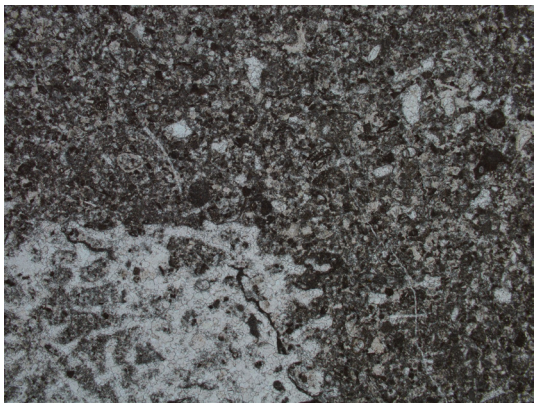

GU3 2.5xPPL.tif

GU29-Fracturing 2.5xPPL.tif

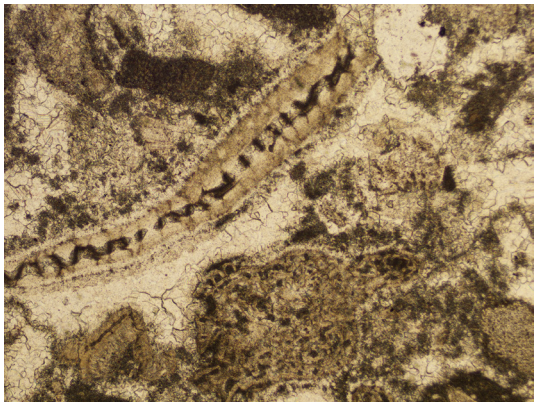

HP05-ReplacedIsopachousFringing 5xPPL.tif

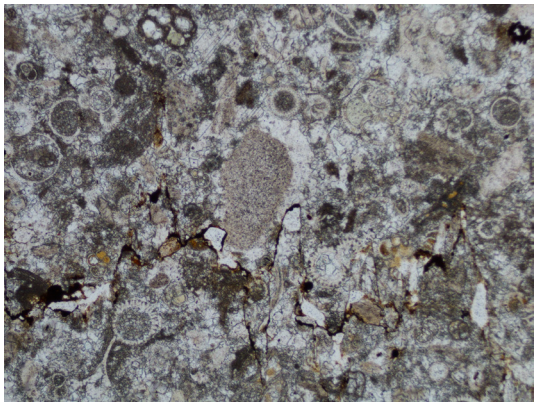

HP19 5xPPL.tif

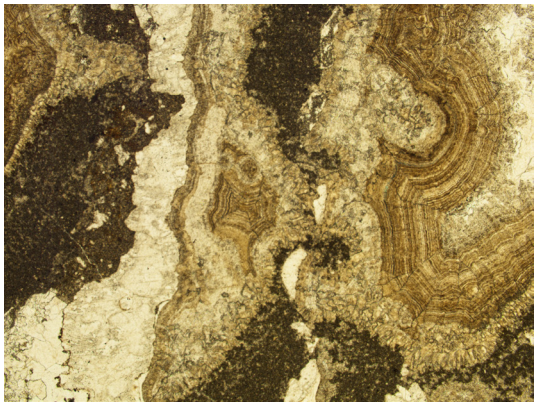

PR05-BandedCement,CavityInfill 2.5xPPL.tif

APPENDIX E

STATEMENT OF THE CONTRIBUTION OF OTHERS

To Whom It May Concern

I, **Robert Henry Christopher Madden**, contributed to all aspects of research including, but not limited to, primary data collection, data processing and analysis, figure drafting and writing for the publications entitled:

"Modern fringing reef carbonates from equatorial SE Asia: an integrated environmental, sediment and satellite characterisation study."

"Diagenesis of Neogene delta-front patch reefs: alteration of coastal siliciclastic influenced carbonates from humid equatorial regions."

"Diagenesis of a SE Asian Cenozoic carbonate platform margin and its adjacent basinal deposits."

RHC MADDEN

Date: 09-01-2013

A realistic breakdown of the contribution by each author is as follows:

Robert H.C. Madden 80%
Dr. Moyra E.J. Wilson 20%

in the case of co-authorship with Maeve O'Shea a realistic breakdown of the contribution by each author is as follows:

Robert H.C. Madden 75%
Dr. Moyra E.J. Wilson 20%
Maeve O'Shea 5%

I, as co-author and supervisor to Robert, endorse that the level of contributions indicated above are accurate. Furthermore I endorse that the level of contribution from Maeve O'Shea (who is not contactable at the time of submission of this thesis) indicated above is accurate.

MEJ WILSON

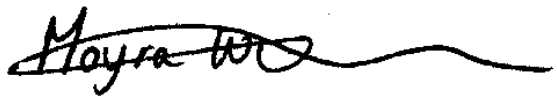

Date: 09-01-2013